

**ON THE REGULATION OF OXYGEN DELIVERY TO THE BRAIN IN  
HUMANS**

by

Ryan Leo Hoiland

BHK., The University of British Columbia, 2013

MSc.. The University of British Columbia, 2015

A THESIS SUBMITTED IN PARTIAL FULLFILLMENT OF  
THE REQUIREMENTS FOR THE DEGREE OF

DOCTOR OF PHILOSOPHY

in

THE COLLEGE OF GRADUATE STUDIES

(Interdisciplinary Studies)

THE UNIVERSITY OF BRITISH COLUMBIA

(Okanagan)

August 2018

©Ryan Leo Hoiland, 2018

The following individuals certify that they have read, and recommend to the College of Graduate Studies for acceptance, a thesis/dissertation entitled:

ON THE REGULATION OF OXYGEN DELIVERY TO THE BRAIN IN HUMANS

---

submitted by Ryan Leo Hoiland in partial fulfillment of the requirements of

the degree of Doctor of Philosophy .

Philip Ainslie, School of Health and Exercise Sciences

---

**Supervisor**

Neil Eves, School of Health and Exercise Sciences

---

**Supervisory Committee Member**

Ali McManus, School of Health and Exercise Sciences

---

**Supervisory Committee Member**

Christopher West, Southern Medical Program

---

**University Examiner**

Kevin Shoemaker, Health Sciences, University of Western Ontario

---

**External Examiner**

## **ABSTRACT**

Intact, coordinated, and precisely regulated increases in cerebral blood flow are required to compensate for reductions in arterial oxygen content and maintain cerebral oxygen delivery. This thesis aimed to determine the physiological processes and regulatory pathways that act to maintain cerebral oxygen delivery in humans and how these processes may be altered by long term exposure to hypoxia at evolutionary and pathological levels. Four studies were conducted to address these objectives. Study 1 investigated the influence of adenosine on the cerebral blood flow response to experimental hypoxemia at sea-level and high altitude. Compared to placebo treatment, adenosine receptor blockade had no impact on the cerebral blood flow response to acute or chronic hypoxemia indicating that adenosine is not an obligatory regulator of cerebral oxygen delivery. Study 2 was designed to determine the role of the erythrocyte in regulating cerebral blood flow and oxygen delivery during two forms of hypoxia: experimental hypoxemia and experimental anemia (hemodilution). The same overall reductions in arterial oxygen content elicited a more robust increase in cerebral blood flow and maintenance of cerebral oxygen delivery during hypoxemia than during hemodilution where cerebral oxygen delivery was reduced. Study 3 compared the regulation of cerebral blood flow and oxygen delivery between lowland natives, and high-altitude natives – the Sherpa – upon graded ascent to 5050m. Sherpa possessed consistently lower cerebral oxygen delivery. However, given their exceptional physical capacity at altitude, this result may indicate a reduced oxygen demand analogous to hypoxia tolerant animals. Study 4 examined the influence of pathological chronic hypoxia on the matching of cerebral blood flow (and therefore oxygen delivery) to metabolic demand in chronic obstructive lung disease patients. Alleviation of hypoxemia with oxygen therapy augmented the flow response to neural activation, indicating chronic hypoxia impairs the mechanisms regulating cerebral oxygen delivery. While signaling mechanisms remain difficult to disentangle in humans, the erythrocyte has emerged as integral to the regulation of cerebral oxygen delivery. Chronic hypoxia at an evolutionary level may lead to positive adaptations related to oxygen demand, whereas pathological chronic hypoxia reduces the capacity to augment flow and oxygen delivery during neural activation.

## **LAY SUMMARY**

This thesis examined the signaling pathways that regulate oxygen delivery to the brain in humans. The red blood cell, through the release of signaling molecules, is integral to the regulation of brain blood flow and oxygen delivery during instances of low blood oxygen levels, termed hypoxia. Individuals of Tibetan descent that have evolved in hypoxia at high-altitude appear to have adapted to require less oxygen. The long term hypoxia characteristic of chronic obstructive pulmonary disease patients, impairs the ability of the brain to increase oxygen delivery when neural activity and oxygen demand are increased. Overall, in healthy humans, oxygen delivery to the brain is consistently maintained, due in part to red blood cell related mechanisms. Evolution at altitude may reduce the oxygen delivery requirements of the brain as a protective response whereas long term hypoxia associated with pathology leads to a dysregulation in the matching oxygen delivery to demand.

## PREFACE

The University of British Columbia Clinical Research Ethics Board approved all experimental chapters in this thesis (CREB IDs: H15-01513; H16-01028; H18-01755; CREB ID: H16-00342; CREB ID: H17-00929).

**Chapter 1.** Chapter one was written by Ryan Hoiland, and edited by Prof. Ainslie.

**Chapter 2.** Aspects of chapter two have been published and/or are under consideration for publication. Sections 2.1, 2.2, and 2.4 are part of an invited manuscript submitted to *Comprehensive Physiology* on May 30<sup>th</sup>, 2018: Hoiland RL, Fisher J & Ainslie PN. Regulation of the Cerebral Circulation by Arterial Carbon Dioxide. *Comprehensive Physiology*. In review. Parts of Section 2.3 were published in the *American Journal of Physiology – Regulatory, Integrative and Comparative Physiology*. Hoiland RL, Bain AR, Rieger MG, Bailey DM, Ainslie PN. (2016) Hypoxemia, oxygen content, and the regulation of cerebral blood flow. *Am J Physiol Regul Integr Comp Physiol*. 310(5): R398-413 as well as in *Clinical Autonomic Research*: Hoiland RL, Howe CA, Coombs GB, Ainslie PN. (2018) Ventilatory and cerebrovascular regulation and integration at high-altitude. *Clinical Autonomic Research*. Doi: 10.1007/s10286-018-0522-2. Ryan Hoiland drafted the majority of each manuscript, was responsible for the majority of figures & tables and is contact author for each manuscript. The specific sections included in this chapter were drafted by Ryan Hoiland with some assistance from Prof. Ainslie and Prof. Fisher.

**Chapter 3.** This chapter was published in the *Journal of Applied Physiology*: Hoiland RL, Bain AR, Tymko MM, Rieger MG, Howe CA, Willie CK, Hansen AB, Fluck D, Wildfong KW, Stembridge M, Subedi P, Anholm J, Ainslie PN. (2017) Adenosine receptor-dependent signaling is not obligatory for normobaric and hypobaric hypoxia-induced cerebral vasodilation in humans. *Journal of Applied Physiology*. 122(4): 795-808. Ryan Hoiland and Prof. Ainslie designed the experimental protocols in this chapter. Ryan Hoiland drafted the manuscript, was responsible for all tables & figures, and is contact author. Co-authors edited and approved the final version of the manuscript. CREB ID: H15-01513.

**Chapter 4.** Aspects of this chapter were presented at the 2017 International Hypoxia symposium by Ryan Hoiland. Aspects of this chapter were also presented at the 2018 Okanagan Cardiovascular and Respiratory Symposium by Ryan Hoiland. Ryan Hoiland and Prof. Ainslie designed the experimental protocols in this chapter. Ryan Hoiland drafted chapter 4 and is responsible for all tables and figures. Prof. Ainslie assisted with drafting and editing of the chapter. CREB ID: H16-01028; H18-01755.

**Chapter 5.** Aspects of this chapter were presented at the 2017 International Hypoxia symposium by Connor Howe. Ryan Hoiland and Prof. Ainslie designed the experimental protocols in this chapter. Ryan Hoiland drafted chapter 5 and is responsible for all tables and figures. Mr. Connor Howe assisted with data analysis. Prof. Ainslie assisted with drafting and editing this chapter. CREB ID: H16-01028.

**Chapter 6.** This chapter was accepted for publication in *Experimental Physiology* on May 29<sup>th</sup>, 2018. Hoiland RL\*, Mladinov S\*, Barak O, Willie CK, Mijacika T, Stembridge M, Dujic Z, Ainslie PN. Oxygen therapy improves cerebral oxygen delivery and neurovascular function in hypoxemic chronic obstructive disease patients. *Experimental Physiology*. Accepted May 29, 2018. (manuscript ID: EP-RP-2018-086994R2). Prof. Ainslie and Prof. Dujic designed the experimental protocols of this chapter. Ryan Hoiland drafted the manuscript and was responsible for all figures and tables. Co-authors edited and approved the manuscript. CREB ID: H16-01028.

**Chapter 7.** Part of this chapter was included in an invited manuscript submitted to *Comprehensive Physiology* on May 30<sup>th</sup>, 2018: Hoiland RL, Fisher J & Ainslie PN. Regulation of the Cerebral Circulation by Arterial Carbon Dioxide. *Comprehensive Physiology*. In review. Other components have been published in the *American Journal of Physiology – Regulatory, Integrative and Comparative Physiology*. Hoiland RL, Bain AR, Rieger MG, Bailey DM, Ainslie PN. (2016) Hypoxemia, oxygen content, and the regulation of cerebral blood flow. *American Journal of Physiology Regulatory Integrative & Comparative Physiology*. 310(5): R398-413. Aspects of this chapter were also been presented at Experimental Biology 2018 by Ryan Hoiland.

**Appendix A.** This appendix was published in the *American Journal of Physiology – Heart and Circulatory Physiology*: Hoiland RL, Smith KJ, Carter HH, Lewis NCS, Tymko MM, Wildfong KW, Bain AR, Green DJ & Ainslie PN. (2017) Shear-mediated dilation of the internal carotid artery occurs independent of hypercapnia. *American Journal of Physiology Heart and Circulatory Physiology*. 313, H24-H31. This project was completed as part of a collaboration between the University of British Columbia Okanagan and the University of Western Australia, whereby Ryan Hoiland traveled to the University of Western Australia having received the UBC Friedman Award for Scholars in Health. Ryan Hoiland, Prof. Philip Ainslie and Prof. Daniel Green conceived the study design. Ryan Hoiland drafted the manuscript and was responsible for all tables and figures. All co-authors edited and approved the manuscript. CREB ID: H16-00342.

## TABLE OF CONTENTS

ABSTRACT.....	III
LAY SUMMARY.....	IV
PREFACE.....	V
TABLE OF CONTENTS .....	VIII
LIST OF FIGURES .....	XV
LIST OF TABLES.....	XVIII
LIST OF EQUATIONS.....	XX
ACKNOWLEDGEMENTS .....	XXI
GLOSSARY.....	XXII
<b>1. CHAPTER 1: INTRODUCTION .....</b>	<b>1</b>
<b>1.1 THESIS OBJECTIVES .....</b>	<b>3</b>
<b>1.2 SPECIFIC AIMS AND HYPOTHESES .....</b>	<b>3</b>
<b>1.2.1 STUDY 1 (CHAPTER 3).....</b>	<b>3</b>
<b>1.2.1.1 STUDY 1 – BACKGROUND .....</b>	<b>3</b>
<b>1.2.1.2 STUDY 1 – AIM.....</b>	<b>4</b>
<b>1.2.1.3 STUDY 1 – HYPOTHESES.....</b>	<b>4</b>
<b>1.2.2 STUDY 2 (CHAPTER 4).....</b>	<b>4</b>
<b>1.2.2.1 STUDY 2 – BACKGROUND .....</b>	<b>4</b>
<b>1.2.2.2 STUDY 2 – AIM .....</b>	<b>5</b>
<b>1.2.2.3 STUDY 2 – HYPOTHESES.....</b>	<b>5</b>
<b>1.2.3 STUDY 3 (CHAPTER 5).....</b>	<b>5</b>
<b>1.2.3.1 STUDY 3 – BACKGROUND .....</b>	<b>5</b>
<b>1.2.3.2 STUDY 3 – AIM.....</b>	<b>6</b>
<b>1.2.3.3 STUDY 3 – HYPOTHESES.....</b>	<b>6</b>
<b>1.2.4 STUDY 4 (CHAPTER 6).....</b>	<b>6</b>
<b>1.2.4.1 STUDY 4 – BACKGROUND .....</b>	<b>6</b>
<b>1.2.4.2 STUDY 4 – AIMS .....</b>	<b>7</b>
<b>1.2.4.3 STUDY 4 – HYPOTHESES.....</b>	<b>7</b>
<b>2. CHAPTER TWO: A REVIEW OF CEREBRAL BLOOD FLOW</b>	
<b>REGULATION .....</b>	<b>8</b>
<b>2.1 CEREBROVASCULAR ANATOMY .....</b>	<b>9</b>

2.1.1	CEREBRAL ARTERIAL ARRANGEMENT .....	9
2.1.2	CEREBRAL VENOUS ARRANGEMENT .....	12
2.2	HISTORICAL PERSPECTIVE ON CEREBRAL BLOOD FLOW .....	14
2.2.1	EARLY PIONEERS IN CEREBROVASCULAR RESEARCH .....	14
2.2.2	MODERN MEASUREMENT TECHNIQUES .....	20
2.2.2.1	<i>THE KETY &amp; SCHMIDT TECHNIQUE</i> .....	22
2.2.2.2	<i>TRANSCRANIAL DOPPLER ULTRASOUND</i> .....	22
2.2.2.3	<i>DUPLEX ULTRASOUND</i> .....	26
2.2.2.4	<i>BLOOD OXYGEN LEVEL DEPENDENT MAGNETIC RESONANCE IMAGING</i> .....	27
2.3	BASICS OF CEREBRAL BLOOD FLOW REGULATION.....	28
2.3.1	CEREBRAL BLOOD FLOW AND MICROVASCULAR PRESSURE WITH CHANGES IN SEGMENTAL VASCULAR RESISTANCE .....	30
2.3.2	CEREBRAL BLOOD FLOW AND BLOOD VISCOSITY .....	34
2.3.3	CEREBRAL BLOOD FLOW AND CRITICAL CLOSING PRESSURE.....	36
2.3.4	CEREBRAL BLOOD FLOW AND ARTERIAL BLOOD GASES .....	37
2.3.5	CEREBRAL BLOOD FLOW AND OXYGEN .....	38
2.3.6	CEREBRAL BLOOD FLOW AND CARBON DIOXIDE.....	40
2.3.7	CEREBRAL BLOOD FLOW AND PERFUSION PRESSURE .....	41
2.3.8	CEREBRAL BLOOD FLOW AND NEUROVASCULAR COUPLING .....	43
2.3.9	CEREBRAL BLOOD FLOW AND CELLULAR REGULATION OF VASCULAR SMOOTH MUSCLE TONE .....	45
2.4	CEREBRAL BLOOD FLOW REGULATION IN HYPOXIA .....	46
2.4.1	RESPONSE CHARACTERISTICS OF CEREBRAL BLOOD FLOW TO HYPOXEMIC HYPOXIA.....	49
2.4.1.1	<i>ACUTE HYPOXEMIC HYPOXIA (SECONDS TO HOURS)</i> .....	49
2.4.1.2	<i>CHRONIC HYPOXEMIC HYPOXIA (DAYS TO YEARS) – EVIDENCE FROM STUDIES AT HIGH-ALTITUDE</i> .....	53
2.4.1.3	<i>CHRONIC ADAPTATION TO HIGH-ALTITUDE:</i> .....	58
2.4.2	ARTERIAL OXYGEN CONTENT AND CEREBRAL BLOOD FLOW: HYPOXEMIC HYPOXIA VERSUS HEMODILUTION .....	60
2.4.3	SIGNALING PATHWAYS IN THE REGULATION OF CEREBRAL BLOOD FLOW DURING HYPOXIA .....	68

<b>2.4.3.1</b>	<b><i>DEOXYHEMOGLOBIN MEDIATED SIGNAL TRANSDUCTION PATHWAYS</i></b>	<b>70</b>
2.4.3.1.1	S- NITROSOHEMOGLOBIN RELEASE FROM ERYTHROCYTES DURING HYPOXIA .....	70
2.4.3.1.2	NITRITE REDUCTION VIA HEMOGLOBIN .....	71
2.4.3.1.3	ADENOSINE TRIPHOSPHATE LIBERATION FROM ERYTHROCYTES DURING HYPOXIA .....	72
<b>2.4.3.2</b>	<b><i>DOWNSTREAM SIGNALING MOLECULES</i></b> .....	<b>72</b>
2.4.3.2.1	HYPOXIA AND ADENOSINE TRI-PHOSPHATE.....	72
2.4.3.2.2	HYPOXIA AND ADENOSINE.....	73
2.4.3.2.3	HYPOXIA AND NITRIC OXIDE .....	74
2.4.3.2.4	HYPOXIA AND PROSTAGLANDINS .....	75
2.4.3.2.5	HYPOXIA AND EPOXYEICOSATRIENOIC ACIDS.....	76
<b>2.4.4</b>	<b>SYNOPSIS OF CEREBRAL BLOOD FLOW REGULATION IN HYPOXIA</b> .....	<b>76</b>
<b>2.5</b>	<b>REGULATION OF CEREBRAL BLOOD FLOW BY CARBON DIOXIDE</b> .....	<b>77</b>
<b>2.5.1</b>	<b>CEREBROVASCULAR CO<sub>2</sub> REACTIVITY</b> .....	<b>80</b>
<b>2.5.2</b>	<b>STANDARDIZATION AND UTILITY OF CEREBROVASCULAR REACTIVITY</b> ....	<b>81</b>
<b>2.5.3</b>	<b>INTRACRANIAL HEMODYNAMICS ASSESSED WITH BOLD</b> .....	<b>83</b>
<b>2.5.4</b>	<b>CO<sub>2</sub>: SITE(S) OF VASCULAR REGULATION</b> .....	<b>86</b>
<b>2.5.5</b>	<b>FACTORS INFLUENCING CEREBROVASCULAR CO<sub>2</sub> REACTIVITY</b> . ....	<b>88</b>
<b>2.5.5.1</b>	<b><i>CO<sub>2</sub> REACTIVITY AND HYPOXIA</i></b> .....	<b>88</b>
<b>2.5.5.2</b>	<b><i>CO<sub>2</sub> REACTIVITY AND BLOOD PRESSURE</i></b> .....	<b>91</b>
<b>2.5.5.3</b>	<b><i>CO<sub>2</sub> REACTIVITY AND SYMPATHETIC NERVOUS ACTIVITY</i></b> .....	<b>94</b>
<b>2.5.5.4</b>	<b><i>CO<sub>2</sub> REACTIVITY AND AGING</i></b> .....	<b>95</b>
<b>2.5.5.5</b>	<b><i>CO<sub>2</sub> REACTIVITY AND SEX DIFFERENCES</i></b> .....	<b>96</b>
<b>2.5.6</b>	<b>SIGNALING PATHWAYS REGULATING CEREBROVASCULAR CO<sub>2</sub></b> <b>REACTIVITY</b> .....	<b>96</b>
<b>2.5.6.1</b>	<b><i>HYPERCAPNIA AND ADENOSINE</i></b> .....	<b>100</b>
<b>2.5.6.2</b>	<b><i>HYPERCAPNIA AND ARACHIDONIC ACID METABOLITES</i></b> .....	<b>101</b>
<b>2.5.6.3</b>	<b><i>HYPERCAPNIA AND NITRIC OXIDE</i></b> .....	<b>104</b>
<b>2.5.6.4</b>	<b><i>HYPERCAPNIA AND ERYTHROCYTE RELEASED ATP AND ENOS</i></b> ....	<b>107</b>
<b>2.5.6.5</b>	<b><i>HYPERCAPNIA AND REACTIVE OXYGEN SPECIES</i></b> .....	<b>108</b>
<b>2.5.6.6</b>	<b><i>HYPERCAPNIA AND SHEAR STRESS</i></b> .....	<b>108</b>

2.5.6.7	<i>HYPERCAPNIA AND POTASSIUM CHANNELS</i> .....	112
2.5.6.8	<i>HYPERCAPNIA AND BICARBONATE ION</i> .....	113
2.5.7	POTENTIAL SIGNALING PATHWAY INTERACTIONS.....	113
2.5.7.1	<i>NITRIC OXIDE AND K<sub>ATP</sub> CHANNELS</i> .....	113
2.5.7.2	<i>CYCLIC NUCLEOTIDE CROSS TALK</i> .....	114
2.5.7.3	<i>ARACHIDONIC ACID PATHWAY AND REACTIVE OXYGEN SPECIES     PRODUCTION</i> .....	117
2.5.8	SYNOPSIS OF CEREBRAL BLOOD FLOW REGULATION BY CARBON DIOXIDE .....	119
2.6	SYNOPSIS OF LITERATURE REVIEW .....	119
3.	<b>CHAPTER 3: ADENOSINE RECEPTOR DEPENDENT SIGNALING IS NOT OBLIGATORY FOR NORMOBARIC AND HYPOBARIC HYPOXIA- INDUCED CEREBRAL VASODILATION IN HUMANS</b> .....	121
3.1	STUDY 2 - METHODS .....	123
3.1.1	STUDY 1 - EXPERIMENTAL MEASURES.....	124
3.1.1.1	<i>CARDIORESPIRATORY MEASURES</i> .....	124
3.1.1.1.1	SEA-LEVEL STUDY. ....	124
3.1.1.1.2	HIGH-ALTITUDE STUDY.....	125
3.1.1.2	<i>DYNAMIC END-TIDAL FORCING</i> .....	125
3.1.1.3	<i>CEREBROVASCULAR MEASURES</i> .....	125
3.1.2	STUDY 1 - EXPERIMENTAL PROTOCOL .....	127
3.1.2.1	<i>SEA-LEVEL STUDY</i> .....	127
3.1.2.2	<i>HIGH-ALTITUDE STUDY</i> .....	128
3.1.2.3	<i>STUDY 1 - CALCULATIONS</i> .....	129
3.1.2.4	<i>STUDY 1 - STATISTICAL ANALYSES</i> .....	131
3.2	STUDY 1 - RESULTS .....	132
3.2.1	SEA LEVEL STUDY .....	132
3.2.1.1	<i>PLACEBO TRIALS</i> .....	132
3.2.1.2	<i>THEOPHYLLINE TRIALS</i> .....	136
3.2.1.3	<i>CEREBROVASCULAR REACTIVITY SLOPES TO HYPOXIA</i> .....	139
3.2.1.4	<i>BETWEEN VESSEL COMPARISONS</i> .....	140
3.2.2	HIGH-ALTITUDE STUDY .....	141
3.3	STUDY 1 - DISCUSSION .....	144

3.3.1	MECHANISMS OF HYPOXIC CEREBRAL VASODILATION.....	145
3.3.2	CEREBRAL BLOOD FLOW AND NORMOBARIC HYPOXIA.....	148
3.3.3	CEREBRAL BLOOD FLOW AND HYPOBARIC HYPOXIA .....	150
3.3.4	ACUTE MOUNTAIN SICKNESS.....	151
3.3.5	METHODOLOGICAL CONSIDERATIONS .....	152
3.4	STUDY 1 - SUMMARY.....	153
4.	ERYTHROCYTE MEDIATED HYPOXIC CEREBRAL VASODILATION IN HUMANS.....	154
4.1	STUDY 2 - METHODS .....	155
4.1.1	PROTOCOL ONE .....	156
4.1.1.1	<i>PROTOCOL ONE - EXPERIMENTAL MEASURES.....</i>	<i>156</i>
4.1.1.1.1	ARTERIAL AND VENOUS CANNULATION.....	156
4.1.1.1.2	ARTERIAL-VENOUS BLOOD ANALYSES.....	157
4.1.1.2	<i>PROTOCOL ONE – EXPERIMENTAL OVERVIEW.....</i>	<i>157</i>
4.1.1.3	<i>PROTOCOL ONE - CALCULATIONS .....</i>	<i>160</i>
4.1.1.4	<i>PROTOCOL ONE - STATISTICAL ANALYSES.....</i>	<i>160</i>
4.1.2	PROTOCOL TWO .....	162
4.1.2.1	<i>PROTOCOL TWO - STATISTICAL ANALYSES.....</i>	<i>163</i>
4.2	STUDY 2 - RESULTS .....	164
4.2.1	RESULTS – PROTOCOL ONE .....	164
4.2.1.1	<i>HYPOXEMIA VERSUS HEMODILUTION .....</i>	<i>164</i>
4.2.1.1.1	CARDIOVASCULAR DATA.....	168
4.2.1.1.2	CEREBROVASCULAR RESPONSES .....	168
4.2.1.2	<i>HYPOXEMIA PRE VERSUS HYPOXEMIA POST.....</i>	<i>173</i>
4.2.1.2.1	CARDIOVASCULAR DATA.....	177
4.2.1.2.2	CEREBRAL BLOOD FLOW RESPONSES .....	177
4.2.1.3	<i>COLLECTIVE COMPARISON OF HYPOXIC CEREBRAL VASODILATION .....</i>	<i>182</i>
4.2.2	RESULTS – PROTOCOL TWO .....	183
4.3	STUDY 2 - DISCUSSION .....	186
4.3.1	WHY IS A LOWER HEMOGLOBIN CONCENTRATION RELATED TO A GREATER HYPOXIC REACTIVITY?.....	187

4.3.2	SEX DIFFERENCES IN THE REGULATION OF HYPOXIC CEREBRAL VASODILATION?.....	189
4.3.3	METHODOLOGICAL CONSIDERATIONS .....	190
4.4	STUDY 2 - SUMMARY.....	191
5.	<b>CHAPTER 4: UBC-NEPAL EXPEDITION: REDUCED CEREBRAL BLOOD FLOW AND OXYGEN DELIVERY IN SHERPA COMPARED TO LOWLANDERS UPON ASCENT TO HIGH-ALTITUDE .....</b>	<b>193</b>
5.1	STUDY 3 - METHODS .....	194
5.1.1	STUDY 3 - EXPERIMENTAL OVERVIEW .....	196
5.1.2	STUDY 3 - EXPERIMENTAL MEASURES .....	196
5.1.3	STUDY 3 - CALCULATIONS .....	197
5.1.4	SUTDY 3 - STATISTICAL ANALYSES.....	197
5.2	STUDY 3 - RESULTS .....	198
5.2.1	ARTERIAL AND VENOUS BLOOD VARIABLES .....	198
5.2.2	CEREBROVASCULAR AND CARDIORESPIRATORY VARIABLES .....	200
5.2.3	PREDICTORS OF GCBF DURING ASCENT.....	203
5.2.4	ASCENT VERSUS ALTITUDE SHERPA COMPARISONS .....	205
5.3	STUDY 3 - DISCUSSION .....	207
5.3.1	CEREBRAL BLOOD FLOW AT ALTITUDE: INFLUENCE OF RACE .....	208
5.3.2	POTENTIAL MECHANISM(S) OF REDUCED CEREBRAL OXYGEN DELIVERY .....	209
5.3.3	METHODOLOGICAL CONSIDERATIONS .....	211
5.4	STUDY 3 - SUMMARY .....	212
6.	<b>OXYGEN THERAPY IMPROVES CEREBRAL OXYGEN DELIVERY AND NEUROVASCULAR FUNCTION IN HYPOXEMIC CHRONIC OBSTRUCTIVE PULMONARY DISEASE PATIENTS.....</b>	<b>213</b>
6.1	STUDY 4 - METHODS .....	214
6.1.1	STUDY 4 - EXPERIMENTAL PROTOCOL .....	216
6.1.2	STUDY 4 - CALCULATIONS .....	217
6.1.3	STUDY 4 - STATISTICAL ANALYSES.....	217
6.2	STUDY 4 - RESULTS .....	218
6.3	STUDY 4 - DISCUSSION .....	225
6.4	STUDY 4 - SUMMARY.....	227

<b>7. CONCLUSION</b> .....	<b>228</b>
<b>7.1 A REVIEW OF THESIS OBJECTIVES</b> .....	<b>228</b>
<b>7.1.1 MECHANISMS LEADING TO A COMPROMISE IN CEREBRAL O<sub>2</sub> DELIVERY</b> <b>DURING HEMODILUTION</b> .....	<b>230</b>
<b>7.1.2 CLINICAL IMPLICATIONS AND FUTURE DIRECTIONS</b> .....	<b>231</b>
<b>7.2 A FRAMEWORK FOR FUTURE INVESTIGATIONS INTO THE SIGNALING PATHWAYS</b> <b>REGULATING HUMAN CEREBRAL BLOOD FLOW</b> .....	<b>232</b>
<b>7.2.1 WHY IS THE DESIGN OF CEREBROVASCULAR EXPERIMENTS SO</b> <b>IMPORTANT?</b> .....	<b>233</b>
<b>7.2.2 COMPONENT 1 - MANIPULATING SIGNALING MOLECULE BIOAVAILABILITY</b> .....	<b>234</b>
<b>7.2.3 COMPONENT 2 - MEASURING CHANGES IN SIGNALING MOLECULE</b> <b>BIOAVAILABILITY</b> .....	<b>235</b>
<b>7.2.4 COMPONENT 3 - MEASUREMENT OF VOLUMETRIC CBF</b> .....	<b>238</b>
<b>7.2.5 WHERE ARE WE NOW?</b> .....	<b>238</b>
<b>7.3 FUTURE DIRECTIONS: NITRIC OXIDE AND HYPOXIC VASODILATION</b> .....	<b>240</b>
<b>7.3.1 AIMS AND HYPOTHESES</b> .....	<b>240</b>
<b>7.3.2 METHODOLOGY</b> .....	<b>240</b>
<b>7.4 FINAL CONSIDERATIONS ON MECHANISTIC INVESTIGATION INTO CEREBRAL</b> <b>BLOOD FLOW REGULATION</b> .....	<b>241</b>
<b>BIBLIOGRAPHY</b> .....	<b>243</b>
<b>APPENDICES</b> .....	<b>315</b>
<b>APPENDIX A: SHEAR-MEDIATED DILATION OF THE INTERNAL CAROTID ARTERY</b> <b>OCCURS INDEPENDENT OF HYPERCAPNIA</b> .....	<b>315</b>

## LIST OF FIGURES

Figure 2.1. Organization of cerebral blood flow and collateral blood flow. ....	10
Figure 2.2. Collateralization across microvascular beds. ....	12
Figure 2.3. Cerebral Blood Flow Measurement Techniques Pioneered by Angelo Mosso. .....	16
Figure 2.4. Early Pioneers in Cerebral Vascular Physiology.....	18
Figure 2.5. The Original Experimental Setup and Recordings for the Nitrous Oxide Technique Developed by Kety & Schmidt. ....	19
Figure 2.6. Influence of changes in middle cerebral artery diameter on the validity of transcranial doppler ultrasound.....	25
Figure 2.7. Duplex ultrasound image of the internal carotid artery and an example of an analysis output. ....	27
Figure 2.8. A simplified schematic of how segmental changes in the resistance of cerebral blood vessels organized in series influence flow and microvascular pressure. ....	32
Figure 2.9. Changes in wall stress along the pial circulation.....	34
Figure 2.10. Basic regulation of cerebral blood flow by oxygen, carbon dioxide, and cerebral perfusion pressure. ....	38
Figure 2.11. Cerebral blood flow reactivity to changes in arterial carbon dioxide. ....	41
Figure 2.12. The classical (left) and contemporary (right) cerebral autoregulation curves. .....	42
Figure 2.13. Feed forward mechanisms in neurovascular coupling. ....	44
Figure 2.14. Diagram of the relationship between oxygen content and the partial pressure of oxygen. ....	48
Figure 2.15. Cerebral blood flow and oxygen delivery during acute hypoxemic hypoxia in humans. ....	51
Figure 2.16. Regional disparities in cerebral oxygen delivery relative to the whole brain during isocapnic hypoxia. ....	52
Figure 2.17. Cerebral blood flow and oxygen delivery at high-altitude.....	54
Figure 2.18. Contribution of changes in partial pressure of oxygen and hemoglobin concentration in the increase in arterial oxygen content during acclimatization at high- altitude.....	55

Figure 2.19. Integrative physiological changes during acclimatization to very high-altitude (~5000m).....	57
Figure 2.20. Cerebral blood flow and oxygen delivery during hemodilution in humans. .	63
Figure 2.21. The relationship between arterial oxygen content, cerebral Blood flow, and cerebral oxygen delivery in anemic, hematologically normal, and polycythemic humans. ....	65
Figure 2.22. Change in cerebral blood flow and oxygen delivery during reductions in arterial oxygen content induced by hypoxemic hypoxia and hemodilution. ....	67
Figure 2.23. Putative pathways regulating cerebral blood flow during hypoxia. ....	69
Figure 2.24. The brain vascular stress test to identify the extent of collateralization in the presence of steno-occlusive vascular disease. ....	85
Figure 2.25. Carbon dioxide mediated alterations in cerebrovascular diameter occurs throughout the entire cerebrovascular tree.....	87
Figure 2.26. Relationship Between the Partial Pressure of Carbon Dioxide and pH With Varying Bicarbonate Ion Concentration. ....	90
Figure 2.27. Effect of a progressive loss of vasodilatory reserve on the response to changes in arterial carbon dioxide. ....	92
Figure 2.28. Increased blood pressure during hypercapnia is related to cerebrovascular reactivity. ....	93
Figure 2.29. Potential pathways regulating cerebrovascular reactivity to carbon dioxide. ....	98
Figure 2.30. Transient increases in shear stress and internal carotid artery vasodilation. ....	111
Figure 2.31. Evidence for cyclic nucleotide cross talk in cerebrovascular regulation. ...	117
Figure 3.1. Adenosine signaling pathways in hypoxia. ....	122
Figure 3.2. Reactivity slopes of extra- and intra-cranial blood vessels in all experimental trials at sea-level. ....	140
Figure 3.3. Global and regional cerebral blood flow during isocapnic hypoxia prior to and following placebo and theophylline interventions. ....	141
Figure 3.4. The relationships between mean arterial pressure and cerebral blood flow variables in the theophylline and placebo trials. ....	147
Figure 3.5. Agreement between measured and calculated arterial oxygen saturation. ....	153
Figure 4.1. Radial artery and internal jugular vein catheters. ....	157

Figure 4.2. Hypoxemia and hemodilution experimental overview.....	160
Figure 4.3. Formalism for the calculation of changes in cerebral blood flow from arterial and jugular venous blood samples. ....	163
Figure 4.4. Key blood parameters from the hypoxemia pre and hemodilution trials. ....	167
Figure 4.5. Cerebrovascular reactivity profiles to hypoxemia and hemodilution.....	172
Figure 4.6. Cerebrovascular reactivity during hypoxemia prior to and following hemodilution. ....	181
Figure 4.7. Cerebral blood flow and oxygen delivery across all three experimental trials. ....	183
Figure 4.8. The relationship between hemoglobin concentration and hypoxic reactivity in males and females. ....	185
Figure 4.9. Relationship between pH and PaCO <sub>2</sub> in eight subjects from the hemodilution study.....	191
Figure 5.1. Regional cerebral blood flow and cerebral oxygen delivery upon ascent to 5050 m in lowlanders and sherpa.....	201
Figure 5.2. Cerebral blood flow distribution in lowlanders and sherpa upon ascent and following acclimatization.....	202
Figure 5.3. Actual versus predicted global cerebral blood flow. ....	205
Figure 5.4. Cerebral blood flow and oxygen delivery in acclimatized lowlanders, sherpa following ascent, and sherpa recruited at altitude.....	206
Figure 5.5. Lowlander and sherpa cerebrovascular reactivity to carbon dioxide. ....	210
Figure 6.1. Cerebral blood flow prior to and following oxygen normalization in chronic obstructive pulmonary disease patients. ....	220
Figure 6.2. Neurovascular coupling responses prior to and following oxygen normalization. ....	223
Figure 6.3. Mean arterial pressure during neurovascular coupling .....	224
Figure 7.1. Differential Changes in Cerebral Blood Flow During Hypoxemic Hypoxia and Hemodilution and the Impact on Cerebral Oxygen Delivery in Animals. ....	231
Figure 7.2. Ozone based chemiluminescence. ....	236
Figure 7.3. Standard curves for ozone based chemiluminescence.....	237
Figure 7.4. Results from the studies by Van Mil in 2002 and Ide in 2007.....	240

## LIST OF TABLES

Table 2.1. The strengths, limitations, and utility of various techniques for the measurement of cerebral blood flow in humans. ....	21
Table 3.1. Cardiorespiratory variables during sea level hypoxia.....	133
Table 3.2. Cerebrovascular variables during sea level hypoxia.....	134
Table 3.3. Theoretical calculations of arterial oxygen content, cerebral oxygen delivery, and cerebral blood flow parameters corrected for carbon dioxide. ....	137
Table 3.4. r-squared values for the linear regression of cerebrovascular reactivity. ....	138
Table 3.5. Cerebral vascular, hemodynamic, and respiratory variables upon exposure to high-altitude. ....	143
Table 4.1. Radial arterial blood data during hypoxemia and hemodilution.....	165
Table 4.2. Jugular venous blood data during hypoxemia and hemodilution. ....	166
Table 4.3. Cardiovascular data during hypoxemia and hemodilution. ....	168
Table 4.4. Cerebral blood flow during hypoxemia and hemodilution. ....	170
Table 4.5. Radial arterial bloods during hypoxemia prior to and following hemodilution. ....	174
Table 4.6 Jugular venous bloods during hypoxemia prior to and following hemodilution. ....	175
Table 4.7. Cardiovascular data during hypoxemia prior to and following hemodilution. ....	176
Table 4.8. Cerebral blood flow during hypoxemia prior to and following hemodilution. ....	179
Table 4.9. Baseline variables for protocol two of study two. ....	184
Table 5.1. Age and time at high-altitude for the sherpa participants. ....	195
Table 5.2. Arterial and venous blood data. ....	199
Table 5.3. Multi-linear regression for the prediction of cerebral blood flow at high-altitude in lowlanders and sherpa.....	204
Table 5.4. Comparison between lowlanders, the ascent sherpa, and the altitude sherpa following arrival at 5050m.....	207
Table 6.1. Chronic obstructive pulmonary disease patient characteristics. ....	215
Table 6.2. Cerebral and cardiovascular variables pre- and post-oxygen normalization in chronic obstructive pulmonary disease patients. ....	219

Table 6.3. Peak changes in neurovascular coupling tests. ....222

## LIST OF EQUATIONS

Equation 2.1: The Kety & Schmidt technique .....	22
Equation 2.2: Cerebral perfusion pressure .....	28
Equation 2.3: Poiseuille's law .....	29
Equation 2.4: Hemodynamic equation for flow, resistance, and pressure (Ohm's law) ...	29
Equation 2.5: Cerebrovascular resistance derived from Poiseuille's law .....	29
Equation 2.6: Cerebrovascular resistance derived from the hemodynamic representation of Ohm's law .....	29
Equation 2.7: Cerebrovascular resistance of parallel vessel beds .....	30
Equation 2.8: Wall stress, the Law of Laplace .....	33
Equation 2.9: Arterial oxygen content .....	39
Equation 2.10: Cerebral oxygen delivery .....	39
Equation 2.11. The Fick Equation .....	39
Equation 3.1. Calculation of volumetric cerebral blood flow .....	126
Equation 3.2. Cerebrovascular conductance .....	126
Equation 3.3. Estimated arterial oxygen content .....	129
Equation 3.4. Estimated cerebral oxygen delivery .....	130
Equation 3.5. Carbon dioxide corrected internal carotid artery blood flow .....	130
Equation 3.6. Carbon dioxide corrected vertebral artery blood flow .....	130
Equation 3.7. Carbon dioxide corrected cerebral blood flow .....	131
Equation 5.1. Shear stress .....	197

## ACKNOWLEDGEMENTS

This thesis is the product of an immense amount of team work. Completed across three continents, and within five laboratories I have been influenced by too many people to list here. Some key individuals that deserve recognition are as follows:

I must thank my supervisor Prof. Philip Ainslie, who through leadership, mentorship, and friendship has been a constant inspiration. It has been the utmost privilege to work with you.

Thank you to my committee members Drs. Neil Eves and Ali McManus for their continued support as well as my PhD external examiners Prof. Kevin Shoemaker and Dr. Chris West. Further, I would like to thank Prof. Damian Bailey for his involvement in my comprehensive examinations and his valuable mentorship that allowed me to add another *arm* to my research portfolio.

Thank you to Dr. Trevor Day for your mentorship, friendship and consistent enthusiasm throughout my time at UBC.

Dr. David MacLeod, your mentorship and leadership have been invaluable and inspiring.

I would like to thank Prof. Danny Green for the opportunity to travel to and study in his laboratory during my PhD.

I would like to recognize the late Dr. Chris Willie who was an invaluable mentor of mine and a good friend.

Dr. Kurt Smith, you have been a big brother to me throughout this entire experience and I cannot thank you enough for everything. Wave Bros.

Finally, I would like to thank my parents Ivar and Marcelle, my brother Randy and sister McKenzie, and my beautiful girlfriend Brooke for their continued support throughout my academic pursuits and otherwise.

## GLOSSARY

- [Hb] – Hemoglobin concentration
- [H<sup>+</sup>] – Hydrogen ion concentration
- [HCO<sub>3</sub><sup>-</sup>]<sub>i</sub> – Concentration of intracellular bicarbonate ion
- [HCO<sub>3</sub><sup>-</sup>]<sub>o</sub> – Concentration of extracellular bicarbonate ion
- ACA – Anterior cerebral artery
- AE-1 – Anion exchanger 1
- AMS – Acute mountain sickness
- ATP – Adenosine tri-phosphate
- β93 Cys – β93 cysteine residue
- BA – Basilar artery
- BK<sub>Ca</sub> channels – Calcium dependent potassium channels
- BOLD – Blood oxygen level dependent
- BMI – Body mass index
- CA – Cerebral autoregulation
- cAMP – Cyclic adenosine monophosphate
- CaO<sub>2</sub> – Arterial oxygen content
- CBF – Cerebral blood flow
- CDO<sub>2</sub> – Cerebral oxygen delivery
- cGMP – Cyclic guanosine monophosphate
- CMRO<sub>2</sub> – Cerebral metabolic rate of oxygen
- COPD – Chronic obstructive pulmonary disease
- corrCBF – Corrected cerebral blood flow
- corrQ<sub>ICA</sub> – Corrected internal carotid artery blood flow
- corrQ<sub>VA</sub> – Corrected vertebral artery blood flow
- COX – Cyclooxygenase
- CPP – Cerebral perfusion pressure
- CrCP – Critical closing pressure
- CSA – Cross sectional area
- CSF – Cerebrospinal fluid
- CVR – Cerebrovascular reactivity
- DO<sub>2</sub> – Delivery of oxygen

eCaO<sub>2</sub> – Estimated arterial oxygen content  
eCDO<sub>2</sub> – Estimated cerebral oxygen delivery  
EET – epoxyeicosatrienoic acid  
eNOS – Endothelial nitric oxide synthase  
F<sub>I</sub>CO<sub>2</sub> – Fraction of inspired CO<sub>2</sub>  
F<sub>I</sub>O<sub>2</sub> – Fraction of inspired oxygen  
gCBF – Global cerebral blood flow  
GOLD – Global Initiative for Obstructive Lung Disease  
GSNO – S-nitrosoglutathione  
HA – High-altitude  
HbFe(II) – Ferrous hemoglobin  
HbFe(III) – Ferric hemoglobin or methemoglobin  
HCT – Hematocrit  
HSp90 – Heat shock protein 90  
ICA – Internal carotid artery  
ICA<sub>v</sub> – Internal carotid artery blood velocity  
ICP – Intracranial blood pressure  
K<sub>ATP</sub> channels – Adenosine tri-phosphate sensitive potassium channels  
L-NMMA – N<sup>G</sup> monomethyl-L-arginine  
MCA – Middle cerebral artery  
MCA<sub>v</sub> – Middle cerebral artery blood velocity  
MHz – Megahertz  
MLCK – Myosin light chain kinase  
MRI – Magnetic resonance imaging  
nNOS – Neuronal nitric oxide synthase  
NO – Nitric oxide  
NO<sub>2</sub> – Nitrite  
NVC – Neurovascular coupling  
N<sub>2</sub>O – Nitrous oxide  
N<sub>2</sub>O<sub>3</sub> – Dinitrogen trioxide  
OH<sup>-</sup> – Hydroxide  
PaCO<sub>2</sub> – Partial pressure of arterial carbon dioxide  
PaO<sub>2</sub> – Partial pressure of arterial oxygen

PCA – Posterior cerebral artery  
PCAv – Posterior cerebral artery blood velocity  
PDE - Phosphodiesterase  
PET – Positron emission tomography  
 $P_{ET}CO_2$  – Partial pressure of end-tidal carbon dioxide  
PG – Prostaglandin  
PGE<sub>2</sub> – Prostaglandin E<sub>2</sub>  
PGI<sub>2</sub> – Prostacyclin  
pH<sub>e</sub> – Extracellular pH  
pH<sub>i</sub> – Intracellular pH  
PO<sub>2</sub> – Partial pressure of oxygen  
PjvO<sub>2</sub> – Partial pressure of jugular venous oxygen  
ROS – Reactive oxygen species  
RSNO – S-nitrosothiols  
SaO<sub>2</sub> – Arterial oxyhemoglobin saturation  
SjvO<sub>2</sub> – Jugular venous oxyhemoglobin saturation  
SNA – Sympathetic nervous activity  
SNO-Hb – S-nitrosohemoglobin  
SpO<sub>2</sub> – Peripheral oxyhemoglobin saturation  
TCD – Transcranial Doppler ultrasound  
TPR – Total peripheral resistance  
VA – Vertebral artery  
VAv – Vertebral artery blood velocity  
V<sub>E</sub> – Minute ventilation  
VEGF – Vascular endothelial growth factor  
VSMC – Vascular smooth muscle cell

## 1 CHAPTER 1: INTRODUCTION

Oxygen is the most vital component of human life. The human organism has evolved to be highly oxygen dependent, and the brain, above all other organs, possesses an unrelenting reliance on oxygen. Requiring >10 times the oxygen expected for its mass, the brain is extremely vulnerable to oxygen deprivation. Complete cessation of cerebral blood supply precipitates unconsciousness in as little as 4 seconds, irreversible neurological damage in minutes, seizure, and death ensues not long thereafter.

To combat this extreme vulnerability to oxygen deprivation, humans possess physiological ‘defense mechanisms’ capable of both maintaining oxygen homeostasis in instances of mild reductions in oxygen availability, and mitigating oxygen deprivation at the tissue level during moderate to severe reductions in oxygen availability. The robustness of these defense mechanisms is evidenced by extreme human feats in low oxygen environments. Examples such as the first ascent of Mt. Everest without oxygen by Reinhold Messner and Peter Habeler in 1978, the world record static apnea of 11:54 by Branko Petrovic in 2014, as well as the residence of populations above 4000m (e.g., Himalayan Sherpa) for millennia, all exemplify the ability of humans to adapt, both acutely and chronically, to oxygen deprivation (i.e. hypoxia). Nonetheless, oxygen deprivation may elicit deleterious physiological deficits as humans are not able to adapt to an extent that completely alleviates deviations from oxygen homeostasis. These debilitating effects of oxygen deprivation are epitomized beautifully by Reinhold Messner as he recounts his state of mind upon Mt. Everest:

*“Not only during the ascent, but also during the descent my willpower is dulled. The longer I climb the less important the goal seems to me, the more indifferent I become to myself. My attention has diminished, my memory is weakened. My mental fatigue is now greater than the bodily. It is so pleasant to sit doing nothing - and therefore so dangerous. Death through exhaustion is like death through freezing - a pleasant one.” – Reinhold Messner, The Crystal Horizon: Everest – The First Solo Ascent.*

Despite the esoteric nature of extreme human feats, understanding the ‘defense mechanisms’ or rather compensatory physiological processes at play in hypoxia is widely significant due to its applicability in clinical populations afflicted with reduced blood oxygen levels. In a normal setting, the brain is able to maintain oxygen supply during hypoxia by increases in cerebral blood flow that are commensurate to any given reduction in blood oxygen levels. This has been demonstrated upon ascent to altitude, prolonged apneas, and in conditions of acute experimental hypoxia. However, the physiological processes underpinning this response, and whether it remains intact in pathological settings, is poorly understood in humans.

The past several decades have seen a rapid growth in the research aiming to understand oxygen homeostasis in humans. At present, investigators are searching for the *sine qua non* of oxygen delivery, although discovery of such a regulator (i.e. mechanism) has yet to occur. As stated by William Blake, a 19th century poet, “*What is now proved was once only imagined*”. While the scientific method does not function to prove *per se*, this quotation highlights the importance of imagination and creativity in science. Today there exists no shortage of substrate for imagination, with an expansive set of modern data that ranges in type from isolated cell cultures, isolated blood vessels, *in vivo* animal models, through to *in vivo* human work. Such research has clearly delineated the potential for various mechanisms in the regulation of oxygen delivery to the brain in humans, but these mechanisms have yet to be translated to *in vivo* human studies or clinical applications. On the other hand, due to the complicated nature of isolating and investigating regulatory pathways in humans, *in vivo* human studies have typically lead to inconsistent and contradictory findings that have yet to be reconciled. Herein, this imaginative substrate has been utilized for the development of experiments that have, as will become clear throughout this thesis, further developed the scientific understanding of how oxygen delivery to the brain is regulated in humans.

This thesis is comprised of seven chapters. Following chapter one, the introduction, chapter two provides a literature review pertinent to the topics investigated: 1) a historical perspective and overview of the measurement techniques used in cerebrovascular research; 2) basic hemodynamic principles that provide the fundamentals for understanding cerebrovascular regulation; 3) the regulation of cerebral blood flow during alterations in

arterial oxygen content; 4) cerebral blood flow regulation during changes in arterial carbon dioxide levels. Chapters three to six comprise the four main experimental chapters of this thesis outlined below (see section “Specific aims and hypotheses”). The final chapter provides a synopsis of all the experimental chapters. Here, future directions, with a focus on the importance of methodological design in human studies, will be discussed.

## **1.1 THESIS OBJECTIVES**

The central aim of this thesis is to determine the physiological processes and regulatory pathways that act to maintain cerebral oxygen delivery in humans and how these processes may be altered by long term exposure to hypoxia at evolutionary and pathological levels. A brief background for each experimental chapter and the specific aims and hypotheses therein are outlined below.

## **1.2 SPECIFIC AIMS AND HYPOTHESES**

### **1.2.1 STUDY 1 (CHAPTER 3)**

#### ***1.2.1.1 STUDY 1 – BACKGROUND***

Animal studies have provided several strong lines of evidence for a role of adenosine in regulating CBF in hypoxia. Hypoxia leads to a rapid and marked increase in endogenous cerebral adenosine production (Winn *et al.*, 1979, 1981*a*), while adenosine receptor antagonism abolishes the CBF response to moderate hypoxia in multiple animal models (Emerson & Raymond, 1981; Morii *et al.*, 1987*a*; Hoffman *et al.*, 2013). These findings in animal studies have undergone an attempt at translation to humans, whereby extravascular adenosine application leads to *ex vivo* dilation of human cerebral arteries (Toda, 1974*a*). *In vivo* human data, however, remains much less clear with observed reductions in CBF at rest following adenosine receptor antagonism (Wechsler *et al.*, 1950; Bowton *et al.*, 1988) but inconclusive data on potential alterations of hypoxic cerebral vasodilation (Bowton *et al.*, 1988; Nishimura *et al.*, 1993).

### **1.2.1.2 STUDY 1 – AIM**

To determine the role of adenosine in mediating cerebral vasodilation during acute experimental hypoxia and upon rapid ascent to high-altitude (HA).

### **1.2.1.3 STUDY 1 – HYPOTHESES**

1) Adenosine receptor antagonism via oral administration of theophylline (3.75 mg/kg) would reduce the CBF response to acute hypoxia in the laboratory setting; 2) Following rapid ascent to 3800m (White Mountain, CA, USA), oral theophylline administration (3.75 mg/kg) would lead to a reduction in CBF.

## **1.2.2 STUDY 2 (CHAPTER 4)**

### **1.2.2.1 STUDY 2 – BACKGROUND**

The role of the erythrocyte in vascular regulation is predicated on three competing, but potentially intertwined theories that either deoxyhemoglobin mediated reduction of nitrite (NO<sub>2</sub>), or deoxyhemoglobin mediated release of s-nitrosothiols (RSNO) and/or adenosine triphosphate (ATP) lead to hypoxic vasodilation (Gladwin *et al.*, 2006; Ellsworth *et al.*, 2009; Doctor & Stamler, 2011). These hypotheses operate on the primary tenets that: 1) the erythrocyte is not just a “sink” for nitric oxide (NO) (i.e. heme scavenging of NO), but that the erythrocyte is also able to confer NO bioactivity, 2) the erythrocyte regulation of NO bioactivation (i.e. NO release) is allosterically linked via the oxygenation/deoxygenation of hemoglobin, and 3) this allosteric link provides a temporal, spatial, and amplitudinal link between O<sub>2</sub> demand and consequent optimization of O<sub>2</sub> delivery. However, despite sharing the same principles, these three hypotheses diverge relative to the specific methods of NO formation, stabilization, and final transduction. Animal data have demonstrated the potential role of these three mechanisms in hypoxic cerebral vasodilation [reviewed in: (Hoiland *et al.*, 2016a)], yet there is no *in vivo* human studies that have attempted to isolate the role of the erythrocyte in the regulation of hypoxic cerebral vasodilation.

### **1.2.2.2 STUDY 2 – AIM**

1) To determine the role of the erythrocyte in the regulation of hypoxic cerebral vasodilation in humans by comparing the cerebrovascular response to hypoxemia and hemodilution; 2) Determine how hemoglobin concentration influence hypoxic cerebral vasodilation through experimental hemodilution; 3) Determine how biological variability in hemoglobin concentration relates to the magnitude of cerebrovascular reactivity to hypoxia.

### **1.2.2.3 STUDY 2 – HYPOTHESES**

1) The cerebral blood flow response to hypoxia will be greater during hypoxemia than during anemic hypoxia (i.e. hemodilution) despite a matched hypoxic stimulus; 2) Reduced hemoglobin concentration would lead to a reduction in hypoxic cerebral vasodilation during hypoxemia; 3) Hemoglobin concentration would be correlated to the magnitude of hypoxic reactivity.

## **1.2.3 STUDY 3 (CHAPTER 5)**

### **1.2.3.1 STUDY 3 – BACKGROUND**

Travel to HA exposes humans to reduced atmospheric pressure and hence oxygen tension. Individuals inhabiting lowland regions experience sub-optimal physical performance upon ascent to altitude. However, HA natives, such as the Himalayan Sherpa possess a legendary physical capacity at HA and consistently out perform their lowland counterparts during HA expeditions. These adapted Sherpa and Tibetans from which they have descended have been demonstrated to possess higher NO bioavailability (Beall *et al.*, 2001; Erzurum *et al.*, 2007) and increased skeletal muscle capillary density (Beall, 2007), compared to lowland natives. However, little is known relative to potential adaptations in cerebral oxygen delivery (CDO<sub>2</sub>) [for review see: (Jansen & Basnyat, 2011; Gilbert-Kawai *et al.*, 2014)]. Evidence to date indicates a high flow adaptation in the brain due to elevated internal carotid artery (ICA) velocity in Tibetan natives compared to lowlanders at 3658 m (Huang *et al.*, 1992). However, a recent cross-sectional study demonstrated lower CDO<sub>2</sub> in Tibetans

than in Han Chinese at sea level and at 3658 m when volumetric CBF was measured (Liu *et al.*, 2016). Contrary to the current high flow hypothesis, one may expect the exceptional performance of the Sherpa in hypoxia to be reflected in a more efficient utilization of oxygen, or reduced need for oxygen, as observed in various hypoxia tolerant species such as the crucian carp (*Carassius carassius*) (Nilsson & Lutz, 2004). Differences in the CBF response to hypoxia during ascent and short-term (i.e. weeks) stay at altitude between lowland natives and Sherpa have yet to be determined using a longitudinal study design and volumetric measures of CBF.

### **1.2.3.2 STUDY 3 – AIM**

To determine potential differences in volumetric CBF and CDO<sub>2</sub> between lowlanders and Sherpa during graded ascent and short term stay at altitude.

### **1.2.3.3 STUDY 3 – HYPOTHESES**

1) During ascent to and upon arrival at 5050 m CBF and CDO<sub>2</sub> would be lower in Sherpa compared to lowlanders; 2) Sherpa that have not descended to low altitude would also possess lower CDO<sub>2</sub> than lowlanders at 5050 m.

## **1.2.4 STUDY 4 (CHAPTER 6)**

### **1.2.4.1 STUDY 4 – BACKGROUND**

Some patients with moderate-to-severe chronic obstructive pulmonary disease (COPD) endure, amongst other pathological factors, a state of chronic hypoxemia. Literature on cerebral vascular regulation in COPD is sparse, which is surprising given the elevated risk of cognitive impairment (Thakur *et al.*, 2010), dementia (Liao *et al.*, 2015) and ischemic stroke (Feary *et al.*, 2010) in this population. If patients are hypoxemic, low flow oxygen (~3L · min<sup>-1</sup>) is typically prescribed (NOTTG, 1980; MRCWP, 1981) with the goal of increasing the partial pressure of arterial oxygen (PaO<sub>2</sub>) to >60mmHg while avoiding hyperoxia (Qaseem *et al.*, 2011). This therapy reduces mortality (NOTTG, 1980; MRCWP, 1981) and the risk of cognitive impairment (Thakur *et al.*, 2010). Given the potential link

between chronic cerebral hypo-perfusion (i.e. vascular insufficiency – reduced CDO<sub>2</sub>) and the pathogenesis of neurovascular injury and dementia (Iadecola, 2010), understanding the influence of oxygen therapy on CBF, CDO<sub>2</sub> and neurovascular function in COPD is of immediate importance.

#### ***1.2.4.2 STUDY 4 – AIMS***

1) Determine the role of chronic hypoxia on regulating basal CBF and CDO<sub>2</sub> in COPD patients; 2) Determine if supplemental O<sub>2</sub> would improve neurovascular function in COPD patients.

#### ***1.2.4.3 STUDY 4 – HYPOTHESES***

1) That CBF would be reduced in COPD patients following O<sub>2</sub> therapy leading to unchanged CDO<sub>2</sub> despite elevated arterial oxygen content (CaO<sub>2</sub>); 2) Despite a reduced CBF and unchanged CDO<sub>2</sub> neurovascular function would be improved.

## 2 CHAPTER TWO: A REVIEW OF CEREBRAL BLOOD FLOW REGULATION

We tend to view the neuronal brain as the base of our perceptions, our personhood, our motivations, our actions, and the repository of the experiences that constitute our lives. However, the brain is not simply a neural organ: it is a neurovascular organ. The vascular component does not merely play a supporting role; it is an intimate and fully integrated partner. The neural component of the brain requires precise control of CBF by the vascular component to maintain  $\text{CDO}_2$ , cerebral metabolic homeostasis, acid-base balance, and to buffer pressure transmission to the microvasculature. Reductions in  $\text{CDO}_2$  can be asymptomatic, or lead to a spectrum of symptoms including cognitive deficits (with or without insight), dizziness, headache, as well as consequences such as unconsciousness, seizure, and ultimately death (Rossen *et al.*, 1943). Acute uncompensated vascular insufficiency may lead to localizing neurological symptoms and signs. In addition, CBF may be sufficient in that baseline flow is adequate for the maintenance of cellular integrity and function, but be insufficient to provide appropriate augmentation to meet the needs of neurovascular activation. Such limitations show few symptoms or signs but are thought to be associated with progressive cognitive decline (Silvestrini *et al.*, 2006; Balucani *et al.*, 2012) and cortical thinning on imaging (Fierstra *et al.*, 2010). Equally important for cerebral function is the maintenance of acid base balance as tight control of cerebral pH is critical for enzymatic function and ultimately cellular survival. Therefore, stringent maintenance of optimal CBF is required to avoid a wide array of perturbations that may jeopardize the health and functioning of the brain.

Cerebrovascular responses to  $\text{PaO}_2$ , the partial pressure of arterial carbon dioxide ( $\text{PaCO}_2$ ), cerebral perfusion pressure (CPP), and neural activation are integral to optimal functioning. While the primary focus of this thesis is the regulation of CBF during hypoxia, given even the slightest alterations in pH (typically via altered  $\text{PaCO}_2$ ) lead to meaningful changes in cerebral vascular smooth muscle cell (VSMC) tone and  $\text{PaO}_2$  and  $\text{PaCO}_2$  are often concurrently altered in free-living environments (such as HA), this thesis provides an extensive review of cerebrovascular regulation by both oxygen and carbon dioxide with a focus on humans where possible.

To begin, cerebrovascular anatomy is outlined. Then the evolution of CBF investigations since their early inception are overviewed in a historical perspective and a summary of key modern measurement techniques. This is followed by an overview of the basics of human CBF regulation and important fundamental hemodynamic concepts. Thereafter, CBF regulation during alterations in  $\text{CaO}_2$  is outlined, while an explanation of CBF regulation during alterations in  $\text{PaCO}_2$  concludes the literature review.

## 2.1 CEREBROVASCULAR ANATOMY

This section provides a general overview of the vascular architecture of cerebral blood vessels as gleaned from 48 autopsy studies in patients between 43-85 years of age reported by Moody *et al.* (Moody *et al.*, 1990) with additional references provided where appropriate. Arteries are defined as thick-walled afferent vessels  $> 100 \mu\text{m}$  in diameter and arterioles defined as vessels  $< 100 \mu\text{m}$  in diameter with at least 1 layer of smooth muscle (Moody *et al.*, 1990).

### 2.1.1 CEREBRAL ARTERIAL ARRANGEMENT

In humans, a bilateral pair of both the ICA and VA supplies blood flow to the brain (**Figure 2.1** Error! Reference source not found.). Following passage through the Foramen Lacerum, the ICA proceeds to the base of the brain where it branches into the MCA, ACA, anterior choroidal, and posterior communicating arteries. It primarily supplies the anterior portion of the brain and bilaterally accounts for  $\sim 70\%$  of global CBF (gCBF). Both vertebral arteries enter the intracranial space through the Foramen Magnum and subsequently confluence into the basilar artery (BA), which then bifurcates into the PCAs and serves  $\sim 30\%$  of total CBF, primarily to the posterior regions of the brain (Zarrinkoob *et al.*, 2015). The MCA, ACA, and PCA through communicating arteries are all conjoined to form an anastomotic ring, the Circle of Willis from which they originate (**Figure 2.1**). This anatomical format serves to provide collateral flow during cases of regional hypoperfusion; however, individual variability in the structure of the Circle of Willis is quite common, with  $\sim 50\%$  of individuals possessing an atypical or incomplete configuration (Alpers *et al.*, 1959; Zarrinkoob *et al.*, 2015).



Once the major arteries (MCA, PCA & ACA) branch outwards from the Circle of Willis, they repeatedly branch into smaller arteries without interconnections en route to the surface of the brain where they lie adjacent to the brain parenchyma and are bathed in cerebrospinal fluid (CSF) within the subarachnoid space. At this juncture they are referred to as pial vessels. Here, an abundant network of inter-arterial anastomoses provide alternate sources of perfusion for penetrating arterioles and important connections between cerebral arterial territories. This provides a secondary safety net for collateral flow in arterial boundary zones (Vander Eecken & Adams, 1953; Coyle & Jokelainen, 1982; Moody *et al.*, 1990). This is of great functional significance, as boundary zones are particularly susceptible to transient episodes of ischemia during instances of hypoperfusion.

Surface pial vessels branch to form penetrating arterioles that advance into the brain parenchyma perpendicular to the cortical surface and supply blood to the cortex (Iadecola, 2004; Nishimura *et al.*, 2007). Entry into the parenchyma occurs via passage through an invagination of the pia mater, termed the Virchow Robin space, following which vessels become encapsulated in astrocytic end feet and are thereafter considered parenchymal arterioles. Although the penetrating arterioles appear to branch to supply silos of tissue, they are also described as richly anastomosing with adjacent vessels, particularly if stimulated to adapt to chronic flow limitations. The extent of developed collateralization across microvascular beds also affects a region's vulnerability to vascular insult (Scharrer, 1940; Moody *et al.*, 1990) (**Figure 2.2**Error! Reference source not found.). A continuous network of capillaries, which extend outwards in radial fashion from parenchymal arterioles, provide a route for perfusion across borders of adjacent arteriolar territories and thereby adjacent pial arterial sources. Notably, capillary density throughout the cerebral parenchyma is relatively heterogeneous, whereby capillary density is generally correlated to metabolic activity (Sokoloff *et al.*, 1977; Göbel *et al.*, 1990).

These anatomical and functional organizations are referred to in a later section that seeks to explain how the analysis of high resolution flow imaging and vasoactive stimuli can be used to investigate vascular physiology and pathology (see section “Standardization and utility of cerebrovascular reactivity”).

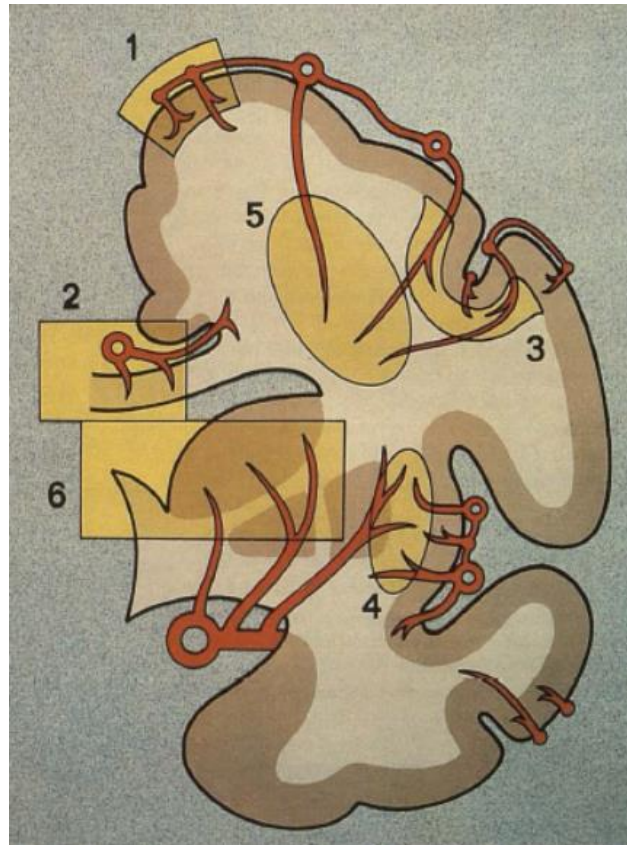


**Figure 2.2. Collateralization across microvascular beds.**

**A.** The vascular supply is outlined in diagrammatic form of a coronal section of the brain. The cortex and corpus callosum (1, 2) are supplied by short arterioles arising from pial arteries supplied by a single cerebral artery. The subcortical association bundles (3) receive a dual supply in the form of terminal twigs of the cortical vessels and long medullary arterioles that traverse the cortex and ramify in the white matter. This provides these areas with an overlap of 2 blood supplies. The external capsule and claustrum (4) have a dual supply from the vessels entering from the insular cortex. The centrum semiovale (5) is supplied by long arteries 2-5 cm entering from the brain surface. These arteries branch but have few communications with other arteries. They tend to form border zones with adjacent afferent arteriolar systems throughout the whole depth of WM. The basal ganglia and thalamus (6) get perfused by long arterioles and long muscular arteries from base of brain. These tend to be end arteries. This leaves border zone at deep portions of centrum semiovale. Reproduced from (Moody *et al.*, 1990) with permission.

### 2.1.2 CEREBRAL VENOUS ARRANGEMENT

By the Monro-Kellie doctrine, the cerebral parenchyma, arterial and venous blood, and CSF, are contained in a very low – but not zero (see below) – compliance container. In adults, the intracranial blood volume component is about 200 mL, and predominantly

venous (Kitano *et al.*, 1964). The balance between arterial and venous flows need to be maintained to a very close tolerance to maintain normal intra-cranial pressure (ICP). Following transit through the capillary system, blood passes through the cerebral veins which terminate in dural sinuses. Here, blood is collected and directed toward the transverse sinus. The blood in the transverse sinus, along with that in the petrosal sinus converge and drain predominantly (~70%) into the internal jugular veins (IJV) when supine (Doepp *et al.*, 2004). In upright posture, the IJV appears collapsed upon ultrasound examination (Dawson *et al.*, 2004; Ogoh *et al.*, 2016) and flow appears to be shifted to the vertebral plexus (Gisolf *et al.*, 2004; Ogoh *et al.*, 2016), the flow capacity of which has been calculated as capable of accommodating the total CBF [see (Gisolf *et al.*, 2004) for discussion]. However, more recent observations indicate that high levels of blood flow continue in the IJV with upright posture, explaining their rapid filling with distal digital obstruction (Yeoh *et al.*, 2017) or Valsalva maneuver. The IJVs have valves that direct centripetal flow, and prevent cephalad transmission of sudden increases in intrathoracic pressure (Fisher *et al.*, 1982). Notably, IJV flow in the upright position is not due to a siphon effect as the IJV walls in the neck collapse and do not transmit negative pressure cephalad. When upright, both venous and CSF pressures are ~0 cm H<sub>2</sub>O (Dawson *et al.*, 2004).

The Monro-Kellie doctrine requires a net zero flow balance on the temporal and volume scales of CBF. However, there are additional volume fluctuations on the scale of arterial pulsations. For these, a crucial element is the compliance of the ‘container’, which exists mostly in the dura around the spinal cord. Arterial pulsations, therefore, induce synchronous movements in the whole brain and CSF directed, like water going into a toilet, towards the tentorial notch and foramen magnum (Greitz *et al.*, 1992). These pulsations also compress the ventricles and support the net intra-ventricular flow of CSF out through the foramen of Monro. For example, in low pressure hydrocephalus, there is insufficient turgor in the brain and intracranial contents for the arterial pressure pulsations to be thus transmitted, and patients become unconscious (mechanism not understood). Consciousness is recovered promptly when venous outflow impediment increases tissue turgor and ICP, providing a medium for arterial pressure transmission, and restores CSF flow in the ventricles (Hatt *et al.*, 2015). Therefore, while venous outflow is not the focus

of this thesis, it is clearly important to remember it is intimately linked to arterial inflow dynamics.

## 2.2 HISTORICAL PERSPECTIVE ON CEREBRAL BLOOD FLOW

### 2.2.1 EARLY PIONEERS IN CEREBROVASCULAR RESEARCH

Following William Harvey's (1578-1657) revolutionary contribution to our understanding of the human circulatory system, detailed anatomical descriptions of the cerebral vasculature emerged in the mid 1600's when Thomas Willis (1621-1675) published his thesis titled *Cerebri Anatome*. This text provided detailed descriptions of the cerebral vasculature, particularly of an anastomotic ring of arterial vessels at the base of the brain, later termed, and still referred to today as, the 'Circle of Willis' (Willis, 1664). However, in-depth study on the function of the cerebral vasculature lagged centuries behind the characterization of its anatomy.

In 1783 Alexander Monro (1733-1817) first described the brain's need for an inordinate supply of blood. His inferences were drawn from comparisons of the cross-sectional area of the ICA and vertebral arteries (VA) to those supplying other vascular beds.

*“...the quantity of [blood] which circulates in the brain is greater than in most organs of the same weight. Thus one of our arms will be found to weigh more than our brain and cerebellum; yet the areaé of the two vertebral and of the two internal carotid arteries, joined together, are much larger than the area of the proper subclavian artery.” – Alexander Monro, Observations on the Structure and Function of the Nervous System, 1783*

However, the most commonly recognized contribution of Monro was the notion that cerebral blood volume should not change, as the cerebral contents are near incompressible and encapsulated within the rigid skull. To this effect he stated:

*“The blood must be continually flowing out of the veins that room may be given to the blood which is entering by the arteries. For, as the substance of the brain, like that of the other solids of our body, is nearly incompressible, the quantity of blood within the head must be the same, or very nearly the same, at all times, whether in health or disease, in life or after death...”* – Alexander Monro, *Observations on the Structure and Function of the Nervous System*, 1783

This notion was supported by George Kellie, a pupil and later collaborator of Monro's, and subsequently coined the Monro-Kellie Doctrine. From the Monro-Kellie Doctrine originated the general understanding that, if intracranial pressure (ICP) is to remain unchanged, increases and decreases in the volume of intracranial contents (brain parenchyma, blood and cerebrospinal fluid) must constantly balance to a resulting zero (or near zero) net change in total cerebral volume (Monro, 1783; Kellie, 1824; Macintyre, 2014).

In the late 1800's, the famed Italian physiologist, Angelo Mosso (1846-1910) made the first estimates of functional changes in CBF in humans (Mosso, 1880). In individuals with skull defects, he directly measured brain pulsations, which were inferred to represent blood flow, using a special plethysmograph of his design (**Figure 2.3**). He demonstrated that mental tasks, such as arithmetic, cause increases in the plethysmographic recordings, and provided the first indications that CBF is linked to cerebral activation.

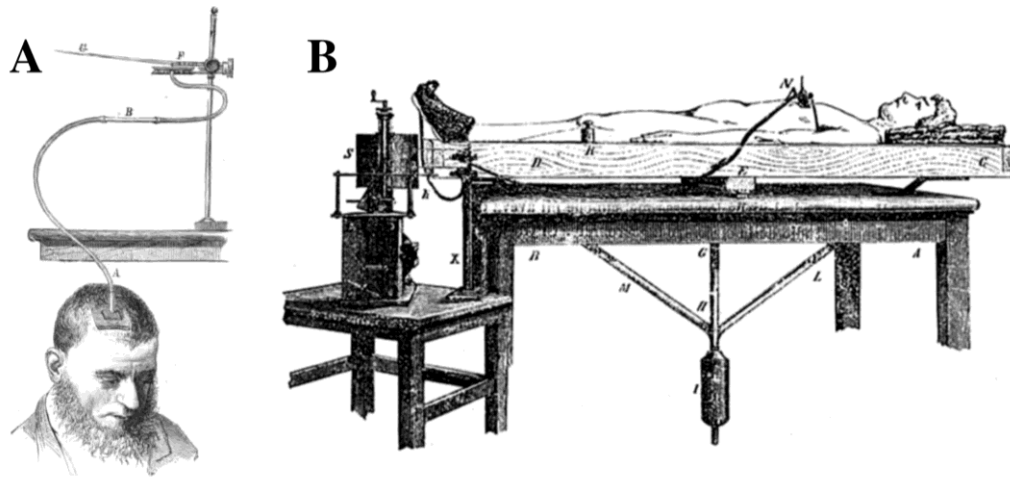


**Figure 2.3. Cerebral Blood Flow Measurement Techniques Pioneered by Angelo Mosso.**

Cerebral blood flow measurement techniques pioneered by Angelo Mosso. A. An illustration of Mosso's self-built plethysmograph from his 1892 manuscript titled: *Die Ermüdung: Aus dem italienischen übersetzt von J. Glinzer*. Here he implemented his invention to study an individual with a congenital skull defect (Mosso & Glinzer, 1892). B. A drawing of Mosso's scale. Reproduced from (Sandrone et al., 2014) with permission.

As this technique precluded the study of healthy individuals, Mosso's curiosity and innovation led to his development of a 'scale' on which one could theoretically measure the distribution of blood travelling through the brain – increased blood flow cephalad would 'tip' the scale in this direction indicating increased CBF (Mosso, 1884) [reviewed in: (Sandrone *et al.*, 2014)]. While this scale was exceptionally crude it illustrates the difficulties in contriving suitable instruments to make direct measurements of the relevant parameters in vascular physiology such as flow, pressure, resistance, oxygenation and related responses to various gases and hormones, neurotransmitters, and neuronal glial activity.

Hitherto unattended, the works of Mosso were extended a decade later by two English physiologists, Charles S. Roy (1854-1897) and Charles S. Sherrington (1857-1952). Their seminal publication, *On the regulation of the blood supply of the brain*, in 1890 confirmed (and often takes credit for) the notion of coupling between CBF (indexed from cerebral volume) and metabolism. To this effect they stated:

*“We conclude then, that the chemical products of cerebral metabolism contained in the lymph which bathes the walls of the arterioles of the brain can cause variations of the calibre of the cerebral vessels: that in this re-action the brain possesses an intrinsic mechanism by which its vascular supply can be varied locally in correspondence with local variations of functional activity.”* Charles Roy & Charles Sherrington – *On the regulation of blood supply of the brain*, 1890

Roy and Sherrington also provided formative evidence towards our current understanding of the relationship between blood pH and CBF, demonstrating increased CBF following infusion of sulphuric acid and decreased CBF following infusion of potassium hydrate. That changes in systemic blood pressure will directly affect CBF was also demonstrated.

*“The higher the arterial pressure, the greater is the amount of blood which passes through the cerebral blood-vessels and vice versa; and, so far as we have been able to learn, this law holds good for all changes in the arterial pressure whatever be their cause.”* Charles Roy & Charles Sherrington – *On the regulation of blood supply of the brain*, 1890

Pertinent to the current thesis, Roy and Sherrington demonstrated that during a period of hypoxia/hypercapnia, resulting from asphyxiation, CBF was dramatically increased. It is particularly noteworthy that, on the highly relevant topic of replication in science [or lack thereof; e.g., (Prinz *et al.*, 2011; Curran-Everett, 2017)], the early works of Roy & Sherrington (Roy & Sherrington, 1890) are remarkably corroborated by the most rigorous studies of the 21<sup>st</sup> century. A summary of these early findings are presented in **Figure 2.4**.

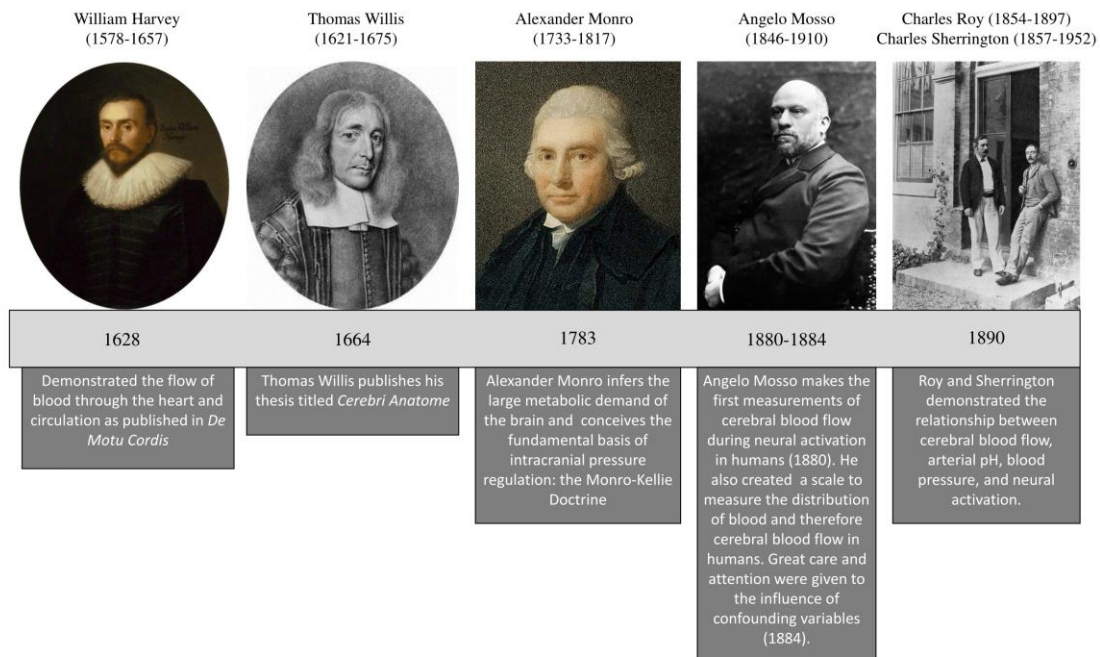


**Figure 2.4. Early Pioneers in Cerebral Vascular Physiology.**

This figure highlights a few (of many) key figures in the early progression of knowledge on cerebral blood flow regulation. Each has provided and been remembered for a major contribution to cerebrovascular physiology.

Photos acquired from:  
[https://en.wikipedia.org/wiki/William\\_Harvey](https://en.wikipedia.org/wiki/William_Harvey) (public domain);  
[https://en.wikipedia.org/wiki/Thomas\\_Willis](https://en.wikipedia.org/wiki/Thomas_Willis) (public domain);  
[https://en.wikipedia.org/wiki/Alexander\\_Monro\\_\(secundus\)](https://en.wikipedia.org/wiki/Alexander_Monro_(secundus)) (public domain);  
[https://en.wikipedia.org/wiki/Angelo\\_Mosso](https://en.wikipedia.org/wiki/Angelo_Mosso) (public domain);  
[https://en.wikipedia.org/wiki/Charles\\_Scott\\_Sherrington](https://en.wikipedia.org/wiki/Charles_Scott_Sherrington) (public domain).

Later breakthroughs in cerebrovascular physiology did not occur until the mid 1900's when Seymour Kety and Carl Schmidt developed the nitrous oxide (N<sub>2</sub>O) technique for measuring volumetric CBF in humans (Kety & Schmidt, 1945, 1948a). Inhalation of low dose N<sub>2</sub>O (15%) and serial measurement of the cerebral arterial-venous difference of N<sub>2</sub>O over a minimum of 10-minutes provided the necessary data to calculate absolute CBF (**Figure 2.5**). Soon thereafter, this technique was utilized for the quantification of resting cerebral metabolism and the impact of changes in arterial blood gases on CBF in healthy humans (Kety & Schmidt, 1948b). The resulting measures of CBF are consistent with normative values that have now been obtained through the use of various modern technologies. However, the N<sub>2</sub>O technique suffered the major limitation of requiring 10-

minutes of quiescence for accurate measurement, and precluded the assessment of dynamic changes in CBF.

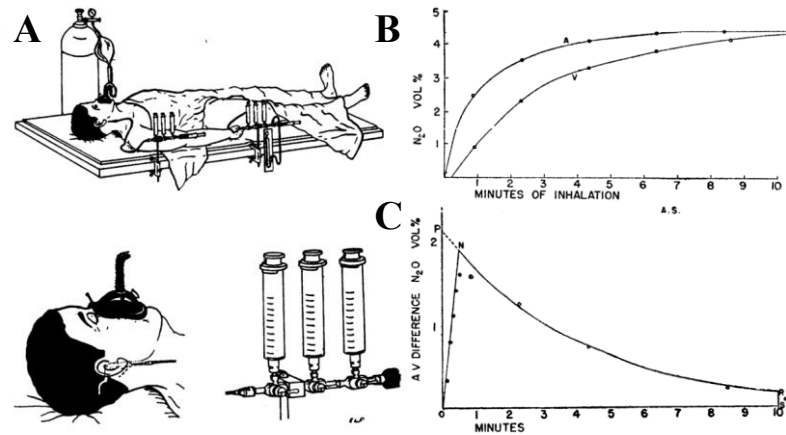


**Figure 2.5. The Original Experimental Setup and Recordings for the Nitrous Oxide Technique Developed by Kety & Schmidt.**

Panel A depicts the subject laying and breathing N<sub>2</sub>O while they have an internal jugular venous and radial arterial catheter for the sampling of blood. Panels B and C depict the temporal dynamics of changes in N<sub>2</sub>O in both jugular and arterial blood (Panel B), and the resulting arterial-venous difference of N<sub>2</sub>O (Panel C) across 10-minutes of N<sub>2</sub>O inhalation. Reproduced from (Kety & Schmidt, 1945) and (Kety & Schmidt, 1948a) with permission.

The utility of Doppler ultrasound for measuring CBF was first described in the early 1960's whereby blood velocity in the carotid arteries was measured (Miyazaki & Kato, 1965). However, attenuation of ultrasonic waves by the skull jeopardized the feasibility of measuring intracranial blood velocity. Then, in 1982, Rune Aaslid and colleagues demonstrated that low frequency ultrasonic waves (1-2MHz) could penetrate the skull. This legitimized the utility of transcranial Doppler (TCD) ultrasound for the measurement of blood velocity (as a surrogate of CBF) in large cerebral arteries, most notably the middle cerebral artery (MCA) (Aaslid *et al.*, 1982). This development truly revolutionized the study of human CBF allowing for the assessment of CBF on a beat-by-beat basis, and in response to many dynamic stimuli, such as transient changes in perfusion pressure (Willie

*et al.*, 2011). More recent advances in methodology are summarized in the following section.

### **2.2.2 MODERN MEASUREMENT TECHNIQUES**

As just highlighted the measurement of CBF has rapidly evolved and now involves the use of more modern techniques including ultrasonography (Willie *et al.*, 2011; Thomas *et al.*, 2015), positron emission tomography (Ito *et al.*, 2003*b*, 2003*a*, 2005*b*, 2005*a*), and multiple magnetic resonance imaging (MRI) techniques such as blood oxygen level-dependent (BOLD) imaging (Bandettini, 2012; Sobczyk *et al.*, 2014; Duffin *et al.*, 2017; Fisher *et al.*, 2017) and arterial spin labelling (St. Lawrence *et al.*, 2002; Verbree *et al.*, 2014; Coverdale *et al.*, 2014; Warnert *et al.*, 2015; Zhou *et al.*, 2015; Lawley *et al.*, 2017) to name a few. Given the prolific use of the Kety-Schmidt technique (albeit much less now), TCD, duplex ultrasound, and BOLD imaging, as well as their relevance to topics discussed hereafter, we have provided an overview of their basic principles and applicability. Other techniques are also briefly considered in **Table 2.1**.

**Table 2.1. The strengths, limitations, and utility of various techniques for the measurement of cerebral blood flow in humans.**

	<b>Method</b>	<b>Strengths</b>	<b>Limitations</b>	<b>Utility</b>
<b>MRI</b>	BOLD (Bandettini, 2012)	1. Assesses regional reactivity 2. High temporal and spatial resolution 3. Non-invasive	1. Influenced by changes in CMRO <sub>2</sub> 2. Not a linear function of flow 3. No volumetric flow measurement	1. Standardized CVR testing 2. CVR ‘mapping’ 3. Track dynamic responses
	Arterial Spin Labelling (Williams <i>et al.</i> , 1992; Telischak <i>et al.</i> , 2015)	1. No contrast needed 2. Non-invasive 3. Volumetric, regional, & global flows	1. Takes several minutes per measure 2. Unknown effects of regional flow variations on signals	1. Measure steady state CBF
<b>Ultrasound</b>	Transcranial Doppler (Aaslid <i>et al.</i> , 1982; Willie <i>et al.</i> , 2011)	1. Portable 2. Non-invasive 3. High temporal resolution 4. Inexpensive	1. Measures velocity, not flow	1. Track dynamic responses
	Duplex Ultrasound (Thomas <i>et al.</i> , 2015)	1. Portable 2. Non-invasive 3. High temporal & spatial resolution 4. Volumetric flow measurement 5. Inexpensive	1. Extra-cranial assessment 2. Contralateral flow differences 3. Requires technical skill	1. Measure CVR 2. Track dynamic responses
<b>Inert gases</b>	Kety Schmidt Technique (Kety & Schmidt, 1945, 1948a, 1948c)	1. Volumetric flow measurement	1. Requires a steady state 2. Invasive cannulation required	1. Measure steady-state changes in CBF

MRI, magnetic resonance imaging; BOLD, Blood oxygen level-dependent; CMRO<sub>2</sub>, cerebral metabolic rate of oxygen; CVR, cerebrovascular reactivity.

### 2.2.2.1 THE KETY & SCHMIDT TECHNIQUE

The serial measurement of N<sub>2</sub>O concentration in arterial and jugular venous blood provides the framework for calculating CBF using the Kety & Schmidt technique (Kety & Schmidt, 1945, 1948a). Throughout ten minutes inhalation of low concentration N<sub>2</sub>O (e.g., 15%) arterial and venous concentration curves of N<sub>2</sub>O volume (%) are determined. The Fick principle, being that the amount of a substance taken up by a tissue (e.g., brain) is equal to the product of the amount of said substance delivered to the tissue and the ensuing arterial-to-venous gradient, is utilized. Therefore the quantity of N<sub>2</sub>O taken up by the brain is equal to the amount supplied by the arterial system less that remaining in the venous system. Following some assumptions, the following equation is derived (**Equation 2.1**):

Equation 2.1: The Kety & Schmidt technique

$$CBF = \frac{100 V_u \cdot S}{\int_0^u (A-V) dt}$$

Where  $V_u$  represents the venous N<sub>2</sub>O concentration for time  $u$ ,  $S$  represents a partition coefficient for nitrous oxide between blood and brain, and  $A$  and  $V$  represent the arterial and venous concentrations of N<sub>2</sub>O multiplied by delta time ( $dt$ ).

The Kety & Schmidt technique revolutionized the study of CBF during its time based on its ability to quantify volumetric CBF. However, several methodological limitations persisted, such as the requirement of a steady state scenario, precluding the measurement of dynamic cerebral responses, as well as the inability to quantify regional CBF.

### 2.2.2.2 TRANSCRANIAL DOPPLER ULTRASOUND

Transcranial Doppler ultrasound, capable of penetrating the skull, was first applied to the study of CBF in 1982 by Aaslid and colleagues (Aaslid *et al.*, 1982). The ease of use, high temporal resolution, low cost, portability, and non-invasiveness of TCD has since led to its widespread use and consequently large impact on our current understanding of CBF regulation in humans (Newell & Aaslid, 1992; Markus, 2000; Willie *et al.*, 2011; Purkayastha & Sorond, 2014). Thin areas of the skull, referred to as ‘acoustic windows’ allow for the transmission of low frequency ultrasound waves (2MHz) through the skull

and insonation of large intracranial cerebral arteries such as the MCA and posterior cerebral artery (PCA). Sound waves are emitted by the ultrasound, which reflect off of red blood cells and travel back to the ultrasound probe. Amplification or dampening of the ultrasound wave indicate the direction of flow away from or to the probe, with the magnitude of amplification or dampening (the Doppler shift) proportional to blood velocity. Live recording of the Doppler shift, and subsequent mathematical considerations, usually inherent within the ultrasound machine, permit beat-by-beat measurement of blood velocity within the large cerebral arteries. How to optimize and standardize the TCD signal has been previously reviewed in detail (Willie *et al.*, 2011) but will be briefly expanded upon here.

The intra-cranial cerebral vessels can be insonated using three primary techniques: (1) the trans-temporal technique, where the probe is placed rostral to the pinna and superior to the zygomatic arch; (2) the trans-ocular technique, where the probe is placed over the closed eye; and (3) the foramen magnum approach, in which the probe is placed on the posterior portion of the head immediately inferior to external occipital protuberance (Willie *et al.*, 2011). These varying probe locations allow for proper signal optimization dependent upon the vessel of interest. To locate the MCA and PCA the trans-temporal approach is used.

Proper determination of absolute MCA and PCA blood velocity (MCA<sub>v</sub> & PCA<sub>v</sub>) is dependent upon correct insonation angle (Willie *et al.*, 2011). The trans temporal technique includes three different approaches for the insonation of the MCA: 1) through the posterior window, where the probe location is directly anterior to the zygomatic arch and immediately rostral of the pinna, 2) through the anterior window, where the probe is placed above the anterior process of the zygomatic arch, and 3) the middle window, which lies between the posterior and anterior window. Ideally the MCA is insonated through the middle window. When there are no anatomical abnormalities this approach provides the lowest insonation angle and thus, most accurate measure of absolute blood velocity.

Two primary benefits of TCD are that it is non-invasive allowing use in a variety of populations, both healthy and clinical, in addition to its high temporal resolution allowing for measurement of dynamic stimulus-response relationships. Highly germane to this review, TCD is often used to assess the cerebral blood velocity response to changes in PaCO<sub>2</sub>, as well as changes in CaO<sub>2</sub> and mean arterial pressure (MAP). This has led to vast

improvements in our knowledge of the temporal dynamics of the CBF response to alterations in arterial blood gases (Poulin *et al.*, 1998), blood pressure (Tzeng *et al.*, 2010) and neural activation (Phillips *et al.*, 2016). Further, TCD has been used in clinical populations for the assessment of cerebral vascular reactivity (CVR) to CO<sub>2</sub> (CVR-CO<sub>2</sub>) and its relationship to stroke risk (Markus & Cullinane, 2001).

Despite the clear utility of TCD, the past 5-10 years have seen its measurement validity widely debated. The primary pitfall of TCD is that it does not provide an index of arterial diameter, and therefore, one must assume that blood velocity is an adequate surrogate of volumetric flow for measurements to be accurate. Recent MRI (Wilson *et al.*, 2011; Verbree *et al.*, 2014; Coverdale *et al.*, 2014, 2015, 2016, Kellawan *et al.*, 2015, 2016; Sagoo *et al.*, 2016; Al-Khazraji *et al.*, 2018) and ultrasound studies (Wilson *et al.*, 2011; Imray *et al.*, 2014; Willie *et al.*, 2014a) have demonstrated changes in larger intra-cranial artery diameter, primarily MCA diameter (**Figure 2.6**), during alteration in blood gases [reviewed in: (Ainslie & Hoiland, 2014; Hoiland & Ainslie, 2016a)]. Earlier study, with data collected during craniotomy indicated MCA diameter may also change during alterations in blood pressure (Giller *et al.*, 1993). Limitations notwithstanding, TCD remains a very valuable tool for CBF measurements. Considerate experimental design and judicious data interpretation facilitate continued use of TCD in the measurement of human CBF.

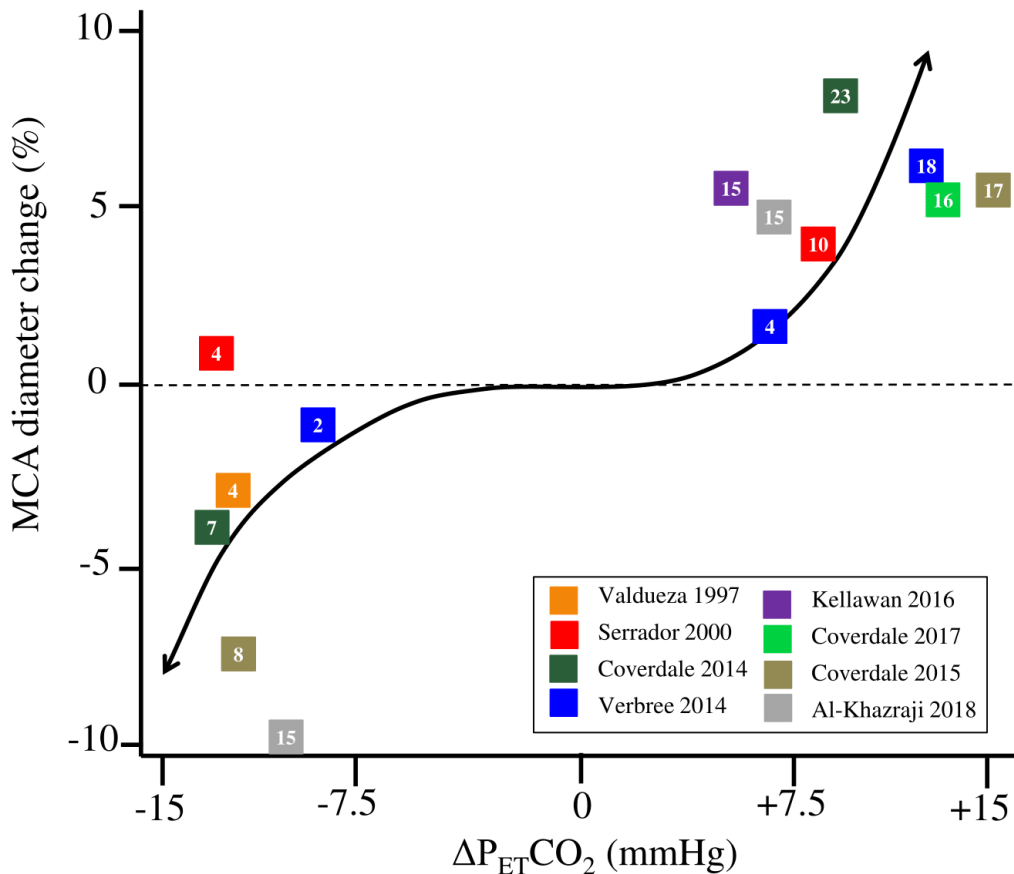


**Figure 2.6. Influence of changes in middle cerebral artery diameter on the validity of transcranial doppler ultrasound.**

Previously reported changes in middle cerebral artery (MCA) diameter (Y axis) and their calculated impact on the discrepancy between flow and velocity measures during changes in end-tidal PCO<sub>2</sub> (PETCO<sub>2</sub>) are depicted. The percent discrepancy between velocity and flow measures are noted as the number within each symbol. To highlight the effect of changes in MCA diameter we estimated the potential difference between CBF and velocity changes using the following formalism. For example: Cross sectional area (CSA; cm<sup>2</sup>) \* Velocity (cm/s) \* 60seconds = Flow (mL/min). Assuming a baseline MCA velocity of 60cm/s (which was done for all studies to facilitate diameter effect comparisons) coupled with the observed alterations in CSA with hyper or hypocapnia (Coverdale *et al.*, 2014), we calculated a representative baseline MCA flow value: 5.6mm<sup>2</sup> \* 60cm/s \* 60s = Flow, therefore: 0.056cm<sup>2</sup> \* 60 cm/s \* 60s = 201.6 mL/min. Assuming previously reported values of cerebrovascular reactivity (Willie *et al.*, 2012), MCA velocity increases ~4% per mmHg increase in P<sub>ET</sub>CO<sub>2</sub>. Assuming this as vessel reactivity (for all studies), we can estimate the volumetric MCA flow during hypercapnia using the reported CSA: 6.5mm<sup>2</sup> \* 84cm/s \* 60s = Flow, therefore: 0.065cm<sup>2</sup> \* 84cm/s \* 60s = 327.6 mL/min. As such, the percent difference for flow between baseline and hypercapnia is: ((327.6-201.6)/201.6)\*100 = 62.5%. While the percent difference in velocity

between baseline and hypercapnia is:  $((84-60)/60)*100 = 40\%$ , indicating that TCD would underestimate the increase in flow of the MCA during hypercapnia (+9mmHg  $P_{ETCO_2}$  from baseline) by >20%. However, if the percent difference is quantified via the magnitude of change in flow and velocity during hypercapnia, the increase in flow is ~50% greater than that of velocity! This can be calculated as: % difference =  $((\% \text{ increase in flow} - \% \text{ increase in velocity}) / \% \text{ increase in velocity}) * 100$ , and therefore  $((62.5-40)/40)*100 = 56.25\%$ . As such, we have conservatively represented the effect of changes in diameter on flow versus velocity discrepancies. For hypocapnia we again assumed a baseline MCA velocity of 60cm/s and used the pre hypocapnia CSA reported (Coverdale *et al.*, 2014) to calculate baseline flow (6):  $5.8\text{mm}^2 * 60\text{cm/s} * 60\text{s} = \text{Flow}$ , therefore:  $0.058\text{cm}^2 * 60\text{cm/s} * 60\text{s} = 208.8\text{mL/min}$ . Incorporating a 2% change in MCA blood velocity per mmHg reduction in  $P_{ETCO_2}$  (Willie *et al.*, 2012), and the associated change in CSA we estimated volumetric MCA flow during hypocapnia (7):  $5.3\text{mm}^2 * 46.8\text{cm/s} * 60\text{s} = \text{Flow}$ , therefore:  $0.053\text{cm}^2 * 46.8\text{cm/s} * 60\text{s} = 148.8 \text{ mL/min}$ . As such, the percent change in flow between baseline and hypocapnia is:  $((148.8-208.8)/208.8)*100 = -28.7\%$ . While the percent difference in velocity between baseline and hypocapnia is:  $((46.8-60)/60)*100 = -22\%$ , indicating that TCD would underestimate the decrease in flow of the MCA during hypocapnia (-13mmHg  $P_{ETCO_2}$  from baseline) by ~7%. Thus, it is evident by these calculations, and those seen above, that small changes in MCA diameter are responsible for large discrepancies between flow and velocity measures. Data are collated from (Valdueza *et al.*, 1997; Serrador *et al.*, 2000; Verbree *et al.*, 2014; Coverdale *et al.*, 2014, 2015, 2016; Kellawan *et al.*, 2015; Al-Khazraji *et al.*, 2018). As noted in the hypercapnic calculations, this graph represents the most conservative way to quantify the percent difference in flow and velocity changes, highlighting the large impact changes in MCA diameter has in quantifying CBF. Further, the shape of the plotted line is theoretical, as data does not exist during modest changes in  $\text{PaCO}_2$ . Modified and updated from (Ainslie & Hoiland, 2014) with permission.

### **2.2.2.3 DUPLEX ULTRASOUND**

The use of duplex ultrasound to measure CBF has recently gained popularity leading to the publication of technical recommendations (Thomas *et al.*, 2015). While it does not penetrate the skull and allow for measurement of intra-cranial blood vessels (e.g. MCA) it allows for measurement of arterial diameter and blood velocity of extra-cranial cerebral conduit arteries, the ICA and VA. Brightness-mode is utilized to visualize arterial diameter in the sagittal axis while pulse-wave mode allows for concurrent measurement of blood velocity (**Figure 2.7**). Duplex ultrasound possesses virtually all the same benefits as TCD, low cost, portability, and non-invasiveness, but while still relatively easy to use it does

require an appreciably greater level of technical expertise (Thomas *et al.*, 2015). However, with adequate training and skill the technical error associated with duplex ultrasonography is minimal [e.g., <2% for arterial diameter (Hoiland *et al.*, 2016b)]. The primary limitation of duplex ultrasound is that contralateral flow may differ between the ICA and VA on each side of the neck. While the potential for these contralateral differences to exist are important to consider, it has been demonstrated that differences in contralateral ICA flows ( $Q_{ICA}$ ) are typically negligible (Schoning *et al.*, 1994; Zarrinkoob *et al.*, 2015). However, there is a tendency for greater flow to occur in the left versus right VA (Schoning *et al.*, 1994). Individuals with large differences in contra-lateral flow can be screened out prior to study. Using  $Q_{ICA}$  to represent CBF is a relatively robust assumption as the ICA does not branch prior to entry into the cranium, and except for a very small proportion of blood (1-2%) that it supplies to the ophthalmic artery, the remainder is distributed to the MCA (~70%) and anterior cerebral artery (ACA; ~30%) (Zarrinkoob *et al.*, 2015). Under a constant distributive relationship between MCA and ACA flow, percent changes in  $Q_{ICA}$  should track changes in MCA and ACA flow.

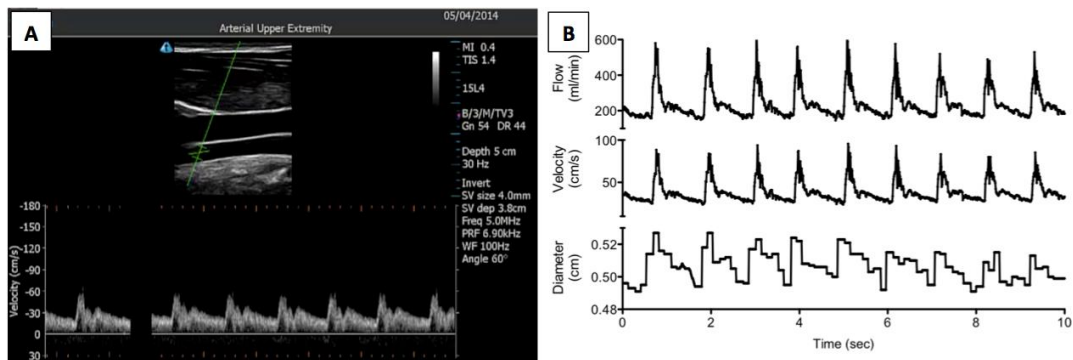


**Figure 2.7. Duplex ultrasound image of the internal carotid artery and an example of an analysis output.**

Simultaneous measurement of the arterial diameter (B-mode image) and the blood velocity (pulse-wave image) enable determination of volumetric flow through extra-cranial cerebral arteries with high temporal and spatial resolution. Reproduced from (Hoiland *et al.*, 2016b) with permission.

#### **2.2.2.4 BLOOD OXYGEN LEVEL DEPENDENT MAGNETIC RESONANCE IMAGING**

For assessing neuronal activation, the most widely used functional MRI technique is BOLD MRI where the MRI signal increases in tandem with blood flow. For the same reason it is

becoming increasingly popular as a non-invasive surrogate measure for assessing the CBF component in CVR measurement (Mikulis *et al.*, 2005; Mandell *et al.*, 2008; Donahue *et al.*, 2012; Sam *et al.*, 2015). The BOLD signal has a high signal-to-noise ratio, as well as high spatial and temporal resolution compared to non-MRI methods used for measuring CBF, such as positron emission tomography (Siero *et al.*, 2015).

The physical basis behind the contrast for BOLD lies in the magnetic susceptibility of blood. Oxygenated hemoglobin (Hb) is diamagnetic and causes little or no distortion to the magnetic field in surrounding tissue which, is also diamagnetic. However, deoxygenated hemoglobin (dOHb) is paramagnetic, attenuating the T2\* signal strength in the surrounding tissue. The rate of attenuation varies directly with [dOHb]. With a constant cerebral metabolic rate of oxygen (CMRO<sub>2</sub>) – and thus constant dOHb production – the [dOHb] will follow a dilution model with CBF. In other words, high CBF results in low [dOHb] and high BOLD signal.

### **2.3 BASICS OF CEREBRAL BLOOD FLOW REGULATION**

Like any other organ, flow to the brain is ultimately regulated by the countervailing influences of, and balance between, perfusion pressure and vascular resistance. Cerebral perfusion pressure (CPP) is defined as the pressure gradient across the brain (input minus output) and often represented by **Equation 2.2**:

Equation 2.2: Cerebral perfusion pressure

$$CPP = MAP - ICP$$

Where MAP represents mean arterial blood pressure, and ICP represents intracranial pressure. Cerebral vascular resistance is determined by the influences of blood viscosity ( $\eta$ ), vessel length ( $L$ ), and the arterial radius ( $r$ ) (or diameter). These factors, in combination with CPP are combined to form Poiseuille's equation, which depicts the overall regulation of CBF (**Equation 2.3**):

Equation 2.3: Poiseuille's law

$$CBF = \frac{CPP \cdot \pi r^4}{8L\eta}$$

Notably, the influence of arterial radius on CBF is not linear with the influence of radius raised to the fourth power, and therefore changes in cerebrovascular tone are the most influential effector of CBF. Analogous to Ohm's law, the previous equation can more simply be represented by

**Equation 2.4:**

Equation 2.4: Hemodynamic equation for flow, resistance, and pressure (Ohm's law)

$$CBF = CPP / \text{cerebrovascular resistance}$$

Thus, cerebrovascular resistance can be represented as (**Equation 2.5**):

Equation 2.5: Cerebrovascular resistance derived from Poiseuille's law

$$\text{Cerebrovascular resistance} = 8L\eta / \pi r^4$$

Or more simply as (**Equation 2.6**):

Equation 2.6: Cerebrovascular resistance derived from the hemodynamic representation of Ohm's law

$$\text{Cerebrovascular resistance} = CPP / CBF$$

Overall, the above formalism represents a simple model for the relationship between pressure, resistance and flow in the brain. Indeed, it represents physical relationships for laminar flow of a Newtonian fluid through a rigid cylindrical tube. However, as highlighted above, the anatomical configuration of the cerebral circulation represents a functional syncytium, versus that of a single tube. For a complex vascular network, as is the cerebral circulation, resistance to any vascular bed may be alternatively, but still simplistically, represented as the sum of parallel vessels (**Equation 2.7**):

Equation 2.7: Cerebrovascular resistance of parallel vessel beds

$$\text{Total Resistance} = 1/R_1 + 1/R_2 + 1/R_3 + \dots 1/R_n$$

Where R indicates resistance of a vessel, and n represents the number of vessels. Here, the diameter dependent influence on viscosity could be taken into account for each independent vessel, increasing the complexity, but also accuracy of determining vascular resistance(s). For the purposes of this thesis, a simple overview on the influence of changes in vascular resistance and blood viscosity follows while hemodynamic influences on flow regulation, and related physical relationships have recently been reviewed in greater detail (Secomb, 2016).

### **2.3.1 CEREBRAL BLOOD FLOW AND MICROVASCULAR PRESSURE WITH CHANGES IN SEGMENTAL VASCULAR RESISTANCE**

In the systemic circulation, vascular resistance is regulated primarily by small muscular arteries/arterioles of the microcirculation. Seemingly as a result, pial arteries are often misconstrued as the primary resistors in the cerebral vascular network, and therefore the primary modulators of CBF. However, extensive differences exist between the systemic and cerebral circulation, such as intrinsic sensitivity to pH (see section “Regulation of cerebral blood flow by carbon dioxide”), encapsulation of microvessels by astrocytic end feet, and the presence of pericytes around capillaries (Hall *et al.*, 2014; Mishra *et al.*, 2016), provide functional and anatomical precedence for a differing segmental regulation of cerebrovascular resistance than that observed in the systemic circulation.

In support of a unique segmental regulation of cerebrovascular resistance, as compared to that of the systemic circulation, animal data dating back as early as the 1950’s has consistently demonstrated that segmental contributions to cerebral vascular resistance along the vasculature, indicated by the consequent and progressive pressure drop across the cerebral circulation (which dictates cerebral microvascular pressure) occur from the larger cerebral arteries through to the smallest pial and parenchymal microvessels (Faraci & Heistad, 1990). Interestingly, this segmental allocation of resistance appears unique to the cerebral circulation (Faraci & Heistad, 1990). Modern technological advances and related

experimental models have confirmed these animal data and have added clarity to our understanding of segmental vascular regulation in humans (Willie *et al.*, 2012; Verbree *et al.*, 2014; Coverdale *et al.*, 2014; Warnert *et al.*, 2015; Kellawan *et al.*, 2016). Overall, the ratio between upstream and downstream resistance governs microvascular pressure (**Figure 2.8**), with implications for regional flow distribution of parallel vessels described in detail later (See section “Standardization and utility of cerebrovascular reactivity”).

In a state of quiescence, approximately 50% of the arterial pressure head is lost by the pial arterioles immediately prior to entry into the parenchyma (Shapiro *et al.*, 1971), indicating a significant contribution to cerebral vascular resistance by upstream vessels; the large vessels proximal to the Circle of Willis (e.g. carotids, vertebrals, and basilar) and those immediately distal (e.g. middle and posterior cerebral arteries). Indeed, approximately 20% of aortic pressure is lost at the level of the BA (Faraci *et al.*, 1988), indicating large arteries proximal to the Circle of Willis contribute ~20% of cerebrovascular resistance, and the larger arteries immediately distal to the Circle of Willis, but proximal to surface pial arteries, contribute the remaining 20-30% of vascular resistance possessed by large arteries (Shapiro *et al.*, 1971; Stromberg & Fox, 1972; Faraci *et al.*, 1988). Further modulation of resistance is consequently at or downstream of pial arterioles and appears to occur even at the level of capillaries via pericyte mediated relaxation and constriction (Hamilton *et al.*, 2010; Hall *et al.*, 2014). Vascular pressure also varies with anatomical location with greater pressures in similar-sized vessels in the brainstem compared to that in the cerebrum (Faraci *et al.*, 1987) possibly due to differences in relative diameter and length of vessels, and differences in branching pattern. It must be noted that this information is derived primarily from animal and *in vitro* models, with limited data in humans (Warnert *et al.*, 2015).

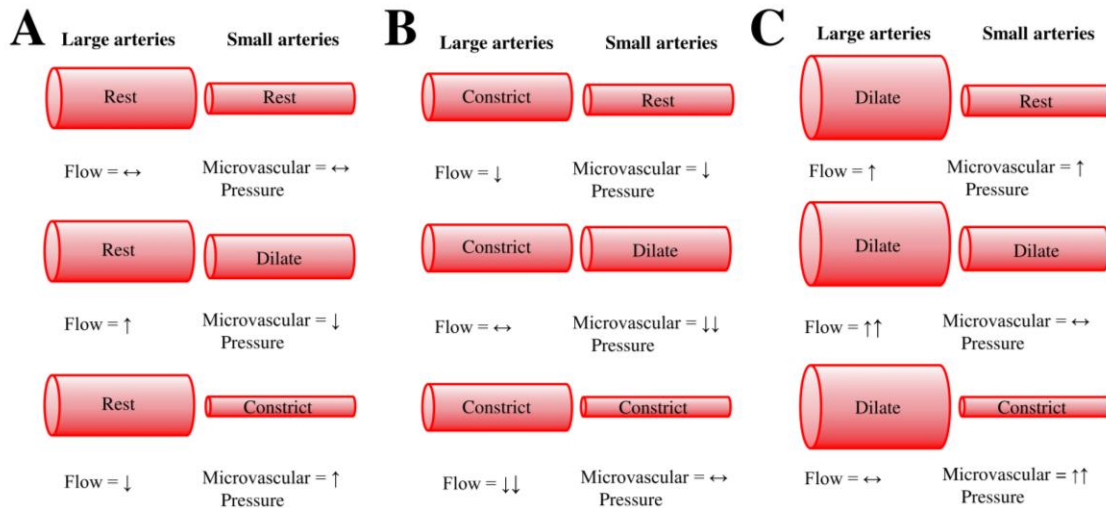


**Figure 2.8. A simplified schematic of how segmental changes in the resistance of cerebral blood vessels organized in series influence flow and microvascular pressure.**

Changes in vasomotor tone (i.e. dilation/constriction) are labelled on each vessel while the resulting directional changes in flow and microvascular pressure are represented below each scenario with arrows. Two arrows simply represent a larger magnitude of effect than one arrow, while a sideways ( $\leftrightarrow$ ) arrow indicates no change. All flow changes are relative to the very top left scenario (resting large vessel & resting small vessel). **A.** In a scenario where larger (and upstream) vessels are in a resting state, dilation smaller (and downstream) vessels will lead to a reduction in microvascular pressure and increase in flow, whereas constriction of smaller vessels will increase microvascular pressure and reduce flow. **B.** Constriction of a large upstream vessel will lead to a reduction in flow and microvascular pressure when the downstream small arteries do not change in diameter. If the downstream small arteries dilate, this will reduce microvascular pressure to an extent that maintains normal flow. However, if the small vessels constrict in concert with the large vessels, this will reduce flow despite unchanged microvascular pressure. **C.** Dilation of a large upstream vessel will lead to an increase in flow and microvascular pressure when the downstream small arteries do not change in diameter. If the downstream small arteries dilate in concert with the large arteries, this will increase flow in the face of unchanged microvascular pressure. However, if the small vessels constrict, flow is unaltered and microvascular pressure is increased. Collectively, this figure represents a simplistic overview of how resistance (dilation versus constriction and driving pressure (effected by changes in microvascular pressure) dictate flow.

This segmental contribution to resistance and related pressure drop possesses important implications for the tangential forces exerted on the vessel wall. As per Laplace's Law (**Equation 2.8**):

Equation 2.8: Wall stress, the Law of Laplace

$$\text{Wall Stress} = \Delta P \cdot r / (2 \cdot T)$$

Where  $\Delta P$  is perfusion pressure,  $r$  is the vessel radius, and  $T$  is the wall thickness, wall stress varies directly with perfusion pressure (or transmural pressure) and inversely to wall thickness.

Therefore, the pressure drop across the cerebral circulation serves to reduce wall stress. Further, changes in the ratio of vessel wall thickness to vessel lumen diameter also serve to reduce wall stress across the cerebral circulation. In human pial vessels resected during surgery for tumor access, Bevan and colleagues (Bevan *et al.*, 1999) investigated how vessel wall and lumen size change in pial arteries ranging from 200-1000 $\mu\text{m}$  in diameter. They demonstrated that as vessel diameter decreases, so does the thickness of the media (**Figure 2.9A**); however, the rate at which the media decreases is less than the diameter, thereby increasing the media thickness to vessel diameter ratio as vessels decrease in size (**Figure 2.9B**). This means that for a given pressure, wall stress is reduced as blood traverses the pial circulation. (**Figure 2.9C**). However, it is important to remember, as previously noted, that pressure drops prior to the pial circulation, as well as across the pial circulation, at least as observed in animals (Shapiro *et al.*, 1971). Therefore, in addition to the increased vessel wall to lumen ratio, reduced pressures further contribute to overall reductions in wall stress (**Figure 2.9C**). The implications of segmental vascular regulation and its contribution to CBF regulation during changes in  $\text{PaCO}_2$  and  $\text{PaO}_2$  are discussed further in later sections (see sections "CO<sub>2</sub>: site(s) of vascular regulation" and "Response characteristics of cerebral blood flow to hypoxemic hypoxia").

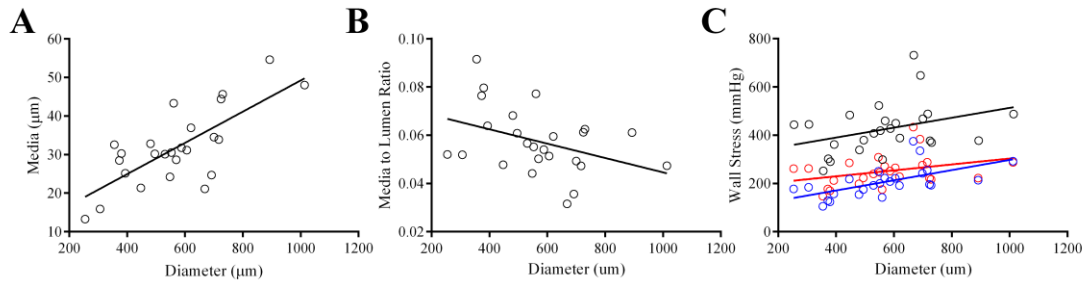


**Figure 2.9. Changes in wall stress along the pial circulation.**

**A.** As diameter decreases so does the thickness of the media (i.e., vessel wall). **B.** As vessel diameter decreases the ratio of wall thickness to luminal diameter increases. **C.** Due to the increase in vessel wall to lumen ratio, wall stress decreases as vessel diameter decreases. The black circles represent the changes in wall stress across the pial circulation if pial artery pressure was the same as systemic blood pressure [e.g. mean arterial pressure =  $93 = (120 \cdot 0.33) / 80 \cdot 0.66$ ]. However, pial artery pressure may approximate 60% of systemic arterial pressure (Shapiro *et al.*, 1971). Therefore, we have re-plotted the wall stress to diameter relationship for 60% of systemic arterial pressure (red-line). Further consideration of how pressure drops across the pial circulation is also required. Using the regression equation for pressure versus pial artery diameter from (Shapiro *et al.*, 1971), we have re-plotted the data taking into consideration the pressure drop across the pial circulation while aligning the pressure for the larger 1000µm on the right side of panel C. This is represented by the blue line where this reduction in pressure across the pial circulation leads to greater drop in wall stress. We acknowledge that applying regression equation derived in animals to human data may not be robust; however, it provides general insight into how wall stress is altered across the cerebral circulation. Data digitized and adapted from (Bevan *et al.*, 1999).

### 2.3.2 CEREBRAL BLOOD FLOW AND BLOOD VISCOSITY

Whole blood viscosity is determined by plasma viscosity, hematocrit (HCT), and mechanical properties (e.g. deformability) of the red blood cell. Blood is a suspension of cells in a relatively homogenous fluid (plasma) and therefore non-Newtonian. Consequently, the behavior of blood with respects to apparent viscosity depends on several factors such as vessel diameter and blood flow velocity. Blood is subject to shear thinning, which is a reduction in viscosity concomitant to increased shear rates, or flow velocity (Bayliss, 1959; Amin & Sirs, 1985). This is due to increased axial migration of red blood cells at increasing blood flow velocities (Bayliss, 1959; Secomb & Pries, 2013). The plasma layer, even if thin (e.g. 1µm) can lead to a large reduction in apparent viscosity, as the

viscosity at the adluminal surface of the vessel wall, or glycocalyx, is the location where viscous energy is primarily dissipated (Secomb & Pries, 2013). Decreasing HCT leads to an increase in the thickness of this marginal cell-free layer and thus reduced blood viscosity. As with laminar flow, velocity across the vessel lumen is parabolic, with velocity highest in the center and lowest (effectively static) at the vessel wall. This increasing velocity from the vessel wall to lumen center underscores the axial drift of red blood cells due to increased speed of flow effectively “pulling” red blood cells towards the center of the vessel (Toksvang & Berg, 2013).

In addition to blood flow velocity as described above, vessel diameter, via the Fåhræus–Lindqvist effect, leads to altered blood viscosity throughout the cerebral circulation (Fåhræus & Lindqvist, 1931). As a tube, or blood vessel, diameter drops below 0.3mm (300µm) HCT is reduced with this effect underlying the variable viscosity observed in microvessels (Fåhræus & Lindqvist, 1931; Pries *et al.*, 1992). This has implications for understanding localized flow distributions and in accordance with the conclusion of Fåhræus and Lindqvist in 1931, “The law of Poiseuille does not apply to the flow of blood in capillary tubes of a diameter below about 0.3mm” (Fåhræus & Lindqvist, 1931). Indeed, cerebrovascular viscosity is variable (Calamante *et al.*, 2016), does not necessarily match the typically assumed 85% of large vessel HCT (Lammertsma *et al.*, 1984), and decreases with increased blood velocity as occurs during hypoxia and hypercapnia (Sakai *et al.*, 1985). The functional significance of the blood flow velocity and diameter dependence of viscosity is that reduced viscosity and related resistive forces in smaller vessels reduces the pressure requirement to maintain adequate tissue perfusion.

Given the physical principles outlined above one would expect changes in viscosity to inversely and proportionately effect changes in flow as per Poiseuille’s Law – at least flows measured in vessels >0.3mm in diameter. However, human studies addressing this phenomenon in the cerebral circulation at rest have demonstrated this to not be the case (Brown & Marshall, 1982, 1985). Importantly, changes in viscosity will elicit commensurate changes in shear stress (i.e., decreases in viscosity lead to decreases in shear stress). Shear stress leads to upregulation of endothelial nitric oxide synthase and consequent nitric oxide mediated vasodilation [(Pohl *et al.*, 1986; Rubanyi *et al.*, 1986) explained later in more detail; see section “Hypercapnia and shear stress”]. Thus, the end

effect may be determined by the consequent balance between the viscosity dependent reduction in resistance, and the potential for reduced NO bioavailability induced increases in resistance. Animal studies have demonstrated that altering this balance between shear and viscosity can even lead to pial vessel constriction (Hudak *et al.*, 1989), although as per previous mentioned studies this effect likely does not occur in humans. As recent evidence indicates that shear stress plays a role in regulating vascular tone of cerebral conduit vessels [e.g., ICA (Carter *et al.*, 2016a; Hoiland *et al.*, 2017c; Smith *et al.*, 2017) (see section “Appendix A”)], and arterioles (Koller & Toth, 2012), it stands to reason that the countervailing influences of reduced viscosity (causing decreased resistance) and reduced shear and consequent constrictor influences (causing increased resistance) balance out for a negligible net effect on CBF at rest *in humans*. This seems to be the case in instances where viscosity is manipulated independent of CaO<sub>2</sub> and PaCO<sub>2</sub> by plasmapheresis (Brown & Marshall, 1982, 1985). One final consideration is that altering large vessel whole blood viscosity by, for example, isovolumic hemodilution (reduced red cell concentration) has been demonstrated to reduce capillary HCT in animals (Todd *et al.*, 1992); however, there is work demonstrating no effect (Hudetz *et al.*, 1999). Therefore it is unknown how influencing large vessel HCT would alter resistive forces at the capillary segment of the vascular network. Whether or not this influence also occurs in small pre-capillary arterioles and/or resistance vessels is less clear, although animal data (Todd *et al.*, 1992) and MRI study in humans indicates that the ratio of tissue to large vessel HCT is reduced with lower large vessel HCT values (e.g. ante-cubital vein versus brain tissue) (Calamante *et al.*, 2016).

### 2.3.3 CEREBRAL BLOOD FLOW AND CRITICAL CLOSING PRESSURE

The discussion of cerebrovascular resistance and CPP as they relate to CBF regulation has thus far been fairly simple. While not erroneous in nature, defining cerebrovascular resistance as CPP/CBF (**Equation 2.6**) and CPP as MAP-ICP (**Equation 2.2**) has been called into question (Panerai, 2003) and may not fully reflect the complexities of the interplay between input pressure, output pressure, vasomotor tone, parenchymal pressure, ICP, cerebrovascular resistance, and their collective influence on CBF. To this effect, there is support in the literature for the use of critical closing pressure (CrCP) as an index of the pressure required to produce forward flow of blood (Dewey *et al.*, 1974). In humans CrCP is derived as the y-intercept (Abscissa = flow; Ordinate = pressure) of linear regression

between CBF and MAP. However, this overestimates CrCP given the relationship becomes non-linear below physiological MAP values limiting the utility of this metric for discerning the state of the cerebral vasculature (Panerai, 2003). Given this limitation it is not often used and will not be considered throughout this thesis. In its place is the use of cerebrovascular conductance or resistance, as well as co-varying for perfusion pressure statistically, such as with linear mixed modelling.

#### **2.3.4 CEREBRAL BLOOD FLOW AND ARTERIAL BLOOD GASES**

Changes in arterial blood gases primarily induce changes in CBF through the vasomotor consequences of altered  $\text{CaO}_2$  and  $\text{PaCO}_2$  (**Figure 2.10**). Changes in cerebrovascular resistance were noted in the early human studies by Kety & Schmidt [e.g.(Kety & Schmidt, 1948b)], and directly visualized even earlier in invasive animal studies (Wolff & Lennox, 1930). Importantly, changes in arterial blood gases also lead to chemoreflex mediated increases in sympathetic nervous activity (SNA) (Xie *et al.*, 2001; Pitsikoulis *et al.*, 2008; Querido *et al.*, 2010) and blood pressure (Willie *et al.*, 2012; Regan *et al.*, 2014) that influence the resulting change in CBF (Przybyłowski *et al.*, 2003; Ainslie *et al.*, 2012; Peebles *et al.*, 2012). Therefore, CBF is the product of cerebral vasomotor tone and systemic reflexes. The same holds true for CBF regulation during alterations in MAP.

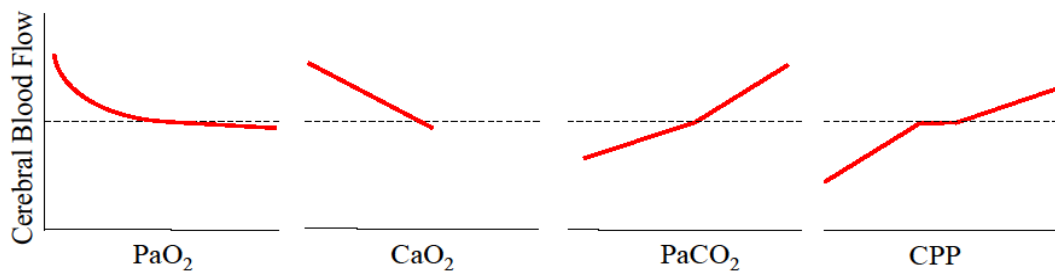


**Figure 2.10. Basic regulation of cerebral blood flow by oxygen, carbon dioxide, and cerebral perfusion pressure.**

The dashed line is representative of resting normative values, with the x-axis variables increasing in the right direction, and decreasing to the left. As the partial pressure of arterial oxygen ( $\text{PaO}_2$ ) decreases CBF increases; however, this response is not linear. Indeed, CBF does not increase appreciably until  $\text{PaO}_2$  drops to approximately 55-60mmHg, the point at which reductions in  $\text{PaO}_2$  lead to appreciable reductions in  $\text{SaO}_2$  and  $\text{CaO}_2$ . When CBF is indexed against changes in  $\text{CaO}_2$  the response is generally linear, with reductions in  $\text{CaO}_2$  leading to increases in CBF. The right portion of the  $\text{CaO}_2$ /CBF relationship is truncated given the inability to significantly increase  $\text{CaO}_2$  above resting values (e.g.,  $20\text{mL} \cdot \text{dL}^{-1}$ ) under physiological conditions. During hyperoxia, where  $\text{CaO}_2$  can be increased by pure oxygen breathing or hyperbaria, the relationship between  $\text{CaO}_2$  and CBF is less clear (Brugniaux *et al.*, 2018). CBF is related to CPP and, when autoregulation is intact, consists of three distinct and adjoining linear components. Within a small range of altered CPP there is no alteration in CBF due to cerebral autoregulation; however, when cerebral autoregulatory mechanisms are exhausted either in a hypo- or hyper- tensive manner, CBF changes linearly with CPP.

### 2.3.5 CEREBRAL BLOOD FLOW AND OXYGEN

In the context of oxygen's influence on CBF, the majority of work has investigated how CBF increases in order to maintain  $\text{CDO}_2$ . Thus, it has been well established that in a normal healthy human, increases in CBF are commensurate in magnitude to the reductions in  $\text{PaO}_2$ ,  $\text{SaO}_2$ , and  $\text{CaO}_2$  associated with arterial hypoxemia (Ainslie & Subudhi, 2014; Hoiland *et al.*, 2016a; Bailey *et al.*, 2017). The  $\text{CaO}_2$  is primarily dependent on hemoglobin concentration ( $[\text{Hb}]$ ) and  $\text{SaO}_2$  as per **Equation 2.9**:

Equation 2.9: Arterial oxygen content

$$\text{CaO}_2 \text{ (mL/dL)} = 1.34 \cdot [\text{Hb}] \cdot (\% \text{SaO}_2 / 100) + 0.003 \cdot \text{PaO}_2$$

Where 1.34 is the Hüfner-number, or binding capacity of oxygen to hemoglobin, and  $0.003 \times \text{PaO}_2$  accounts for the net solubility of  $\text{O}_2$  per dL of blood (vs. plasma) as a function of  $\text{PaO}_2$ .

The  $\text{CDO}_2$  is then calculated as (**Equation 2.10**):

Equation 2.10: Cerebral oxygen delivery

$$\text{CDO}_2 \text{ (mL/min)} = \text{gCBF (mL/min)} \cdot \text{CaO}_2 \text{ (mL/dL)} / 100$$

In experimental paradigms that allow for the sampling of trans-cerebral arterial blood gases, the  $\text{CMRO}_2$  can be calculated using the Fick equation as per (**Equation 2.11**).

Equation 2.11. The Fick Equation

$$\text{CMRO}_2 \text{ (mL/min)} = \text{gCBF (mL/min)} \cdot [\text{CaO}_2 \text{ (mL/dL)} - \text{CvO}_2 \text{ (mL/dL)}] / 100$$

Where  $\text{CvO}_2$  represents the cerebral venous content of oxygen, and  $\text{CaO}_2 - \text{CvO}_2$  represents the arterial-venous difference in oxygen content (mL/dL).

The relationship between  $\text{CaO}_2$ , CBF, and  $\text{CDO}_2$  is illustrated by the changes in CBF that occur during exposure to, and prolonged stay at, HA (Ainslie & Subudhi, 2014; Hoiland *et al.*, 2018a). Increases in minute ventilation ( $V_E$ ) resulting from acid-base compensation increase  $\text{PaO}_2$  (and the partial pressure of alveolar oxygen) as well as the  $\text{O}_2$  binding capacity of hemoglobin (Balaban *et al.*, 2013) (i.e., shift the oxyhemoglobin curve to the left) throughout acclimatization. Additionally, erythropoietin mediated increases in [Hb] also occur, and these factors collectively leading to a progressive increase in  $\text{CaO}_2$ . This leads to a reduction in CBF following the zenith observed at altitude in a very tightly

coupled manner. The result is maintained CDO<sub>2</sub> across acclimatization (Ainslie & Subudhi, 2014).

### 2.3.6 CEREBRAL BLOOD FLOW AND CARBON DIOXIDE

Increases and decreases in PaCO<sub>2</sub> lead to increases and decreases respectively in CBF (Kety & Schmidt, 1948c; Sato *et al.*, 2012a; Willie *et al.*, 2012; Smith *et al.*, 2014) (**Figure 2.11**). Alterations in PaCO<sub>2</sub> mediate changes in extracellular pH (Lambertsen *et al.*, 1961; Harper & Bell, 1963; Kontos *et al.*, 1977b, 1977a) within cerebral vessels and hence the regulation of CBF. Changes in PaCO<sub>2</sub> further influence pH of the cerebrospinal fluid bathing the ventrolateral medulla, which is important in ventilatory control (Ainslie & Duffin, 2009) and mitigating deviation from acid-base homeostasis (Hoiland *et al.*, 2018a).

The magnitude of the increase in CBF per unit change in PaCO<sub>2</sub> (mmHg), is termed cerebrovascular reactivity (CVR). This CVR represents the slope relationship between PaCO<sub>2</sub> and CBF, and can be represented as both the absolute (cm/s or mL/min) and relative percent (%) change in CBF per unit change in PaCO<sub>2</sub>. The use of absolute or relative reactivity is typically dependent on the research question and/or hypothesis (Ainslie & Duffin, 2009).

Measures of CVR are used to index the ‘responsiveness’ of the cerebral vasculature, and often targeted experimentally as an index of cerebrovascular health. Indeed, CVR has long been used as an indicator of the hemodynamic significance of stenotic arterial lesions and as a predictor for risk of stroke in related clinical populations (Ringelstein *et al.*, 1988; Kleiser & Widdern, 1992; Markus & Cullinane, 2001; Gupta *et al.*, 2012; Reinhard *et al.*, 2014). Importantly, and often overlooked, however, is the fact that CO<sub>2</sub> reactivity has yet to provide any utility for the prediction of stroke risk in apparently healthy cohorts (Portegies *et al.*, 2014). Therefore, more research is needed to determine the feasibility of classifying stroke risk with CO<sub>2</sub> reactivity in individuals without any pre-existing cerebrovascular disease.

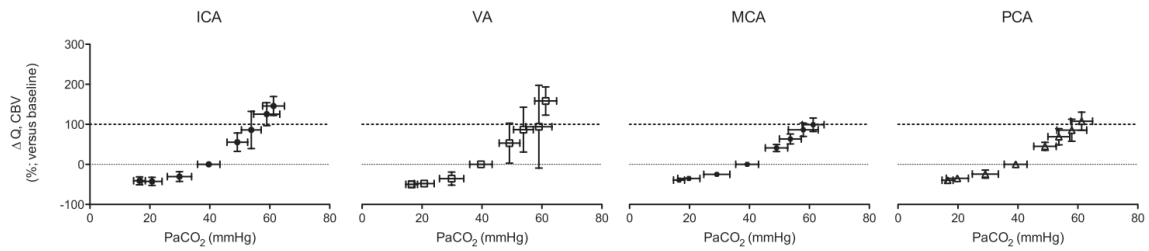


**Figure 2.11. Cerebral blood flow reactivity to changes in arterial carbon dioxide.**

Changes in blood flow (ICA & VA) and blood velocity (MCA & PCA) are plotted during alterations in the partial pressure of arterial carbon dioxide ( $\text{PaCO}_2$ ). When comparing the ICA and VA to their upstream intra-cranial vessel (MCA and PCA, respectively) it is apparent that flow reactivity assessed in the ICA and VA with duplex ultrasound is approximately 50% greater than that assessed in the MCA and PCA with transcranial Doppler ultrasound. The reasons underlying this difference have been discussed in sections “*Transcranial Doppler Ultrasound*” and “*Duplex Ultrasound*” and Figure 4 legend. Changes in flow/velocity in response to hypercapnia ( $\text{PaCO}_2 > 40 \text{ mmHg}$ ) lead to approximately 100% change in flow than that which occurs during hypocapnia ( $\text{PaCO}_2 < 40 \text{ mmHg}$ ) for a matched change in  $\text{PaCO}_2$  (e.g.  $+10 \text{ mmHg}$  vs.  $-10 \text{ mmHg}$ ). The presented data are mean  $\pm$  standard deviation. Reproduced from (Willie *et al.*, 2012) with permission. © 2012 The Authors. The Journal of Physiology © 2012 The Physiological Society.

### 2.3.7 CEREBRAL BLOOD FLOW AND PERFUSION PRESSURE

As described above, CPP is a primary determinant of CBF in all scenarios, and while it regulates CBF in an independent manner (**Figure 2.10 & Figure 2.12**), CPP often changes during physiological perturbations and is therefore highly relevant when considering the integration of various regulatory factors. Classic dogma has long posited that CBF remains constant during alterations in MAP due to counter-regulatory or ‘auto-regulatory’ mechanisms consisting of adjustments in cerebrovascular resistance. A seminal review published by Lassen in 1959 described the notion that CBF remains constant in an MAP range of 60 to 150 mmHg (Lassen, 1959). This relationship, or cerebral autoregulation (CA) curve, was notably formulated from 7 different studies with 11 different subject groups. The subject groups’ CBF was measured at a single MAP value and was not observed throughout a range in MAP. Furthermore, these subjects had a pathological condition and/or were taking pharmaceuticals. This classic report has often been

misconstrued to depict a mean curve for intra-subject CA relationships collected over a range of MAP values versus its true representation of connected individual inter-subject data points. Indeed, fixing a line through several singular subject MAP/CBF relationships ignores the potential of varying MAP/CBF relationships in different pathologies (Nobili *et al.*, 1993; Warnert *et al.*, 2016). Upon closer examination of the response for CBF (or a related index of CBF) to a change in MAP, recent studies have revealed that this relationship appears to be more pressure passive than previously described (Numan *et al.*, 2014). In other words, changes in MAP lead to directionally consistent changes in CBF. Consequently, contemporary understanding now holds that the autoregulatory plateau is much narrower than previously thought, and may encompass a mere 5-10mmHg range in healthy humans (Lucas *et al.*, 2010; Tan, 2012; Numan *et al.*, 2014; Tzeng & Ainslie, 2014) (Figure 2.12).

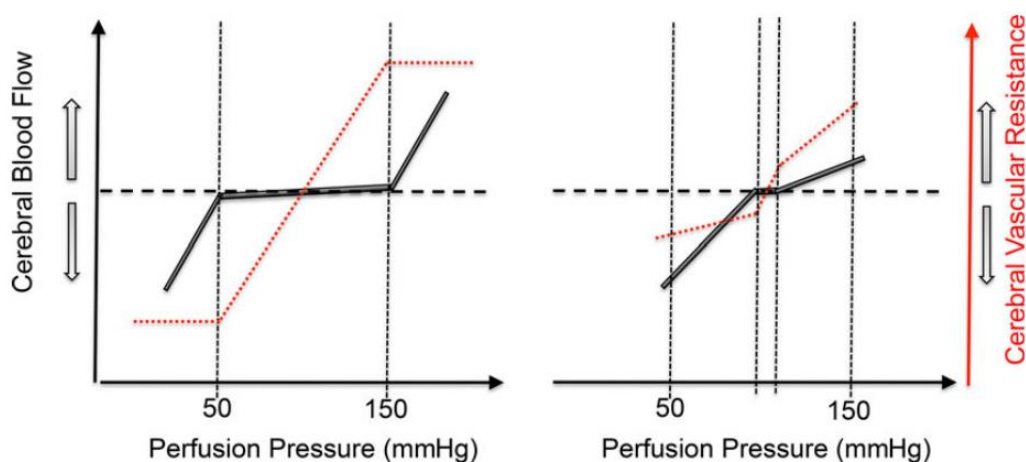


**Figure 2.12. The classical (left) and contemporary (right) cerebral autoregulation curves.**

Changes in cerebral perfusion pressure are buffered by intrinsic vascular mechanisms (Fog, 1937, 1939). Following the review paper published by Lassen in 1959 (Lassen, 1959), it was thought that CBF remained constant between an arterial blood pressure of 50 to 150 mmHg (left panel). However, at least within-subjects, it has now been well established that this autoregulation mechanism does not maintain constant perfusion over as wide of a range in arterial blood pressure (Tan, 2012; Numan *et al.*, 2014; Hori *et al.*, 2017). Reproduced from (Willie *et al.*, 2014b) with permission. © 2014 The Authors. The Journal of Physiology © 2014 The Physiological Society.

### 2.3.8 CEREBRAL BLOOD FLOW AND NEUROVASCULAR COUPLING

Increases in cerebral metabolic demand necessitate increases in substrate and oxygen delivery as originally demonstrated in the classic works by Mosso (Mosso, 1880) and Roy and Sherrington (Roy & Sherrington, 1890). Complex processes that may involve both feed forward and feedback mechanisms match CBF to metabolic demand, with this response termed neurovascular coupling (NVC) (Attwell *et al.*, 2010; Phillips *et al.*, 2016; Wei *et al.*, 2016). Regulation of NVC occurs at the neurovascular unit, which is made up of three components that allow for spatial and temporal matching of flow to metabolic demand: 1) the blood vessel or vascular smooth muscle, 2) the astrocyte, and 3) the neuron. Together these three components form the structural unit responsible for coupling CBF to metabolic demand. Extensive details on the mechanisms that mediate NVC and the related clinical implications have been recently outlined elsewhere (Iadecola, 2017); however, given the use of NVC in Study 4, a few aspects are outlined here for clarity.

Both feed forward and feedback mechanisms are thought to underly the NVC response. Feed forward mechanisms are related to increased glutamatergic signaling (from increased neural activity) (**Figure 2.13**). These processes are as follows: 1) Activation of post-synaptic N-methyl-D-aspartate receptors leads to an increase in the intracellular concentration of neuronal  $\text{Ca}^{2+}$  (Attwell *et al.*, 2010). This stimulates the increased production of prostaglandins (PG) and NO related to the  $\text{Ca}^{2+}$  dependence of their enzymatic production. 2) Binding of metabotropic glutamate receptors on astrocytes leads to an increase in their intracellular  $[\text{Ca}^{2+}]$ . These mechanisms have been primarily investigated following stimulation of neurons and/or astrocytes with exogenous glutamate (Gordon *et al.*, 2008), photolytic uncaging of intracellular  $\text{Ca}^{2+}$  (Gordon *et al.*, 2008), and/or utilization of the whisker-barrel cortex reflex (Adachi *et al.*, 1994; Liu *et al.*, 2012a). Feed back mechanisms are related to drops in tissue  $\text{PO}_2$  and the related build up of metabolic byproducts [e.g.  $\text{CO}_2$  (Howarth *et al.*, 2017)] in addition to direct influences of the red blood cell (Wei *et al.*, 2016). Overall, these two mechanisms lead to vasodilation occurring from the level of the capillaries (Hall *et al.*, 2014) through to pial vessels, with the vast locale of this response governed by retrograde propagation of vasodilatory signals [reviewed in: (Iadecola, 2017)].

While mechanistic delineation of NVC has taken place primarily in animal models, some researchers have begun to turn their focus to the investigation of NVC in humans (Phillips *et al.*, 2016). Here it has been demonstrated that PaCO<sub>2</sub> influences NVC (Szabo *et al.*, 2011), but whether or not there is an influence of O<sub>2</sub> on NVC is less clear (Caldwell *et al.*, 2017, 2018). However, in clinical populations where vascular dysfunction is manifest, the NVC response is reduced [reviewed in: (Phillips *et al.*, 2016)].

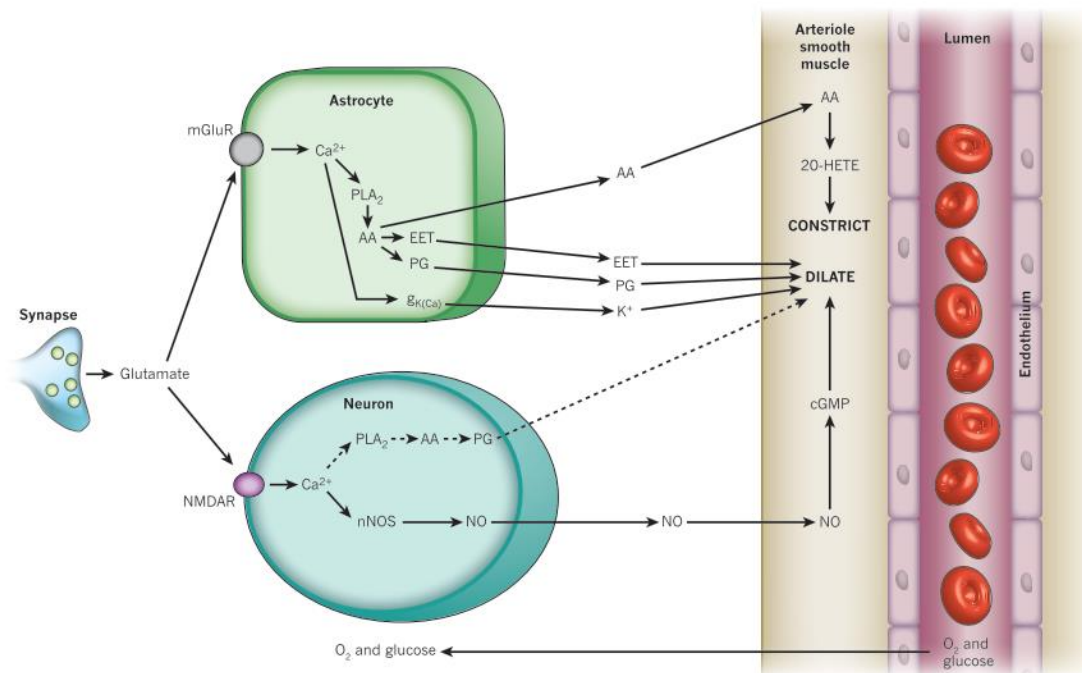


**Figure 2.13. Feed forward mechanisms in neurovascular coupling.**

Feed forward control of blood flow during localized increases in cerebral metabolic activity and oxygen demand are due to glutamatergic signaling. Glutamate acts on both neurons and astrocytes to increase the production of vasodilators. See text for details. From (Attwell *et al.*, 2010) with permission. 20-HETE, 20-hydroxyeicosatetraenoic acid; AA, arachidonic acid; Ca<sup>2+</sup>, calcium; EET, epoxyeicosatrienoic acids; g<sub>K(Ca)</sub>, calcium gated potassium channels; K<sup>+</sup>, potassium, mGluR, metabotropic glutamate receptor; NMDAR, N-methyl-D-aspartate receptor; nNOS, neuronal nitric oxide synthase; NO, nitric oxide; PG, prostaglandin; PLA<sub>2</sub>, phospholipase 2. Reproduced from (Attwell *et al.*, 2010) with permission.

### 2.3.9 CEREBRAL BLOOD FLOW AND CELLULAR REGULATION OF VASCULAR SMOOTH MUSCLE TONE

Fundamentally, there are two primary ways in which smooth muscle tone is regulated: 1) through changes in intracellular calcium concentration or calcium influx, and 2) through changes in vascular smooth muscle cell calcium sensitivity. Calcium entry into cells is governed largely by voltage-gated calcium channels. Hyperpolarization of the vascular smooth muscle cells by potassium efflux will downregulate calcium channel activity, making potassium channel conductance another highly relevant factor in the regulation of smooth muscle tone (Nelson *et al.*, 1990a). Calcium sensitivity is dependent upon the phosphorylation (activation) of myosin, by myosin light chain kinase (MLCK), which itself is dependent on cyclic nucleotide (cyclic adenosine and guanosine monophosphate, cAMP & cGMP) activity (Adelstein *et al.*, 1978).

Increased conductance of potassium channels effluxes potassium, hyperpolarizes cells, decreases membrane potential and ultimately inhibits activity of voltage-gated calcium channels (Nelson *et al.*, 1990a; Faraci & Sobey, 1998). Several vasoactive factors affect potassium channel conductance. Adenosine, through binding of smooth muscle A<sub>2A</sub> receptors, and vasodilator PGs [e.g., prostacyclin (PGI<sub>2</sub>) and prostaglandin E<sub>2</sub> (PGE<sub>2</sub>)] through binding of smooth muscle IP and EP receptors (Davis *et al.*, 2004), increase intracellular cAMP concentrations (Narumiya *et al.*, 1999; Hein *et al.*, 2013), which results in increased potassium channel conductance. Moreover, epoxyeicosatrienoic acids (EETs) (Gebremedhin *et al.*, 1992) and NO (Bolotina *et al.*, 1994) may mediate cerebrovascular dilation through modulation of calcium-activated potassium channel conductance.

Cyclic nucleotides (cAMP and cGMP) exert vasodilatory effects (Triner *et al.*, 1971) primarily via two pathways; 1) by increasing conductance through potassium channels (Song & Simard, 1995), and 2) by decreasing vascular smooth muscle cell calcium sensitivity. Cyclic nucleotides reduce smooth muscle cell calcium sensitivity by increasing cAMP- and cGMP-dependent protein kinase-mediated phosphorylation of myosin light chain kinase, which leads to its deactivation, and a consequent reduced myosin-actin binding (Adelstein *et al.*, 1978; Kerrick & Hoar, 1981). Several vasoactive signaling molecules may mediate vasodilation through increased cyclic nucleotide activity. For

example, ATP degradation to adenosine, through subsequent binding of adenosine A<sub>2A</sub> receptors (Kalaria & Harik, 1988; Hein *et al.*, 2013), increases cAMP levels (Sattin & Rall, 1970; Nordstrom *et al.*, 1977). In addition, PG binding of IP and EP receptors (Davis *et al.*, 2004) leads to increased intracellular cAMP (Narumiya *et al.*, 1999), while NO upregulates cGMP production (Pearce *et al.*, 1990).

## **2.4 CEREBRAL BLOOD FLOW REGULATION IN HYPOXIA**

Here, and throughout this thesis, hypoxia is defined as a scenario in which tissue hypoxia will manifest. Under this umbrella term, there are four specific types of hypoxia that may occur: hypoxemia, anemia, stagnant hypoxia, and histotoxic hypoxia. This thesis focuses on hypoxemia and anemia. Herein hypoxemia (or hypoxemic hypoxia) is defined here as a reduction in the amount of oxygen in the blood ( $\downarrow PaO_2$ ) whereby hemoglobin desaturation ensues ( $\downarrow SaO_2$ ). Anemia (or anemic hypoxia or hemodilution) is defined here as a reduction in hemoglobin concentration that reduces the oxygen carrying capacity of the blood ( $\downarrow [Hb]$ ). This thesis will simply refer to hypoxia, unless experimental nuances require the specific mention of hypoxemia or anemia (hemodilution).

Relative to other species, the human brain has evolved to be approximately three times larger than expected for body size due to increases in the frontal lobe, temporal lobe, and cerebellum (Schoenemann, 2006). The increase in brain volume occurred during the early evolution of the genus *Homo* and was especially pronounced in *Homo erectus* likely due to selection pressures associated with greater social complexity, enhanced ecological demands on cognition and increased physical activity (Holloway, 2008; Sherwood *et al.*, 2008; Raichlen & Polk, 2013). As a consequence, the brain has evolved into a highly oxidative organ accounting for a disproportionate 20% of the basal oxygen demand which is 10 times higher than what would be expected from its weight (Raichle & Gusnard, 2002). The ability to process large amounts of O<sub>2</sub> over a relatively small tissue mass is required to support the high rate of ATP production needed to maintain an electrically active state for the continual transmission of neuronal signals [reviewed in: (Bailey *et al.*, 2009a)]. However, this obligatory high rate of CMRO<sub>2</sub> is associated with a commensurately high “vulnerability for failure”. In light of this vulnerability, adequate CDO<sub>2</sub> via precise regulation of CBF is vital to maintain optimal function and avoid cellular damage and/or

death. Describing the influence of O<sub>2</sub> availability on CBF and brain metabolism is an essential step towards a better understanding of brain energy homeostasis and associated clinical implications.

An appropriate and commonly employed model to investigate the acute and chronic cerebrovascular effects of reduced O<sub>2</sub> availability involves exposure to normobaric hypoxia or ascent to HA (over 3,000m above sea level). It has been well documented that CBF increases in response to the severity of hypoxic stimuli in humans via cerebral vasodilation (Severinghaus *et al.*, 1966a; Ainslie & Poulin, 2004; Ainslie & Ogoh, 2010; Willie *et al.*, 2012, 2014c; Ainslie *et al.*, 2014; Ainslie & Subudhi, 2014). These compensatory increases in CBF upon exposure to normo- and hypo- baric (sea level and HA, respectively) hypoxia are adequate to maintain CDO<sub>2</sub> [reviewed in: (Ainslie & Subudhi, 2014)]. The mechanisms underlying the influence of hypoxia upon CBF are complex and involve interactions of many physiological, metabolic and biochemical processes. For example, potential mechanisms of cerebrovascular dilation likely change depending on the magnitude and duration of exposure to hypoxia, the degree of acid-base adjustment, intrinsic cerebral reactivity to changes in O<sub>2</sub>, CO<sub>2</sub>, and pH, as well as release of local vasoactive factors [e.g., NO (Van Mil *et al.*, 2002a) and adenosine (Bowton *et al.*, 1988; Nishimura *et al.*, 1993) to name but a few].

The PaO<sub>2</sub> dissolved in the plasma contributes little to the total CaO<sub>2</sub> as previously described (see section “Cerebral Blood Flow and oxygen” and **Figure 2.14**); however, because the partial pressure gradient between arterial blood and tissue facilitates diffusion of O<sub>2</sub> into the cell, PaO<sub>2</sub> is often presumed to be the cerebral vascular stimulus during hypoxia. Yet, blood flow to contracting skeletal muscles is regulated by CaO<sub>2</sub>, not PaO<sub>2</sub> (Roach *et al.*, 1999; González-Alonso *et al.*, 2001), with deoxyhemoglobin being both the primary O<sub>2</sub> sensor and upstream response effector; there are data in humans indicating the same might be true for CBF regulation. Moreover, in clinical and environmental conditions where CaO<sub>2</sub> is elevated, there is evidence that CBF is reduced (Milledge & Sorensen, 1972; Humphrey *et al.*, 1980b).

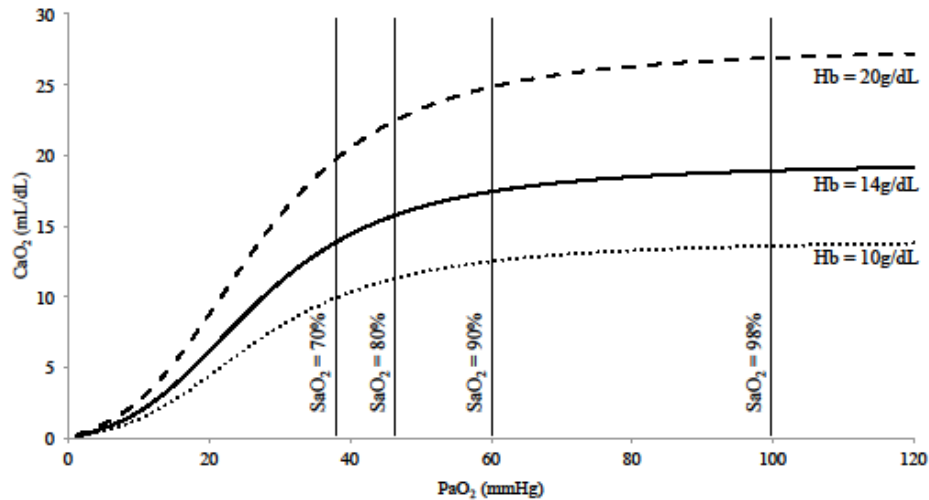


**Figure 2.14. Diagram of the relationship between oxygen content and the partial pressure of oxygen.**

Reduced hemoglobin (Hb) concentration during anemia or following hemodilution (lower dotted curve) decreases  $\text{CaO}_2$ . Increased hemoglobin as would occur in polycythemia (upper dashed curve) increases  $\text{CaO}_2$ . The middle solid line denotes normal resting values. Figure derived from equation (3)  $\text{CaO}_2$  ( $\text{mL} \cdot \text{dL}^{-1}$ ) =  $[\text{Hb}] \cdot 1.36 \cdot (\% \text{SaO}_2/100) + 0.003 \cdot \text{PaO}_2$ . Reproduced from (Hoiland *et al.*, 2016a), permission not required.

Herein, for both physiological and to a lesser extent pathophysiological settings, this section (Cerebral blood flow regulation in hypoxia) reviews the current knowledge of CBF regulation with changes in  $\text{PaO}_2$  and/or  $\text{CaO}_2$ . Emerging evidence suggests that deoxyhemoglobin is the primary biological regulator of CBF, and therefore consequently  $\text{CDO}_2$  and brain tissue oxygenation, during changes in  $\text{CaO}_2$  originating from alterations in  $\text{O}_2$  tension (i.e., hypoxemic hypoxia), hemodilution, and anemia. First, an overview of how CBF is regulated under acute (seconds to hours), chronic (days to years) and lifetime conditions of hypoxemic hypoxia, is provided with the evidence supporting the sufficient maintenance of  $\text{CDO}_2$  highlighted. Second, this section reviews the studies to date that have examined (directly or indirectly) the relationship between  $\text{CaO}_2$  and CBF in the absence of changes in  $\text{PaO}_2$  (hemodilution), and contrast the CBF response with those where  $\text{PaO}_2$  is reduced (hypoxemic hypoxia). Further, we consider the varying levels of deoxyhemoglobin produced between these different experimental paradigms. Finally, we

provide an overview of the molecular underpinnings that regulate CBF during hypoxemia or during independent changes in  $\text{CaO}_2$ .

#### **2.4.1 RESPONSE CHARACTERISTICS OF CEREBRAL BLOOD FLOW TO HYPOXEMIC HYPOXIA**

It is well established that inhalation of hypoxic gas mixtures causes dilation of the pial vessels, a reduction in cerebral vascular resistance, and increases CBF in humans (Kety & Schmidt, 1948c; Cohen *et al.*, 1967). However, while hypoxia *per se* is a cerebral vasodilator, reflected in a rise in CBF in proportion to the severity of isocapnic hypoxia [reviewed in; (Willie *et al.*, 2014c; Ainslie & Subudhi, 2014)], in normal conditions the hypoxia-induced activation of peripheral chemoreceptor activity leads to hyperventilatory-induced lowering of  $\text{PaCO}_2$  and subsequent cerebral vasoconstriction. Over time, metabolic compensation occurs in response to the respiratory alkalosis and CBF is normalized to the lowered  $\text{PaCO}_2$  (Willie *et al.*, 2015a). Although often viewed in isolation, the interaction between  $\text{PaCO}_2$  and  $\text{PaO}_2$  dramatically alters the CBF response, and varies with exposure time.

##### **2.4.1.1 ACUTE HYPOXEMIC HYPOXIA (SECONDS TO HOURS)**

The cerebral vasculature is responsive to hypoxia, but only below a  $\text{PaO}_2$  of ~50-60mmHg. This response is dependent on the prevailing  $\text{PaCO}_2$  – hypercapnia increases and hypocapnia decreases the vasodilatory response to a hypoxic stimulus (Mardimae *et al.*, 2012) due to the independent vasoactive effects of  $\text{PaCO}_2$  / pH on CBF (Willie *et al.*, 2014c). For a given severity of isocapnic hypoxia, studies incorporating a range of techniques to quantify CBF report a 0.5 to 2.5% increase in CBF per percent reduction in  $\text{SaO}_2$  (Cohen *et al.*, 1967; Shapiro *et al.*, 1970; Jensen *et al.*, 1996; Querido *et al.*, 2008; Reichmuth *et al.*, 2009; Willie *et al.*, 2012; Querido *et al.*, 2013; Hoiland *et al.*, 2015). However, this response is not uniform across the brain. For example, for a given severity of isocapnic hypoxia, blood flow to the brain stem increases more than that to the middle and anterior regions, as assessed by flow through the VA and ICA, respectfully (Willie *et al.*, 2012; Ogoh *et al.*, 2013a; Lewis *et al.*, 2014b; Hoiland *et al.*, 2015). Data collected using congruous positron emission tomography scans during isocapnic hypoxia also

indicate that cortical blood flow is less responsive to hypoxia than phylogenetically older areas of the brain (Binks *et al.*, 2008). Although the cerebral areas responsible for increased blood flow to hypoxia were traditionally thought to fall exclusively at the small pial vessels (Wolff & Lennox, 1930), recent data now indicates that cerebral vasodilation also occurs at the larger intra-cranial cerebral (e.g., MCA) (Wilson *et al.*, 2011; Imray *et al.*, 2014; Willie *et al.*, 2014a) and extra-cranial cerebral vessels (e.g., ICA & VA) (Lewis *et al.*, 2014b). This dilation has been observed when SaO<sub>2</sub> falls to ~80% for both the large intra- (Imray *et al.*, 2014) and extra- (Lewis *et al.*, 2014b) cranial cerebral vessels.

Although the underlying mechanisms have not been fully elucidated in awake humans (see section “Signaling pathways in the regulation of cerebral blood flow during hypoxia”), upon re-analysis of the key studies to date (see **Figure 2.15**), the elevation in CBF in response to acute hypoxemic hypoxia seems to be entirely appropriate to maintain CDO<sub>2</sub>.

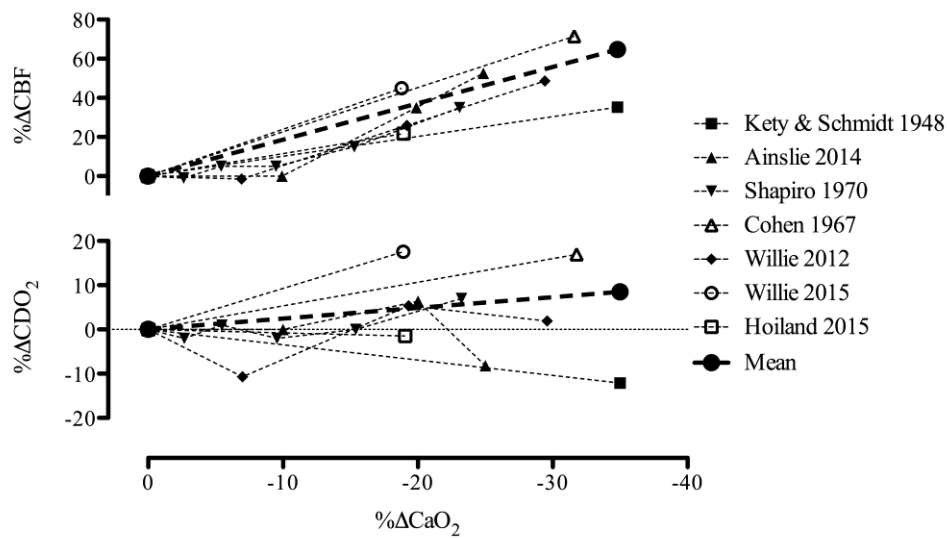


**Figure 2.15. Cerebral blood flow and oxygen delivery during acute hypoxemic hypoxia in humans.**

Data taken from five studies during hypoxemic hypoxia with concurrent measures of CBF and arterial blood gases. As exceptions we used data from (Shapiro *et al.*, 1970; Hoiland *et al.*, 2015), where Equation 2.9 was used to calculate  $\text{CaO}_2$  with  $\text{SaO}_2$  estimated using the Severinghaus equation (Severinghaus, 1979b). Data from 55 healthy subjects are depicted; i.e.,  $n =$  seven (Kety & Schmidt, 1948c), ten (Ainslie *et al.*, 2014), six (Shapiro *et al.*, 1970), nine (Cohen *et al.*, 1967), ten (Willie *et al.*, 2012), nine (Willie *et al.*, 2015a), and four (Hoiland *et al.*, 2015). The mean lines for both CBF and  $\text{CDO}_2$  have been calculated as the linear slope from the mean data of each study weighted for sample size. All studies were conducted under isocapnic conditions except for (Kety & Schmidt, 1948c), where  $\text{PaCO}_2$  was reduced by 4mmHg during the hypoxic exposure. Reproduced from (Hoiland *et al.*, 2016a), permission not required.

While global  $\text{CDO}_2$  is maintained during hypoxemic hypoxia, there appears to be a moderately heterogeneous response throughout the brain, related to regional disparities in CBF and hypoxic reactivity (**Figure 2.16**) and an overall drop in the tissue's partial pressure of oxygen ( $\text{PO}_2$ ; as inferred from jugular venous  $\text{PO}_2$ ,  $\text{PjvO}_2$ ) (Ainslie *et al.*, 2014). These disparities in the maintenance of  $\text{CDO}_2$ , and thus specific regional variations in tissue  $\text{PO}_2$ , in concert with selective vulnerability of specific regions (i.e., selective neuronal vulnerability) to hypoxia (Pulsinelli, 1985) are likely implicated in cerebral dysfunction (e.g., reduced cognitive capacity). Additionally, independent of  $\text{CDO}_2$ , tissue  $\text{PO}_2$  levels can directly regulate neuronal ion channel function (Jiang & Haddad, 1994) and alter

neurotransmitter production (e.g., glutamate, serotonin, acetylcholine) due to a low  $kM$  for oxygen (Gibson *et al.*, 1981; Hackett, 1999). Cerebral dysfunction in hypoxia has been reviewed in detail elsewhere (Gibson *et al.*, 1981; Bailey *et al.*, 2009a).

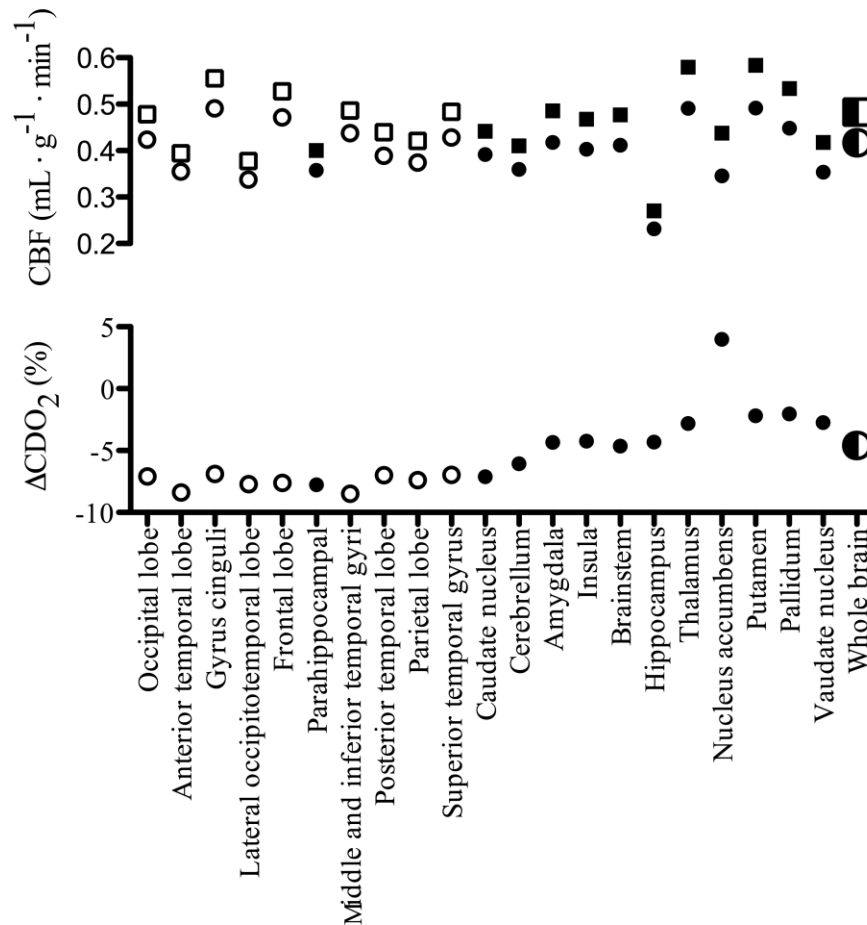


**Figure 2.16. Regional disparities in cerebral oxygen delivery relative to the whole brain during isocapnic hypoxia.**

The top panel depicts regional cerebral blood flow during normoxia (circles) and hypoxia ( $F_{I}O_2 = 0.10$ ; squares) in phylogenetically new (open symbols) and old (closed symbols) brain regions as measured by positron emission tomography. These values can be compared to their respective whole brain flow values (half-filled symbols). The lower panel highlights the heterogeneous changes in  $CDO_2$  relative to the whole brain (half-filled circle), and a trend for  $CDO_2$  of newer brain regions to be less impacted by hypoxia than phylogenetically older regions.  $CDO_2$  was calculated assuming a uniform [Hb] of 15g/dL and O<sub>2</sub> affinity of 1.34. Data adapted from (Binks *et al.*, 2008). Reproduced from (Hoiland *et al.*, 2016a), permission not required.

#### **2.4.1.2 CHRONIC HYPOXEMIC HYPOXIA (DAYS TO YEARS) – EVIDENCE FROM STUDIES AT HIGH-ALTITUDE**

The influence of  $\text{CaO}_2$  on CBF is contingent on the balance between the degree and duration of hypoxia and ensuing hypocapnia. In turn, the extent to which the cerebral vasculature responds to HA hypoxia is dependent upon four key integrated reflexes: 1) hypoxic cerebral vasodilation; 2) hypocapnic cerebral vasoconstriction; 3) the hypoxic ventilatory response; and, 4) the hypercapnic ventilatory response [reviewed in: (Ainslie & Subudhi, 2014; Hoiland *et al.*, 2018a)]. Indeed, because pH and  $\text{CaO}_2$  change throughout the acclimatization process to hypoxia (i.e., metabolic compensation for the respiratory alkalosis, which returns pH towards baseline, and progressive increases  $\text{CaO}_2$  from hemoconcentration), the CBF response to hypoxia will follow accordingly.

At least eight studies have measured CBF during acclimatization to HA (> 3400 m) using a variety of techniques (e.g., Kety Schmidt,  $\text{Xe}^{133}$ , vascular ultrasound, transcranial, and transcranial color coded Doppler; for review of measurement techniques see section “Modern measurement techniques”) to identify consistent increases in CBF following exposure to HA; however, the degree of hypoxia and duration of time at altitude is inconsistent and variable (Severinghaus *et al.*, 1966a; Huang *et al.*, 1987; Jensen *et al.*, 1990; Baumgartner *et al.*, 1994; Lucas *et al.*, 2011; Rupp *et al.*, 2014; Subudhi *et al.*, 2014b; Willie *et al.*, 2014a). What is noteworthy, as illustrated in **Figure 2.17**, is that the ~20-60% increase in CBF in each of the cited studies is closely matched to the reduction in  $\text{CaO}_2$  in a reciprocal manner;  $\text{CDO}_2$  is therefore well maintained across acclimatization.

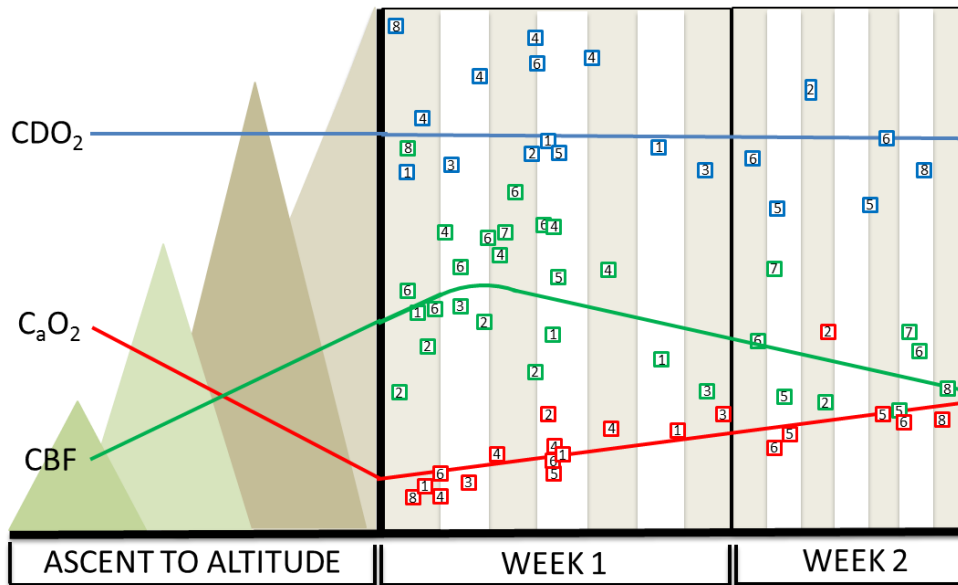


**Figure 2.17. Cerebral blood flow and oxygen delivery at high-altitude.**

Following initial exposure to high-altitude, arterial oxygen content ( $C_{aO_2}$ ) is reduced and cerebral blood flow (CBF) is commensurately increased. Increases and decreases in  $C_{aO_2}$  and CBF, respectively, then mirror each other throughout acclimatization and maintain constant cerebral oxygen delivery ( $CDO_2$ ). Alternating vertical bars represent individual days at altitude. Data are labelled based on their corresponding study. 1: (Severinghaus *et al.*, 1966b), 2: (Huang *et al.*, 1987), 3: (Jensen *et al.*, 1990), 4: (Baumgartner *et al.*, 1994), 5: (Lucas *et al.*, 2011), 6: (Willie *et al.*, 2014a), 7: (Willie *et al.*, 2014a), 8: (Subudhi *et al.*, 2014b). From (Hoiland *et al.*, 2018a) with permission.

An important factor that has been largely ignored in the regulation of CBF at HA is changes in  $C_{aO_2}$  and blood viscosity (see section “cerebral blood flow and blood viscosity” for discussion of blood viscosity and CBF regulation). As outlined in **Figure 2.17**,  $C_{aO_2}$  is progressively increased after approximately the first week at HA due to ventilatory acclimatization, hemoconcentration and acid-base changes. Over the first few weeks at altitude HCT is increased by 10-15% (Lucas *et al.*, 2011) and therefore, due to the consequent elevation in  $C_{aO_2}$ , also tends to lower CBF. The magnitude by which HCT and  $PaO_2$  affect  $C_{aO_2}$ , and thereby would be expected to influence CBF at altitude is depicted in **Figure 2.18**. Experimental evidence from our group indicate that following 1 week at 5050m, hemoconcentration does indeed contribute to ~75% of the change (i.e. decrease) in CBF during acclimatization (Howe *et al.*, n.d.).

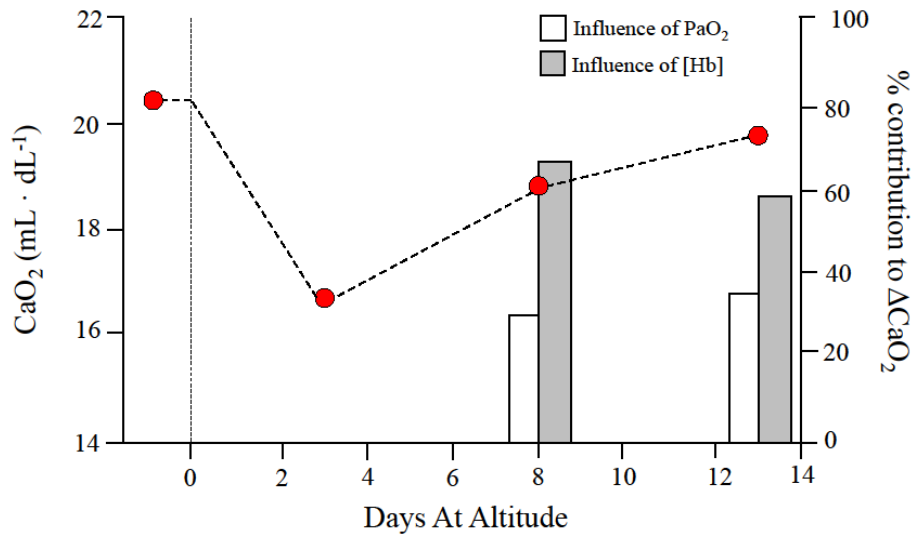


**Figure 2.18. Contribution of changes in partial pressure of oxygen and hemoglobin concentration in the increase in arterial oxygen content during acclimatization at high-altitude.**

Upon exposure to altitude, PaO<sub>2</sub> is reduced, thereby reducing SaO<sub>2</sub> and CaO<sub>2</sub>. Hyperventilation mitigates but does not alleviate this drop in PaO<sub>2</sub>. Ventilatory acclimatization to high-altitude contributes to progressive increases in V<sub>E</sub> and leads to elevations in PaO<sub>2</sub>, SaO<sub>2</sub>, and CaO<sub>2</sub>. Respiratory alkalosis induced diuresis leads to the early increase in [Hb], with erythropoiesis contributing to later increases in [Hb], both aiding in the increase of CaO<sub>2</sub> across acclimatization. The red dots denote CaO<sub>2</sub> across acclimatization, with the white and grey bars representing the influence of PaO<sub>2</sub> and [Hb] on CaO<sub>2</sub>, respectively. Given the linear relationship between CaO<sub>2</sub> and CBF, it is inferred that the % contribution of PaO<sub>2</sub> and [Hb] to CaO<sub>2</sub> during acclimatization possess the same % contribution to changes in CBF. Determined using data from (Lucas *et al.*, 2011). From (Hoiland *et al.*, 2018a) with permission.

Acute changes in blood viscosity may also affect endothelial functioning via changes in shear stress, and research has indeed shown that the cerebral vasculature exhibits a degree of autoregulation in response to both acute increases and decreases in plasma viscosity (Muizelaar *et al.*, 1986). The magnitude and direction of the change in viscosity may therefore affect the capacity of the blood vessel to respond to further changes in CaO<sub>2</sub>. Alternatively, in conditions where viscosity is *chronically* increased (e.g. chronic mountain sickness, sickle cell disease), endothelial functioning is often blunted as increases in shear stress are offset by secondary complications such as heightened SNA and systemic inflammation (Bailey *et al.*, 2013b). Irrespective of potential influences on endothelial

function, viscosity is likely to have little to no effect on CBF at altitude based on current evidence in humans (see section “cerebral blood flow and blood viscosity”).

Alterations in cerebral vascular reactivity to both O<sub>2</sub> and CO<sub>2</sub> may also be implicated in CBF regulation at HA (Lucas *et al.*, 2011). Both increases (Lucas *et al.*, 2011; Flück *et al.*, 2015) and no change (Rupp *et al.*, 2014; Willie *et al.*, 2015a) in hypocapnic cerebral vasoconstriction have been demonstrated upon ascent to and acclimatization at altitude. Therefore, given methodological (technical & logistical) differences between studies, physiological differences (e.g., acid-base balance) and the consequent inconsistency of results, it remains relatively unclear how altered hypocapnic vasoconstriction may contribute to the progressively reduced CBF throughout acclimatization. Relative to cerebral sensitivity to O<sub>2</sub>, one study to date has conducted repeated measures indicating that hypoxic cerebral vasodilation is increased at altitude (Jensen *et al.*, 1996), which is corroborated by more well-controlled laboratory studies (Poulin *et al.*, 2002). Yet, changes in hypoxic vasodilation with acclimatization have not been examined using volumetric measures of CBF, necessitating judicious interpretation of the currently available data. Nonetheless, the observed increase in hypoxic cerebral vasodilation may counteract the vasoconstrictor stimulus consequent to reduced PaCO<sub>2</sub> and underscore, in part, the net vasodilatory stimulus and maintained CDO<sub>2</sub> observed upon exposure to HA. Collectively, gCBF at altitude mirrors changes in CaO<sub>2</sub> and although PaCO<sub>2</sub>/pH is a very potent regulator of tone, following initial exposure to altitude, arterial pH is minimally altered (**Figure 2.19**). Therefore, it appears that a change in CaO<sub>2</sub>, in the absence of altered pH, is the primary factor governing the pattern by which gCBF changes following initial exposure to HA. Potential alterations in reactivity at altitude may further “fine tune” the observed changes in CBF.

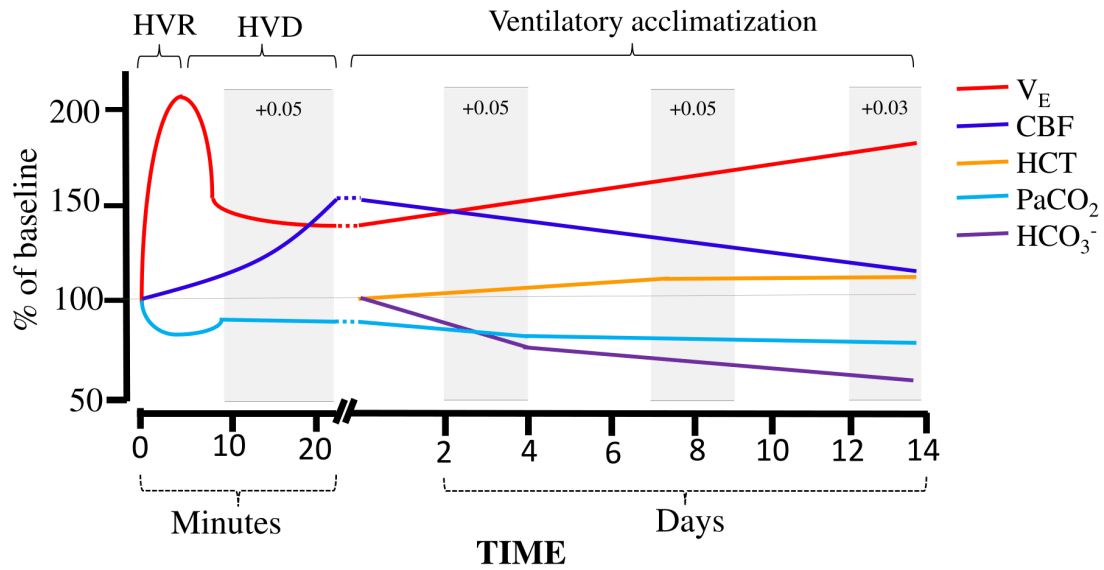


**Figure 2.19. Integrative physiological changes during acclimatization to very high-altitude (~5000m).**

Ascent to altitude stimulates a multitude of physiological adaptations. The immediate response to hypoxia involves a brisk increase in ventilation ( $V_E$ ) (red line) and cerebral blood flow (CBF) (dark blue line), with a concurrent drop in  $PaCO_2$  (light blue line). Hypoxic ventilatory decline ensues leading to a small attenuation of the drop in  $PaCO_2$ . Throughout acclimatization,  $V_E$  and CBF begin to progressively increase and decrease, respectively. Due to the respiratory alkalosis that follows the hypoxic ventilatory response, arterial and CSF pH (denoted by vertical grey bars) is increased; however, renal bicarbonate ( $HCO_3^-$ , purple line) excretion increases progressively leading to a stabilization of pH, and potential mitigation of respiratory alkalosis as acclimatization progresses. Finally, hematocrit (HCT) increases following ascent to altitude and throughout acclimatization. This figure represents general trends based on data from: (Lucas *et al.*, 2011; Ainslie *et al.*, 2013; Ryan *et al.*, 2014; Subudhi *et al.*, 2014a; Willie *et al.*, 2014a; Ainslie & Subudhi, 2014). Reproduced with permission from (Hoiland *et al.*, 2018a).

Although global changes in CBF have been shown to maintain  $CDO_2$  in hypobaric hypoxia throughout ascent and stay at HA, regional differences in the flow response to altitude have been demonstrated (Subudhi *et al.*, 2014b; Hoiland *et al.*, 2017b). These altitude studies, and those conducted in well controlled laboratory settings (Binks *et al.*, 2008; Subudhi *et al.*, 2014b; Hoiland *et al.*, 2017b; Lawley *et al.*, 2017) display preferential blood flow distribution to the posterior circulation, which perfuses brain regions such as the brainstem, hypothalamus, thalamus and cerebellum (Binks *et al.*, 2008). Despite no relationship between gCBF and AMS (Ainslie & Subudhi, 2014) and failure of globally maintained

CDO<sub>2</sub> to explain cognitive deficits in hypoxia, the aforementioned regionalization of CBF is suggested to be responsible for AMS (Feddersen *et al.*, 2015) as well as cognitive impairment (Lawley *et al.*, 2017) at altitude. However, given the number of inconsistent studies (Ainslie & Subudhi, 2014; Liu *et al.*, 2017), sufficient data is still lacking with regard to the intricacies of regionalized CBF regulation and its consequent impact(s). Nevertheless, regionally differential distribution of CBF likely occurs as a survival mechanism to prioritize delivery to the posterior areas of the brain responsible for controlling functional and homeostatic processes while consequently reducing delivery to areas responsible for higher cognitive function. Although this section intentionally focuses on CBF (i.e., inflow), it should be noted that a mismatch between cerebral inflow and venous outflow is critical in the pathophysiology of AMS (Wilson & Imray, 2016) and potentially cerebral edema (Sagoo *et al.*, 2016). In the latter landmark study, it was reported that CDO<sub>2</sub> was maintained via increased arterial inflow (i.e., CBF) and this preceded the development of cerebral edema thus implicating venous outflow restriction as a key mechanism (Sagoo *et al.*, 2016).

Technological advancements in imaging modalities have greatly improved the quantification of CBF (e.g., MRI), yet difficulties persist with regards to the portability and feasibility of such equipment during HA studies. As such, transcranial Doppler and portable duplex ultrasound devices remain standard tools for assessment of CBF during HA expeditions. Although the latter approach can be quite accurate and effective (Willie *et al.*, 2014a; Thomas *et al.*, 2015; Hoiland *et al.*, 2017b), the former fails to provide a complete assessment of CBF (Kellawan *et al.*, 2016; Sagoo *et al.*, 2016). Thus, changes in flow as reported through changes in blood velocity using transcranial Doppler ultrasound measurements should be interpreted cautiously in hypoxic environments. This discrepancy between imaging techniques largely underlies the methodological differences that make comparing HA studies difficult.

#### **2.4.1.3 CHRONIC ADAPTATION TO HIGH-ALTITUDE:**

Although hypoxia is a major physiological stress, several human populations have survived for millennia at HA, suggesting they have adapted to hypoxic conditions. Three primary patterns of human adaptation to HA hypoxia have been documented (Beall, 2006): Andean

(i.e., erythrocytosis with arterial hypoxemia) (Beall, 2007); Tibetan (i.e., marginally elevated venous hemoglobin concentration with arterial hypoxemia) (Beall, 2006); and the recently identified Ethiopian - Amhara highlanders living at ~3500m - pattern (i.e., normal venous hemoglobin concentration and arterial oxygen saturation within the normal range of sea level populations (Beall, 2006). Of note, the Amhara pattern of adaptation exhibits higher O<sub>2</sub> saturation and less erythrocytosis than their Omotic Ethiopian counterparts (Simonson, 2015).

Early studies have reported that native Andeans living at HA (~4200m) have 20% lower CBF values compared to sea-level natives [reviewed in: (Ainslie & Subudhi, 2014)]. The main mechanism underpinning the ~20% lower CBF of HA residents is the reported elevation in HCT and consequently increased CaO<sub>2</sub>. These conclusions are largely based on the inverse relationship between CaO<sub>2</sub> and CBF that has been demonstrated at rest and with carbon monoxide exposure or hemodilution (Paulson *et al.*, 1973; Brown *et al.*, 1985) (see section “Arterial oxygen content and cerebral blood flow: hypoxemic hypoxia versus hemodilution”). The lower CBF in HA residents may also be attributed to the passive changes in blood viscosity associated with increased HCT (Milledge & Sorensen, 1972) and active cerebral vasoconstriction (Rebel *et al.*, 2001, 2003), although as previously mentioned the likelihood of this playing a significant role is very small. The cerebral arterio-venous oxygen content difference is approximately proportional to the HCT level in HA natives (Milledge & Sorensen, 1972), but this may simply represent the relationship between flow (inferred from oxygen extraction) and CaO<sub>2</sub> (inferred from HCT). However, via theoretical corrections in CBF for the elevations in HCT, it was calculated by Jansen & Basnyat that CBF is still ~5% lower in HA Andean natives (Jansen & Basnyat, 2011). The mechanism underlying this as of yet experimentally demonstrated, and thus completely speculative difference has yet to be resolved. Nevertheless, it appears, at least at sea level, that blood viscosity does not affect CBF and that the observed reductions are simply due to the corresponding elevation in CaO<sub>2</sub> (see section “Arterial oxygen content and cerebral blood flow: hypoxemic hypoxia versus hemodilution”). Therefore, increased CaO<sub>2</sub> is likely the primary factor governing the reduction in CBF noted in HA natives.

Although CBF in Tibetan HA residents at ~4200m seems 5-10% lower than lowlanders, these data are limited and based on blood velocity indices of the middle cerebral artery

(MCA) (Jansen *et al.*, 1999, 2000, 2007). Jansen and Basnyat 2011 (Jansen & Basnyat, 2011) contended that velocities in the ICA and MCA were 11.7% and 3.4% (mean 6.2%) higher, respectively, compared to lowlanders, yet still within the range of expected variation at sea level reported by others (Scheel *et al.*, 2000a, 2000b). Also, HCT and CaO<sub>2</sub> in Tibetan (Sherpa) HA residents (Winslow *et al.*, 1989) is slightly increased compared to sea-level (by roughly 10%) but comparable to well-acclimatized lowlanders (Rahn & Otis, 1949; Fan *et al.*, 2010a; Lucas *et al.*, 2011; Foster *et al.*, 2014). Despite the need for experimental evidence, an increased NO bioavailability in Himalayans has been speculated to explain differences in CBF between Tibetan and Andean populations (Droma *et al.*, 2006; Beall *et al.*, 2012). Likewise, although the cerebral circulation of Ethiopian HA dwellers seems to be insensitive to hypoxia and may represent a positive adaptation (unlike Andean HA dwellers), this is also solely based on MCA velocity (Claydon *et al.*, 2008). Since the MCA has been demonstrated to dilate in hypoxia (Wilson *et al.*, 2011; Imray *et al.*, 2014; Willie *et al.*, 2014a), past indices of CBF at altitude based on MCA velocity need to be interpreted with caution. Investigation of cerebral vascular regulation in Tibetan descendant – the Sherpa – forms the basis of the third experimental chapter of this thesis (see section “Chapter 4: UBC-nepal expedition: reduced cerebral blood flow and oxygen delivery in Sherpa compared to lowlanders upon ascent to high-altitude”).

#### **2.4.2 ARTERIAL OXYGEN CONTENT AND CEREBRAL BLOOD FLOW: HYPOXEMIC HYPOXIA VERSUS HEMODILUTION**

As has been well established thus far, the magnitude of the CBF response is proportional to the severity of hypoxic stimuli and is appropriate to maintain CDO<sub>2</sub> and hence offset the hypoxemic hypoxia-induced reductions in CaO<sub>2</sub> (Severinghaus *et al.*, 1966a; Ainslie & Poulin, 2004; Ainslie & Ogoh, 2010; Willie *et al.*, 2012, 2014c; Ainslie *et al.*, 2014; Ainslie & Subudhi, 2014). However, an important prevailing question in human cerebrovascular physiology is whether the primary regulator of CBF is the total amount of O<sub>2</sub> (i.e., CaO<sub>2</sub>) or the O<sub>2</sub> dissolved in plasma (i.e., PaO<sub>2</sub>). The amount of oxygen bound to hemoglobin and PaO<sub>2</sub> determine CaO<sub>2</sub>, as per **Equation 2.9**.

Although PaO<sub>2</sub> (dissolved O<sub>2</sub>) only minimally contributes to the total CaO<sub>2</sub> when breathing room air, because it facilitates diffusion of oxygen into the cell, PaO<sub>2</sub> is often presumed to

be the cerebral vascular stimulus. Yet, as previously discussed, CBF does not decrease until a PaO<sub>2</sub> of ~50-60mmHg, the point whereby the reduction in CaO<sub>2</sub> (and SaO<sub>2</sub>) accelerates with further decreases in PaO<sub>2</sub> (**Figure 2.14**). Reductions in CaO<sub>2</sub> with maintained PaO<sub>2</sub> resulting from either carbon monoxide exposure (Paulson *et al.*, 1973), acute or chronic anemia (Brown *et al.*, 1985; Hare, 2004), and hemodilution (Paulson *et al.*, 1973), all increase CBF. Moreover, CBF varies inversely with HCT in many species in both acute (e.g., acute anemia) and chronic experimental conditions (e.g., erythropoiesis / polycythemia). While all three of these experimental paradigms (anemia, hemodilution, & carbon monoxide exposure) highlight the coupling of CBF to CaO<sub>2</sub>, it is important to consider their biological differences. For example, carbon monoxide is a cerebral vasodilator independent of inhibiting the formation of oxyhemoglobin (Leffler *et al.*, 2006), and elicits a greater increase in CBF for a given reduction in CaO<sub>2</sub> than hemodilution (Paulson *et al.*, 1973). Therefore, comparing the differences in vasodilation mediated by hypoxemic hypoxia (i.e., ↓PaO<sub>2</sub>) and isovolumic hemodilution (simulated acute anemic hypoxia) represents a more robust model, than using carbon monoxide. As the underlying mechanism(s) remain largely theoretical, it has been speculated that; (1) the hemorheologic consequences of reductions in blood viscosity (which is derived from plasma viscosity, HCT, and mechanical properties of red blood cells) mediate the increases in CBF noted during hemodilution [e.g., (Thomas *et al.*, 1977a, 1977b)] – although this is unlikely; and (2) reductions in CaO<sub>2</sub> elicit vasodilatory responses in order to maintain CDO<sub>2</sub> [e.g., (Brown & Marshall, 1985; Brown *et al.*, 1985)].

The majority of animal studies have indicated that viscosity is an important regulator of CBF during hemodilution (Hudak *et al.*, 1986; Korosue & Heros, 1992; Tomiyama *et al.*, 1999b); however, this is not a universal finding (Waschke *et al.*, 1994). Moreover, studies in humans provide evidence against an appreciable role of viscosity. Indeed, despite the initial few human studies supporting that viscosity is a primary regulator of CBF during changes in HCT (Thomas *et al.*, 1977b; Humphrey *et al.*, 1979, 1980b; Grotta *et al.*, 1982), the potential implications of changes in CaO<sub>2</sub>, and its consequent effects on CDO<sub>2</sub> were ignored. To partition the influence of blood viscosity independently of HCT and CaO<sub>2</sub>, Humphrey *et al.*, (Humphrey *et al.*, 1980a) investigated the difference in CBF between paraproteinemic (patients with high plasma protein concentration and elevated plasma viscosity) and non-paraproteinemic patients (Humphrey *et al.*, 1980a). However, both HCT

and PaCO<sub>2</sub> differed between groups. If the average CBF difference between paraproteinemic and non-paraproteinemic groups are corrected for the differences in HCT (assumed to be indicative of differences in CaO<sub>2</sub>), and PaCO<sub>2</sub> [using the linear slope presented in **Figure 2.20** and the known ~7% increase in volumetric CBF per mmHg change in PaCO<sub>2</sub> above eupneic levels (Kety & Schmidt, 1948c; Willie *et al.*, 2012), respectively], the observed difference in CBF is abolished. The limitations of this study were addressed in a later study by Brown & Marshall in 1985 (Brown & Marshall, 1985); here, changes in viscosity failed to alter CBF when CaO<sub>2</sub> and PaCO<sub>2</sub> remained constant. In turn, the authors suggested that independently viscosity is an insignificant factor in CBF regulation after accounting for changes in CaO<sub>2</sub> (Brown *et al.*, 1985). This finding has been replicated in other clinical populations possessing intact cerebrovascular function and normal HCT during isovolumic conditions (Brown & Marshall, 1982) as well as during hemodilution mediated hypoxia in animals using high and low viscosity replacement fluids (Waschke *et al.*, 1994). Therefore, it seems the impact of viscosity may be negligible in the hypoxic brain at rest, and relative to hypoxic CBF reactivity where the vascular bed becomes vasodilated. Nevertheless, theoretically, Poiseuille's Law demonstrates that changes in viscosity will have pronounced effects on flow, as per **Equation 2.3** .

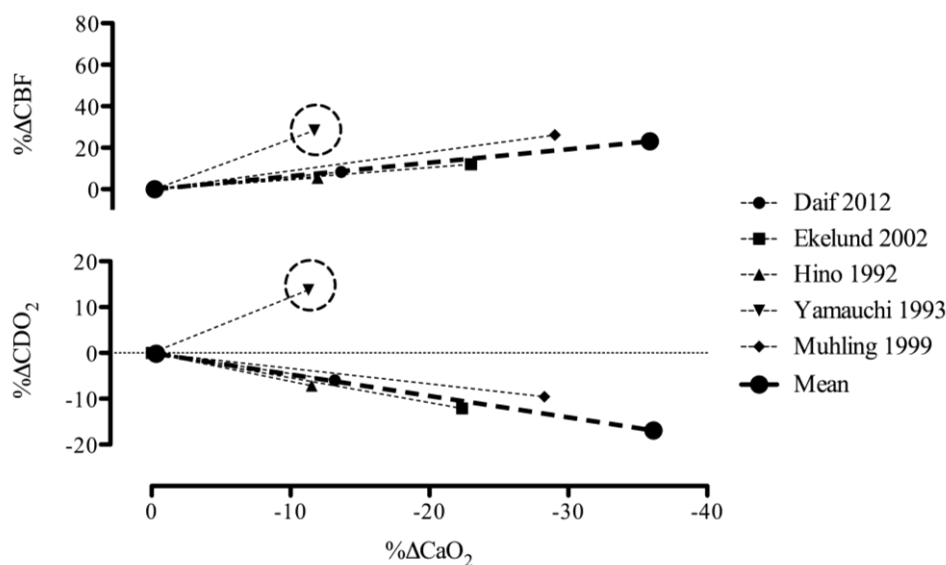


**Figure 2.20. Cerebral blood flow and oxygen delivery during hemodilution in humans.**

Data taken from five studies utilizing hemodilution and concurrent measures of CBF and arterial blood gases. The subject samples include 20 anesthetized tumor resection patients prior to surgery (filled circle) (Daif *et al.*, 2012), eight patients with vasospasm following aneurysmal subarachnoid hemorrhage (filled square) (Ekelund *et al.*, 2002), eight young healthy volunteers (upwards triangle) (Hino *et al.*, 1992), five patients with unilateral internal carotid artery occlusion in addition to previous stroke or transient ischemic attacks (downwards triangle) (Yamauchi *et al.*, 1993), and 11 healthy young volunteers (filled diamond) (Mühling *et al.*, 1999), totally 47 subjects. As all of the data collected in clinical patients, except for that of (Yamauchi *et al.*, 1993) (circled data point), followed the same trend as the studies using healthy patients, the data from (Yamauchi *et al.*, 1993) has been excluded from our representation of mean data. Indeed, the unilateral internal carotid artery occlusion would have influenced CBF regulation and in turn likely explains the larger increase in CBF (on the patent side). The mean lines for both the CBF and CDO<sub>2</sub> graphs have been calculated as the linear slope from the mean data of each study weighted for sample size. Reproduced from (Hoiland *et al.*, 2016a), permission not required.

Indeed, according to Poiseuille's Law, viscosity is directly and inversely related to flow. The disparity between physiological conditions (turbulent flow and non-Newtonian fluid) and those that define Poiseuille's Law likely explain the negative findings regarding an effect of viscosity on CBF during hemodilution, and hypoxia in humans (Brown *et al.*, 1985). Moreover, if viscosity was the primary factor regulating CBF during hemodilution, one might expect that blood flow to all organs would increase to the same magnitude. The greater blood flow increase to the cerebral circulation relative to other organs indicates a

selective active regulation (van Bommel *et al.*, 2002), which is further supported by data demonstrating increased cerebral blood volume during hemodilution – interpreted to indicate increased vascular cross-sectional area due to vasodilation (Todd *et al.*, 1992). Collectively, analysis of 20 studies shows that  $\text{CaO}_2$  is inversely related to CBF (**Figure 2.21**).

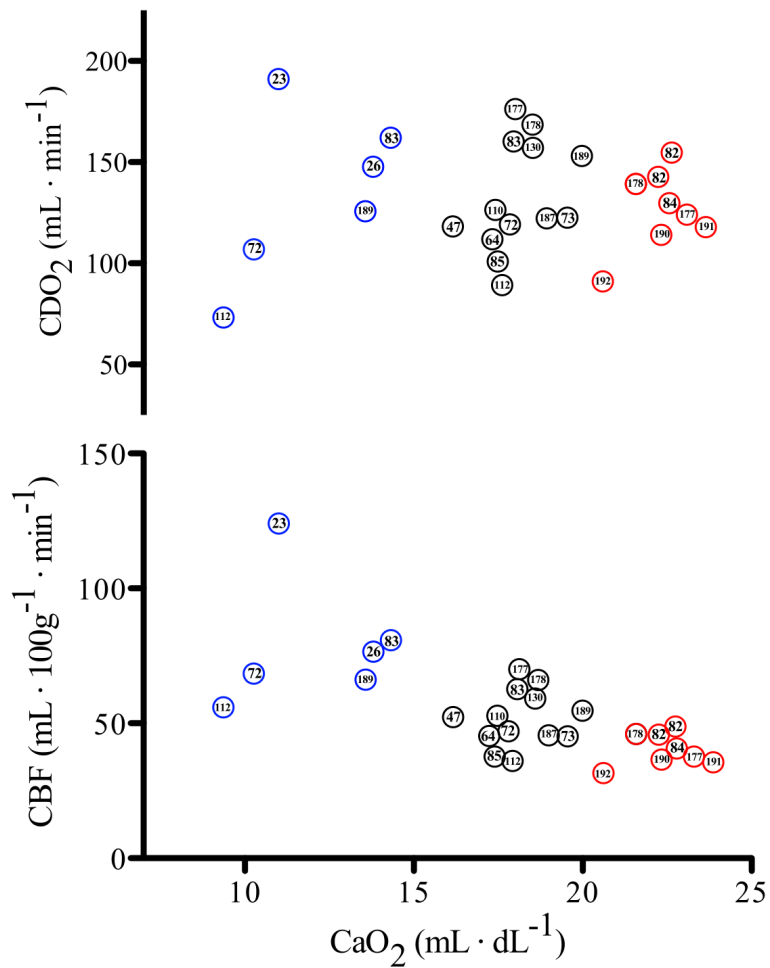


**Figure 2.21. The relationship between arterial oxygen content, cerebral Blood flow, and cerebral oxygen delivery in anemic, hematologically normal, and polycythemic humans.**

Data were collated from 20 separate studies to highlight the relationship between CaO<sub>2</sub> and CBF. **A.** Across studies there appears to be a relatively linear inverse relationship between CaO<sub>2</sub> and CBF, with higher CaO<sub>2</sub> concomitant to a reduced CBF, and lower CaO<sub>2</sub> concomitant to increased CBF. **B.** Despite reductions in CaO<sub>2</sub>, the CBF increase is adequate to maintain CDO<sub>2</sub>. Across the presented studies there appears to be variability in CDO<sub>2</sub> at any given CaO<sub>2</sub>; however, there is no distinct relationship between changes in CaO<sub>2</sub> and CDO<sub>2</sub>. Thus, it seems that CDO<sub>2</sub> is preserved in anemic hypoxia, and maintains a normal level during polycythemia due to a reduced CBF. Data are collated from (Heyman *et al.*, 1952; Thomas *et al.*, 1977b, 1977a, Humphrey *et al.*, 1979, 1980a, 1980b, Wade *et al.*, 1980, 1981; Grotta *et al.*, 1982; Wade, 1983; Brown & Marshall, 1985; Korosue *et al.*, 1988; Brass *et al.*, 1991; Vorstrup *et al.*, 1992; Hino *et al.*, 1992; Tu & Liu, 1996; Mühling *et al.*, 1999; Kuwabara *et al.*, 2002; Ekelund *et al.*, 2002; Ibaraki *et al.*, 2010) with the number corresponding to the specific study as noted in (Hoiland *et al.*, 2016a). Reproduced from (Hoiland *et al.*, 2016a), permission not required.

The CBF response during hemodilution and hypoxemic hypoxia is tightly coupled to reductions in  $\text{CaO}_2$  for isovolumic hemodilution [e.g., (Hino *et al.*, 1992; Yamauchi *et al.*, 1993; Mühling *et al.*, 1999; Ekelund *et al.*, 2002; Daif *et al.*, 2012)]; and for hypoxemic hypoxia; see **Figure 2.15 & Figure 2.20** (Kety & Schmidt, 1948c; Cohen *et al.*, 1967; Willie *et al.*, 2012; Ainslie *et al.*, 2014). Thus, in both otherwise healthy individuals and those with pathology (e.g., polycythemia, paraproteinemic), with normal (Brown & Marshall, 1985) or high HCT (Humphrey *et al.*, 1980b), isovolumic hemodilution leads to an increase in CBF. The key point here though, is that the slope increase in CBF during isovolumic hemodilution is markedly (3-fold) reduced compared to during hypoxemic hypoxia (**Figure 2.22**). The mean slope increase in CBF during isovolumic hemodilution is  $0.66\% \text{CBF} \cdot -\% \text{CaO}_2^{-1}$ , whereas the mean slope increase in CBF during hypoxemic hypoxia is  $1.85\% \text{CBF} \cdot -\% \text{CaO}_2^{-1}$  (see **Figure 2.15 & Figure 2.20** legends for explanation of calculations). The blunted cerebrovascular response to hemodilution compared to hypoxemic hypoxia results in a lowered  $\text{CDO}_2$  (**Figure 2.22**). When assessing the long-term influence of  $\text{CaO}_2$  from altered hemoglobin mass in anemia and polycythemia, it is apparent that  $\text{CDO}_2$  is not impaired (**Figure 2.21**). Indeed, patients with anemia possess a relatively high CBF that maintains  $\text{CDO}_2$  despite reduced  $\text{CaO}_2$ , and the reduction in CBF that is typical of polycythemic patients is not large enough to reduce  $\text{CDO}_2$ , which appears to remain normal in these patients. This indicates compensation by via other signaling pathways during chronic changes in [Hb].

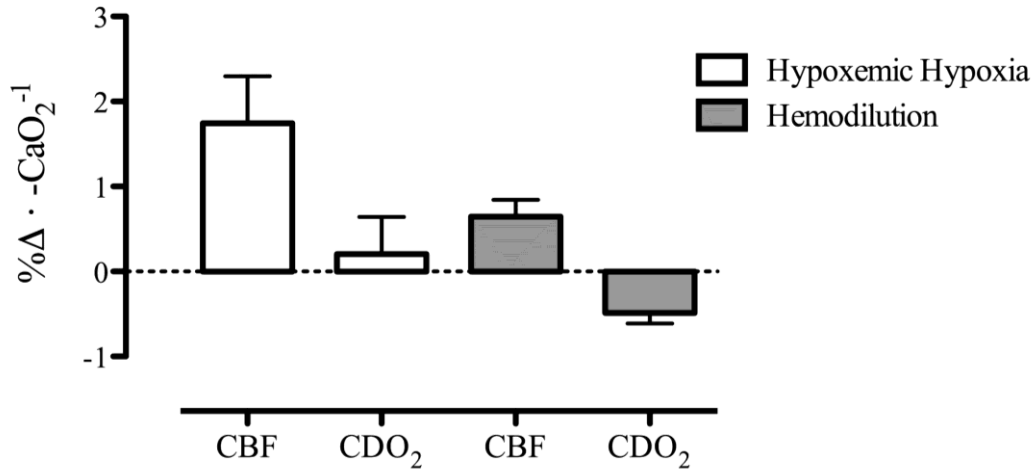


**Figure 2.22. Change in cerebral blood flow and oxygen delivery during reductions in arterial oxygen content induced by hypoxemic hypoxia and hemodilution.**

The mean slope increase in CBF is  $0.66\% \text{ CBF} \cdot -\% \text{ CaO}_2^{-1}$  during hemodilution and  $1.85\% \text{ CBF} \cdot -\% \text{ CaO}_2^{-1}$  during hypoxemic hypoxia. During hypoxemic hypoxia CDO<sub>2</sub> is maintained with a  $0.24\% \text{ CDO}_2 \cdot -\% \text{ CaO}_2^{-1}$  slope response, whereas during hemodilution, CDO<sub>2</sub> is compromised with a  $-0.47\% \text{ CDO}_2 \cdot -\% \text{ CaO}_2^{-1}$  slope decrease with reduced CaO<sub>2</sub>. Error bars represent standard deviation of the mean slopes from each study used in **Figure 2.15** and **Figure 2.20**. Reproduced from (Hoiland *et al.*, 2016a), permission not required.

In the study by Daif *et al.*, (Daif *et al.*, 2012) where jugular venous samples were collected, an approximate 10% reduction in CMRO<sub>2</sub> during hemodilution was estimated (Daif *et al.*, 2012). This is in contrast to the multiple studies assessing CMRO<sub>2</sub> during hypoxemic hypoxia, where a  $\leq 35\%$  reduction in CaO<sub>2</sub> does not result in an altered CMRO<sub>2</sub> (Kety & Schmidt, 1948c; Cohen *et al.*, 1967; Ainslie *et al.*, 2014). Whether the reduction in estimated CMRO<sub>2</sub> calculated by Daif *et al.*, (Daif *et al.*, 2012) is due to the impaired CDO<sub>2</sub> following hemodilution, or simply confounded by the concurrent anesthesia, is unknown (Oshima *et al.*, 2002). The remainder of human (Paulson *et al.*, 1973; Hino *et al.*, 1992), and animal (Todd *et al.*, 1994) data indicate that CMRO<sub>2</sub> remains unchanged during hemodilution despite a CaO<sub>2</sub> reduction of  $\leq 30\%$ , due to a compensatory increase in cerebral O<sub>2</sub> extraction (Hino *et al.*, 1992; Todd *et al.*, 1994).

While within subject manipulation of CaO<sub>2</sub> through various methods (e.g. hemodilution vs. hypoxemic hypoxia) to assess cerebral vascular regulation to hypoxia has yet to be done in

healthy human subjects, we speculate that the supposed differential response between hemodilution and hypoxemic hypoxia (that is, greater CBF increase with hypoxemic hypoxia compared to hemodilution) is due to the fundamental mechanisms governing hypoxic cerebral vasodilation.

### **2.4.3 SIGNALING PATHWAYS IN THE REGULATION OF CEREBRAL BLOOD FLOW DURING HYPOXIA**

Although the cerebrovascular responses to acute and chronic hypoxia during both normobaria and hypobaria have been well characterized in humans, there remains a paucity of data related to the cellular mechanisms that govern it. Ultimately, it seems that hemoglobin in the erythrocyte functions as the primary O<sub>2</sub> sensor and upstream response effector governing the regulation of vascular tone in hypoxia. Three principle mechanisms have been proposed for erythrocyte-dependent hypoxic vasodilation and include: 1) ATP release and subsequent activation of endothelial nitric oxide synthase (eNOS); 2) nitrite reduction to NO by deoxyhemoglobin, and 3) S-nitrosohemoglobin (SNO-Hb) mediated bioactivity, which are all dependent on transition of hemoglobin from the relaxed (R) state to tense (T) state. These processes have direct vasomotor effects and influence release and/or formation of specific signaling molecules that are integral to the vasodilatory response. Candidate mechanisms (see **Figure 2.23**) responsible for vasodilation downstream of deoxyhemoglobin include: NO, adenosine, PGs, and EETs.

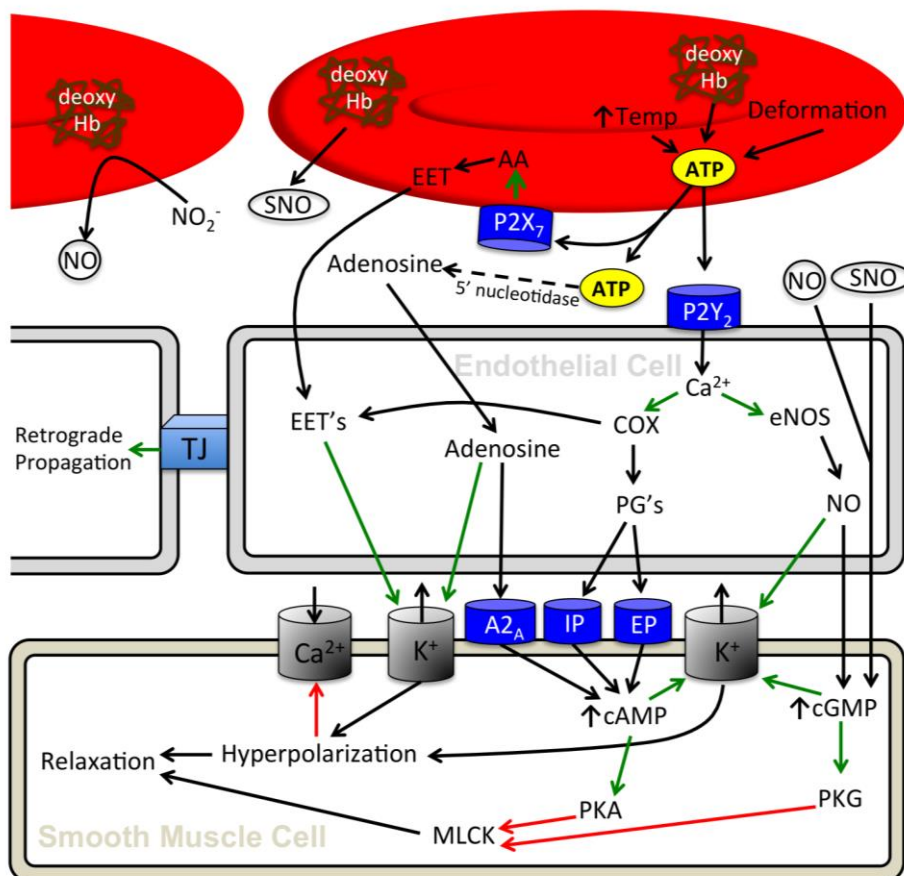


**Figure 2.23. Putative pathways regulating cerebral blood flow during hypoxia.**

Increased temperature, erythrocyte deformation, and the conformational change concomitant to transition of oxy- to deoxy-hemoglobin all signal erythrocyte mediated release of ATP (Bergfeld & Forrester, 1992; Ellsworth *et al.*, 1995; Sprague *et al.*, 1998; Kalsi & González-Alonso, 2012). Released ATP can then bind to the erythrocyte P2X<sub>7</sub> receptor in an autocrine fashion to induce erythrocyte mediated EET release (Jiang *et al.*, 2007), which will increase vascular smooth muscle cell K<sup>+</sup> channel conductance (Gebremedhin *et al.*, 1992). The released ATP also binds endothelial P2Y<sub>2</sub> receptors to initiate a signal cascade involving NO and potentially PGs (You *et al.*, 1997). Moreover, ATP will breakdown into AMP and subsequently adenosine (Fuentes & Palomo, 2015) that will also exert a vasodilatory effect on vascular smooth muscle through binding adenosine A<sub>2A</sub> receptors (Kalaria & Harik, 1988; Hein *et al.*, 2013), increasing cAMP levels (Sattin & Rall, 1970; Nordstrom *et al.*, 1977) and also through increasing inward rectify potassium channel conductance (Hein *et al.*, 2013). Prostaglandins, if implicated, bind IP and EP receptors (Davis *et al.*, 2004) which increases intracellular cAMP (Narumiya *et al.*, 1999). NO, derived from the endothelium, through the nitrite reductase activity of erythrocytes (Cosby *et al.*, 2003), and s-nitrosohemoglobin (Stamler *et al.*, 1997a; Lima *et al.*, 2010) will lead to increased guanylate cyclase activity and cGMP (Pearce *et al.*, 1990) as

well as directly increase K<sup>+</sup> channel conductance (Bolotina *et al.*, 1994). Cyclic nucleotides will upregulate cAMP dependent protein kinase (PKA) and cGMP dependent protein kinase (PKG) activity, which act to inhibit myosin light chain kinase (MLCK; 1), and therefore, reduce smooth muscle tone (Kerrick & Hoar, 1981). Cyclic nucleotides will also increase potassium channel conductance (Song & Simard, 1995), with increased potassium efflux hyperpolarizing cells and reducing activity of voltage gated Ca<sup>2+</sup> channels (Nelson *et al.*, 1990*b*). Overall, ATP leads to vasodilation that can be conducted through gap junctions (Dietrich *et al.*, 1996; Kajita *et al.*, 1996). Green arrows represent activation of a downstream factor, and red arrows represent inhibition of downstream factors. Reproduced from (Hoiland *et al.*, 2016*a*), permission not required.

The site of hemoglobin deoxygenation (R → T allosteric shift) is not exclusive to the capillaries as over 66% of blood oxygen may be removed in the upstream cerebral arterial circulation prior to reaching the capillaries (Duling & Berne, 1970; Tsai *et al.*, 2003). This highlights that erythrocyte release of ATP, SNO, and NO<sub>2</sub> reductase activity can mediate dilation throughout the cerebral arterial tree. Moreover, these signals can be propagated (Ellsworth *et al.*, 1995; Dietrich *et al.*, 1996, 2008; Kajita *et al.*, 1996), and therefore, likely impact further upstream resistance vessels that only see oxygenated blood. Indeed, hypoxemia has been shown to dilate the MCA (Wilson *et al.*, 2011; Imray *et al.*, 2013; Willie *et al.*, 2014*a*), ICA (Lewis *et al.*, 2014*b*), and VA (Lewis *et al.*, 2014*b*) in humans.

The following sections aim to outline the key concepts underlying erythrocyte mediated signaling. The S-nitrosohemoglobin pathway, nitrite reductase pathways, and erythrocyte released ATP pathway are considered. Following this, other downstream molecules and their contribution to hypoxic vasodilation are outlined. While mechanistic data is derived primarily from *ex vivo* or animal models, these studies form the basis of each topic; however, the relevance for human physiology, and consideration of human data, if available is noted.

### **2.4.3.1 DEOXYHEMOGLOBIN MEDIATED SIGNAL TRANSDUCTION PATHWAYS**

#### **2.4.3.1.1 S- NITROSOHEMOGLOBIN RELEASE FROM ERYTHROCYTES DURING HYPOXIA**

Transport to, and release of NO in the microvasculature is achieved in part through S-nitrosylation of hemoglobin. Formation of S-nitrosohemoglobin (SNO-Hb) in the lung

occurs due to covalent bonding of NO with the  $\beta$ -chain of hemoglobin on the  $\beta$ 93 cysteine residue (Cys  $\beta$ 93) (Jia *et al.*, 1996). S-nitrosylation of Hb to form S-nitrosohemoglobin occurs most effectively in the R-state and allows for transport of vasoactive NO to the cerebral vasculature, where s-nitrosothiols (RSNO) are released upon deoxygenation of hemoglobin and transition to the T-state (Stamler *et al.*, 1997a). When released, RSNOs provide the chemical stability required for NO to reach the endothelium as free NO would be scavenged too quickly to elicit vasodilation (Tsoukias, 2008). The presence of a negative arterial to jugular venous RSNO gradient indicates its transport and release in the rat brain (Jia *et al.*, 1996). Moreover, it seems that the oxygenation state of cerebral tissue PO<sub>2</sub> affects the vasodilatory influence of RSNO (Stamler *et al.*, 1997a), and regulates its role across physiological oxygen gradients.

#### 2.4.3.1.2 NITRITE REDUCTION VIA HEMOGLOBIN

As NO is quickly scavenged, NO<sub>2</sub> acts as a valuable storage pool of NO. There is accumulating evidence that its reduction by deoxyhemoglobin during hypoxia is an integral component of NO mediated vasodilation (Doyle *et al.*, 1981; Cosby *et al.*, 2003). The time course for NO<sub>2</sub> reduction by hemoglobin is in the order of seconds to minutes (Doyle *et al.*, 1981), and thus likely contributes primarily to steady state CBF versus that of the initial upslope upon hypoxic exposure. In humans, after nine hours of passive exposure to normobaric hypoxia, the arterial delivery of NO<sub>2</sub> to the brain was reduced indicating that it was either reduced by deoxyhemoglobin to increase circulating NO, reappportioned towards erythrocyte bound species that also display bioactivity (NO<sub>2</sub>, Hb-SNO, or HbNO), and/or in part scavenged by oxidizing free radical species (Bailey *et al.*, 2009b). Similar responses have been observed in extreme apnea (Bain *et al.*, 2017b), but given how little data exists on this mechanism in intact humans, its involvement remains equivocal. Of note, circulating nitrite anions may also participate in direct vasodilation (Demoncheaux *et al.*, 2002). However the specific role of direct cerebral vasodilation from circulating nitrite in hypoxia remains undetermined.

#### 2.4.3.1.3 ADENOSINE TRIPHOSPHATE LIBERATION FROM ERYTHROCYTES DURING HYPOXIA

Hypoxia induces ATP release from the erythrocyte (Bergfeld & Forrester, 1992; Ellsworth *et al.*, 1995, 2009). In isolated single cerebral arterioles, reduction of tissue PO<sub>2</sub> in the presence of erythrocytes results in both vessel dilation and marked increases in effluent [ATP]; however, hypoxia without the presence of erythrocytes possesses no dilatory effect, while effluent [ATP] remains unchanged (Dietrich *et al.*, 2000). The importance of deoxyhemoglobin in this response is further highlighted in that the presence of oxyhemoglobin in isolated rat penetrating arterioles significantly inhibits both dilation to low dose [ATP] in a tissue bath, and the propagated dilation to intraluminally applied ATP (Kajita *et al.*, 1996). Moreover, hypoxia induced via carbon monoxide inhalation, which precludes the conformational change associated with offloading O<sub>2</sub>, does not change ATP levels (Jagger *et al.*, 2001). Yet, data assessing cerebral efflux of ATP during hypoxia are scarce, and collectively difficult to interpret.

#### **2.4.3.2 DOWNSTREAM SIGNALING MOLECULES**

##### 2.4.3.2.1 HYPOXIA AND ADENOSINE TRI-PHOSPHATE

ATP is a potent cerebral vasodilator. Intraluminal ATP dilates the MCA of rats *in vitro* (You *et al.*, 1997, 1999; Horiuchi *et al.*, 2001; Crossland *et al.*, 2013), while *in vivo* intra-carotid infusion of ATP increases pial vessel diameter in cats and global CBF in baboons (Forrester *et al.*, 1979). This ATP mediated dilation is endothelium dependent (You *et al.*, 1997, 1999) through binding of P2Y<sub>2</sub> purinoceptors (Martin *et al.*, 1985; Dietrich *et al.*, 2008), is capable of retrograde propagation (Dietrich *et al.*, 1996; Kajita *et al.*, 1996), and acts through initiating downstream signal cascades. The candidate downstream signals responsible for ATP mediated changes in vascular tone include NO (You *et al.*, 1997), adenosine (Fuentes & Palomo, 2015), EETs (Jiang *et al.*, 2007; Dietrich *et al.*, 2008), and PGs (McCalden *et al.*, 1984; Leffler & Parfenova, 1997). Collectively, these vasoactive factors increase K<sup>+</sup> channel conductance (Ikeuchi & Nishizaki, 1995; Horiuchi *et al.*, 2003), hyperpolarize the vascular smooth muscle (Kajita *et al.*, 1996; You *et al.*, 1999; Dietrich *et al.*, 2008), and/or decrease smooth muscle cell calcium sensitivity (Adelstein *et al.*, 1978; Kerrick & Hoar, 1981). Evidence for an important role of these factors downstream of ATP

binding to endothelial P2Y<sub>2</sub> receptors, which we propose as one of the initial steps mediating the CBF response to hypoxia (see section “Adenosine triphosphate liberation from erythrocytes during hypoxia”) is discussed, with particular focus on data in humans.

#### 2.4.3.2.2 HYPOXIA AND ADENOSINE

Extravascular adenosine application leads to *in vitro* dilation of animal (Dietrich *et al.*, 1996) and human (Toda, 1974*b*) cerebral vessels and *in vivo* (Berne *et al.*, 1974; Wahl & Kuschinsky, 1976; Morii *et al.*, 1987*a*) dilation of animal cerebral vessels. This dilatory response is capable of retrograde propagation (Kajita *et al.*, 1996) and is mediated in part through increases in NO, inward rectifying potassium channel conductance (Hein *et al.*, 2013), and increased cAMP levels (Sattin & Rall, 1970; Nordstrom *et al.*, 1977).

Hypoxia leads to an increase in the endogenous cerebral production of adenosine (Berne *et al.*, 1974; Winn *et al.*, 1979, 1981*b*; Phillis *et al.*, 1993). Production of adenosine in cerebral tissue is vital as negligible amounts of adenosine are thought to cross the blood brain barrier and thus intravascular adenosine likely plays a limited role in CBF regulation during hypoxia (Berne *et al.*, 1974). Administration of adenosine receptor antagonists (e.g., theophylline) abolishes the CBF increase to moderate hypoxia (i.e., PaO<sub>2</sub> = 40-50 mmHg) and all but one study in animals, albeit CBF was still moderately reduced (Pinard *et al.*, 1989), indicate a reduced CBF increase to severe hypoxia (i.e., PaO<sub>2</sub> = 20-30 mmHg) by ~50% (Emerson & Raymond, 1981; Hoffman *et al.*, 1984*a*; Morii *et al.*, 1987*a*). This effect of attenuating CBF during hypoxia by adenosine receptor antagonism is reflected in reductions of pial arteriolar dilation to hypoxia subsequent to administration of adenosine deaminase (Armstead, 1997) and theophylline (Pelligrino *et al.*, 1995*a*; Armstead, 1997). However, this latter finding is not universal (Haller & Kuschinsky, 1987) and may depend on the severity of hypoxia. Adenosine A<sub>2A</sub> receptor knock out mice possess a markedly attenuated CBF response to acute hypoxia (Miekisiak *et al.*, 2008), while A<sub>2B</sub> receptor antagonism has no effect on CBF, highlighting the predominant role of A<sub>2A</sub> receptors in mediating hypoxic vasodilation by adenosine (Liu *et al.*, 2015). Adenosine mediated regulation of CBF in humans is also likely mediated by A<sub>2</sub> receptors (Kalaria & Harik, 1988); however, a distinction between A<sub>2A</sub> and A<sub>2B</sub> receptors in mediating this response is still vague.

In keeping with animal data, aminophylline – an adenosine receptor antagonist – reduces CBF both at rest (Wechsler *et al.*, 1950; Gottstein & Paulson, 1972; Magnussen & Hoedt-Rasmussen, 1977) and during hypoxia in humans; however, the slope of the CBF response to hypoxia does not seem to differ pre and post aminophylline infusion (Bowton *et al.*, 1988; Nishimura *et al.*, 1993). This would suggest there is no effect of adenosine on the cerebrovascular response to hypoxia in humans, yet the methodological limitations of the xenon-133 technique (Obrist *et al.*, 1975) used by Bowton *et al.*, 1988 and indirect quantification of CBF by Nishimura *et al.*, 1993 precludes a definitive conclusion. In summary, it remains possible, yet unconfirmed in humans, that adenosine contributes to the hypoxic cerebrovascular response.

#### 2.4.3.2.3 HYPOXIA AND NITRIC OXIDE

The potent vasodilatory and cardiovascular properties of NO are well documented (Bohlen, 2015), and likely extend into hypoxic CBF regulation. Increased NO levels induce vasodilation through increases in cGMP (Pearce *et al.*, 1990) and directly mediated increases in K<sup>+</sup> channel conductance (Bolotina *et al.*, 1994). Notionally, hypoxia increases neuronal nitric oxide synthase activity (nNOS) (Hudetz *et al.*, 1998; Santizo *et al.*, 2000; Bauser-Heaton & Bohlen, 2007), releases NO from NO<sub>2</sub> (Cosby *et al.*, 2003) and SNO-Hb (Lima *et al.*, 2010) (discussed in previous sections), and leads to endothelial NO release downstream of ATP signaling (You *et al.*, 1997). In turn, NO is consistently involved with *in vivo* and *in vitro* animal cerebral hypoxic vasodilation (Pearce *et al.*, 1989; Koźniewska *et al.*, 1992; Pelligrino *et al.*, 1995a; Takuwa *et al.*, 2010). In awake humans, intravenous infusion of N<sup>G</sup>-monomethyl-L-arginine (L-NMMA), a NOS inhibitor, reduces the hypoxic CBF response, as assessed via MRI (Van Mil *et al.*, 2002a). In contrast, Ide *et al.*, 2007 (Ide *et al.*, 2007) reported that NOS inhibition with L-NMMA does not influence the CBF response to acute hypoxia, as assessed by MCA velocity measures. The latter finding, however, is confounded by recent MRI and ultrasound evidence demonstrating that the MCA dilates in normobaric hypoxia (Wilson *et al.*, 2011; Imray *et al.*, 2014). As previously highlighted in **Equation 2.3**, even the slightest changes in MCA diameter will have a profound effect on flow, due to their exponential relationship. Increases in shear stress via increased velocity through cerebral vessels during hypoxia likely provide an additional

stimulus to upregulate endothelial NOS (Dimmeler *et al.*, 1999) and modulate NO signaling (see section Appendix A). Experiments implementing pharmacological blockade of NOS (e.g., via L-NMMA) do not however provide a complete indication of the vasoactive influence of NO from Hb-SNO and NO<sub>2</sub> reduction, which retain some bioavailability. Indeed, data in rabbits (Stamler *et al.*, 1992) and rats (Jia *et al.*, 1996) indicate that L-NMMA infusion reduces circulating RSNOs by ~80%. The relevance of this remaining 20% of RSNOs to hypoxic vasodilation in NOS blockade studies is not clear.

#### 2.4.3.2.4 HYPOXIA AND PROSTAGLANDINS

Indomethacin, a non-steroidal anti-inflammatory drug that non-selectively and reversibly inhibits cyclooxygenase (COX) activity, and consequently PG synthesis, has no effect on the CBF response to severe hypoxia (PaO<sub>2</sub> = 25mmHg) *in vivo* in rats (Sakabe & Siesjö, 1979) and newborn pigs (Coyle *et al.*, 1993; Leffler & Parfenova, 1997), despite abolishing hypoxic dilation *in vitro* (Fredricks *et al.*, 1994). Further evidence highlights that PGs are not one of the endothelium derived hyperpolarizing factors released downstream of ATP binding P2Y<sub>2</sub> receptors (Horiuchi *et al.*, 2003; Dietrich *et al.*, 2008). However, hypoxia increases cerebral 6-keto-PGF<sub>1α</sub> (a stable prostacyclin metabolite), which is indicative of increased PG production (McCalden *et al.*, 1984; Leffler & Parfenova, 1997).

In humans, one study (Hoiland *et al.*, 2015), but not all (Fan *et al.*, 2011; Harrell & Schrage, 2014) report that indomethacin reduces MCA velocity reactivity to hypoxia. However, volumetric flow reactivity of the ICA during hypoxia is unaffected (Hoiland *et al.*, 2015). In contrast, hypoxic reactivity seems to be reduced in the posterior circulation, assessed by Q<sub>VA</sub>, following COX inhibition with indomethacin (Hoiland *et al.*, 2015). While these data indicate that COX may be selectively mediating hypoxic dilation in the posterior cerebral circulation, they are not conclusive. For example, indomethacin selectively reduces cerebral reactivity to hypercapnia (elevated arterial CO<sub>2</sub>) whereas other COX inhibitors such as Aspirin and Naproxen have no effect (Eriksson *et al.*, 1983; Markus *et al.*, 1994). These findings suggest indomethacin may influence CBF responses via a PG independent mechanism. Indeed, indomethacin inhibits cAMP dependent protein kinase activity (Kantor & Hampton, 1978; Goueli & Ahmed, 1980), which will directly impact smooth muscle tone (Adelstein *et al.*, 1978; Kerrick & Hoar, 1981) (see section “Cerebral blood

flow and Cellular Regulation of Vascular Smooth Muscle Tone”). More work is required to establish a role (if any) of PGs in the cerebral hypoxic vasodilatory response in humans.

#### 2.4.3.2.5 HYPOXIA AND EPOXYEICOSATRIENOIC ACIDS

Epoxyeicosatrienoic acids dilate cerebral blood vessels (Gebremedhin *et al.*, 1992) and are released from erythrocytes both spontaneously (Jiang *et al.*, 2005) and by ATP binding of P2X<sub>7</sub> receptors (Jiang *et al.*, 2007). Notably, this ATP binding also inhibits erythrocyte release of the vasoconstrictor 20-hydroxyeicosatrienoic acid (Jiang *et al.*, 2007, 2010). During hypoxia, both inhibition of EET synthesis and EET antagonism markedly reduces the CBF response to hypoxia in rats (Liu *et al.*, 2015) and newborn pigs (Leffler *et al.*, 1997). While EETs may represent an endothelium derived hyperpolarizing factor that is a relevant regulator of CBF during hypoxia, this has not been verified in humans.

#### 2.4.4 SYNOPSIS OF CEREBRAL BLOOD FLOW REGULATION IN HYPOXIA

During hypoxemic hypoxia at both sea-level and HA in healthy humans, elevations in CBF are intimately matched to reductions in CaO<sub>2</sub> in order to maintain CDO<sub>2</sub>. Studies employing hemodilution, and those of patients with anemia and polycythemia, support the notion that CaO<sub>2</sub> has an independent influence on CBF; yet, in the majority of cases when CaO<sub>2</sub> is reduced by hemodilution, CDO<sub>2</sub> is compromised. The mechanisms regulating CBF during changes in CaO<sub>2</sub> are multifactorial but primarily triggered by deoxygenation of hemoglobin (R → T allosteric shift) and consequent erythrocyte release of ATP and SNO, and deoxyhemoglobin nitrite reductase activity. Downstream of this initial process, additional chemical mediators include adenosine, nitric oxide, and epoxyeicosatrienoic acids. The relatively lower CBF increase with hemodilution compared to hypoxemic hypoxia (due to ↓[Hb] and higher jugular venous O<sub>2</sub> saturation) provides strong evidence for the role of deoxyhemoglobin as the primary regulator of CBF in hypoxia. Although studies to date support the role of CaO<sub>2</sub> as a biological regulator of CBF, due to the dependence of key regulatory mechanisms on the oxygenation state of hemoglobin, maintenance of O<sub>2</sub> delivery via CBF is better established during hypoxemic hypoxia, compared to hemodilution.

## 2.5 REGULATION OF CEREBRAL BLOOD FLOW BY CARBON DIOXIDE

While this thesis is focused on CBF regulation in instances of altered  $\text{CaO}_2$ , in a free-living scenario,  $\text{CaO}_2$  and  $\text{PaCO}_2$  often change simultaneously. Therefore, cerebrovascular regulation by  $\text{PaCO}_2$  is important to properly understand the cerebrovascular response to hypoxia and will be reviewed hereafter.

During wakefulness in otherwise healthy and normoxic humans,  $\text{PaCO}_2$  is the most potent regulator of cerebrovascular tone. The cerebral vascular response to  $\text{CO}_2$  is characterized as the unit (i.e., mL/min), or percent, change in CBF per unit change in either the partial pressure of end-tidal  $\text{CO}_2$  ( $\text{P}_{\text{ETCO}_2}$ ) or  $\text{PaCO}_2$ . When discussing the vasomotor action of  $\text{PaCO}_2$ , two important factors require consideration: 1) in a general sense, how is  $\text{CO}_2$  eliciting its effect? 2) What is the site(s) of action/sensitivity for  $\text{CO}_2$ ?

Changes in  $\text{PCO}_2$  mediate alterations in CBF locally via changes in perivascular pH (Wahl *et al.*, 1970; Betz *et al.*, 1973; Kontos *et al.*, 1977b; Liu *et al.*, 2012b), evidenced experimentally by the vascular reactions to acidic and alkaline superfusates delivered with the cranial window technique. Acidic hypercapnic and acidic isocapnic superfusates lead to a similar magnitude of vasodilation in cat pial arteriole cranial window preps *in vivo* (Kontos *et al.*, 1977a) while isolated changes in intraluminal  $\text{CO}_2$  (Kontos *et al.*, 1977b) or pH (Lambertsen *et al.*, 1961; Harper & Bell, 1963) do not influence vessel tone as a result of unchanged pH within the vascular wall. For example, modulation of arterial pH in the presence of unchanged  $\text{PaCO}_2$  produces no change in CBF in humans (Lambertsen *et al.*, 1961) or animals (Harper & Bell, 1963), while application of minute volumes of acidic/alkalotic fluid into the perivascular space leads to highly localized changes in pial arteriolar diameter (Wahl *et al.*, 1970). Further, pretreatment of artificial CSF with sodium bicarbonate to maintain normal pH abolishes pial vessel dilation in response to intraluminal hypercapnia (Kontos *et al.*, 1977b; Koehler & Traystman, 1982). Indeed, if superfusate is euhydric, no vasomotor response will occur irrespective of local changes in  $\text{PCO}_2$  (Wahl *et al.*, 1970; Kontos *et al.*, 1977b, 1977a).

The importance of perivascular pH has been further delineated in *in vitro* animal models, whereby acidosis reduces L-type  $\text{Ca}^{2+}$  channel conductance (Klößner & Isenberg, 1994a),

intracellular calcium concentration  $[Ca^{2+}]_i$  (Boedtkjer *et al.*, 2016), and induces vasodilation of isolated cerebral arterioles (Peng *et al.*, 1998) independent of  $CO_2$  and bicarbonate  $HCO_3^-$ . The magnitude of contraction following membrane depolarization (Boedtkjer *et al.*, 2016) or calcium channel activation (Dabertrand *et al.*, 2012) is also reduced in acidosis independent of  $CO_2$  and  $HCO_3^-$ . Similar to *in vivo* studies, acidic hypercapnic and acidic isocapnic superfusate leads to similar vasodilation in isolated arterioles *in vitro* (You *et al.*, 1994; Tian *et al.*, 1995; Peng *et al.*, 1998). Conversely, increases in  $CO_2$  without alterations in pH or  $[HCO_3^-]$ , or euhydric hypercapnia, does not induce vasodilation *in vitro* (Nakahata *et al.*, 2003). Although there is a small amount of evidence for an independent role of  $PCO_2$  on cerebrovascular  $CO_2$  reactivity (Harder & Madden, 1985; Yoon *et al.*, 2012), such as a modest persistence of vasorelaxation in isolated vessels during transition from severe hypercapnia to euhydric hypercapnia (Toda *et al.*, 1989), these data have recently come under criticism (Boedtkjer, 2017). Given the inevitable interconversion between  $CO_2$ ,  $H^+$ , and  $HCO_3^-$  (i.e.,  $CO_2 + H_2O \rightleftharpoons H_2CO_3 \rightleftharpoons HCO_3^- + H^+$ ), it has been argued that the aforementioned studies may not have appropriately isolated  $PCO_2$ . Recent use of out of equilibrium superfusion, which hypothetically circumvents this issue of interconversion, indicates that changes in  $PCO_2$  while  $[HCO_3^-]_o$  and  $pH_o$  are held constant at normal values does not affect resting tone or sensitivity to vasoconstrictor stimuli (Boedtkjer *et al.*, 2016), corroborating the notion that perivascular pH is the regulator of cerebrovascular tone downstream of alterations in  $PaCO_2$ .

Therefore, the overarching insight gained from these studies is that movement of  $CO_2$  through the vessel wall and consequent alteration of perivascular pH is necessary to stimulate alterations in vasomotor tone (Kontos *et al.*, 1977b, 1977a; Tian *et al.*, 1995). It is important to note, however, that this represents a slightly generalized overview of  $PaCO_2$ -mediated vasodilation. Indeed, separate and integrated roles of vascular smooth muscle cell intracellular ( $pH_i$ ) and extracellular ( $pH_o$ ) pH may be operational within the vascular wall. These details have been recently reviewed (Boedtkjer, 2017); therefore, this review will only provide a brief summary.

Animal models have demonstrated that alterations in  $pH_i$  (Klöckner & Isenberg, 1994b; Schubert *et al.*, 2001) and  $pH_o$  (West *et al.*, 1992; Klöckner & Isenberg, 1994a) may influence ion channel conductance of vascular smooth muscle (e.g., potassium & calcium

channels) as well as enzymatic function (e.g. NOS activity) within vascular smooth muscle and endothelial cells (Fleming *et al.*, 1994; Boedtkjer *et al.*, 2011). Further, alterations in  $\text{Ca}^{2+}$  sensitivity (Boedtkjer *et al.*, 2016) and contractile function (Gardner & Diecke, 1988) are also influenced by alterations in  $\text{pH}_i$  and  $\text{pH}_o$ , respectively with independent influences of  $\text{HCO}_3^-$  also apparent (Boedtkjer *et al.*, 2016). Determining the specific components of  $\text{CO}_2$  related cerebrovascular regulation is inherently difficult and as such some hypotheses are based in part upon data in peripheral VSMCs, and cerebral specific regulation has yet to be fully delineated [reviewed in: (Boedtkjer, 2017)]. However, several inferences may be drawn from the data collected in cerebral specific models: 1) *in vitro* changes in VSMC  $\text{pH}_i$ ,  $\text{pH}_o$ , and extracellular  $\text{HCO}_3^-$  possess independent influences on cerebral vascular tone (Boedtkjer *et al.*, 2016), although a role for  $\text{pH}_i$  remains a topic of contention (Tian *et al.*, 1995); 2) VSMC  $\text{pH}_i$  does not decrease as much as  $\text{pH}_o$  during acidosis (Boedtkjer *et al.*, 2016); 3) in the more complex *in vivo* setting, altered pH in cranial window superfusate alters cerebral vascular tone irrespective of superfusate  $\text{CO}_2$  or  $\text{HCO}_3^-$  levels indicating a lack of direct effects of  $\text{CO}_2$  (Kontos *et al.*, 1977a); 4) manipulation of intraluminal arterial pH produces no vascular effect when  $\text{CO}_2$  is constant in *in vivo* animal (Kontos *et al.*, 1977a) and human models (Lambertsen *et al.*, 1961), indicating  $\text{CO}_2$  must be altered, diffuse across the vascular wall, and then change pH within the extra- and potentially intracellular domains. It is also important to consider the influence of endothelial  $\text{pH}_i$  (versus that of VSMC  $\text{pH}_i$ ), which is implicated in the regulation of NOS activity – NOS activity in cultured human endothelial cells is greatest at a  $\text{pH}_i$  of 7.5 (Fleming *et al.*, 1994). However, while VSMC  $\text{pH}_i$  will decrease in hypercapnia (or normocapnic acidosis), endothelial  $\text{pH}_i$  would be expected to increase as occurs with endothelial stimulation with bradykinin (Fleming *et al.*, 1994). Resolution of the *in vitro* and *in vivo* data has yet to be achieved, with the current differences potentially a result of varying experimental techniques, more robust isolation *in vitro*, and/or a lack of an appreciable independent effect of  $\text{HCO}_3^-$  and  $\text{CO}_2$  *in vivo* due to the inherent complexity of a living organism.

In light of the complexities of  $\text{CO}_2$  dependent influences on the cerebral vasculature, this thesis will for the purpose of simplicity commonly refer to  $\text{PaCO}_2$  as the response effector given it is the variable often manipulated experimentally, at least in human studies. In instances where  $\text{PaCO}_2$  is no longer as simply related to the pH stimulus [e.g. during chronic acid-base balance changes in disease or at HA (Willie *et al.*, 2015a)] this thesis

will re-address the relationship between PaCO<sub>2</sub> and pH. This influence of PaCO<sub>2</sub>/pH on CBF regulation is unique and distinctly different from that of the peripheral circulation (Lennox & Gibbs, 1932; Ainslie *et al.*, 2005) where there is a limited influence of PaCO<sub>2</sub> on vasomotor tone in humans.

### 2.5.1 CEREBROVASCULAR CO<sub>2</sub> REACTIVITY

Cerebrovascular CO<sub>2</sub> reactivity is a relatively linear response during both hypo and hypercapnia (Harper & Glass, 1965*b*; Shapiro *et al.*, 1966; Willie *et al.*, 2012; Skow *et al.*, 2013*a*). However, this relationship deviates from linearity at the limits of vasoconstrictive and vasodilator capacity, whereby further changes in PaCO<sub>2</sub> no longer induce changes in vasomotor tone and CBF, resulting in a sigmoidal relationship. Reaching these limits requires considerable alterations in PaCO<sub>2</sub>, which are difficult to tolerate by awake research subjects. Between these extremes, the relationship is effectively linear. Increases and decreases in CBF with hyper- and hypo- capnia, respectively are due to both alterations in blood vessel diameter and blood velocity, indicated by changes in cerebral blood volume and transit times (Ito *et al.*, 2003*a*). Furthermore, there is evidence of a modest hysteresis in the CBF response to altered PaCO<sub>2</sub>, whereby transitioning from a low to high PaCO<sub>2</sub> produces greater changes in flow compared to transitioning from a high PaCO<sub>2</sub> to lower PaCO<sub>2</sub> (Ide *et al.*, 2003).

When comparing reactivity in the hyper- versus hypo- capnic ranges volumetric blood flow reactivity during hypercapnia is near double that during hypocapnia (i.e., hypercapnia ~  $\Delta 6\text{-}8\%$  CBF/mmHg PaCO<sub>2</sub> vs. hypocapnia ~  $\Delta 3\text{-}4\%$  CBF/mmHg PaCO<sub>2</sub>) as assessed by the Kety & Schmidt technique (Kety & Schmidt, 1948*c*), duplex ultrasound (Willie *et al.*, 2012), MRI (Coverdale *et al.*, 2014)], and PET (Ramsay *et al.*, 1993; Ito *et al.*, 2000, 2003*a*) (see **Figure 2.11**). This pattern of vasoreactivity appears unaltered with anesthesia (Grüne *et al.*, 2015). Indexing reactivity with TCD shows an approximate 50% underestimation of volumetric reactivity (Willie *et al.*, 2012; Coverdale *et al.*, 2014; Hoiland *et al.*, 2015, 2016*b*), although the difference between hypercapnic and hypocapnic reactivity remains (TCD: hypercapnia ~  $\Delta 3\text{-}4\%$  CBF/mmHgPaCO<sub>2</sub> vs. hypocapnia ~  $\Delta 2\%$  CBF/mmHgPaCO<sub>2</sub>) (Ide *et al.*, 2003). While these reactivity values are standard for

healthy populations, reactivity is largely variable across disease populations [e.g. (Markus & Cullinane, 2001; Lavi, 2006; Warnert *et al.*, 2016)].

Regional differences in the magnitude of reactivity between the anterior and posterior circulation (Skow *et al.*, 2013b) as well as between grey and white matter (Ramsay *et al.*, 1993) are evident. The posterior circulation possesses an approximately 50% reduced absolute reactivity ( $\text{cm} \cdot \text{s}^{-1} \cdot \text{mmHg PaCO}_2^{-1}$ ) compared to the anterior circulation (Willie *et al.*, 2012; Hoiland *et al.*, 2015); however, this difference is minimized or eliminated when reactivity is scaled to resting blood flow and/or velocity and represented as a % change from baseline (Sato *et al.*, 2012b; Willie *et al.*, 2012; Hoiland *et al.*, 2015). Relative reactivity is also similar between the MCA and BA (Park *et al.*, 2003). Although there is near-unanimous support for the notion that the anterior circulation has a higher absolute reactivity than that of the posterior circulation including that from both TCD as well as volumetric CBF studies, similar MCAv and PCAv reactivity has been observed during end-tidal forcing through an extreme range of changes in PaCO<sub>2</sub> [i.e. 15-65mmHg; (Willie *et al.*, 2012)] and during hyperventilation and changes in fractional inspired CO<sub>2</sub> (Ogawa *et al.*, 1988). Differences between studies may also be due to differences in statistical power (i.e., sample size), or analytical techniques such as non-linear analysis versus linear regression (Ogawa *et al.*, 1988; Willie *et al.*, 2012; Skow *et al.*, 2013a). Relative to grey and white matter comparisons, reactivity of the insular cortex (grey matter) possesses an apparent 2 to 3-fold greater absolute CO<sub>2</sub> reactivity compared to the centrum semiovale (white matter) when measured with PET (Ramsay *et al.*, 1993). Similar findings are evident in studies utilizing BOLD sequences (Thomas *et al.*, 2014; Bhogal *et al.*, 2015).

### **2.5.2 STANDARDIZATION AND UTILITY OF CEREBROVASCULAR REACTIVITY**

Cerebrovascular reactivity represents the slope relationship between the stimulus and the change in flow. As the acquisition of PaCO<sub>2</sub> measures, which necessitates an arterial puncture or catheterization for repeat measures, was thought to be an invasive measure, noninvasive surrogates have been employed widely: the concentration of inspired CO<sub>2</sub> [See: (Fisher, 2016) for discussion]; the duration of a breath-hold (Kastrup *et al.*, 1999b). However, it had been noted by Swenson *et al.*, in 1994 (Swenson *et al.*, 1994) that end-inspiratory PCO<sub>2</sub> equalized the PCO<sub>2</sub> between arterial and end-tidal gas, allowing the latter

to be used as a measure of the former. This has been validated in animals with pneumonia (Fierstra *et al.*, 2011) and in humans (Ito *et al.*, 2008) and used to apply precise PaCO<sub>2</sub> targeting as a vasoactive stimulation (Fierstra *et al.*, 2013). As CBF is difficult to measure non-invasively [although possible via ASL or duplex ultrasound (see **Table 2.1**)] other non-invasive measures are predominantly surrogates leaving measures as a relative percent (%) change in CBF. The use of absolute or relative reactivity is typically dependent on the research question and/or hypothesis (Ainslie & Duffin, 2009).

For example, if CBF increased from 750mL/min to 1012.5mL/min following an increase in PaCO<sub>2</sub> from 40mmHg to 45mmHg, cerebrovascular CO<sub>2</sub> reactivity would be calculated as follows:

$$\begin{aligned}\text{Absolute (mL/min/mmHg) CO}_2 \text{ reactivity} &= (1012.5-750) / (45-40) \\ &= 262.5 / 5 \\ &= 52.5\text{mL/min/mmHg}\end{aligned}$$

$$\begin{aligned}\text{Relative (\%) CO}_2 \text{ reactivity} &= (((1012.5-750)/750)*100) / (45-40) \\ &= 35 / 5 \\ &= 7\%/\text{mmHg}\end{aligned}$$

Such determination of reactivity as noted above is simple, but applicable, and commonly utilized with global measures of CBF, such as duplex ultrasound. While the experimental chapters of this thesis (Chapters 3-6) use ultrasonography to quantify CBF, the utilization of BOLD imaging provides in-depth data on regional reactivity, and locally specific cerebrovascular disease and is therefore outlined here.

Standardization of CVR, across a variety of vasoactive stimuli and surrogate measures of regional blood flow, is not feasible. For a given flow measuring method, say BOLD imaging, the stimulus must also be consistent in type, magnitude, duration, and pattern. The various vasoactive stimuli that are used, typically consisting of intravenous drugs (usually acetazolamide) or CO<sub>2</sub> in the form of hypercapnia are not compatible and thus not comparable. Even with a constant injected dose normalized for body weight, acetazolamide produces variable blood concentration levels, possesses an unknown time

course, and an unknown subject susceptibility to side effects [see: (Fierstra *et al.*, 2013)]. Similarly, there are challenges associated with controlling/standardizing CO<sub>2</sub> as well. With breath-holds, PaCO<sub>2</sub> levels may not rise, are constantly changing and the time course of PaCO<sub>2</sub> changes and peak response are unknown; furthermore, it is accompanied by hypoxia which also confounds the stimulus effect [see: (Fierstra *et al.*, 2013) for review and discussion]. Administering a fixed inspired concentration of CO<sub>2</sub> is intuitively attractive, but does not result in a predictable, fixed, or even known PaCO<sub>2</sub> (Fisher, 2016). Even if invasive arterial cannulation is performed to directly measure the PaCO<sub>2</sub> stimulus, it still cannot be fixed or predicted and remains highly variable within and between subjects. Indeed, repeatedly and accurately targeting PaCO<sub>2</sub> across subjects and within subjects over time is not a trivial undertaking and has required a new conceptual framework for blood gas control (Slessarev *et al.*, 2007; Fierstra *et al.*, 2013; Fisher *et al.*, 2016) and computerized gas control to execute effectively (Tymko *et al.*, 2015, 2016a; Fisher, 2016). In its technical embodiment, it can be used to implement precise PaCO<sub>2</sub> targeting as vasoactive stimulation for measuring CVR [see: (Fierstra *et al.*, 2013) for review].

Even so, changes in a flow signal (i.e., BOLD) need to be normalized for signal size and anatomical location. As the BOLD response is not a linear function of PaCO<sub>2</sub>, the simplification of  $\Delta\text{BOLD}/\Delta\text{PaCO}_2$  is inconsistent at different PaCO<sub>2</sub> ranges and stimulus sizes. As discussed above, the relationship between PaCO<sub>2</sub> and BOLD signal also depends on the absolute values of PaCO<sub>2</sub> (hypocapnic, hypercapnic), direction (from hypocapnic to hypercapnic or vice versa) as well as its range (i.e.,  $\Delta\text{PaCO}_2$ ). All of these need to be standardized to generate comparable data.

### **2.5.3 INTRACRANIAL HEMODYNAMICS ASSESSED WITH BOLD**

Localized differences in regional reactivity can often be compensated during normal activity of everyday life by autoregulation, which modulates the resistance in vessels with upstream flow limitations or reductions in perfusion pressure. The modulations are in the direction of maintaining constant blood perfusion. Autoregulation would thus obscure any indication of flow limitation when CBF is measured at rest. Therefore, a provocative vasoactive stimulus is required to perturb this equilibrium to reveal any occult flow limitations (Sobczyk *et al.*, 2014). This is explained by reference to the model illustrated

in **Figure 2.24**. While this steal phenomenon was demonstrated experimentally in animal models as early as 50 years ago (Brawley, 1968; Symon, 1968), it has recently been revived and applied to humans using precise, characterizable vasoactive stimuli and a non-invasive high temporal and spatial resolution surrogate measure of CBF, BOLD imaging (Sobczyk *et al.*, 2014). The simple single vessel models of Brawley and Symon (Brawley, 1968; Symon, 1968) have been expanded to account for changes in flow signal throughout the brain. A global cerebral vasodilatory stimulus induces a strong distal vasodilatory stimulus (e.g., at the pial vessels) that exceeds the inflow capacity (through a shared conduit) and thus reduces the perfusion pressure distal to the carotid arteries and at each branch. Perfusion is determined by the ability of distal vessels to vasodilate by autoregulation. Vessels distal to a stenosis have encroached on their vasodilatory reserve, as they vasodilate in resting conditions to maintain adequate flow. Therefore, they have a limited capacity to dilate in response to a stimulus and in turn a reduction in perfusion pressure results in a reduction in flow (**Figure 2.24**, blue coloration of the axial slices in the upper left panel). In the lower panel the CVR is normalized despite the same fully occluded vessel. The lower right panel shows the mechanism for normalization being the presence of collateral blood flow.

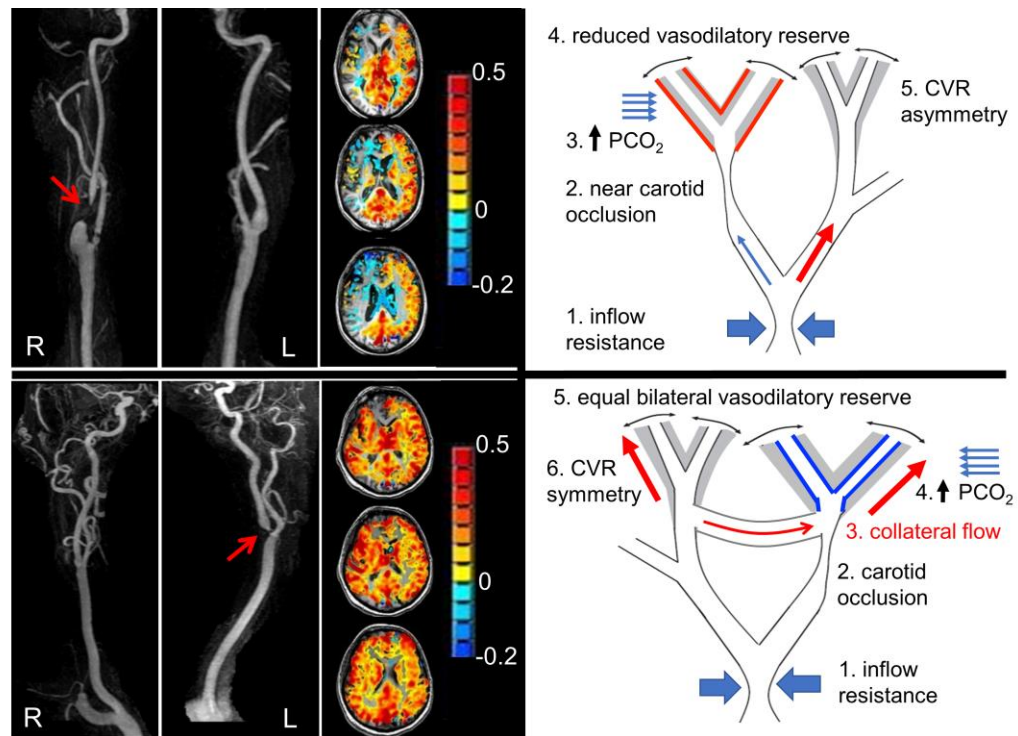


**Figure 2.24. The brain vascular stress test to identify the extent of collateralization in the presence of steno-occlusive vascular disease.**

Left panel shows angiograms from two patients with near occluded carotid arteries (red arrow). Next to each, are axial slices from the CVR test. The CVR for each voxel is color coded according to the color scheme shown, and mapped onto the corresponding voxel of the anatomical scan. The upper panel shows steal physiology due to lack of collateral blood flow, and the lower one shows near compensatory collateral blood flow. The mechanism is shown in the schematic diagram to the right of each. Further discussion of the mechanism is in the text. Reproduced with permission from Fisher et al. Stroke 2018.

With reference to the model shown in **Figure 2.24**, progressive increases in PaCO<sub>2</sub>, result in progressive reductions in cerebrovascular resistance, even in the presence of upstream resistance and encroachment on the cerebrovascular vasodilatory reserve. The same principle applies in vascular beds compromised by localized cerebrovascular disease. **Figure 2.24** shows that despite a global vasoactive stimulus, asymmetrical vasodilatory reserves or responses result in an increase in flow in some distal vessels and reductions in others. Indeed, there is an interaction between the two resistances (Faraci & Heistad, 1990), such that any increase in flow to these two regions produces a decrease in their shared perfusion pressure. An extreme example of this regional interaction can occur, where one

region cannot vasodilate to maintain flow in the face of the perfusion pressure reduction driven mainly by the other region, resulting in its decreased flow: the steal phenomenon.

#### 2.5.4 CO<sub>2</sub>: SITE(S) OF VASCULAR REGULATION

While previously a contentious matter (Serrador *et al.*, 2000; Giller, 2003), evidence continues to emerge supporting the theory that alterations in PaCO<sub>2</sub> lead to vasomotor changes throughout the entire cerebral circulation implicating both large cerebral arteries through to pial, penetrating, and micro vessels in the regulation of cerebrovascular resistance during PaCO<sub>2</sub> perturbations (Wolff & Lennox, 1930; Willie *et al.*, 2012; Verbree *et al.*, 2014; Coverdale *et al.*, 2014, 2015; Howarth *et al.*, 2017) (**Figure 2.25**). Previous animal data corroborates this recent paradigm shift in human cerebrovascular regulation (Heistad *et al.*, 1978; Faraci & Heistad, 1990). This multi-segment response is, however, likely not uniform and has been shown to vary between small and large pial vessels in animals (Morii *et al.*, 1986). In keeping, the underlying mechanism(s) governing changes in arterial/arteriole caliber throughout the vasculature are also unlikely to be uniform (Faraci & Heistad, 1990). Pial vessels demonstrate an intrinsic sensitivity to pH, whereby changes in PaCO<sub>2</sub> lead to immediate changes in vessel diameter. This tight temporal relationship between PaCO<sub>2</sub> and smaller arteries/arterioles (e.g. pial vessels) has been demonstrated in animal studies (Wolff & Lennox, 1930) and is demonstrated by a near immediate increase in MCAv and BOLD in humans (Poulin *et al.*, 1996; Poublanc *et al.*, 2015) due to the preceding reductions in downstream resistance. However, larger intracranial cerebral arteries (e.g. MCA) and extracranial cerebral conduit arteries (e.g. internal carotid artery) display a delayed vasomotor response to PaCO<sub>2</sub>, which are likely unrelated to direct pH sensitivity and may be due to changes in shear stress subsequent to altered pial vessel resistance (Carter *et al.*, 2016a; Hoiland *et al.*, 2017c). Indeed, vasomotor changes of both the MCA (Coverdale *et al.*, 2015) and ICA (Carter *et al.*, 2016a; Hoiland *et al.*, 2017c) occur in similar temporal fashion (e.g. 30-60s onset delay) as endothelium-dependent shear stress-mediated dilation of peripheral blood vessels (Thijssen *et al.*, 2011). As the specific signaling pathway(s) regulating large intracranial and cerebral conduit artery vasodilation have received little attention to date, further research is needed to determine their regulation, and overall contribution to PaCO<sub>2</sub> mediated cerebral vascular reactivity.

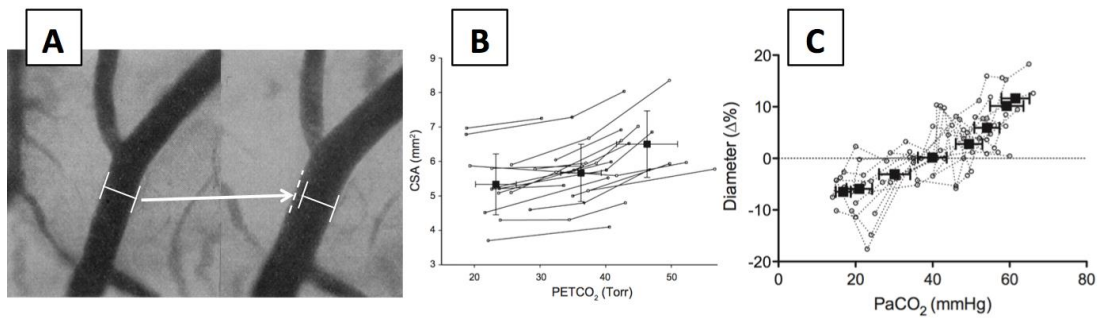


**Figure 2.25. Carbon dioxide mediated alterations in cerebrovascular diameter occurs throughout the entire cerebrovascular tree.**

**A.** Classic data from Wolff & Lennox (Wolff & Lennox, 1930) depicting hypercapnic vasodilation of pial arterioles in anesthetized cats. Two vessels can be seen; the one on the left is an image during craniotomy in the resting state, while the one on the right is during hypercapnia. The difference in diameter can be visualized by the addition of the dotted line to the diameter of the vessel in the right image. These data, along with extrapolation from others (Serrador *et al.*, 2000), led to the belief that CBF regulation during changes in PaCO<sub>2</sub> was mediated solely by pial arteries / arterioles. Adapted from Wolff & Lennox, 1930 with permission. **B.** Changes in diameter of the MCA as assessed by high resolution (3T) MRI in humans during changes in end-tidal carbon dioxide (P<sub>ET</sub>CO<sub>2</sub>). Reproduced from Coverdale *et al.*, 2014 with permission. **C.** Data depicting changes in diameter of the internal carotid artery (ICA) in humans throughout a wide range of PaCO<sub>2</sub>. It is now, therefore, established that changes in diameter of large intra- and extra-cranial cerebral arteries occurs in response to changes in PaCO<sub>2</sub> along with changes at the pial artery and arteriolar level. Reproduced from Willie *et al.*, 2012 with permission.

As previously mentioned, cerebral vessels are unique to those in the periphery in regard to their intrinsic sensitivity to chemical changes (e.g. PaCO<sub>2</sub>). However, where this transition between vessels intrinsically sensitive to pH occurs is unknown in humans. It is also unknown if this transition is definitive at one point, or occurs across a gradual continuum. While animal data indicates this “transition site” may occur abruptly and near the distal end of the vertebral artery and internal carotid artery (Bevan, 1979), human data may be inferred to suggest that the transition site occurs distal to the large arteries originating from the Circle of Willis given the vasomotor delay following alterations in PaCO<sub>2</sub>. For example, the MCA does not seem to be intrinsically sensitive to pH changes given the lack of temporal coupling between MCA vasodilation and PaCO<sub>2</sub> changes.

### 2.5.5 FACTORS INFLUENCING CEREBROVASCULAR CO<sub>2</sub> REACTIVITY.

Cerebrovascular CO<sub>2</sub> reactivity is subject to between test and between subject variability and can be altered by a myriad of potential concurrent physiological effectors. Consideration of potential interactions with other primary regulators of CBF (hypoxia, neuronal activity, blood pressure, and autonomic inputs) is pivotal in fully understanding CO<sub>2</sub> induced changes in vasomotor tone. Further consideration of factors such as altered acid-base balance, age and sex, are also important.

#### 2.5.5.1 CO<sub>2</sub> REACTIVITY AND HYPOXIA

It has been previously demonstrated that alterations in PaO<sub>2</sub> will interact with PaCO<sub>2</sub> perturbations to collectively dictate cerebrovascular reactivity. Specifically, hypoxia will elevate CBF across a wide range of PaCO<sub>2</sub> in both the hypo and hypercapnic CO<sub>2</sub> range (Ainslie & Poulin, 2004; Mardimae *et al.*, 2012). In instances of severe hypoxia (i.e., PaO<sub>2</sub> ≈ 40mmHg), CBF remains above baseline despite pronounced hypocapnia (Mardimae *et al.*, 2012). The interaction between hypoxia and CO<sub>2</sub> on CBF has been demonstrated as a simple additive effect (Poulin *et al.*, 1996; Ainslie & Burgess, 2008) where CO<sub>2</sub> reactivity is unaltered, or a synergistic effect (Mardimae *et al.*, 2012), with between study differences being potentially due to analytical methods. Regardless, no study has assessed this interactive nature of hypoxia and CO<sub>2</sub> on CBF regulation using volumetric measures of CBF – this is requisite to provide confirmatory evidence for either above mentioned theory. Indeed, while CO<sub>2</sub> (see section “CO<sub>2</sub>: site(s) of vascular regulation”) and O<sub>2</sub> (Giller *et al.*, 1993; Wilson *et al.*, 2011; Imray *et al.*, 2014; Kellawan *et al.*, 2016; Sagoo *et al.*, 2016; Hoiland *et al.*, 2017b) possess individual influences on arterial diameter throughout the cerebral circulation, their combined influences on vascular diameter has yet to be comprehensively examined, and possesses obvious implications for the use of TCD.

In addition to the acute influences of hypoxia, the acid base changes associated with prolonged hypoxia, such as ascent to and stay at altitude are implicated in the regulation of cerebrovascular CO<sub>2</sub> reactivity [reviewed in: (Hoiland *et al.*, 2018a)]. For example, one to two weeks leads to significant excretion of HCO<sub>3</sub><sup>-</sup> subsequent to respiratory alkalosis, which steepens the [H<sup>+</sup>]/PaCO<sub>2</sub> relationship (Willie *et al.*, 2015a) (**Figure 2.26**). As

outlined above, perivascular pH is the stimulus for CO<sub>2</sub> mediated alterations in vasomotor tone; thus, this altered [H<sup>+</sup>]/PaCO<sub>2</sub> relationship has obvious implications for cerebral vascular control. Indeed, hypercapnic CO<sub>2</sub> reactivity, when indexed against PaCO<sub>2</sub> is elevated at HA (Ainslie *et al.*, 2012; Willie *et al.*, 2015a; Flück *et al.*, 2015). This finding consistent with a rebreathing study conducted at the same altitude (5050 m) (Fan *et al.*, 2010a). Yet, there are findings to the contrary (i.e., CO<sub>2</sub> reactivity is reduced); however, these studies are limited by concurrent hyperoxia (Ainslie *et al.*, 2007; Ainslie & Burgess, 2008; Lucas *et al.*, 2011), lack of iso-oxia (Jansen *et al.*, 1999) and non-volumetric indices of CBF (Jansen *et al.*, 1999; Ainslie *et al.*, 2007; Ainslie & Burgess, 2008; Lucas *et al.*, 2011; Rupp *et al.*, 2014). Different altitudes may also underscore between study differences.

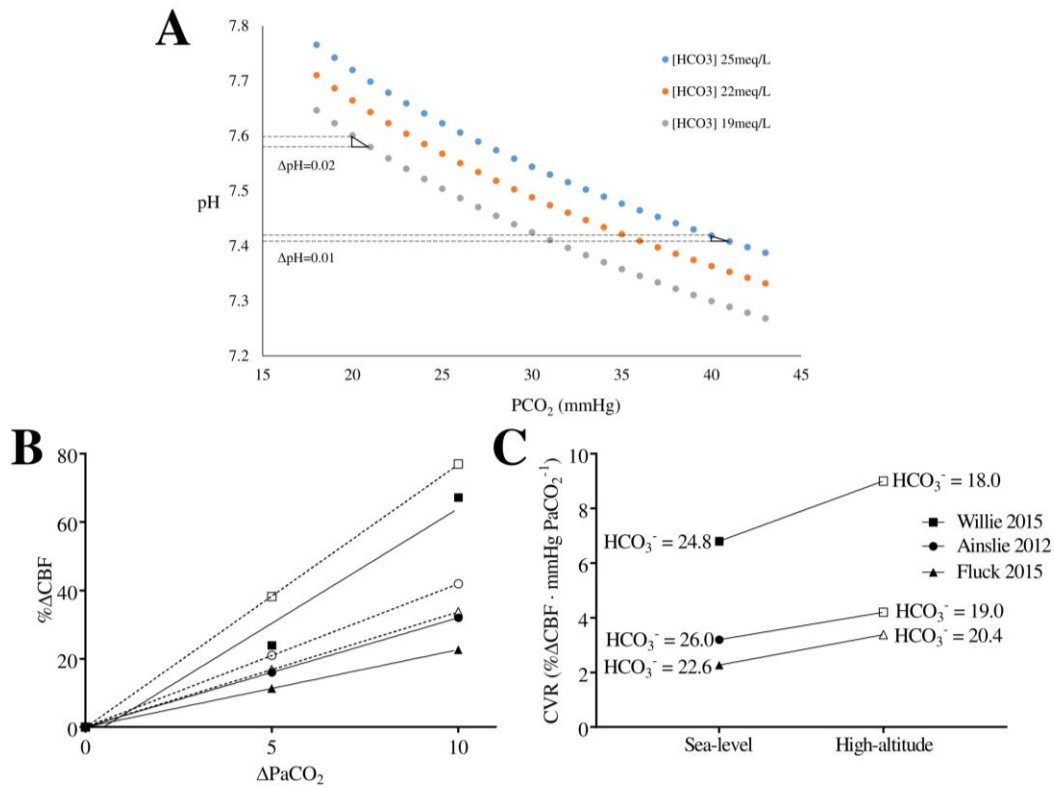


**Figure 2.26. Relationship Between the Partial Pressure of Carbon Dioxide and pH With Varying Bicarbonate Ion Concentration.**

This figure highlights how, according to the Henderson-Hasselbalch equation, the magnitude of pH changes with varying PCO<sub>2</sub> are augmented at altitude following renal compensation for respiratory alkalosis (Panel A). At sea level, where [HCO<sub>3</sub><sup>-</sup>] approximates 25 meq/L (Willie *et al.*, 2015a), an increase in resting PaCO<sub>2</sub> from 40 to 41 mmHg would lead to a reduction in pH of 0.01. Conversely, at altitude where [HCO<sub>3</sub><sup>-</sup>] may approximate 19 meq/L, an increase in resting PaCO<sub>2</sub> from 20 to 21 mmHg would lead to a reduction in pH of 0.02. Panels B and C indicate how the magnitude increase in CBF per increase in PaCO<sub>2</sub> is increased following acclimatization (Panel B), with the resulting CVR values and their related arterial [HCO<sub>3</sub><sup>-</sup>] concentrations in in Panel C. Panel A was reproduced with permission from (Hoiland *et al.*, 2018a). Panels B and C created from the data of (Ainslie *et al.*, 2012; Willie *et al.*, 2015b; Flück *et al.*, 2015).

Both increases (Lucas *et al.*, 2011; Flück *et al.*, 2015), no change (Rupp *et al.*, 2014; Willie *et al.*, 2015a) and decreases (Ainslie *et al.*, 2007) in hypocapnic cerebral vasoconstriction have been demonstrated upon ascent to and acclimatization at altitude. Therefore, given methodological (technical & logistical) differences between studies, physiological differences (e.g., acid-base balance) and the resultant inconsistency of results, it remains relatively unclear how altered hypocapnic vasoconstriction may contribute to the

progressively reduced CBF throughout acclimatization. Importantly, the study by Willie *et al.*, 2015 was conducted under iso-oxic conditions (Willie *et al.*, 2015a). In studies where PaO<sub>2</sub> was not purposefully controlled, the hyperventilation necessary to reduce PaCO<sub>2</sub> leads to concomitant increases in PaO<sub>2</sub>. This point holds relevance for the assessment of hypocapnic CO<sub>2</sub> reactivity at altitude given it may ‘withdraw’ some of the hypoxic vasodilatory stimulus (Møller, 2010), and thus an overestimation of the vasoconstrictive effect of hypocapnia may occur.

#### ***2.5.5.2 CO<sub>2</sub> REACTIVITY AND BLOOD PRESSURE***

Blood pressure regulation is relevant for the regulation of CO<sub>2</sub> reactivity in two contexts: 1) the relationship between resting, or steady state, MAP and CO<sub>2</sub> reactivity, and 2) the influence of the CO<sub>2</sub> induced vasopressor response on CO<sub>2</sub> reactivity.

A seminal study conducted in 1965 by Harper & Glass, showed that progressive decreases in MAP up to a reduction of 66% below baseline, causes marked reductions in cerebrovascular CO<sub>2</sub> reactivity to hypo and hypercapnia (Harper & Glass, 1965a) (**Figure 2.27**). Indeed, progressive hypotension leads to graded reductions in CBF during hypercapnia, where at extreme hypotension there is no apparent hypercapnia related elevation in CBF (Iwabuchi *et al.*, 1973). Collectively, these studies indicate that in the instance of severe hypotension, autoregulatory vasodilation is of a magnitude that appreciably exhausts the vasodilatory reserve of the cerebral vasculature rendering it incapable to further dilate in response to acidosis. Conversely, hypotension induced dilation also appears to counteract the vasoconstrictive stimulus of hypocapnia, reducing and/or abolishing the normally expected reductions in flow.

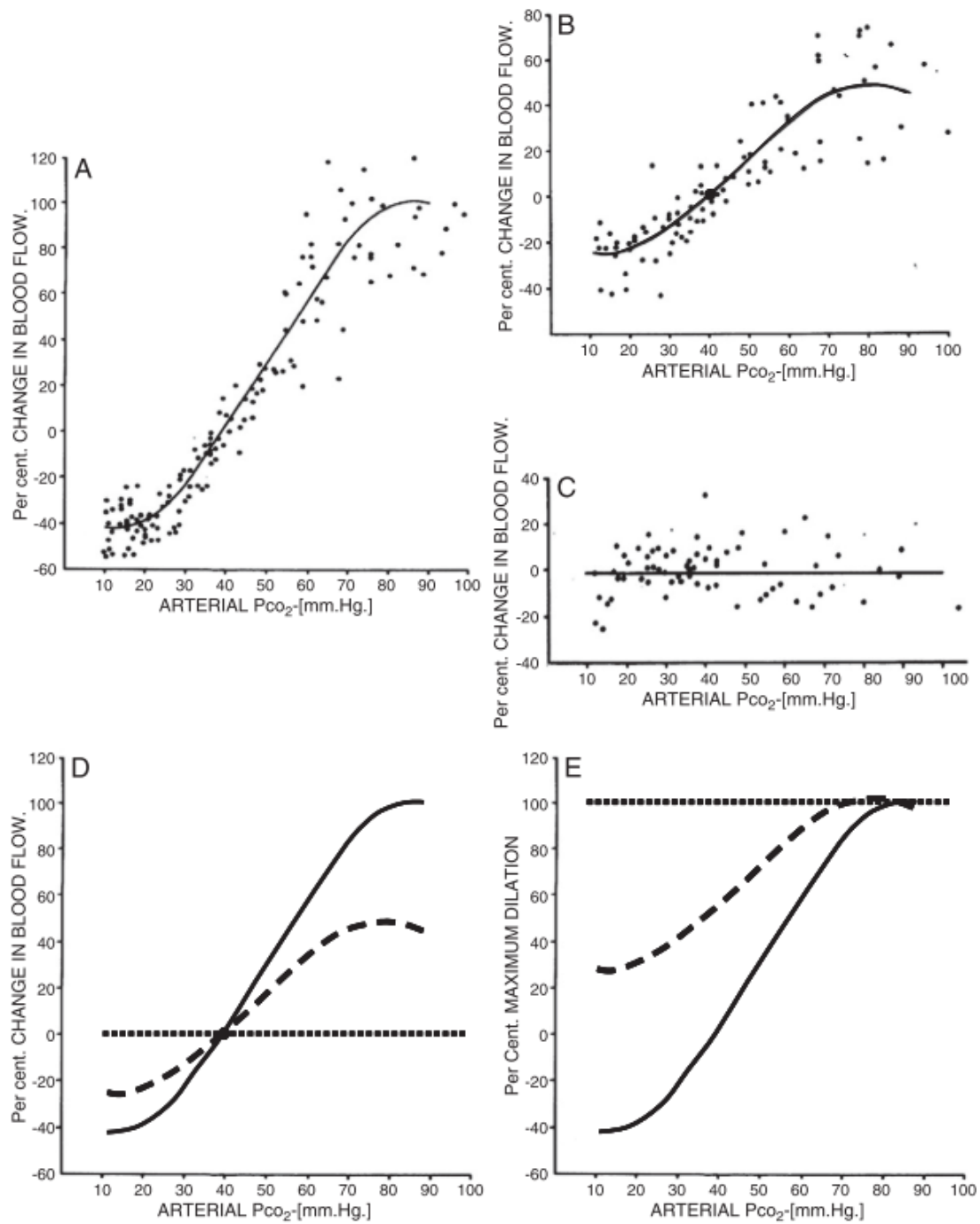


**Figure 2.27. Effect of a progressive loss of vasodilatory reserve on the response to changes in arterial carbon dioxide.**

Results redrawn from experiments in dogs by Harper and Glass (1965; Figs. A, B, and C) showing the effects of reducing perfusion pressure on the CBF response to CO<sub>2</sub>. A) Normotensive; B) Hypotensive; C) Extreme hypotension; D) An overlay of the fitted responses in A and B drawn to the same scale; E) The fitted responses presented as the % of maximum vasodilation. Reproduced from (Sobczyk *et al.*, 2014) with permission.

Elevations in PaCO<sub>2</sub> result in concomitant increases in blood pressure due to increased SNA (Ainslie *et al.*, 2005). When the elevations in blood pressure are sustained, they are generally related to the magnitude of the flow response to hypercapnia (**Figure 2.28**) (Willie *et al.*, 2012; Regan *et al.*, 2014). Thus, it is important to consider the influence of systemic blood pressure in the cerebrovascular response to CO<sub>2</sub>. If flow is considered in isolation, than an individual with an exaggerated vasopressor response to CO<sub>2</sub> may be mistaken as possessing a high CO<sub>2</sub> reactivity. Therefore, the relationship between cerebrovascular conductance (mL · min<sup>-1</sup> · mmHg<sup>-1</sup>) and/or cerebrovascular resistance (mmHg<sup>-1</sup> · mL<sup>-1</sup> · min<sup>-1</sup>) and changes in PaCO<sub>2</sub> are commonly assessed to provide further insight into vasomotor changes occurring independent of changes in MAP.

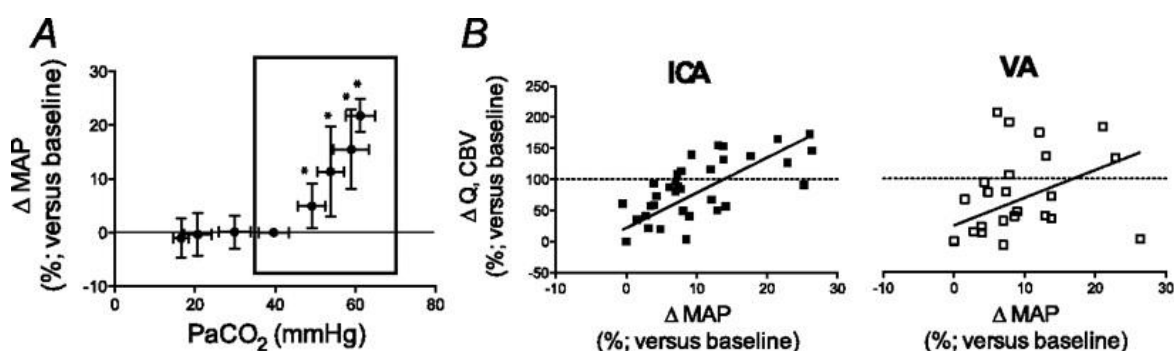


**Figure 2.28. Increased blood pressure during hypercapnia is related to cerebrovascular reactivity.**

Panel A depicts the changes in mean arterial pressure (MAP) that occur during hypercapnia (highlighted by the box). Panel B shows the relationship between changes in MAP from baseline (rest) and changes in internal carotid (ICA) and vertebral artery (VA) flow during hypercapnia. As depicted, there is a linear relationship whereby increases in MAP are related to the increase in flow (ICA & VA) and thus important to consider when measuring cerebrovascular reactivity. Figure reproduced from (Willie *et al.*, 2012) with permission. © 2012 The Authors. The Journal of Physiology © 2012 The Physiological Society.

Importantly, when considering the influence of MAP on CO<sub>2</sub> reactivity, is the potential for concurrent changes in CPP (i.e. MAP-ICP) alongside a vasopressor response. Hypercapnia increases, while hypocapnia decreases cerebral blood volume (Ito *et al.*, 2003a) with implications for alterations in ICP. Indeed, hypocapnia reduces ICP (Steiner *et al.*, 2005), but does not seem to appreciably alter MAP, even with extreme hypocapnia (e.g. 15mmHg PaCO<sub>2</sub>) (Willie *et al.*, 2012). This may lead to over estimation of hypocapnic reactivity if

the hydraulic pressure head is slightly reduced. Conversely, hypercapnia increases ICP, with inhalation of 5% cCO<sub>2</sub> (5% F<sub>I</sub>CO<sub>2</sub>; 21% F<sub>I</sub>O<sub>2</sub>; N<sub>2</sub> balance) demonstrated to increase ICP by as much as 20 mmHg (Asgari *et al.*, 2011). Therefore, careful consideration must be given as to how blood pressure influences CO<sub>2</sub> reactivity, with further consideration of how MAP and ICP are concurrently changing and collectively determining CPP.

### **2.5.5.3 CO<sub>2</sub> REACTIVITY AND SYMPATHETIC NERVOUS ACTIVITY**

Chemoreflex activation via acidosis increases SNA (Steinback *et al.*, 2009, 2010b, 2010a) and may, therefore, be implicated in modulating cerebrovascular CO<sub>2</sub> reactivity. Increasing SNA through various techniques such as handgrip exercise (Ainslie *et al.*, 2005) and lower body negative pressure (LeMarbre *et al.*, 2003) does not alter reactivity in either the hyper and hypocapnic range; however, pharmacological blockade of SNA has been reported to reduce both hypocapnic (Peebles *et al.*, 2012) and hypercapnic (Przybyłowski *et al.*, 2003) reactivity. A reduction in hypercapnic reactivity via pharmacological SNA blockade is likely mediated by an abolished pressor response (Przybyłowski *et al.*, 2003; Ainslie *et al.*, 2012) which, as mentioned, normally contributes to the flow response (Willie *et al.*, 2012; Regan *et al.*, 2014). There is, however, data indicating that the CVR is augmented by ganglionic blockade (Jordan *et al.*, 2000) although it is still strongly related to the magnitude of change in MAP. Overall it appears that SNA activity contributes to CO<sub>2</sub> reactivity, particularly in the hypercapnic range, by eliciting a pressor response, versus possessing a limiting effect through vascular ‘constraint’. However, given increased muscle SNA is related to increased resistance of larger cerebral arteries proximal to, and at the level of, the Circle of Willis (Warnert *et al.*, 2015; Verbree *et al.*, 2017), these inferences, which are based on velocity, but not flow measurements, (i.e. TCD) may require future reconsideration. A recent study that elicited sympathoexcitation, with unaltered MAP, using lower body negative pressure demonstrated this had no influence on the increase in cerebrovascular conductance associated with hypercapnia (Iwamoto *et al.*, 2018). Notably, this is the first study to investigate the role of SNA on CO<sub>2</sub> reactivity with volumetric CBF measures (duplex ultrasound) (Iwamoto *et al.*, 2018).

#### **2.5.5.4 CO<sub>2</sub> REACTIVITY AND AGING**

Population based study has demonstrated in ~1700 people that hypercapnic CO<sub>2</sub> reactivity is progressively reduced with aging past 65 years (Bakker *et al.*, 2004). Many smaller studies corroborate this notion across the entire adult lifespan, with cerebral vascular CO<sub>2</sub> reactivity to hypercapnia impaired in elderly compared to young individuals (Reich & Rusinek, 1989; Ito *et al.*, 2002a; Lu *et al.*, 2011; Barnes *et al.*, 2012; Bailey *et al.*, 2013a; Thomas *et al.*, 2013; Flück *et al.*, 2014; Jaruchart *et al.*, 2016) with reductions in reactivity potentially more pronounced in females than males (Kastrup *et al.*, 1998). Reductions in the vasodilatory response of the MCA to hypercapnia in old versus young has also been demonstrated (Coverdale *et al.*, 2016). The significance of this latter finding is two-fold: 1) reductions in reactivity with aging occur in part in large arteries distal to the Circle of Willis, and 2) transcranial Doppler determination of reduced CO<sub>2</sub> reactivity with aging will under-estimate the true magnitude of differences given the change in MCA diameter that is not accounted for with this technique. When grey matter and white matter are considered separately, there appears to be a reduced grey matter reactivity in older individuals (Thomas *et al.*, 2014; Leoni *et al.*, 2017), although this may be a function of reduced grey matter volume (Coverdale *et al.*, 2016), while white matter reactivity may conversely be greater in old versus young (Thomas *et al.*, 2014). Contrary to these recent MRI studies, cortical and white matter CO<sub>2</sub> reactivity have been shown to similarly decrease with age when measured with the xenon-133 technique (Reich & Rusinek, 1989).

Despite the large amount of data demonstrating that normal aging reduces CO<sub>2</sub> reactivity, there are studies to the contrary, demonstrating unaltered (Galvin *et al.*, 2010; Oudegeest-Sander *et al.*, 2014; Madureira *et al.*, 2017) or even higher (Zhu *et al.*, 2013) reactivity with aging. While some have attributed this difference to the method of CO<sub>2</sub> administration or measurement of CBF (e.g., TCD vs BOLD) (Tarumi & Zhang, 2017), differences in the proportion of male and female participants (Kastrup *et al.*, 1998) or arterial stiffness (Flück *et al.*, 2014; Jaruchart *et al.*, 2016), the reasons underlying these divergent findings remains unknown.

#### 2.5.5.5 CO<sub>2</sub> REACTIVITY AND SEX DIFFERENCES

Premenopausal women, at least as assessed using transcranial Doppler, have higher CO<sub>2</sub> reactivity than similarly aged men (Kastrup *et al.*, 1997, 1999a; Matteis *et al.*, 1998). Women also appear to have higher cerebrovascular reactivity (Karnik *et al.*, 1996) in response to acetazolamide infusion, although this sex difference is small or negligible when relative (%) reactivity is considered (Nirkko & Baumgartner, 1996). In the hypocapnic range, cerebrovascular CO<sub>2</sub> reactivity appears similar between sexes (Vriens *et al.*, 1989). Notably, these aforementioned studies did not specify any standardization of menstrual phase for reactivity testing. This could have implications for reactivity given the fluctuations in estrogen across the menstrual cycle of premenopausal women (Marsh *et al.*, 2011). Increased CO<sub>2</sub> reactivity in women would potentially be due to a role of estrogen in increasing NO related signaling (Hisamoto *et al.*, 2001; Florian *et al.*, 2004) or an increase in the ratio of vasodilator to vasoconstrictor PGs (Ospina *et al.*, 2003) although contrary to this point a lack of change in CO<sub>2</sub> reactivity across the menstrual cycle has been reported (Peltonen *et al.*, 2016). Given this was a small study that utilized TCD, not a measure of volumetric flow, more data is needed to firmly conclude how CO<sub>2</sub> reactivity may be altered across the menstrual cycle and how this contributes to potential sex differences. If sex differences in CO<sub>2</sub> reactivity are present, however, it is more likely that differences would be attributable to NO than PGs (see section “Signaling pathways regulation cerebrovascular CO<sub>2</sub> reactivity”). Notably, if testing in women is standardized to take place in the early follicular phase, where estrogen levels are the lowest (Marsh *et al.*, 2011) and comparable to men (Peltonen *et al.*, 2015), there is no detectable sex differences for CO<sub>2</sub> reactivity (Willie *et al.*, 2012; Peltonen *et al.*, 2015). In older adults there is conflicting data as to whether cerebrovascular CO<sub>2</sub> reactivity is higher in men (Matteis *et al.*, 1998; Bakker *et al.*, 2004) or women (Deegan *et al.*, 2011).

#### 2.5.6 SIGNALING PATHWAYS REGULATING Cerebrovascular CO<sub>2</sub> REACTIVITY

Regulation of CBF at the cellular level in response to varying stimuli is a multifaceted and complex process. See **Figure 2.29** for a generalized overview of cerebrovascular smooth muscle cell regulation by CO<sub>2</sub>. Overall, potassium channels, calcium channels and vasoactive factors such as adenosine, NO, EETs, PGs, and reactive oxygen species (ROS)

may all potentially mediate cerebral vasomotor changes in response to alterations in PaCO<sub>2</sub>. While the role of any of these candidate molecules in CO<sub>2</sub> reactivity could be the topic of their own dedicated review, this thesis comprehensively but also concisely outlines their individual roles below.

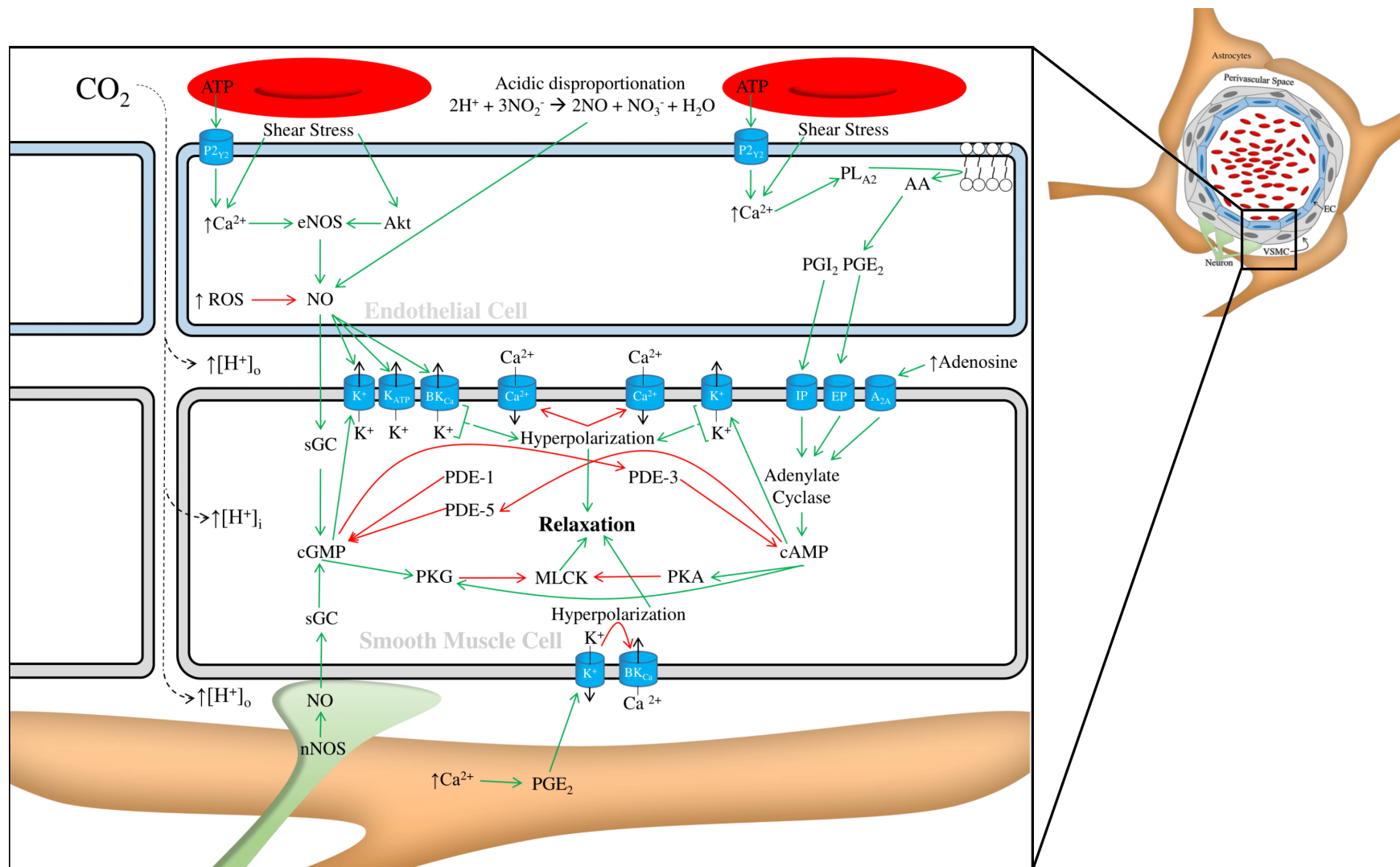


**Figure 2.29. Potential pathways regulating cerebrovascular reactivity to carbon dioxide.**

Hypercapnia leads to an increase in intra- and extracellular hydrogen ion concentration ( $[H^+]_o$  and  $[H^+]_i$ , respectively) (Boedtkjer, 2017). While all the depicted cellular processes act to induce smooth muscle cell relaxation, these processes initiate in various locales. In the vessel lumen, the red blood cell can release adenosine triphosphate (ATP) following deformation (or shear) (Wan *et al.*, 2008), which through binding of purinergic ( $P2_{Y2}$ ) receptors leads to endothelial nitric oxide synthase (eNOS) activation (Sprague *et al.*, 1996), in addition to shear dependent serine threonine specific protein kinase (Akt) activation of eNOS (Dimmeler *et al.*, 1998, 1999; Fulton *et al.*, 1999). Further, acidosis itself stimulates ATP release from red blood cells (Bergfeld & Forrester, 1992; Ellsworth *et al.*, 1995). Finally, within the lumen, acidic disproportionation (note: non-enzymatic production) of nitrite ( $NO_2^-$ ) into NO can occur (Zweier *et al.*, 1995; Modin *et al.*, 2001). Within endothelial cells (EC), NO production occurs as a result of the aforementioned shear and ATP mechanisms. In addition, activation of phospholipase- $A_2$  (PLA $_2$ ) hydrolyzes arachidonic acid (AA) from membrane phospholipids which is then, via cyclooxygenase, converted into prostaglandins (PGs), with the relevant vasodilator prostaglandins being PGE $_2$  and PGI $_2$ . Increased PG synthesis also occurs in astrocytes in response to hypercapnia (Howarth *et al.*, 2017). Prostaglandin production leads to concurrent reactive oxygen species (ROS) production (Kontos *et al.*, 1980, 1985) which may influence CO $_2$  reactivity by direct vasodilator effects (Rosenblum, 1983*b*) or NO scavenging (Thomas *et al.*, 2008), although experimental evidence for this is lacking (see text). At the level of the vascular smooth muscle cells (VSMC), increased adenosine levels (Phillis & O'Regan, 2003; Dulla *et al.*, 2005) leads to binding of A $2A$  receptors and consequent adenylate cyclase activation. Activation of EP and IP prostaglandin receptors on the VSMC (Narumiya *et al.*, 1999; Davis *et al.*, 2004) also contribute to adenylate cyclase activation. Adenylate cyclase activation leads to upregulation of cyclic adenosine monophosphate (cAMP) activity. This cAMP acts via activation of cAMP dependent protein kinase, also termed protein kinase-A (PKA), as well as by increasing potassium ( $K^+$ ) channel conductance (Song & Simard, 1995). Soluble guanylate cyclase (sGC) activation occurs downstream of NO production (Arnold *et al.*, 1977; Miki *et al.*, 1977), from both the endothelial cells (eNOS derived) and from neurons [neuronal NOS (nNOS) derived] (Wang *et al.*, 1995; Iadecola & Zhang, 1996; Okamoto *et al.*, 1997). This leads to upregulation of cyclic guanosine monophosphate (cGMP) and consequent activation of cGMP dependent protein kinase, also termed protein kinase-G (PKG) (Rapoport & Murad, 1983; Rapoport *et al.*, 1983). Cross talk between cGMP and cAMP should also be considered (see text). Both NO (Bolotina *et al.*, 1994) and cGMP (Archer *et al.*, 1994; Han *et al.*, 2001; Chai *et al.*, 2011) also increase  $K^+$  channel conductance. Overall, the increases in  $K^+$  channel conductance may lead to VSMC hyperpolarization, inhibiting calcium ( $Ca^{2+}$ ) influx through voltage dependent  $Ca^{2+}$  channels while both PKA and PKG phosphorylate and deactivate myosin light chain kinase (MLCK) leading to reduced calcium sensitivity of the VSMC and vasodilation (relaxation) (Adelstein *et al.*, 1978; Kerrick & Hoar, 1981).

### ***2.5.6.1 HYPERCAPNIA AND ADENOSINE***

Purinergic P<sub>1</sub> receptors that respond to adenosine are located on vascular smooth muscle cells, with their stimulation leading to vasodilation (Hardebo *et al.*, 1987). Adenosine A<sub>2A</sub> receptors are the main class of P<sub>1</sub> receptors that transduce the vasodilatory signal of adenosine (Ngai *et al.*, 2001) and are expressed on human cerebral blood vessels (Kalaria & Harik, 1988). Their stimulation occurs both on the extracellular surface and intracellularly as demonstrated in feline, but not human pial arterioles (Hardebo *et al.*, 1987). Increased adenosine and A<sub>2A</sub> stimulation leads to the activation of adenylate cyclase (Anand-Srivastava *et al.*, 1982) and therefore cAMP.

Increases in CO<sub>2</sub> have been demonstrated to increase cerebral adenosine levels *in vitro* (Dulla *et al.*, 2005) and *in vivo* (Phillis & O'Regan, 2003). *In vivo* adenosine receptor antagonism (Phillis & DeLong, 1987; Estevez & Phillis, 1997) and application of adenosine deaminase (Simpson & Phillis, 1991) both reduce CBF or pial arteriolar dilation to hypercapnia in animals. Moreover, the response to hypercapnia is potentiated by the administration of dipyridamole and adenosine deaminase inhibitors, which both increase adenosine concentrations (Phillis & DeLong, 1987). While some studies do not provide experimental support for a role of adenosine in hypercapnic vasodilation (Morii *et al.*, 1987b; Pelligrino *et al.*, 1995b; Meno *et al.*, 2001; Phillis & O'Regan, 2003), the production of adenosine during hypercapnia (Phillis & O'Regan, 2003) in addition to the low concentrations of adenosine required to induce vasodilation, at least in animal models (Morii *et al.*, 1986), strongly support the notion that adenosine is implicated in hypercapnic CBF regulation.

The rat model has demonstrated a high sensitivity to adenosine, with a 10<sup>-8</sup>M adenosine superfusate dilating pial arterioles (Morii *et al.*, 1986) with other species also demonstrating dilation to adenosine (Joshi *et al.*, 2002). However, despite dilation of *in vitro* human pial arterioles to ~10<sup>-5</sup>M adenosine, cerebral blood concentrations of approximately 10<sup>-6</sup> to 10<sup>-5</sup>M secondary to intracarotid adenosine infusion do not alter CBF in living, albeit anesthetized (fentanyl, midazolam, droperidol & propofol), humans (Joshi *et al.*, 1998). In keeping with the different cerebrovascular sensitivities to adenosine between rat and humans, the role of adenosine in hypercapnic vasodilation observed in animals does not appear operational in humans. Although findings regarding basal CBF and increases (e.g.,

dipyridamole) or decreases (e.g., caffeine) in adenosine mediated signal transduction are highly variable – likely due to poorly managed MAP and/or PaCO<sub>2</sub> (Cameron *et al.*, 1990; Ito *et al.*, 1999, 2002*b*; Kruuse *et al.*, 2000; Blaha *et al.*, 2007; Xu *et al.*, 2015) – the available studies indicate CO<sub>2</sub> reactivity is unaltered following adenosine receptor antagonism (Blaha *et al.*, 2007; Chen & Parrish, 2009). It is, however, important to consider the washout time for caffeine prior to these studies in humans. For example, as the half-life of caffeine is approximately 5.5 hours (Statland & Demas, 1980), and subjects in the study by Blaha *et al.*, were only asked to refrain from caffeine containing beverages for 6 hours, pre-existing caffeine may have contaminated baseline recordings making it difficult to draw strong conclusions (Blaha *et al.*, 2007). Further, the animal studies demonstrating increased adenosine concentration with hypercapnia utilized a 10% CO<sub>2</sub> stimulus, whereas the human studies conducted to date have utilized 5% (Chen & Parrish, 2009) and 6% (Blaha *et al.*, 2007) CO<sub>2</sub> challenges. A greater severity of hypercapnia is required to determine if the role of adenosine in CO<sub>2</sub> reactivity is negligible as current data suggest, or rather severity dependent. Researchers investigating the role of adenosine in human cerebrovascular CO<sub>2</sub> reactivity must also consider the complexities associated with using non-selective antagonists (Chen *et al.*, 2013). Further, methylxanthines (e.g. caffeine & theophylline) also inhibit phosphodiesterase (PDE) activity (Poison *et al.*, 1978; Beavo, 1995). This has obvious implications for VSMC tone, given PDE inhibition related reductions in the enzymatic degradation of cGMP and cAMP (Rybalkin *et al.*, 2003; Bubb *et al.*, 2014), which may increase CBF (Yu *et al.*, 2000).

#### **2.5.6.2 HYPERCAPNIA AND ARACHIDONIC ACID METABOLITES**

Prostaglandins are produced from arachidonic acid (Weksler *et al.*, 1977) downstream of phospholipase activity (Kunze & Vogt, 1971). It is important to also consider that lipoxygenase and epoxygenase utilize arachidonic acid as substrate to produce 20-hydroxyeicosatetraenoic acid and epoxyeicosatrienoic acids, respectively. The potential roles of these two eicosanoids will be briefly discussed following a focus on PGs.

Cyclooxygenase is one of two main enzymes involved in converting arachidonic acid to PGs (Smith *et al.*, 1991; Smith, 1992), thus the majority of studies investigating the role of PGs in CO<sub>2</sub> reactivity have implemented COX inhibition. As PGI<sub>2</sub> has a relatively short half-life (~30 seconds) and the more stable PG's are quickly metabolized, it is likely that

PG's primarily mediate effects localized to their production site, thus necessitating this production via cerebral vessels (Narumiya *et al.*, 1999).

The production of PG's appears to occur in both endothelial (Weksler *et al.*, 1977; Messina *et al.*, 1992; Hsu *et al.*, 1993) and smooth muscle (Parfenova *et al.*, 1995a) cells, with the presence of PG synthases (Boullin *et al.*, 1979) and PG production in the cerebral circulation of animals (Hagen *et al.*, 1979; Gecse *et al.*, 1982; Parfenova *et al.*, 1995b) and humans (Boullin *et al.*, 1979; Abdel-halim *et al.*, 1980) demonstrated *in vitro*. More recently, a role for astrocytic PGE<sub>2</sub> production in response to hypercapnia has been demonstrated as well (Howarth *et al.*, 2017). Addition of exogenous PG's to *in vitro* tissue baths, such as PGE<sub>2</sub>, PGI<sub>2</sub> and iloprost (a synthetic PGI<sub>2</sub> analogue) dilate larger cerebral arteries (e.g., VA, MCA and BA) in animals (Boullin *et al.*, 1979; Paul *et al.*, 1982; Whalley *et al.*, 1989; Parsons & Whalley, 1989) and humans (Boullin *et al.*, 1979; Paul *et al.*, 1982; Parsons & Whalley, 1989; Davis *et al.*, 2004) as well as the pial arterioles (Welch *et al.*, 1974; Ellis *et al.*, 1979). This signal transduction occurs via stimulation of the EP and IP prostaglandin receptors (Narumiya *et al.*, 1999; Davis *et al.*, 2004). However, the vasodilatory effect of PGE<sub>2</sub> appears exclusive to the anterior circulation as it dilates MCA segments (Davis *et al.*, 2004), but constricts BA segments (Toda & Miyazaki, 1978; Parsons & Whalley, 1989). These regional differences may be due to differences in dish preparation, pre-contractile agents, and concentrations of PGI<sub>2</sub> (or related analogues) used (Uski *et al.*, 1983); such differences could also be indicative of regionally specific cerebrovascular regulation by PG's.

*In vivo* topical application of arachidonic acid (e.g., 200µg/mL in artificial cerebrospinal fluid) stimulates increased cerebral PG production (Kontos *et al.*, 1985; Ellis *et al.*, 1990; Leffler *et al.*, 1993) and subsequent pial vessel dilation in various animal models (Wei *et al.*, 1980; Kontos *et al.*, 1984; Ellis *et al.*, 1990; Leffler *et al.*, 1990, 1993), while application of PGs themselves possesses the same effect (Wahl *et al.*, 1973, 1989, Leffler & Busija, 1985, 1987; Parfenova *et al.*, 1995b). Similar to topical application of arachidonic acid, hypercapnia increases cerebral PG synthesis *in vivo* (Leffler *et al.*, 1993; Parfenova *et al.*, 1994) and in cultured endothelial cells (Parfenova & Leffler, 1996). Inhibition of PG synthesis with the administration of indomethacin, a non-selective COX inhibitor results in a marked reduction of cerebrovascular CO<sub>2</sub> reactivity in animals (Pickard & MacKenzie, 1973; Wagerle & Mishra, 1988; Leffler *et al.*, 1993, 1994). However, it seems

indomethacin more consistently reduces CO<sub>2</sub> reactivity than other COX inhibitors (Chemtob *et al.*, 1991; Parfenova *et al.*, 1995b) with two studies also suggesting a specific role of cyclooxygenase-1 (COX<sub>1</sub>) inhibition in reducing CO<sub>2</sub> reactivity (Niwa *et al.*, 2001; Howarth *et al.*, 2017). This unique influence of indomethacin in animal studies is in accordance with human studies. Indeed, irrespective of the measurement technique used, non-selective COX inhibition with indomethacin causes an approximate 20-30% reduction in resting CBF. This has been exemplified in studies utilizing TCD (Markus *et al.*, 1994; Kastrup *et al.*, 1999a; Xie *et al.*, 2006a; Fan *et al.*, 2010b), duplex ultrasound (Hoiland *et al.*, 2015, 2016b), the Kety & Schmidt technique (Eriksson *et al.*, 1983; Wennmalm *et al.*, 1984), and various MRI techniques (Bruhn *et al.*, 2001; St. Lawrence *et al.*, 2002). Yet, resting CBF is largely unaffected by a wide array of other COX inhibitors such as acetylsalicate (Eriksson *et al.*, 1983; Wennmalm *et al.*, 1984; Markus *et al.*, 1994; Bruhn *et al.*, 2001), naproxen (Eriksson *et al.*, 1983; Wennmalm *et al.*, 1984; Hoiland *et al.*, 2016b), sulindac (Markus *et al.*, 1994), and ketorolac (Hoiland *et al.*, 2016b) [See Table 1 in (Hoiland & Ainslie, 2017)]. One study to date has reported a reduction in baseline CBF in response to Naproxen; however, this study used peak systolic MCAv as its index of flow, which is a poor index of true volumetric flow (Szabo *et al.*, 2014). Infusion of PGI<sub>2</sub> counter-intuitively causes a slight reduction in CBF in humans (~8%); however, it is likely that this effect is due systemic vasodilation related reductions in MAP (Brown & Pickles, 1982; Pickles *et al.*, 1984).

Cerebrovascular CO<sub>2</sub> reactivity is reduced by approximately 40-60% following indomethacin (Eriksson *et al.*, 1983; Wennmalm *et al.*, 1984; Kastrup *et al.*, 1999a; Xie *et al.*, 2006b; Hoiland *et al.*, 2015, 2016b), with reductions apparently greater in grey matter than white matter (St. Lawrence *et al.*, 2002). Similar to the effect reported on resting CBF, reductions in cerebrovascular CO<sub>2</sub> reactivity following COX inhibition are exclusive to the use of indomethacin, despite other drugs (i.e., aspirin & naproxen) effectively inhibiting PG synthesis (Eriksson *et al.*, 1983). Upon chronic use of indomethacin (e.g., three days) CO<sub>2</sub> reactivity is apparently restored to normal (Pickles *et al.*, 1984). However, chronic treatment with indomethacin for one week has been contrastingly shown to reduce CO<sub>2</sub> reactivity (Eriksson *et al.*, 1983). Whether this difference over time (i.e., three days versus one week) is a result of methodological differences between studies or a time dependent effect of indomethacin is unclear. Due to the unique ability of indomethacin to reduce CO<sub>2</sub> reactivity it has been proposed - although not clearly established - that indomethacin

induced impairments in resting CBF and CO<sub>2</sub> reactivity are due to a mechanism independent of PG synthesis inhibition (Eriksson *et al.*, 1983; Markus *et al.*, 1994; Hoiland & Ainslie, 2016b, 2017; Hoiland *et al.*, 2016b). This unique influence of indomethacin is likely related to its inhibition of cAMP dependent protein kinase (Kantor & Hampton, 1978; Goueli & Ahmed, 1980). Indeed, as highlighted throughout this thesis, cAMP is an integral component of many signaling pathways that are relevant for cerebrovascular regulation.

As previously mentioned, flux through the arachidonic acid pathway produces three potential end products; PG's (via COX); 20-hydroxyeicosatetraenoic acid (20-HETE; via lipoxygenases); and EET's (via epoxygenases). There are multiple EETs (5,6-EET; 8,9-EET; 11,12-EET; and 14,15-EET), all of which may confer vasodilatory responses (Leffler & Fedinec, 1997), but there is evidence rather that 5,6-EET is the most, if not only, vasoactive EET (Ellis *et al.*, 1990). As EETs are formed downstream of arachidonic acid, and phospholipase inhibition has been demonstrated to inhibit the CBF response to hypercapnia, at least in newborn piglets, it stands to reason that EET dependent mechanisms may be in part responsible for CO<sub>2</sub> mediated cerebral vasodilation (Wagerle & Mishra, 1988). 20-HETE is a vasoconstrictor eicosanoid. Inhibition of lipoxygenase, which inhibits the production of 20-HETE augments CO<sub>2</sub> reactivity in newborn piglets (Wagerle & Mishra, 1988) indicating it may normally counteract a portion of CO<sub>2</sub> induced vasodilation. The influence of EETs and 20-HETE on cerebrovascular CO<sub>2</sub> reactivity in humans has yet to be investigated.

### **2.5.6.3 HYPERCAPNIA AND NITRIC OXIDE**

Hypercapnia increases brain cGMP *in vivo* in rats, indicating a role for NO in mediating the observed hypercapnic vasodilation (Irikura *et al.*, 1994). Intravenous administration of non-selective NOS inhibitors reduces pial vessel dilation and/or CBF in response to hypercapnia in multiple *in vivo* animal models (Wang *et al.*, 1992, 1994a, 1994b; Niwa *et al.*, 1993; Pelligrino *et al.*, 1993; Bonvento *et al.*, 1994; Faraci *et al.*, 1994; Goadsby, 1994; Horvath *et al.*, 1994; Iadecola & Zhang, 1994, 1996; Sandor *et al.*, 1994; Thompson *et al.*, 1996; Estevez & Phillis, 1997; Smith *et al.*, 1997a, 1997b). This reduction in pial vessel dilation occurs in concert with reduced brain cGMP levels (Irikura *et al.*, 1994). The level of contribution of NO to hypercapnic vasodilation appears to vary with the severity of

hypercapnia, with its influence decreasing as the level of hypercapnia increases (Faraci *et al.*, 1994; Iadecola & Zhang, 1994; Wang *et al.*, 1994b). This may be related to upregulation of other signaling pathways in response to severe acidosis. Independent of CO<sub>2</sub> levels NOS inhibition reduces pial vessel dilation to superfusion of acidic mock-CSF, indicating that the effects of NOS inhibition are indeed related to blocking of pH mediated signal transduction versus that of direct CO<sub>2</sub> effects (Niwa *et al.*, 1993). While the above studies indicate a role of NO at the level of the pial vessels, the vasodilatory response of *in vitro* excised cerebral parenchymal vessels appears unaffected by L-NAME, indicating the role of NO may possess segmental variation (Dabertrand *et al.*, 2012), methodological differences acknowledged. Overall, *in vivo* animal studies indicate that NO is integral to cerebral vasodilation during hypercapnia.

In studies where NO donors or cGMP analogues, but not NO independent vasodilators (Iadecola *et al.*, 1994), were administered to restore baseline flow and vessel tone in the presence of NOS inhibition, the CBF response to hypercapnia was no longer impaired (Iadecola *et al.*, 1994; Sandor *et al.*, 1994; Iadecola & Zhang, 1996; Smith *et al.*, 1997b; Wang *et al.*, 1998). These findings lead to the hypothesis that the presence of NO is required for normal hypercapnic vasodilation, but that NO may regulate cerebrovascular CO<sub>2</sub> through permissive action rather than CO<sub>2</sub>/pH mediated NOS upregulation (Brian, 1998). This permissive action may represent a downstream interaction with other signaling pathways. However, an elegant study by Wang and colleagues in 1998 demonstrated that potassium channel blockade does not reduce cerebral vasodilation during severe hypercapnia under normal conditions, but in rats under systemic NOS blockade, potassium channel blockade abolished the restored vasodilation associated with cGMP repletion and hypercapnia (Wang *et al.*, 1998). These findings indicate that the mechanistic control of these two pathways (normal CO<sub>2</sub> reactivity versus NOS blockade and cGMP replete reactivity) possess differing regulation, or, both involve redundant overlap of NOS and potassium channel regulation that is only unmasked following multiple blockades. Indeed, nitric oxide (Bolotina *et al.*, 1994) and cGMP dependent protein kinase (Archer *et al.*, 1994; Han *et al.*, 2001; Chai *et al.*, 2011) have been shown to directly affect calcium-dependent potassium channel conductance.

Genetic knockout models have sought to further attribute the regulation of CO<sub>2</sub> reactivity to specific NOS isoforms, nNOS and eNOS, given most studies use non-selective NOS

inhibitors (e.g., L-NMMA). In a nNOS genetic knockout model, non-selective NOS inhibition has no effect on the CBF response to hypercapnia, despite causing marked reductions in reactivity in wild-type mice expressing nNOS within cerebral arterioles, which clearly demonstrates an integral role of nNOS in CO<sub>2</sub> reactivity (Irikura *et al.*, 1995). In keeping, inhibition of cerebrovascular CO<sub>2</sub> reactivity by selective nNOS inhibition has been demonstrated in multiple studies (Wang *et al.*, 1995; Iadecola & Zhang, 1996; Okamoto *et al.*, 1997). Studies demonstrating maintained hypercapnic reactivity following endothelial injury (Wang *et al.*, 1994a) or denudation (Toda *et al.*, 1993) further support a specific role for nNOS derived NO in cerebrovascular CO<sub>2</sub> reactivity. Shortly after systemic infusion of a non-selective NOS inhibitor (<15min), acetylcholine mediated dilation is nearly abolished yet pial arteriolar dilation to hypercapnia is largely preserved further supporting the notion eNOS derived NO may not be integral for hypercapnic CO<sub>2</sub> reactivity (Irikura *et al.*, 1994). The relevant nNOS for hypercapnic NO mediated vasodilation is seemingly located throughout the parenchyma and mediated by central pathways, as transection of perivascular nitrenergic nerves originating from the sphenopalatine ganglia does not influence hypercapnic CO<sub>2</sub> reactivity, at least in rats (Iadecola *et al.*, 1993).

*In vitro*, hypercapnia has been demonstrated to increase NO in isolated human cerebrovascular endothelial cells and astrocytes (Fathi *et al.*, 2011). Few studies have been conducted in humans examining the influence of NOS blockade on cerebrovascular CO<sub>2</sub> reactivity. Intra-carotid infusion of L-NMMA reduces basal CBF as determined by the Xe<sup>133</sup> injection/scintillation technique in anesthetized patients (Joshi *et al.*, 2000). Cerebrovascular CO<sub>2</sub> reactivity studies using TCD have produced conflicting results demonstrating blunted CO<sub>2</sub> reactivity following NOS blockade (Schmetterer *et al.*, 1997) or no affect (White *et al.*, 1998; Ide *et al.*, 2007). Further, no influence of NOS blockade on acetazolamide stimulated CBF increases has also been reported (Lassen *et al.*, 2005). Notably, these aforementioned studies did not quantify changes in NO bioavailability or the magnitude of their blockade following NOS inhibition, while animal studies indicate >45% blockade of NOS activity is required to reduce CO<sub>2</sub> reactivity (Irikura *et al.*, 1994). This latter point may be due to compensation via cyclic nucleotide cross talk (see section “Cyclic nucleotide cross Talk”).

Administration of NO donors (e.g. sodium nitroprusside) have been demonstrated to increase (Jahshan *et al.*, 2017) or not affect (Lavi *et al.*, 2003) cerebral reactivity to hypercapnia. While animal studies largely support the notion nNOS primarily regulates NO-mediated hypercapnic vasodilation, classic work in animals as well as recent work in humans indicates shear stress may be an important regulatory factor secondary to the initial hypercapnic hyperemia implicating eNOS as an important CBF regulator for human cerebrovascular CO<sub>2</sub> reactivity (see following section “Hypercapnia and shear stress”). Further, patients with impaired endothelial function also possess a reduced CO<sub>2</sub> reactivity, indicating an important role of the endothelium in this response (Lavi, 2006).

While the above animal evidence for the dependence of cerebrovascular CO<sub>2</sub> reactivity on nNOS mediated NO formation but lack of NO dependence in humans are difficult to reconcile, other potential contributing “storage pools” of NO should be considered. Indeed, acidic disproportionation of nitrite to NO (Zweier *et al.*, 1995; Weitzberg & Lundberg, 1998) contributes to acidosis dependent vasorelaxation as demonstrated *in vitro* (Modin *et al.*, 2001). Increased plasma nitrite formation across the brain during hypercapnia has been demonstrate in humans that underwent radial arterial and jugular venous catheterization (Peebles *et al.*, 2008). While not explicitly demonstrated in the cerebral circulation, forearm blood flow studies in humans indicate that red blood cell bound and/or plasma nitrite (i.e., intravascular nitrite) contributes significantly to increases in blood flow during exercise, even in the setting of NOS inhibition (Gladwin *et al.*, 2000). Whether such compensation via non-enzymatic NO production exists during the cerebrovascular challenge of hypercapnia has yet to be determined in humans, but if present, may in part explain unaltered CO<sub>2</sub> reactivity following L-NMMA infusion in humans.

#### **2.5.6.4 HYPERCAPNIA AND ERYTHROCYTE RELEASED ATP AND ENOS**

Low pH (e.g. 7.0) settings, as would occur in hypercapnia, lead to release of ATP from erythrocytes (Bergfeld & Forrester, 1992; Ellsworth *et al.*, 1995). Further, increased shear/deformation of erythrocytes, which would follow hypercapnia induced hyperemia, also leads to ATP release from erythrocytes (Sprague *et al.*, 1996; Sprung *et al.*, 2002; Price *et al.*, 2004, 2006; Wan *et al.*, 2008). These ATP molecules then bind to endothelial purinergic receptors and upregulate eNOS activity and NO bioavailability (Sprague *et al.*, 1996). However, it should be noted that hypercapnia reduces the deformability of

erythrocytes (Kikuchi, 1979), which has implications for the magnitude of deformation induced erythrocyte release of ATP (Fischer *et al.*, 2003), and makes the potential role of this mechanism in hypercapnic cerebral vasodilation of humans unclear.

#### **2.5.6.5 HYPERCAPNIA AND REACTIVE OXYGEN SPECIES**

The role of ROS in the regulation of CVR-CO<sub>2</sub> should be considered in two separate contexts: 1) the role of ROS on cerebrovascular tone and the influence of free radical scavenging during hypercapnia, and 2) influence of chronically elevated ROS levels and how consequent reductions in endothelial function influence CVR-CO<sub>2</sub>. In animals, acute increases in ROS levels have been demonstrated to dilate pial vessels (Rosenblum, 1983*b*); however, cerebrovascular CO<sub>2</sub> reactivity is unaffected in animals by superoxide dismutase and/or catalase application (Rosenblum, 1983*b*; Kontos *et al.*, 1984; Wagerle & Mishra, 1988; Leffler *et al.*, 1991). This is in agreement with recently published data in healthy humans where antioxidant loading has no influence on CO<sub>2</sub> reactivity (Hansen *et al.*, 2018). When considering the chronic impact of ROS, it has been demonstrated that clinical populations (e.g., diabetes & hypertension) with endothelial dysfunction possess reduced CO<sub>2</sub> reactivity (Lavi, 2006). This would seemingly be due, at least in part, to the NO scavenging activity of free radicals, for example the scavenging of NO by superoxide (O<sub>2</sub><sup>-</sup>) to form peroxynitrite (ONOO<sup>-</sup>) (i.e. O<sub>2</sub><sup>-</sup> + NO → ONOO<sup>-</sup>) (Thomas *et al.*, 2008). Indeed, a recent study in COPD patients demonstrated using covariate analyses that ROS may underscore the impaired CO<sub>2</sub> reactivity in this population when compared to age matched controls (Hartmann *et al.*, 2012). Future studies that experimentally manipulate ROS, for example by antioxidant supplementation, will provide further insight into the role of ROS on CVR-CO<sub>2</sub> impairments in clinical populations.

#### **2.5.6.6 HYPERCAPNIA AND SHEAR STRESS**

The investigation of shear-mediated regulation of the cerebral vasculature in humans has received newfound attention (see section “Appendix A”). However, fifty years ago, it was demonstrated that increases in CBF in response to hypercapnia take about 30-60 seconds to complete and reach steady state (Shapiro *et al.*, 1966), which may be a result of the time needed for larger cerebral vessel dilation to occur and, therefore, indicate a role for endothelial released NO. Such is the case in the large peripheral arteries (e.g., brachial),

where shear stress mediated dilation takes ~30 seconds to occur (Black *et al.*, 2008) and is driven largely by NO (Green *et al.*, 2014). Further, steady state elevations in CBF are reported to have higher cerebral vascular reactivity than non-steady state tests [e.g., rebreathing (Pandit *et al.*, 2003)]. This disparity in reactivity may be explained by the time dependent nature of shear-mediated eNOS upregulation and consequent NO mediated vasodilation, which may not be fully engaged at the termination of a progressive and dynamic stimulus.

Since the study by Shapiro and Colleagues (Shapiro *et al.*, 1966), *in vivo* and *ex vivo* studies of cerebrovascular shear-mediated dilation have demonstrated disparate results (Koller & Toth, 2012), with *in vivo* study demonstrating shear-mediated regulation of CBF, but *ex vivo* study producing inconsistent results (i.e., dilation, constriction, biphasic responses). Of note, there are two stark differences between *ex vivo* and *in vivo* preparations that will impact shear-mediated responses. First, *ex vivo* preparations typically using physiological salt solution do not simulate the viscosity of blood, and typically lack pulsatile flow pumps. The only *ex vivo* studies demonstrating a role for shear-mediated CBF regulation used a peristaltic pump (Drouin & Thorin, 2009; Drouin *et al.*, 2011), which may have provided adequate simulation of *in vivo* hemodynamics, although to what extent is unknown. Second, relating *ex vivo* to *in vivo* preparations is further limited in that *ex vivo* responses to increased intraluminal shear using physiological salt solution appear to be endothelium independent (Garcia-Roldan & Bevan, 1991; Madden & Christman, 1999). This endothelium independent response may be due to the low relative viscosity of physiological salt solution compared to blood (~1 vs. 4, respectively) and consequent inability to appropriately stimulate the endothelium. However, *in vivo* animal models have collectively demonstrated cerebral shear-mediated dilation (Fujii *et al.*, 1991, 1992; Paravicini *et al.*, 2006). Indeed, a more recent study, in a well-controlled mouse model, demonstrated that the cerebrovascular endothelium optimally couples shear stress to eNOS-mediated dilation under physiological pulse pressures, in contrast to static flow conditions (Raignault *et al.*, 2016). These findings strongly infer that changes in the diameter of cerebral arteries are responsive to a pulsatile environment and that shear stress sensitivity and consequent production of NO are optimized under *in vivo* conditions.

Recent experiments in humans from our group (Carter *et al.*, 2016a; Hoiland *et al.*, 2017c; Smith *et al.*, 2017) (**Figure 2.30**) and others (Iwamoto *et al.*, 2018) provide preliminary

evidence of shear-mediated regulation of CBF, as demonstrated in hypercapnia. Importantly, *in vitro* study has demonstrated increased NO bioavailability in cerebral artery endothelial cells exposed to shear stress (Mashour & Boock, 1999). While the importance of shear-mediated dilation in CO<sub>2</sub> reactivity has yet to be demonstrated following pharmacological NOS blockade, that vasodilatory responses of large cerebral arteries such as the ICA (Carter *et al.*, 2016a; Hoiland *et al.*, 2017c) and MCA (Coverdale *et al.*, 2015) are delayed by ~60 seconds, and occur independent of sustained hypercapnia (Hoiland *et al.*, 2017c), indicate the potential of an endothelium dependent shear-mediated regulation of cerebrovascular CO<sub>2</sub> reactivity in these arteries. Notably, while SNA has been demonstrated not to influence CVR (i.e., flow response; see section “CO<sub>2</sub> reactivity and sympathetic nervous activity”), it does possess an independent influence on vessel diameter whereby sympathoexcitation from lower body negative pressure (-20mmHg) reduces shear mediated dilation of the ICA (Iwamoto *et al.*, 2018). Given the importance of larger cerebral conduit arteries in cerebral vascular regulation and CO<sub>2</sub> reactivity (See section “CO<sub>2</sub>: site(s) of vascular regulation”), future research is imperative to fully understand the contribution of shear-mediated dilation of large resistance vessels in the brain (see section “Appendix A”).

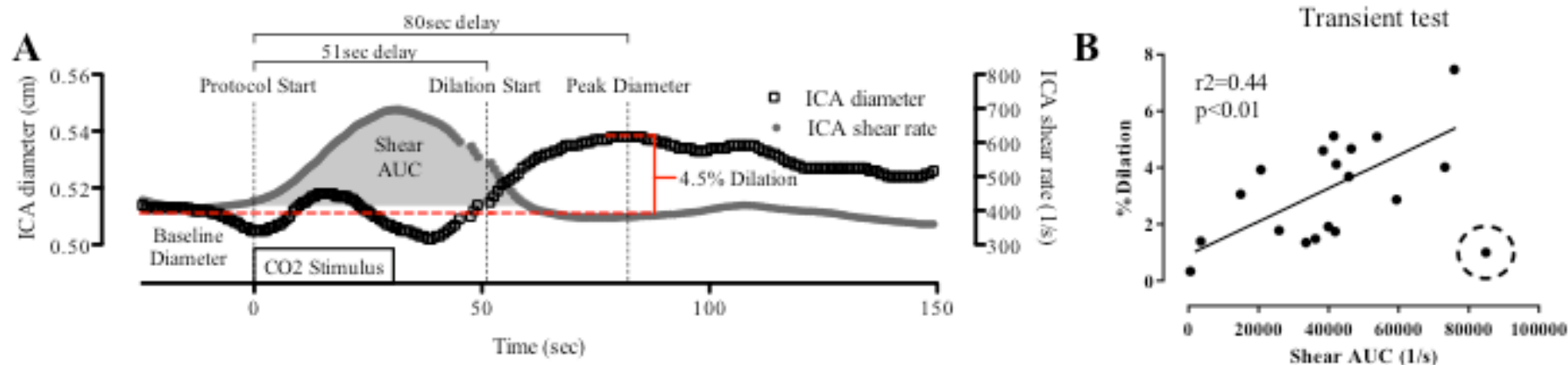


**Figure 2.30. Transient increases in shear stress and internal carotid artery vasodilation.**

Panel A. Via carbon dioxide manipulation, a transient (~30 second) increase in shear stress elicits vasodilation of the internal carotid artery. This increase in internal carotid artery (ICA) diameter occurs following return of carbon dioxide and shear to baseline levels, and follows similar temporal pattern to that of a brachial FMD test. (Thijssen *et al.*, 2011) Panel B. In the transient carbon dioxide test shown on the left, shear stress area under the curve (AUC) was positively correlated to the magnitude of vasodilation (following removal of a statistical outlier — circled). This implicates shear as a potential regulator of cerebral conduit artery vasomotor tone. This represents data recently published by our group. (Hoiland *et al.*, 2017c). Reproduced with permission.

### 2.5.6.7 HYPERCAPNIA AND POTASSIUM CHANNELS

Potassium ( $K^+$ ) channels are present in cerebrovascular smooth muscle cells and their impact on membrane potential is an important regulator of vascular tone (Faraci & Sobey, 1998; Rosenblum, 2003). Activation of  $K^+$  channels increases  $K^+$  conductance resulting in efflux of  $K^+$  from vascular smooth muscle cells and consequent hyperpolarization and relaxation. Inhibition of  $K^+$  channels contrastingly reduces  $K^+$  conductance resulting in depolarization and constriction.

*In vitro* evidence, albeit from non-cerebral preparations, indicate that a reduction in pH activates ATP sensitive potassium channels ( $K_{ATP}$  channels) (Davies, 1990; Wang *et al.*, 2003), which would lead to vasodilation. In keeping, outward  $K^+$  current of cerebral smooth muscle cells is markedly increased following a reduction in pH (Bonnet *et al.*, 1991) and increased perivascular  $[K^+]$  relaxes cerebral VSMCs (Kuschinsky *et al.*, 1972). While some studies suggest a negligible role of  $K_{ATP}$  channels in cerebral vascular regulation *in vitro* (Dabertrand *et al.*, 2012),  $K_{ATP}$  activation dilates cerebral arteries (Nagao *et al.*, 1996) and channel blockade has been demonstrated to completely abolish parenchymal arteriole dilation to hypercapnia in rat brain slices (Nakahata *et al.*, 2003). Importantly, acidosis leads to increased activation of calcium sensitive potassium channels ( $BK_{Ca}$ ) in isolated parenchymal cerebral arteries (Dabertrand *et al.*, 2012).

Looking at the *in vivo* model, pharmacological activation of  $K_{ATP}$  channels increases CBF in eucapnic conditions, demonstrating the vasomotor influence of  $K_{ATP}$  channel conductance (Reid *et al.*, 1995). During acidosis, with, or without (Santa *et al.*, 2003) elevated  $PaCO_2$ ,  $K_{ATP}$  channel blockade reduces the vasodilatory response. However, reductions in pial vessel dilation seemingly occur only during moderate hypercapnia (e.g., ~55 mmHg) (Faraci *et al.*, 1994; Kontos & Wei, 1996), with no effect at more severe levels (e.g., ~65 mmHg) (Reid *et al.*, 1993, 1995; Faraci *et al.*, 1994). An attenuated CBF response to severe hypercapnia (67mmHg) following  $K_{ATP}$  channel blockade has, however, been demonstrated in cats (Kontos & Wei, 1996) suggesting  $K_{ATP}$  channel activation is obligatory for hypercapnic vasodilation irrespective of the severity of hypercapnia. That the role of potassium channel inhibition on the CBF response to hypercapnia is important, but reduced at higher levels of  $PaCO_2$  is corroborated by *in vitro* studies on basilar artery relaxation to acidosis (Kinoshita & Katusic, 1997).

To our knowledge, only one study has assessed the role of  $K_{ATP}$  channels in the regulation of CVR in healthy humans. The primary finding was that inhibition of  $K_{ATP}$  channels with glibenclamide has no effect on the blood velocity response through the MCA during hypercapnia (Bayerle-Eder *et al.*, 2000); however, as  $K_{ATP}$  channels directly affect vascular tone it is difficult to extrapolate velocity measures to represent volumetric CBF in this instance.

Overall, potassium channels regulate cerebrovascular smooth muscle tone (at least in animals) downstream of several vasoactive factors which are implicated in  $CO_2$  mediated cerebrovascular vasodilation: NO [via cyclic guanosine monophosphate (cGMP)], Adenosine, EETs, and PGs [via cyclic adenosine monophosphate (cAMP)].

#### **2.5.6.8 HYPERCAPNIA AND BICARBONATE ION**

There is some evidence that alterations in  $[HCO_3^-]$  may possess independent influences on  $CO_2$  reactivity. For example, reductions in  $[HCO_3^-]_o$  directly increases cerebral vascular tone via a mechanism that requires receptor protein tyrosine phosphatase binding in isolated rat BAs, which is an endothelium dependent response (Boedtkjer *et al.*, 2016). In support of this data is that  $HCO_3^-$  appears to stimulate soluble adenylyate cyclase activity in a manner independent of pH (Chen, 2000). In humans, arterial  $[HCO_3^-]$  increases modestly during a hypercapnic challenge ( $\uparrow 1$  meq/L) (unpublished observations), which would theoretically facilitate  $CO_2$  reactivity when considering the aforementioned animal data. Given the minimal numbers of studies investigating the independent influence of  $HCO_3^-$ , more studies are required to determine if it plays an important role in  $CO_2$  reactivity, especially in humans.

### **2.5.7 POTENTIAL SIGNALING PATHWAY INTERACTIONS**

#### **2.5.7.1 NITRIC OXIDE AND $K_{ATP}$ CHANNELS**

$K_{ATP}$  channel blockade does not influence cerebral artery dilation to exogenous NO donors or acetylcholine, indicating that  $K_{ATP}$  channel activation does not possess an obligatory contribution to vasodilation following increased NO (Faraci *et al.*, 1994; Kontos & Wei,

1996; Kinoshita & Katusic, 1997) (see section “Hypercapnia and nitric oxide”). Yet, NOS blockade abolishes pial arteriolar dilation to cromakalim, indicating increased  $K_{ATP}$  channel conductance may be dependent upon increases in NO. In terms of hypercapnic reactivity, following a blunting of the CBF response to  $CO_2$  by  $K_{ATP}$  channel blockade, nitro-L-arginine (a NOS inhibitor) provides no additional attenuation of hypercapnic  $CO_2$  reactivity (Kontos & Wei, 1996), further supporting the notion that  $K_{ATP}$  conductance may underlie, at least in part, a component of NO mediated hypercapnic vasodilation. In line with this notion, inhibition of NOS or soluble guanylate cyclase eliminates increases in  $K_{ATP}$  channel conductance that occur subsequent to increased cGMP (Miyoshi *et al.*, 1994). However, it is unclear exactly how NO activates  $K_{ATP}$  channels, with the method of action (e.g., direct NO effect, cGMP, or S-nitrosylation) variable depending on the prep used (Miyoshi *et al.*, 1994; Han *et al.*, 2001, 2002; Lin *et al.*, 2004; Kawano *et al.*, 2009). Of note, the study by Miyoshi *et al.*, demonstrating a reduced  $K_{ATP}$  channel conductance with soluble guanylate cyclase inhibition was conducted in vascular smooth muscle cells (Miyoshi *et al.*, 1994). The importance of an additional mechanism(s) for NO mediated signal transduction is highlighted in that inhibition of soluble guanylate cyclase does not reduce hypercapnic  $CO_2$  reactivity in cats or rats, indicating pathways apart from the prototypical NO/cGMP pathway are acting (Kontos & Wei, 1996; Rosenblum *et al.*, 2002). Thus increases in  $K_{ATP}$  channel conductance may fill this ‘gap’, although this atypical action of NO may also be in part related to increased conductance of  $BK_{Ca}$  channels (Robertson *et al.*, 1993; Bolotina *et al.*, 1994). Indeed, blockade of calcium activated potassium channels reduces the hypercapnic vasodilatory response to acidosis, with dilation to increased calcium activated potassium channel conductance dependent on NO activity (Lindauer *et al.*, 2003).

### ***2.5.7.2 CYCLIC NUCLEOTIDE CROSS TALK***

The potential for cyclic nucleotide interactions in VMSC control, or “cross talk”, in regulating cerebrovascular regulation is important to consider when investigating pathways that ostensibly regulate cAMP or cGMP levels in an independent manner. For example, as both PG and NO formation are predominantly endothelium dependent they are commonly thought to interact. While PGs lead to increased cAMP production (Leffler & Balabanova, 2001) and NO leads to increased cGMP production (Irikura *et al.*, 1994), interpretation of isolated blockade studies requires an understanding of how cerebral VSMC tone is influenced when one of these cyclic nucleotides, cAMP or cGMP, remains operational

(Pelligrino & Wang, 1998). The same is relevant for the potential interactions between adenosine related signaling ( $\uparrow$ cAMP) and NO signaling ( $\uparrow$ cGMP) (Kurtz, 1987).

Phosphodiesterases (PDEs) hydrolyze cyclic nucleotides and provide an avenue by which cyclic nucleotide cross talk may occur (Pelligrino & Wang, 1998). Different PDE isoforms possess greater reaction constants for either cyclic nucleotide, cAMP or cGMP, enabling diverse regulatory influences. Isoforms PDE-1 (Kakkar *et al.*, 1999) and PDE-5 primarily hydrolyze cGMP, while PDE-3 primarily hydrolyzes cAMP (Sharma, 1995). Conversely, cyclic nucleotides are also able to influence PDE activity. Indeed, cGMP inhibits PDE-3 (Degerman *et al.*, 1997) and PDE-4 (Willette *et al.*, 1997) activity, while cAMP and cAMP dependent protein kinase also reduce PDE activity (Sharma, 1995).

The importance of cyclic nucleotides and PDEs in cerebrovascular CO<sub>2</sub> reactivity is apparent in that hypercapnia leads to an increase in cAMP and cGMP concentrations (Parfenova *et al.*, 1993; Irikura *et al.*, 1994), while inhibiting PDE mediated hydrolysis of these cyclic nucleotides augments cerebrovascular CO<sub>2</sub> reactivity (Parfenova *et al.*, 1993). The cross talk between these cyclic nucleotides is outlined hereafter. In anesthetized rats with an installed cranial window, following nNOS blockade, superfusion of non-hydrolyzable cAMP or cGMP analogue restores CO<sub>2</sub> reactivity to baseline values. However, for example, independent superfusion of an adenylate cyclase activator (to increase endogenous cAMP production) or a PDE-3 inhibitor, do not appreciably restore CO<sub>2</sub> reactivity, although combined infusion returns CO<sub>2</sub> reactivity to near baseline values. This indicates that while following nNOS blockade, CO<sub>2</sub> reactivity is impaired to an extent by reduced signal transduction through the prototypical cGMP pathway, the disinhibition of PDE-3 following nNOS blockade and consequently increased hydrolysis of cAMP also contributes to the impaired reactivity. In other words, both endogenous production of cAMP, and reduced hydrolysis of this cAMP were required to elicit somewhat normal vascular reactivity. Further, it has been shown that increasing cAMP levels leads to increases in cGMP levels and pial vasodilation, but that this effect is minimized if tested subsequent to inhibition of the cGMP selective PDE-5, indicating that cAMP also influences cGMP mediated signal transduction via modulation of PDE-5 activity (Wright *et al.*, 1994). This latter point highlights the important of cyclic nucleotide “cross talk” in the regulation of cerebrovascular CO<sub>2</sub> reactivity. Additional avenues for cross talk is evidenced in that both cGMP and cAMP can activate cGMP dependent protein kinase

(Lincoln *et al.*, 1990; Jiang *et al.*, 1992; Francis & Corbin, 1994). Thus, there is a probable interaction between NO ( $\uparrow$ cGMP) and adenosine and/or PG ( $\uparrow$ cAMP) as both influence cGMP dependent protein kinase activation. This may explain why singular inhibition of various pathways seems ineffective in human cerebrovascular models (Markus *et al.*, 1994; White *et al.*, 1998; Bayerle-Eder *et al.*, 2000; Ide *et al.*, 2007; Hoiland *et al.*, 2016b). In support of this notion, following blockade of cGMP pathways (e.g., via NOS blockade) cAMP dependent process would theoretically still operate via both cAMP dependent protein kinase (Song & Simard, 1995) and cross-activation of cGMP dependent protein kinase as mentioned above.

In animal models the magnitude of reduction in reactivity with sequential blockade of PKG and PKA (in either order) is less following the second blockade than the first, indicating that by eliminating one protein's action you are in actuality reducing the function of both through direct [ $\downarrow$  activation of target protein (e.g. cGMP dependent protein kinase)] and indirect [ $\downarrow$ disinhibition of the degradation of the other protein by PDE's (e.g. PKA)] influences (**Figure 2.31**). This leads to an attenuated reduction of CO<sub>2</sub> reactivity following the second blockade given much of the role of that target protein was previously diminished in the first blockade (Pelligrino & Wang, 1998). An improved (Phillis & O'Regan, 2003) or complete (Estevez & Phillis, 1997) blockade of CO<sub>2</sub> reactivity is observed when both an adenosine receptor antagonist (non-selective or A<sub>2A</sub> elective) and L-NAME are combined. However, in human studies, independent administration of multiple different pharmacological enzyme or receptor blockers (e.g., L-NMMA, aminophylline/theophylline, ibuprofen or naproxen) does not reduce reactivity. In this context, perhaps, in contrast to the animal data, the un-targeted protein (e.g., cAMP dependent protein kinase when L-NMMA is infused) is able to compensate by upregulation. A potential explanation of this is modulation of phosphodiesterase hydrolyzation of the untargeted protein (either cAMP or cGMP) or activation of cGMP dependent protein kinase by cAMP (Lincoln *et al.*, 1990; Jiang *et al.*, 1992; Francis & Corbin, 1994) as discussed above. While necessary to determine this speculative point, signaling pathway interaction studies on human CBF regulation have not been conducted, likely due to the typical use of systemic blockades and potential dangers of drug interactions.

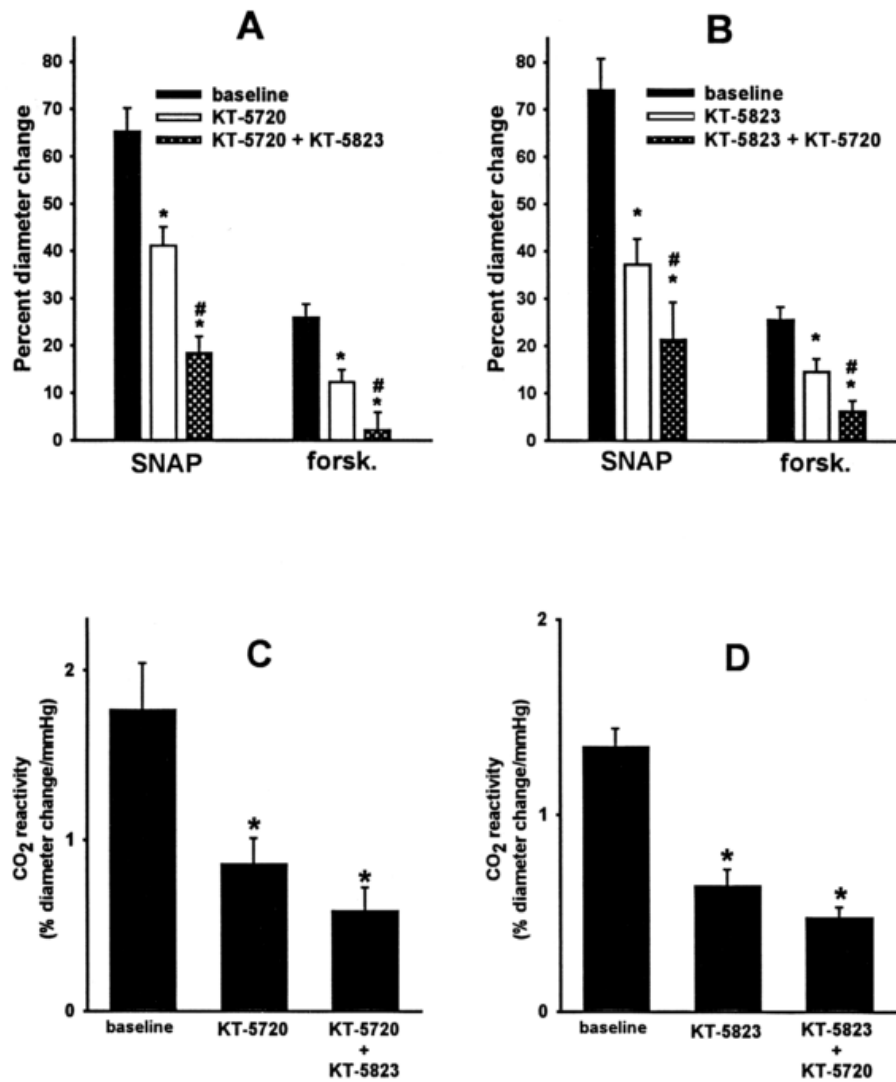


**Figure 2.31. Evidence for cyclic nucleotide cross talk in cerebrovascular regulation.**

This figure depicts the influence of cyclic nucleotide kinase blockers on the pial arteriolar diameter increases accompanying topical applications of the NO donor, SNAP and the adenylate cyclase activator, forskolin (A,B) and exposure to hypercapnia ( $\text{PaCO}_2 = 60\text{mmHg}$ ) (C,D). KT-5720, PKA-selective inhibitor; KT-5720, PKG selective inhibitor. Reproduced from (Pelligrino & Wang, 1998) with permission.

### 2.5.7.3 ARACHIDONIC ACID PATHWAY AND REACTIVE OXYGEN SPECIES PRODUCTION

Increased PG production, induced via topical application of arachidonic acid within a cranial window, leads to concomitant ROS production in cats (Kontos *et al.*, 1980, 1985) due to hydroperoxidase conversion of Prostaglandin-G to Prostaglandin-H (Kontos *et al.*, 1980; Kukreja *et al.*, 1986). The production of ROS resulting from the application of

arachidonic acid is inhibited to the same extent by superoxide dismutase and non-selective COX inhibition with indomethacin, suggesting that the increase in ROS are mediated via COX (or downstream enzyme, e.g. hydroperoxidase) activity (Kontos *et al.*, 1985).

Superoxide dismutase greatly reduces ( $\geq 50\%$ ) the cerebral dilation response to topical application of bradykinin (a peptide that causes downstream PG production and COX activity), in normal mice (Rosenblum, 1987; Niwa *et al.*, 2001), but not COX<sub>1</sub> null mice (Niwa *et al.*, 2001). This suggests COX<sub>1</sub> may be responsible for ROS release during flux through the arachidonic acid pathway (Niwa *et al.*, 2001). In addition to their effects on ROS production, superoxide dismutase and indomethacin equally block vasodilation to both 5,6-EET and arachidonic acid (Ellis *et al.*, 1990). The eicosanoid 5,6-EET is a COX substrate providing further evidence that COX dependent ROS formation results in cerebral vasodilation (Ellis *et al.*, 1990). While the implications of concurrent ROS production during PG synthesis in regulating cerebrovascular tone is unknown in humans, it has been shown that ROS inhibition with superoxide dismutase and catalase nearly abolishes the vasodilatory response to topical arachidonic acid application in cats (Kontos *et al.*, 1984) and rabbits (Ellis *et al.*, 1990). Further, pial arterioles of cats (Wei *et al.*, 1985), mice (Rosenblum, 1983a) and newborn pigs (Leffler *et al.*, 1990) dilate in response to increased ROS production. Taken together, at least at rest in animals, these studies indicate that pial vessel dilation in response to flux through the arachidonic acid pathway is largely due to ROS production secondary to COX activity.

There is some (Leffler *et al.*, 1991), albeit inconsistent (Ellis *et al.*, 1980) evidence that hypercapnia increases flux through the arachidonic acid pathway and consequent PG synthesis (Leffler *et al.*, 1991); Yet, contrary to topical administration of arachidonic acid, combined superoxide dismutase and catalase do not attenuate the vasodilatory response to increased PaCO<sub>2</sub> in cats (Kontos *et al.*, 1984), newborn pigs (Wagerle & Mishra, 1988; Leffler *et al.*, 1991) and mice (Rosenblum, 1983a). Interpretation of these inter-species data is, however, difficult given hypercapnic vasodilation in cats and rabbits does not appear to be related to PGs (Wei *et al.*, 1980; Busija, 1983; Busija & Heistad, 1983). Despite these species differences, reductions in hypercapnia mediated dilation following COX inhibition are likely attributable to a reduction in PGs rather than COX mediated ROS production (Leffler *et al.*, 1991). These studies highlight that the effects of ROS on vascular tone during increased PG synthesis at rest cannot be extrapolated to hypercapnic challenges, and

an interaction between the eicosanoid production and ROS mediated dilation does not appear relevant to hypercapnic vasodilation in animal models. This phenomenon remains to be studied in humans, but is likely also not relevant given PG synthesis, and therefore COX activity, do not appear obligatory for hypercapnic vasodilation (Eriksson *et al.*, 1983; Markus *et al.*, 1994; Hoiland *et al.*, 2016b; Hoiland & Ainslie, 2017) (see section “Hypercapnia and arachidonic acid metabolites”).

### **2.5.8 SYNOPSIS OF CEREBRAL BLOOD FLOW REGULATION BY CARBON DIOXIDE**

Even the slightest changes in PaCO<sub>2</sub> lead to meaningful alterations in CBF, with PaCO<sub>2</sub> the most potent regulator of CBF in healthy awake humans. Increases in PaCO<sub>2</sub> lead to elevations in CBF, while reductions in PaCO<sub>2</sub> decrease CBF. The cerebral vasculature is notably about twice as sensitive to increases in PaCO<sub>2</sub> than decreases; however, as outlined, multiple factors such as blood pressure influence reactivity and likely underlie this difference in CVR to hyper- and hypo- capnia. As CVR is widely measured, comparisons across laboratories are important for repeatability and accelerated development of knowledge unhindered by methodological disparities. Volumetric flow analyses such as duplex ultrasound, and high-spatial resolution techniques such as BOLD imaging are attractive avenues for the development of standardized CVR tests when utilized in conjunction with advanced gas control systems. While there is a relatively large amount of data characterizing CVR responses in humans, the majority of our understanding on which molecular pathways govern CVR is derived from animal studies. Human studies have to date produced equivocal results. Future research is required in humans to better understand the relevant signaling pathways underlying CVR.

### **2.6 SYNOPSIS OF LITERATURE REVIEW**

This literature review overviewed the history of cerebrovascular physiology and relevant advancements in measurement techniques. Further, following an outline of fundamental hemodynamic and vascular principles, CBF regulation in response to hypoxia and alterations in PaCO<sub>2</sub> were review in detail. Several patterns have hence emerged, and underlie several key considerations:

- 1) Cerebrovascular research is to a large extent limited by the inability to utilize direct measures of CBF (at least intra-cranially). This has led to poor reproducibility and difficulty in comparing results between studies, ultimately hindering forward movement in the investigation of cerebrovascular regulation. Thus, contriving suitable surrogate measures of CBF has been a constant focus of investigators.
- 2) The cerebral vasculature is exquisitely sensitive to changes in  $\text{CaO}_2$  and  $\text{PaCO}_2$ , with precise regulation in the face of arterial blood gas perturbations requisite for optimal functioning.
- 3) The mechanisms governing CBF regulation are poorly understood in humans. Despite clear mechanistic delineation in animal models, translation of these findings into applicable human models has yet to materialize.

The experimental chapters herein contain experimental protocols designed with these three points in mind. Rigorous measures, characterization of responses, and interrogation of signaling pathways are utilized to further our knowledge on hypoxic cerebral vasodilation in humans.

### 3 CHAPTER 3: ADENOSINE RECEPTOR DEPENDENT SIGNALING IS NOT OBLIGATORY FOR NORMOBARIC AND HYPOBARIC HYPOXIA-INDUCED CEREBRAL VASODILATION IN HUMANS

Reductions in  $\text{CaO}_2$  invoke increases in CBF (Kety & Schmidt, 1948c; Cohen *et al.*, 1967; Shapiro *et al.*, 1970; Hoiland *et al.*, 2016a) in order to maintain  $\text{CDO}_2$  in normobaric (Willie *et al.*, 2012; Ainslie *et al.*, 2014) and hypobaric hypoxia (Imray *et al.*, 2014; Ainslie & Subudhi, 2014). This increase in CBF occurs at a  $\text{PaO}_2$  of approximately 50-55 mmHg, where reductions in  $\text{PaO}_2$  lead to appreciable reductions in  $\text{CaO}_2$  – i.e., upon descending from the flat portion of the oxygen dissociation curve. For example, hypoxia leads to an increase in blood velocity through the MCA and PCA (Willie *et al.*, 2012; Ogoh *et al.*, 2013b; Hoiland *et al.*, 2015), and an increase in blood flow through the ICA and VA thus increasing gCBF (Lewis *et al.*, 2014b); however, this has been previously demonstrated to not occur until  $\text{PaO}_2$  has been reduced to a level below 60mmHg (Willie *et al.*, 2012). At HA, CBF is similarly increased, but compared to isocapnic sea-level conditions the magnitude of vasodilation is contingent on individual variability of the hypoxic ventilatory response, and consequent hypocapnic vasoconstriction (Ainslie & Subudhi, 2014). While the regulation of hypoxic cerebral vasodilation is complex and undoubtedly involves a multitude of signaling pathways [reviewed in: (Hoiland *et al.*, 2016a)], several factors are commonly recognized as the likely key mediators of this response. These include, but are not limited to: nitric oxide (Van Mil *et al.*, 2002b), adenosine triphosphate (Ellsworth *et al.*, 1995), and adenosine (Berne *et al.*, 1974; Winn *et al.*, 1981c).

Adenosine is vasoactive in the cerebral vasculature through binding of  $\text{A}_{2\text{A}}$  receptors (Miekisiak *et al.*, 2008; Liu *et al.*, 2015) secondary to endogenous production during hypoxia (Berne *et al.*, 1974; Winn *et al.*, 1979, 1981a; Phillis *et al.*, 1993) (**Figure 3.1**). Extensive animal data has highlighted a prominent role of adenosine in the regulation of hypoxic cerebral vascular vasodilation. For example, extravascular application of adenosine dilates pial vessels *in vivo* (Berne *et al.*, 1974; Wahl & Kuschinsky, 1976; Morii *et al.*, 1987a), while adenosine receptor antagonism markedly blunts the vasodilatory response to moderate and severe hypoxia in dogs (Emerson & Raymond, 1981) and rats (Hoffman *et al.*, 1984a; Morii *et al.*, 1987a). However, whether adenosine plays a significant role in hypoxic cerebrovascular vasodilation in *humans* remains to be determined.

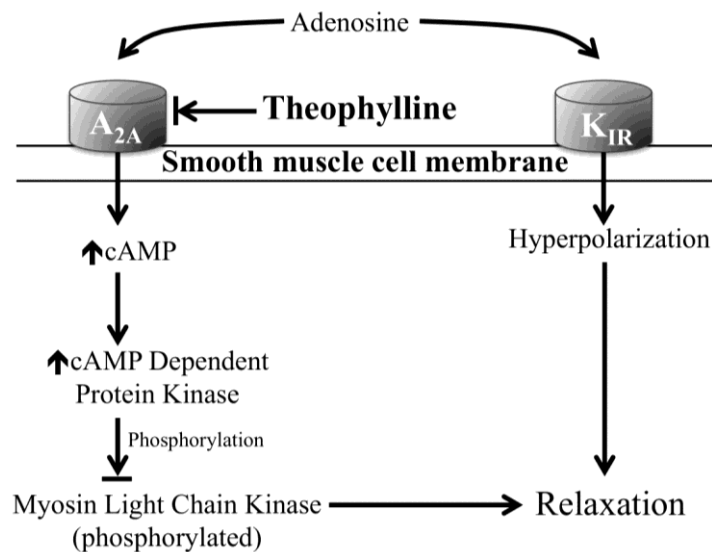


**Figure 3.1. Adenosine signaling pathways in hypoxia.**

Adenosine may lead to vasodilation (i.e., smooth muscle cell relaxation) by binding to adenosine A<sub>2A</sub> receptors, or by increasing inward rectifying potassium (K<sub>IR</sub>) channel conductance. A<sub>2A</sub> receptor binding activates (→) (cAMP), leading to up-regulation of cAMP dependent protein kinase and subsequent inhibition (→|) of myosin light chain kinase (Adelstein *et al.*, 1978). By inhibiting this response, downstream phosphorylation of myosin light chain and its consequent contribution to contraction does not occur, resulting in smooth muscle cell relaxation, and/or vasodilation (Kerrick & Hoar, 1981). Theophylline is a non-selective adenosine receptor antagonist, and therefore, does not allow for insight into how adenosines action on K<sub>IR</sub> channels may influence CBF regulation in hypoxia. cAMP, cyclic adenosine monophosphate; K<sub>IR</sub>, inward rectifying potassium channels. Reproduced from (Hoiland *et al.*, 2017b), permission not required.

In humans during normoxic rest, adenosine receptor antagonism (intravenous aminophylline) reduces CBF (Wechsler *et al.*, 1950; Gottstein & Paulson, 1972; Magnussen & Hoedt-Rasmussen, 1977). Similarly, CBF is lowered by aminophylline during acute normobaric hypoxia (Bowton *et al.*, 1988), but reactivity (i.e., the magnitude of the vasodilatory response per unit reduction in saturation) to hypoxia does not appear altered (Bowton *et al.*, 1988; Nishimura *et al.*, 1993). However, due to methodological limitations of the xenon-133 technique (Obrist *et al.*, 1975) used Bowton *et al.*, 1988 (Bowton *et al.*, 1988) and indirect inference of changes in CBF by Nishimura *et al.*, 1993 (Nishimura *et al.*, 1993), the direct role of adenosine in hypoxic cerebral vasodilation in

humans remains unclear in normobaric hypoxia. Moreover, the putative role of adenosine in cerebral vasodilation has not been investigated in hypobaric conditions where the magnitude of elevations in CBF can be markedly variable [reviewed in: (Ainslie & Subudhi, 2014; Hoiland *et al.*, 2016a)]. Although posterior cerebrovascular reactivity to isocapnic hypoxia is reportedly greater than that of anterior cerebrovascular reactivity (Willie *et al.*, 2012) it has yet to be investigated if regional differences in CBF regulation are attributable to adenosine.

Using a double blinded, randomized, placebo controlled and counter balanced design, the primary purpose of this study was to determine the effect of non-selective adenosine receptor antagonism with theophylline on the cerebral vascular response to normobaric isocapnic hypoxia *and* during exposure to hypobaric hypoxia. We hypothesized that: 1) normobaric isocapnic hypoxia would increase gCBF and induce vasodilation of the ICA & VA, 2) that this response would be attenuated following theophylline, and 3) based upon previous studies (Willie *et al.*, 2012; Ogoh *et al.*, 2013b; Lewis *et al.*, 2014b) posterior cerebral vascular reactivity (i.e., VA flow) would be greater than that of the anterior circulation (i.e., Q<sub>ICA</sub>). To follow up our sea-level study, we examined the effect of theophylline on cerebral vasodilation during acute exposure to hypobaric hypoxia following a rapid ascent profile to 3800m. We further hypothesized that ICA and VA diameter would increase upon exposure to HA, and that theophylline would again reduce the magnitude of observed vasodilation.

### **3.1 STUDY 2 - METHODS**

Twelve healthy young individuals (age: 26.0±5.6 years; body mass index: 22.9±2.3 kg/m<sup>2</sup>; 2 female) were recruited to participate in both the sea-level and HA component of this study. The sea-level portion of the study preceded the HA experiment. All participants provided written informed consent prior to arrival at the laboratory for a familiarization session. Participants were screened to ensure that reliable ICA and VA ultrasound images could be acquired and then familiarized with the remaining experimental equipment and procedures. All participants were free of cardiovascular, respiratory & cerebrovascular disease, were non-diabetic, and were not taking any prescription drugs (other than oral contraceptives, n=1) at their time of participation, as determined by a screening questionnaire. This study was approved by the University of British Columbia Clinical

Research Ethics Board and conformed to standards set by the Declaration of Helsinki and the Canadian Government Tri-Council Policy Statement for Integrity in Research.

### **3.1.1 STUDY 1 - EXPERIMENTAL MEASURES**

Collection and analysis of all cardiorespiratory and cerebrovascular variables for the entire study was completed while blinded to the specific protocols (e.g., placebo vs. theophylline).

#### **3.1.1.1 CARDIORESPIRATORY MEASURES**

##### **3.1.1.1.1 SEA-LEVEL STUDY.**

All cardiorespiratory variables were sampled continuously throughout the protocol at 1KHz via an analogue-to-digital converter (Powerlab, 16/30; ADInstruments, Colorado Springs, CO). A 3-lead electrocardiogram was used to measure HR (ADI bioamp ML132), and beat-to-beat blood pressure was measured by finger photoplethysmography (Finometer PRO, Finapres Medical Systems, Amsterdam, Netherlands). The Finometer reconstructed brachial waveform was used for the calculation of MAP after values were back calibrated to the average of three automated brachial blood pressure measurements made over five-minutes at rest (Tango+; SunTech, Morrisville, NC). Both  $P_{ET}CO_2$  and  $P_{ET}O_2$  were sampled at the mouth and recorded by a calibrated gas analyzer (ML206, ADInstruments, Colorado, CO, USA), while respiratory flow and  $V_E$  were measured by a pneumotachograph (HR800L, HansRudolph, Shawnee, KS) connected in series to a bacteriological filter. Due to the time delay associated with pulse-oximeter based estimation of arterial oxyhemoglobin saturation ( $SaO_2$ ), and assuming a constant  $P_a-P_{ET}O_2$  gradient throughout isocapnic hypoxia (Tymko *et al.*, 2015),  $SaO_2$  was calculated from  $P_{ET}O_2$  using a previously validated equation (Severinghaus, 1979a). This equation has been previously demonstrated to have a maximum error of 0.55%  $SaO_2$  when pH is standardized (Severinghaus, 1979a). Given that the experimental protocol was conducted under isocapnic conditions (i.e., stable pH), this calculation should accurately represent changes in  $SaO_2$ . Measurements of CBF were conducted as describe below (see section “Study 1 - Experimental measures”). Average values for the last minute of each stage were recorded (see section “Study 1 - Experimental protocol”).

#### 3.1.1.1.2 HIGH-ALTITUDE STUDY.

Cardiorespiratory variables were sampled continuously at 1KHz (Powerlab, 16/30; ADInstruments). Respiratory flow was measured by a pneumotachograph (HR 800L, HansRudolph, location), while  $P_{ET}O_2$  and  $P_{ET}CO_2$  were sampled continuously at the mouth by a calibrated gas analyzer (ML206, ADInstruments). Similar to the sea-level study, changes in  $SaO_2$  were estimated from  $P_{ET}O_2$  (Severinghaus, 1979a). The established changes in pH at 3800m (Severinghaus *et al.*, 1966b) were used to correct for  $P_{ET}O_2$  prior to  $SaO_2$  calculation (Severinghaus, 1979a). An automated brachial blood pressure cuff was used to measure HR and blood pressure (HEM-775CAN, Omron Healthcare, Illinois). Measurements of CBF were conducted as describe below (see section “Cerebrovascular measures”).

#### **3.1.1.2 DYNAMIC END-TIDAL FORCING**

The  $P_{ET}O_2$  and  $P_{ET}CO_2$  were controlled by a portable dynamic end-tidal forcing system. This system has been described in detail elsewhere (Tymko *et al.*, 2015, 2016b). End-tidal steady-state for each stage (see section “Study 1 - Experimental protocol”) was determined once values were within one-mmHg of the desired target point for at least three consecutive breaths. Our end-tidal forcing system effectively controls end-tidal gases through wide ranges of  $P_{ET}CO_2$  and  $P_{ET}O_2$ , independent of  $V_E$  at low (Tymko *et al.*, 2015, 2016b), and HA (Tymko *et al.*, 2015).

#### **3.1.1.3 CEREBROVASCULAR MEASURES**

Blood velocity through the right MCA and left PCA was measured using a 2MHz TCD (Spencer Technologies, Seattle, WA). The TCD probes were attached to a specialized headband (model M600 bilateral head frame, Spencer Technologies), and secured in place. Insonation was achieved through the trans-temporal window using previously described location and standardization techniques (Willie *et al.*, 2011). Based upon these guidelines a satisfactory PCAv signal could not be acquired in one participant, rendering a sample size of 11 for this metric.

Blood velocity and vessel diameter of the ICA and VA were measured using a 10MHz multi-frequency linear array duplex ultrasound (Terason T3200, Teratech, Burlington, MA). Arterial diameter was measured with B-mode imaging while pulse-wave mode was used to simultaneously measure peak blood velocity. Measures of  $Q_{ICA}$  and  $Q_{VA}$  were made ipsilateral to the MCA and PCA, respectively. The ICA diameter and velocity were measured at least 1.5 cm distal to the common carotid bifurcation to eliminate recordings of turbulent and retrograde flow, while VA diameter and velocity were measured between C4-C5, C5-C6, or proximal to entry into the vertebral column. The location was determined on an individual basis in an attempt to select the most reproducible measures, with the same location repeated within participants and between trials. For all experimental sessions, upon acquisition of the first ultrasound image there was no alteration of B-mode gain to avoid any artificial changes in arterial wall brightness/thickness.

Ultrasound recordings were screen captured and stored as video files for offline analysis. Concurrent measures of arterial diameter and peak blood velocity were acquired at 30Hz using customized edge detection and wall tracking software designed to mitigate observer bias (Woodman *et al.*, 2001). No less than 12 consecutive cardiac cycles were used to determine  $Q_{ICA}$  or  $Q_{VA}$ . Volumetric blood flow was calculated using the following formula (**Equation 3.1**):

Equation 3.1. Calculation of volumetric cerebral blood flow

$$Q_{ICA \text{ or } Q_{VA}} = \frac{\text{Peak Envelope Velocity}}{2} \cdot [\pi(0.5 \cdot \text{Diameter})^2]$$

Of note, half of peak envelope velocity equals mean blood velocity through a vessel (Evans, 1985; Secomb, 2016). To account for MAP in our analysis of the CBF responses, CVC was subsequently calculated for both the ICA and VA (e.g.,  $Q_{ICA}/MAP$ ) (**Equation 3.2**).

Equation 3.2. Cerebrovascular conductance.

$$CVC = CBF / MAP$$

Due to the high  $V_E$  associated with hypoxia and associated neck movement (particularly during sea-level experimentation), acquisition of adequate quality images was not achieved in all participants. The resulting sample sizes for  $Q_{VA}$  and  $gCBF$  at sea-level was 8 participants (out of 12), and at HA was 11 participants (out of 12), while all ICA images ( $n=12$ ) were used for both studies. We conducted our ultrasound scanning in accordance with published guidelines (Thomas *et al.*, 2015) and have previously reported a within and between day coefficient of variation for extra-cranial artery scanning of 1.5 and 4.4%, respectively (Hoiland *et al.*, 2016b).

### **3.1.2 STUDY 1 - EXPERIMENTAL PROTOCOL**

The sea-level portion of this study was carried out in the Centre for Heart, Lung and Vascular Health at the University of British Columbia's Okanagan Campus, Kelowna, British Columbia, Canada (344 m) one month prior to the HA investigations. The HA portion of this study was carried out upon arrival (day 1) to the Barcroft Station, located on White Mountain, CA, USA (3800 m).

#### **3.1.2.1 SEA-LEVEL STUDY**

This study consisted of two laboratory visits: a placebo day and the drug intervention day, which were counter balanced, and double blinded. Participants attended the laboratory having abstained from exercise and alcohol for  $\geq 24$  hours and were fasted for a minimum of two hours. Given the use of an adenosine receptor antagonist in the protocol, participants were instructed to strictly abstain from methyl xanthine containing products (e.g., caffeine, chocolate) for  $\geq 48$  hours prior to each testing day. Upon arrival, participants lay supine and rested for 15-minutes, during which time they were instrumented with the experimental equipment.

Following instrumentation and five minutes of baseline measurements (HR, MAP,  $V_E$ ,  $MCA_V$ ,  $PCA_V$ ,  $Q_{ICA}$ ,  $Q_{VA}$ ,  $P_{ET}O_2$ , and  $P_{ET}CO_2$ ) the participant completed an isocapnic hypoxia test. Participants breathed simulated room air (e.g.,  $P_{ET}O_2$  and  $P_{ET}CO_2$  were approximately 100 mmHg and 40 mmHg, respectively) on the end-tidal forcing system for a five-minute period prior to commencing three hypoxic stages. To achieve the target  $SaO_2$  values of 90%, 80%, and 70%,  $P_{ET}O_2$  was lowered in three sequential steps to 60 mmHg,

45 mmHg, and 37 mmHg, with each stage lasting five-minutes once steady state was reached. Following the last stage participants returned to breathing room air. Participants then orally ingested either 3.75 mg/kg of theophylline or a placebo pill (sugar pill matched for capsule size, color, and weight). Sustained release theophylline pills have been shown to reach peak plasma concentration between five & seven hours post-ingestion with plasma concentration stable during that time period (Dederich *et al.*, 1981; Tulain & Nisar-Ur-Rahman, 2008). Therefore, the post intervention test took place six-hours following ingestion of theophylline or placebo. On the second day of testing, participants received the opposite intervention as day one, but completed the same hypoxic protocols. Testing days were on average separated by three days (range: two to eight days). Importantly, co-infusion of aminophylline (similar to theophylline) and adenosine has been shown to produce less forearm vasodilation than adenosine infusion alone, indicating the efficacy of aminophylline (and therefore theophylline) in reducing adenosine dependent vasodilation (Leuenberger *et al.*, 1999).

### **3.1.2.2 HIGH-ALTITUDE STUDY**

The study participants were split into a placebo and theophylline group (n=6 for each). Participants awoke at 5am and were transported by two vans from Palm Springs, CA (146 m) to the Barcroft Station, White Mountain Research Center, White Mountain, CA (3800 m) in approximately six-hours. One participant slept in Bishop, CA (1265 m) the night prior to arrival and arrived at the same time as the other participants from Palm Springs. Participants arrived at the laboratory having abstained from methyl-xanthine containing products (e.g., chocolate & caffeine) for  $\geq 48$  hours, exercise and alcohol for  $\geq 24$  hours, and were fasted for a minimum of 2 hours. Participants in the placebo and theophylline group were tested  $125 \pm 32$  (mean  $\pm$  standard deviation) and  $128 \pm 31$  minutes following arrival to 3800 m, respectively. Following initial testing, the placebo or theophylline capsule was ingested, and post testing for the placebo and theophylline groups occurred  $315 \pm 13$  and  $300 \pm 0$  minutes later, respectively. A double blinded study design was utilized.

Upon initial arrival participants were tested in the supine position after 15-minutes of rest, during which they were instrumented with the experimental equipment. Resting measurements of HR, MAP,  $Q_{ICA}$ ,  $Q_{VA}$ ,  $P_{ET}O_2$ , and  $P_{ET}CO_2$  were collected for a five-minute period ( $V_E$  was not assessed at this time point due to logistical issues). For the post

intervention (i.e. placebo/drug) testing, participants again rested supine for 15-minutes prior to measurement. Measurements were collected over five-minutes of room air breathing. To account for any between group differences in  $V_E$  due to theophylline as well as inherent variability in the hypoxic ventilatory response, participants were then controlled at the same  $P_{ET}O_2$  and  $P_{ET}CO_2$  using the portable end-tidal forcing system for 5-minutes prior to the second set of measurements. The clamped  $P_{ET}O_2$  and  $P_{ET}CO_2$  were determined from the mean values of all participants during the pre drug/placebo testing upon arrival (52 mmHg  $P_{ET}O_2$  & 33 mmHg  $P_{ET}CO_2$ ). This end-tidal clamping was initiated immediately following the post-intervention measure. Therefore, data were collected over three distinct time points: 1) two hours following arrival to the laboratory; 2) five-hours post drug/placebo ingestion (seven-hours after arrival), and; 3) post intervention with controlled  $P_{ET}CO_2$  and  $P_{ET}O_2$  (seven-hours after arrival). Prior to testing at the arrival time point, and post drug time point, as well as during the following morning, each participant completed the Lake Louise Acute Mountain Sickness (AMS) questionnaire (Roach *et al.*, 1993) to assess any symptoms of AMS.

### 3.1.2.3 STUDY 1 - CALCULATIONS

Arterial oxygen content was estimated ( $eCaO_2$ ) using the following equation (**Equation 3.3**):

Equation 3.3. Estimated arterial oxygen content

$$eCaO_2(\text{ml. dl}^{-1}) = [\text{Hb}] \cdot 1.36 \cdot \frac{\text{SaO}_2(\%)}{100} + 0.003 \cdot P_{ET}O_2$$

Where  $[\text{Hb}]$  is the concentration of hemoglobin, which we have assumed to be 15.5 g/dL, 1.36 is the affinity of  $O_2$  for hemoglobin,  $\text{SaO}_2$  is arterial oxygen saturation calculated using the Severinghaus equation (Severinghaus, 1979a), and 0.003 is the solubility of oxygen dissolved in the blood. We replaced  $\text{PaO}_2$  with  $P_{ET}O_2$  for our estimation of  $\text{CaO}_2$ .

Cerebral oxygen delivery was subsequently estimated ( $eCDO_2$ ) by using  $eCaO_2$  in the following equation (**Equation 3.4**):

Equation 3.4. Estimated cerebral oxygen delivery

$$eCDO_2(\text{ml. min}^{-1}) = eCaO_2 \cdot \frac{\text{gCBF}}{100}$$

In this study the end-tidal forcing baseline for each trial was determined individually pre- and post-intervention based on  $P_{ET}O_2$  and  $P_{ET}CO_2$  measured during the 5-minutes of resting room air breathing. While theophylline and/or time of day may have caused post-intervention end-tidal gases to deviate from their respective pre-intervention trials, it was determined *a priori* to adopt this approach so that each trial began from a natural baseline. Given interaction between  $O_2$  and  $CO_2$  on cerebral reactivity (Mardimae *et al.*, 2012) we chose not to manipulate  $P_{ET}CO_2$  from resting values to normalize between pre- and post-intervention baselines. Therefore, following analysis of the respiratory data we noted a difference in  $P_{ET}CO_2$  in the theophylline trial. Specifically,  $P_{ET}CO_2$  was lower post-theophylline than pre-theophylline trial (see section “Study 1 - results”), which necessitated mathematical corrections for the effect of  $P_{ET}CO_2$  on CBF. Therefore, we corrected the CBF variables for changes in  $P_{ET}CO_2$ . The following equations were used to correct for changes in  $P_{ET}CO_2$  (**Equation 3.5**):

Equation 3.5. Carbon dioxide corrected internal carotid artery blood flow

$$corrQ_{ICA} = Q_{ICA} + [P_{ET}CO_2(Pre) - P_{ET}CO_2(Post)] \cdot (0.084 \cdot bQ_{ICA})$$

Where for a given stage of hypoxia,  $corrQ_{ICA}$  is the estimated  $Q_{ICA}$  following correction for  $CO_2$ ,  $P_{ET}CO_2(Pre)$  is the  $P_{ET}CO_2$  of that stage pre-theophylline,  $P_{ET}CO_2(Post)$  is the  $P_{ET}CO_2$  of that stage post-theophylline, 0.084 is the reactivity of the ICA to a 1 mmHg change in  $P_{ET}CO_2$  (i.e., 8.4%) (Hoiland *et al.*, 2015), and  $bQ_{ICA}$  is the baseline  $Q_{ICA}$  prior to hypoxic exposure. The percent reactivity was applied to the baseline  $Q_{ICA}$  so that the impact of  $CO_2$  was not inflated by the increase of  $Q_{ICA}$  during the hypoxic stages (**Equation 3.6**).

Equation 3.6. Carbon dioxide corrected vertebral artery blood flow

$$corrQ_{VA} = Q_{ICA} + [P_{ET}CO_2(Pre) - P_{ET}CO_2(Post)] \cdot (0.076 \cdot bQ_{VA})$$

Where for a given stage of hypoxia,  $corrQ_{VA}$  is the estimated  $Q_{VA}$  following correction for  $CO_2$ ,  $P_{ETCO_2}(Pre)$  is the  $P_{ETCO_2}$  of that stage pre-theophylline,  $P_{ETCO_2}(Post)$  is the  $P_{ETCO_2}$  of that stage post-theophylline, 0.076 is the reactivity of the VA to a 1 mmHg change in  $P_{ETCO_2}$  (i.e., 7.6%) (Hoiland *et al.*, 2015), and  $bQ_{VA}$  is the baseline  $Q_{VA}$  prior to hypoxic exposure (**Equation 3.7**).

Equation 3.7. Carbon dioxide corrected cerebral blood flow

$$corrCBF = (corrQ_{ICA} + corrQ_{VA}) \cdot 2$$

Where  $corrCBF$  is the  $gCBF$  corrected for the change in  $P_{ETCO_2}$  following theophylline.

Absolute and relative (i.e., %) reactivity for  $gCBF$ ,  $Q_{ICA}$ ,  $ICA_v$ ,  $Q_{VA}$ ,  $VA_v$ ,  $MCA$ , and  $PCA_v$  was calculated using linear regression analysis.

#### **3.1.2.4 STUDY 1 - STATISTICAL ANALYSES**

For the sea level testing, all cardiovascular, cerebrovascular and respiratory variables were analyzed within trial (i.e., placebo & theophylline) using two-way repeated measures ANOVAs. Post-hoc comparisons were made using a Bonferroni correction. Sphericity of data was confirmed using Mauchly's test of sphericity. When the test of sphericity was not passed, the Greenhouse-Geisser correction was used. Data did not significantly differ from a normal distribution as determined by the Shapiro-Wilks test. A sub analysis was performed where the reactivity slopes from the pre placebo, post placebo, pre theophylline, and post theophylline trials were compared using a one-way repeated measures ANOVA. These reactivity slopes were calculated using linear regression (Willie *et al.*, 2012; Skow *et al.*, 2013b). Regional differences in vessel reactivity were analyzed pre and post theophylline using a mixed design ANOVA (between subject factor: vessel; within subject factor: trial). Differences in confluent vessel blood flow (ICA & VA) and velocity (MCA<sub>v</sub> & PCA<sub>v</sub>) reactivity were analyzed using a mixed design ANOVA (between subject factor: vessel; within subject factor: trial). The relationship between MAP and CBF variables was assessed using a Pearson r correlation between the  $\% \Delta MAP$  and  $\% \Delta CBF$  variables for each experimental trial.

The HA data were analyzed using a mixed design ANOVA (between subject factor: drug; within subject factor: exposure time). Post-hoc comparisons were made using a Bonferroni correction. When the test of sphericity was not passed, the Greenhouse-Geisser correction was used. Data did not significantly differ from a normal distribution as determined by the Shapiro-Wilks test. All data were analyzed using SPSS (Version 22, IBM statistics) and are expressed as mean  $\pm$  standard deviation with *a priori* statistical significance set at  $P < 0.05$ .

## **3.2 STUDY 1 - RESULTS**

### **3.2.1 SEA LEVEL STUDY**

#### **3.2.1.1 PLACEBO TRIALS**

Cardiovascular variables at all stages of hypoxia during placebo trials are presented in **Table 3.1**. Under placebo conditions HR and VE increased at all stages of hypoxia pre and post intervention while MAP increased at 90% and 70% hypoxia. A main effect of placebo on MAP was observed; here, MAP was higher post placebo ( $P=0.03$ ).

Cerebral vascular variables at all stages of hypoxia during placebo trials are presented in **Table 3.1**.  $Q_{ICA}$ , ICA CVC, and ICA<sub>v</sub> increased pre and post placebo at 80% and 70% SaO<sub>2</sub> while ICA diameter and MCA<sub>v</sub> increased at all stages of hypoxia. Hypoxia increased  $Q_{VA}$ , VA<sub>v</sub>, VA diameter and PCA<sub>v</sub> pre and post placebo at 80% and 70% SaO<sub>2</sub> while VA CVC increased at 70% SaO<sub>2</sub>. Pre and post placebo, gCBF and gCBF CVC increased at 80% and 70% SaO<sub>2</sub>. Hypoxia increased eCDO<sub>2</sub> at 70% SaO<sub>2</sub>, while there was no effect of placebo on eCDO<sub>2</sub> (**Table 3.2**).

**Table 3.1. Cardiorespiratory variables during sea level hypoxia.**

		Placebo				Theophylline			
		Baseline	90% SaO <sub>2</sub>	80% SaO <sub>2</sub>	70% SaO <sub>2</sub>	Baseline	90% SaO <sub>2</sub>	80% SaO <sub>2</sub>	70% SaO <sub>2</sub>
		<i>Pre vs. Post: P=0.285; O<sub>2</sub>: P&lt;0.001; Interaction: P=0.281</i>				<i>Pre vs. Post: P=0.494; O<sub>2</sub>: P&lt;0.001; Interaction: P=0.784</i>			
<b>P<sub>ET</sub>O<sub>2</sub></b> (mmHg)	Pre	93.5±7.1	59.3±1.2*	45.3±1.0*	37.1±0.7*	94.4±4.0	59.7±1.6*	45.0±1.1*	37.1±1.0*
	Post	95.2±4.9	59.3±1.8*	45.2±1.0*	37.3±0.6*	95.2±8.2	59.8±1.5*	45.7±1.2*	37.4±0.7*
		<i>Pre vs. Post: P=0.419; O<sub>2</sub>: P=0.295; Interaction: P=0.847</i>				<b>Pre vs. Post: P=0.001; O<sub>2</sub>: P=0.526; Interaction: P=0.087</b>			
<b>P<sub>ET</sub>CO<sub>2</sub></b> (mmHg)	Pre	40.4±3.0	40.4±3.1	40.2±3.2	40.2±3.2	41.2±1.9	41.1±2.0	41.1±2.0	41.1±2.1
	Post	39.9±2.9	40.0±2.9	39.9±2.9	39.9±2.8	38.8±2.5	39.0±2.4	38.9±2.6	38.8±2.5
		<i>Pre vs. Post: P=0.188; O<sub>2</sub>: P&lt;0.001; Interaction: P=0.349</i>				<b>Pre vs. Post: P=0.029; O<sub>2</sub>: P=0.001; Interaction: P=0.162</b>			
<b>VE</b> (L · min <sup>-1</sup> )	Pre	11.3±1.2	17.9±7.2*	30.3±14.4*	46.5±22.4*	13.2±3.8	21.2±7.1*	34.6±15.3*	50.2±24.3*
	Post	12.2±1.9	22.4±11.2*	34.2±16.0*	47.6±25.1*	13.1±2.6	18.5±4.8*	30.2±15.3*	42.3±25.4*
		<i>Pre vs. Post: P=0.026; O<sub>2</sub>: P=0.005; Interaction: P=0.521</i>				<i>Pre vs. Post: P=0.324; O<sub>2</sub>: P=0.002; Interaction: P=0.001</i>			
<b>MAP</b> (mmHg)	Pre	76.2±3.8	78.3±5.4*	81.4±5.7	83.6±13.1*	79.3±7.0	80.9±6.7	86.1±6.9	90.4±7.1*‡
	Post	78.3±6.0	83.4±5.9*	81.7±13.0	89.7±7.8*	81.6±6.2	83.0±6.9	82.7±6.3	85.0±5.5*
		<i>Pre vs. Post: P=0.872; O<sub>2</sub>: P&lt;0.001; Interaction: P=0.984</i>				<i>Pre vs. Post: P=0.065; O<sub>2</sub>: P&lt;0.001; Interaction: P=0.019</i>			
<b>HR</b> (beats · min <sup>-1</sup> )	Pre	62.2±15.0	70.3±12.7*	81.1±14.4*	92.1±16.5*	63.5±15.4	71.3±19.0*	82.4±19.7*	94.7±19.4*
	Post	62.4±15.1	70.9±13.4*	81.4±15.2*	93.0±19.7*	62.4±13.3	68.1±15.4*	77.5±16.9*	88.3±15.9*

**Bolded Pre or Post** indicates main effect of the intervention, with the bolded trial significantly greater. \*signifies a significant difference from baseline. ‡ indicates significant interaction between pre and post. n=12 for all measurements.

**Table 3.2. Cerebrovascular variables during sea level hypoxia.**

		Placebo				Theophylline			
		Baseline	90%	80%	70%	Baseline	90%	80%	70%
		<i>Pre vs. Post: P=0.562; O<sub>2</sub>: P&lt;0.001; Interaction: P=0.722</i>				<i>Pre vs. Post: P=0.315; O<sub>2</sub>: P&lt;0.001; Interaction: P=0.083</i>			
<b>SaO<sub>2</sub></b> (% oxyhemoglobin)	Pre	97.2±0.6	90.3±0.5*	81.0±1.0*	70.7±1.2*	97.3±0.3	90.4±0.7*	80.6±1.1*	70.7±1.5*
	Post	97.4±0.3	90.2±0.8*	80.9±1.0*	71.0±1.0*	97.3±0.7	90.5±0.7*	81.3±1.1*	71.1±1.1*
		<i>Pre vs. Post: P=0.852; O<sub>2</sub>: P&lt;0.001; Interaction: P=0.377</i>				<i>Pre vs. Post: P&lt;0.001; O<sub>2</sub>: P&lt;0.001; Interaction: P=0.211</i>			
<b>Q<sub>ICA</sub></b> (mL · min <sup>-1</sup> )	Pre	276.5±57.7	292.9±68.1	357.6±91.8*	465.2±105.3*	273.2±38.9	309.8±54.5*	358.2±64.1*	465.3±75.4*
	Post	280.6±75.3	282.5±112.9	369.8±92.1*	451.34±110.3*	236.4±37.2	258.8±50.6*	310.7±54.3*	404.0±69.3*
		<i>Pre vs. Post: P=0.854; O<sub>2</sub>: P&lt;0.01; Interaction: P=0.050</i>				<i>Pre vs. Post: P=0.001; O<sub>2</sub>: P&lt;0.001; Interaction: P=0.796</i>			
<b>ICAv</b> (cm · s <sup>-1</sup> )	Pre	47.9±7.3	48.5±6.2	56.3±8.6*	69.3±9.7*	48.1±7.2	51.3±8.6	57.5±10.6*	68.7±10.1*
	Post	48.8±9.3	50.9±10.9	57.1±11.8*	66.2±13.0*	41.7±7.1	43.3±7.9	49.6±9.3*	61.4±9.8*
		<i>Pre vs. Post: P=0.841; O<sub>2</sub>: P&lt;0.001; Interaction: P=0.124</i>				<i>Pre vs. Post: P=0.498; O<sub>2</sub>: P&lt;0.001; Interaction: P=0.512</i>			
<b>ICA diameter</b> (mm)	Pre	4.94±0.57	5.03±0.51*	5.17±0.58*	5.32±0.56*	4.91±0.43	5.07±0.51*	5.17±0.52*	5.37±0.54*
	Post	4.91±0.51	5.00±0.46*	5.23±0.53*	5.37±0.52*	4.92±0.43	5.03±0.41*	5.16±0.43*	5.29±0.45*
		<i>Pre vs. Post: P=0.211; O<sub>2</sub>: P&lt;0.001; Interaction: P=0.178</i>				<i>Pre vs. Post: P&lt;0.001; CO<sub>2</sub>: P&lt;0.001; Interaction: P=0.126</i>			
<b>ICA CVC</b> (mL · min <sup>-1</sup> · mmHg <sup>-1</sup> )	Pre	3.62±0.67	3.72±0.70	4.37±0.93*	5.73±1.81*	3.46±0.56	3.84±0.72*	4.17±0.78*	5.16±0.81*
	Post	3.57±0.85	3.39±1.27	4.58±1.03*	5.06±1.30*	2.91±0.51	3.12±0.57*	3.77±0.68*	4.76±0.84*
		<i>Pre vs. Post: P=0.436; O<sub>2</sub>: P&lt;0.001; Interaction: P=0.156</i>				<i>Pre vs. Post: P=0.020; O<sub>2</sub>: P&lt;0.001; Interaction: P=0.125</i>			
<b>Q<sub>VA</sub> (n=8)</b> (mL · min <sup>-1</sup> )	Pre	109.3±36.0	106.1±31.3	127.0±30.7*	179.3±46.7*	111.8±30.4	121.7±28.6	133.3±31.0*	188.7±46.8*
	Post	106.7±33.4	114.3±30.9	146.1±38.5*	178.8±37.2*	98.9±22.3	101.7±19.8	123.7±22.3*	162.5±32.7*
		<i>Pre vs. Post: P=0.108; O<sub>2</sub>: P&lt;0.001; Interaction: P=0.090</i>				<i>Pre vs. Post: P=0.011; O<sub>2</sub>: P&lt;0.001; Interaction: P=0.265</i>			
<b>VA<sub>v</sub> (n=8)</b> (cm · s <sup>-1</sup> )	Pre	25.1±4.6	24.5±4.6	28.4±4.2*	37.5±6.3*	25.5±4.9	26.9±3.1	29.6±5.2*	39.2±6.7*
	Post	26.1±6.3	27.5±5.4	33.1±6.6*	38.3±5.8*	23.2±3.7	23.4±3.1	27.6±4.0*	34.6±6.5*
		<i>Pre vs. Post: P=0.420; O<sub>2</sub>: P&lt;0.001; Interaction: P=0.272</i>				<i>Pre vs. Post: P=0.305; O<sub>2</sub>: P&lt;0.001; Interaction: P=0.219</i>			
<b>VA diameter (n=8)</b> (mm)	Pre	4.16±0.43	4.16±0.40	4.24±0.39*	4.38±0.38*	4.17±0.45	4.23±0.46	4.24±0.44	4.38±0.43*
	Post	4.05±0.35	4.09±0.35	4.21±0.36*	4.43±0.26*	4.12±0.39	4.16±0.42	4.24±0.41	4.36±0.39*

		Placebo				Theophylline			
		Baseline	90%	80%	70%	Baseline	90%	80%	70%
		<i>Pre vs. Post: P=0.918; O<sub>2</sub>: P&lt;0.001; Interaction: P=0.097</i>				<i>Pre vs. Post: P=0.022; O<sub>2</sub>: P&lt;0.001; Interaction: P=0.060</i>			
<b>VA CVC</b> (n=8) (mL · min <sup>-1</sup> · mmHg <sup>-1</sup> )	Pre	1.43±0.40	1.37±0.36	1.60±0.33	2.19±0.42*	1.37±0.37	1.48±0.35	1.51±0.35	2.05±0.48*
	Post	1.36±0.38	1.36±0.32	1.84±0.72	1.98±0.45*	1.21±0.32	1.21±0.21	1.47±0.24	1.89±0.34*
		<i>Pre vs. Post: P=0.821; O<sub>2</sub>: P&lt;0.001; Interaction: P=0.395</i>				<i>Pre vs. Post: P=0.004; O<sub>2</sub>: P&lt;0.001; Interaction: P=0.199</i>			
<b>gCBF</b> (n=8) (mL · min <sup>-1</sup> )	Pre	758.0±183.7	780.2±192.8	941.8±246.4*	1245.5±262.2*	757.4±113.6	849.8±138.6*	955.1±151.6*	1270.2±137.3*
	Post	736.4±193.1	755.5±290.9	983.6±238.9*	1215.6±281.7*	672.4±111.1	712.8±133.5*	864.4±131.2*	1108.3±158.6*
		<i>Pre vs. Post: P=0.195; O<sub>2</sub>: P&lt;0.001; Interaction: P=0.228</i>				<i>Pre vs. Post: P=0.002; O<sub>2</sub>: P&lt;0.001; Interaction: P=0.072</i>			
<b>gCBF CVC</b> (n=8) (mL · min <sup>-1</sup> · mmHg <sup>-1</sup> )	Pre	9.92±1.94	10.02±2.02	11.80±2.41*	15.78±4.54*	9.27±1.30	10.30±1.61*	10.85±1.80*	13.86±1.39*
	Post	9.38±2.21	9.00±3.16	12.59±3.40*	13.41±3.16*	8.20±1.68	8.47±1.42*	10.32±1.51*	12.95±1.76*
		<i>Pre vs. Post: P=0.968; O<sub>2</sub>: P&lt;0.001; Interaction: P=0.540</i>				<i>Pre vs. Post: P=0.037; O<sub>2</sub>: P&lt;0.001; Interaction: P=0.500</i>			
<b>MCAv</b> (cm · s <sup>-1</sup> )	Pre	58.0±11.6	61.2±11.8*	71.1±13.2*	86.6±16.2*	62.0±11.1	66.6±11.8*	76.7±14.8*	90.0±18.1*
	Post	58.0±10.0	62.2±10.4*	70.9±12.1*	85.0±16.4*	57.1±11.2	60.3±12.0*	69.6±16.1*	83.73±16.8*
		<i>Pre vs. Post: P=0.192; O<sub>2</sub>: P&lt;0.001; Interaction: P=0.554</i>				<i>Pre vs. Post: P=0.003; O<sub>2</sub>: P&lt;0.001; Interaction: P=0.151</i>			
<b>PCAv</b> (cm · s <sup>-1</sup> )	Pre	39.9±6.4	41.3±6.1	48.4±7.4*	58.5±10.5*	44.1±9.3	47.1±10.1*	55.1±12.4*	65.5±15.9*
	Post	36.9±7.2	39.2±8.7	45.5±10.5*	54.8±12.0*	38.8±7.1	40.2±7.4*	46.3±10.5*	58.4±11.3*

**Bolded Pre or Post** indicates main effect of the intervention, with the bolded trial significantly greater. \*signifies a significant difference from baseline. ‡ indicates significant difference between pre and post. n=12 unless otherwise specified.

### 3.2.1.2 THEOPHYLLINE TRIALS

Cardiovascular variables at all stages of isocapnic hypoxia during theophylline trials are presented in **Table 3.1**. Hypoxia elevated HR and VE at all stages pre and post theophylline trials, while MAP was only elevated at 70% SaO<sub>2</sub> and was higher pre-theophylline (P=0.02). Following theophylline, VE was lower at all stages (main effect: P=0.03) concomitant to a lower P<sub>ET</sub>CO<sub>2</sub> clamp (main effect: P<0.01).

Cerebral vascular variables at all stages of hypoxia during the theophylline trials are presented in **Table 3.2**. Pre and post theophylline Q<sub>ICA</sub>, ICA CVC, ICA diameter, and MCA<sub>v</sub> increased during all stages of hypoxia while ICA<sub>v</sub> increased at 80% and 70% SaO<sub>2</sub>. There was a main effect of theophylline on Q<sub>ICA</sub>, ICA CVC, ICA<sub>v</sub>, and MCA<sub>v</sub> with all variables lower post theophylline (all, P<0.05); however, this coincided with the previously mentioned lower P<sub>ET</sub>CO<sub>2</sub> (main effect: P<0.01). Following correction for P<sub>ET</sub>CO<sub>2</sub>, there was no main effect of theophylline on corrQ<sub>ICA</sub> (P=0.29; **Table 3.3**).

Pre and post theophylline, Q<sub>VA</sub> and VA<sub>v</sub> increased at 80% and 70% SaO<sub>2</sub> while VA diameter and VA CVC only increased at 70% SaO<sub>2</sub>; PCA<sub>v</sub> also increased, during all stages of hypoxia both pre and post intervention. There was a main effect of theophylline on Q<sub>VA</sub>, VA CVC, VA<sub>v</sub> and PCA<sub>v</sub> with all variables lower post theophylline. Following correction for P<sub>ET</sub>CO<sub>2</sub>, however, there was no main effect of theophylline on corrQ<sub>VA</sub> (P=0.85; **Table 3.3**). Hypoxia increased gCBF and gCBF CVC across all stages pre and post theophylline while there was a main effect of theophylline to lower gCBF (P<0.01) and gCBF CVC (P<0.01). Following correction for P<sub>ET</sub>CO<sub>2</sub>, there was no main effect of theophylline on corrCBF (P=0.80; **Table 3.3**). Hypoxia increased eCDO<sub>2</sub> at 70% SaO<sub>2</sub>, while there was no effect of theophylline on eCDO<sub>2</sub>.

**Table 3.3. Theoretical calculations of arterial oxygen content, cerebral oxygen delivery, and cerebral blood flow parameters corrected for carbon dioxide.**

For both the placebo and theophylline trial, CaO<sub>2</sub> and CDO<sub>2</sub> were estimated (eCaO<sub>2</sub> & eCDO<sub>2</sub>, respectively). Due to the difference in P<sub>ET</sub>CO<sub>2</sub> between the pre and post theophylline trials, Q<sub>ICA</sub>, Q<sub>VA</sub>, and gCBF post theophylline (corrQ<sub>ICA</sub>, corrQ<sub>VA</sub> & corrCBF, respectively) were all corrected for differences in P<sub>ET</sub>CO<sub>2</sub> (explained in methods section “calculations”).

		Placebo			
		Baseline	90%	80%	70%
		<i>Pre vs. Post: P=0.275; O<sub>2</sub>: P&lt;0.001; Interaction: P=0.808</i>			
<b>eCaO<sub>2</sub></b> (mL·dL <sup>-1</sup> )	Pre	20.77±0.14	19.21±0.12*	17.21±0.22*	15.01±0.25*
	Post	20.81±0.09	19.20±0.18*	17.19±0.21*	15.09±0.21*
		<i>Pre vs. Post: P=0.846; O<sub>2</sub>: P&lt;0.001; Interaction: P=0.067</i>			
<b>eCDO<sub>2</sub></b> (mL·min <sup>-1</sup> )	Pre	152.2±36.1	145.0±35.6	156.9±41.1	179.6±35.8*
	Post	148.3±38.4	139.9±53.8	163.6±38.4	176.3±38.7*
		Theophylline			
		Baseline	90%	80%	70%
		<i>Pre vs. Post: P=0.527; O<sub>2</sub>: P&lt;0.001; Interaction: P=0.294</i>			
<b>eCaO<sub>2</sub></b> (mL·dL <sup>-1</sup> )	Pre	20.80±0.08	19.24±0.15*	17.13±0.24*	15.01±0.32*
	Post	20.80±0.17	19.25±0.14*	17.28±0.14*	15.11±0.23*
		<i>Pre vs. Post: P=0.004; O<sub>2</sub>: P&lt;0.001; Interaction: P=0.314</i>			
<b>eCDO<sub>2</sub></b> (mL·min <sup>-1</sup> )	Pre	152.6±23.0	158.3±26.0	157.7±24.9	183.1±20.6*
	Post	135.4±22.3	133.0±25.1	144.4±21.1	162.1±22.5*
		<i>Pre vs. Post: P=0.797; O<sub>2</sub>: P&lt;0.001; Interaction: P=0.032</i>			
<b>gCBF</b> <b>corrCBF</b>	Pre	757.0±128.3	850.7±150.6*	927.3±165.6*	1260.3±145.4*
	Post	766.2±146.7	804.5±147.2*	973.9±122.5*	1213.8±141.6*
		<i>Pre vs. Post: P=0.294; O<sub>2</sub>: P&lt;0.001; Interaction: P=0.067</i>			
<b>Q<sub>ICA</sub></b> (n=12) <b>corrQ<sub>ICA</sub></b>	Pre	273.2±38.9	309.8±54.5*	358.2±64.1*	465.3±75.4*
	Post	280.3±42.6	296.3±46.1*	349.2±46.8*	444.9±71.4*
		<i>Pre vs. Post: P=0.850; O<sub>2</sub>: P=0.001; Interaction: P=0.160</i>			
<b>Q<sub>VA</sub></b> <b>corrQ<sub>VA</sub></b>	Pre	111.8±30.1	121.7±28.6	133.3±31.0*	188.7±46.8*
	Post	117.1±34.0	117.3±29.1	139.7±26.7*	178.3±36.2*

**Bolded Pre or Post** indicates main effect of the intervention, with the bolded trial significantly greater. \*signifies a significant difference from baseline. ‡ indicates significant interaction between pre and post. n=8 unless otherwise specified.

**Table 3.4. r-squared values for the linear regression of cerebrovascular reactivity.**

	<b>Pre-theophylline</b>	<b>Post-theophylline</b>	<b>Pre-placebo</b>	<b>Post-placebo</b>
<b>MCA<sub>v</sub></b>	0.97±0.03	0.90±0.10	0.95±0.03	0.90±0.16
<b>PCA<sub>v</sub></b>	0.95±0.05	0.89±0.08	0.92±0.05	0.90±0.08
<b>Q<sub>ICA</sub></b>	0.92±0.08	0.94±0.05	0.93±0.05	0.94±0.04
<b>ICA<sub>v</sub></b>	0.88±0.16	0.90±0.12	0.89±0.05	0.88±0.12
<b>Q<sub>VA</sub></b>	0.84±0.10	0.89±0.15	0.84±0.10	0.90±0.16
<b>VA<sub>v</sub></b>	0.84±0.08 (n=8)	0.86±0.17 (n=8)	0.74±0.10 (n=8)	0.88±0.22 (n=8)
<b>gCBF</b>	0.90±0.08 (n=8)	0.93±0.08 (n=8)	0.91±0.05 (n=8)	0.95±0.03 (n=8)

n=12 unless otherwise specified.

### **3.2.1.3 Cerebrovascular Reactivity Slopes to Hypoxia**

The r-squared values for each CBF variable in the pre-theophylline, theophylline, pre-placebo, and placebo trials are reported in **Table 3.4**. These analyses were conducted to discern if the main effect of theophylline on CBF variables was simply a product of differing  $P_{ET}CO_2$  values between trials and to determine between vessel differences in reactivity. The response slopes for absolute changes of  $MCA_v$  ( $P=0.89$ ),  $PCA_v$  ( $P=0.504$ ),  $Q_{ICA}$  ( $P=0.348$ ),  $ICA_v$  ( $P=0.231$ ),  $Q_{VA}$  ( $P=0.890$ ),  $VA_v$  ( $P=0.950$ ), and  $gCBF$  ( $P=0.694$ ) were not different between the pre-placebo, post-placebo, pre-theophylline, and post-theophylline trials. The response slopes for percent changes of  $MCA_v$  ( $P=0.598$ ),  $PCA_v$  ( $P=0.753$ ),  $Q_{ICA}$  ( $P=0.707$ ),  $ICA_v$  ( $P=0.08$ ),  $Q_{VA}$  ( $P=0.860$ ),  $VA_v$  ( $P=0.989$ ), and  $gCBF$  ( $P=0.953$ ) were not different between the pre-placebo, post-placebo, pre-theophylline, and post-theophylline trials (**Figure 3.2**). The percent changes in  $gCBF$ ,  $Q_{ICA}$ , and  $Q_{VA}$  at each stage of hypoxia for all trials are depicted in **Figure 3.3**.

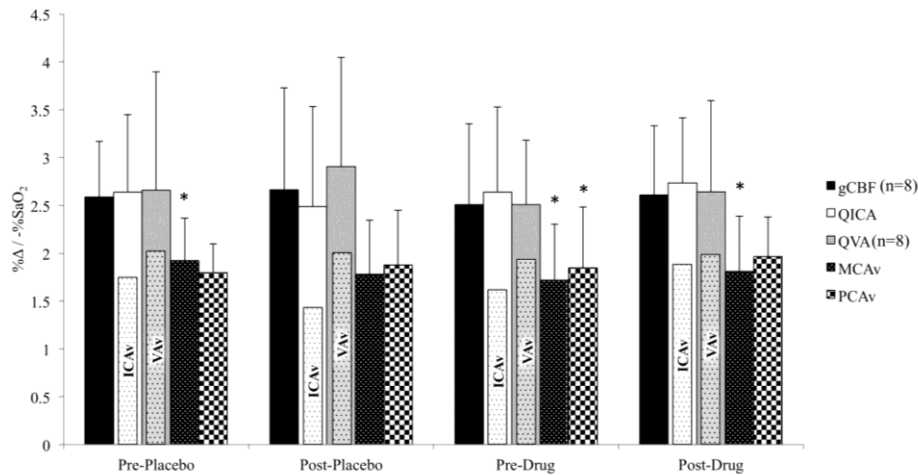


**Figure 3.2. Reactivity slopes of extra- and intra-cranial blood vessels in all experimental trials at sea-level.**

The percent increase in CBF per percent drop in SaO<sub>2</sub> is depicted for each vessel insonated, during all trials. Volumetric reactivity (gCBF, Q<sub>ICA</sub>, Q<sub>VA</sub>) was not different within or between trials, while MCA<sub>v</sub> and PCA<sub>v</sub> reactivity were lower than Q<sub>ICA</sub> (main effect: P<0.001) and Q<sub>VA</sub> (main effect: P=0.008) reactivity respectively in all trials. The percent reactivity of ICA<sub>v</sub> and VAV are superimposed onto their respective flow reactivity columns to highlight the contribution of velocity versus diameter changes in determining overall flow reactivity. gCBF, global cerebral blood flow; Q<sub>ICA</sub>, internal carotid artery blood flow; Q<sub>VA</sub>, vertebral artery blood flow; MCA<sub>v</sub>, middle cerebral artery blood velocity; PCA<sub>v</sub>, posterior cerebral artery blood velocity; ICA<sub>v</sub>, internal carotid artery blood velocity; VAV, vertebral artery blood velocity. \* indicates significant difference between confluent vessel velocity and volumetric reactivity (e.g., Q<sub>ICA</sub> vs MCA<sub>v</sub>), P<0.05 after correction for multiple comparisons. n=12 unless otherwise specified. Reproduced from (Hoiland *et al.*, 2017b), permission not required.

#### **3.2.1.4 BETWEEN VESSEL COMPARISONS**

There was no main effect of theophylline (P=0.45) or vessel (P=0.41) on the percent reactivity of the MCA<sub>v</sub> versus PCA<sub>v</sub> to hypoxia. Similarly, for Q<sub>ICA</sub> versus Q<sub>VA</sub> there was no main effect of theophylline (P=0.97) or vessel (p=0.69). Volumetric reactivity through the ICA (Q<sub>ICA</sub>) was greater than velocity reactivity of the MCA (main effect of vessel: P<0.001), while Q<sub>VA</sub> reactivity was greater than PCA<sub>v</sub> reactivity (main effect of vessel: P=0.008) (Figure 3.2).

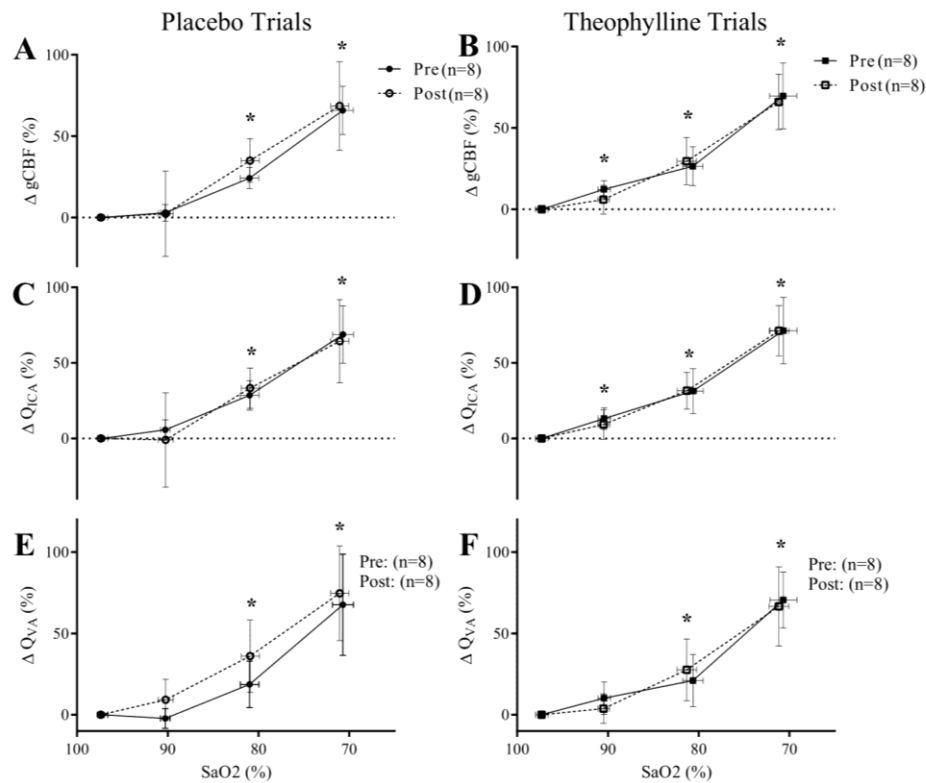


**Figure 3.3. Global and regional cerebral blood flow during isocapnic hypoxia prior to and following placebo and theophylline interventions.**

The three panels on the left depict CBF (gCBF,  $Q_{ICA}$ ,  $Q_{VA}$ ) responses pre (●) and post (○) placebo, while the three panels on the right depict the CBF responses pre (■) and post (□) theophylline. Data are presented as the percent change of each variable from baseline. There was no effect of theophylline treatment on the %changes in CBF from baseline. \* indicates a post-hoc derived significant change from baseline ( $P < 0.05$ ) following a main effect of  $SaO_2$  on CBF variables ( $P < 0.05$ ).  $n = 12$  unless otherwise specified. Reproduced from (Hoiland *et al.*, 2017b), permission not required.

### 3.2.2 HIGH-ALTITUDE STUDY

The resting room air baseline measurements for the sea-level placebo trial (pre-intervention) were used as the sea-level baseline for comparison to the HA data. Cerebrovascular, hemodynamic and respiratory variables for the sea-level baseline and at HA are presented in **Table 3.5**. Compared to sea-level,  $V_E$ , HR and MAP were increased (main effect, all  $P < 0.05$ ) at all HA time points, while  $SaO_2$ ,  $P_{ET}O_2$ ,  $P_{ET}CO_2$  were reduced (main effect, all  $P < 0.05$ ) at all time points. Six hours post-intervention  $Q_{VA}$  was

significantly lower in the theophylline trial compared to placebo ( $P=0.047$ ), while there was a tendency for gCBF to be lower in the theophylline group ( $P=0.058$ ). However, these differences were abolished when end-tidal gases were matched between groups and to the initial exposure time (**Table 3.5**). There was no elevation in  $Q_{ICA}$  at HA as compared to sea-level baseline and  $eCDO_2$  was not different from sea-level to HA or between groups.

**Table 3.5. Cerebral vascular, hemodynamic, and respiratory variables upon exposure to high-altitude.**

The sea-level baseline was selected from the pre-placebo trial, while the time after arrival to the Barcroft Laboratory is indicated in brackets for each high-altitude time point.

		Sea-Level (344m)	High-Altitude (3800m)		
		Kelowna	Initial exposure (2hrs)	5 hours post drug (7hrs)	5 hours post drug clamped (7hrs)
<i>Drug vs. Placebo: P=0.062; O<sub>2</sub>: P&lt;0.001; Interaction: P=0.247</i>					
SaO <sub>2</sub> (% oxyhemoglobin)	Drug	97.5±0.4	89.2±1.1*	87.3±0.7*	88.0±0.4*
	Placebo	97.4±0.3	87.7±1.7*	85.8±2.3*	87.9±0.7*
<i>Drug vs. Placebo: P=0.124; O<sub>2</sub>: P&lt;0.001; Interaction: P=0.671</i>					
P <sub>ET</sub> O <sub>2</sub> (mmHg)	Drug	96.9±6.4	57.1±2.2*	53.4±1.2*	54.7±0.7*
	Placebo	95.3±3.3	54.4±2.7*	51.4±3.6*	54.5±1.3*
<i>Drug vs. Placebo: P=0.368; O<sub>2</sub>: P&lt;0.001; Interaction: P=0.724</i>					
P <sub>ET</sub> CO <sub>2</sub> (mmHg)	Drug	39.7±4.1	32.6±1.4*	34.7±2.5*	33.0±0.5*
	Placebo	41.4±2.2	33.1±1.5*	35.5±2.0*	33.0±0.4*
<i>Drug vs. Placebo: P=0.069; O<sub>2</sub>: P&lt;0.001; Interaction: P=0.636</i>					
V <sub>E</sub> (L · min <sup>-1</sup> )	Drug	9.6±2.0		13.3±1.5*	18.5±2.6*
	Placebo	10.7±2.5		14.5±2.4*	21.4±5.5*
<i>Drug vs. Placebo: P=0.430; O<sub>2</sub>: P&lt;0.001; Interaction: P=0.075</i>					
MAP (mmHg)	Drug	78.0±3.8	83.5±5.9*	84.9±7.6*	86.9±8.8*
	Placebo	76.7±5.0	87.6±2.0*	91.9±7.1*	85.7±3.9*
<i>Drug vs. Placebo: P=0.156; O<sub>2</sub>: P&lt;0.001; Interaction: P=0.666</i>					
HR (beats · min <sup>-1</sup> )	Drug	56.2±14.1	63.2±7.6	62.5±11.4	72.5±8.7*
	Placebo	65.4±11.7	74.5±23.3	79.8±19.9	85.4±25.2*
<i>Drug vs. Placebo: P=0.094; O<sub>2</sub>: P=0.032; Interaction: P=0.189</i>					
gCBF (mL · min <sup>-1</sup> )	Drug	682.5±96.6 (n=5)	778.0±80.6 (n=5)	706.9±67.7 (n=5)	693.9±56.4 (n=5)
	Placebo	748.7±108.5	850.7±94.0	898.3±126.7	822.8±111.9
<i>Drug vs. Placebo: P=0.462; O<sub>2</sub>: P=0.618; Interaction: P=0.222</i>					
Q <sub>ICA</sub> (mL · min <sup>-1</sup> )	Drug	271.1±70.5	272.7±33.8	255.6±31.5	260.7±47.9
	Placebo	256.1±28.2	288.1±44.5	297.4±54.1	281.1±36.9
<i>Drug vs. Placebo: P=0.093; O<sub>2</sub>: P=0.541; Interaction: P=0.256</i>					
ICA <sub>v</sub> (cm · s <sup>-1</sup> )	Drug	45.1±6.8	43.8±3.4	42.2±6.2	42.7±7.0
	Placebo	48.4±6.4	48.1±7.7	55.4±12.0	50.5±10.4
<i>Drug vs. Placebo: P=0.372; O<sub>2</sub>: P=0.132; Interaction: P=0.478</i>					
ICA diameter (mm)	Drug	5.02±0.60	5.14±0.43	5.08±0.42	5.09±0.44
	Placebo	4.74±0.42	5.05±0.33	4.80±0.47	4.88±0.26
<i>Drug vs. Placebo: P=0.117; O<sub>2</sub>: P=0.039; Interaction: P=0.038</i>					
Q <sub>VA</sub> (mL · min <sup>-1</sup> )	Drug	96.4±25.6 (n=5)	121.0±31.9 (n=5)	98.5±25.9‡ (n=5)	102.1±28.4 (n=5)
	Placebo	118.2±28.4	137.2±27.4	151.8±29.6	130.4±31.6

		Sea-Level (344m)	High-Altitude (3800m)		
		Kelowna	Initial exposure (2hrs)	5 hours post drug (7hrs)	5 hours post drug clamped (7hrs)
<i>Drug vs. Placebo: P=0.053; O<sub>2</sub>: P=0.002; Interaction: P=0.001</i>					
VA <sub>v</sub> (cm · s <sup>-1</sup> )	<b>Drug</b>	22.6±5.0 (n=5)	26.6±6.7 (n=5)	21.7±5.4 (n=5)	21.8±4.8 (n=5)
	<b>Placebo</b>	26.5±1.8	28.7±4.1	34.2±3.7*‡	30.1±6.4
<i>Drug vs. Placebo: P=0.532; O<sub>2</sub>: P=0.008; Interaction: P=0.493</i>					
VA diameter (mm)	<b>Drug</b>	4.22±0.27 (n=5)	4.41±0.20 (n=5)	4.31±0.34 (n=5)	4.12±0.35 (n=5)
	<b>Placebo</b>	4.31±0.43	4.49±0.24	4.32±0.33	4.28±0.31
<i>Drug vs. Placebo: P=0.129; O<sub>2</sub>: P=0.226; Interaction: P=0.195</i>					
eCDO <sub>2</sub> (mL · min <sup>-1</sup> )	<b>Drug</b>	137.9±16.7	143.8±14.1	127.0±12.0	125.9±9.9
	<b>Placebo</b>	150.9±21.7	153.6±17.0	158.5±22.0	149.0±20.9

**Bolded Drug or Placebo** indicates main effect of the intervention, with the bolded trial significantly greater,  $P < 0.05$ . \*signifies a significant difference from baseline,  $P < 0.05$ . ‡ indicates significant difference between drug and placebo, corrected for multiple comparisons,  $P < 0.05$ .  $n = 6$  unless otherwise specified.

In the placebo group, Lake Louise AMS scores did not change from initial exposure ( $2.4 \pm 1.5$ ) to six hours post intervention ( $4.4 \pm 3.1$ ) or the following morning ( $2.6 \pm 0.9$ ) ( $P = 0.585$ ). Similarly, in the theophylline group there was no difference in AMS scores from initial exposure ( $2.8 \pm 2.5$ ) to six hours post intervention ( $2.3 \pm 3.0$ ) or the following morning ( $2.8 \pm 3.2$ ) ( $P = 0.585$ ). There was no main effect of theophylline on AMS scores compared to placebo ( $P = 0.723$ ).

### 3.3 STUDY 1 - DISCUSSION

At sea-level and under the conditions of isocapnic hypoxia the novel findings of this study are; 1) hypoxic vasodilation of the ICA, while confirming earlier reports of hypoxic vasodilation of the VA (Willie *et al.*, 2012); 2) the vasomotor response of these extracranial arteries and overall gCBF is unaffected by non-selective adenosine receptor antagonism during all stages of isocapnic hypoxia, and 3) anterior ( $Q_{ICA}$ ) and posterior ( $Q_{VA}$ ) cerebrovascular reactivity to isocapnic hypoxia were not different. At HA under the conditions of poikilocapnic hypoxia, adenosine receptor antagonism reduced  $Q_{VA}$  compared to the placebo group, however, this difference was abolished when end-tidal gases were matched between groups. Collectively, these results indicate adenosine receptor

dependent signaling is not obligatory for hypoxic cerebral vasodilation under the conditions of normobaric and hypobaric hypoxia.

### 3.3.1 MECHANISMS OF HYPOXIC CEREBRAL VASODILATION

Hypoxia increases production of adenosine in cerebral tissue (Winn *et al.*, 1981a; Kulik *et al.*, 2010), which, in animal models, is reflected in cerebral arteriolar vasodilation (Berne *et al.*, 1974). However, the present study provides evidence that, in humans, adenosine receptor dependent signaling is not an obligatory regulator of CBF during normobaric or hypobaric hypoxia. This is consistent with previous studies that have utilized pharmacological adenosine receptor antagonism under less controlled conditions (Bowton *et al.*, 1988; Nishimura *et al.*, 1993). Our current findings are further consistent with studies utilizing pharmacological inhibition of cAMP prior to a hypoxic exposure (Fan *et al.*, 2011; Harrell & Schrage, 2014; Hoiland *et al.*, 2015; Peltonen *et al.*, 2015). Given that cAMP inhibition with indomethacin (Kantor & Hampton, 1978; Goueli & Ahmed, 1980) does not affect reactivity of cerebral vessels to hypoxia, and adenosine induces vasodilation largely through increasing cAMP levels (Sattin & Rall, 1970; Nordstrom *et al.*, 1977) downstream of A<sub>2A</sub> receptor binding (Miekisiak *et al.*, 2008; Liu *et al.*, 2015), it is perhaps not surprising that adenosine receptor antagonism had no effect on CBF in the current study. Nevertheless, adenosine has also been reported to induce cerebral vasodilation through increasing inward rectifying potassium channel conductance (Hein *et al.*, 2013). While inward rectifying potassium channels have been shown to regulate skeletal muscle blood flow, it remains to be investigated if adenosine regulates hypoxic cerebral vasodilation in humans via action on inward rectifying potassium channels.

This study and others indicating an insignificant role of cAMP in hypoxic cerebral vasodilation (Fan *et al.*, 2011; Harrell & Schrage, 2014; Hoiland *et al.*, 2015; Peltonen *et al.*, 2015), lead to the speculation that signaling pathways relying on cGMP (not cAMP) must be the primary regulators of CBF during hypoxia. This is consistent with the notion that red blood cell mediated release of s-nitrosohemoglobin and adenosine triphosphate in addition to nitrite reductase activity, which all lead to up-regulation of cGMP, are the primary regulators of hypoxic cerebral vasodilation (Ellsworth *et al.*, 1995; Jia *et al.*, 1996; Hoiland *et al.*, 2016a). Furthermore, given recent evidence that shear stress contributes to vasodilation of cerebral conduit arteries [e.g. ICA; (Carter *et al.*, 2016a)], this mechanism

may also contribute to hypoxic cerebral vasodilation. These latter possibilities remain to be established.

In addition to hypoxia induced upregulation of specific signaling pathways, the potential for other physiological factors to influence gCBF and the diameter of the ICA and VA remains. For example, MAP directly influences CBF (Lucas *et al.*, 2010; Numan *et al.*, 2014) but increases in MAP do not seem to affect the %change in MCAv for a given CO<sub>2</sub> stimulus. Indeed, a pressor response of <10 mmHg or >10 mmHg increase in MAP does not lead to a difference in %MCAv reactivity, however, conductance is affected given the difference in denominator for calculating CVC (Regan *et al.*, 2014). Similarly, changes in MAP were not related to changes in CBF variables in previous investigation under hypoxic conditions (Willie *et al.*, 2012). While there was a significant relationship between MAP and CBF variables pre theophylline and placebo (but not post either intervention; **Figure 3.4**), the presence of ICA vasodilation (**Table 3.2**) prior to an increased MAP (**Table 3.1**) in all trials (irrespective of correlation with MAP) infers active, not passive, changes in vessel caliber and a relatively small role of MAP in our diameter responses. Nonetheless, direct pressure passive effects on CBF (Lucas *et al.*, 2010), and the potential for pressure mediated vessel distension cannot be discounted as contributors to the integrative regulation of CBF during hypoxia.

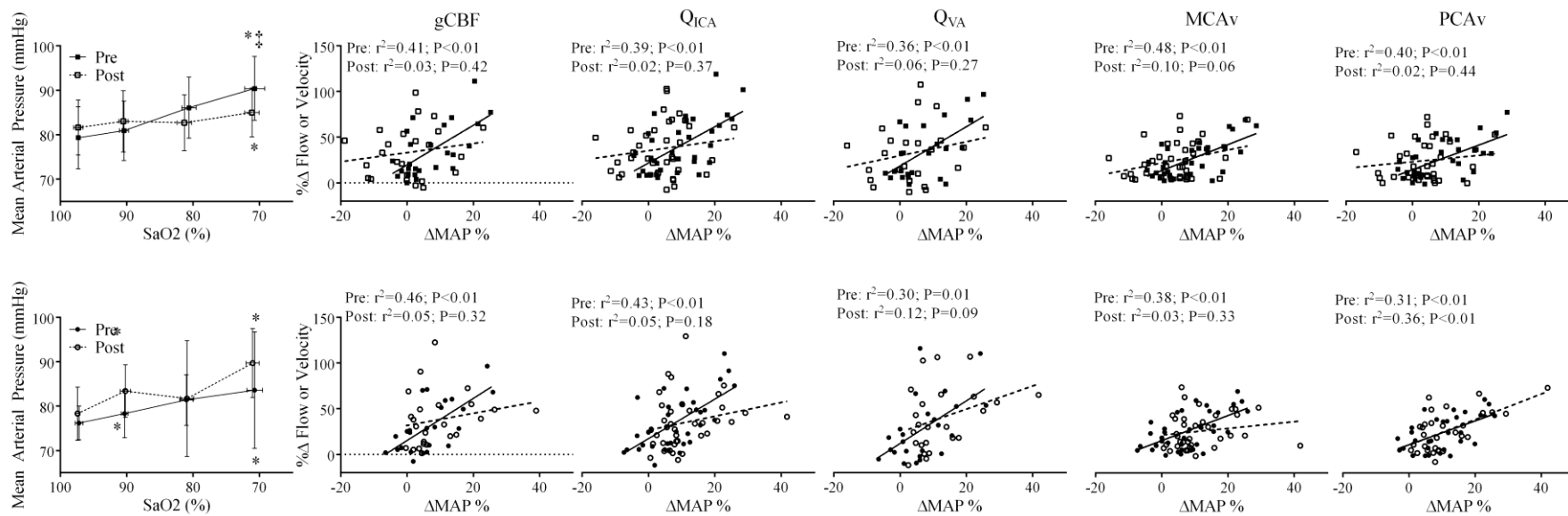


**Figure 3.4. The relationships between mean arterial pressure and cerebral blood flow variables in the theophylline and placebo trials.**

The two left panels represent the changes in MAP during a reduction in arterial oxygen saturation during the theophylline (upper panel) and placebo (lower panel) trials. The upper row of correlations depict the relationship between the percent change in MAP (%ΔMAP) and the percent change in CBF variables (%ΔFlow or Velocity) pre (■) and post (□) theophylline, while the bottom row shows the same data, but for the pre (●) and post (○) placebo trials. \* indicates a significant difference from baseline,  $P<0.05$ ; ‡ indicates significant difference between drug and placebo,  $P<0.05$ .  $n=12$  unless otherwise specified. Reproduced from (Hoiland *et al.*, 2017b), permission not required.

As per previous studies utilizing drug interventions, this study highlights the necessity of using a placebo time control trial for proper interpretation (Peebles *et al.*, 2012). Much like a previous study by Peebles and colleagues if we had not had a placebo trial it would have led to the erroneous conclusion that theophylline, while not affecting overall reactivity, diminishes the influences of MAP on CBF in hypoxia. However, while speculative, given the similar lack of correlation between MAP and CBF variables following placebo (**Figure 3.4**), it appears that this may be a result of repeated within day exposure to hypoxia, or a time of day effect as the pre versus post trials were separated by six hours. In other words, that the placebo and theophylline trial showed the same change in the MAP and CBF relationship indicates this is not an adenosine related change. As CBF reactivity to hypoxia was not different, in the presence or absence of a correlation with MAP, suggests indirectly that MAP did not appreciably influence CBF in the present study i.e., correlation does not reflect causation. This finding is noteworthy as reductions in resting MAP or the MAP response during hypercapnia results in a blunting of CBF reactivity to CO<sub>2</sub> (Harper & Glass, 1965b; Ainslie *et al.*, 2012); thus, it seems plausible that the influence of MAP on CBF differs depending on the prevailing blood gas stimulus.

### **3.3.2 CEREBRAL BLOOD FLOW AND NORMOBARIC HYPOXIA**

At sea-level, there is conflicting evidence regarding hypoxic vasodilation of the extracranial cerebral arteries (ICA & VA) (Willie *et al.*, 2012; Ogoh *et al.*, 2013b; Lewis *et al.*, 2014b). Our study supports previous work (Willie *et al.*, 2012; Subudhi *et al.*, 2014b; Lewis *et al.*, 2014b) demonstrating vasodilation of the VA during hypoxia, although this has not been consistently reported (Ogoh *et al.*, 2013b). Differences in methodological and analytical factors may explain these differences. For example, in the study by Ogoh *et al.*, manual measurements of vessel diameter were used to detect hypoxic vasodilation, whereas automated edge-detection software was used in the current study and our previous work (Willie *et al.*, 2012; Lewis *et al.*, 2014b). Our automated edge-detection software, which has been validated using phantom models (Woodman *et al.*, 2001), possess a lower intra-observer error than manual caliper measurements of arterial diameter (Woodman *et al.*, 2001; Thomas *et al.*, 2015). Moreover, we observed hypoxic vasodilation of the ICA, the occurrence of which there is similarly both support for (Lewis *et al.*, 2014b) and against (Willie *et al.*, 2012; Ogoh *et al.*, 2013b; Subudhi *et al.*, 2014b). This study is the first to report ICA vasodilation during normobaric isocapnic hypoxia.

Contrary to previous studies investigating cerebral vascular reactivity to isocapnic hypoxia (Willie *et al.*, 2012), we report no difference in anterior vs. posterior relative (%) reactivity. As approximately 25-40% of the increase in  $Q_{ICA}$  and  $Q_{VA}$  may be attributable to vasodilation (**Figure 3.2**), the regional differences observed by Willie *et al.*, 2012 may be due to a failure to detect ICA vasodilation in the face of VA vasodilation (Willie *et al.*, 2012). In addition to the small sample size ( $n=7$  for ICA), and a prolonged stage of hypoxia (15-minutes), a technical consideration is the quality of the ultrasound used by Willie *et al.*, 2012 (Terason t3000) versus that used in the present study (Terason t3200). For example, advances in spatial resolution of other imaging techniques (i.e., MRI) have produced new insight into vascular control during alterations in arterial blood gases [reviewed in: (Hoiland & Ainslie, 2016a)]. We feel technical, not physiological, differences between studies may have precluded the ability to detect small, yet significant, changes in ICA diameter and lead to between study differences. Further, vasodilation of the ICA is consistent with downstream increases in MCA diameter that have been demonstrated with both MRI (Wilson *et al.*, 2011; Sagoo *et al.*, 2016) and transcranial color coded ultrasound (Wilson *et al.*, 2011; Imray *et al.*, 2014), indicating vasodilation to hypoxia throughout the cerebrovascular tree. Despite no differences between posterior and anterior reactivity, it is important to note there still exists a heterogeneous reactivity among specific brain regions (Binks *et al.*, 2008). While increases in CBF act to maintain  $CDO_2$  in the face of arterial hypoxemia [reviewed in: (Hoiland *et al.*, 2016a)], our calculation of  $eCDO_2$  indicates that adequate  $CDO_2$  was likely maintained during isocapnic hypoxia, and is not dependent on an adenosine receptor dependent signaling pathway.

Despite a lower CBF during hypoxia in the theophylline trial, our data still provides evidence that cerebral vasodilation is unaltered by adenosine receptor antagonism. The lower CBF can be attributed to the lower  $P_{ET}CO_2$  throughout the theophylline trial, as evidenced by the lack of difference between trials once CBF is mathematically corrected for the difference in  $P_{ET}CO_2$  using standard volumetric reactivity values. Further, indicating unaltered vascular responsiveness, the reactivity slopes of  $Q_{ICA}$ ,  $Q_{VA}$ , and  $gCBF$  were not different pre versus post theophylline. While our experimental design allowed for the quantification of extra-cranial cerebral artery vasodilation, which was unaltered (**Table 3.2**), the unaltered  $gCBF$  provides indirect evidence that adenosine receptor dependent signaling also has no effect on downstream resistance vessels (e.g., pial vessels). The lack

of effect of theophylline is highlighted by the tight overlap of CBF during hypoxia pre- versus post-theophylline (**Figure 3.3**).

### 3.3.3 CEREBRAL BLOOD FLOW AND HYPOBARIC HYPOXIA

Measurements of CBF at HA have consistently demonstrated that CBF increases to an extent that compensates for the reductions in  $\text{CaO}_2$  (or  $\text{SaO}_2$ ) to maintain  $\text{CDO}_2$  [reviewed in: (Ainslie & Subudhi, 2014; Hoiland *et al.*, 2016a)]. Our calculations provide indirect evidence of adequate maintenance of  $\text{CDO}_2$  and further demonstrate that maintenance of  $\text{CDO}_2$  at HA is not dependent on adenosine receptor dependent signaling (**Table 3.3**). Given that hemoglobin concentration is likely unaltered (Severinghaus *et al.*, 1966b) or even slightly increased (Subudhi *et al.*, 2014b) within 8 hours following rapid ascent to HA, an unaltered CBF and  $\text{SaO}_2$  in the face of adenosine receptor antagonism provides compelling evidence, albeit inferential, that  $\text{CDO}_2$  is commensurately unaltered. Despite no main effect of  $\text{O}_2$  (i.e., HA) on  $\text{Q}_{\text{ICA}}$ , contrary to previous study showing increased  $\text{Q}_{\text{ICA}}$  upon ascent to HA (Subudhi *et al.*, 2014b), the maintenance of  $\text{eCDO}_2$  (i.e., global delivery) indicates adequate responsiveness of the cerebral vasculature as a whole to the hypoxic stimulus. No change in  $\text{Q}_{\text{ICA}}$  may simply reflect the lower hypoxic stimulus (3800m,  $\text{SaO}_2 \sim 87\%$ ) in the present study versus that of Subudhi *et al.*, (5260m,  $\text{SaO}_2 \sim 76\%$ ). In keeping,  $\text{Q}_{\text{ICA}}$  was only modestly elevated at 90% $\text{SaO}_2$  in the sea level theophylline trials and did not significantly increase until  $\text{SaO}_2$  dropped to 80% in the sea-level placebo trials (**Table 3.2**); therefore, it is perhaps not surprising that  $\text{Q}_{\text{ICA}}$  was not statistically elevated at HA where the relatively mild hypoxic stimulus (87%  $\text{SaO}_2$ ) is occurring simultaneous to moderate hypocapnia ( $\text{P}_{\text{ETCO}_2} \approx 32\text{-}34\text{mmHg}$ ). The latter response, which acts to constrict the cerebral vessels, likely balanced with the vasodilatory influence of the mild hypoxic stimulus to produce no overall change in diameter. However, given the small sample size ( $n=6$ ) in each group for the HA data, it is important to interpret these data judiciously and consider them more exploratory than confirmatory. Power calculations indicate that given the change in CBF observed a sample size of  $n=12$  in each group would be necessary to observe a significant difference with a power of 0.80. Therefore, further study using a larger sample size is needed to make firm conclusions regarding adenosine receptor antagonism and CBF regulation at HA.

### 3.3.4 ACUTE MOUNTAIN SICKNESS

Theophylline has been demonstrated to reduce AMS symptoms at 3454m (Fischer *et al.*, 2000) and 4559m (Kupper *et al.*, 2008), which was speculated to be due to a reduction in gCBF (Fischer *et al.*, 2000). However, given the speculative role of gCBF in the pathogenesis of AMS (Ainslie & Subudhi, 2014; Sagoo *et al.*, 2016) we aimed to concurrently assess AMS and CBF following theophylline treatment at HA (3800m). Contrary to previous study (Fischer *et al.*, 2000; Kupper *et al.*, 2008) we demonstrate no effect of theophylline on AMS scores when end-tidal gases were matched; however, this (end-tidal clamping) is not reflective of normal physiology upon sojourn to HA. Indeed, CBF did not increase following theophylline, despite seemingly, although not statistically, increasing (+20%) in the placebo trial, under poikilocapnic (natural) conditions. Therefore, as there was no difference when end-tidals were matched, it seems that theophylline may act indirectly via hyperventilation-induced hypocapnia (not adenosine receptor antagonism) to reduce CBF. While AMS was not statistically different between the placebo and theophylline group, it was 48% lower (concomitant to a tendency for lower gCBF). These differences in CBF and AMS following theophylline, if confirmed in a larger sample size, may be meaningful despite the lack of significance (note, n=6 in each group). For example, at a power of 0.8, a sample size of n=12 would be required for each group to detect a statistical difference when CBF increases to the magnitude observed in the present study. Therefore, although not through a direct effect on the vasculature, theophylline may indeed be prophylactic in treating AMS by causing hyperventilation-induced hypocapnia and consequent reductions in CBF via vasoconstriction. This finding provides preliminary data that CBF is potentially implicated in previously observed theophylline induced reductions in AMS (Fischer *et al.*, 2000). However, the effect of theophylline on AMS may simply also be attributable to other factors such as an elevated resting SaO<sub>2</sub> (Fischer *et al.*, 2000). Collectively, given the small sample size for both AMS and CBF it is difficult to draw firm conclusions from the current study. Further research is needed to determine if CBF regulation and/or improved oxygenation due to hyperventilation is related to potential benefits of theophylline on AMS severity.

### 3.3.5 METHODOLOGICAL CONSIDERATIONS

In the present study, SaO<sub>2</sub> and CaO<sub>2</sub> were estimated from P<sub>ET</sub>O<sub>2</sub> and normative values for hemoglobin. With direct measures of PaO<sub>2</sub> occurring in the following study (see section Erythrocyte mediated hypoxic cerebral vasodilation in humans) it is important to consider the agreement between our calculated versus experimentally measured variables. As depicted in **Figure 3.5**, there is a mean bias where measured SaO<sub>2</sub> is lower than estimated SaO<sub>2</sub> when determined from the Severinghaus equation (Severinghaus, 1979a). This indicates subjects may have been slightly more hypoxic than reported with our estimations in the current study. However, what is important to note is that this difference would persist between trials and not introduce error related to the comparison of the hypoxic stimulus between each condition. In other words, this would lead to a systematic error, not random error, and therefore, not influence our primary findings.

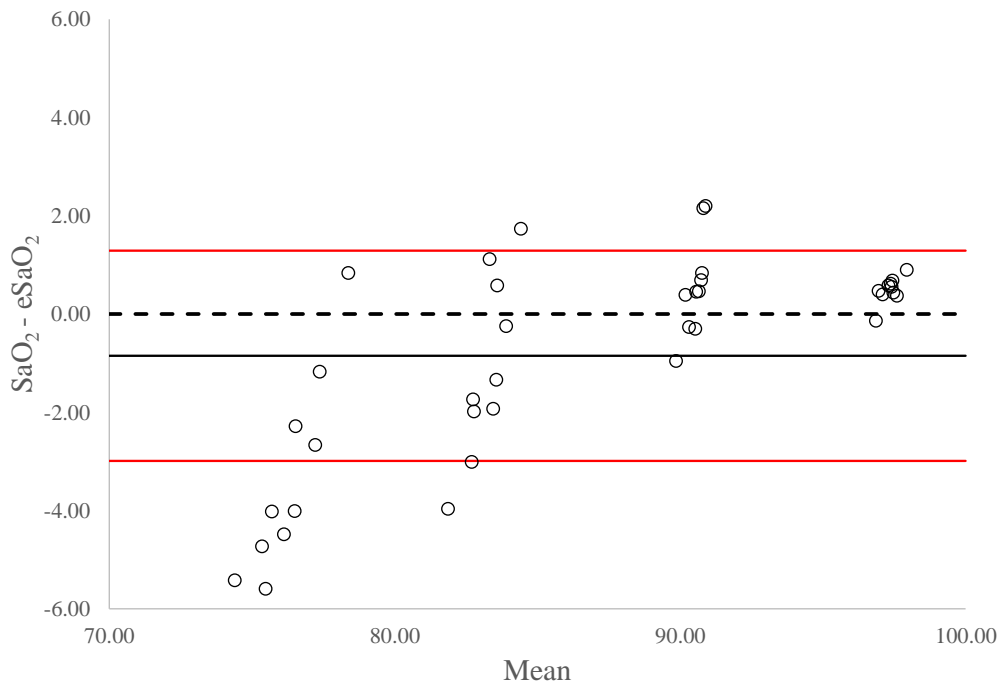


**Figure 3.5. Agreement between measured and calculated arterial oxygen saturation.**

The above figure is a bland altman plot of data from Study 2 of this thesis. Here, measured arterial oxygen saturation ( $SaO_2$ ) and estimated arterial oxygen saturation ( $eSaO_2$ ) are depicted. The black dashed line indicates zero on the Y-axis, whereas the solid black line indicates mean bias, which was  $-0.85$  in this case. This indicates that arterial  $SaO_2$  is lower than  $eSaO_2$  when estimated using the severinhaus equation (Severinghaus, 1979a). The lower and upper limits of agreement are plotted as red lines.

### **3.4 STUDY 1 - SUMMARY**

We demonstrated that the ICA and VA dilate during isocapnic hypoxia at sea-level and that this vascular response to hypoxia is unaltered by adenosine receptor dependent signaling. Contrary to previous studies we demonstrate that anterior and posterior reactivity, indexed by  $Q_{ICA}$  and  $Q_{VA}$  respectively, does not differ during hypoxia. We extend these findings to highlight that theophylline does not affect regional reactivity in a differential manner. Following rapid ascent to HA, CBF is unaltered by theophylline when arterial blood gases are controlled. Collectively, our sea-level and HA data indicate that adenosine receptor dependent signaling is not obligatory for cerebral vasodilation during hypoxia.

#### 4 ERYTHROCYTE MEDIATED HYPOXIC CEREBRAL VASODILATION IN HUMANS

In humans, reductions in  $\text{CaO}_2$  initiate a signaling cascade that increases CBF to maintain  $\text{CDO}_2$  (Ainslie *et al.*, 2014; Hoiland *et al.*, 2016a). Human research aimed at determining these signaling pathways is sparse, and difficult to conduct due to the invasive nature of mechanistic studies and the usual necessity of pharmacological blockade. Currently, there is evidence that neither adenosine (Bowton *et al.*, 1988; Nishimura *et al.*, 1993; Hoiland *et al.*, 2017b), PGs (Fan *et al.*, 2011; Hoiland *et al.*, 2015; Peltonen *et al.*, 2015) or SNA (Lewis *et al.*, 2014b) play an obligatory role in human hypoxic cerebral vasodilation. However, there is some data supporting the notion that NO mediates hypoxic cerebral vasodilation (Van Mil *et al.*, 2002b; Peebles *et al.*, 2008), although this has not been consistently demonstrated (Ide *et al.*, 2007).

In agreement with the idea that NO may regulate hypoxic cerebral vasodilation in humans, a large body of research has now implicated erythrocyte mediated signal transduction as a primary regulator of systemic (e.g., forearm) hypoxic vasodilation (Gladwin *et al.*, 2006; Ellsworth *et al.*, 2009; Doctor & Stamler, 2011). These results have also been extended to vasodilation in the cerebral circulation of rats (Jia *et al.*, 1996; Stamler *et al.*, 1997b). This is in agreement with a multitude of pharmacological blockade studies in animals demonstrating reduced hypoxic cerebral vasodilation following NOS inhibition [reviewed in: (Hoiland *et al.*, 2016a)]. This role of NO is hypothesized to be attributable to one of three erythrocyte dependent pathways: 1) deoxyhemoglobin mediated release of ATP (Ellsworth *et al.*, 1995), 2) deoxyhemoglobin mediated release of SNO-Hb (Stamler *et al.*, 1997b), and 3)  $\text{NO}_2$  reduction to bioactive NO species by deoxyhemoglobin (Gladwin *et al.*, 2006). All three of these processes have been studied extensively, and ultimately hinge on the R-state to T-state allosteric shift associated with the desaturation of hemoglobin (Stamler *et al.*, 1997b; Jagger *et al.*, 2001; Huang *et al.*, 2005).

Differential reactivity between hypoxemia and hemodilution in humans has been speculated to indicate an important role of the erythrocyte in hypoxic cerebral vasodilation [reviewed in: (Hoiland *et al.*, 2016a)]. However, a comparison between hypoxemia and hemodilution has yet to be conducted within-subjects. Further, in healthy humans, the role of biological variability in resting [Hb] on the magnitude of hypoxic cerebral vasodilation

has yet to be explored. Indeed, if the red blood cell is integral to hypoxic vasodilation, one may expect differences in [Hb] between individuals to confer variations in vasodilation to a hypoxic stimulus that would be reflected in a relationship between [Hb] and cerebrovascular reactivity to hypoxia. Therefore, the two primary purposes of this study were to: 1) assess hypoxic cerebrovascular reactivity to hypoxia during experimental hypoxemia and hemodilution; 2) determine if experimental manipulations of [Hb] as well as biological variability in resting [Hb] are related to the magnitude of hypoxic cerebral vasodilation. It was hypothesized that, 1) compared to hypoxemia, the CBF response to hemodilution would be attenuated; 2) Experimental *within subject* reductions in [Hb] would be reflected in an attenuated hypoxic reactivity, with the same relationship between [Hb] and reactivity occurring *between subjects* as a result of natural biological variability in resting [Hb].

#### **4.1 STUDY 2 - METHODS**

Following an outline of the experimental measures, two separate protocols will be described. The first protocol addresses purpose 1 of the study by comparing the CBF response to hypoxemia with that of hemodilution. The first protocol also addresses purpose 2 using a *within* subjects design, where the influence of [Hb] on hypoxic reactivity to hypoxemia is assessed. Ten young healthy male participants were recruited to partake in the first protocol (Age:  $29\pm 7$  years; body mass index:  $23\pm 2$  Kg · m<sup>-2</sup>).

The second protocol addresses purpose 2 of the study by assessing the relationship between [Hb] and hypoxic reactivity in a large subject sample. Therefore, *between* subject differences in [Hb] and hypoxic reactivity were determined. A data repository that contained data on 199 young healthy subjects was analyzed for this study (Age:  $26\pm 6$  years; body mass index:  $24\pm 3$ ).

All participants were engaged in a conversation on the experimental protocol and associated risks. Informed consent was then obtained in writing. This study adhered to the standards outlined in Declaration of Helsinki and the Canadian Tri-council Policy Statement for Integrity in Research and was approved by the University of British Columbia Clinical Research Ethics Board (CREB ID: H16-01028; H18-01755).

## 4.1.1 PROTOCOL ONE

### 4.1.1.1 PROTOCOL ONE - EXPERIMENTAL MEASURES

Cardiovascular and cerebrovascular measures were conducted as outlined previously in Study 1 (e.g., MAP, SV, CO & TPR determined from the Finometer). Further, the same end-tidal forcing apparatus was utilized to target specific blood gas values. Measurements unique to this study are outlined below.

#### 4.1.1.1.1 ARTERIAL AND VENOUS CANNULATION

Using sterile technique, a 20G arterial catheter (Arrow, Markham, ON) was advanced into the left radial artery under local anesthesia (Lidocaine, 1.0%) (**Figure 4.1**). This technique was assisted via the use of ultrasound guidance. Subsequently, a 13G central venous catheter (Cook Medical, Bloomington, IN) was advanced into the right internal jugular vein, again under sterile conditions and with the use of local anesthesia and ultrasound guidance (**Figure 4.1**). The catheter was then advanced up to 15 cm cephalad (Schell & Cole, 2000). This technique has been previously demonstrated to lead to catheter tip placement in the jugular bulb, which is importantly proximal to the facial vein (Ainslie *et al.*, 2014). Further, correct placement was additionally determined by participants noting a sensation in their ear upon full insertion of the catheter (Schell & Cole, 2000). Fulfilment of these techniques leads to  $\leq 3\%$  contamination by extra-cerebral blood (Schell & Cole, 2000). Finally, an 18G venous catheter (Insyte™ Autoguard™, Becton Dickinson, USA) was inserted into the median ante-cubital vein.

The radial arterial and jugular venous catheters were both attached to an in-line and waste-less sampling system (VAMP system, Edwards Life Sciences). This allows for serial blood sampling (see section “Protocol one – experimental overview”) and the continuous measurement of radial arterial and jugular venous blood pressure (Truwave Transducer, Edwards Life Sciences).

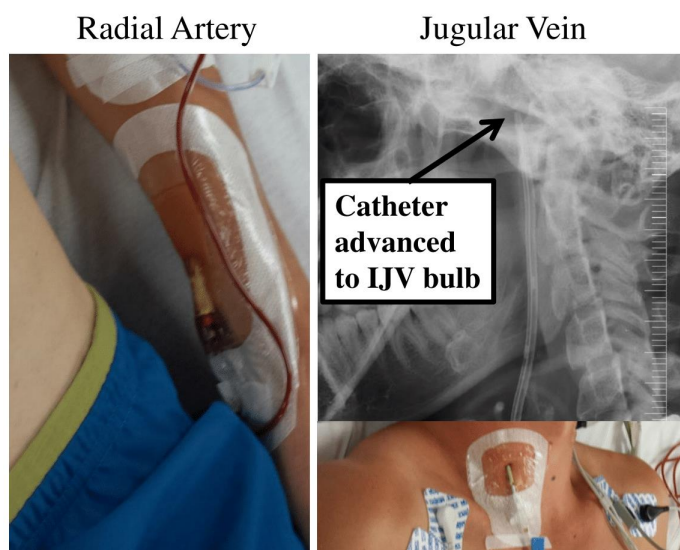


**Figure 4.1. Radial artery and internal jugular vein catheters.**

The radial artery catheter is displayed in the left panel, while the internal jugular vein catheter is depicted in the right panel. Notably, the catheter tip is advanced to the jugular bulb as indicated in the X-ray image. IJV, internal jugular vein.

#### 4.1.1.1.2 ARTERIAL-VEIN BLOOD ANALYSES

At each stage of hypoxia (see section “Protocol one – experimental overview”) ~1.0mL of radial arterial and jugular venous blood were simultaneously drawn into pre-heparinized syringes (SafePICO, Radiometer, Copenhagen, Denmark) and analyzed immediately using a commercial blood gas analyzer (ABL90 FLEX, Radiometer). This analysis included measurement of PaO<sub>2</sub>, PaCO<sub>2</sub>, SaO<sub>2</sub>, CaO<sub>2</sub>, pH, [H<sup>+</sup>], [HCO<sub>3</sub><sup>-</sup>], [Hb] and HCT. Jugular venous blood was also analyzed for whole blood viscosity. Venous blood was drawn into a Lithium Heparin Vacutainer® (Becton Dickinson, USA). Blood viscosity was measured within 15 minutes of blood sample acquisition at a shear rate of 225 s<sup>-1</sup> at 37.0°C with a cone-and-plate viscometer (Model DV2T, Brookfield, USA).

#### **4.1.1.2 PROTOCOL ONE – EXPERIMENTAL OVERVIEW**

Participants arrived to laboratory having abstained from alcohol, caffeine and exercise for 24 hours, were fasted for 4 hours, but drank water *ad libitum*. Further instructions were given to avoid food/drink high in antioxidants (e.g., orange juice, vitamin supplements) 24

hours prior to arrival to the laboratory. Half the participants began the protocol at 0600 h and the other half at 1300 h.

Upon arrival, participants assumed the supine position and were instrumented with the radial arterial, jugular venous, and ante-cubital venous catheters. Twenty minutes was provided for subjects to rest following cannulation, at which time the rest of the experimental set-up was performed (e.g., TCD and Finometer).

The order of experiments is depicted in **Figure 4.2** and outlined below. Following instrumentation and 5 min of baseline measurements (HR, MAP, VE, MCAV, PCAV, Q<sub>ICA</sub>, Q<sub>VA</sub>, P<sub>ET</sub>O<sub>2</sub>, and P<sub>ET</sub>CO<sub>2</sub>, and blood gases etc.) the participant completed an isocapnic hypoxemia test. Participants breathed simulated room air (e.g., P<sub>ET</sub>O<sub>2</sub> and P<sub>ET</sub>CO<sub>2</sub> were ~100 mmHg and 40 mmHg, respectively) on the end-tidal forcing system for a 5-min period before commencing three sequential hypoxic stages. To achieve the target SaO<sub>2</sub> values of 90, 80, and 70%, P<sub>ET</sub>O<sub>2</sub> was lowered in three sequential steps to 60, 48, and 43 mmHg, with each stage lasting 5 min once steady state was reached. These P<sub>ET</sub>O<sub>2</sub> values were predicted to achieve the desired SaO<sub>2</sub> values by accounting for the known end-tidal-to-arterial gradient with our breathing apparatus (Tymko *et al.*, 2015) and the known relationship between PaO<sub>2</sub> and SaO<sub>2</sub> (Severinghaus, 1979a).

Prediction of PaO<sub>2</sub> from P<sub>ET</sub>O<sub>2</sub> (Tymko *et al.*, 2015):

$$\text{PaO}_2 = -6.024 + (0.986 \cdot \text{P}_{\text{ET}}\text{O}_2)$$
$$R^2 = 0.94; P < 0.001$$

Prediction of SaO<sub>2</sub> from estimated PaO<sub>2</sub> value (Severinghaus, 1979a):

$$\text{SaO}_2 = (((\text{PaO}_2^3 + 150 \cdot \text{PaO}_2)^{-1} \cdot 23400) + 1)^{-1}$$

Following the last stage of end-tidal forcing, participants returned to breathing room air. Measurements of Q<sub>ICA</sub>, Q<sub>VA</sub>, and radial arterial and jugular venous blood samples were made at baseline and each stage of isocapnic hypoxemia.

Following the first isocapnic hypoxemia test, the isovolumic hemodilution was initiated. Whole blood was transferred into an Anticoagulant Citrate Phosphate Dextrose Solution BLOOD-PACK™ (4R0012MC, Fenwal, USA) through a plasma transfer kit (4C2240, Fenwal, USA) to collect up to 450mL of whole blood per BLOOD-PACK for short term storage. This blood was stored at room temperature on an orbital agitator.

The hemodilution protocol was conducted in two stages aimed at removing/replacing blood in 10% increments (i.e., 10% of whole blood volume). Thus approximately 10% of whole blood was removed and then replaced with an equal volume of 5% human serum albumin (Alburex 5%). Adequate hemodilution ( $\pm 1\%$  of target) was confirmed with an arterial [Hb] measurement. Subsequently, end-tidal forcing was utilized to return end-tidal gases to normal resting values, in the event that any respiratory changes and end-tidal gas deviations had occurred during hemodilution. Here, an ICA and VA measurement were conducted simultaneous to a radial arterial and jugular venous blood sample. The first stage of blood removal took  $27 \pm 7$  minutes, while replacement with albumin took  $15 \pm 3$  minutes. The time lapse between completion of the first hemodilution stage and subsequent measurements was  $14 \pm 7$  minutes. The second stage of blood removal took  $26 \pm 6$  minutes, while blood replacement with albumin took  $14 \pm 5$  minutes. Finally, measurements commenced again  $28 \pm 15$  minutes following the second stage of hemodilution. These two stages of hemodilution were designed to match the hypoxemic stimulus at 90% and 80% SaO<sub>2</sub>.

Following hemodilution a second hypoxemic trial was conducted. Here, as done prior to hemodilution, the participant completed an isocapnic hypoxemia test. Target SaO<sub>2</sub> values were 90, 80 & 70% and each stage lasted for 5-minutes following steady-state conditions. Following completion of the entire protocol, each subjects' blood was re-infused using a blood component recipient set (Fenwal, 4C2160).

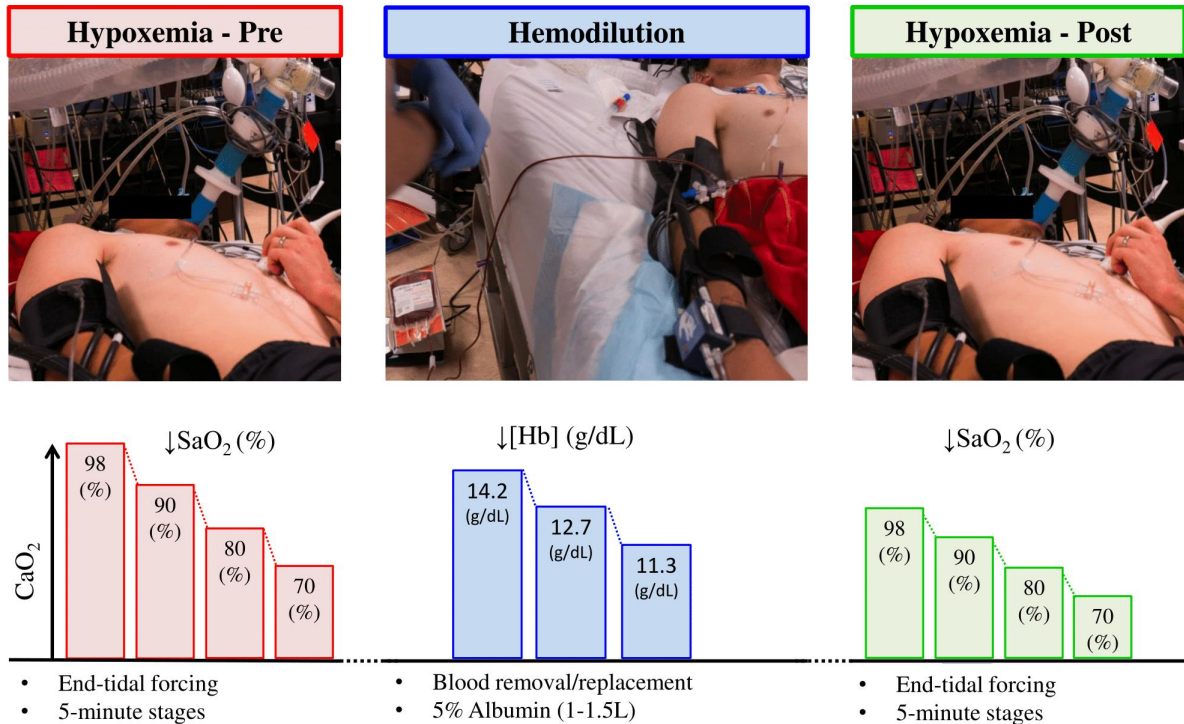


**Figure 4.2. Hypoxemia and hemodilution experimental overview.**

Moving left to right, hypoxemia was first performed prior to our hemodilution intervention. Hypoxemia was isocapnic, with each stage lasting 5-minutes once steady state was reached. Targeted SaO<sub>2</sub> values of 90, 80, and 70% SaO<sub>2</sub>. The second protocol was hemodilution, where in two separate steps, 10% of blood volume was removed and replaced with 5% human serum albumin for a total of 20% dilution (hemoglobin values noted in the blue bars). Finally, the post hemodilution hypoxemia trial was performed. As noted by the shorter bars (green bars) subjects began this protocol at a lower arterial oxygen content (CaO<sub>2</sub>) due to the previous hemodilution stage.

#### 4.1.1.3 PROTOCOL ONE - CALCULATIONS

While intrinsic to the blood gas analyzer, CaO<sub>2</sub> was calculated as per **Equation 2.9**. The CDO<sub>2</sub> was calculated as the product of gCBF and CaO<sub>2</sub> as per **Equation 2.10**. To calculate CPP, jugular venous pressure was used as a surrogate of ICP (i.e., CPP = MAP – Jugular venous pressure).

#### 4.1.1.4 PROTOCOL ONE - STATISTICAL ANALYSES

To address the first hypothesis, CBF during the initial hypoxemic stimulus and CBF during hemodilution were compared. As only a 20% reduction in CaO<sub>2</sub> could be achieved with

hemodilution, only the first and second stage of hypoxemia (i.e., stage 1, ~90% SaO<sub>2</sub>; stage 2, ~80% SaO<sub>2</sub>) were compared to hemodilution (i.e., stage 1, 10% blood volume removal; stage 2, 20% blood volume removal). Data from these two trials were compared using a repeated measures ANOVA (factors: trial and stage). Sphericity was assessed using Mauchly's test. When data significantly deviated from sphericity, the Greenhouse-Geisser correction was used. If a significant interaction was detected, bonferroni corrected post-hoc tests were utilized for pairwise comparisons.

As the hypoxic stimulus varied between hypoxemia and hemodilution (see section Study 2 - results), CBF responses were analyzed using linear regression analysis. This allowed for the determination of the slope (i.e. reactivity) and comparison of CBF responses without the confounding influence of a variable stimulus. Reactivity slopes were compared using paired t-tests.

To address the second hypothesis, CBF during initial hypoxemic stimulus (hypoxemia pre) and CBF during the second hypoxemic stimulus (hypoxemia post) were compared. These responses were compared across the entire isocapnic hypoxia trial (rest, 90, 80, 70%). Data from these two trials were compared using a repeated measures ANOVA (factors: Trial and stage). Sphericity was tested using Mauchly's test. When data significantly deviated from sphericity, the Greenhouse-Geisser correction was used. If a significant interaction was detected, bonferroni corrected post-hoc tests were utilized for pairwise comparisons.

To compare the gCBF response across all three trials, cerebrovascular reactivity to hypoxia was analyzed using linear mixed effects modelling. This method has been previously described, and possesses greater statistical power than conducting t-tests between individual subject reactivity slopes (Atkinson *et al.*, 2011). Fixed effects were CaO<sub>2</sub>, the experimental trial (hypoxemia pre, hemodilution, hypoxemia post), with trial and subject included as random effects with random intercepts. This model was tested against the same model, but with CPP included as a co-variate. Inclusion of CPP significantly improved the model (-2 log likelihood of 1286.76 versus 1293.72; Chi-Sq P=0.008). Thus, CPP was accounted for as a co-variate in our analyses of CBF reactivity. Residuals were examined for parity to normality. For all statistical tests, significance was set at an alpha level of  $\alpha=0.05$ .

#### 4.1.2 PROTOCOL TWO

Data were analyzed from a repository made available through a collaboration with Duke University (Durham, NC, USA). The data repository analyzed for this study consisted of nine separate experiments conducted between 2004 and 2016. Each study consisted of an isocapnic hypoxemia test to 70% SaO<sub>2</sub>, although given the different experiments the data are derived from, the number of stages was variable ranging from four to seven stages. The hypoxemia tests were conducted using the RespirAct™ (Thornhill Medical, Toronto) (Slessarev *et al.*, 2007).

Subjects underwent the previously described radial arterial and jugular venous cannulation (see section “Arterial and venous cannulation”). This blood was analyzed as previously described (see section “Arterial-venous blood analyses”). Trans-cerebral blood draws were acquired serially at each stage of hypoxemia. However, in contrast to protocol one, CBF was not measured using ultrasound. Percent changes in CBF were determined as follows:

Based upon the Fick equation (**Equation 2.11**), CMRO<sub>2</sub> is the product of CBF and the arterio-venous difference of oxygen (AvDO<sub>2</sub>). Therefore, CBF is the quotient of CMRO<sub>2</sub> and the AvDO<sub>2</sub>. As CMRO<sub>2</sub> is constant in hypoxia (Ainslie *et al.*, 2014) CBF is inversely proportional to AvDO<sub>2</sub> and percent reductions in AvDO<sub>2</sub> with hypoxia indicate percent increases in CBF (see **Figure 4.3**).

## Fick Equation

$$CMRO_2 = CBF \cdot AvDO_2$$

$$CBF = \frac{CMRO_2}{AvDO_2}$$

CMRO<sub>2</sub> is constant during hypoxia  
(Ainslie *et al.*, 2014, *Clin Sci*)

$$CBF \propto \frac{1}{AvDO_2}$$

### Figure 4.3. Formalism for the calculation of changes in cerebral blood flow from arterial and jugular venous blood samples.

The above formalism was utilized to calculate changes in cerebral blood flow from changes in the cerebral arterial venous difference of oxygen using the principles of the Fick equation. Note data exists to suggest CMRO<sub>2</sub> is not constant during hypoxia as well (Vestergaard *et al.*, 2015), albeit with the use of differing methodology (MRI).

As noted, the number of hypoxemic stages was variable; however, given the CBF response in this range of hypoxemia is linear (**Table 3.4**), reactivities (i.e. slope responses) are comparable across all experiments included. Therefore, hypoxemic reactivity was calculated as the slope of the linear regression between percent changes in CBF and reductions in CaO<sub>2</sub> [i.e., %ΔCBF · ΔCaO<sub>2</sub> (mL/dL)].

#### 4.1.2.1 PROTOCOL TWO - STATISTICAL ANALYSES

Prior to further data and statistical analyses, this data repository was scrutinized for data quality control purposes. The following data exclusion criteria were used:

- 1) Data were excluded if one or more of the primary parameters for analysis (CaO<sub>2</sub>, C<sub>jv</sub>O<sub>2</sub>, & [Hb]) were missing;
- 2) If the participant terminated the isocapnic protocol prior to reaching 70% SaO<sub>2</sub>;
- 3) If the relationship between CBF and CaO<sub>2</sub> was not linear (R<sup>2</sup> < 0.7 arbitrary cutoff);
- 4) If there was a PaCO<sub>2</sub> deviation of ≥ 3 mmHg during any stage.

This resulted in the exclusion of 65 participants and a sample size of 134 (79 male, 55 female).

The relationship between resting [Hb] and hypoxic reactivity was assessed using Pearson r correlations. Males and females were also analyzed separately. Here, reactivity was again related to [Hb] with Pearson r correlations. Further, baseline variables and reactivity were compared between males and females using unpaired t-tests. Significance was determined *a priori* as an alpha level of  $\alpha=0.05$ .

## **4.2 STUDY 2 - RESULTS**

### **4.2.1 RESULTS – PROTOCOL ONE**

#### **4.2.1.1 *HYPOXEMIA VERSUS HEMODILUTION***

Arterial blood data are presented in **Table 4.1**. Notably,  $\text{CaO}_2$  was reduced during hypoxemia and hemodilution; however, the reduction in  $\text{CaO}_2$  during hemodilution was slightly greater than hypoxemia for the corresponding first ( $P<0.01$ ) and second ( $P<0.01$ ) stages of the protocol (e.g. 90%  $\text{SaO}_2$  vs. 10% blood volume removal). Hypoxemia reduced  $\text{CaO}_2$  due to a reduction in  $\text{PaO}_2$  and  $\text{SaO}_2$  at each stage ( $P<0.01$  for all), whereas hemodilution reduced  $\text{CaO}_2$  due to a reduction in [Hb] and HCT at each stage ( $P<0.01$  for all) (**Figure 4.4**). Arterial pH was lower during each stage of hemodilution compared to hypoxemia ( $P<0.01$  for both stages) owing to a reduced  $[\text{HCO}_3^-]$  ( $P<0.01$  for both stages).

**Table 4.1. Radial arterial blood data during hypoxemia and hemodilution.**

	Hypoxemia			Hemodilution		
	Baseline	90% SaO <sub>2</sub>	80% SaO <sub>2</sub>	Baseline	10% removal	20% removal
<b>PaO<sub>2</sub></b> (mmHg)	93.3±4.0	59.2±1.7*	46.8±1.8*	93.3±4.0	94.6±5.5†	92.4±4.4†
	<i>Trial, P&lt;0.01; Stage, P&lt;0.01; Interaction, P&lt;0.01</i>					
<b>SaO<sub>2</sub></b> (%)	97.6±0.4	90.8±0.8*	82.7±1.6*	97.6±0.4	97.7±0.5†	97.6±0.4†
	<i>Trial, P&lt;0.01; Stage, P&lt;0.01; Interaction, P&lt;0.01</i>					
<b>CaO<sub>2</sub></b> (mL·dL <sup>-1</sup> )	19.3±1.1	18.0±0.9*	16.5±1.0*	19.3±1.1	17.3±0.8*†	15.4±0.7*†
	<i>Trial, P&lt;0.01; Stage, P&lt;0.01; Interaction, P&lt;0.01</i>					
<b>[Hb]</b> (g·dL <sup>-1</sup> )	14.2±0.9	14.3±0.8	14.4±0.8*	14.2±0.9	12.7±0.6*†	11.3±0.5*†
	<i>Trial, P&lt;0.01; Stage, P&lt;0.01; Interaction, P&lt;0.01</i>					
<b>HCT</b> (%)	43.5±2.6	43.7±2.5*	44.1±2.6*	43.5±2.6	38.9±1.8*†	34.6±1.7*†
	<i>Trial, P&lt;0.01; Stage, P&lt;0.01; Interaction, P&lt;0.01</i>					
<b>PaCO<sub>2</sub></b> (mmHg)	41.9±1.9	41.6±2.1	41.8±2.0	41.9±1.9	41.3±2.1	41.5±1.6
	<i>Trial, P=0.20; Stage, P=0.05; Interaction, P=0.47</i>					
<b>[HCO<sub>3</sub><sup>-</sup>]</b> (mmol·L <sup>-1</sup> )	25.6±0.9	25.7±1.1	25.8±1.0*	25.6±0.9	24.7±1.0*†	24.5±0.8*†
	<i>Trial, P&lt;0.01; Stage, P&lt;0.01; Interaction, P&lt;0.01</i>					
<b>pH</b>	7.394±0.019	7.400±0.018*	7.400±0.018*	7.394±0.019	7.386±0.017*†	7.379±0.016*†
	<i>Trial, P&lt;0.01; Stage, P=0.04; Interaction, P&lt;0.01</i>					
<b>[H<sup>+</sup>]</b> (nmol·L <sup>-1</sup> )	40.4±1.7	39.9±1.7*	39.9±1.6	40.4±1.7	41.2±1.7*†	41.8±1.6*†
	<i>Trial, P&lt;0.01; Stage, P=0.04; Interaction, P&lt;0.01</i>					

\*indicates a change from baseline, P<0.05; † indicates a difference between hypoxemia and hemodilution for corresponding stages, P<0.05.

Jugular venous blood gas data are presented in **Table 4.2**. Hypoxemia led to a greater reduction in PjvO<sub>2</sub> during stage 1 (P<0.01) and stage 2 (P<0.01) compared to hemodilution. This was reflected in a similarly lower SjvO<sub>2</sub> during each stage of hypoxemia compared to hemodilution (P<0.01 for each stage) (**Figure 4.4**).

**Table 4.2. Jugular venous blood data during hypoxemia and hemodilution.**

	Hypoxemia			Hemodilution		
	Baseline	90% SaO <sub>2</sub>	80% SaO <sub>2</sub>	Baseline	10% removal	20% removal
<b>P<sub>jv</sub>O<sub>2</sub></b> (mmHg)	37.0±2.7	33.8±2.6*	31.6±2.3*	37.0±2.7	37.0±2.5†	37.1±2.2†
	<i>Trial, P&lt;0.01; Stage, P&lt;0.01; Interaction, P&lt;0.01</i>					
<b>S<sub>jv</sub>O<sub>2</sub></b> (%)	66.5±4.5	61.4±4.7*	57.4±4.3*	66.5±4.5	65.9±4.3†	66.3±3.9†
	<i>Trial, P&lt;0.01; Stage, P&lt;0.01; Interaction, P&lt;0.01</i>					
<b>C<sub>jv</sub>O<sub>2</sub></b> (mL·dL <sup>-1</sup> )	13.0±1.3	12.1±1.3*	11.3±1.3*	13.0±1.3	11.5±1.0*†	10.3±0.7*†
	<i>Trial, P&lt;0.01; Stage, P&lt;0.01; Interaction, P&lt;0.01</i>					
<b>P<sub>jv</sub>CO<sub>2</sub></b> (mmHg)	51.6±1.3	50.6±1.4*	49.3±1.4*	51.6±1.3	50.6±1.2*	49.9±1.6*†
	<i>Trial, P=0.06; Stage, P&lt;0.01; Interaction, P=0.04</i>					
<b>[HCO<sub>3</sub><sup>-</sup>]</b> (mmol·L <sup>-1</sup> )	28.4±0.7	28.4±0.7	28.1±0.6*	28.4±0.7	27.3±0.7*†	26.6±0.7*†
	<i>Trial, P&lt;0.01; Stage, P&lt;0.01; Interaction, P&lt;0.01</i>					
<b>pH</b>	7.348±0.015	7.358±0.014*	7.364±0.015*	7.348±0.015	7.340±0.014*†	7.336±0.014*†
	<i>Trial, P&lt;0.01; Stage, P=0.50; Interaction, P&lt;0.01</i>					
<b>[H<sup>+</sup>]</b> (nmol·L <sup>-1</sup> )	44.9±1.6	43.9±1.4*	43.3±1.5*	40.4±1.7	41.2±1.7*†	41.8±1.6*†
	<i>Trial, P&lt;0.01; Stage, P=0.59; Interaction, P&lt;0.01</i>					

\*indicates a change from baseline, P<0.05; † indicates a difference between hypoxemia and hemodilution for corresponding stages, P<0.05.

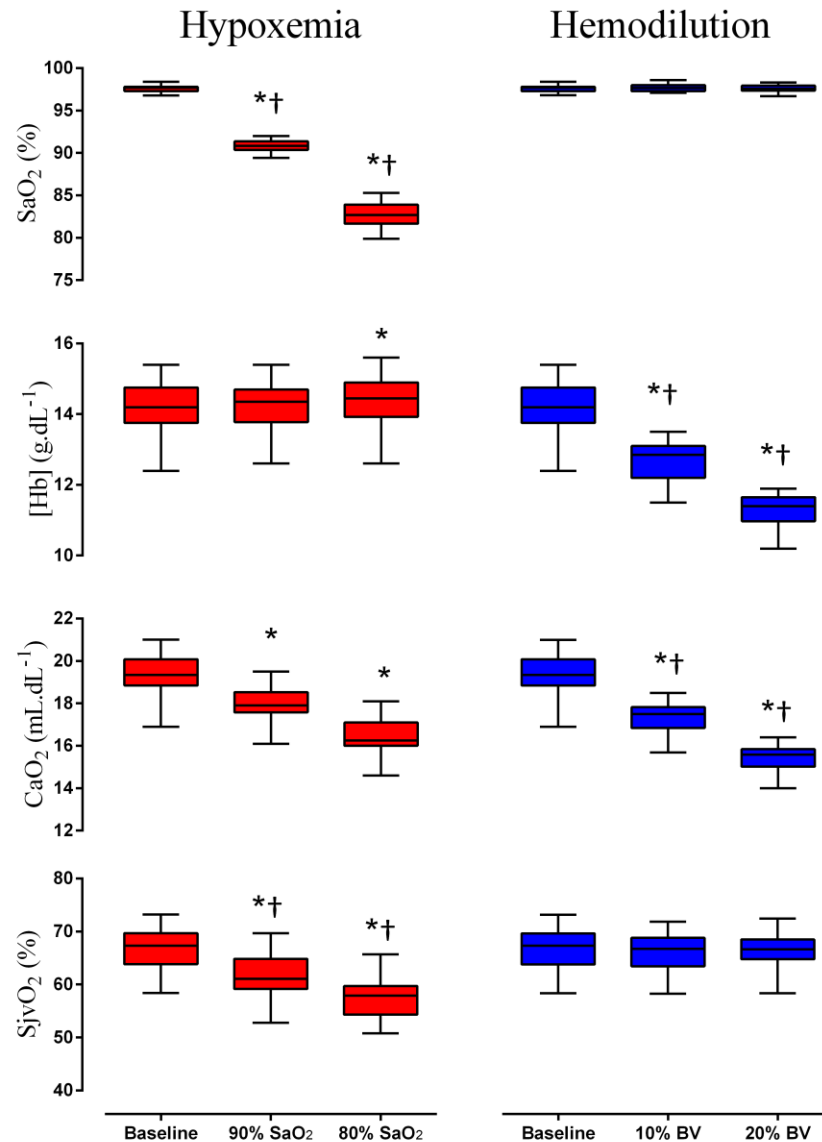


**Figure 4.4. Key blood parameters from the hypoxemia pre and hemodilution trials.**

The hypoxemia trial lead to progressive reductions in arterial oxyhemoglobin saturation (SaO<sub>2</sub>) and the partial pressure of oxygen (PaO<sub>2</sub>), whereas these parameters were unaltered during hemodilution. However, hemodilution reduced hemoglobin concentration [Hb]. Overall both trial lead to a reduction in arterial oxygen content (CaO<sub>2</sub>), although CaO<sub>2</sub> was lower at each corresponding level of hemodilution compared to hypoxemia. BV, blood volume. \*indicates a change from baseline, P<0.05; † indicates a difference between hypoxemia and hemodilution for corresponding stages, P<0.05.

#### 4.2.1.1.1 CARDIOVASCULAR DATA

Cardiovascular data are presented in **Table 4.3**. MAP was unchanged across each trial, which coupled with no changes in jugular venous blood pressure, produced no changes in CPP. Heart rate was elevated during hypoxemia at each stage, but was unaltered during hemodilution. Estimated cardiac output (Finometer) increased in stage 2 of hypoxemia ( $P=0.02$ ), but did not change during hemodilution. Hypoxemia reduced TPR in stage 1 ( $P=0.03$ ) and stage 2 ( $P=0.02$ ); however, TPR was unaltered by hemodilution.

**Table 4.3. Cardiovascular data during hypoxemia and hemodilution.**

	Hypoxemia			Hemodilution		
	Baseline	90% SaO <sub>2</sub>	80% SaO <sub>2</sub>	Baseline	10% removal	20% removal
<b>HR</b> (bpm)	61.6±11.8	71.0±11.6*	80.0±11.0*	61.6±11.8	63.9±12.0†	64.6±10.3†
	<i>Trial, P&lt;0.01; Stage, P&lt;0.01; Interaction, P&lt;0.01</i>					
<b>Radial BP</b> (mmHg)	99.2±5.6	100.9±7.5	103.0±10.3	99.2±5.6	97.8±5.1	96.9±4.5
	<i>Trial, P=0.09; Stage, P=0.78; Interaction, P=0.07</i>					
<b>Jugular BP</b> (mmHg)	6.7±1.8	7.0±1.7	7.1±1.8	6.7±1.8	6.4±1.4†	6.5±1.5
	<i>Trial, P=0.05; Stage, P=0.83; Interaction, P=0.11</i>					
<b>CPP</b> (mmHg)	92.5±4.5	94.0±6.4	95.8±9.4	92.5±4.5	91.4±5.7	90.4±4.7
	<i>Trial, P=0.11; Stage, P=0.84; Interaction, P=0.11</i>					
<b>SV</b> (mL)	106.4±9.7	107.2±8.2	107.7±9.3	106.4±9.7	103.0±7.6	115.5±17.1
	<i>Trial, P=0.41; Stage, P=0.08; Interaction, P=0.05</i>					
<b>CO</b> (L/min)	6.6±1.4	7.7±1.2	8.7±0.9*	6.6±1.4	6.7±1.4	7.5±1.4†
	<i>Trial, P=0.32; Stage, P=0.01; Interaction, P=0.27</i>					
<b>TPR</b> (mmHg/L/min)	16.1±5.1	13.7±3.0*	12.1±2.0*	16.1±5.1	15.4±3.8†	13.5±2.6†
	<i>Trial, P&lt;0.01; Stage, P&lt;0.01; Interaction, P=0.01</i>					

\*indicates increase from baseline,  $P<0.05$ ; † indicates a difference between hypoxemia and hemodilution for corresponding stages,  $P<0.05$ .

#### 4.2.1.1.2 CEREBROVASCULAR RESPONSES

Cerebrovascular data during hypoxemia and hemodilution are presented in **Table 4.4**. Hypoxemia and hemodilution increased  $Q_{ICA}$  at each stage ( $P<0.01$  for all stages), with  $Q_{ICA}$  elevated to a greater extent in the second stage of hypoxemia than hemodilution ( $P=0.02$ ). This response was due to a differential response of ICA diameter, which was unaltered in hypoxemia, but decreased in hemodilution ( $P=0.02$  for stage 1 &  $P=0.04$  for stage 2). Hypoxemia and hemodilution elicited a similar  $Q_{VA}$  response, which was

increased at stage 2 (main effect,  $P < 0.01$ ), while gCBF was increased during both stages of hypoxemia ( $P < 0.01$  for both stages) and hemodilution ( $P < 0.01$  for both stages). These blood flow responses lead to a maintenance of  $\text{CDO}_2$  during hypoxemia where  $\text{CDO}_2$  was in fact elevated in stage 2 ( $P = 0.04$ ); however, in contrast, the blood flow response during hemodilution was not adequate enough to maintain  $\text{CDO}_2$ , leading to a  $4.8 \pm 4.6\%$  reduction in  $\text{CDO}_2$  ( $P = 0.04$ ).

**Table 4.4. Cerebral blood flow during hypoxemia and hemodilution.**

	Hypoxemia			Hemodilution		
	Baseline	90% SaO <sub>2</sub>	80% SaO <sub>2</sub>	Baseline	10% removal	20% removal
<b>ICA<sub>v</sub></b> (cm/s)	43.0±5.8	46.8±8.1*	52.3±9.4*	43.0±5.8	52.0±9.5*†	54.6±8.3*
	<i>Trial, P&lt;0.01; Stage, P&lt;0.01; Interaction, P=0.01</i>					
<b>ICA diameter</b> (mm)	5.39±0.41	5.41±0.44	5.50±0.35	5.39±0.41	5.24±0.41*†	5.21±0.27*†
	<i>Trial, P&lt;0.01; Stage, P=0.29; Interaction, P&lt;0.01</i>					
<b>Q<sub>ICA</sub></b> (mL/min)	297±52	325±71*	377±84*	297±52	338±69*	351±63*†
	<i>Trial, P=0.47; Stage, P&lt;0.01; Interaction, P&lt;0.01</i>					
<b>ICA CVC</b> (mL/min/mmHg)	3.20±0.54	3.45±0.74*	3.95±0.92*	3.20±0.54	3.72±0.87*	3.89±0.75*
	<i>Trial, P=0.38; Stage, P&lt;0.01; Interaction, P=0.04</i>					
<b>ICA DO<sub>2</sub></b> (mL/min)	57.3±9.9	58.3±12.5	62.0±13.8*	57.3±9.9	58.3±10.8	54.0±9.4*†
	<i>Trial, P=0.03; Stage, P=0.61; Interaction, P&lt;0.01</i>					
<b>VA<sub>v</sub></b> (cm/s)	21.6±5.5	23.0±5.8*	25.0±5.4*	21.6±5.5	23.7±4.4*	28.0±7.2*
	<i>Trial, P=0.08; Stage, P&lt;0.01; Interaction, P&lt;0.06</i>					
<b>VA diameter</b> (mm)	4.11±0.27	4.15±0.29	4.21±0.29*	4.11±0.27	3.95±0.31*†	3.97±0.25†
	<i>Trial, P&lt;0.01; Stage, P=0.08; Interaction, P&lt;0.01</i>					
<b>Q<sub>VA</sub></b> (mL/min)	86.0±22.5	94.6±28.0	104.9±27.0*	86.0±22.5	87.6±20.8	105.2±29.6*
	<i>Trial, P=0.53; Stage, P&lt;0.01; Interaction, P=0.47</i>					
<b>VA CVC</b> (mL/min/mmHg)	0.93±2.4	1.01±0.29	1.10±0.28*	0.93±2.4	0.96±0.23	1.16±0.32*
	<i>Trial, P=0.85; Stage, P&lt;0.01; Interaction, P=0.37</i>					
<b>VA DO<sub>2</sub></b> (mL/min)	16.6±4.2	16.9±4.7	17.2±4.3	16.6±4.2	15.2±3.6	16.2±4.4
	<i>Trial, P=0.14; Stage, P=0.25; Interaction, P=0.27</i>					
<b>gCBF</b> (mL/min)	765±105	839±145*	963±177*	765±105	851±136*	912±120*
	<i>Trial, P=0.36; Stage, P&lt;0.01; Interaction, P=0.02</i>					
<b>gCBF CVC</b> (mL/min/mmHg)	8.27±1.05	8.92±1.44*	10.09±1.90*	8.27±1.05	9.37±1.80*	10.11±1.42*
	<i>Trial, P=0.36; Stage, P&lt;0.01; Interaction, P=0.22</i>					
<b>CDO<sub>2</sub></b> (mL/min)	148±19	150±24	158±29*	148±19	147±20	140±17*†
	<i>Trial, P=0.01; Stage, P=0.78; Interaction, P&lt;0.01</i>					
<b>MCA<sub>v</sub></b> (cm/s)	68.0±13.8	71.2±16.3	77.3±17.5*	68.0±13.8	71.7±12.6	76.7±12.7*
	<i>Trial, P=0.97; Stage, P&lt;0.01; Interaction, P=0.83</i>					
<b>PCA<sub>v</sub></b> (cm/s)	42.9±9.1	43.9±9.4	46.9±10.3*	42.9±9.1	48.5±15.8	48.7±15.6*
	<i>Trial, P=0.22; Stage, P&lt;0.01; Interaction, P=0.21</i>					
<b>ICA shear stress</b> (dyne/cm <sup>2</sup> )	11.6±2.1	12.2±2.6*	13.4±2.7*	12.0±2.0†	12.6±2.6	11.6±1.7†
	<i>Trial, P=0.40; Stage, P=0.02; Interaction, P&lt;0.01</i>					
<b>VA shear Stress</b> (dyne/cm <sup>2</sup> )	7.3±1.8	7.7±1.6	8.3±1.6*	7.8±1.9†	7.6±1.3	7.8±2.1
	<i>Trial, P=0.98; Stage, P=0.05; Interaction, P=0.04</i>					

\*indicates increase from baseline, P<0.05; † indicates a difference between hypoxemia and hemodilution for the same reduction in CaO<sub>2</sub>, P<0.05.

Given the distinct difference in blood gases at each stage of hypoxemia versus hemodilution, such as the greater hypoxic stimulus (lower  $\text{CaO}_2$ ) at each stage of hemodilution compared to hypoxemia (**Figure 4.4**), data were also analyzed as reactivity slopes to account for the stimulus magnitude.

Reactivity of  $Q_{\text{ICA}}$  ( $P < 0.01$ ; **Figure 4.5A**), ICA CVC ( $P = 0.01$ ; **Figure 4.5D**), and ICA  $\text{DO}_2$  ( $P < 0.01$ ; **Figure 4.5G**) were all reduced in response to hemodilution compared to hypoxemia. However, reactivity of  $Q_{\text{VA}}$  ( $P = 0.36$ ; **Figure 4.5B**), VA CVC ( $P = 0.91$ ; **Figure 4.5E**), and VA  $\text{DO}_2$  ( $P = 0.28$ ; **Figure 4.5F**) were unaltered in response to hemodilution. The collective impact of the ICA and VA responses following hemodilution on gCBF were as follows: gCBF reactivity was reduced by  $38 \pm 35\%$  ( $P < 0.01$ ; **Figure 4.5C**), gCBF CVC reactivity displayed a mean decrease of  $12 \pm 42\%$  that was not significant ( $P = 0.07$ ; **Figure 4.5F**), and gCBF  $\text{DO}_2$  reactivity decreased by  $170 \pm 182\%$  ( $P < 0.01$ ) (**Figure 4.5I**). This change in gCBF  $\text{DO}_2$  represented a change from increasing  $\text{DO}_2$  with progressive hypoxemia, to decreasing  $\text{DO}_2$  with hemodilution.

While absolute reactivity of the ICA was greater than that of the VA during hypoxemia ( $-27.8 \pm 11.7$  vs.  $-6.3 \pm 3.8 \text{ mL} \cdot \text{min}^{-1} \cdot \text{mL}^{-1} \cdot \text{dL}^{-1}$ ;  $P < 0.01$ ) and hemodilution ( $-13.6 \pm 4.9$  vs.  $-4.6 \pm 3.0 \text{ mL} \cdot \text{min}^{-1} \cdot \text{mL}^{-1} \cdot \text{dL}^{-1}$ ;  $P < 0.01$ ), relative percent reactivity was not different between vessels during hypoxemia ( $-9.1 \pm 3.5$  vs.  $-7.6 \pm 5.0 \text{ \%} \cdot \text{mL}^{-1} \cdot \text{dL}^{-1}$ ;  $P = 0.45$ ) or hemodilution ( $-4.6 \pm 1.6$  vs.  $-5.5 \pm 3.2 \text{ \%} \cdot \text{mL}^{-1} \cdot \text{dL}^{-1}$ ;  $P = 0.45$ ).

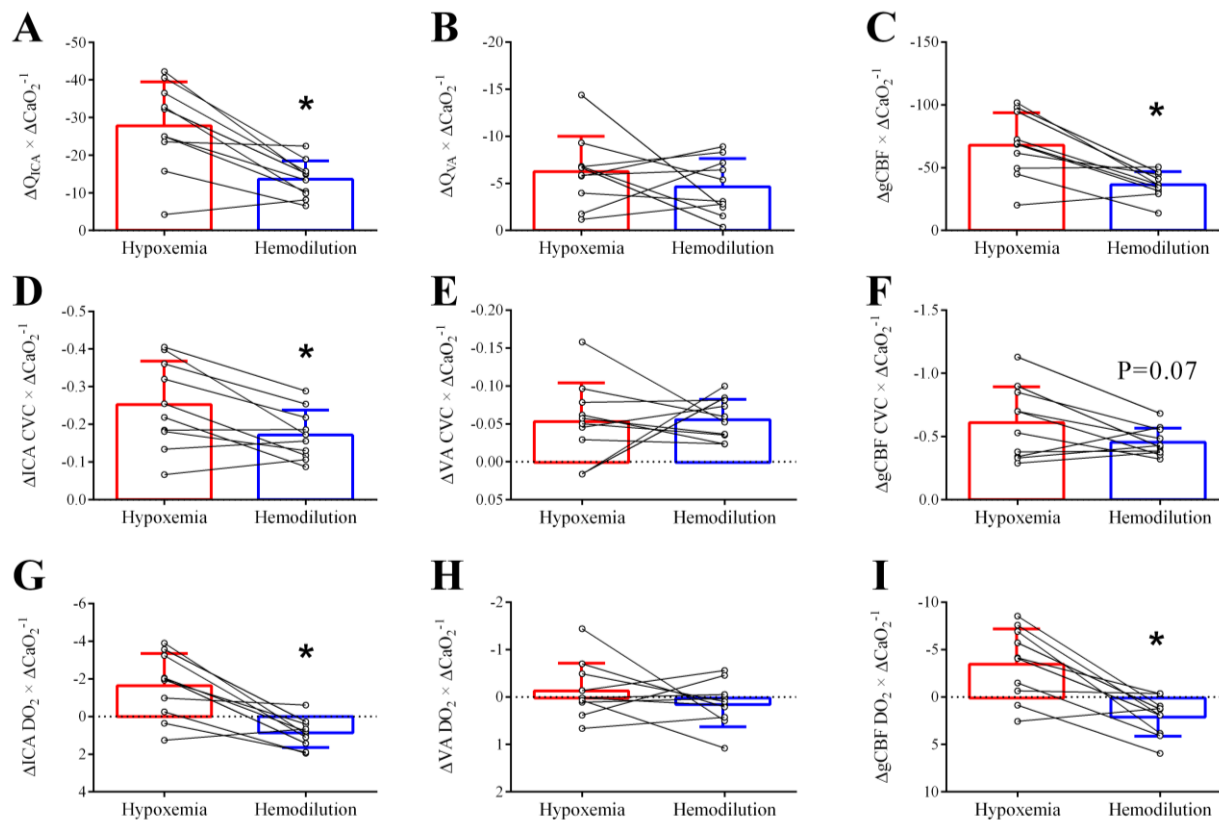


**Figure 4.5. Cerebrovascular reactivity profiles to hypoxemia and hemodilution.**

Cerebrovascular reactivity during hypoxemia is denoted by the red bars (mean  $\pm$  standard deviation) while hemodilution is denoted by the blue bars. Reactivity slopes for cerebral blood flow (e.g.  $\Delta Q_{ICA} \times \Delta CaO_2^{-1}$ ) represent the volumetric flow (mL/min) changes per unit reduction in  $CaO_2$  (mL/dL). Cerebrovascular conductance (CVC) slopes are mL/min/mmHg per unit reduction in  $CaO_2$  (mL/dL). Slopes for oxygen delivery ( $DO_2$ ) are in mL/min per unit reduction in  $CaO_2$  (mL/dL).  $Q_{ICA}$ , internal carotid artery blood flow;  $Q_{VA}$  vertebral artery blood flow; gCBF, global cerebral blood flow; CVC, cerebrovascular conductance;  $DO_2$ , oxygen delivery. \*denotes a significant difference between hypoxemia and hemodilution,  $P < 0.05$

#### **4.2.1.2 HYPOXEMIA PRE VERSUS HYPOXEMIA POST**

Arterial blood data are presented in **Table 4.5**. Both [Hb] and HCT were lower during hypoxemia post hemodilution (main effect,  $P=0.02$  for [Hb] and  $P=0.03$  for HCT). While  $\text{PaO}_2$  and  $\text{SaO}_2$  were similarly reduced at each stage of hypoxemia pre and post hemodilution,  $\text{CaO}_2$  was lower at every stage of hypoxemia post hemodilution compared to pre hemodilution ( $P<0.01$  for all stages). While  $\text{PaCO}_2$  was held constant and not different between hypoxemia trials pre and post hemodilution, pH was lower at each stage of hypoxemia following hemodilution ( $P=0.04$  at baseline, and  $P<0.01$  for all other stages) due to a lower  $[\text{HCO}_3^-]$  at each stage of hypoxemia following hemodilution ( $P<0.01$  for all stages).

All jugular venous blood data are presented in **Table 4.6**. There were similar reductions in  $\text{PjvO}_2$  and  $\text{SjvO}_2$  during hypoxemia both pre and post, however,  $\text{CjvO}_2$  was lower at each stage of hypoxemia following hemodilution ( $P<0.01$  for each stage), owing to the reduction in [Hb] (**Table 4.1**). Jugular venous pH and  $[\text{HCO}_3^-]$  were lower across the hypoxemia trial following hemodilution compared to the pre hemodilution trial (main effect,  $P<0.01$  for both).

**Table 4.5. Radial arterial bloods during hypoxemia prior to and following hemodilution.**

	Hypoxemia - Pre				Hypoxemia - Post			
	Baseline	90% SaO <sub>2</sub>	80% SaO <sub>2</sub>	70% SaO <sub>2</sub>	Baseline	90% SaO <sub>2</sub>	80% SaO <sub>2</sub>	70% SaO <sub>2</sub>
<b>PaO<sub>2</sub></b> (mmHg)	93.3±4.0	59.2±1.7*	46.8±1.8*	39.9±1.7*	95.9±7.2	58.1±2.4*	45.8±2.3*	39.9±2.4*
	<i>Trial, P=0.94; Stage, P&lt;0.01; Interaction, P=0.06</i>							
<b>SaO<sub>2</sub></b> (%)	97.6±0.4	90.8±0.8*	82.7±1.6*	74.6±2.1*	97.8±0.6	90.3±1.4*	81.3±2.7*	73.9±3.7*
	<i>Trial, P=0.20; Stage, P&lt;0.01; Interaction, P=0.16</i>							
<b>CaO<sub>2</sub></b> (mL·dL <sup>-1</sup> )	19.3±1.1	18.0±0.9*	16.5±1.0*	15.0±1.0*	15.7±0.7†	14.4±0.6*†	13.3±0.7*†	11.9±0.8*†
	<i>Trial, P&lt;0.01; Stage, P&lt;0.01; Interaction, P&lt;0.01</i>							
<b>[Hb]</b> (g·dL <sup>-1</sup> )	14.2±0.9	14.3±0.8	14.4±0.8	14.5±0.8*	11.4±0.5	11.5±0.5	11.8±0.6	11.7±0.5*
	<i>Trial, P&lt;0.01; Stage, P=0.02; Interaction, P=0.26</i>							
<b>HCT</b> (%)	43.5±2.6	43.7±2.5	44.1±2.6	44.5±2.4*	35.0±1.6	35.2±1.5	36.1±2.0	35.7±1.4*
	<i>Trial, P&lt;0.01; Stage, P=0.03; Interaction, P=0.23</i>							
<b>PaCO<sub>2</sub></b> (mmHg)	41.9±1.9	41.6±2.1	41.8±2.0	42.1±2.1	41.4±1.9	41.4±1.9	42.4±2.1†	42.1±1.8
	<i>Trial, P=0.56; Stage, P&lt;0.01; Interaction, P&lt;0.01</i>							
<b>[HCO<sub>3</sub><sup>-</sup>]</b> (mmol·L <sup>-1</sup> )	25.6±0.9	25.7±1.1	25.8±1.0*	25.6±0.9*	24.6±1.0	24.8±1.0	25.2±0.9*	25.0±0.6*
	<i>Trial, P&lt;0.01; Stage, P&lt;0.01; Interaction, P=0.35</i>							
<b>pH</b>	7.394±0.019	7.399±0.018*	7.400±0.18*	7.397±0.019	7.382±0.013†	7.386±0.012†	7.382±0.013†	7.381±0.016†
	<i>Trial, P&lt;0.01; Stage, P=0.03; Interaction, P=0.04</i>							
<b>[H<sup>+</sup>]</b> (nmol·L <sup>-1</sup> )	40.4±1.7	39.9±1.7*	39.9±1.6	40.2±1.6	41.5±1.3†	41.1±1.1†	41.5±1.2†	41.6±1.5†
	<i>Trial, P&lt;0.01; Stage, P=0.04; Interaction, P=0.04</i>							

\*indicates increase from baseline, P<0.05; † indicates a difference between hypoxemia pre and hypoxemia post for corresponding stages, P<0.05.

**Table 4.6 Jugular venous bloods during hypoxemia prior to and following hemodilution.**

	Hypoxemia - Pre				Hypoxemia - Post			
	Baseline	90% SaO <sub>2</sub>	80% SaO <sub>2</sub>	70% SaO <sub>2</sub>	Baseline	90% SaO <sub>2</sub>	80% SaO <sub>2</sub>	70% SaO <sub>2</sub>
<b>PjvO<sub>2</sub></b> (mmHg)	37.0±2.7	33.8±2.6*	31.6±2.3*	29.9±2.0*	37.2±2.3	34.1±2.4*	32.2±1.8*	30.0±1.5*
	<i>Trial, P=0.14; Stage, P&lt;0.01; Interaction, P=0.35</i>							
<b>SjvO<sub>2</sub></b> (%)	66.5±4.5	61.4±4.7*	57.4±4.3*	53.9±4.2*	66.8±3.9	61.8±4.6*	58.7±4.0*	54.2±3.6*
	<i>Trial, P=0.11; Stage, P&lt;0.01; Interaction, P=0.13</i>							
<b>CjvO<sub>2</sub></b> (mL·dL <sup>-1</sup> )	13.0±1.3	12.1±1.3*	11.3±1.3*	10.7±1.3*	10.6±0.8†	9.8±0.8*†	9.4±0.8*†	8.9±0.8*†
	<i>Trial, P&lt;0.01; Stage, P&lt;0.01; Interaction, P&lt;0.01</i>							
<b>PjvCO<sub>2</sub></b> (mmHg)	51.6±1.3	50.6±1.4*	49.3±1.4*	47.6±2.4*	50.2±1.6	48.8±1.3*	48.1±1.5*	47.0±1.7*
	<i>Trial, P&lt;0.01; Stage, P&lt;0.01; Interaction, P=0.17</i>							
<b>[HCO<sub>3</sub><sup>-</sup>]</b> (mmol·L <sup>-1</sup> )	28.4±0.7	28.4±0.7	28.1±0.6*	27.3±1.5*	27.0±0.8	26.9±0.7	26.7±0.8*	26.2±0.5*
	<i>Trial, P&lt;0.01; Stage, P&lt;0.01; Interaction, P=0.32</i>							
<b>pH</b>	7.348±0.015	7.358±0.014*	7.364±0.015*	7.367±0.014*	7.339±0.012	7.349±0.011*	7.353±0.011*	7.355±0.012*
	<i>Trial, P&lt;0.01; Stage, P&lt;0.01; Interaction, P=0.25</i>							
<b>[H<sup>+</sup>]</b> (nmol·L <sup>-1</sup> )	44.9±1.6	43.9±1.4*	43.3±1.5*	43.0±1.4*	45.9±1.2	44.8±1.2*	44.4±1.1*	44.2±1.2*
	<i>Trial, P&lt;0.01; Stage, P&lt;0.01; Interaction, P=0.30</i>							

\*indicates increase from baseline, P<0.05; † indicates a difference between hypoxemia pre and hypoxemia post for corresponding stages, P<0.05.

**Table 4.7. Cardiovascular data during hypoxemia prior to and following hemodilution.**

	Hypoxemia - Pre				Hypoxemia - Post			
	Baseline	90% SaO <sub>2</sub>	80% SaO <sub>2</sub>	70% SaO <sub>2</sub>	Baseline	90% SaO <sub>2</sub>	80% SaO <sub>2</sub>	70% SaO <sub>2</sub>
<b>HR</b> (bpm)	61.6±11.8	71.0±11.6*	80.0±11.0*	84.0±15.1*	64.0±11.1	76.5±13.8*	88.4±14.7*†	95.2±16.1*†
	<i>Trial, P=0.01; Stage, P&lt;0.01; Interaction, P=0.01</i>							
<b>Radial BP</b> (mmHg)	99.2±5.6	100.9±7.5	103.0±10.3	107.2±14.2	98.2±4.5	103.0±7.2	106.7±10.3	106.6±8.4
	<i>Trial, P=0.16; Stage, P=0.01; Interaction, P=0.06</i>							
<b>Jugular BP</b> (mmHg)	6.7±1.8	7.0±1.7	7.1±1.8	7.9±1.7*	6.5±1.3	6.7±1.6	7.2±1.9	7.5±2.1*
	<i>Trial, P=1.00; Stage, P&lt;0.01; Interaction, P=0.79</i>							
<b>CPP</b> (mmHg)	92.5±4.5	94.0±6.4	95.8±9.4	99.3±13.3	91.7±5.0	96.2±7.0	99.4±9.7*	99.1±8.0†
	<i>Trial, P=0.15; Stage, P=0.03; Interaction, P=0.04</i>							
<b>SV</b> (mL)	106.4±9.7	107.2±8.2	107.7±9.3	108.2±8.0	118.9±17.1	114.1±16.1	114.8±13.3	114.6±11.5
	<i>Trial, P=0.02; Stage, P=0.88; Interaction, P=0.09</i>							
<b>CO</b> (L/min)	6.6±1.4	7.7±1.2*	8.7±0.9*	9.2±1.5*	7.7±1.4	8.8±1.4*	10.3±1.6*	11.2±1.7*
	<i>Trial, P&lt;0.01; Stage, P&lt;0.01; Interaction, P=0.06</i>							
<b>TPR</b> (mmHg/L/min)	16.1±5.1	13.7±3.0	12.1±2.0	12.1±2.7	13.3±2.7	12.1±2.4	10.7±2.1	9.8±1.3
	<i>Trial, P=0.09; Stage, P=0.51; Interaction, P=0.07</i>							

\*indicates increase from baseline, P<0.05; † indicates a difference between hypoxemia pre and hypoxemia post for corresponding stages, P<0.05.

#### 4.2.1.2.1 CARDIOVASCULAR DATA

Cardiovascular variables during hypoxemia prior to and following hemodilution are reported in **Table 4.7**. Hypoxemia elevated HR in both trials, with the increase in HR in stage 2 and 3 greater in the post hemodilution trial ( $P<0.01$  for both stages). There was a main effect for increased radial BP ( $P=0.01$ ), jugular venous BP ( $P<0.01$ ), and CPP ( $P<0.01$ ) during hypoxemia. Both SV and TPR were unaltered, although CO increased at each stage of hypoxemia (main effect,  $P<0.01$ ).

#### 4.2.1.2.2 CEREBRAL BLOOD FLOW RESPONSES

While hypoxemia increased  $Q_{ICA}$  at each stage for both trials (**Table 4.8**),  $Q_{ICA}$  was higher at every stage of hypoxemia following hemodilution compared to hypoxemia prior to hemodilution ( $P<0.01$  for each stage). Similarly,  $Q_{VA}$  was elevated at each stage of hypoxemia following to hemodilution compared to the pre-trial ( $P\leq 0.01$  for all stages). These changes in  $Q_{ICA}$  and  $Q_{VA}$  were reflected in an increased gCBF at each stage of hypoxemia with gCBF higher at each stage of hypoxemia following hemodilution compared to pre hemodilution ( $P<0.01$  for each stage). The  $CDO_2$  was unaltered during hypoxemia prior to and following hemodilution.

Reactivity data from the hypoxemia trials prior to and following hemodilution are presented in **Figure 4.6**. Reactivity of  $Q_{ICA}$  ( $P<0.01$ ; **Figure 4.6A**), ICA CVC ( $P=0.01$ ; **Figure 4.6D**), and ICA  $DO_2$  ( $P=0.01$ ; **Figure 4.6G**) were all greater in the hypoxemia trial following hemodilution. Similarly,  $Q_{VA}$  ( $P<0.01$ ; **Figure 4.6B**), VA CVC ( $P<0.01$ ; **Figure 4.6E**), and VA  $DO_2$  ( $P<0.01$ ; **Figure 4.6F**) were greater following hemodilution. The collective impact of the ICA and VA responses on gCBF following hemodilution were as follows: gCBF reactivity was increased by  $118\pm 69\%$  ( $P<0.01$ ; **Figure 4.6C**), gCBF CVC reactivity increased by  $269\pm 549\%$  ( $P<0.01$ ; **Figure 4.6F**), and gCBF  $DO_2$  reactivity increased by  $227\pm 262\%$  ( $P<0.01$ ; **Figure 4.6I**).

Regional reactivity through the ICA was greater than that of the VA during hypoxemia pre ( $-33.7\pm 11.1$  vs.  $-6.9\pm 4.6$   $mL \cdot min^{-1} \cdot mL^{-1} \cdot dL^{-1}$ ;  $P<0.01$ ) and hypoxemia post ( $65.5\pm 21.7$  vs.  $-18.8\pm 9.0$   $mL \cdot min^{-1} \cdot mL^{-1} \cdot dL^{-1}$ ;  $P<0.01$ ). However, regional percent reactivity was

not different between the ICA and VA during hypoxemia pre ( $-11.2 \pm 2.9$  vs  $-8.1 \pm 5.1$  %  $\cdot$   $\text{mL}^{-1} \cdot \text{dL}^{-1}$ ;  $P=0.10$ ) or hypoxemia post ( $-19.2 \pm 5.4$  vs.  $-17.9 \pm 8.3$   $\cdot$   $\text{mL}^{-1} \cdot \text{dL}^{-1}$ ;  $P=0.67$ ).

**Table 4.8. Cerebral blood flow during hypoxemia prior to and following hemodilution.**

	Hypoxemia - Pre				Hypoxemia - Post			
	Baseline	90% SaO <sub>2</sub>	80% SaO <sub>2</sub>	70% SaO <sub>2</sub>	Baseline	90% SaO <sub>2</sub>	80% SaO <sub>2</sub>	70% SaO <sub>2</sub>
<b>ICA<sub>v</sub></b> (cm/s)	43.0±5.8	46.8±8.1*	52.3±9.4*	58.3±8.5*	52.7±8.1†	60.0±13.1†	68.5±10.9*†	78.5±13.7*†
	<i>Trial, P&lt;0.01; Stage, P&lt;0.01; Interaction, P&lt;0.01</i>							
<b>ICA diameter</b> (mm)	5.39±0.41	5.41±0.44	5.50±0.35*	5.62±0.39*	5.24±0.30	5.37±0.33	5.24±0.30*	5.37±0.33*
	<i>Trial, P=0.29; Stage, P&lt;0.01; Interaction, P=0.08</i>							
<b>Q<sub>ICA</sub></b> (mL/min)	297±52	325±71*	377±84*	439±94*	344±74†	410±100*†	482±109*†	576±121*†
	<i>Trial, P&lt;0.01; Stage, P&lt;0.01; Interaction, P&lt;0.01</i>							
<b>ICA CVC</b> (mL/min/mmHg)	3.20±0.54	3.45±0.74	3.95±0.92*	4.48±1.10*	3.76±0.80†	4.25±0.95*†	4.83±0.96*†	5.81±1.1*†
	<i>Trial, P&lt;0.01; Stage, P&lt;0.01; Interaction, P=0.02</i>							
<b>ICA DO<sub>2</sub></b> (mL/min)	57.3±9.9	58.3±12.5	62.0±13.8*	65.8±13.5*	53.8±11.3	59.1±14.8	63.7±13.6*	68.6±13.6*
	<i>Trial, P=0.88; Stage, P&lt;0.01; Interaction, P=0.12</i>							
<b>VA<sub>v</sub></b> (cm/s)	21.6±5.5	23.0±5.8	25.0±5.4*	27.6±7.2*	26.8±5.7†	29.5±6.4†	34.5±7.9*†	39.3±7.1*†
	<i>Trial, P&lt;0.01; Stage, P&lt;0.01; Interaction, P&lt;0.01</i>							
<b>VA diameter</b> (mm)	4.11±0.27	4.15±0.29	4.21±0.29	4.19±0.31	4.09±0.26	4.13±0.32	3.82±1.26	4.26±0.37
	<i>Trial, P=0.97; Stage, P&lt;0.01; Interaction, P=0.31</i>							
<b>Q<sub>VA</sub></b> (mL/min)	86.0±22.5	94.6±28.0	104.9±27.0*	115.6±35.8*	106.8±28.4†	120.9±33.1†	144.2±37.6†	170.2±43.9*†
	<i>Trial, P&lt;0.01; Stage, P&lt;0.01; Interaction, P&lt;0.01</i>							
<b>VA CVC</b> (mL/min/mmHg)	0.93±2.4	1.01±0.29	1.10±0.28*	1.17±0.35*	1.16±0.29†	1.26±0.32†	1.46±0.36†	1.73±0.45*†
	<i>Trial, P&lt;0.01; Stage, P&lt;0.01; Interaction, P&lt;0.01</i>							
<b>VA DO<sub>2</sub></b> (mL/min)	16.6±4.2	16.9±4.7	17.2±4.3	17.2±5.2	16.7±4.6	17.4±4.6	19.0±4.8†	20.3±5.4†
	<i>Trial, P=0.04; Stage, P=0.04; Interaction, P&lt;0.01</i>							
<b>gCBF</b>	765±105	839±145*	963±177*	1109±208*	902±130†	1061±192*†	1252±230*†	1492±248*†

	Hypoxemia - Pre				Hypoxemia - Post			
	Baseline	90% SaO <sub>2</sub>	80% SaO <sub>2</sub>	70% SaO <sub>2</sub>	Baseline	90% SaO <sub>2</sub>	80% SaO <sub>2</sub>	70% SaO <sub>2</sub>
(mL/min)	<i>Trial, P&lt;0.01; Stage, P&lt;0.01; Interaction, P&lt;0.01</i>							
<b>gCBF CVC</b>	8.27±1.05	8.92±1.44*	10.09±1.90*	11.30±2.47*	9.84±1.33†	11.01±1.71*†	12.58±1.91*†	15.07±2.33*†
(mL/min/mmHg)	<i>Trial, P&lt;0.01; Stage, P&lt;0.01; Interaction, P&lt;0.01</i>							
<b>CDO<sub>2</sub></b>	148±19	150±24	158±29	166±29	141±19	153±28	166±28	178±28
(mL/min)	<i>Trial, P=0.91; Stage, P=0.14; Interaction, P=0.57</i>							
<b>MCAv</b>	68.0±13.8	71.2±16.3	77.3±17.5*	87.7±19.1*	77.0±12.8†	84.8±16.7*†	93.2±17.5*†	96.6±10.2*†
(cm/s)	<i>Trial, P&lt;0.01; Stage, P&lt;0.01; Interaction, P&lt;0.01</i>							
<b>PCAv</b>	42.9±9.1	43.9±9.4	46.9±10.3*	51.8±11.4*	48.4±14.2†	52.1±16.3*†	54.9±15.9*†	55.3±8.7*†
(cm/s)	<i>Trial, P&lt;0.01; Stage, P&lt;0.01; Interaction, P&lt;0.01</i>							

\*indicates increase from baseline, P<0.05; † indicates a difference between hypoxemia pre and hypoxemia post for corresponding stages, P<0.05.

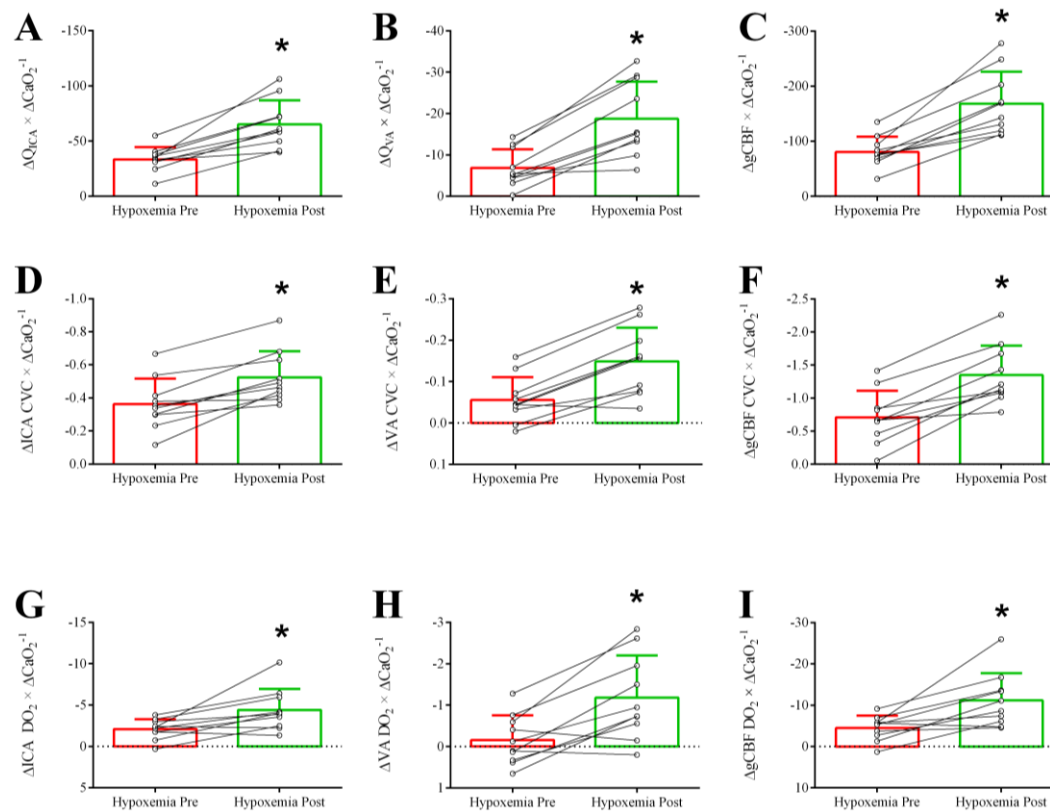


**Figure 4.6. Cerebrovascular reactivity during hypoxemia prior to and following hemodilution.**

Cerebrovascular reactivity during hypoxemia pre is denoted by the red bars (mean  $\pm$  standard deviation) while hypoxemia post is denoted by the green bars. Reactivity slopes for cerebral blood flow (e.g.  $\Delta Q_{ICA} \times \Delta CaO_2^{-1}$ ) represent the volumetric flow (mL/min) changes per unit reduction in  $CaO_2$  (mL/dL). Cerebrovascular conductance (CVC) slopes are mL/min/mmHg per unit reduction in  $CaO_2$  (mL/dL). Slopes for oxygen delivery ( $DO_2$ ) are in mL/min per unit reduction in  $CaO_2$  (mL/dL).  $Q_{ICA}$ , internal carotid artery blood flow;  $Q_{VA}$  vertebral artery blood flow; gCBF, global cerebral blood flow; CVC, cerebrovascular conductance;  $DO_2$ , oxygen delivery. \*denotes a significant difference between hypoxemia and hemodilution,  $P < 0.05$ .

#### 4.2.1.3 COLLECTIVE COMPARISON OF HYPOXIC CEREBRAL VASODILATION

The data presented here, from the linear mixed effects modelling, are reported as mean  $\pm$  standard error. Absolute gCBF reactivity to hypoxemia prior to hemodilution was  $-70.63 \pm 6.68 \text{ mL} \cdot \text{min}^{-1} \cdot \text{mL}^{-1} \cdot \text{dL}^{-1}$ . Reactivity to the hemodilution protocol was  $\sim 45\%$  lower than that during hypoxemia ( $-44.35 \pm 9.62 \text{ mL} \cdot \text{min}^{-1} \cdot \text{mL}^{-1} \cdot \text{dL}^{-1}$ ;  $P < 0.01$ ), whereas reactivity was  $\sim 100\%$  greater than the normal hypoxemia test during hypoxemia following hemodilution ( $-144.42 \pm 10.23 \text{ mL} \cdot \text{min}^{-1} \cdot \text{mL}^{-1} \cdot \text{dL}^{-1}$ ;  $P < 0.01$ ) (**Figure 4.7**). Absolute CDO<sub>2</sub> reactivity to hypoxemia prior to hemodilution was  $-3.74 \pm 0.83 \text{ mL} \cdot \text{min}^{-1} \cdot \text{mL}^{-1} \cdot \text{dL}^{-1}$ . The increase in CDO<sub>2</sub> seen in the hypoxemia trial was reversed, with CDO<sub>2</sub> decreasing in response to hemodilution ( $0.95 \pm 1.19 \text{ mL} \cdot \text{min}^{-1} \cdot \text{mL}^{-1} \cdot \text{dL}^{-1}$ ;  $P < 0.01$ ). Conversely, CDO<sub>2</sub> reactivity was  $\sim 150\%$  greater in the hypoxemia trial post hemodilution compared to pre hemodilution ( $P < 0.01$ ) (**Figure 4.7**).

Absolute ICA flow reactivity to hypoxemia prior to hemodilution was  $-28.76 \pm 2.91 \text{ mL} \cdot \text{min}^{-1} \cdot \text{mL}^{-1} \cdot \text{dL}^{-1}$ . Reactivity to the hemodilution protocol was  $\sim 38\%$  lower than that during hypoxemia ( $-17.58 \pm 4.17 \text{ mL} \cdot \text{min}^{-1} \cdot \text{mL}^{-1} \cdot \text{dL}^{-1}$ ;  $P < 0.01$ ), whereas reactivity was  $\sim 100\%$  greater than the normal hypoxemia test during hypoxemia following hemodilution ( $-55.74 \pm 4.47 \text{ mL} \cdot \text{min}^{-1} \cdot \text{mL}^{-1} \cdot \text{dL}^{-1}$ ;  $P < 0.01$ ). Absolute VA flow reactivity to hypoxemia prior to hemodilution was  $-6.68 \pm 1.23 \text{ mL} \cdot \text{min}^{-1} \cdot \text{mL}^{-1} \cdot \text{dL}^{-1}$ . Reactivity to the hemodilution protocol appeared  $\sim 25\%$  lower than that during hypoxemia but was not statistically lower ( $-4.95 \pm 1.79 \text{ mL} \cdot \text{min}^{-1} \cdot \text{mL}^{-1} \cdot \text{dL}^{-1}$ ;  $P = 0.34$ ). In contrast, VA reactivity was  $\sim 140\%$  greater than the normal hypoxemia test during hypoxemia following hemodilution ( $-16.11 \pm 1.86 \text{ mL} \cdot \text{min}^{-1} \cdot \text{mL}^{-1} \cdot \text{dL}^{-1}$ ;  $P < 0.01$ ).

Absolute MCAv reactivity to hypoxemia prior to hemodilution was  $-3.69 \pm 0.34 \text{ cm} \cdot \text{s}^{-1} \cdot \text{mL}^{-1} \cdot \text{dL}^{-1}$ . Reactivity to the hemodilution was  $\sim 40\%$  lower than that during hypoxemia ( $-2.21 \pm 0.48 \text{ cm} \cdot \text{s}^{-1} \cdot \text{mL}^{-1} \cdot \text{dL}^{-1}$ ;  $P < 0.01$ ), whereas reactivity was  $\sim 35\%$  greater than the normal hypoxemia test during hypoxemia following hemodilution ( $-4.97 \pm 0.51 \text{ cm} \cdot \text{s}^{-1} \cdot \text{mL}^{-1} \cdot \text{dL}^{-1}$ ;  $P = 0.01$ ). Absolute PCAv reactivity to hypoxemia prior to hemodilution was  $-1.60 \pm 0.28 \text{ cm} \cdot \text{s}^{-1} \cdot \text{mL}^{-1} \cdot \text{dL}^{-1}$ . Although reactivity to the hemodilution was  $\sim 35\%$  lower than that during hypoxemia, this was not statistically significant ( $-1.02 \pm 0.42 \text{ cm} \cdot \text{s}^{-1} \cdot \text{mL}^{-1} \cdot \text{dL}^{-1}$ ;  $P = 0.17$ ). Likewise, again not statistically significant, reactivity appeared to be

~50% greater than the normal hypoxemia test during hypoxemia following hemodilution ( $-2.39 \pm 0.43 \text{ cm} \cdot \text{s}^{-1} \cdot \text{mL}^{-1} \cdot \text{dL}^{-1}$ ;  $P=0.07$ ).

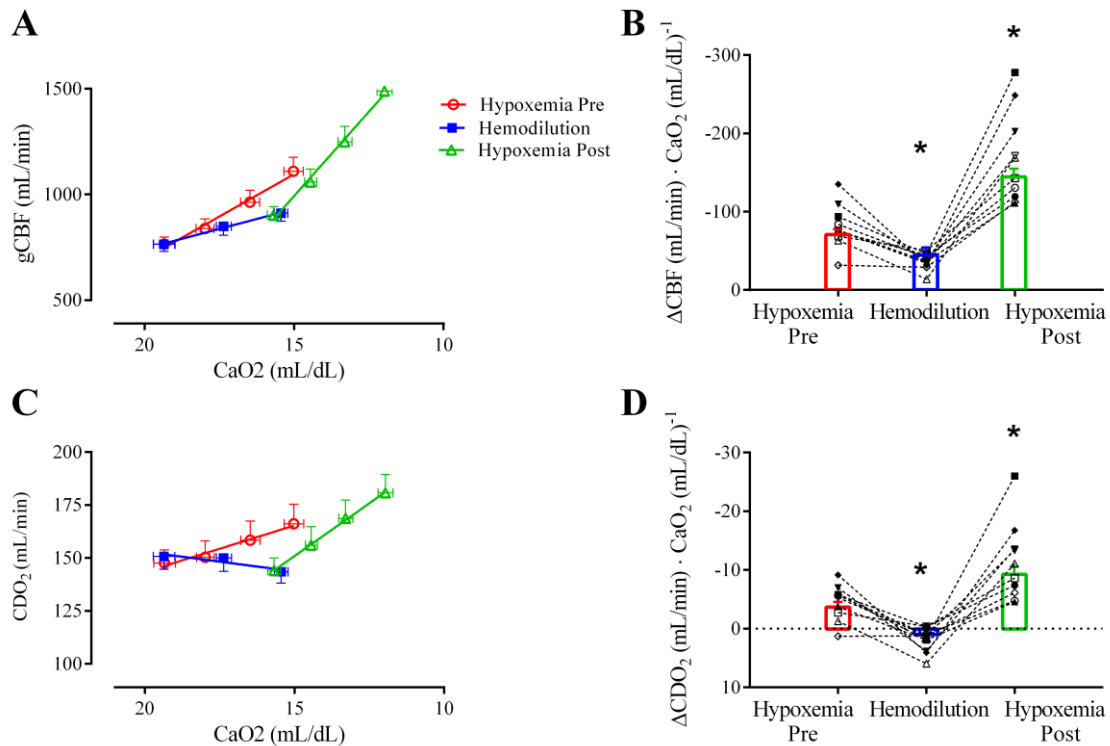


**Figure 4.7. Cerebral blood flow and oxygen delivery across all three experimental trials.**

Panel A depicts the cerebral blood flow (CBF) response to hypoxia, with hypoxemia pre in red, hemodilution in blue, and the post hemodilution hypoxemia trial in green. The slope of the CBF response to hypoxia was different between all trials. The corresponding individual data for the reactivity slopes are presented in panel B, where the bar graphs represent the mean  $\pm$  standard error. Panel C depicts the cerebral oxygen delivery (CDO<sub>2</sub>) response to hypoxia, with hypoxemia pre in red, hemodilution in blue, and the post hemodilution hypoxemia trial in green. The slope of the CDO<sub>2</sub> response to hypoxia was different between all trials. The corresponding individual data for the reactivity slopes are presented in panel B, where the bar graphs represent the mean  $\pm$  standard error. \* denotes a significant difference from the Hypoxemia Pre trial,  $P < 0.05$ .

#### 4.2.2 RESULTS – PROTOCOL TWO

Baseline variables for protocol two are listed in **Table 4.9**. While males and females did not differ in age, the males were taller, heavier, and had a higher body mass index. Further,

males possessed a higher MAP, [Hb], and HCT, although hypoxic reactivity was not different between males and females.

**Table 4.9. Baseline variables for protocol two of study two.**

<b>Variable</b>	<b>All Subjects</b>	<b>n</b>	<b>Male</b>	<b>n</b>	<b>Female</b>	<b>n</b>	<b>P-value</b>
Subjects, n	134		79		55		
Age, years	26 ± 6	(117)	26 ± 6	(69)	25 ± 4	(55)	0.10
Height, cm	173 ± 9	(116)	179 ± 6	(68)	165 ± 7	(55)	< <b>0.01</b>
Weight, kg	72 ± 13	(116)	79 ± 11	(68)	62 ± 8	(55)	< <b>0.01</b>
BMI, kg/m <sup>2</sup>	24 ± 3	(116)	25 ± 3	(68)	23 ± 3	(55)	< <b>0.01</b>
MAP, mmHg	86.6 ± 9.3	(86)	89.2 ± 9.4	(36)	83.7 ± 8.2	(30)	< <b>0.01</b>
[Hb], g/dL (arterial)	14.1 ± 1.3	(134)	14.8 ± 1.0	(79)	13.1 ± 1.2	(55)	< <b>0.01</b>
HCT, % (arterial)	41.7 ± 3.8	(120)	43.6 ± 3.2	(67)	39.3 ± 3.1	(55)	< <b>0.01</b>
%ΔCBF · ΔCaO <sub>2</sub>	-7.86 ± 3.6	(134)	-7.54 ± 4.13	(79)	-8.32 ± 2.71	(55)	0.22

Data are presented as mean ± standard deviation. The P-value represents the statistical output for a t-test between men and women.

Across all subjects, there was a significant correlation between hypoxic reactivity and [Hb] at rest (**Figure 4.8A**). This relationship remained evident when males were assessed independently (**Figure 4.8B**); however, no correlation was observed in the female participants (**Figure 4.8C**).

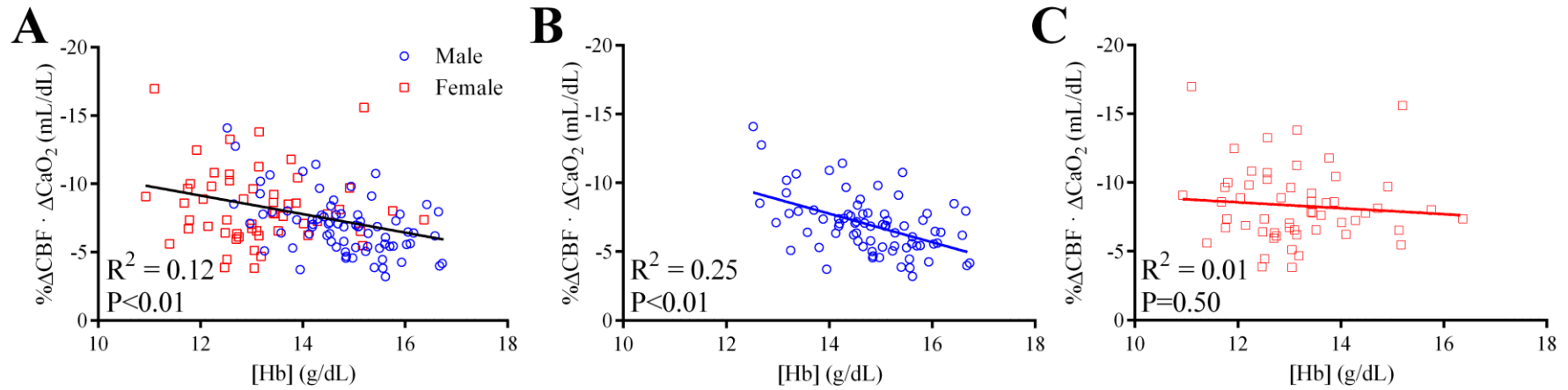


**Figure 4.8. The relationship between hemoglobin concentration and hypoxic reactivity in males and females.**

Panel A depicts the relationship between hypoxic reactivity and [Hb] for all subjects. Panel B depicts the relationship between hypoxic reactivity and [Hb] for males. Panel C depicts the relationship between hypoxic reactivity and [Hb] for females.

### 4.3 STUDY 2 - DISCUSSION

The primary findings of this study are: 1) The CBF response to hemodilution is impaired in comparison to hypoxemia; 2) The blunted CBF response to hemodilution lead to a ~5% reduction in CDO<sub>2</sub>. These two findings indicate that deoxyhemoglobin mediated signaling is integral to the CBF response to hypoxia and the maintenance of CDO<sub>2</sub> in humans. Finally, contrary to our second hypothesis, the CBF response to hypoxemia following hemodilution was greater than the response to hypoxemia prior to hemodilution. This finding was further reflected between subjects, where a lower [Hb] was related to a greater hypoxic reactivity in males but not females. Therefore, there appears to be an interaction between [Hb] and hypoxia in the control of human CBF that is specific to males.

An important role of erythrocyte dependent mechanisms (SNO-Hb, NO<sub>2</sub>, & ATP) in the regulation of hypoxic vasodilation has been demonstrated in a multitude of isolated vessel preps [e.g., (Dietrich *et al.*, 2000; Jagger *et al.*, 2001)] and animal models [ e.g., (Jia *et al.*, 1996; Stamler *et al.*, 1997b)]. Importantly, these three mechanisms all operate via increasing NO bioavailability/bioactivity, which has also been shown as integral to the CBF response to hypoxia in numerous studies utilizing pharmacological blockade (Pearce *et al.*, 1989; Koźniewska *et al.*, 1992; Pelligrino *et al.*, 1995a; Takuwa *et al.*, 2010). Human studies to date have provided equivocal results with regard to whether or not NO is integral to hypoxic cerebral vasodilation in humans (Van Mil *et al.*, 2002a; Ide *et al.*, 2007), with no studies specifically investigating the role of erythrocyte dependent signaling. The current study bridges this gap by demonstrating through the use of hypoxemia and hemodilution that the erythrocyte is an important regulator of hypoxic cerebral vasodilation in humans. Indeed, as is the case in animals where hemodilution does not produce an increase in cGMP (Todd *et al.*, 1997), the reduction in reactivity observed here is likely due to a reduction in NO mediated signaling.

Interestingly, the reduction in gCBF hypoxic reactivity and the related reduction in CDO<sub>2</sub> during hemodilution manifested solely within the anterior circulation, as indicated by reductions in ICA specific reactivity and CDO<sub>2</sub> (**Figure 4.5**), whereas VA reactivity and its DO<sub>2</sub> were unaltered. This differential response between the posterior and anterior circulation may indicate a fundamental difference in vascular control on the teleological basis of prioritizing flow to vital areas such as the brainstem. Although experimental data

are lacking, this teleological prioritization is often speculated when a greater posterior than anterior reactivity to hypoxemia is observed (Binks *et al.*, 2008; Willie *et al.*, 2012; Ogoh *et al.*, 2013a; Subudhi *et al.*, 2014b; Lewis *et al.*, 2014b). However, the present study, and others (Hoiland *et al.*, 2015, 2017a) have shown no difference between the relative reactivity of the ICA and VA during isocapnic hypoxemia. Reasons for the disparate results between the current study and others have been discussed in Study 1 (see section “Cerebral blood flow and normobaric hypoxia”). Therefore, the potential mechanisms underlying the differential ICA and VA response to hemodilution when compared to hypoxemia remains unclear.

#### **4.3.1 WHY IS A LOWER HEMOGLOBIN CONCENTRATION RELATED TO A GREATER HYPOXIC REACTIVITY?**

Contrary to our second hypothesis, hypoxic reactivity was increased in the post-hemodilution hypoxemia trial. Further, when assessed across a large sample size, lower [Hb] was also related to higher hypoxic reactivity. While it was originally speculated that reactivity would be reduced due to a lower deoxyhemoglobin mass, there are several mechanisms that may explain the observed increase in reactivity with lower [Hb]:

1) *The severity of hypoxia* – The severity of hypoxia (i.e., reduction in  $\text{CaO}_2$ ) is greater in the post hemodilution hypoxemia trial despite matched  $\text{SaO}_2$  as a result of the lower [Hb]. Typically, human studies only reduced  $\text{CaO}_2$  by up to ~30% from baseline, as occurs when  $\text{SaO}_2$  is lowered to 70% [e.g., (Willie *et al.*, 2012; Ainslie *et al.*, 2014; Hoiland *et al.*, 2017b)]. Here,  $\text{CaO}_2$  was reduced by  $38 \pm 2\%$  to a  $\text{CaO}_2$  of 12mL/dL in the post hypoxemia trial compared to a  $\text{CaO}_2$  of 15mL/dL in the pre hypoxemia trial. As there is little data on CBF at this severity of hypoxia in humans it is unknown if the reactivity of cerebral vessels increases simply by virtue of a greater hypoxic stimulus. This greater overall hypoxia may engage other regulatory pathways such as carbon monoxide and hydrogen sulfide based signaling mechanisms (Morikawa *et al.*, 2012), adenosine and/or PGs. While we acknowledge that there is no evidence for adenosine and PGs as regulators of hypoxic cerebral vasodilation in humans [reviewed in (Hoiland *et al.*, 2016a)], this may be due to redundant pathways that compensate when pharmacological blockades are used. However, in an instant of severe hypoxia, these compensatory mechanisms may be engaged to promote the larger CBF requirements. Evidence in animals indicate the endogenous

cerebral adenosine production does not occur until ~30mmHg PaO<sub>2</sub> (Winn *et al.*, 1981a), which may serve to facilitate dilation during severe hypoxia. Analogous to this point is the observation that during hypercapnia, more severe levels of hypercapnia reduce the contribution of NO to the vasodilatory response (see section “Hypercapnia and nitric oxide”) indicating the potential necessity of other vasoactive factors to contribute during extreme blood gas perturbations. However, given the lack of human data at these levels of hypoxia, the latter point is merely speculation.

2) *Altered half-life of NO* – While deoxyhemoglobin appears to convey vasodilatory signaling, theoretically via an NO dependent pathway, it is important to remember that hemoglobin also operates as an NO scavenger (Thomas *et al.*, 2008). Indeed, *in vitro* experiments have indicated that a reduction in HCT leads to an increase in the half-life of NO (Azarov *et al.*, 2005). Specifically, a reduction of HCT from 50% to 15% triples (+200%) the half-life of NO *in vitro*. This could be taken to indicate that that the ~8% reduction in HCT we observed would increase the half-life of NO by ~50%. Considering that NO is a potent vasodilator despite an exceptionally short half-life (a few milliseconds) it is conceivable that even a small increase in the stability (i.e. half-life) of NO in the blood will translate to profound changes in a vasodilatory response. In line with our hypothesis, there may in fact be a reduction in deoxyhemoglobin mediated NO bioactivation, but NO signal transduction may be sensitized resulting in a net increase in vasodilation despite lower signaling molecule release.

3) *Reduced blood viscosity* – This thesis has consistently argued against a role of viscosity in regulating CBF in humans. For example, no effect of plasmapheresis in paraproteinemic patients stands as the strongest evidence against a role for blood viscosity [reviewed in: (Hoiland *et al.*, 2016a)]. It has been speculated that this is due to a net balance between reduced resistive forces of blood viscosity and reduced shear mediated relaxation of blood vessels (Hoiland *et al.*, 2016a). However, there is evidence in animals that blood viscosity plays a larger role when CBF is increased (Tomiya *et al.*, 2000). Perhaps, in a scenario where CBF is elevated there is an adequate shear stimulus to maintain the same vasodilatory stimulus despite reduced viscosity, hence driving a shift in the balance to a reduction in viscosity dependent resistance increasing CBF.

#### 4.3.2 SEX DIFFERENCES IN THE REGULATION OF HYPOXIC CEREBRAL VASODILATION?

Sex differences in cerebrovascular regulation have only recently begun to receive attention (Barnes, 2017). This study demonstrates that while [Hb] is correlated to hypoxic reactivity in males, it is not in females, indicating a potential sex difference in cerebrovascular regulation. Given the paucity of data on sex differences and cerebrovascular control it is unclear what mechanism(s) may be underlying the differential relationships in males versus females that were observed. On this note, two speculative points require further discussion:

1) *Contamination by unstandardized menstrual phase* – Plasma estradiol levels change throughout the menstrual phase (Peltonen *et al.*, 2016) and estradiol may influence cerebrovascular tone through NO dependent mechanisms (Pelligrino *et al.*, 2000; Momoi *et al.*, 2003). This holds relevance for the erythrocyte signaling mechanisms linked to deoxyhemoglobin. Menstrual cycle was not controlled in the present study, although a recent study has demonstrated that hypoxic reactivity does not change across the menstrual cycle in women (Peltonen *et al.*, 2016). This study, however, utilized TCD, and therefore the findings are difficult to interpret as one may expect variations in NO dependent signaling across the menstrual phase in relation to altered estradiol levels (Marsh *et al.*, 2011; Peltonen *et al.*, 2016). The impact of these potential changes in NO signaling on MCA diameter and TCD validity are unclear in the context of the study by Peltonen *et al.*, (Peltonen *et al.*, 2016), although it is likely changes in NO would have resulted in alterations in MCA diameter (Schulz *et al.*, 2018).

2) *A legitimate sex difference in the regulation of hypoxic reactivity* – Alternatively, the observed differences may indeed reflect sex differences in the regulation of hypoxic reactivity. To the best of our knowledge, there are no sex specific differences in hemoglobin that would influence the SNO-Hb, NO<sub>2</sub>, or ATP signaling mechanisms. Therefore, it is more likely that rather than NO signaling (relative to [Hb]) being different, the proportion of vasodilation attributable to NO may differ – perhaps NO plays a larger role in mediating hypoxic cerebral vasodilation in males leading to the observed correlation. However, no study has aimed to determine the sex specific contribution of NO dependent mechanisms to hypoxic vasodilation in humans. The observed differences may also be related to a difference in one of the aforementioned mechanism that may explain increased reactivity

with lower [Hb] (see section “Why is a lower hemoglobin concentration related to a greater hypoxic reactivity?”).

### 4.3.3 METHODOLOGICAL CONSIDERATIONS

While this study is the first to indicate an important role of the erythrocyte in regulating hypoxic cerebral vasodilation, it does not provide information on which erythrocyte mechanism(s) is/are at play or the most important. This is a relevant next step for researchers as it will illuminate a molecular target for the purposes of perfusion management and pharmacology.

We have manipulated [Hb] as measured in large vessels (i.e., radial artery), it is unclear how this change in [Hb] manifests in the cerebral pial and micro circulation where reductions in arterial diameter change [Hb] due to the Fåhræus-Lindqvist effect. Animal data are inconsistent, suggesting hemodilution reduces (Todd *et al.*, 1992) or does not affect (Hudetz *et al.*, 1999) capillary [Hb]. Data in humans, based on indices derived from MRI suggest that hemodilution indeed would reduce, at least modestly, microvessel and capillary [Hb] (Calamante *et al.*, 2016). If so, this would in turn reduce the mass of deoxyhemoglobin transiting the vascular bed for a given flow rate.

Hemodilution, likely a result of albumin acting as a weak acid (Stewart, 1983), led to a slight reduction in pH at hemodilution stage one and two as well as during the post hypoxemia trial. Relative to the hemodilution trial, this may have led to an underestimation of the difference between hypoxemia and hemodilution (i.e., the hemodilution reactivity was inflated by reductions in pH). Using the regression formula presented in **Figure 4.9**, we can infer the level of stimulus the change in pH would have elicited. For example, the changes in pH at stage one and two of hemodilution would be equivalent in stimulus to a ~1mmHg and ~1.75 mmHg change in PaCO<sub>2</sub>, respectively. The changes in gCBF in hemodilution were +11.2% at stage one and +19.2% at stage two. If a general correction factor is assumed at 7% change in gCBF per mmHg change in PaCO<sub>2</sub> (Willie *et al.*, 2012), then the portion of the hemodilution response at stage one and two attributable to hypoxia may only be ~4% (stage one) and 7% (stage 2). Therefore, the magnitude difference in CBF responses may be underestimated in the current study, further strengthening our conclusion that the erythrocyte is integral for the regulation of hypoxic cerebral vasodilation. Relative

to comparing pre hypoxemia to post hypoxemia, the change in PaCO<sub>2</sub> would be equivalent to a ~1-1.5mmHg change in PaCO<sub>2</sub> depending on the stage of hypoxemia. This may be important given the potential for an interaction between PaCO<sub>2</sub> and CaO<sub>2</sub> related cerebrovascular reactivity (Mardimae *et al.*, 2012). However, the study by Mardimae *et al.*, which observed unremarkable changes in O<sub>2</sub> reactivity with large (10mmHg) changes in PaCO<sub>2</sub>, indexed their hypoxic reactivity to PaO<sub>2</sub>, not SaO<sub>2</sub> or CaO<sub>2</sub>. Their measured stimulus of PaO<sub>2</sub> is not appropriate as pH will alter the relationship between PaO<sub>2</sub> and SaO<sub>2</sub> (Bohr effect) and confound these results. Therefore, given the very minimal change in pH, and index of reactivity slopes to CaO<sub>2</sub>, which takes into account a potential Bohr effect, it does not appear as though the hemodilution mediated decrease in pH would have influenced our pre and post hypoxemia comparison.

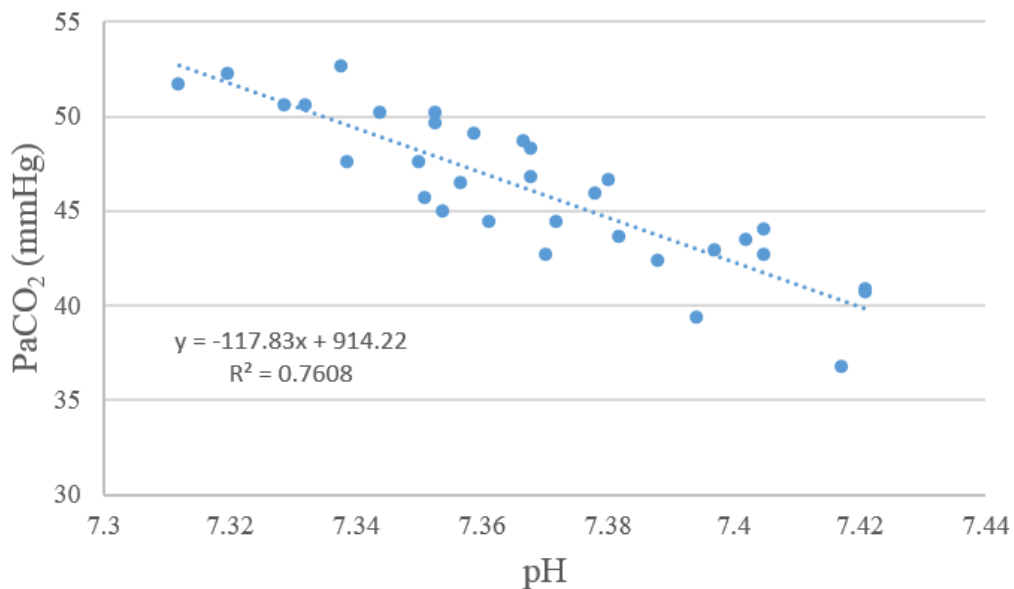


**Figure 4.9. Relationship between pH and PaCO<sub>2</sub> in eight subjects from the hemodilution study**

Data were collected during a euoxic hypercapnia trial. The above data represent the relationship between PaCO<sub>2</sub> and pH across all eight subjects during four stages of end-tidal forcing.

#### 4.4 STUDY 2 - SUMMARY

This study demonstrated that erythrocyte mediated signaling is integral to cerebral hypoxic vasodilation in humans. However, while lower [Hb] was related to higher reactivity in

males it was not in females. Therefore, it remains uncertain if the differences we observed between hypoxemic and hemodilution reactivity (protocol one) would manifest in female subjects. Future work is needed to determine the potential presence of and mechanisms governing sex differences in the regulation of hypoxic cerebral vasodilation.

## 5 CHAPTER 4: UBC-NEPAL EXPEDITION: REDUCED CEREBRAL BLOOD FLOW AND OXYGEN DELIVERY IN SHERPA COMPARED TO LOWLANDERS UPON ASCENT TO HIGH-ALTITUDE

The dramatically low atmospheric oxygen levels of the Tibetan Plateau represent one of the most hostile living conditions of modern human habitation. While this environment is debilitating for most humans, and can be fatal for those who ascend too high and fast, it has been inhabited for millennia (>25,000 years) by a lineage of Sherpa (Zhang & Li, 2002; Aldenderfer, 2011). The Sherpa, a highlander population of the Nepalese Khumbu region that shares a common genetic origin with Tibetans (Lu *et al.*, 2016; Zhang *et al.*, 2017), have clearly evolved under the selection pressures imposed by hypoxia through natural selection and are consequently better suited for life at altitude than lowland natives (Lahiri & Milledge, 1965; Moore, 2017). Of critical importance in the setting of hypoxia is the oxygen sensitive brain, which due to a high metabolic demand and limited substrate storage is highly susceptible to metabolic deficiency and ensuing hypoxic damage [reviewed in: (Bailey *et al.*, 2009a)]. Therefore, increases in CBF are integral to maintain  $\text{CDO}_2$  in the face of hypoxemia and resultant reductions in  $\text{CaO}_2$  (see **Equation 2.10**).

While several examples of phenotypical adaptations distinct from those in lowlanders have been observed in the oxygen cascade of Tibetans, such as a higher nitric oxide bioavailability (Beall *et al.*, 2001; Erzurum *et al.*, 2007) and increased skeletal muscle capillary density (Beall, 2007), and improved muscle energetics in Sherpa (Horscroft *et al.*, 2017), little is known relative to potential adaptations in cerebral oxygen delivery/utilization [for review see: (Jansen & Basnyat, 2011; Gilbert-Kawai *et al.*, 2014)]. Tibetans' display a "high flow" phenotype to maintain oxygen delivery to various peripheral tissues in the presence of unremarkable arterial  $\text{SaO}_2$  and [Hb] (Beall, 2007). Preliminary evidence indicated a similar high flow adaptation in the brain due to elevated ICAv in Tibetan natives compared to lowlanders at 3658 m (Huang *et al.*, 1992). However, a recent cross-sectional study demonstrated lower  $\text{CDO}_2$  in Tibetans than in Han Chinese at sea level and at 3658 m (Liu *et al.*, 2016). Given that velocity is a poor index of flow (and therefore  $\text{CDO}_2$ ; see section "transcranial doppler ultrasound") in the setting of altered intra-cranial cerebral arterial diameter (Ainslie & Hoiland, 2014), which occurs at altitude (Wilson *et al.*, 2011; Imray *et al.*, 2014; Willie *et al.*, 2014a), previous theories related to a high-flow adaptation in the Sherpa brain (Huang *et al.*, 1992; Gilbert-Kawai *et al.*, 2014)

need to be re-considered. Elucidation of hypoxia tolerant adaptation in humans may provide insight into potential therapeutic targets in chronic hypoxic diseases and further our basic understanding of human responses to low oxygen conditions.

It is well established that  $\text{CDO}_2$  is maintained during ascent and at altitude in lowlanders [reviewed in: (Ainslie & Subudhi, 2014)]. However, volumetric CBF and  $\text{CDO}_2$  have yet to be compared between lowlanders and Sherpa following a short duration at altitude (e.g., days). It is also unknown if lowlander CBF responds differentially to that of Sherpa during graded ascent to altitude. During ascent to and upon arrival at 5050 m, we hypothesized that CBF and  $\text{CDO}_2$  would be lower in Sherpa compared to lowlanders. To examine these novel hypotheses, Sherpa and lowlanders were studied using a longitudinal experimental design during ascent to altitude. Further, Sherpa recently exposed to altitude for a short duration (those who ascended) and long duration (those residing at altitude) were compared to lowlanders using a cross-sectional design following arrival at 5050 m. Further mechanistic insight was also obtained within these groups via the concurrent assessment of established factors in the regulation of CBF [e.g. arterial blood gases (Kety & Schmidt, 1948c), MAP (Lucas *et al.*, 2010; Numan *et al.*, 2014) and blood viscosity (Hoiland *et al.*, 2016a)].

## **5.1 STUDY 3 - METHODS**

This study involved the recruitment of three distinct subject groups. First, the lowlander group comprised of 21(1 female) healthy individuals (mean $\pm$ SD, Age: 29 $\pm$ 6 years; BMI: 23 $\pm$ 2kg/m<sup>2</sup>) who were recruited at the University of British Columbia's Okanagan campus and were part of the research team. All lowlander participants were free of cardiovascular, respiratory and neurological diseases and were non-smokers.

The second group of participants comprised of 12 HA Sherpa (Age: 34 $\pm$ 11, BMI: 24 $\pm$ 4). These Sherpa were of Tibetan lineage. The Sherpa participants were recruited from local villages in the Solukhumbu Valley (**Table 5.1**) and descended to Kathmandu prior to baseline testing (see section "Study 3 - experimental overview"). Four Sherpa were current smokers, with an average of 1.3 $\pm$ 1.1 pack years in the current smokers. The Sherpa were free of cardiovascular, respiratory and neurological diseases. This cohort of Sherpa will be referred to as the "Ascent Sherpa" throughout the manuscript. Notably, three of the Sherpa

in this group had summited Mount Everest (8848 m) in the previous year, while the remaining Sherpa had reached maximum altitude of 4800 m to 7800 m (median: 5545 m) in the last year.

**Table 5.1. Age and time at high-altitude for the sherpa participants.**

Ascent Sherpa					Altitude Sherpa				
Subject Number	Age	Childhood Residence	Altitude (m)	Total Years at altitude	Subject Number	Age	Childhood Residence	Altitude (m)	Total Years at altitude
101	22	Thame	3800	16.5	113	43	Pangbouche	3985	43
102	31	Thamo	3440	31	114	19	Khunde	3800	14
103	30	Namche	3400	12	115	23	Darjeeling	2040	6
104	25	Thamo	3440	25	116	26	Pheriche	4371	26
105	38	Salleri	2300	24	117	18	Thame	3800	18
106	39	Khumjung	3790	39	118	20	Thame	3800	16
107	44	Khumjung	3790	44	120	18	Thame	3800	18
108	26	Thamo	3440	21	121	20	Thame	3800	20
109	44	Pangbouche	3985	41	122	23	Thamo	3440	23
110	22	Thamo	3440	20	123	24	Thamo	3440	25
111	59	Khunde	3840	59	124	20	Thamo	3440	10
112	31	Pheriche	4371	16					

The third group of participants included 11 Sherpa of Tibetan lineage (Age:  $23\pm 7$ , BMI:  $21\pm 2$ ) that were recruited from local villages in the Solukhumbu Valley (**Table 5.1**); however, unlike the Ascent Sherpa, these Sherpa were recruited while the research team was at the Ev-K2-CNR Pyramid laboratory. Therefore, these Sherpa did not descend to Kathmandu prior to testing. Five Sherpa were current smokers, with an average of  $0.4\pm 0.1$  pack years. All Sherpa were free of cardiovascular, respiratory and neurological diseases. This cohort of Sherpa will be referred to as the “Altitude Sherpa” throughout the manuscript. Notably, two of the Sherpa in this group had summited Mount Everest in the previous year, while the remaining Sherpa had reached a maximum altitude of 4200 m to 5545 m (median: 5300 m).

This study was approved by the Clinical Research Ethics Board of the University of British Columbia and the Nepal Health Research Council. All lowlander participants gave written informed consent in English prior to participating. All Sherpa participants read an in-depth

study information form, spoke with a Nepalese doctor and gave written informed consent in Nepalese prior to participating.

### **5.1.1 STUDY 3 - EXPERIMENTAL OVERVIEW**

All lowlander participants spent 3-9 days in Kathmandu (1400 m) prior to flying to Lukla (2860 m) to begin the ascent to the EV-K2-CNR Pyramid Research laboratory (5050 m), while the Ascent Sherpa group descended to Kathmandu and remained there for 5-15 days (median: 7) prior to flying to Lukla with the lowlanders. Ascent to the Pyramid Laboratory took place over a slow and safe 9-day trekking protocol without the use of any acute mountain sickness prophylactics (e.g., acetazolamide). Participants spent one night in Monjo (2800 m), three nights in Namche Bazaar (3400 m), one night in Deboche (3820 m), and then three nights in Pheriche (4371 m) followed by the final trekking day to 5050 m.

In Kathmandu prior to the ascent and on the day following arrival to Namche, Pheriche, and the Pyramid laboratory, all participants underwent experimental measurement of arterial blood gases, venous blood viscosity, MAP, HR, and CBF. The protocol for venous blood viscosity, MAP, HR, and CBF have been previously described in Study 1. Other relevant measurements are detailed below (see section “Study 3 - experimental measures”).

Following approximately two-weeks of stay at the Pyramid Laboratory, a second experimental protocol was completed on the Altitude Sherpa group. The Altitude Sherpa group were all living at HA prior to arrival at the Pyramid, ascended from 3400-4200 m in 1-2 days, and were tested 1-2 days following arrival. They completed the same experimental protocol as the lowlanders and Ascent Sherpa (described below).

### **5.1.2 STUDY 3 - EXPERIMENTAL MEASURES**

Following 10-minutes supine rest at each location during the ascent and after approximately 2 weeks at HA when the Altitude Sherpa were tested, arterial blood samples were taken from the radial artery. A 23-G self-filling catheter (SafePico, Radiometer) was advanced into the radial artery under local anesthesia (Lidocaine, 1.0%) and ultrasound guidance (Terason, uSmart 3300). Approximately 1mL of blood was withdrawn anaerobically and immediately assessed using an arterial blood gas analyzer for PaO<sub>2</sub>, PaCO<sub>2</sub>, pH, [HCO<sub>3</sub><sup>-</sup>],

[Hb], and HCT (i-STAT 1, Abbott Point of Care). Further, following venipuncture of the median ante-cubital vein (21G needle, BD Vacutainer eclipse) blood was collected for the measurement of whole blood viscosity. This venous blood was drawn into a Lithium Heparin Vacutainer® (Becton Dickinson, USA). Blood viscosity was measured within 15 minutes of blood sample acquisition at a shear rate of  $225 \text{ s}^{-1}$  at  $37.0^\circ\text{C}$  with a cone-and-plate viscometer (Model DV2T, Brookfield, USA). Resting gCBF was also measured using previously described techniques (see section “Cerebrovascular measures”).

In an attempt to better understand the underlying physiology regulating gCBF in Sherpa and lowlanders we measured cerebral vascular reactivity to  $\text{CO}_2$  using the hyperoxic rebreathe technique (Fan *et al.*, 2010b). These data were collected in 13 lowlanders and five Sherpa on our 2008 expedition to Nepal, where lowlander subjects underwent a similar ascent protocol, and were tested following  $>2$  weeks acclimatization (Lucas *et al.*, 2011). These data have not been previously published.

### 5.1.3 STUDY 3 - CALCULATIONS

To account for the influence of changes in blood pressure on CBF upon ascent to HA, we calculated CVC as gCBF divided by MAP (**Equation 3.2**). Shear stress in the ICA and VA were also calculated (**Equation 5.1**).

Equation 5.1. Shear stress.

$$\begin{aligned}\text{Shear Stress} &= \text{Shear rate} * \text{blood viscosity} \\ \text{Shear Stress} &= (4 * \text{velocity} / \text{diameter}) * \text{blood viscosity}\end{aligned}$$

### 5.1.4 STUDY 3 - STATISTICAL ANALYSES

Data were analyzed using a linear mixed model with a compound symmetry co-variance structure. The selected factors were altitude and race. When significant main effects were detected, Bonferroni corrected post-hoc tests were used to make pairwise comparisons. Significance was assumed at  $P < 0.05$ . There was no difference in the primary outcome variables between current and non-smokers in either Sherpa group.

To further ascertain the underlying components regulating gCBF (dependent variable) during ascent in lowlanders and Sherpa, we ran a forward stepwise linear regression model including the following input variables: Altitude, race, CaO<sub>2</sub>, PaCO<sub>2</sub>, pH, venous whole blood viscosity, and both systolic and diastolic blood pressures. These variables were chosen as they are considered important regulators of CBF in humans (Willie *et al.*, 2014c).

Differences between acclimatized lowlanders, the ascent Sherpa, and altitude Sherpa at 2-weeks were compared using a one-way ANOVA. When significant main effects were detected, Bonferroni corrected post-hoc tests were used to make pairwise comparisons. Sherpa versus lowlander cerebral vascular CO<sub>2</sub> reactivity were compared using a Mann-Whitney U test.

## 5.2 STUDY 3 - RESULTS

### 5.2.1 ARTERIAL AND VENOUS BLOOD VARIABLES

All arterial and venous blood data are summarized in **Table 5.2**. Notably, CaO<sub>2</sub>, SaO<sub>2</sub>, and PaO<sub>2</sub> did not differ between Lowlanders and Sherpa at any HA location. Although a reduction in PaCO<sub>2</sub> was observed in both groups, PaCO<sub>2</sub> was higher in Sherpa at 4371 m and 5050 m (vs. lowlanders P<0.01). In keeping, there was a main effect for lower pH in Sherpa across all altitudes (P<0.01). At 1400 m Sherpa had an elevated [Hb] relative to lowlanders (P<0.01), but following an increase in lowlander [Hb] at 3400 m (P<0.01), there was no difference present between groups throughout the remainder of the ascent. Both HCT and venous whole blood viscosity followed the same pattern as [Hb], with Sherpa HCT and viscosity elevated compared to lowlanders at 1400 m, but not different during the remainder of ascent.

**Table 5.2. Arterial and venous blood data.**

		Kathmandu (1400m)	Namache (3400m)	Pheriche (4371m)	Pyramid (5050m)
CaO <sub>2</sub> (ml · dl <sup>-1</sup> )		<i>Race: P=0.244; Altitude: P&lt;0.001; Interaction: P=0.005</i>			
	Lowlander	17.8±1.1†	17.3±1.0	16.7±0.9*	15.6±1.4*
	Sherpa	19.3±1.1	17.3±1.4*	16.8±1.0*	15.7±1.4*
SaO <sub>2</sub> (%)		<i>Race: P=0.152; Altitude: P&lt;0.001; Interaction: P=0.809</i>			
	Lowlander	95.4±1.2	87.4±2.7*	84.5±3.2*	79.0±4.9*
	Sherpa	94.5±1.9	86.7±3.2*	82.5±4.5*	77.4±4.5*
PaO <sub>2</sub> (mmHg)		<i>Race: P=0.523; Altitude: P&lt;0.001; Interaction: P=0.693</i>			
	Lowlander	77.0±6.5	51.8±4.1*	47.6±3.7*	41.2±4.4*
	Sherpa	74.8±7.6	52.2±4.6*	46.7±4.5*	40.6±4.3*
PaCO <sub>2</sub> (mmHg)		<i>Race: P=0.050; Altitude: P&lt;0.001; Interaction: P=0.011</i>			
	Lowlander	40.3±2.6	34.5±1.4*	32.2±1.6*†	29.9±1.9*†
	Sherpa	39.8±1.6	35.4±2.3*	34.3±2.9*	32.1±2.7*
pH		<i>Race: P&lt;0.001; Altitude: P&lt;0.001; Interaction: P=0.918</i>			
	<b>Lowlander</b>	7.42±0.02	7.44±0.02*	7.43±0.02	7.46±0.02*
	Sherpa	7.40±0.01	7.41±0.02*	7.40±0.02	7.44±0.02*
HCO <sub>3</sub> <sup>-</sup> (mEq · L <sup>-1</sup> )		<i>Race: P=0.111; Altitude: P&lt;0.001; Interaction: P=0.002</i>			
	Lowlander	26.33±1.42*†	23.57±1.21*†	21.55±1.34*	21.37±1.57*
	Sherpa	24.55±1.24*	22.32±1.63*	21.47±1.83*	21.66±2.01*
BE <sub>ecf</sub> (mEq · L <sup>-1</sup> )		<i>Race: P=0.034; Altitude: P&lt;0.001; Interaction: P=0.029</i>			
	<b>Lowlander</b>	1.95±1.56*†	-0.62±1.40*†	-2.81±1.60*	-2.39±1.93*
	Sherpa	-0.11±1.45*	-2.18±1.83*	-3.27±2.15*	-2.67±2.17*
[Hb] (g · dl <sup>-1</sup> )		<i>Race: P=0.017; Altitude: P=0.012; Interaction: P=0.001</i>			
	Lowlander	13.56±0.80†	14.46±0.70*	14.44±0.52*	14.46±0.72*
	<b>Sherpa</b>	14.83±0.92	14.50±0.75	14.85±0.89	14.81±0.65
HCT (%)		<i>Race: P=0.020; Altitude: P=0.010; Interaction: P=0.001</i>			
	Lowlander	39.90±2.39†	42.52±2.04*	42.48±1.54*	42.78±2.24*
	<b>Sherpa</b>	43.64±2.69	42.64±2.20	43.64±2.62	43.66±2.17
Venous viscosity (cP)		<i>Race: P=0.240; Altitude: P&lt;0.001; Interaction: P=0.004</i>			
	Lowlander	3.78±0.48†	4.41±0.30*	4.53±0.43*	4.78±0.36*
	Sherpa	4.32±0.40	4.46±0.67	4.63±0.58	4.62±0.29

**Bolded Lowlander or Sherpa** indicates a main effect of race, with the bolded group possessing a higher value

\* Significant difference from baseline, P<0.05

† Significant difference between Sherpa and Lowlander within an altitude, P<0.05

CaO<sub>2</sub>, arterial oxygen content; SaO<sub>2</sub>, arterial oxyhemoglobin saturation; PaO<sub>2</sub>, partial pressure of arterial oxygen; PaCO<sub>2</sub>, partial pressure of arterial carbon dioxide; HCO<sub>3</sub><sup>-</sup>, bicarbonate ion; BE<sub>ecf</sub>, base excess extracellular fluid; [Hb], hemoglobin concentration; HCT, hematocrit.

### 5.2.2 CEREBROVASCULAR AND CARDIORESPIRATORY VARIABLES

In Lowlanders, gCBF was unchanged from Kathmandu (1400 m) values at 3400 m and 4371 m ( $+0.4\pm 15.5\%$  &  $-0.1\pm 21.5\%$ , respectively), but increased by  $23.3\pm 26.1\%$  at 5050 m (main effect of altitude,  $P<0.01$ ) (**Figure 5.1**). Flow through the ICA and VA followed a similar pattern – both were unaltered at 3400 m or 4371 m, but were elevated by  $18.4\pm 26.2\%$  and  $24.6\pm 31.9\%$  at 5050 m, respectively (main effect of altitude,  $P<0.01$ ). In the Sherpa, gCBF was  $21.3\pm 24.0\%$  lower at 3400 m compared to Kathmandu, returned to baseline by 4371 m ( $-4.3\pm 8.8\%$ ), and was elevated by  $13.5\pm 22.3\%$  at 5050 m (main effect of altitude,  $P<0.01$ ). Regional flow through the ICA and VA appeared to follow differential patterns in the Sherpa, with  $Q_{ICA}$  reduced by  $22.8\pm 21.6\%$  at 3400 m compared to Kathmandu, returned to baseline by 4371 m ( $-5.8\pm 11.1\%$ ), and then elevated by  $10.0\pm 22.8\%$  at 5050 m. However, VA flow was unaltered at 3400 m ( $-5.9\pm 44.2\%$ ), albeit this response showed substantial inter-individual variability (**Figure 5.1**). At 4371 m, VA flow in the Sherpa was slightly elevated by  $10.6\pm 51.2\%$ , with a further significant elevation at 5050 m where VA flow was  $20.7\pm 31.8\%$  greater than in Kathmandu (main effect of altitude,  $P<0.01$ ). There was a significant main effect of race, with  $Q_{ICA}$ , VA flow, and gCBF greater in lowlanders compared to Sherpa across all altitudes (**Figure 5.1**). Anterior (i.e.  $Q_{ICA}$ ) versus posterior (i.e. VA flow) distributions of CBF in lowlanders and Sherpa are presented in **Figure 5.2**. Sherpa had a lower posterior distribution of CBF than lowlanders across all altitudes during ascent (main effect of race,  $P=0.018$ ).

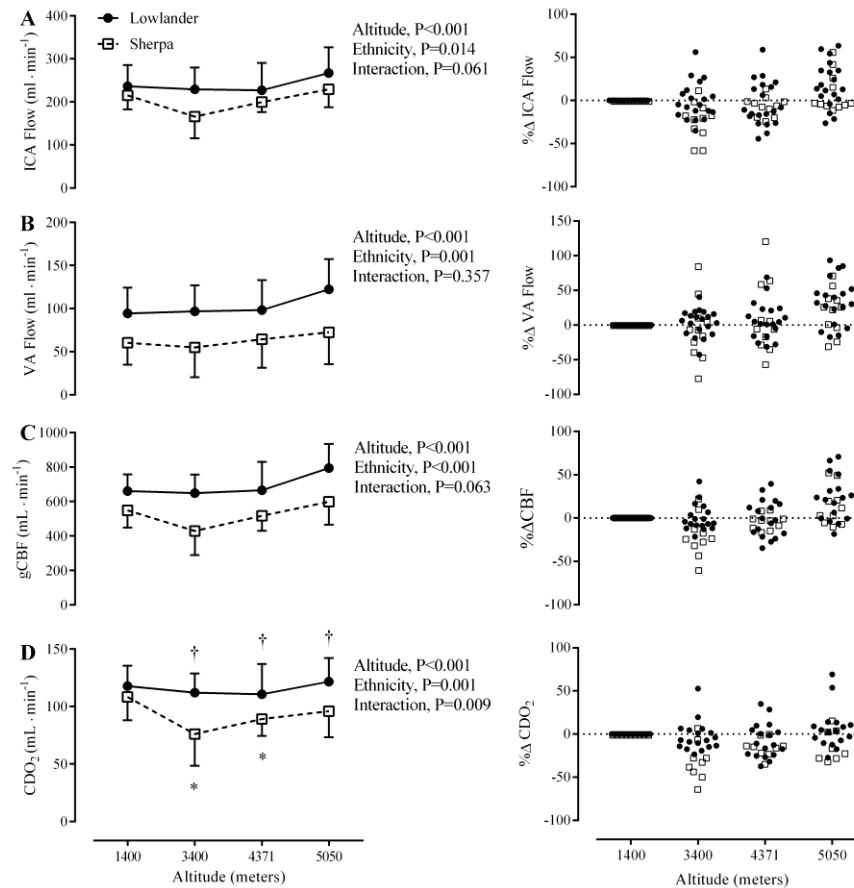


**Figure 5.1. Regional cerebral blood flow and cerebral oxygen delivery upon ascent to 5050 m in lowlanders and sherpa.**

For all panels lowlanders are denoted by the filled circle symbol (●), and Sherpa by the open square symbol (□). **A.** Internal carotid artery (ICA) flow in lowlander and Sherpa. ICA flow (i.e.  $Q_{ICA}$ ) was reduced across groups at 3400 m (marginal means,  $P=0.01$ ) and increased across groups at 5050 m (marginal means,  $P=0.02$ ). **B.** Vertebral artery (VA) flow in lowlander and Sherpa. VA flow was increased across groups at 5050 m (marginal means,  $P<0.01$ ). **C.** Global cerebral blood flow (gCBF) in lowlander and Sherpa. gCBF was reduced across groups at 3400 m (marginal means,  $P=0.038$ ) and increased across groups at 5050 m (marginal means,  $P<0.01$ ). **D.** Cerebral oxygen delivery ( $CDO_2$ ) in lowlander and Sherpa.  $CDO_2$  was lower in Sherpa compared to lowlanders at 3400 m ( $P<0.01$ ), 4371 m ( $P=0.03$ ), and 5050 m ( $P<0.01$ ). While lowlander  $CDO_2$  was maintained across ascent, Sherpa  $CDO_2$  decreased from Kathmandu values at 3400 m ( $P<0.01$ ) and 4731 m ( $P=0.04$ ). In all panels, the % change from Kathmandu values for lowlanders and Sherpa throughout ascent are presented in the right figures.

\* Denotes a significant change from Kathmandu values ( $P<0.05$ )

† Denotes a significant difference between lowlanders and Sherpa at a given altitude ( $P<0.05$ )

The CDO<sub>2</sub> was maintained in the lowlanders during ascent. In contrast, Sherpa CDO<sub>2</sub> was reduced at 3400 m ( $-30.3 \pm 21.6\%$ ;  $P < 0.01$ ), 4371 m ( $-14.2 \pm 10.7\%$ ;  $P = 0.03$ ), but was not statistically different from Kathmandu at 5050 m ( $-12.0 \pm 18.0\%$ ;  $P = 0.28$ ). Compared to lowlanders, Sherpa CDO<sub>2</sub> was lower at 3400 m ( $P < 0.01$ ), 4371 m ( $P = 0.03$ ), and 5050 m ( $P < 0.01$ ) (**Figure 5.1**).

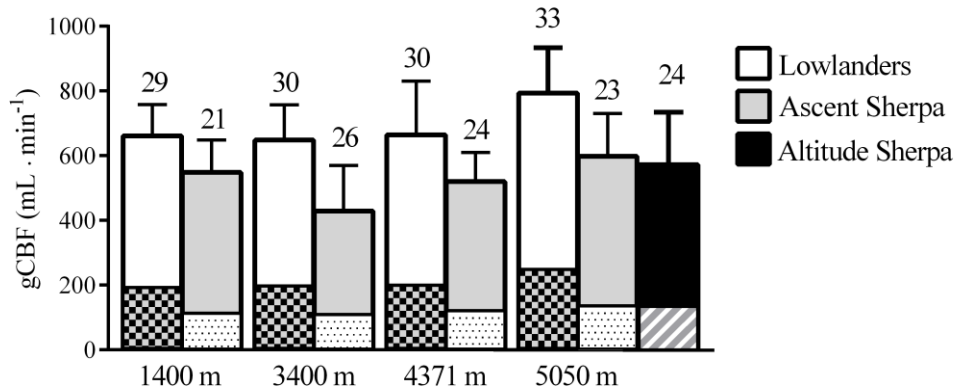


**Figure 5.2. Cerebral blood flow distribution in lowlanders and sherpa upon ascent and following acclimatization.**

The presented data are global cerebral blood flow (gCBF) with open bars for the lowlanders, grey bars for the ascent sherpa and a black bar for the altitude sherpa. Overlaid on the gCBF data, a patterned bar, is an estimate of bilateral VA flow ( $2 \cdot$  unilateral VA flow), with the estimated %contribution of VA flow to gCBF denoted above each time point. For the ascent protocol a 2-way ANOVA was used for statistical comparisons (Factors: Race and Altitude). There was a main effect of Race ( $P = 0.018$ ) with the %CBF distribution to the posterior circulation less in Sherpa across altitudes. Following 2-weeks at 5050 m, the three groups (right side of figure) were compared using a 1-way ANOVA. Both the ascent Sherpa ( $P < 0.01$ ) and altitude Sherpa ( $P < 0.01$ ) had lower VA distribution than lowlanders following arrival at 5050 m.

Lowlander MAP was lower in Kathmandu compared to Sherpa ( $84.5 \pm 6.3$  vs.  $95.2 \pm 9.2$  mmHg;  $P < 0.01$ ), and increased from Kathmandu at each altitude ( $P < 0.01$  for all altitudes), while MAP in the Sherpa did not increase at altitude. At 3400 m ( $93.4 \pm 9.1$  vs.  $101.5 \pm 10.7$  mmHg;  $P = 0.02$ ) and 4371 m ( $93.9 \pm 8.6$  vs.  $100.7 \pm 9.6$  mmHg;  $P = 0.03$ ), lowlander MAP was lower than that of the Sherpa. At 5050 m there was no difference between lowlander and Sherpa MAP ( $99.9 \pm 10.2$  vs.  $96.5 \pm 5.3$  mmHg;  $P = 0.38$ ). The combination of changes in

gCBF and MAP lead to a main effect of both altitude ( $P < 0.001$ ) and race ( $P < 0.001$ ) on cerebrovascular conductance (CVC; interaction,  $P = 0.166$ ). Lowlander ( $7.91 \pm 1.42$  vs.  $6.97 \pm 1.32$  mL  $\cdot$  min<sup>-1</sup>  $\cdot$  mmHg<sup>-1</sup>) and Sherpa ( $5.80 \pm 1.32$  vs.  $4.02 \pm 1.15$  mL  $\cdot$  min<sup>-1</sup>  $\cdot$  mmHg<sup>-1</sup>) were reduced at 3400 m compared to Kathmandu (main effect of altitude,  $P = 0.001$ ). Lowlander and Sherpa CVC were not different from baseline at 4371 m ( $7.04 \pm 1.58$  &  $5.22 \pm 1.23$  mL  $\cdot$  min<sup>-1</sup>  $\cdot$  mmHg<sup>-1</sup>, respectively) or 5050 m ( $7.99 \pm 1.74$  &  $6.41 \pm 1.64$  mL  $\cdot$  min<sup>-1</sup>  $\cdot$  mmHg<sup>-1</sup>, respectively).

### 5.2.3 PREDICTORS OF gCBF DURING ASCENT

Forward stepwise linear regression revealed that race, altitude, CaO<sub>2</sub>, pH and viscosity were all important predictors of gCBF during ascent (**Table 5.3**). Our model (see **Table 5.3**; and **Figure 5.3**) resulted in an  $r^2$  of 0.36. The standard error of estimate between actual and predicted gCBF was 72.08 mL  $\cdot$  min<sup>-1</sup>. The significant coefficient of 172.6 for race corroborates the main effect of race detected with the mixed model analysis, and is extremely comparable to the mean differences in lowlander and Sherpa gCBF at each altitude seen in **Figure 5.1**.

**Table 5.3. Multi-linear regression for the prediction of cerebral blood flow at high-altitude in lowlanders and sherpa.**

Stepwise Multi-linear Regression Output		
$\text{gCBF} = 8976.751 + 172.639(\text{Race}) - 84.635(\text{Namche}) - 63.915(\text{Pheriche}) + 36.877(\text{Pyramid}) - 25.580(\text{CaO}_2) - 1104.140(\text{pH}) + 48.488(\text{Viscosity})$		
Input Variable	Coefficient	P-value
Race	172.639	<b>&lt;0.001</b>
Altitude (Namche)	-84.635	<b>0.035</b>
Altitude (Pheriche)	-63.915	0.161
Altitude (Pyramid)	36.877	0.551
CaO <sub>2</sub>	-25.580	0.036
pH	-1104.140	0.075
Viscosity	48.488	0.119

Race is a nominal variable with 0=Sherpa and 1=lowlander. Altitude is an ordinal variable, where 1 is entered in for the current altitude, and zero for the other altitudes. The true values for CaO<sub>2</sub>, pH and viscosity are used. For example, a lowlander in Namche (3400 m) with a CaO<sub>2</sub> of 17.3mL · dL<sup>-1</sup>, pH of 7.44, and viscosity of 4.41 would be represented by the following equation:  $\text{gCBF} = 8976.751 + 172.639(1) - 84.635(1) - 63.915(0) + 36.877(0) - 25.580(17.3) - 1104.140(7.44) + 48.488(4.41)$ . This predicts a gCBF of 621.25 mL · min<sup>-1</sup>.

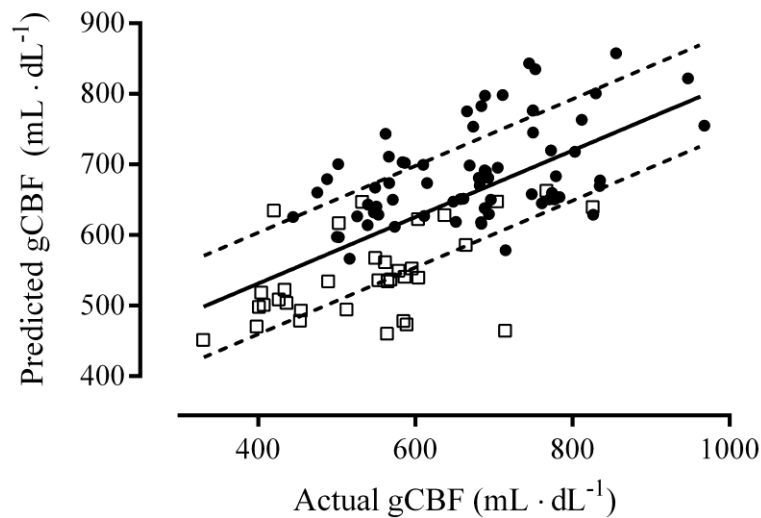


**Figure 5.3. Actual versus predicted global cerebral blood flow.**

This figure depicts actual CBF in lowlander and Sherpa versus their predicted values using our stepwise linear regression model. The standard error of the estimate between actual and predicted values was  $72.1 \text{ mL} \cdot \text{min}^{-1}$ . The regression equation used was:  $\text{gCBF} = 8976.751 + 172.639(\text{Race}) - 84.635(\text{Namche}) - 63.915(\text{Pheriche}) + 36.877(\text{Pyramid}) - 25.580(\text{CaO}_2) - 1104.140(\text{pH}) + 48.488(\text{Viscosity})$ . Lowlanders are denoted by the filled circle symbol (•), and Sherpa by the open square symbol (□).

#### 5.2.4 ASCENT VERSUS ALTITUDE SHERPA COMPARISONS

Comparison of lowlanders to both the ‘Ascent’ Sherpa and ‘Altitude’ Sherpa at 5050 m revealed their gCBF were similarly 24% ( $P < 0.01$ ) and 27% ( $P < 0.01$ ) lower, respectively (**Figure 5.4**). While differences in  $Q_{\text{ICA}}$  between groups approached statistical significance (main effect,  $P = 0.06$ ), the difference in gCBF between lowlanders and both Sherpa groups is largely attributable to a 40% (Ascent Sherpa,  $P < 0.01$ ) and 44% (Altitude Sherpa,  $P < 0.01$ ) lower VA flow. This is consistent with the largely reduced posterior CBF distribution in both Sherpa groups compared to lowlanders at 5050 m ( $P < 0.05$  for both; **Figure 5.2**). These differences in CBF, in the face of similar  $\text{CaO}_2$  values (**Table 5.4**) lead to a 21% ( $P = 0.02$ ) and 22% ( $P < 0.01$ ) lower  $\text{CDO}_2$  in the Ascent Sherpa and Altitude Sherpa, respectively. Cerebral vascular  $\text{CO}_2$  reactivity was not different between Sherpa and lowlanders ( $5.4 \pm 2.1$  vs.  $5.0 \pm 1.1 \text{ \%} \cdot \text{mmHg}^{-1}$ ;  $P = 0.77$ ) at 5050 m.

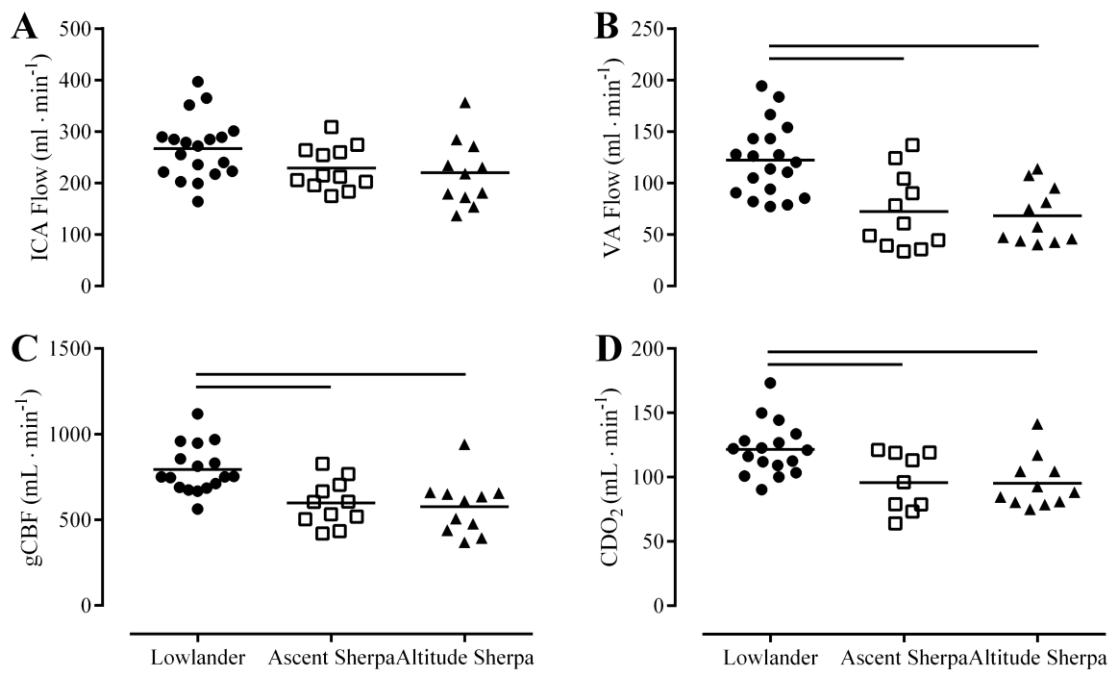


**Figure 5.4. Cerebral blood flow and oxygen delivery in acclimatized lowlanders, sherpa following ascent, and sherpa recruited at altitude.**

In all panels, lowlanders are denoted by the filled circle symbol, Sherpa that took part in the ascent with the open square symbol, and Sherpa who were recruited at altitude by the filled triangle. ICA, internal carotid artery; VA, vertebral artery; gCBF, global cerebral blood flow; CDO<sub>2</sub>, cerebral oxygen delivery. Horizontal bars indicate a significant difference from lowlanders.

**Table 5.4. Comparison between lowlanders, the ascent sherpa, and the altitude sherpa following arrival at 5050m.**

	Lowlander	Ascent Sherpa	Altitude Sherpa	ANOVA
CaO <sub>2</sub> (ml · dl <sup>-1</sup> )	15.66±1.35	15.68±1.35	16.95±2.36	0.102
SaO <sub>2</sub> (%)	78.95±4.94	77.43±6.32	86.73±3.42*†	< <b>0.001</b>
PaO <sub>2</sub> (mmHg)	41.20±4.44	40.58±4.25	41.65±6.23	0.876
PaCO <sub>2</sub> (mmHg)	29.93±1.58	32.06±2.71*	31.88±2.44	<b>0.020</b>
pH	7.46±0.02	7.44±0.02*	7.41±0.02*†	< <b>0.001</b>
HCO <sub>3</sub> <sup>-</sup> (mEq · L <sup>-1</sup> )	21.37±1.57	21.66±2.01	20.26±1.56	0.123
BE <sub>ecf</sub> (mEq · L <sup>-1</sup> )	-2.39±1.93	-2.67±2.17	-4.35±1.69*	<b>0.030</b>
[Hb] (g · dl <sup>-1</sup> )	14.46±0.72	14.81±0.65	15.94±1.03*†	< <b>0.001</b>
HCT (%)	42.78±2.24	43.66±2.17	47.05±3.58*†	< <b>0.001</b>
MAP (mmHg)	99.86±10.22	96.55±5.30	88.87±7.69*	<b>0.006</b>
CVC (ml · min <sup>-1</sup> · mmHg <sup>-1</sup> )	7.99±1.74	6.41±1.64	6.54±1.99	<b>0.047</b>

\*denotes a significant difference from lowlanders; †, denotes a significant difference from the ascent Sherpa group. CaO<sub>2</sub>, arterial oxygen content; SaO<sub>2</sub>, arterial oxyhemoglobin saturation; PaO<sub>2</sub>, partial pressure of arterial oxygen; PaCO<sub>2</sub>, partial pressure of arterial carbon dioxide; HCO<sub>3</sub><sup>-</sup>, bicarbonate ion; BE<sub>ecf</sub>, base excess extracellular fluid; [Hb], hemoglobin concentration; HCT, hematocrit; MAP, mean arterial pressure; CVC, cerebral vascular conductance.

### **5.3 STUDY 3 - DISCUSSION**

The present study examined the novel hypothesis that CBF and CDO<sub>2</sub> would be lower in Sherpa compared to lowlanders during ascent to HA. To address this question, unique comparisons of CBF, CDO<sub>2</sub> and related physiological parameters were made between lowlanders and partially de-acclimatized Sherpa during graded ascent to 5050 m. Further comparisons were made between lowlanders, the Sherpa that had ascended (Ascent Sherpa), and Sherpa that were residing at altitude prior to travel to the Pyramid Laboratory (Altitude Sherpa). The primary findings are: 1) gCBF during ascent to HA is significantly lower in the Sherpa with an approximate 175 mL · min<sup>-1</sup> of the difference in gCBF between lowlanders and Sherpa attributable to factors associated with race; 2) consequently, upon ascent to HA, CDO<sub>2</sub> is higher in lowlanders compared to Sherpa, and higher than both the Ascent and Altitude Sherpa at 5050 m.; and 3) CBF distribution to the posterior circulation

was lower across all altitudes during ascent in Sherpa compared to lowlanders, and lower in both Sherpa groups compared to lowlanders at 5050 m. Collectively, these data indicate that there is a unique role of race in governing differential CBF regulation between lowlanders and Sherpa, irrespective of partial de-acclimatization, implicating long-term (i.e., generational) adaptations in the regulation of  $\text{CDO}_2$ .

### 5.3.1 CEREBRAL BLOOD FLOW AT ALTITUDE: INFLUENCE OF RACE

Our study corroborates recent research demonstrating that Tibetans' possess lower CBF than lowlanders at altitude (Liu *et al.*, 2016) (**Figure 5.1; Table 5.3**). Although not quantified in this latter study (Liu *et al.*, 2016), we extend these findings using a longitudinal design to show that these differences are present despite a similar blood gas profile during ascent between groups. Notably, however, pH was lower, and  $\text{PaCO}_2$  was higher in the Sherpa (typically these two factors would increase gCBF in Sherpa relative to lowlanders – see section “Potential mechanism(s) of reduced cerebral oxygen delivery”). When lowlander CBF was compared to Sherpa that had not recently descended to low altitude, lowlander CBF remained higher; therefore, irrespective of recent time at altitude, Sherpa possess lower CBF than lowlanders. Yet, the recent study by Lui *et al.*, reported similar CBF at sea level between Tibetans and Han-Chinese (Liu *et al.*, 2016). Our group has also recently demonstrated that gCBF is lower in Sherpa children compared to lowlander children, which given the consistently lower CBF across the lifespan, suggests developmental differences across a single lifespan do not account for our observation of lower CBF in Sherpa at HA compared to lowlanders (Flück *et al.*, 2017). Further research, using a longitudinal study design where Tibetans/Sherpa born at sea-level ascend to altitude is necessary to explicitly determine the influence of Tibetan genetic adaptation on CBF regulation independent of previous hypoxic exposure. Overall, the lower gCBF in Sherpa during ascent, and in both Sherpa groups at 5050 m, led to a lower  $\text{CDO}_2$  in Sherpa compared to lowlanders at every HA time point.

Previous studies have indicated a greater preservation of VA flow (i.e. posterior oxygen delivery) relative to  $Q_{\text{ICA}}$  (i.e. anterior oxygen delivery) in both HA natives (Liu *et al.*, 2016) and lowlanders rapidly ascending to 5260 m (Subudhi *et al.*, 2014b). In other words, reactivity of the posterior circulation to altitude appears greater than the anterior circulation, with posterior oxygen delivery not changing from normoxic values. These findings are

further corroborated by the present study (**Figure 5.1**) where posterior CBF distribution did not decrease during ascent in lowlanders or Sherpa. However, the Ascent and Altitude Sherpa demonstrated a lower percentage of gCBF distributed to the posterior circulation across all altitudes when compared to the lowlanders (**Figure 5.2**). At 5050 m lower posterior CBF distribution appeared to represent the majority of the lower gCBF in both Sherpa groups compared to lowlanders.

### 5.3.2 POTENTIAL MECHANISM(S) OF REDUCED CEREBRAL OXYGEN DELIVERY

Several factors that are implicated in the integrative regulation of CBF should theoretically be cause for a *higher* – rather than the observed *lower* - CBF in Sherpa compared to lowlanders in the present study. For example, a lower pH and higher PaCO<sub>2</sub> in addition to a higher MAP in Sherpa compared to lowlanders (**Table 5.2**) should all contribute to a higher CBF (Kety & Schmidt, 1948c; Lucas *et al.*, 2010). The similar CaO<sub>2</sub>, [Hb], and blood viscosity throughout ascent would not contribute to the lower CBF in Sherpa in the face of higher MAP and PaCO<sub>2</sub>. That race came out as an independent predictor of gCBF at altitude (~172 mL · min<sup>-1</sup>; **Table 5.3**; ~25% of resting lowlander CBF) further affirms that the difference in CBF between groups cannot be explained by our measured variables. When considering cerebrovascular responsiveness to the aforementioned inputs (e.g. CaO<sub>2</sub>, PaCO<sub>2</sub>, MAP, etc.) there remains no apparent explanation of reduced CBF and CDO<sub>2</sub> in Sherpa during ascent. For example, cerebrovascular CO<sub>2</sub> reactivity is not different between lowlander and Sherpa at altitude during ascent at 4371 m (Jansen *et al.*, 1999) and following acclimatization to 5050 m (**Figure 5.5**). Further, we have demonstrated previously that the cerebrovascular response to driven changes in MAP (i.e. cerebral autoregulation) does not differ between Sherpa and partially acclimatized lowlanders (Smirl *et al.*, 2014), although this has not been consistently demonstrated during infusion of the vasoactive drug phenylephrine (Jansen *et al.*, 2014). Notably, however, infusion of a vasoactive drug likely invalidates TCD as an index of CBF as used in the aforementioned study by Jansen and coworkers (Hoiland & Ainslie, 2016a). Endothelial function, as indexed in the peripheral vasculature, also appears similar between Sherpa and lowlanders at HA (Lewis *et al.*, 2014a) eliminating another potential explanation for reduced CDO<sub>2</sub> in the Sherpa during ascent.

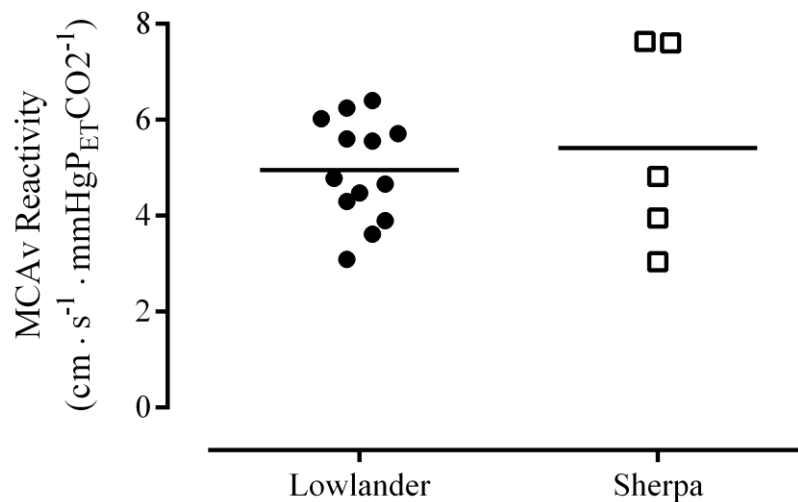


**Figure 5.5. Lowlander and sherpa cerebrovascular reactivity to carbon dioxide.**

The presented cerebrovascular reactivity data are the relative reactivity (i.e. %change) values for lowlanders and Sherpa collected at 5050 m in 2008. The hyperoxic rebreathe technique was used for these tests [Previously described: (Fan *et al.*, 2010*b*)]. There is no difference in CO<sub>2</sub> reactivity between Sherpa and acclimatized lowlanders as determined by the non-parametric Mann Whitney U Test (P=0.77).

While cerebral metabolism does not differ between Sherpa and lowlanders at sea level (Hochachka *et al.*, 1996), it has not been compared between groups following acclimatization or prolonged stay at altitude and may represent the most tenable mechanism for reduced CDO<sub>2</sub>. In keeping, CDO<sub>2</sub> did not differ between groups at 1400 m where metabolism is apparently not different after a similar duration of de-acclimatization (Hochachka *et al.*, 1996); however, upon hypoxic exposure (3400 m and above) CDO<sub>2</sub> was lower in Sherpa, which, if coupled to cerebral metabolic demand (as it is at sea-level) (Ainslie *et al.*, 2014), is perhaps related to some form of hypoxia induced hypometabolism. This may represent a genetic/hypoxic interaction, whereby adaptive phenotypes only present following exposure to hypoxia (i.e., genotype-phenotype interaction). Such a hypometabolic adaptation is key for the purposes of oxygen conservation in various vertebrates such as the crucian carp and some fresh water turtles that possess an ability to reduce cerebral metabolism among a number of other adaptive physiological processes to tolerate hypoxic and anoxic environments (Nilsson & Lutz, 2004). Further, greater mitochondrial efficiency has recently been demonstrated in skeletal muscle of Sherpa compared to lowlanders (Horscroft *et al.*, 2017), which if such a phenomenon is present in

cerebral tissue may be related to the differential flow regulation observed in the present study. However, if the difference in  $\text{CDO}_2$  is unrelated to metabolic differences between lowlander and Sherpa (i.e., no difference in cerebral metabolism), perhaps there is a role of elevated angiogenesis and capillary density (Xu & Lamanna, 2006) in Sherpa that allows for a greater extraction of oxygen. If the case, this would necessitate less bulk flow to maintain metabolic homeostasis as is seen in skeletal muscle of varying capillary density (Gayeski *et al.*, 1988); however, one would expect this to be reflected by a higher (not lower as we observed) cerebrovascular conductance in the Sherpa group. Although these mechanism(s) remain to be established, it would seem reasonable to suggest that the observed reductions in  $\text{CDO}_2$  in the Sherpa are adaptive rather than maladaptive (see section “Study 3 - Summary”).

### 5.3.3 METHODOLOGICAL CONSIDERATIONS

This study demonstrated that in lowlanders ascending to altitude, CBF does not increase until approximately 5050 m (**Figure 5.1**). This CBF pattern is distinctly different from that demonstrated in individuals performing a similar ascent profile with concurrent acetazolamide prescription for AMS prophylaxis (Willie *et al.*, 2014a). However, given the maintenance of  $\text{CDO}_2$  despite unaltered CBF, and the disconnect between CBF at altitude and AMS severity (Ainslie & Subudhi, 2014), there appears no likely maladaptive consequences of the present CBF response to altitude. This is also likely the case for Sherpa, who despite reduced  $\text{CDO}_2$  present with no AMS symptoms.

Following >2 years of de-acclimatization, Tibetans possess a reduced [Hb] compared to lowlanders at low altitude (Liu *et al.*, 2016); however, in the present study Sherpa [Hb] was elevated above lowlanders following 5-15 days of de-acclimatization in Kathmandu (**Table 5.2**). In lowlanders returning from altitude, [Hb] has been shown to return to baseline values within one to two weeks (Ryan *et al.*, 2014; Siebenmann *et al.*, 2015) although this did not appear to be the case for the Sherpa population we tested. There was no correlation between the variability in duration (days) of de-acclimatization with [Hb] in Kathmandu ( $r < 0.01$ ;  $P = 0.87$ ). Whether a greater extent of chronic hypoxia in the Sherpa prolongs the presence of elevated [Hb] (or Hb mass) is currently unknown. Nevertheless, upon reaching 3400 m, there were no recorded hematological differences between groups. This indicates that

differences in CBF and CDO<sub>2</sub> throughout ascent cannot be attributed to [Hb], as it was similar between groups.

Typically, Sherpa are of smaller weight and stature than that of western counterparts (as in the present study), which may be cause to scale CBF to body size. However, there appears to be no relationship between stature and brain weight (Heymsfield *et al.*, 2009), indicating that scaling to body size may not be appropriate. Indeed, cerebral metabolism is not different between Sherpa and lowlanders near sea-level (Hochachka *et al.*, 1996), which may be indicative of similar brain mass. Therefore, if there is indeed a lower cerebral metabolism in Sherpa at altitude, as speculated, this is more likely due to a signaled down-regulation of metabolic processes, versus that of a size principle (i.e., lower brain mass = lower cerebral metabolism).

#### **5.4 STUDY 3 - SUMMARY**

Since their early involvement in the attempted conquests of Mt. Everest in the early 1920's, HA native Sherpa have been recognized for their exceptional performance at altitude and tolerance to hypoxia. In contrast to lowland native mountaineers who display deleterious consequences of ascent above 8000 m such as cortical atrophy and/or hyper-intensities (Garrido *et al.*, 1993; Paola *et al.*, 2008), Sherpa are unaffected in this regard (Garrido *et al.*, 1996), indicating the presence of functional adaptations that proffer protection to the brain. Therefore, it stands to reason that the reduced CBF observed herein represents a positive adaptation. While lower CBF and CDO<sub>2</sub> may indicate a hypometabolic adaptation in Sherpa, as speculated above, the potential implications of reduced CBF extend beyond that of metabolic homeostasis. For example, reduced CBF may predispose Sherpa to a lower risk of vasogenic edema and/or intracranial hypertension (Lawley *et al.*, 2015; Sagoo *et al.*, 2016) than lowlanders (Schoonman *et al.*, 2008). This may be of particular importance at extreme altitudes (e.g. ≥8000 m) where lowlander CBF is reportedly 200% greater than at sea-level (Wilson *et al.*, 2011). Overall, it remains to be determined why Sherpa possess a lower CDO<sub>2</sub> at a given altitude than lowlanders, yet it seems most likely such a difference represents a positive physiological adaptation.

## **6 OXYGEN THERAPY IMPROVES CEREBRAL OXYGEN DELIVERY AND NEUROVASCULAR FUNCTION IN HYPOXEMIC CHRONIC OBSTRUCTIVE PULMONARY DISEASE PATIENTS**

Some patients with moderate-to-very severe COPD endure a state of chronic hypoxemia - a consequence of sub optimal gas exchange. Literature on cerebral vascular regulation in COPD is sparse (Beaudin *et al.*, 2017), despite an elevated risk of cognitive impairment (Thakur *et al.*, 2010), dementia (Liao *et al.*, 2015) and ischemic stroke (Feary *et al.*, 2010); this risk increases in proportion to disease severity (Portegies *et al.*, 2016). Further, greater brain atrophy has been observed in COPD patients compared to age and sex matched controls (Zhang *et al.*, 2013). Physiological links between COPD, cerebrovascular dysfunction and risk of the aforementioned diseases have yet to be established.

In healthy individuals, a reduction in  $CaO_2$  leads to an increase in CBF due to cerebral vasodilator mechanisms (Kety & Schmidt, 1948c; Hoiland *et al.*, 2016a), which may be continuously active in hypoxemic COPD patients. Indeed, CBF is elevated in COPD commensurate to the level of hypoxemia (Albayrak *et al.*, 2006); however, whether this elevated CBF is great enough in magnitude to maintain  $CDO_2$  is unknown. If patients are hypoxemic, low flow oxygen (e.g.  $3L \cdot min^{-1}$ ) is typically prescribed (NOTTG, 1980; MRCWP, 1981) with the goal of increasing  $PaO_2$  to  $>60mmHg$  while avoiding hyperoxia (Qaseem *et al.*, 2011). This therapy reduces mortality (NOTTG, 1980; MRCWP, 1981) and the risk of cognitive impairment (Thakur *et al.*, 2010). Given the potential link between chronic cerebral hypo-perfusion (i.e. vascular insufficiency – reduced  $CDO_2$ ) and the pathogenesis of neurovascular injury and dementia (Iadecola, 2010), understanding the influence of oxygen therapy on CBF,  $CDO_2$  and neurovascular function in COPD is of immediate importance.

We examined two primary hypotheses: 1) that CBF would be reduced in COPD patients following  $O_2$  normalization leading to unchanged  $CDO_2$  despite elevated  $CaO_2$ , and 2) in the face of unaltered  $CDO_2$  no change in neurovascular function would be observed.

## **6.1 STUDY 4 - METHODS**

The study was approved by the institutional Ethics Committee (University of Split, Croatia; Reg. no. 2181-198-03-03-13-0017) and the University of British Columbia Clinical Research Ethics Board (H16-01028). Written informed consent was obtained from all participants and all experimental procedures conformed to the standards set by the *Declaration of Helsinki*, except for registration in a database.

At the Split Clinical Hospital Centre Pulmonary Diseases Clinic (Split, Croatia), 342 COPD patients were screened for eligibility during hospital stays or ambulatory visits. Diagnosis of COPD was classified according to the criteria of the Global Initiative for Obstructive Lung Disease (GOLD) (Vestbo *et al.*, 2013). The primary inclusion criterion was chronic hypoxemia defined as arterial oxygen saturation of  $\leq 93\%$  objectively confirmed on at least two different occasions during the six previous months (n=84). The related arterial blood gas values from these measurements are reported in **Table 6.1**. Patients who had suffered from an acute exacerbation, active respiratory infection or infection of other localization within six weeks prior to the visit were excluded (n=32). Likewise, patients who had a relevant coexisting condition such as interstitial lung disease, cancer, renal failure, thromboembolic disease or major cardiovascular event during the previous year were also excluded (n=25). Those patients who could not provide informed consent or comply with the study protocol due to a mental or physical condition were also excluded (n=10). One patient did not participate due to scheduling conflicts. Details on the remaining 16 patients included in the present study are presented in **Table 6.1**.

**Table 6.1. Chronic obstructive pulmonary disease patient characteristics.**

	COPD (n=16)
Age (years), mean (SD)	69.4 (8.7)
Sex (male), No. (%)	11 (68.8)
Height (cm), mean (SD)	171.8 (6.5)
Weight (kg), mean (SD)	75.6 (14.2)
Body mass index (kg/m <sup>2</sup> ), mean (SD)	25.6 (4.6)
<b>Cigarette smoking status</b>	
Current, No. (%)	6 (37.5)
Former, No. (%)	8 (50.0)
Non-smoker, No. (%)	2 (12.5)
Smoking pack-years, mean (SD)	50.1 (44.6)
<b>Co-morbidities</b>	
Hypertension, No. (%)	9 (56.3)
Diabetes mellitus, No. (%)	3 (18.8)
Coronary artery disease, No. (%)	1 (6.3)
Peripheral artery disease, No. (%)	2 (12.5)
<b>Medication use</b>	
β-blockers, No. (%)	4 (25.0)
Calcium channel blockers, No. (%)	3 (18.8)
ACE inhibitors or angiotensin antagonists, No. (%)	8 (50.0)
Diuretics, No. (%)	12 (75.0)
Statins, No. (%)	1 (6.3)
Acetylsalicylic acid, No. (%)	2 (12.5)
Inhaled corticosteroids, No. (%)	14 (87.5)
Systemic corticosteroids, No. (%)	1 (6.3)
Short-acting β-agonists, No. (%)	4 (25.0)
Long-acting β-agonists, No. (%)	16 (100.0)
Short-acting anticholinergics, No. (%)	4 (25.0)
Long-acting anticholinergics, No. (%)	11 (68.8)
Theophylline, No. (%)	8 (50.0)
Roflumilast, No. (%)	1 (6.3)
Methylidigoxine, No. (%)	1 (6.3)
<b>Cardiorespiratory Variables</b>	
Systolic blood pressure (mm Hg), mean (SD)	132 (25)
Diastolic blood pressure (mm Hg), mean (SD)	77 (13)
FEV1 (% of predicted), mean (SD)	32.9 (12.7)
FVC (% of predicted), mean (SD)	55.1 (15.2)
FEV1/FVC ratio (%), mean (SD)	44.9 (9.6)
SaO <sub>2</sub> (%), mean (SD)	88.8 (4.0)
PaO <sub>2</sub> (kPa), mean (SD)	7.5 (1.1)
PaCO <sub>2</sub> (kPa), mean (SD)	6.2 (0.9)
pH, mean (SD)	7.43 (0.03)
[Hb] (g/dL) mean (SD)	13.9 (1.4)

	COPD (n=16)
Home oxygen therapy, No. (%)	12 (75.0)
O <sub>2</sub> washout period (h), mean (SD)	6.5(5.8)
Severity of airflow limitation (GOLD)	
Stage 1, No. (%)	0 (0.0)
Stage 2, No. (%)	2 (12.5)
Stage 3, No. (%)	5 (31.3)
Stage 4, No. (%)	9 (56.3)
Dyspnea grade (mMRC), mean (SD)	3.2 (0.5)
Acute exacerbations $\geq 2$ per year, No. (%)	13 (81.3)
Combined COPD assessment	
Group A, No. (%)	0 (0.0)
Group B, No. (%)	1 (6.3)
Group C, No. (%)	0 (0.0)
Group D, No. (%)	15 (93.8)

ACE, angiotensin converting enzyme; FEV<sub>1</sub>, forced expiratory volume in one second; FVC, forced vital capacity; SaO<sub>2</sub>, arterial oxyhemoglobin saturation; PaO<sub>2</sub>, partial pressure of arterial oxygen; PaCO<sub>2</sub>, partial pressure of arterial carbon dioxide; [Hb], hemoglobin concentration.

### 6.1.1 STUDY 4 - EXPERIMENTAL PROTOCOL

Patients arrived at the laboratory having abstained from exercise, alcohol and caffeine for a minimum of 12 hours. Additionally, the patients had fasted for four hours, and current smokers had their last cigarette a minimum of eight hours prior to testing.

All cardiorespiratory and cerebrovascular variables (HR, MAP, SpO<sub>2</sub>, MCA<sub>v</sub>, PCA<sub>v</sub>, Q<sub>ICA</sub> and Q<sub>VA</sub>) were measured as previously described study 1 (see sections “Cardiorespiratory measures” and “Cerebrovascular measures”).

Following at least 20 minutes of supine rest, resting volumetric CBF was measured alongside the other cardiovascular variables. Reliable images of the ICA were collected in all patients; however, due to excessive neck movement from respiration (e.g. sternocleidomastoid contraction), reliable VA images were only captured in seven patients. Therefore, the resulting sample size for VA and gCBF is based on n=7.

After the resting measures, the NVC response was assessed. For this test, participants performed five cycles of 30-seconds eyes open followed by 30-seconds eyes closed while PCA<sub>v</sub> and MCA<sub>v</sub> were recorded. During the 30-seconds of eyes open patients read standardized material. This test was conducted in accordance to published guidelines (Phillips *et al.*, 2016). The hemodynamic response to the five cycles was averaged and used for analysis.

Following initial resting measurements and NVC, low flow O<sub>2</sub> was administered via nasal cannula to normalize SpO<sub>2</sub> to  $\geq 96\%$  for 20 minutes, following which time resting measurements and NVC were repeated while O<sub>2</sub> supplementation was continued. Therefore, measurements of NVC and gCBF occurring  $26.5 \pm 3$  and  $30.0 \pm 5.5$  minutes following onset of O<sub>2</sub> normalization, respectively. Two subjects withdrew for reasons unstated, rendering the final maximum sample size as n=14 for pre- and post- O<sub>2</sub> normalization data.

#### 6.1.2 STUDY 4 - CALCULATIONS

To provide further insight into the role of oxygen therapy on cerebral vascular function we have estimated CDO<sub>2</sub> by combining our pulse-oximetry data and gCBF according to **Equation 3.3** and **Equation 3.4**. In the COPD patients [Hb] was taken from two separate arterial blood gases over 6-months prior to testing (i.e. same values as in **Table 6.1**).

#### 6.1.3 STUDY 4 - STATISTICAL ANALYSES

Sample size was determined *a priori* based upon similar studies (Patterson *et al.*, 1952; Albayrak *et al.*, 2006) and sample size calculations (G\*Power, V3.1). It was determined that with a power of 0.8, 15 subjects would be required to detect a  $100 \text{ mL} \cdot \text{min}^{-1}$  change in gCBF (e.g., 13% change from typical value of  $750 \text{ mL} \cdot \text{min}^{-1}$ ) – or  $25 \text{ mL} \cdot \text{min}^{-1}$  change in unilateral Q<sub>ICA</sub>. Resting variables pre- and post- O<sub>2</sub> normalization, as well as NVC parameters were compared using two-tailed paired t-tests. When significant main effects were determined Bonferroni post hoc tests were ran, and corrected for multiple comparisons. Effect size was calculated as the mean difference divided by the standard deviation of the difference. Statistical analyses were performed in the Statistical Package for the Social Sciences (V24) with significance determined *a priori* as  $P < 0.05$ .

## 6.2 STUDY 4 - RESULTS

In total, 14 participants completed both pre and post O<sub>2</sub> normalization testing. Resting variables are presented in **Table 6.2**. As expected, SpO<sub>2</sub> increased following O<sub>2</sub> normalization from 91.0±3.3 to 97.4±3.0 % (P<0.01). There was no change in internal carotid artery flow (Q<sub>ICA</sub>), vertebral artery flow (Q<sub>VA</sub>), gCBF (**Figure 6.1**), MCA<sub>V</sub>, PCA<sub>V</sub>, or MAP following O<sub>2</sub> normalization; however, there was a reduction in HR (P=0.03). Maintained gCBF in combination with elevated SpO<sub>2</sub> resulted in improved *e*CDO<sub>2</sub> in the COPD patients (98.1±25.7 vs. 108.7±28.4 mL · dL<sup>-1</sup>; P=0.02). The sample sizes for each comparison are noted in **Table 6.2**.

**Table 6.2. Cerebral and cardiovascular variables pre- and post-oxygen normalization in chronic obstructive pulmonary disease patients.**

	Room air	O <sub>2</sub> normalization	n	P-Value	Effect size
Q <sub>ICA</sub> (mL · min <sup>-1</sup> )	231.2±59.0	231.6±68.0	14	0.97	0.01
ICA <sub>v</sub> (cm · sec <sup>-1</sup> )	29.72±7.25	30.62±8.06	14	0.27	0.31
ICA diameter (mm)	5.81±0.98	5.73±1.05	14	0.13	0.43
Q <sub>VA</sub> (mL · min <sup>-1</sup> )	61.4±35.1	70.2±49.3	7	0.32	0.41
VA <sub>v</sub> (cm · sec <sup>-1</sup> )	18.32±5.81	18.72±5.66	7	0.55	0.24
VA diameter (mm)	3.82±0.85	3.73±0.92	7	0.49	0.28
gCBF (mL · min <sup>-1</sup> )	593.0±162.8	590.1±138.5	7	0.91	0.05
MCA <sub>v</sub> (cm · sec <sup>-1</sup> )	51.4±10.4	51.5±5.6	9	0.96	0.24
PCA <sub>v</sub> (cm · sec <sup>-1</sup> )	36.4±11.1	36.5±12.8	12	0.93	0.03
MAP (mmHg)	90.2±17.3	96.3±18.4	14	0.14	0.42
HR (beats · min <sup>-1</sup> )	81.5±16.0	77.7±13.0*	14	<b>0.03</b>	0.65
SV (mL)	81.5±39.1	85.5±50.8	14	0.63	0.13
CO (L · min <sup>-1</sup> )	6.4±2.6	6.4±3.3	14	0.99	0.00
SaO <sub>2</sub> (%)	91.0±3.3	97.4±3.0*	14	<b>&lt;0.01</b>	1.41
eCaO <sub>2</sub> (mL · dL <sup>-1</sup> )	17.2±2.0	18.4±1.9*	14	<b>&lt;0.01</b>	1.39
eCDO <sub>2</sub> (mL · min <sup>-1</sup> )	98.1±25.7	108.7±28.4	7	<b>0.02</b>	1.17

Data are presented as mean ± standard deviation. \* denotes a significant change from room air, P<0.05.

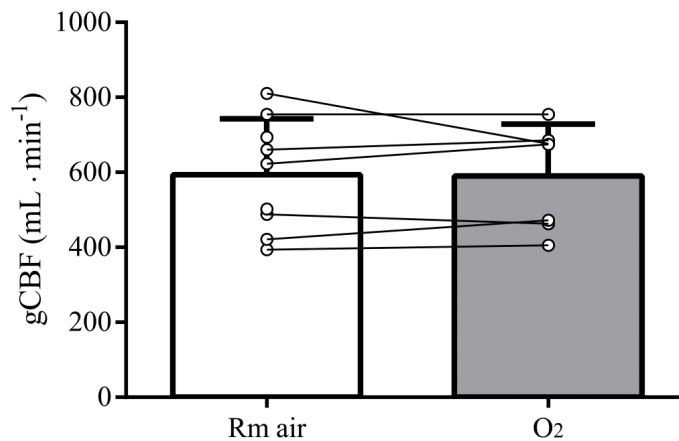


**Figure 6.1. Cerebral blood flow prior to and following oxygen normalization in chronic obstructive pulmonary disease patients.**

Individual data for the COPD patients are depicted with the open circle symbol ( $\circ$ ) with the mean and standard deviation superimposed as bar graphs (pre: white bar, post: grey bar). The resulting sample sizes were  $n=7$  for the COPD. There was no change in global cerebral blood flow (gCBF) following  $O_2$  normalization. Reproduced from (Hoiland *et al.*, 2018b) with permission.

Results from the neurovascular coupling trials ( $n=11$ ) pre and post  $O_2$  normalization are presented in **Table 6.3** and **Figure 6.2**. Notably, the peak relative and absolute increases in PCAv were unaltered following  $O_2$  normalization (**Table 6.3** & **Figure 6.2**). Despite this the peak percent increase in PCA cerebrovascular conductance (CVC) upon transition from eyes closed to eyes open increased by  $\sim 40\%$  (from  $20.4 \pm 9.9$  to  $28.0 \pm 10.4\%$ ) following  $O_2$  normalization ( $P=0.04$ ). Accordingly, the peak drop in PCA cerebrovascular resistance (CVR) was also increased from  $-16.7 \pm 7.3$  to  $-21.4 \pm 6.6\%$  ( $P=0.04$ ) following  $O_2$  normalization. We also observed a significant improvement in the magnitude of the peak absolute reduction in CVR ( $-0.46 \pm 0.25$  vs.  $-0.64 \pm 0.27$ ;  $P < 0.01$ ). The lack of change in PCAv despite the apparent influence on changes in vasomotor tone (i.e. CVC & CVR) following can be attributed to a differing MAP response during NVC prior to and during  $O_2$  normalization (**Figure 6.3**). It can be seen by the mean trace (**Figure 6.3A**) and the peak (**Figure 6.3B**) and average (**Figure 6.3C**) change in MAP during NVC that the greater average and peak increase in MAP during room air breathing facilitated the increase in PCAv during NVC. Therefore, the same magnitude of PCAv response (**Figure 6.2A, B &**

C) despite a lower driving force (i.e. MAP) resulted in the larger changes in vasomotor tone during O<sub>2</sub> normalization (**Figure 6.2**, panels D-I).

**Table 6.3. Peak changes in neurovascular coupling tests.**

	Absolute data				Relative data			
	Room air	O <sub>2</sub> normalization	P-Value	Effect size	Room air	O <sub>2</sub> normalization	P-Value	Effect Size
$\Delta$ PCAv (cm · s <sup>-1</sup> )	7.81±4.57	7.87±4.31	0.93	0.03	24.2±12.3	23.1±12.0	0.41	0.26
Time to peak (s)	13.29±4.73	16.09±4.60	0.10	0.54				
$\Delta$ MAP (mmHg)	8.2±3.5	5.5±2.7	<b>0.01</b>	0.91	10.1±4.8	6.0±3.2	<b>&lt;0.01</b>	1.20
Time to peak (s)	12.8±6.5	9.4±8.0	0.23	0.39				
$\Delta$ PCAv CVC (cm · s <sup>-1</sup> · mmHg <sup>-1</sup> )	0.08±0.05	0.11±0.06	0.27	0.35	20.4±9.9	28.0±10.4	<b>0.04</b>	0.71
Time to peak (s)	9.25±6.28	12.93±5.05	0.09	0.56				
$\Delta$ PCAv CVR (mmHg · cm <sup>-1</sup> · s <sup>-1</sup> )	-0.46±0.25	-0.64±0.27	<b>&lt;0.01</b>	1.38	-16.7±7.3	-21.4±6.6	<b>0.04</b>	0.69
Time to peak (s)	9.8±6.2	12.91±5.02	0.17	0.44				

N=11. PCAv, posterior cerebral artery blood velocity; CVC, cerebrovascular conductance; CVR, cerebrovascular resistance.

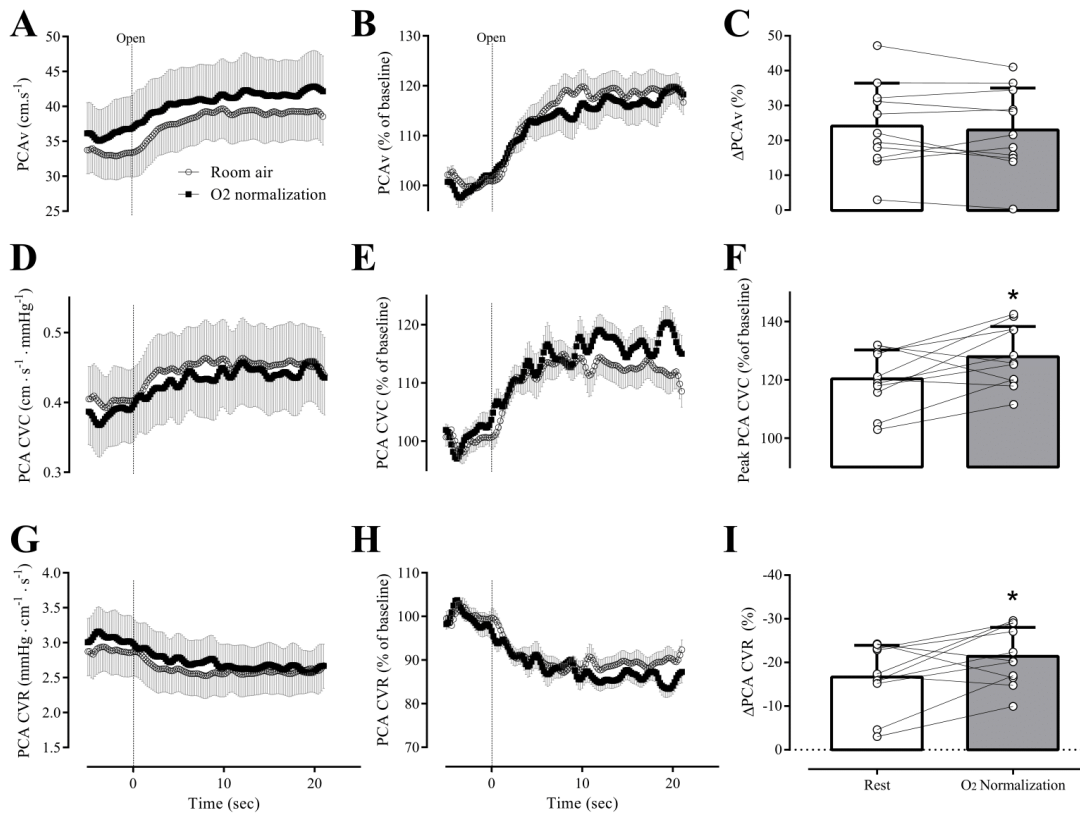


**Figure 6.2. Neurovascular coupling responses prior to and following oxygen normalization.**

For panels A, B, D, E, G & H pre oxygen normalization data are represented by the open circles ( $\circ$ ), while the post  $O_2$  normalization data are represented by the closed square symbol ( $\blacksquare$ ) with error bars representing the standard error. Panel A depicts the absolute PCAv response to NVC, while Panel B depicts the relative (%) change in PCAv during NVC. Panel C highlights the individual %peak changes in PCAv during NVC prior to and following  $O_2$  normalization – there was no significant difference ( $P=0.41$ ; Effect size=0.26). Panel D depicts the absolute PCA cerebrovascular conductance (CVC) response during NVC, while Panel E depicts the relative (%) change in PCA CVC during NVC. Panel F highlights the individual %peak changes in PCA CVC during NVC prior to and following  $O_2$  normalization – the CVC response was improved during  $O_2$  normalization ( $P=0.04$ ; Effect size=0.71). Panel G depicts the absolute PCA cerebrovascular resistance (CVR) response during NVC, while Panel H depicts the relative (%) change in PCA CVR during NVC. Panel I highlights the %peak changes in PCA CVR during NVC prior to and following  $O_2$  normalization - the CVR response was improved during  $O_2$  normalization ( $P=0.04$ ; Effect size=0.69). \* denotes  $P<0.05$ .  $N=11$  for NVC comparisons. Reproduced from (Hoiland *et al.*, 2018b) with permission.

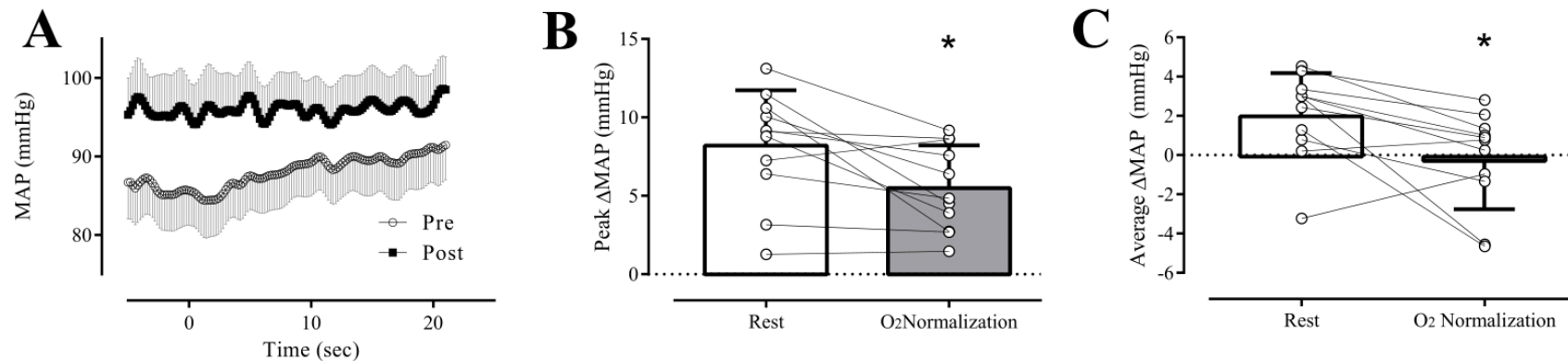


**Figure 6.3. Mean arterial pressure during neurovascular coupling**

In Panel A pre oxygen normalization data are represented by the open circles ( $\circ$ ), while the post O<sub>2</sub> normalization data are represented by the closed square symbol ( $\blacksquare$ ) with error bars representing the standard error. Panel B highlights the individual data for the peak absolute (mmHg) change in mean arterial pressure (MAP) during NVC – the MAP response was significantly lower during O<sub>2</sub> normalization ( $P=0.01$ ; Effect size=0.91). Panel C highlights the individual data for the average absolute (mmHg) change in mean arterial pressure (MAP) during NVC (analogous to area under the curve as time is matched between trials) – the MAP response was significantly lower during O<sub>2</sub> normalization ( $P=0.02$ ; Effect size=0.84). Reproduced from (Hoiland *et al.*, 2018b) with permission.

### 6.3 STUDY 4 - DISCUSSION

The primary novel findings of the current study are that, contrary to our hypothesis, acute normalization of SpO<sub>2</sub> with low flow supplemental O<sub>2</sub> does not alter resting CBF in COPD patients; however, O<sub>2</sub> normalization improves both CDO<sub>2</sub> and NVC (a functional marker of cerebrovascular health). Collectively our results indicate that O<sub>2</sub> therapy is related to an improvement in neurovascular function in COPD, potentially related to improved CDO<sub>2</sub>. Further, our results indicate a cerebrovascular insensitivity to normalization of SpO<sub>2</sub> in patients with COPD; however, this insensitivity of CBF to acute increases in SpO<sub>2</sub> appears to possess a positive effect, as increased CaO<sub>2</sub> without a reduction in gCBF is responsible for the improved CDO<sub>2</sub> in COPD.

There is a paucity of experimental studies examining how altered resting arterial blood gases effect CBF in COPD patients (Beaudin *et al.*, 2017). Herein we have provided support for the notion that O<sub>2</sub> normalization does not affect CBF in moderate-to-very severe COPD patients. While we are aware our gCBF measures are limited in sample size (n=7), we did collect Q<sub>ICA</sub> and intracranial velocity data in a larger percentage of our subjects (n=14 for Q<sub>ICA</sub>) and these data reinforce our gCBF findings of no change with O<sub>2</sub> normalization. In comparison, the first study to investigate the influence of oxygen on CBF in COPD patients was in 1952, where investigators administered 85-100% oxygen to hypoxemic emphysema patients for 20-minutes increasing SaO<sub>2</sub> from 68 to 93% (Patterson *et al.*, 1952). While one would expect removal of a hypoxic stimulus to reduce CBF secondary to disengaging hypoxic cerebral vasodilation, the opposite effect was observed - CBF was elevated by ~14% (Patterson *et al.*, 1952). However, this elevation in CBF was likely due to the 12 mmHg increase in the partial pressure of carbon dioxide that occurred during O<sub>2</sub> breathing (presumably as a result of hypoventilation). More recently, a transcranial Doppler study by Cannizzaro and colleagues observed no influence of O<sub>2</sub> normalization on intra-cranial cerebral blood velocity in hypercapnic COPD patients (Cannizzaro *et al.*, 1997). These latter findings may be due to: 1) transcranial Doppler ultrasound is limited in its capacity to assess changes in volumetric CBF due to exclusively quantifying blood velocity (Ainslie & Hoiland, 2014; Hoiland & Ainslie, 2016a); 2) the hypercapnic vasodilation typically associated with the high PaCO<sub>2</sub> observed in the patients (mean: 64.7mmHg) may have overridden any influence of disengaging hypoxic cerebral vasodilation to hypoxia; or 3) there is no influence of O<sub>2</sub> normalization on CBF in COPD

patients (i.e. a lack of O<sub>2</sub> sensitivity). Our study supports the notion that O<sub>2</sub> normalization does not affect CBF in moderate to very severe COPD patients.

Our data in COPD patients are at odds with those previously collected in healthy individuals whereby a reduction in gCBF is observed following O<sub>2</sub> normalization 1 week after arrival to 5050 m (Willie *et al.*, 2015a). Indeed, the prototypical response to withdrawal of a hypoxic stimulus is a reduction in CBF. This indicates that the lack of responsiveness to O<sub>2</sub> normalization in COPD is not representative of normal cerebrovascular function. To judiciously interpret this notion, it is important to consider that differences between healthy individuals and COPD patients to O<sub>2</sub> normalization may be the result of differences in systemic inflammation, oxidative stress, age, or medications and their potential influences in vascular control (Hoffman *et al.*, 1984b; Barnes, 2014; Austin *et al.*, 2016). Importantly, this abnormal response (i.e. lack of response) in COPD patients to O<sub>2</sub> normalization underlies the primary finding of unchanged CBF with concurrently improved CDO<sub>2</sub> and NVC following O<sub>2</sub> normalization in COPD. Of relevance to the experimental stimulus, previous data providing similar O<sub>2</sub> supplementation have shown an increase in PaO<sub>2</sub> without a concurrent change in PaCO<sub>2</sub> (van Helvoort *et al.*, 2006) in COPD patients indicating the lack of change of gCBF in our COPD patients is unlikely due to altered PaCO<sub>2</sub> but related to vascular changes that may be a result of their disease and/or medications. However, while it cannot be ignored that the physiological consequences of O<sub>2</sub> normalization depend to an extent on whether the stimulus is poikilocapnic or isocapnic, our current experimental design reflects the stimulus associated with home O<sub>2</sub> therapy.

A recently conducted clinical trial (LTOTTR, 2017) has called into question the efficacy of long-term oxygen therapy on reducing mortality in COPD patients although previous landmark trials have displayed a reduction in mortality with long-term oxygen therapy (NOTTG, 1980; MRCWP, 1981). Differences in study patients notwithstanding, this important question arises: Are there other potential benefits of long-term oxygen therapy worth considering? For example, there is an increased risk of stroke, dementia, and mild cognitive impairment in patients with COPD [reviewed in: (Lahousse *et al.*, 2015)]. However, the physiological pathways linking COPD to deteriorated cerebral vascular function and increased risk have yet to be disentangled. While cerebrovascular insufficiency is a contributory factor to coinciding cerebral vascular dysfunction and neurodegeneration (Iadecola, 2010), O<sub>2</sub> therapy reduces the

risk of cognitive impairment in COPD patients (Thakur *et al.*, 2010). Thus, it stands to reason that a mechanism for this is an improvement in CDO<sub>2</sub>. Indeed, the observed improvement in NVC coincided with improved CDO<sub>2</sub> and may represent a physiological link between long-term O<sub>2</sub> therapy and the reduced risk for dementia. As CDO<sub>2</sub> is the product of CaO<sub>2</sub> and CBF, an increase in SaO<sub>2</sub> will improve CDO<sub>2</sub> if the consequent increase in CaO<sub>2</sub> is not outweighed by disengagement of hypoxic cerebral vasodilation and a reduction in CBF. The lack of sensitivity to O<sub>2</sub> normalization observed in our COPD patients contributed to the increase in CDO<sub>2</sub> with low flow supplementation O<sub>2</sub> and may be fortuitously beneficial in the context of low O<sub>2</sub> therapy and cerebrovascular function.

#### **6.4 STUDY 4 - SUMMARY**

Although low flow supplemental O<sub>2</sub> does not alter volumetric gCBF in COPD patients, the increased SpO<sub>2</sub> results in improved CDO<sub>2</sub> and neurovascular function. This improvement in CDO<sub>2</sub> and neurovascular function with supplemental O<sub>2</sub> may underscore the cognitive benefits, and reduced risk of cognitive impairment associated with O<sub>2</sub> therapy in COPD.

## 7 CONCLUSION

### 7.1 A REVIEW OF THESIS OBJECTIVES

This thesis aimed to determine the primary physiological processes and regulatory pathways that act to maintain cerebral oxygen delivery in humans. Study 1 (chapter 3) investigated the role of adenosine in regulating hypoxic vasodilation at sea-level and HA and determined that non-selective adenosine receptor antagonism does not influence the CBF response during hypoxia. This finding is inferred to indicate that adenosine is not an obligatory mediator of hypoxic cerebral vasodilation. However, as previously noted (see **Figure 3.1**) adenosine may also influence hypoxia independent of adenosine receptors via increasing  $K^+$  channel conductance. This latter point highlights the complexities associated with truly isolating a pathway from any signaling molecule, as there are typically several routes by which they act.

As adenosine was, to some extent, determined not to underlie hypoxic cerebral vasodilation, Study 2 aimed to investigate the relevance of a different signaling pathway. Here, the focus was to investigate the role of the erythrocyte, which may regulate hypoxic cerebral vasodilation via several pathways as previously outlined. By hemodiluting participants and reducing [Hb] we were, in theory, able to manipulate the magnitude of erythrocyte mediated signaling (see section “Mechanisms leading to a compromise in cerebral O<sub>2</sub> delivery during hemodilution” for an explanation). Hemodilution elicited a less robust CBF response compared to hypoxemia, which lead to a reduction in CDO<sub>2</sub>. Conversely, when hypoxemia was induced following hemodilution it led, in contrast to our second hypothesis, to an augmented CBF response. Unexpected, given the lower [Hb], several factors such as the severity of hypoxia, engagement of additional signaling pathways, altered transduction of NO signaling, or a high-flow dependent effect of viscosity have all been proposed as potential factors underlying this surprising finding. Notably, this increased reactivity with experimentally lowered [Hb] concentration *within subjects* was consistent with *between subject* data demonstrating that a lower [Hb] is correlated to a higher reactivity to hypoxia. How hemodilution leads to a reduction in erythrocyte signaling and impairs CDO<sub>2</sub> is considered in a subsequent section (see section “Mechanisms leading to a compromise in cerebral O<sub>2</sub> delivery during hemodilution”).

Collectively, these two studies have furthered the general understanding of the mechanisms that underlie hypoxic cerebral vasodilation in the *in vivo* human model. Building on previous studies (Bowton *et al.*, 1988; Nishimura *et al.*, 1993) that suffered several methodological limitations, Study 1 determined adenosine receptor dependent (not K<sup>+</sup> channel) signaling is not obligatory for hypoxic vasodilation in humans. Study 2, for the first time in humans, was designed specifically to investigate the role of deoxyhemoglobin mediated signaling in the regulation of hypoxic cerebral vasodilation in humans. This study is the first to indicate that the erythrocyte is a key regulator of the hypoxic cerebral vasodilation response and requisite for the maintenance of CDO<sub>2</sub>.

To further address the thesis objectives, this thesis aimed to better understanding how long term exposure to hypoxia at evolutionary and pathological levels influence cerebrovascular regulation. In study 3, Sherpa, who have lived at altitude for millennia were tested alongside lowlanders during progressive ascent to high-altitude to investigate how evolutionary adaptations to hypoxia may influence the regulation of CDO<sub>2</sub>. Here, it was determined that Sherpa possess a lower CDO<sub>2</sub> during ascent to altitude. It therefore appears that the Sherpa, who experience less cerebral specific deficits in function than lowlanders (Garrido *et al.*, 1993, 1996), may possess improved oxygen utilization and/or a reduced oxygen metabolism. This speculation is supported by evidence suggesting other key regulators of CBF (e.g., blood pressure, endothelial function, dynamic autoregulation, CO<sub>2</sub> reactivity, etc.) do not explain the observed differences between Sherpa and lowlanders. Further, a reduced metabolic demand is characteristic of hypoxia tolerant animals [e.g. crucian carp (Nilsson & Lutz, 2004)] as well as elite breath hold divers (Bain *et al.*, 2016, 2017a, 2017b, 2018; Bailey *et al.*, 2017). Such an adaptation may manifest, albeit to a lesser extent, in the clearly hypoxia tolerant Sherpa.

To investigate the influence of pathological hypoxia on CBF, NVC was assessed in COPD patients. Here, alleviation of hypoxia with low flow oxygen therapy led to an improvement in the cerebral vasomotor response to neural activation. In other words, the magnitude of NVC was increased and indicates that chronic hypoxia in a pathological context impairs the mechanisms that regulate CDO<sub>2</sub>. Such findings hold great relevance as neurovascular dysfunction (Nicolakakis & Hamel, 2011) and the related hypoperfusion (Iadecola, 2010) are thought to underlie, at least in part, the pathogenesis of dementia. For example, oxygen levels have been demonstrate to influence the accumulation of  $\beta$ -amyloid (Salminen *et al.*, 2017).

Therefore, future work should aim to understand what mechanisms are leading to this hypoxia induced reduction in neurovascular function.

### 7.1.1 MECHANISMS LEADING TO A COMPROMISE IN CEREBRAL O<sub>2</sub> DELIVERY DURING HEMODILUTION

In agreement with Study 2, previous data collected in humans (Hino *et al.*, 1992; Mühlhling *et al.*, 1999; Ekelund *et al.*, 2002; Daif *et al.*, 2012) and animals (Todd *et al.*, 1994, 1997; Tomiyama *et al.*, 1999a) (**Figure 7.1**) indicated that CDO<sub>2</sub> is impaired during reductions in CaO<sub>2</sub> via hemodilution. Why this impairment is thought to occur and the fundamental basis for our experimental design is as follows: 1) a reduction of total hemoglobin levels during hemodilution compared to hypoxemic hypoxia will reduce erythrocyte mediated signaling, and 2) a reduction of deoxyhemoglobin produced during hemodilution compared to hypoxemic hypoxia (i.e., smaller percentage of deoxyhemoglobin) will reduce erythrocyte mediated signaling. In humans, during hemodilution, jugular venous saturation is not appreciably reduced (<3% change) compared to baseline (Paulson *et al.*, 1973; Daif *et al.*, 2012) (**Figure 4.4**), whereas during hypoxemic hypoxia jugular venous saturation is reduced progressively (up to ~20%) with increases in severity (Ainslie *et al.*, 2014) (**Figure 4.4**). The higher SaO<sub>2</sub> during hemodilution would result in reduced deoxyhemoglobin mediated ATP release, NO<sub>2</sub> reductase activity, and NO release from RSNOs (Lima *et al.*, 2010). The downstream mechanisms governing this difference in reactivity between hypoxemic hypoxia and hemodilution are thought to be related to K<sub>ATP</sub> channel conductance (Tomiyama *et al.*, 1999a), which is largely responsible for ATP mediated dilation through vascular smooth muscle hyperpolarization (Kajita *et al.*, 1996; You *et al.*, 1999; Dietrich *et al.*, 2008) as well as reduced NO signaling demonstrated by no increase in cGMP during hemodilution (Todd *et al.*, 1997). These two aforementioned studies indicate a large mechanistic disparity between the regulation of hypoxemia induced cerebral vasodilation and the less effective hemodilution induced cerebral vasodilation.

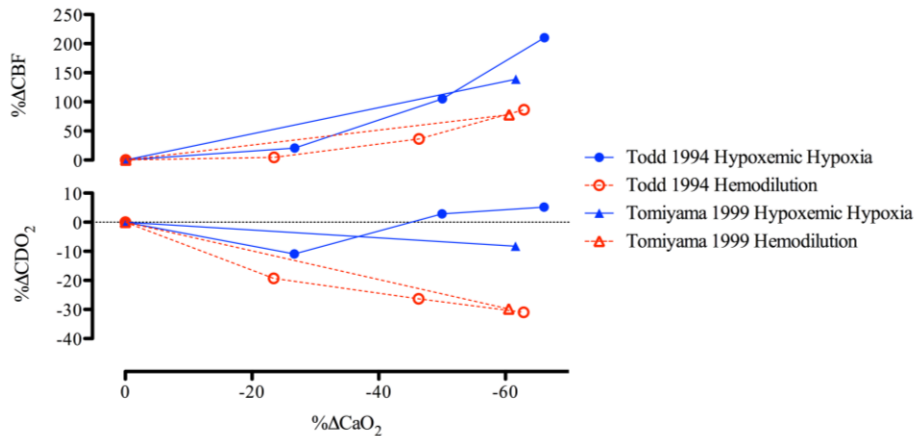


**Figure 7.1. Differential Changes in Cerebral Blood Flow During Hypoxemic Hypoxia and Hemodilution and the Impact on Cerebral Oxygen Delivery in Animals.**

The cerebral blood flow (CBF) response to both hypoxemic hypoxia and hemodilution in animals is presented (Todd *et al.*, 1994; Tomiyama *et al.*, 1999a). Despite similar reductions in arterial oxygen content (CaO<sub>2</sub>) between conditions, the CBF response (%Δ from baseline) is ~100% greater during hypoxemic hypoxia than hemodilution. Consequently, cerebral oxygen delivery (CDO<sub>2</sub>) is reduced during hemodilution but not hypoxemic hypoxia. Reproduced from (Hoiland *et al.*, 2016a), permission not required.

Although the CBF response to a reduction in CaO<sub>2</sub> is impaired during hemodilution, it is not abolished; thus, it seems that some regulatory mechanisms remain intact. These may be a residual component of the interrogated pathways (i.e., retention of partial NO signaling) or compensation via other pathways. Some animal studies suggests that NO is a primary factor mediating the CBF response to hemodilution predominantly through upregulation of neuronal nitric oxide synthase (Hudetz *et al.*, 1998; McLaren *et al.*, 2009), but, as stated, others have indicated hemodilution occurs via mechanisms other than NO related signal transduction (Todd *et al.*, 1997). Whether there is a differential influence from eNOS or nNOS that underlies the difference in vasodilation that occurs in response to hypoxemia and hemodilution remains to be determined.

### 7.1.2 CLINICAL IMPLICATIONS AND FUTURE DIRECTIONS

During or following major surgery (e.g., cardiac artery bypass, grafts, transplant, etc.), patients often become acutely hemodiluted and are at risk of suffering acute neurological injury and long-term neurological impairment (Murkin, 2005; Scott *et al.*, 2014). Indeed, evidence from

animal models indicates that hemodilution reduces tissue oxygenation during cardiopulmonary bypass (Duebener *et al.*, 2001) and increases neuronal and mitochondrial injury (Dian-San *et al.*, 2006). For example, in patients refusing blood transfusion during surgery (for religious reasons), preoperative [Hb] <8g/dL increased the risk of death 16-fold compared with those of higher [Hb] (Carson *et al.*, 1988). During anesthesia, hemodilution leads to a reduction in CMRO<sub>2</sub> (Daif *et al.*, 2012), which may be indicative that CDO<sub>2</sub> is not adequate to maintain metabolic homeostasis, as would normally occur during hypoxemic hypoxia (Ainslie *et al.*, 2014). Moreover, the occurrence of tissue hypoxia in traumatic brain injury patients with a tissue oxygenation probe, was greater in patients with a [Hb] of 7g/dL vs. a [Hb] of 10g/dL (Yamal *et al.*, 2015). Whether the reduced vasomotor response and thus impaired maintenance of CDO<sub>2</sub> during hemodilution is implicated in the risk for neurological injury in humans during major surgeries requires further investigation (Hare, 2006). In addition to the implications for various surgical interventions, elucidation of these mechanistic CBF relationships is paramount to our comprehension of pathologies associated with arterial hypoxemia (e.g., sleep apnea, chronic lung diseases, and heart failure) and/or alterations in blood viscosity or hemoglobin levels (e.g., anemic or polycythemic pathologies including von Hippel-Landau or Chuvash diseases). Uncovering the molecular basis of hypoxic adaptation in humans will both inform understanding of hematological and other adaptations involved in hypoxia tolerance and form the basis of novel methods for treating conditions of pathological brain hypoxia. Optimizing CDO<sub>2</sub> via multi-modal imaging and/or molecular approaches may provide new insight into the treatment of many hypoxemic, anemic, or polycythemic pathologies and that associated with cerebrovascular complications.

## **7.2 A FRAMEWORK FOR FUTURE INVESTIGATIONS INTO THE SIGNALING PATHWAYS REGULATING HUMAN CEREBRAL BLOOD FLOW**

This thesis has noted several times that human cerebrovascular investigations are plagued by inconsistent results that are difficult or impossible to reconcile and/or reproduce. Therefore, improvements in methodology and appropriate experimental design are required. This section outlines a framework for future investigations aiming to elucidate the signaling pathways underlying hypoxic cerebral vasodilation using an *in vivo* human model.

### 7.2.1 WHY IS THE DESIGN OF CEREBROVASCULAR EXPERIMENTS SO IMPORTANT?

Stroke is the second leading cause of death world-wide (11.8% of all deaths) (Feigin *et al.*, 2017) and the overall incidence of first strokes has increased markedly (up 68%) over the past two decades (Feigin *et al.*, 2014). The prevalence of other vascular brain pathologies, such as dementia, are also increasing (>35 million people globally with dementia) (Prince *et al.*, 2013). Aging is a major risk factor for these brain-related diseases, which, coupled with a global increase in life expectancy (Salomon *et al.*, 2012), will perpetuate the already substantial global burden of brain vascular disease. Extensive pre-clinical data on vascular brain pathology exists, yet there is a developing crisis whereby pre-clinical data is failing to translate at an alarming rate; <5% of pre-clinically discovered “targets” translate to successful drug development (Paul *et al.*, 2010; Collins, 2011; Dirnagl *et al.*, 2013).

*“Although the scientific substrate for drug discovery has never been more abundant, a more complete understanding of human (disease) biology will still be required before many true breakthrough medicines emerge” – Paul, et al., Nat Rev Drug Discov, 2010 (Paul et al., 2010)*

The above quotation is an appropriate call to action as we still possess a poor understanding of the basic mechanisms of *in vivo* human brain blood flow regulation and lack a robust physiological assay of brain blood vessel health. Thus, human studies are urgently needed to better predict/stratify stroke and/or dementia risk. A leading example of our inadequate knowledge of human brain blood regulation is the lack of data on NO. In other vascular beds the function of NO is predictive of cardiovascular risk (Green *et al.*, 2011). However, despite the notion that NO is integral to human CBF regulation (Toda *et al.*, 2009), comprehensive and definitive demonstration of NO’s role in regulating human CBF does not exist (published work is inconsistent and severely limited) (Schmetterer *et al.*, 1997; White *et al.*, 1998, 1999; Van Mil *et al.*, 2002b; Ide *et al.*, 2007). Indeed, throughout this thesis, a theme has emerged: animal studies highlight multiple important signaling pathways in the regulation of CBF (during hypoxia or otherwise), yet human studies fail to observe meaningful influences of these candidate signaling molecules (e.g. NO). Even when studies demonstrate that a molecule is important in a CBF response, such as that demonstrated by Van Mil *et al.*, (Van Mil *et al.*, 2002b), whereby infusion of the NOS inhibitor L-NMMA reduced CBF, findings to the

contrary exist (Ide *et al.*, 2007). Further, methodological limitations with regards to measuring blood velocity raise doubt on the interpretation of the Van Mil and Ide studies (Schulz *et al.*, 2018). To date, human studies have, as a whole, provided an unremarkable step forward in our knowledge of signaling pathways in CBF control. Expensive, invasive, and logistically complex, these studies are not typically repeated. Therefore, it is critical to utilize an appropriate experimental protocol to investigate the pathway of interest.

To illustrate in greater detail why it is difficult to delineate signaling pathways in humans, as well as why it is difficult to reconcile between study differences, the juxtaposition of two studies with disparate results is utilized. A “framework” for cerebrovascular experiments is proposed, the extent to which the two studies of interest (Van Mil *et al.*, 2002*b*; Ide *et al.*, 2007) adhered to this framework is assessed, and future studies derived from this framework are suggested.

Three fundamental components of an experimental design should be considered pre-requisites to effectively investigate signaling pathways in human cerebrovascular regulation: 1) Manipulation of the pathway of interest; 2) Assessment of changes in that signaling pathway and molecular bioavailability; 3) Utilization of measures of CBF *per se*, rather than the use of surrogate indices.

### **7.2.2 COMPONENT 1 - MANIPULATING SIGNALING MOLECULE BIOAVAILABILITY**

Various methods can be employed for the purpose of manipulating a signaling pathway of interest. Typically, pharmacology is used to either increase [e.g., (Jahshan *et al.*, 2017)] or decrease [e.g., (Van Mil *et al.*, 2002*b*; Ide *et al.*, 2007)] signaling molecule bioavailability or to reduce downstream signal transduction [e.g., block a specific receptor (Bowton *et al.*, 1988)]. If the overall goal is to simulate a disease state, or replicate potential impairments in signaling that may manifest with disease, it seems most appropriate to decrease signaling molecule bioavailability or downstream signal transduction. However, as outlined in the following section (see section “Component 2 - measuring changes in signaling molecule bioavailability”), manipulating signaling molecule bioavailability, at least with regards to NO, may stand alone as the most appropriate method. Such an undertaking involves the use of a NOS inhibitor, for which L-NMMA is typically employed in humans (Van Mil *et al.*, 2002*b*; Ide *et al.*, 2007). Of

note, asymmetrical dimethyl arginine, given its endogenous production (Leiper & Vallance, 1999) and increased concentration in disease models (Faraci, 2011), may also be suitable. Asymmetrical dimethyl arginine has been used safely in humans previously (Kielstein *et al.*, 2004, 2006). It is important to also note, that while reducing molecular bioavailability will provide insight in to pathological changes with disease, increasing molecular bioavailability may be more suitable for understanding how administering a potential treatment, to alleviate pathological deficits in signaling, will effect physiological function. In this regard, administration of NO donors is also important (Jahshan *et al.*, 2017; Schulz *et al.*, 2018).

### 7.2.3 COMPONENT 2 - MEASURING CHANGES IN SIGNALING MOLECULE BIOAVAILABILITY

If a study utilizes a pharmacological blockade (e.g. L-NMMA) and observes no vascular consequence, the first question to arise is: Was the blockade effective? Thus, it is critical to evaluate the extent to which a pharmacological blockade is reflected in altered signaling molecule bioavailability. Continuing to use NO as the example, it is extremely difficult to measure NO activity. Indeed, given the half-life of NO is in the magnitude of milliseconds, studies in living humans do not have the capacity to measure NO directly. However, NO bioavailability can be measured via several related and bioactive NO species. Both SNO-Hb and NO<sub>2</sub> are derived from NO and convey NO bioactivity – notably, this bioactivity underscored the rationale for study 2. These NO species can be measured using a technique called ozone based chemiluminescence (**Figure 7.2**) (MacArthur *et al.*, 2007; Pinder *et al.*, 2009).

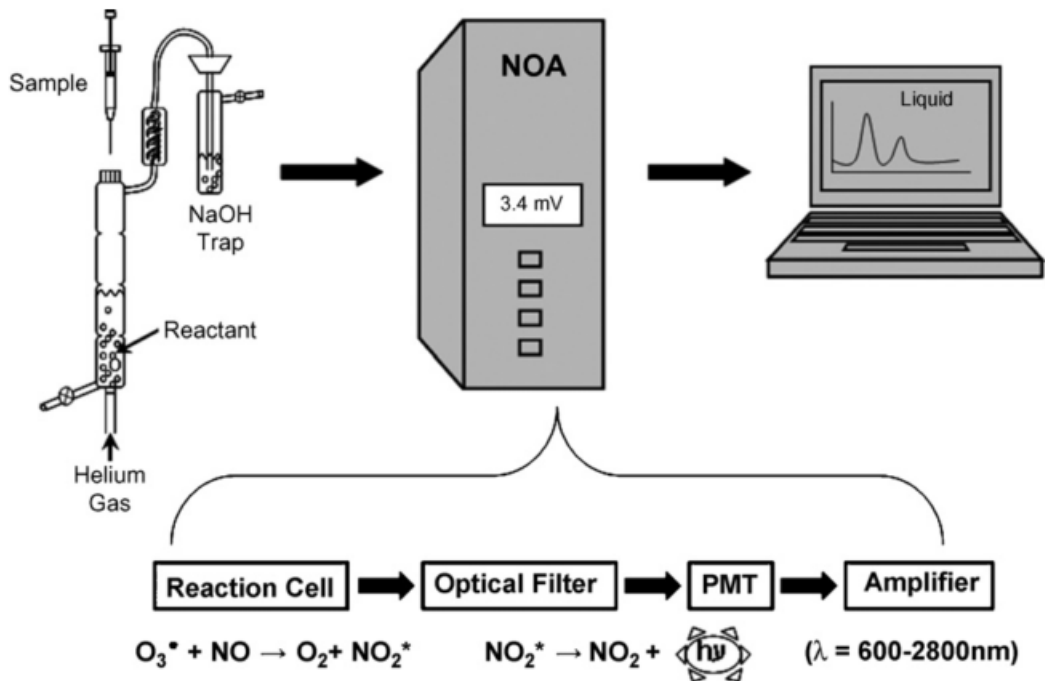


**Figure 7.2. Ozone based chemiluminescence.**

This technique functions through the use of a reductive solution (typically tri-iodide), whereby injection of a sample (plasma or red blood cells) into a purge vessel (left of figure) leads to the reduction of all NO compounds and liberation of NO gas from the solution. Constant bubbling of an inert gas (e.g., helium) carries this NO gas through the system and into the nitric oxide analyzer (NOA), where it is charged with ozone. As the NO transitions from this high energy state to a low energy state it releases a photon, which is the measured signal. This signal is outputted to a program (Liquid – noted on laptop image) and data are extracted.

This technique is effective as it is sensitive to 1nM (**Figure 7.3**). Another advantage of this technique is that it allows for the measurement of NO species specific to red blood cells and the plasma. As highlighted in the literature review (see section “Deoxyhemoglobin mediated signal transduction pathways”), these species may move between locales (erythrocyte/plasma) as well as SNO-Hb and NO<sub>2</sub> may be interconverted to one another. As such it is imperative to measure both plasma and red blood cell NO species to account for total NO bioavailability and potential reapportionment during gas exchange with cerebral tissue.

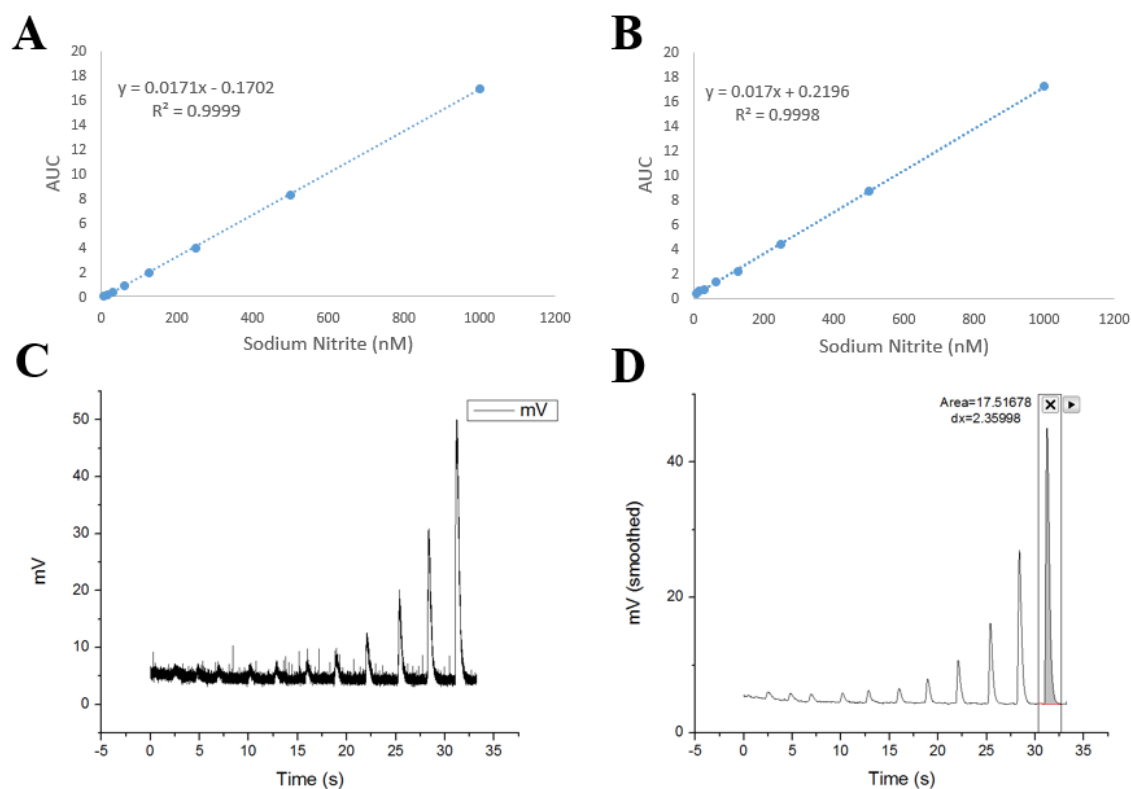


**Figure 7.3. Standard curves for ozone based chemiluminescence.**

The above two curves represent the standard curves derived using known sodium nitrite concentrations. Panels A and B represent curves determined on two separate days. Note the high r-squared value as well as the similar slopes (0.0171 vs 0.017). The only difference is the y-intercept, which is a product of varying nitrite levels in the water used to create the dilution. High-performance liquid chromatography water is utilized, but given the ubiquity of nitrite, some contamination is inevitable. However, this is accounted for when calculating sample concentrations. As depicted in Panels C and D, the nitric oxide analyzer (Seivers, NOA 280i) outputs a millivolt signal. Panel C displays the raw signal, which is then smoothed using a 150 window adjacent averaging function. The area under the curve of this signal (Panel D) is calculated at each concentration of sodium nitrite and then used to create the standard curve. Note the most rightward peak is highlighted grey and has a corresponding area under the curve output.

A methodological process for the measurement of NO has been outlined; however, consideration of how the study design impacts the capacity to measure changes in a signal transduction pathway warrants further discussion. Downstream of NO, upregulation of soluble guanylyl cyclase and cGMP lead to VSMC relaxation. Thus, soluble guanylyl cyclase may appear to be an attractive target for pharmacological interventions. Previous studies in animals have utilized methylene blue infusions to inhibit soluble guanylyl cyclase activity (Pearce *et*

*al.*, 1990) and it has been used in humans for other purposes (Hosseinian *et al.*, 2016). However, it would not be possible in humans to measure VSMC cGMP levels, where the influence of methylene blue infusion occurs. This lack of ability to assess the effectiveness of the intervention indicates methylene blue may not be an appropriate intervention. Therefore, careful consideration of the pharmacological intervention to be utilized is paramount in study design of mechanistic cerebrovascular experiments.

#### **7.2.4 COMPONENT 3 - MEASUREMENT OF VOLUMETRIC CBF**

Multiple techniques are now utilized to measure, or index, CBF responses during hypoxia (see section “Modern measurement techniques”). As has been outlined in the literature review each technique possesses its own strengths and limitations. For the purpose of determining a mechanistic pathway, volumetric measurements should be utilized. Simply, the method of choice should not be confounded by the vasoactive influence of a pharmacological intervention. Such a requirement precludes the use of TCD in research aiming explore mechanistic pathways, especially related to NO, which has been shown to cause MCA vasodilation (Schulz *et al.*, 2018). Techniques such as arterial spin labelling MRI and duplex ultrasound appear to hold more merit. Importantly, arterial spin labelling, and duplex ultrasound, due to their volumetric measures, allow for the calculation of the net exchange (uptake or release) of a relevant signaling molecule (e.g., SNO-Hb). These approaches are integral for the determination of signaling molecule bioavailability across the brain.

#### **7.2.5 WHERE ARE WE NOW?**

The above sections have provided a framework for investigating signaling pathways that may regulate hypoxic cerebral vasodilation in humans. Here, the extent to which Van Mil *et al.*, (Van Mil *et al.*, 2002a) and Ide *et al.*, (Ide *et al.*, 2007) adhered to this framework, and how this impacts one’s ability to reconcile their disparate results is discussed.

Van Mil *et al.*, (Van Mil *et al.*, 2002a) have demonstrated that NO is an important regulator of hypoxic cerebral vasodilation, whereas Ide *et al.*, (Ide *et al.*, 2007) have demonstrated that NO does not influence CBF in hypoxia. Both studies utilized L-NMMA to non-selectively inhibit NOS activity. Van Mil *et al.*, administered a 3mg/kg bolus following 30-minutes of hypoxia

(SpO<sub>2</sub> ~80%), whereas Ide *et al.*, performed a hypoxic reactivity test (P<sub>ET</sub>O<sub>2</sub> = 50mmHg, didn't measure SpO<sub>2</sub>) followed by a 5mg/kg bolus and 50µg/Kg/min maintenance dose (**Figure 7.4**). Following initiation of the maintenance dose a second reactivity test was performed. So with relevance to component one of the proposed experimental framework, Van Mil *et al.*, and Ide *et al.*, adhered to the requirements by utilizing a pharmacological NOS blockade. However, neither Van Mil *et al.*, nor Ide *et al.*, undertook any measurements to determine the effectiveness of their blockades, failing to adhere to component two of the proposed framework.

Relative to component three, the study by Van Mil *et al.*, used phase contrast MRI to index CBF (Van Mil *et al.*, 2002a). Importantly, phase contrast measures cerebral blood velocity, not flow. Similarly, Ide *et al.*, also measured cerebral blood velocity, not flow, albeit with TCD. Therefore, neither study possessed a measure of volumetric CBF. Further, under the assumption (and hypothesis) that NO influences CBF, one would expect it to influence vascular diameter and invalidate velocity measures. This has recently been demonstrated following sodium nitroglycerin administration and CBF measurement with a 7 Tesla MRI (Schulz *et al.*, 2018)

Given the disparate results between studies, one must look at each experimental component to determine if one study can be considered to provide the more accurate and meaningful findings. However, as the effectiveness of the blockades were not measured, it is not possible to discern if study differences are related to differences in NO bioavailability post-intervention. Further, it is not possible to determine if the indexes of CBF utilized provide an accurate representation of the underlying physiology. For example, perhaps flow was decreased in both studies due to a reduction in MCA diameter, which seems plausible given NO can dilate the MCA (Schulz *et al.*, 2018), but this reduction was not detectable with the methods used. Such a conundrum perpetuates the issue whereby inconsistent and methodologically limited data in humans are hindering our understanding of the mechanistic pathways that regulate hypoxic cerebral vasodilation. Future studies must address these gaps in the literature (see section “Future directions: nitric oxide and hypoxic vasodilation”)

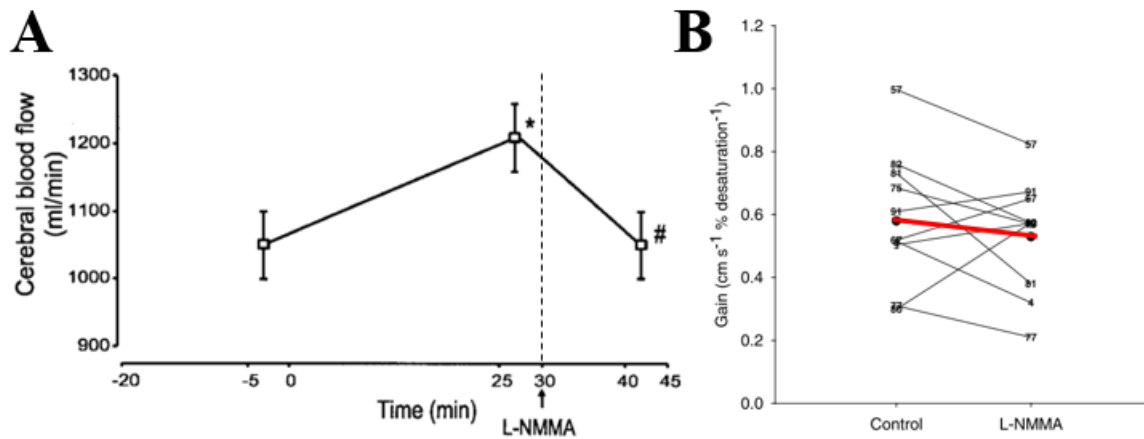


**Figure 7.4. Results from the studies by Van Mil in 2002 and Ide in 2007.**

Panel A outlines the experimental protocol and cerebral blood flow (CBF) results from Van Mil *et al.*, 2002. Hypoxia increased CBF, while subsequent infusion of L-NMMA reduced CBF to baseline levels. Panel B depicts the individual reactivity data for the study by Ide *et al.*, 2007 with the mean change denoted by the red line. Here reactivity was determined as the stimulus-response relationship both prior to and following L-NMMA infusion, which was unaltered. Reproduced from (Ide *et al.*, 2007) with permission as well as from (Van Mil *et al.*, 2002b), permission not required.

### 7.3 FUTURE DIRECTIONS: NITRIC OXIDE AND HYPOXIC VASODILATION

In light of the outlined pitfalls in cerebrovascular research, future studies must aim to use innovative and valid methodologies to provide significant steps forward in our understanding of cerebrovascular regulation. Below, a study designed to investigate the role of NO in regulating human CBF during hypoxia is outlined as a logical future direction.

#### 7.3.1 AIMS AND HYPOTHESES

1) To determine the impact of NOS blockade on CBF regulation during hypoxia.

- We hypothesize that NOS blockade will reduce the increase in CBF observed during hypoxia.

#### 7.3.2 METHODOLOGY

To address the project aims, CBF will be measured using duplex ultrasound of the ICA and VA. Measurement of signaling molecule bioavailability will be achieved through radial arterial and jugular venous cannulation, with serial sampling at each experimental stage. Samples will be analyzed for standard blood gas parameters (PaO<sub>2</sub>, PaCO<sub>2</sub>, [Hb], HCT, pH, [HCO<sub>3</sub><sup>-</sup>], etc.) while SNO-Hb and NO<sub>2</sub> will be measured using ozone base chemiluminescence. Systemic L-NMMA infusions (5mg/kg bolus and 50µg/Kg/min maintenance dose etc.) will be utilized to manipulate NO levels, with hypoxic reactivity measured prior to and during infusion. End-tidal forcing will be utilized to target the desired blood gas values as was done in studies 1 and 2.

#### **7.4 FINAL CONSIDERATIONS ON MECHANISTIC INVESTIGATION INTO CEREBRAL BLOOD FLOW REGULATION**

Throughout this thesis a recurrent theme has emerged. First, there has been an extensive amount of research into signaling pathways using *in vitro* and *in vivo* animal models. These studies have produced variable results, although the majority consistently demonstrate the importance of each signaling pathway (K<sub>ATP</sub> channels, adenosine, NO, PGs, etc.). However, data in humans are scarce, and while variable, often support the notion that the prototypical candidate signaling molecules do not regulate hypoxic vasodilation in humans. It is important to consider that the technological and safety constraints inherent to cerebrovascular investigations in humans largely precludes the use of highly valid metrics and leads to relatively unfounded speculations. Thus, several key considerations are required when juxtaposing animal and human research in cerebrovascular regulation:

- 1) It is important to be cognizant of the fact that animal studies measuring pial arteriolar dilation have not necessarily measured “flow”. Given changes in vascular resistance can occur throughout the entire arterial circulation (see section “Cerebral blood flow and microvascular pressure with changes in Segmental ” and “CO<sub>2</sub>: site(s) of vascular regulation”), the collective proportional changes in each segment influence flow, not just the pial arteriolar changes in resistance.
- 2) Studies conducted using *in vivo* animal models typically involve the use of anesthesia. Anesthetics can affect the level of neural activity/metabolism, cyclic nucleotide levels, nNOS activity, and impact on calcium channels to name but a few confounding actions [reviewed in: (Tran & Gordon, 2015)].

- 3) Differences in cerebral vascular anatomy and structure exist between species that may be important when considering difference between species (Edvinsson & Krause, 2002).
- 4) Hypoxia elicits an integrative physiological response that may activate multiple regulatory pathways, not just those relevant to hypoxia based alterations in vascular tone. Acknowledgement of the potential for extraneous influences is necessary, although difficult to handle in human research. Nevertheless, appropriate experimental and statistical considerations can mitigate this issue.
- 5) Typically, authors of “negative finding” studies call upon redundant mechanisms as the reason for no influence of a pharmacological blockade (e.g. L-NMMA) on hypoxic vasodilation. However, the intricacies required to manipulate, measure, and detect relevant signaling pathways are typically absent in the discussion of human research. Systemic versus localized infusions, limits to drug dosage, and non-invasive measurements/indices of flow are typical, and essentially required given the safety concerns of more invasive techniques. However, as has become clear throughout this thesis, the regulatory pathways of interest are exceptionally complex and highly unlikely to be mediated via one or two molecules alone.
- 6) In humans consideration needs to be given as to where in the signaling cascade experimental manipulations are being made. For example, to investigate the role of NO in hypoxic cerebral vasodilation, one could theoretically inhibit NOS activity (e.g. L-NMMA infusion) or cGMP activity (e.g. Methylene Blue infusion). A consideration, however, is which target may be better suited for analytical and interpretive purposes. Blockade of NOS will lead to measureable reductions in NO bioavailability, thus providing an index of blockade efficacy, whereas determining the impact of cGMP blockade would not be possible *in vivo* given the localization of relevant cyclic nucleotides to the VSMCs.

## BIBLIOGRAPHY

- Aaslid R, Markwalder TM & Nornes H (1982). Noninvasive transcranial Doppler ultrasound recording of flow velocity in basal cerebral arteries. *J Neurosurg* **57**, 769–774.
- Abdel-halim MS, Holst H Von, Meyerson B, Sachs C & Anggard E (1980). Prostaglandin Profiles in Tissue and Blood Vessels from Human Brain. *J Neurochem* **34**, 1331–1333.
- Adachi K, Takahashi S, Melzer P, Campos KL, Nelson T, Kennedy C & Sokoloff L (1994). Increases in local cerebral blood flow associated with somatosensory activation are not mediated by NO. *Am J Physiol* **267**, H2155-62.
- Adelstein R, Conti MA, Adelstein S, Conti MA & Hathaway DR (1978). Phosphorylation of Smooth Muscle Myosin Light Chain Kinase by the Catalytic Subunit of Adenosine 3': 5'-Monophosphate-dependent Protein Kinase. *J Biol Chem* **253**, 8347–8350.
- Ainslie PN, Ashmead JC, Ide K, Morgan BJ & Poulin MJ (2005). Differential responses to CO<sub>2</sub> and sympathetic stimulation in the cerebral and femoral circulations in humans. *J Physiol* **566**, 613–624.
- Ainslie PN, Burgess K, Subedi P & Burgess KR (2007). Alterations in cerebral dynamics at high altitude following partial acclimatization in humans: wakefulness and sleep. *J Appl Physiol* **102**, 658–664.
- Ainslie PN & Burgess KR (2008). Cardiorespiratory and cerebrovascular responses to hyperoxic and hypoxic rebreathing: Effects of acclimatization to high altitude. *Respir Physiol Neurobiol* **161**, 201–209.
- Ainslie PN & Duffin J (2009). Integration of cerebrovascular CO<sub>2</sub> reactivity and chemoreflex control of breathing: mechanisms of regulation, measurement, and interpretation. *Am J Physiol Regul Integr Comp Physiol* **296**, R1473-95.
- Ainslie PN & Hoiland RL (2014). Transcranial Doppler Ultrasound: Valid, Invalid, or Both? *J Appl Physiol* **117**, 1081–1083.
- Ainslie PN, Lucas SJE & Burgess KR (2013). Breathing and sleep at high altitude. *Respir Physiol Neurobiol* **188**, 233–256.
- Ainslie PN, Lucas SJE, Fan J-L, Thomas KN, Cotter JD, Tzeng YC & Burgess KR (2012). Influence of sympathoexcitation at high altitude on cerebrovascular function and

- ventilatory control in humans. *J Appl Physiol* **113**, 1058–1067.
- Ainslie PN & Ogoh S (2010). Regulation of cerebral blood flow in mammals during chronic hypoxia: a matter of balance. *Exp Physiol* **95**, 251–262.
- Ainslie PN & Poulin MJ (2004). Ventilatory, cerebrovascular, and cardiovascular interactions in acute hypoxia: regulation by carbon dioxide. *J Appl Physiol* **97**, 149–159.
- Ainslie PN, Shaw AD, Smith KJ, Willie CK, Ikeda K, Graham J & Macleod DB (2014). Stability of cerebral metabolism and substrate availability in humans during hypoxia and hyperoxia. *Clin Sci (Lond)* **126**, 661–670.
- Ainslie PN & Subudhi AW (2014). Cerebral blood flow at high altitude. *High Alt Med Biol* **15**, 133–140.
- Al-Khazraji BK, Shoemaker LN, Gati JS, Szekeres T & Shoemaker JK (2018). Reactivity of larger intracranial arteries using 7 T MRI in young adults. *J Cereb Blood Flow Metab*0271678X1876288.
- Albayrak R, Fidan F, Unlu M, Sezer M, Degirmenci B, Acar M, Haktanir A & Yaman M (2006). Extracranial carotid Doppler ultrasound evaluation of cerebral blood flow volume in COPD patients. *Respir Med* **100**, 1826–1833.
- Aldenderfer M (2011). Peopling the Tibetan Plateau: Insights from Archaeology. *High Alt Med Biol* **12**, 141–147.
- Alpers BJ, Berry RG & Paddison RM (1959). Anatomical studies of the circle of Willis in normal brain. *Arch Neurol Psychiatry* **81**, 409.
- Amin TM & Sirs JA (1985). The blood rheology of man and various animal species. *Q J Exp Physiol* **70**, 37–49.
- Anand-Srivastava MB, Franks DJ, Cantin M & Genest J (1982). Presence of “Ra” and “P”-site receptors for adenosine coupled to adenylate cyclase in cultured vascular smooth muscle cells. *Biochem Biophys Res Commun* **108**, 213–219.
- Archer SL, Huang JMC, Hampl V, Nelson DP, Shultz PJ & Weir EK (1994). Nitric oxide and cGMP cause vasorelaxation by activation of a charybdotoxin-sensitive K channel by cGMP-dependent protein kinase. *Proc Natl Acad Sci* **91**, 7583–7587.
- Armstead WM (1997). Role of nitric oxide, cyclic nucleotides, and the activation of ATP-sensitive K<sup>+</sup> channels in the contribution of adenosine to hypoxia-induced pial artery

- dilation. *J Cereb Blood Flow Metab* **17**, 100–108.
- Arnold WP, Mittal CK, Katsuki S & Murad F (1977). Nitric oxide activates guanylate cyclase and increases guanosine 3':5'-cyclic monophosphate levels in various tissue preparations. *Proc Natl Acad Sci* **74**, 3203–3207.
- Asgari S, Bergsneider M, Hamilton R, Vespa P & Hu X (2011). Consistent changes in intracranial pressure waveform morphology induced by acute hypercapnic cerebral vasodilatation. *Neurocrit Care* **15**, 55–62.
- Atkinson CL, Carter HH, Naylor LH, Dawson EA, Marusic P, Hering D, Schlaich MP, Thijssen DH & Green DJ (2015). Opposing effects of shear-mediated dilation and myogenic constriction on artery diameter in response to handgrip exercise in humans. *J Appl Physiol* **119**, 858–864.
- Atkinson G & Batterham AM (2013). Allometric scaling of diameter change in the original flow-mediated dilation protocol. *Atherosclerosis* **226**, 425–427.
- Atkinson G, Batterham AM, Jones H, Taylor CE, Willie CK & Tzeng YC (2011). Appropriate within-subjects statistical models for the analysis of baroreflex sensitivity. *Clin Physiol Funct Imaging* **31**, 80–82.
- Atkinson G, Batterham AM, Thijssen DHJ & Green DJ (2013). A new approach to improve the specificity of flow-mediated dilation for indicating endothelial function in cardiovascular research. *J Hypertens* **31**, 287–291.
- Attwell D, Buchan AM, Charpak S, Lauritzen M, MacVicar BA & Newman EA (2010). Glial and neuronal control of brain blood flow. *Nature* **468**, 232–243.
- Austin V, Crack PJ, Bozinovski S, Miller AA & Vlahos R (2016). COPD and stroke: are systemic inflammation and oxidative stress the missing links? *Clin Sci* **130**, 1039–1050.
- Azarov I, Huang KT, Basu S, Gladwin MT, Hogg N & Kim-shapiro DB (2005). Nitric Oxide Scavenging by Red Blood Cells as a Function of Hematocrit and Oxygenation \*. **280**, 39024–39032.
- Bailey DM, Bärtsch P, Knauth M & Baumgartner RW (2009a). Emerging concepts in acute mountain sickness and high-altitude cerebral edema: From the molecular to the morphological. *Cell Mol Life Sci* **66**, 3583–3594.
- Bailey DM, Marley CJ, Brugniaux J V., Hodson D, New KJ, Ogoh S & Ainslie PN (2013a).

Elevated aerobic fitness sustained throughout the adult lifespan is associated with improved cerebral hemodynamics. *Stroke* **44**, 3235–3238.

Bailey DM, Rimoldi SF, Rexhaj E, Pratali L, Salmòn CS, Villena M, McEneny J, Young IS, Nicod P, Allemann Y, Scherrer U & Sartori C (2013b). Oxidative-nitrosative stress and systemic vascular function in highlanders with and without exaggerated hypoxemia. *Chest* **143**, 444–451.

Bailey DM, Taudorf S, Berg RMG, Jensen LT, Lundby C, Evans KA, James PE, Pedersen BK & Moller K (2009b). Transcerebral Exchange Kinetics of Nitrite and Calcitonin Gene-Related Peptide in Acute Mountain Sickness: Evidence Against Trigeminovascular Activation? *Stroke* **40**, 2205–2208.

Bailey DM, Willie CK, Hoiland RL, Bain AR, MacLeod DB, Santoro MA, DeMasi DK, Andrijanic A, Mijacika T, Barak OF, Dujic Z & Ainslie PN (2017). Surviving Without Oxygen: How Low Can the Human Brain Go? *High Alt Med Biol* **18**, 73–79.

Bain AR, Ainslie PN, Barak OF, Hoiland RL, Drvis I, Mijacika T, Bailey DM, Santoro A, DeMasi DK, Dujic Z & MacLeod DB (2017a). Hypercapnia is essential to reduce the cerebral oxidative metabolism during extreme apnea in humans. *J Cereb Blood Flow Metab*; DOI: 10.1177/0271678X16686093.

Bain AR, Ainslie PN, Hoiland RL, Barak OF, Cavar M, Drvis I, Stembridge M, MacLeod DM, Bailey DM, Dujic Z & MacLeod DB (2016). Cerebral oxidative metabolism is decreased with extreme apnoea in humans; impact of hypercapnia. *J Physiol* **594**, 5317–5328.

Bain AR, Ainslie PN, Hoiland RL, Barak OF, Drvis I, Stembridge M, MacLeod DM, McEneny J, Stacey BS, Tuailon E, Marchi N, De Maudave AF, Dujic Z, MacLeod DB & Bailey DM (2017b). Competitive apnea and its effect on the human brain: focus on the redox-regulation of blood–brain barrier permeability and neuronal–parenchymal integrity. *FASEB J*fj.201701031R.

Bain AR, Drvis I, Dujic Z, MacLeod DB & Ainslie PN (2018). Physiology of static breath holding in elite apneists. *Exp Physiol* 1–49.

Bakker SLM, de Leeuw FE, den Heijer T, Koudstaal PJ, Hofman A & Breteler MMB (2004). Cerebral Haemodynamics In The Elderly: The Rotterdam Study. *Neuroepidemiology* **23**, 178–184.

- Balaban DY, Duffin J, Preiss D, Mardimae A, Vesely A, Slessarev M, Zubieta-Calleja GR, Greene ER, MacLeod DB & Fisher JA (2013). The in-vivo oxyhaemoglobin dissociation curve at sea level and high altitude. *Respir Physiol Neurobiol* **186**, 45–52.
- Balanos GM, Talbot NP, Dorrington KL & Robbins PA (2003). Human pulmonary vascular response to 4 h of hypercapnia and hypocapnia measured using Doppler echocardiography. *J Appl Physiol* **94**, 1543–1551.
- Balucani C, Viticchi G & Falsetti L (2012). Cerebral hemodynamics and cognitive performance in bilateral asymptomatic carotid stenosis. ; DOI: 10.1212/WNL.0b013e318270402e.
- Bandettini PA (2012). Twenty years of functional MRI: The science and the stories. *Neuroimage* **62**, 575–588.
- Barnes JN (2017). Sex specific factors regulating pressure and flow. *Exp Physiol* **11**, 1385–1392.
- Barnes JN, Schmidt JE, Nicholson WT & Joyner MJ (2012). Cyclooxygenase inhibition abolishes age-related differences in cerebral vasodilator responses to hypercapnia. *J Appl Physiol* **112**, 1884–1890.
- Barnes PJ (2014). Cellular and Molecular Mechanisms of Chronic Obstructive Pulmonary Disease. *Clin Chest Med* **35**, 71–86.
- Baumgartner RW, Bartsch P, Maggiorini M, Waber U & Oelz O (1994). Enhanced cerebral blood flow in acute mountain sickness. *Aviat Sp Environ Med* **65**, 726–729.
- Bauser-Heaton HD & Bohlen HG (2007). Cerebral microvascular dilation during hypotension and decreased oxygen tension: a role for nNOS. *Am J Physiol Heart Circ Physiol* **293**, H2193–H2201.
- Bayerle-Eder M, Wolzt M, Polska E, Langenberger H, Pleiner J, Teherani D, Rainer G, Polak K, Eichler HG & Schmetterer L (2000). Hypercapnia-induced cerebral and ocular vasodilation is not altered by glibenclamide in humans. *Am J Physiol Regul Integr Comp Physiol* **278**, R1667-73.
- Bayliss LE (1959). The Axial Drift of the Red Cells When Blood Flows in A Narrow Tube. *J Physiol* **149**, 593–613.
- Beall CM (2006). Andean, Tibetan, and Ethiopian patterns of adaptation to high-altitude

- hypoxia. *Integr Comp Biol* **46**, 18–24.
- Beall CM (2007). Two routes to functional adaptation: Tibetan and Andean high-altitude natives. *Proc Natl Acad Sci U S A* **104**, 8655–8660.
- Beall CM, Laskowski D & Erzurum SC (2012). Nitric oxide in adaptation to altitude. *Free Radic Biol Med* **52**, 1123–1134.
- Beall CM, Laskowski D, Strohl KP, Soria R, Villena M, Vargas E, Alarcon a M, Gonzales C & Erzurum SC (2001). Pulmonary nitric oxide in mountain dwellers. *Nature* **414**, 411–412.
- Beaudin AE, Hartmann SE, Pun M & Poulin MJ (2017). Human cerebral blood flow control during hypoxia: focus on chronic pulmonary obstructive disease and obstructive sleep apnea. *J Appl Physiol* **123**, 1350–1361.
- Beavo JA (1995). Cyclic nucleotide phosphodiesterases: functional implications of multiple isoforms. *Physiol Rev* **75**, 725–748.
- Berdeaux A, Ghaleh B, Dubois-Randé JL, Vigué B, Drieu La Rochelle C, Hittinger L & Giudicelli JF (1994). Role of vascular endothelium in exercise-induced dilation of large epicardial coronary arteries in conscious dogs. *Circulation* **89**, 2799–2808.
- Bergfeld GR & Forrester T (1992). Release of ATP from human erythrocytes in response to a brief period of hypoxia and hypercapnia. *Cardiovasc Res* **26**, 40–47.
- Berne RM, Rubio R & Curnish RR (1974). Release of Adenosine from Ischemic Brain: Effect on Cerebral Vascular Resistance and Incorporation into Cerebral Adenine Nucleotides. *Circ Res* **35**, 262–271.
- Bertalanffy H, Kawase T & Toya S (1993). In vivo Effect of Visible Light on Feline Cortical Microcirculation. *Acta Neurochir* **121**, 174–180.
- Betz E, Enzenrob HG & Vlahov V (1973). Interaction of H<sup>+</sup> and Ca<sup>++</sup> in the Regulation of Local Pial Vascular Resistance. **88**, 79–88.
- Bevan JA (1979). Sites of Transition Between Functional Systemic and Cerebral Arteries of Rabbits Occur at Embryological Junctional Sites. *Science (80- )* **204**, 635–637.
- Bevan JA, Dodge J, Walters CL, Wellman T & Bevan RD (1999). As human pial arteries (internal diameter 200 - 1000 µm) get smaller, their wall thickness and capacity to develop tension relative to their diameter increase. *Life Sci* **65**, 1153–1161.

- Bhogal AA, Philippens MEP, Siero JCW, Fisher JA, Petersen ET, Luijten PR & Hoogduin H (2015). Examining the regional and cerebral depth-dependent BOLD cerebrovascular reactivity response at 7T. *Neuroimage* **114**, 239–248.
- Bijari PB, Wasserman BA & Steinman DA (2014). Carotid bifurcation geometry is an independent predictor of early wall thickening at the carotid bulb. *Stroke* **45**, 473–478.
- Binks AP, Cunningham VJ, Adams L & Banzett RB (2008). Gray matter blood flow change is unevenly distributed during moderate isocapnic hypoxia in humans. *J Appl Physiol* **104**, 212–217.
- Black MA, Cable NT, Thijssen DHJ & Green DJ (2008). Importance of measuring the time course of flow-mediated dilatation in humans. *Hypertension* **51**, 203–210.
- Blaha M, Benes V, Douville CM & Newell DW (2007). The effect of caffeine on dilated cerebral circulation and on diagnostic CO<sub>2</sub> reactivity testing. *J Clin Neurosci* **14**, 464–467.
- Boedtker E (2017). Acid – base regulation and sensing: Accelerators and brakes in metabolic regulation of cerebrovascular tone. *J Cereb Blood Flow Metab*; DOI: 10.1177/0271678X17733868.
- Boedtker E, Hansen KB, Boedtker DM, Aalkjaer C & Boron WF (2016). Extracellular H<sub>2</sub>O<sub>3</sub> is sensed by mouse cerebral arteries: Regulation of tone by receptor protein tyrosine phosphatase  $\gamma$ . *J Cereb Blood Flow Metab* **36**, 965–980.
- Boedtker E, Praetorius J, Matchkov V V., Stankevicius E, Mogensen S, Füchtbauer AC, Simonsen U, Füchtbauer EM & Aalkjaer C (2011). Disruption of NA<sup>+</sup>,HCO<sub>3</sub><sup>-</sup> cotransporter NBCn1 (slc4a7) Inhibits no-mediated vasorelaxation, smooth muscle Ca<sup>2+</sup>Sensitivity, and hypertension development in mice. *Circulation* **124**, 1819–1829.
- Bohlen HG (2015). Nitric Oxide and the Cardiovascular System. *Compr Physiol* **5**, 808–823.
- Bolduc V, Thorin-Trescases N & Thorin E (2013). Endothelium-dependent control of cerebrovascular functions through age: exercise for healthy cerebrovascular aging. *Am J Physiol Heart Circ Physiol* **305**, H620-33.
- Bolotina VM, Najibi S, Palacino JJ, Pagano PJ & Cohen R a (1994). Nitric oxide directly activates calcium-dependent potassium channels in vascular smooth muscle. *Nature* **368**, 850–853.

- van Bommel J, Trouwborst A, Schwarte L, Siegemund M, Ince C & Henny CP (2002). Intestinal and cerebral oxygenation during severe isovolemic hemodilution and subsequent hyperoxic ventilation in a pig model. *Anesthesiology* **97**, 660–670.
- Bonnet P, Rusch NJ & Harder DR (1991). Characterization of an outward K<sup>+</sup> current in freshly dispersed cerebral arterial muscle cells. *Pflugers Arch* **418**, 292–296.
- Bonvento G, Seylaz J & Lacombe P (1994). Widespread attenuation of the cerebrovascular reactivity to hypercapnia following inhibition of nitric oxide synthase in the conscious rat. *J Cereb Blood Flow Metab* **14**, 699–703.
- Boullin D, Bunting S, Blaso WP, Hunt TM & Moncada S (1979). Responses of human and baboon arteries to prostaglandin endoperoxides and biologically generated and synthetic prostacyclin: their relevance to cerebral arterial spasm in man. *Br J Pharmacol* 139–147.
- Bowton DL, Haddon WS, Prough DS, Adair N, Alford PT & Stump DA (1988). Theophylline effect on the cerebral blood flow response to hypoxemia. *Chest* **94**, 371–375.
- Brass L, Prohovnik I, Pavlakis S, DeVivo D, Piomelli S & Mohr J (1991). Middle cerebral artery blood velocity and cerebral blood flow in sickle cell disease. *Stroke* **22**, 27–30.
- Brassard P, Tymko MM & Ainslie PN (2016). Sympathetic control of the brain circulation: Appreciating the complexities to better understand the controversy. *Auton Neurosci Basic Clin* **207**, 37–47.
- Brawely B (1968). The Pathophysiology of Intracerebral Steal Following Carbon Dioxide Inhalation, an Experimental Study. *Scandinavian J Clin Lab Investig* **102**, XIII.
- Brian JE (1998). Carbon dioxide and the cerebral circulation. *Anesthesiology* **88**, 1365–1386.
- Brown M, Wade J & Marshall J (1985). Fundamental Importance of Arterial Oxygen Content in the Regulation of Cerebral Blood Flow in Man. *Brain* **108**, 81–93.
- Brown MM & Marshall J (1982). Effect of plasma exchange on blood viscosity and cerebral blood flow. *Br Med J* **284**, 1733–1736.
- Brown MM & Marshall J (1985). Regulation of Cerebral Blood Flow in Response to Changes in Blood Viscosity. *Lancet* **1**, 604–609.
- Brown MM & Pickles H (1982). Effect of epoprostenol ( prostacyclin , PGI<sub>2</sub> ) on cerebral blood flow in man. *J Neurol Neurosurg Psychiatry* **45**, 1033–1036.

- Brugniaux J V, Coombs GB, Barak OF, Dujic Z, Sekhon MS & Ainslie PN (2018). Highs and Lows of Hyperoxia: Physiological, Performance, and Clinical Aspects. *Am J Physiol - Regul Integr Comp Physiol*; DOI: 10.1093/cid/ciy165/4922283.
- Bruhn H, Fransson P & Frahm J (2001). Modulation of cerebral blood oxygenation by indomethacin: MRI at rest and functional brain activation. *J Magn Reson Imaging* **13**, 325–334.
- Bubb KJ, Trinder SL, Baliga RS, Patel J, Clapp LH, MacAllister RJ & Hobbs AJ (2014). Inhibition of phosphodiesterase 2 augments cGMP and cAMP signaling to ameliorate pulmonary hypertension. *Circulation* **130**, 496–507.
- Busija D (1983). Role of Prostaglandins in the Response of the Cerebral Circulation to Carbon Dioxide in Conscious Rabbits. *J Cereb Blood Flow Metab* 376–380.
- Busija D & Heistad D (1983). Effects of indomethacin on cerebral blood flow during hypercapnia in cats. *Am J Physiol Heart Circ Physiol* **244**, H519–H524.
- Calamante F, Ahlgren A, van Osch MJ & Knutsson L (2016). A novel approach to measure local cerebral haematocrit using MRI. *J Cereb Blood Flow Metab* **36**, 768–780.
- Caldwell HG, Ainslie PN, Ellis LA, Phillips AA & Flück D (2017). Stability in neurovascular function at 3800 m. *Physiol Behav* **182**, 62–68.
- Caldwell HG, Coombs GB, Tymko MM, Nowak-Flück D & Ainslie PN (2018). Severity-dependent influence of isocapnic hypoxia on reaction time is independent of neurovascular coupling. *Physiol Behav* **188**, 262–269.
- Cameron OG, Modell JG & Hariharan M (1990). Caffeine and Human Cerebral Blood Flow: a Positron Emission Tomography Study. *Life Sci* **47**, 1141–1146.
- Cannizzaro G, Garbin L, Clivati A & Pesce LI (1997). Correction of hypoxia and hypercapnia in COPD patients: effects on cerebrovascular flow. *Monaldi Arch Chest Dis* **52**, 9–12.
- Carson JL, Poses RM, Spence RK & Bonavita G (1988). Severity of anaemia and operative mortality and morbidity. *Lancet* **1**, 727–729.
- Carter HH, Atkinson CL, Heinonen IHA, Haynes A, Robey E, Smith KJ, Ainslie PN, Hoiland RL & Green DJ (2016a). Evidence for shear stress – mediated dilation of the internal carotid artery in humans. *Hypertension* **68**, 1217–1224.

- Carter HH, Atkinson CL, Heinonen IHA, Haynes A, Robey E, Smith KJ, Ainslie PN, Hoiland RL & Green DJ (2016b). Evidence for shear stress-mediated dilation of the internal carotid artery in humans. *Hypertension* **68**, 1217–1224.
- Celermajer DS, Sorensen KE, Gooch VM, Spiegelhalter J, Miller OI, Sullivan ID, Lloyd JK & Deanfield JE (1992). Non-invasive detection of endothelial dysfunction in children and adults at risk of atherosclerosis. *Lancet* **340**, 1111–1115.
- Chai Y, Zhang DM & Lin YF (2011). Activation of cGMP-dependent protein kinase stimulates cardiac ATP-sensitive potassium channels via a ROS/calmodulin/CaMKII signaling cascade. *PLoS One*; DOI: 10.1371/journal.pone.0018191.
- Chemtob S, Beharry K, Barna T, Varma DR & Aranda J V (1991). Differences in the effects in the newborn piglet of various nonsteroidal antiinflammatory drugs on cerebral blood flow but not on cerebrovascular prostaglandins. *Pediatr Res* **30**, 106–111.
- Chen JF, Eltzschig HK & Fredholm BB (2013). Adenosine receptors as drug targets-what are the challenges? *Nat Rev Drug Discov* **12**, 265–286.
- Chen Y (2000). Soluble Adenylyl Cyclase as an Evolutionarily Conserved Bicarbonate Sensor. *Science (80- )* **289**, 625–628.
- Chen Y & Parrish TB (2009). Caffeine's effects on cerebrovascular reactivity and coupling between cerebral blood flow and oxygen metabolism. *Neuroimage* **44**, 647–652.
- Claydon VE, Gulli G, Slessarev M, Appenzeller O, Zenebe G, Gebremedhin A & Hainsworth R (2008). Cerebrovascular responses to hypoxia and hypocapnia in Ethiopian high altitude dwellers. *Stroke* **39**, 336–342.
- Cohen PJ, Alexander SC, Smith TC, Reivich M & Wollman H (1967). Effects of hypoxia and normocarbica on cerebral blood flow and metabolism in conscious man. *J Appl Physiol* **23**, 183–189.
- Collins FS (2011). Reengineering Translational Science: The Time Is Right. *Sci Transl Med* **3**, 1–6.
- Cosby K, Partovi KS, Crawford JH, Patel RP, Reiter CD, Martyr S, Yang BK, Waclawiw MA, Zalos G, Xu X, Huang KT, Shields H, Kim-Shapiro DB, Schechter AN, Cannon RO & Gladwin MT (2003). Nitrite reduction to nitric oxide by deoxyhemoglobin vasodilates the human circulation. *Nat Med* **9**, 1498–1505.

- Coverdale NS, Badrov MB & Kevin Shoemaker J (2016). Impact of age on cerebrovascular dilation versus reactivity to hypercapnia. *J Cereb Blood Flow Metab*; DOI: 10.1177/0271678X15626156.
- Coverdale NS, Gati JS, Opalevych O, Perrotta A & Shoemaker JK (2014). Cerebral blood flow velocity underestimates cerebral blood flow during modest hypercapnia and hypocapnia. *J Appl Physiol* **117**, 1090–1096.
- Coverdale NS, Lalande S, Perrotta A & Shoemaker JK (2015). Heterogeneous patterns of vasoreactivity in the middle cerebral and internal carotid arteries. *Am J Physiol Heart Circ Physiol* **308**, H1030-1038.
- Coyle MG, Oh W & Stonestreet BS (1993). Effects of indomethacin on brain blood flow and cerebral metabolism in hypoxic newborn piglets. *Am J Physiol* **264**, H141–H149.
- Coyle P & Jokelainen PT (1982). Dorsal cerebral arterial collaterals of the rat. *Anat Rec* **203**, 397–404.
- Crossland RF, Durgan DJ, Lloyd EE, Phillips SC, Reddy AK, Marrelli SP & Bryan RM (2013). A new rodent model for obstructive sleep apnea: effects on ATP-mediated dilations in cerebral arteries. *Am J Physiol Regul Integr Comp Physiol* **305**, R334-42.
- Curran-Everett D (2017). CORP: Minimizing the chances of false positives and false negatives. *J Appl Physiol* **122**, 91–95.
- Dabertrand F, Nelson MT & Brayden JE (2012). Acidosis dilates brain parenchymal arterioles by conversion of calcium waves to sparks to activate BK channels. *Circ Res* **110**, 285–294.
- Daif AAA, Hassan YMAEM, Ghareeb NAE-G, Othman MM & Mohamed SAM (2012). Cerebral Effect of Acute Normovolemic Hemodilution During Brain Tumor Resection. *J Neurosurg Anesthesiol* **24**, 19–24.
- Davies NW (1990). Modulation of ATP-sensitive K<sup>+</sup> channels in skeletal muscle by intracellular protons. *Nature* **343**, 375–377.
- Davis RJ, Murdoch CE, Ali M, Purbrick S, Ravid R, Baxter GS, Tilford N, Sheldrick RLG, Clark KL & Coleman RA (2004). EP4 prostanoid receptor-mediated vasodilatation of human middle cerebral arteries. *Br J Pharmacol* **141**, 580–585.
- Dawson EA, Rathore S, Cable NT, Wright DJ, Morris JL & Green DJ (2010). Impact of

- catheter insertion using the radial approach on vasodilatation in humans. *Clin Sci* **118**, 633–640.
- Dawson EA, Secher NH, Dalsgaard MK, Ogoh S, Yoshiga CC, Gonza J, Steensberg A & Raven PB (2004). Standing up to the challenge of standing : a siphon does not support cerebral blood flow in humans. *Am J Physiol - Regul Integr Comp Physiol* **287**, 911–914.
- Dederich RA, Szeffler SJ & Green ER (1981). Intrasubject variation in sustained-release theophylline absorption. *J Allergy Clin Immunol* **67**, 465–471.
- Deegan BM, Sorond FA, Galica A, Lipsitz LA, O’Laighin G & Serrador JM (2011). Elderly women regulate brain blood flow better than men do. *Stroke* **42**, 1988–1993.
- Degerman E, Belfrage P & Manganiello VC (1997). Regulation of cGMP-inhibited Phosphodiesterase ( PDE3 )\*. *J Biol Chem* **272**, 6823–6827.
- Demoncheaux EAG, Higenbottam TW, Foster PJ, Borland CDR, Smith APL, Marriott HM, Bee D, Akamine S & Davies MB (2002). Circulating nitrite anions are a directly acting vasodilator and are donors for nitric oxide. *Clin Sci* **102**, 77–83.
- Dewey RC, Pieper HP & Hunt WE (1974). Experimental cerebral hemodynamics. Vasomotor tone, critical closing pressure, and vascular bed resistance. *J Neurosurg* **41**, 597–606.
- Dian-San S, Xiang-Rui W, Yongjun Z & Yan-Hua Z (2006). Low hematocrit worsens cerebral injury after prolonged hypothermic circulatory arrest in rats. *Can J Anaesth* **53**, 1220–1229.
- Dietrich HH, Ellsworth ML, Sprague RS & Dacey RG (2000). Red blood cell regulation of microvascular tone through adenosine triphosphate. *Am J Physiol Heart Circ Physiol* **278**, H1294–H1298.
- Dietrich HH, Horiuchi T, Xiang C, Hongo K, Falck JR & Dacey RG (2008). Mechanism of ATP-induced local and conducted vasomotor responses in isolated rat cerebral penetrating arterioles. *J Vasc Res* **46**, 253–264.
- Dietrich HH, Kajita Y & Dacey RG (1996). Local and conducted vasomotor responses in isolated rat cerebral arterioles. *Am J Physiol* **271**, H1109–H1116.
- Dimmeler S, Assmus B, Hermann C, Haendeler J & Zeiher AM (1998). Fluid Shear Stress

- Stimulates Phosphorylation of Akt in Human Endothelial Cells: Involvement in Suppression of Apoptosis. *Circ Res* **83**, 334–341.
- Dimmeler S, Fleming I, Fisslthaler B, Hermann C, Busse R & Zeiher AM (1999). Activation of nitric oxide synthase in endothelial cells by Akt-dependent phosphorylation. *Nature* **399**, 601–605.
- Dirnagl U, Hakim A, Macleod M, Fisher M, Howells D, Alan SM, Steinberg G, Planas A, Boltze J, Savitz S, Iadecola C & Meairs S (2013). A Concerted Appeal for International Cooperation in Preclinical Stroke Research. *Stroke* **44**, 1754–1760.
- Doctor A & Stamler JS (2011). Nitric Oxide Transport in Blood : A Third Gas in the Respiratory Cycle. *Compr Physiol* **1**, 541–568.
- Doepp F, Schreiber SJ, von Münster T, Rademacher J, Klingebiel R & Valdueza JM (2004). How does the blood leave the brain? A systematic ultrasound analysis of cerebral venous drainage patterns. *Neuroradiology* **46**, 565–570.
- Donahue MJ, Strother MK & Hendrikse J (2012). Novel MRI approaches for assessing cerebral hemodynamics in ischemic cerebrovascular disease. *Stroke* **43**, 903–915.
- Doyle MP, Pickering RA, DeWeert TM, Hoekstra JW & Pater D (1981). Kinetics and mechanism of the oxidation of human deoxyhemoglobin by nitrites. *J Biol Chem* **256**, 12393–12398.
- Droma Y, Hanaoka M, Basnyat B, Arjyal A, Neupane P, Pandit A, Sharma D, Miwa N, Ito M, Katsuyama Y, Ota M & Kubo K (2006). Genetic contribution of the endothelial nitric oxide synthase gene to high altitude adaptation in sherpas. *7*, 209–220.
- Drouin A, Bolduc V, Thorin-Trescases N, Belanger E, Fernandes P, Baraghis E, Lesage F, Gillis MA, Villeneuve L, Hamel E, Ferland G & Thorin E (2011). Catechin treatment improves cerebrovascular flow-mediated dilation and learning abilities in atherosclerotic mice. *Am J Physiol Hear Circ Physiol* **300**, H1032-43.
- Drouin A & Thorin E (2009). Flow-Induced Dilation Is Mediated By Akt-Dependent Activation of Endothelial Nitric Oxide Synthase-Derived Hydrogen Peroxide in Mouse Cerebral Arteries. *Stroke* **40**, 1827–1833.
- Duebener LF, Sakamoto T, Hatsuoka S, Stamm C, Zurakowski D, Vollmar B, Menger MD, Schäfers HJ & Jonas RA (2001). Effects of hematocrit on cerebral microcirculation and

- tissue oxygenation during deep hypothermic bypass. *Circulation* **104**, I260–I264.
- Duffin J, Sobczyk O, Crawley A, Poublanc J, Venkatraghavan L, Sam K, Mutch A, Mikulis D & Fisher J (2017). The Role of Vascular Resistance in BOLD Responses to Progressive Hypercapnia. *Hum Brain Mapp*; DOI: 10.1002/hbm.23751.
- Duling BBR & Berne RM (1970). Longitudinal Gradients in Periarteriolar Oxygen Tension. *Circ Res* **27**, 669–678.
- Dulla CG, Dobelis P, Pearson T, Frenguelli BG, Staley KJ & Masino SA (2005). Adenosine and ATP link PCO<sub>2</sub> to cortical excitability via pH. *Neuron* **48**, 1011–1023.
- Edvinsson L & Krause DN (2002). *Cerebral Blood Flow And Metabolism*, Second. Lippincott Williams & Wilkins.
- Vander Eecken HM & Adams RD (1953). The anatomy and functional significance of the meningeal arterial anastomoses of the human brain. *J Neuropathol Exp Neurol* **12**, 132–157. Available at: <http://www.ncbi.nlm.nih.gov/pubmed/13053234>.
- Ekelund A, Reinstrup P, Ryding E, Andersson AM, Molund T, Kristiansson KA, Romner B, Brandt L & Säveland H (2002). Effects of Iso- and hypervolemic hemodilution on regional cerebral blood flow and oxygen delivery for patients with vasospasm after aneurysmal subarachnoid hemorrhage. *Acta Neurochir (Wien)* **144**, 703–713.
- Ellis EF, Police RJ, Yancey L, McKinney JS & Amruthesh SC (1990). Dilation of cerebral arterioles by cytochrome p-450 metabolites of arachadonic acid. *Am J Physiol Heart Circ Physiol* **259**, 1171–1177.
- Ellis EF, Wei EP, Cockrell CS, Traweek DL, Saady JJ & Kontos HA (1980). The Effect of O<sub>2</sub> and CO<sub>2</sub> on Prostaglandin Levels in the Cat Cerebral Cortex. *Circ Res* **51**, 652–657.
- Ellis EF, Wei EP & Kontos A (1979). Vasodilation of cat cerebral prostaglandins arterioles by prostaglandins D<sub>2</sub>, E<sub>2</sub>, G<sub>2</sub>, and I<sub>2</sub>. *Am J Physiol Heart Circ Physiol* **6**, H381–H385.
- Ellsworth ML, Ellis CG, Goldman D, Stephenson AH, Dietrich HH & Sprague RS (2009). Erythrocytes: oxygen sensors and modulators of vascular tone. *Physiology (Bethesda)* **24**, 107–116.
- Ellsworth ML, Forrester T, Ellis CG & Dietrich HH (1995). The erythrocyte as a regulator of vascular tone. *Am J Physiol* **269**, H2155–H2161.
- Emerson TE & Raymond RM (1981). Involvement of adenosine in cerebral hypoxic

- hyperemia in the dog. *Am J Physiol Circ Physiol* **241**, H134–H138.
- Eriksson S, Hagenfeldt L, Law D, Patrono C, Pinca E & Wennmalm A (1983). Effect of prostaglandin synthesis inhibitors on basal and carbon dioxide stimulated cerebral blood flow in man. *Acta Physiol Scand* **117**, 203–211.
- Erzurum SC, Ghosh S, Janocha AJ, Xu W, Bauer S, Bryan NS, Tejero J, Hemann C, Hille R, Stuehr DJ, Feelisch M & Beall CM (2007). Higher blood flow and circulating NO products offset high-altitude hypoxia among Tibetans. *Proc Natl Acad Sci U S A* **104**, 17593–17598.
- Estevez AY & Phillis JW (1997). Hypercapnia-induced increases in cerebral blood flow: Roles of adenosine, nitric oxide and cortical arousal. *Brain Res* **758**, 1–8.
- Evans D (1985). On the measurement of the mean velocity of blood flow over the cardiac cycle using Doppler ultrasound. *Ultrasound Med Biol* **11**, 735–741.
- Faber JE, Chilian WM, Deindl E, Van Royen N & Simons M (2014). A brief etymology of the collateral circulation. *Arterioscler Thromb Vasc Biol* **34**, 1854–1859.
- Fåhræus R & Lindqvist T (1931). The Viscosity of the Blood in Narrow Capillary Tubes. *Am J Physiol* **96**, 562–568.
- Fan J-L, Burgess KR, Basnyat R, Thomas KN, Peebles KC, Lucas SJE, Lucas RAI, Donnelly J, Cotter JD & Ainslie PN (2010a). Influence of high altitude on cerebrovascular and ventilatory responsiveness to CO<sub>2</sub>. *J Physiol* **588**, 539–549.
- Fan JL et al. (2011). Influence of indomethacin on the ventilatory and cerebrovascular responsiveness to hypoxia. *Eur J Appl Physiol* **111**, 601–610.
- Fan JL, Burgess KR, Thomas KN, Peebles KC, Lucas SJE, Lucas RAI, Cotter JD & Ainslie PN (2010b). Influence of indomethacin on the ventilatory and cerebrovascular responsiveness to CO<sub>2</sub> and breathing stability: the influence of PCO<sub>2</sub> gradients. *Am J Physiol - Regul Integr Comp Physiol* **298**, R1648–R1658.
- Fanou EM, Knight XJ, Aviv RI, Hojjat S, Symons SP, Zhang L & Wintermark XM (2015). Effect of Collaterals on Clinical Presentation , Baseline Imaging , Complications , and Outcome in Acute Stroke.
- Faraci FM (2011). Protecting against vascular disease in brain. *Am J Physiol Hear Circ Physiol* **300**, H1566–H1582.

- Faraci FM, Baumbach GL & Heistad DD (1989). Myogenic mechanisms in the cerebral circulation. *J Hypertens* **7**, S61–S64.
- Faraci FM, Breese KR & Heistad DD (1994). Cerebral vasodilation during hypercapnia: Role of Glibenclamide-Sensitive Potassium Channels and Nitric Oxide. *Stroke* **25**, 1679–1683.
- Faraci FM & Heistad DD (1990). Regulation of large cerebral arteries and cerebral microvascular pressure. *Circ Res* **66**, 8–17.
- Faraci FM, Mayhan WG & Heistad DD (1987). Segmental vascular responses to acute hypertension in cerebrum and brain stem. *Am J Physiol Hear Circ Physiol* **252**, H738–H742.
- Faraci FM, Mayhan WG, Schmid PG & Heistad DD (1988). Effects of arginine vasopressin on cerebral microvascular pressure. *Am J Physiol* **255**, H70-6.
- Faraci FM & Sobey CG (1998). Role of potassium channels in regulation of cerebral vascular tone. *J Cereb blood flow Metab* **18**, 1047–1063.
- Fathi AR, Yang C, Bakhtian KD, Qi M, Lonser RR & Pluta RM (2011). Carbon dioxide influence on nitric oxide production in endothelial cells and astrocytes: Cellular mechanisms. *Brain Res* **1386**, 50–57.
- Feary JR, Rodrigues LC, Smith CJ, Hubbard RB & Gibson JE (2010). Prevalence of major comorbidities in subjects with COPD and incidence of myocardial infarction and stroke: a comprehensive analysis using data from primary care. *Thorax* **65**, 956–962.
- Fedderson B, Neupane P, Thanbichler F, Hadolt I, Sattelmeyer V, Pfefferkorn T, Waanders R, Noachtar S & Ausserer H (2015). Regional differences in the cerebral blood flow velocity response to hypobaric hypoxia at high altitudes. *J Cereb Blood Flow Metab* **35**, 1–6.
- Feigin VL et al. (2014). Global and regional burden of stroke during 1990-2010: findings from the Global Burden of Disease Study 2010. *Lancet (London, England)* **383**, 245–254.
- Feigin VL, Norrving B & Mensah GA (2017). Global Burden of Stroke. *Circ Res* **120**, 439–448.
- Fierstra J, MacHina M, Battisti-Charbonney A, Duffin J, Fisher JA & Minkovich L (2011).

- End-inspiratory rebreathing reduces the endtidal to arterial PCO<sub>2</sub> gradient in mechanically ventilated pigs. *Intensive Care Med* **37**, 1543–1550.
- Fierstra J, Poublanc J, Han JS, Silver F, Tymianski M, Crawley AP, Fisher JA & Mikulis DJ (2010). Steal physiology is spatially associated with cortical thinning. *J Neurol Neurosurg Psychiatry* **81**, 290–293.
- Fierstra J, Sobczyk O, Battisti-Charbonney A, Mandell DM, Poublanc J, Crawley AP, Mikulis DJ, Duffin J & Fisher JA (2013). Measuring cerebrovascular reactivity: what stimulus to use? *J Physiol* **591**, 5809–5821.
- Fischer DJ, Torrence NJ, Sprung RJ & Spence DM (2003). Determination of erythrocyte deformability and its correlation to cellular ATP release using microbore tubing with diameters that approximate resistance vessels in vivo. *Analyst* **128**, 1163–1168.
- Fischer R, Lang SM, Steiner U, Toepfer M, Hautmann H, Pongratz H & Huber RM (2000). Theophylline improves acute mountain sickness. *Eur Respir J* **15**, 123–127.
- Fisher J, Vaghaiwalla F, Tsitlik J, Levin H, Brinker J, Weisfeldt M & Yin F (1982). Determinants and clinical significance of jugular venous valve competence. *Circulation* **65**, 188–196.
- Fisher JA (2016). The CO<sub>2</sub> stimulus for cerebrovascular reactivity: Fixing inspired concentrations vs . targeting end-tidal partial pressures. *J Cereb Blood Flow Metab* **36**, 1004–1011.
- Fisher JA, Iscoe S & Duffin J (2016). Sequential gas delivery provides precise control of alveolar gas exchange. *Respir Physiol Neurobiol* **225**, 60–69.
- Fisher JA, Sobczyk O, Crawley A, Poublanc J, Dufort P, Venkatraghavan L, Sam K, Mikulis D & Duffin J (2017). Assessing Cerebrovascular Reactivity by the Pattern of Response to Progressive Hypercapnia. *Hum Brain Mapp*; DOI: 10.1002/hbm.23598.
- Fleming I, Hecker M & Busse R (1994). Intracellular alkalinization induced by bradykinin sustains activation of the constitutive nitric oxide synthase in endothelial cells. *Circ Res* **74**, 1220–1226.
- Florian M, Lu Y, Angle M & Magder S (2004). Estrogen induced changes in Akt-dependent activation of endothelial nitric oxide synthase and vasodilation. **69**, 637–645.
- Flück D, Beaudin AE, Steinback CD, Kumarpillai G, Shobha N, McCreary CR, Peca S,

- Smith EE & Poulin MJ (2014). Effects of aging on the association between cerebrovascular responses to visual stimulation, hypercapnia and arterial stiffness. *Front Physiol* **5**, 1–12.
- Flück D, Morris LE, Niroula S, Tallon CM, Sherpa KT, Stembridge M, Ainslie PN & McManus AM (2017). UBC-Nepal Expedition: Markedly lower cerebral blood flow in high altitude Sherpa children compared to children residing at sea-level. *J Appl Physiol*; DOI: 10.1152/jappphysiol.00292.2017.
- Flück D, Siebenmann C, Keiser S, Cathomen A & Lundby C (2015). Cerebrovascular reactivity is increased with acclimatization to 3,454 m altitude. *J Cereb blood flow Metab* **35**, 1323–1330.
- Fog M (1937). Cerebral Circulation: The Reaction Of The Pial Arteries To A Fall In Blood Pressure. *Arch Neurol Psychiatry* **37**, 351–364.
- Fog M (1939). Cerebral Circulation II: Reaction of Pial Arteries To Increase In Blood Pressure. *Arch Neurol Psychiatry* **41**, 260–268.
- Forrester T, Harper AM, MacKenzie ET & Thomson EM (1979). Effect of adenosine triphosphate and some derivatives on cerebral blood flow and metabolism. *J Physiol* **296**, 343–355.
- Foster GE, Ainslie PN, Stembridge M, Day TA, Bakker A, Lucas SJE, Lewis NCS, MacLeod DB & Lovering AT (2014). Resting pulmonary haemodynamics and shunting: a comparison of sea-level inhabitants to high altitude Sherpas. *J Physiol* **592**, 1397–1409.
- Francis SH & Corbin JD (1994). Structure and function of cyclic nucleotide-dependent protein kinases. *Annu Rev Physiol* **56**, 237–272.
- Fredricks KT, Liu Y, Rusch NJ & Lombard JH (1994). Role of endothelium and arterial K<sup>+</sup> channels in mediating hypoxic dilation of middle cerebral arteries. *Am J Physiol* **267**, H580–H586.
- Fuentes E & Palomo I (2015). Extracellular ATP metabolism on vascular endothelial cells: A pathway with pro-thrombotic molecules. *Vascul Pharmacol*; DOI: 10.1016/j.vph.2015.05.002.
- Fujii K, Heistad DD & Faraci FM (1991). Flow-mediated dilatation of the basilar artery in vivo. *Circ Res* **69**, 697–705.

- Fujii K, Heistad DD & Faraci FM (1992). Effect of diabetes mellitus on flow-mediated and endothelium-dependent dilation of the rat basilar artery. *Stroke* **23**, 1494–1498.
- Fulton D, Gratton J, McCabe TJ, Fontana J, Fujio Y, Walsh K, Franke TF, Papapetropoulos A & Sessa WC (1999). Regulation of endothelium-derived nitric oxide production by the protein kinase Akt. **399**, 597–601.
- Galvin SD, Celi LA, Thomas KN, Clendon TR, Galvin IF, Bunton RW & Ainslie PN (2010). Effects of age and coronary artery disease on cerebrovascular reactivity to carbon dioxide in humans. *Anaesth Intensive Care* **38**, 710–717.
- Garcia-Roldan JL & Bevan JA (1991). Augmentation of endothelium-independent flow constriction in pial arteries at high intravascular pressures. *Hypertension* **17**, 870–874.
- Gardner JP & Diecke FP (1988). Influence of pH on isometric force development and relaxation in skinned vascular smooth muscle. *Pflugers Arch Eur J Physiol* **412**, 231–239.
- Garrido E, Castelló A, Ventura JL, Capdevila A & Rodríguez FA (1993). Cortical atrophy and other brain magnetic resonance imaging (MRI) changes after extremely high-altitude climbs without oxygen. *Int J Sports Med* **14**, 232–234.
- Garrido E, Segura R, Capdevila A, Pujol J, Javierre C & Li Ventura J (1996). Are Himalayan Sherpas Better Protected against Brain Damage Associated with Extreme Altitude Climbs? *Clin Sci* **90**, 81–85.
- Gayeski TE, Federspiel WJ & Honig CR (1988). A graphical analysis of the influence of red cell transit time, carrier-free layer thickness, and intracellular PO<sub>2</sub> on blood-tissue O<sub>2</sub> transport. *Adv Exp Med Biol* **222**, 25–35.
- Gebremedhin D, Ma YH, Falck JR, Roman RJ, VanRollins M & Harder DR (1992). Mechanism of action of cerebral epoxyeicosatrienoic acids on cerebral arterial smooth muscle. *Am J Physiol* **263**, H519–H525.
- Gecse A, Ottlecz A, Mezei Z, Telegdy G & Joo F (1982). Prostacyclin and prostaglandin synthesis in isolated brain capillaries. *Prostaglandins*.
- Gibson GE, Pulsinelli W, Blass JP & Duffy TE (1981). Brain dysfunction in mild to moderate hypoxia. *Am J Med* **70**, 1247–1254.
- Gilbert-Kawai ET, Milledge JS, Grocott MPW & Martin DS (2014). King of the Mountains:

- Tibetan and Sherpa Physiological Adaptations for Life at High Altitude. *Physiology* **29**, 388–402.
- Giller C (2003). The Emperor Has No Clothes: Velocity, Flow, and the Use of TCD. *J Neuroimaging* **13**, 97–98.
- Giller CA, Bowman G, Dyer H, Mootz L & Krippner W (1993). Cerebral arterial diameters during changes in blood pressure and carbon dioxide during craniotomy. *Neurosurgery* **32**, 737–741.
- Gisolf J, van Lieshout JJ, van Heusden K, Pott F, Stok WJ & Karemaker JM (2004). Human cerebral venous outflow pathway depends on posture and central venous pressure. *J Physiol* **560**, 317–327.
- Gladwin MT, Raat NJH, Shiva S, Dezfulian C, Hogg N, Kim-Shapiro DB & Patel RP (2006). Nitrite as a vascular endocrine nitric oxide reservoir that contributes to hypoxic signaling, cytoprotection, and vasodilation. *Am J Physiol Heart Circ Physiol* **291**, H2026–H2035.
- Gladwin MT, Shelhamer JH, Schechter AN, Pease-Fye ME, Waclawiw MA, Panza JA, Ognibene FP & Cannon RO (2000). Role of circulating nitrite and S-nitrosohemoglobin in the regulation of regional blood flow in humans. *Proc Natl Acad Sci* **97**, 11482–11487.
- Glagov S, Zarins C, Giddens DP & Ku DN (1988). Hemodynamics and atherosclerosis. Insights and perspectives gained from studies of human arteries. *Arch Pathol Lab Med* **112**, 1018–1031.
- Glodzik L, Randall C, Rusinek H & de Leon M (2013). Cerebrovascular reactivity to carbon dioxide in Alzheimer’s disease. A review. *J Alzheimer’s Dis* **35**, 427–440.
- Goadsby PJ (1994). Nitric oxide is not the sole determinant of hypercapnic or metabolically driven vasodilation in the cerebral circulation. *J Auton Nerv Syst* **49**, 67–72.
- Göbel U, Theilen H & Kuschinsky W (1990). Congruence of total and perfused capillary network in rat brains. *Circ Res* **66**, 271–281.
- González-Alonso J, Richardson RS & Saltin B (2001). Exercising skeletal muscle blood flow in humans responds to reduction in arterial oxyhaemoglobin, but not to altered free oxygen. *J Physiol* **530**, 331–341.

- Gordon GRJ, Choi HB, Rungta RL, Ellis-Davies GCR & MacVicar BA (2008). Brain metabolism dictates the polarity of astrocyte control over arterioles. *Nature* **456**, 745–750.
- Gottstein U & Paulson OB (1972). The Effect of Intracarotid Aminophylline Infusion on the Cerebral Circulation. *Stroke* **3**, 560–565.
- Goueli SA & Ahmed K (1980). Indomethacin and inhibition of protein kinase reactions. *Nature* **287**, 171–172.
- Green DJ, Dawson EA, Groenewoud HMM, Jones H & Thijssen DHJ (2014). Is flow-mediated dilation nitric oxide mediated?: A meta-analysis. *Hypertension* **63**, 376–382.
- Green DJ, Hopman MTE, Padilla J, Laughlin MH & Thijssen DHJ (2017). Vascular Adaptation to Exercise in Humans: Role of Hemodynamic Stimuli. *Physiol Rev* **97**, 495–528.
- Green DJ, Jones H, Thijssen D, Cable NT & Atkinson G (2011). Flow-Mediated Dilation and Cardiovascular Event Prediction: Does Nitric Oxide Matter ? *Hypertension* **57**, 363–369.
- Greitz D, Wirestam R, Franck A, Nordell B, Thomsen C & Ståhlberg F (1992). Pulsatile brain movement and associated hydrodynamics studied by magnetic resonance phase imaging. The Monro-Kellie doctrine revisited. *Neuroradiology* **34**, 370–380.
- Grotta J, Ackerman R, Correia J, Fallick G & Chang J (1982). Whole blood viscosity parameters and cerebral blood flow. *Stroke* **13**, 296–301.
- Grüne F, Kazmaier S, Stolker RJ, Visser GH & Weyland A (2015). Carbon dioxide induced changes in cerebral blood flow and flow velocity: role of cerebrovascular resistance and effective cerebral perfusion pressure. *J Cereb Blood Flow Metab* **35**, 1470–1477.
- Gupta A, Chazen JL, Hartman M, Delgado D, Anumula N, Shao H, Mazumdar M, Segal AZ, Kamel H, Leifer D & Sanelli PC (2012). Cerebrovascular reserve and stroke risk in patients with carotid stenosis or occlusion: A systematic review and meta-analysis. *Stroke* **43**, 2884–2891.
- Hackett PH (1999). The cerebral etiology of high-altitude cerebral edema and acute mountain sickness. *Wilderness Environ Med* **10**, 97–109.
- Hagen AA, White RP & Robertson JT (1979). Synthesis of prostaglandins and thromboxane B<sub>2</sub> by cerebral arteries. *Stroke* **10**, 306–309.

- Hall CN, Reynell C, Gesslein B, Hamilton NB, Mishra A, Sutherland BA, O'Farrell FM, Buchan AM, Lauritzen M & Attwell D (2014). Capillary pericytes regulate cerebral blood flow in health and disease. *Nature* **508**, 55–60.
- Haller C & Kuschinsky W (1987). Moderate hypoxia: reactivity of pial arteries and local effect of theophylline. *J Appl Physiol* **63**, 2208–2215.
- Hamilton NB, Attwell D & Hall CN (2010). Pericyte-mediated regulation of capillary diameter: a component of neurovascular coupling in health and disease. *Front Neuroenergetics* **2**, 1–14.
- Han J, Kim N, Joo H, Kim E & Earm YE (2002). ATP-sensitive K<sup>+</sup> channel activation by nitric oxide and protein kinase G in rabbit ventricular myocytes. *Am J Physiol Hear Circ Physiol* **283**, 1545–1554.
- Han J, Kim N, Kim E, Ho W-KK & Earm YE (2001). Modulation of ATP-sensitive Potassium Channels by cGMP-dependent Protein Kinase in Rabbit Ventricular Myocytes. *J Biol Chem* **276**, 22140–22147.
- Hansen AB, Hoiland RL, Lewis NCS, Tymko MM, Tremblay JC, Stembridge M, Nowak-Flück D, Carter HH, Bailey DM & Ainslie PN (2018). UBC-Nepal expedition: The use of oral antioxidants does not alter cerebrovascular function at sea level or high altitude. *Exp Physiol*; DOI: 10.1113/EP086887.
- Hardebo JE, Kåhrström J & Owman C (1987). P<sub>1</sub>- and P<sub>2</sub>-purine receptors in brain circulation. *Eur J Pharmacol* **144**, 343–352.
- Harder DR & Madden JA (1985). Cellular mechanism of force development in cat middle cerebral artery by reduced PCO<sub>2</sub>. *Pflugers Arch* **403**, 402–406.
- Hare GMT (2004). Anaemia and the brain. *Curr Opin Anaesthesiol* **17**, 363–369.
- Hare GMT (2006). At what point does hemodilution harm the brain? *Can J Anaesth* **53**, 1171–1174.
- Harper a M & Glass HI (1965a). Effect of alterations in the arterial carbon dioxide tension on the blood flow through the cerebral cortex at normal and low arterial blood pressures. *J Neurol Neurosurg Psychiatry* **28**, 449–452.
- Harper AM & Bell RA (1963). The effect of metabolic acidosis and alkalosis on the blood flow through the cerebral cortex. *J Neurol Neurosurg Psychiatry* **471**, 341–345.

- Harper AM & Glass HI (1965*b*). Effects of alterations in the arterial CO<sub>2</sub> tension on the blood flow through the cerebral cortex at normal and low arterial blood pressures. *J Neurol Neurosurg Psychiat* **28**, 449–453.
- Harrell JW & Schrage WG (2014). Cyclooxygenase-derived vasoconstriction restrains hypoxia-mediated cerebral vasodilation in young adults with metabolic syndrome. *Am J Physiol Heart Circ Physiol* **306**, H261-9.
- Hartmann SE, Pialoux V, Leigh R & Poulin MJ (2012). Decreased cerebrovascular response to CO<sub>2</sub> in post-menopausal females with COPD: Role of oxidative stress. *Eur Respir J* **40**, 1354–1361.
- Hatt A, Cheng S, Tan XK, Sinkus R & Bilston LE (2015). MR elastography can be used to measure brain stiffness changes as a result of altered cranial venous drainage during jugular compression. *Am J Neuroradiol* **36**, 1971–1977.
- Hearon CM & Dinunno FA (2016). Regulation of skeletal muscle blood flow during exercise in ageing humans. *J Physiol* **594**, 2261–2273.
- Hedera P, Bujdaková J & Traubner P (1994). Compressions of Carotid and Vertebral Arteries in Assessment of Intracranial Collateral Flow: Correlation Between Angiography and Transcranial Doppler Ultrasonography. *Angiology* **45**, 1039–1045.
- Hein TW, Xu W, Ren Y & Kuo L (2013). Cellular signalling pathways mediating dilation of porcine pial arterioles to adenosine A<sub>2A</sub> receptor activation. *Cardiovasc Res* **99**, 156–163.
- Heistad DD, Marcus ML & Abboud FM (1978). Role of large arteries in regulation of cerebral blood flow in dogs. *J Clin Invest* **62**, 761.
- Heitzer T, Schlinzig T, Krohn K, Meinertz T & Münzel T (2001). Endothelial Dysfunction, Oxidative Stress, and Risk of Cardiovascular Events in Patients With Coronary Artery Disease. *Circulation* **104**, 2673–2678.
- van Helvoort HAC, Heijdra YF, Heunks LMA, Meijer PLM, Ruitenbeek W, Thijs HMM & Dekhuijzen PNR (2006). Supplemental oxygen prevents exercise-induced oxidative stress in muscle-wasted patients with chronic obstructive pulmonary disease. *Am J Respir Crit Care Med* **173**, 1122–1129.
- Heyman BA, Patterson JL & Duke TW (1952). Cerebral circulation and metabolism in sickle

- cell and other chronic anemias, with observations on the effects of oxygen inhalation. *J Clin Invest* **824–828**.
- Heymsfield SB, Chirachariyavej T, Rhyu IJ, Roongpisuthipong C, Heo M & Pietrobelli A (2009). Differences between brain mass and body weight scaling to height: potential mechanism of reduced mass-specific resting energy expenditure of taller adults. *J Appl Physiol* **106**, 40–48.
- Hino A, Ueda S, Mizukawa N, Imahori Y & Tenjin H (1992). Effect of hemodilution on cerebral hemodynamics and oxygen metabolism. *Stroke* **23**, 423–426.
- Hisamoto K, Ohmichi M, Kurachi H, Hayakawa J, Kanda Y, Nishio Y, Adachi K, Tasaka K, Miyoshi E, Fujiwara N, Taniguchi N & Murata Y (2001). Estrogen Induces the Akt-dependent Activation of Endothelial Nitric-oxide Synthase in Vascular Endothelial Cells \*. *276*, 3459–3467.
- Hochachka PW, Clark CM, Monge C, Stanley C, Brown WD, Stone CK, Nickles RJ & Holden JE (1996). Sherpa brain glucose metabolism and defense adaptations against chronic hypoxia. *J Appl Physiol (Bethesda, Md 1985)* **81**, 1355–1361.
- Hoffman WE, Albrecht RF & Miletich DJ (1984a). The role of adenosine in CBF increases during hypoxia in young vs aged rats. *Stroke* **15**, 124–129.
- Hoffman WE, Albrecht RF & Miletich DJ (1984b). Cerebrovascular Response to Hypoxia in Young vs Aged Rats. *Stroke* **15**, 141–143.
- Hoffman WE, Albrecht RF & Miletich DJ (2013). The role of adenosine in CBF increases during hypoxia in young vs aged rats. *Stroke* **15**, 124–129.
- Hoi Y, Gao L, Tremmel M, Paluch RA, Siddiqui AH, Meng H & Mocco J (2008). In vivo assessment of rapid cerebrovascular morphological adaptation following acute blood flow increase. *J Neurosurg* **109**, 1141–1147.
- Hoiland RL & Ainslie PN (2016a). CrossTalk proposal: The middle cerebral artery diameter does change during alterations in arterial blood gases and blood pressure. *J Physiol* **594**, 4073–4075.
- Hoiland RL & Ainslie PN (2016b). Rebuttal from Ryan L. Hoiland and Philip N. Ainslie. *J Physiol* **0**, 4081.
- Hoiland RL & Ainslie PN (2017). Reply from Ryan L. Hoiland. *J Physiol* **595**, 3673–3675.

- Hoiland RL, Ainslie PN, Wildfong KW, Smith KJ, Bain AR, Willie CK, Foster G, Monteleone B & Day TA (2015). Indomethacin-induced impairment of regional cerebrovascular reactivity: Implications for respiratory control. *J Physiol* **593**, 1291–1306.
- Hoiland RL, Bain AR, Rieger MG, Bailey DM & Ainslie PN (2016a). Hypoxemia, oxygen content, and the regulation of cerebral blood flow. *Am J Physiol - Regul Integr Comp Physiol* **310**, R398–R413.
- Hoiland RL, Bain AR, Tymko MM, Rieger MG, Howe CA, Willie CK., Hansen AB, Flück D, Wildfong KWWKW, Stembridge M, Subedi P, Anholm JD & Ainslie PN (2017a). Adenosine receptor-dependent signaling is not obligatory for normobaric and hypobaric hypoxia-induced cerebral vasodilation in humans. *J Appl Physiol* **122**, 795–808.
- Hoiland RL, Bain AR, Tymko MM, Rieger MG, Howe CA, Willie CK, Hansen AB, Flück D, Wildfong KW, Stembridge M, Subedi P, Anholm JD & Ainslie PN (2017b). Adenosine receptor dependent signaling is not obligatory for normobaric and hypobaric hypoxia-induced cerebral vasodilation in humans. *J Appl Physiol* **122**, 795–808.
- Hoiland RL, Howe CA, Coombs GB & Ainslie PN (2018a). Ventilatory and cerebrovascular regulation and integration at high-altitude. *Clin Auton Res*; DOI: 10.1007/s10286-018-0522-2.
- Hoiland RL, Mijacika T, Mladinov S, Stembridge M, Barak OF, Dujic Z, Willie CK & Ainslie PN (2018b). Oxygen therapy improves cerebral oxygen delivery and neurovascular function in hypoxaemic chronic obstructive pulmonary disease patients. 1–8.
- Hoiland RL, Smith KJ, Carter HH, Lewis NCS, Tymko MM, Wildfong KW, Bain AR, Green DJ & Ainslie PN (2017c). Shear-mediated dilation of the internal carotid artery occurs independent of hypercapnia. *Am J Physiol - Hear Circ Physiol* **313**, 24–31.
- Hoiland RLRL, Tymko MMMM, Bain ARAR, Wildfong KWKW, Monteleone B & Ainslie PNP (2016b). Carbon dioxide mediated vasomotion of extra-cranial cerebral arteries in humans: A role for prostaglandins? *J Physiol* **594**, 3463–3481.
- Holloway RL (2008). The Human Brain Evolving: A Personal Retrospective. *Annu Rev Anthropol* **37**, 1–19.
- Hori D, Nomura Y, Ono M, Joshi B, Mandal K, Cameron D, Kocherginsky M & Hogue CW

- (2017). Optimal blood pressure during cardiopulmonary bypass defined by cerebral autoregulation monitoring. *J Thorac Cardiovasc Surg* **154**, 1590–1598.e2.
- Horiuchi T, Dietrich HH, Hongo K & Dacey RG (2003). Comparison of P2 receptor subtypes producing dilation in rat intracerebral arterioles. *Stroke* **34**, 1473–1478.
- Horiuchi T, Dietrich HH, Tsugane S & Dacey RG (2001). Analysis of purine- and pyrimidine-induced vascular responses in the isolated rat cerebral arteriole. *Am J Physiol Heart Circ Physiol* **280**, H767–H776.
- Horscroft JA et al. (2017). Metabolic basis to Sherpa altitude adaptation. *Proc Natl Acad Sci* **114**, 6382–6387.
- Horvath I, Sandor NT, Ruttner Z & McLaughlin a C (1994). Role of nitric oxide in regulating cerebrocortical oxygen consumption and blood flow during hypercapnia. *J Cereb blood flow Metab* **14**, 503–509.
- Hosseini L, Weiner M, Levin MA & Fischer GW (2016). Methylene Blue: Magic Bullet for Vasoplegia? *Anesth Analg* **122**, 194–201.
- Howarth C, Sutherland BA, Choi HB, Martin C, Lind BL, Khennouf L, LeDue JM, Pakan JMP, Ko RWY, Ellis-Davies G, Lauritzen M, Sibson NR, Buchan AM & MacVicar BA (2017). A Critical Role for Astrocytes in Hypercapnic Vasodilation in Brain. *J Neurosci* **37**, 2403–2414.
- Howe CA, Hoiland RL, MacLeod DB, Tremblay JC, Carter HH, Patrician A, Stembridge M, Williams A, Delorme E, Rieger MG, Tymko MM, Gasho C, Santoro A, Green DJ & Ainslie PN (n.d.). UBC-Nepal Expedition: Peripheral and Cerebral Blood Flow and Blood Vessel Function Following Hemodilution at High-Altitude.
- Hsu P, Shibata M & Leffler C (1993). Prostanoid synthesis in response to high CO<sub>2</sub> in newborn pig brain microvascular endothelial cells. *Am J ...* **264**, H1485–H1492.
- Huang SY, Moore LG, McCullough RE, McCullough RG, Micco AJ, Fulco C, Cymerman A, Manco-Johnson M, Weil J V & Reeves JT (1987). Internal carotid and vertebral arterial flow velocity in men at high altitude. *J Appl Physiol* **63**, 395–400.
- Huang SY, Sun S, Droma T, Zhuang J, Tao JX, McCullough RG, McCullough RE, Micco a J, Reeves JT & Moore LG (1992). Internal carotid arterial flow velocity during exercise in Tibetan and Han residents of Lhasa (3,658 m). *J Appl Physiol* **73**, 2638–2642.

- Huang Z, Shiva S, Kim-Shapiro DB, Patel RP, Ringwood LA, Irby CE, Huang KT, Ho C, Hogg N, Schechter AN & Gladwin MT (2005). Enzymatic function of hemoglobin as a nitrite reductase that produces NO under allosteric control. *J Clin Invest* **115**, 2099–2107.
- Hudak ML, Jones MD, Popel AS, Koehler RC, Traystman RJ & Zeger SL (1989). Hemodilution causes size-dependent constriction of pial arterioles in the cat. *Am J Physiol* **257**, H912–7.
- Hudak ML, Koehler C, Rosenberg AA, Traystman RJ & Jones MD (1986). Effect of hematocrit on cerebral blood flow. *Am J Physiol* **251**, 63–70.
- Hudetz a G, Shen H & Kampine JP (1998). Nitric oxide from neuronal NOS plays critical role in cerebral capillary flow response to hypoxia. *Am J Physiol* **274**, H982–H989.
- Hudetz AG, Wood JD, Biswal BB, Krolo I & Kampine JP (1999). Effect of hemodilution on RBC velocity, supply rate, and hematocrit in the cerebral capillary network. *J Appl Physiol* **87**, 505–509.
- Humphrey PR, du Boulay GH, Marshall J, Pearson TC, Russell RW, Slater NG, Symon L, Wetherley-Mein G & Zilkha E (1980a). Viscosity, cerebral blood flow and haematocrit in patients with paraproteinaemia. *Acta Neurol Scand* **61**, 201–209.
- Humphrey PR, Du Boulay GH, Marshall J, Pearson TC, Russell RW, Symon L, Wetherley-Mein G & Zilkha E (1979). Cerebral blood-flow and viscosity in relative polycythaemia. *Lancet* **2**, 873–877.
- Humphrey PR, Michael J & Pearson TC (1980b). Management of relative polycythaemia: studies of cerebral blood flow and viscosity. *Br J Haematol* **46**, 427–433.
- Iadecola C (2004). Neurovascular regulation in the normal brain and in Alzheimer’s disease. *Nat Rev Neurosci* **5**, 347–360.
- Iadecola C (2010). The overlap between neurodegenerative and vascular factors in the pathogenesis of dementia. *Acta Neuropathol* **120**, 287–296.
- Iadecola C (2017). The Neurovascular Unit Coming of Age: A Journey through Neurovascular Coupling in Health and Disease. *Neuron* **96**, 17–42.
- Iadecola C & Zhang F (1994). Nitric oxide-dependent and -independent components of cerebrovasodilation elicited by hypercapnia. *Am J Physiol* **266**, R546–R552.

- Iadecola C & Zhang F (1996). Permissive and obligatory responses of NO in cerebrovascular responses to hypercapnia and acetylcholine. *Am J Physiol Regul Integr Comp Physiol* **271**, R990–R1001.
- Iadecola C, Zhang F & Xu X (1993). Role of nitric oxide synthase-containing vascular nerves in cerebrovasodilation elicited from cerebellum. *Am J Physiol* **264**, R738–R746.
- Iadecola C, Zhang F & Xu X (1994). SIN-1 reverses attenuation of hypercapnic cerebrovasodilation by nitric oxide synthase inhibitors. *Am J Physiol* **267**, R228–35.
- Ibaraki M, Shinohara Y, Nakamura K, Miura S, Kinoshita F & Kinoshita T (2010). Interindividual variations of cerebral blood flow, oxygen delivery, and metabolism in relation to hemoglobin concentration measured by positron emission tomography in humans. *J Cereb blood flow Metab* **30**, 1296–1305.
- Ide K, Eliasziw M & Poulin MJ (2003). Relationship between middle cerebral artery blood velocity and end-tidal PCO<sub>2</sub> in the hypocapnic-hypercapnic range in humans. *J Appl Physiol* **95**, 129–137.
- Ide K, Worthley M, Anderson T & Poulin MJ (2007). Effects of the nitric oxide synthase inhibitor L-NMMA on cerebrovascular and cardiovascular responses to hypoxia and hypercapnia in humans. *J Physiol* **584**, 321–332.
- Ikeuchi Y & Nishizaki T (1995). ATP activates the potassium channel and enhances cytosolic Ca<sup>2+</sup> release via a P2Y purinoceptor linked to pertussis toxin-insensitive G-protein in brain artery endothelial cells. *Biochem Biophys Res Commun* **215**, 1022–1028.
- Imray CHE, Chan CWM, Stubbings A, Rhodes H, Patey S, Wilson MH, Bailey DM & Wright AD (2013). Time course variations in the mechanisms by which cerebral oxygen delivery is maintained on exposure to hypoxia/altitude. *High Alt Med Biol* **11**, 1–18.
- Imray CHE, Chan CWM, Stubbings A, Rhodes H, Patey S, Wilson MH, Bailey DM & Wright AD (2014). Time course variations in the mechanisms by which cerebral oxygen delivery is maintained on exposure to hypoxia/altitude. *High Alt Med Biol* **15**, 21–27.
- Irikura K, Huang PL, Ma J, Lee WS, Dalkara T, Fishman MC, Dawson TM, Snyder SH & Moskowitz MA (1995). Cerebrovascular alterations in mice lacking neuronal nitric oxide synthase gene expression. *Proc Natl Acad Sci U S A* **92**, 6823–6827.
- Irikura K, Maynard KI, Lee WS & Moskowitz MA (1994). L-NNA decreases cortical

- hyperemia and brain cGMP levels following CO<sub>2</sub> inhalation in Sprague-Dawley rats. *Am J Physiol Hear Circ Physiol* **267**, H837–H843.
- Ito H, Ibaraki M, Kanno I, Fukuda H & Miura S (2005a). Changes in the Arterial Fraction of Human Cerebral Blood Volume during Hypercapnia and Hypocapnia Measured by Positron Emission Tomography. *J Cereb Blood Flow Metab* **25**, 852–857.
- Ito H, Kanno I & Fukuda H (2005b). Human cerebral circulation: positron emission tomography studies. *Ann Nucl Med* **19**, 65–74.
- Ito H, Kanno I, Ibaraki M & Hatazawa J (2002a). Effect of aging on cerebral vascular response to Paco<sub>2</sub> changes in humans as measured by positron emission tomography. *J Cereb Blood Flow Metab* **22**, 997–1003.
- Ito H, Kanno I, Ibaraki M, Hatazawa J & Miura S (2003a). Changes in Human Cerebral Blood Flow and Cerebral Blood Volume During Hypercapnia and Hypocapnia Measured by Positron Emission Tomography. *J Cereb Blood Flow Metab* **23**, 665–670.
- Ito H, Kanno I, Takahashi K, Ibaraki M & Miura S (2003b). Regional distribution of human cerebral vascular mean transit time measured by positron emission tomography. *Neuroimage* **19**, 1163–1169.
- Ito H, Kinoshita T, Tamura Y, Yokoyama I & Iida H (1999). Effect of intravenous dipyridamole on cerebral blood flow in humans. A PET study. *Stroke* **30**, 1616–1620.
- Ito H, Yokoyama I, Iida H, Kinoshita T, Hatazawa J, Shimosegawa E, Okudera T & Kanno I (2000). Regional differences in cerebral vascular response to PaCO<sub>2</sub> changes in humans measured by positron emission tomography. *J Cereb Blood Flow Metab* **20**, 1264–1270.
- Ito H, Yokoyama I, Tamura Y, Kinoshita T, Hatazawa J, Kawashima R & Iida H (2002b). Regional Changes in Human Cerebral Blood Flow during Dipyridamole Stress: Neural Activation in the Thalamus and Prefrontal Cortex. *Neuroimage* **16**, 788–793.
- Ito S, Mardimae A, Han J, Duffin J, Wells G, Fedorko L, Minkovich L, Katznelson R, Meineri M, Arenovich T, Kessler C & Fisher JA (2008). Non-invasive prospective targeting of arterial PCO<sub>2</sub> in subjects at rest. *J Physiol* **586**, 3675–3682.
- Iwabuchi T, Kutsuzawa T, Ikeda K & Nakamura T (1973). Effects of blood gases on the pressure-flow relationships in canine cerebral circulation. *Stroke* **4**, 65–72.
- Iwamoto E, Bock JM & Casey DP (2018). Blunted shear-mediated dilation of the internal but

not common carotid artery in response to lower body negative pressure. ; DOI:  
10.1074/jbc.M109.090936.

Jagger JE, Bateman RM, Ellsworth ML, Ellis CG, Justin E & Ells- ML (2001). Role of erythrocyte in regulating local O<sub>2</sub> delivery mediated by hemoglobin oxygenation. *Am J Physiol Heart Circ Physiol* **280**, H2833-9.

Jahshan S, Dayan L & Jacob G (2017). Nitric oxide-sensitive guanylyl cyclase signaling affects CO<sub>2</sub> -dependent, but not pressure-dependent regulation of cerebral blood flow. *Am J Physiol - Regul Integr Comp Physiol* **312**, R948–R955.

Jansen GFA et al. (2014). Role of the altitude level on cerebral autoregulation in residents at high altitude. 518–523.

Jansen GFA & Basnyat B (2011). Brain blood flow in Andean and Himalayan high-altitude populations: evidence of different traits for the same environmental constraint. *J Cereb blood flow Metab* **31**, 706–714.

Jansen GFA, Krins A & Basnyat B (1999). Cerebral vasomotor reactivity at high altitude in humans. *J Appl Physiol* **86**, 681–686.

Jansen GFA, Krins A, Basnyat B, Bosch A & Odoom JA (2000). Cerebral autoregulation in subjects adapted and not adapted to high altitude. *Stroke* **31**, 2314–2318.

Jansen GFA, Krins A, Basnyat B, Odoom JA & Ince C (2007). Role of the altitude level on cerebral autoregulation in residents at high altitude. *J Appl Physiol* **103**, 518–523.

Jaruchart T, Suwanwela NC, Tanaka H & Suksom D (2016). Arterial stiffness is associated with age-related differences in cerebrovascular conductance. *Exp Gerontol* **73**, 59–64.

Jensen JB, Sperling B, Severinghaus JW & Lassen NA (1996). Augmented hypoxic cerebral vasodilation in men during 5 days at 3,810 m altitude. *J Appl Physiol* **80**, 1214–1218.

Jensen JB, Wright AD, Lassen NA, Harvey TC, Winterborn MH, Raichle ME & Bradwell AR (1990). Cerebral blood flow in acute mountain sickness. *J Appl Physiol* **69**, 430–433.

Jia L, Bonaventura C, Bonaventura J & Stamler JS (1996). S-nitrosohaemoglobin: a dynamic activity of blood involved in vascular control. *Nature* **380**, 221–226.

Jiang C & Haddad GG (1994). A direct mechanism for sensing low oxygen levels by central neurons. *Proc Natl Acad Sci U S A* **91**, 7198–7201.

- Jiang H, Anderson GD & McGiff JC (2010). Red blood cells (RBCs), epoxyeicosatrienoic acids (EETs) and adenosine triphosphate (ATP). *Pharmacol Reports* **62**, 468–474.
- Jiang H, Colbran JL, Francis SH & Corbin JD (1992). Direct Evidence for Cross-activation of cGMP-dependent Protein Kinase by cAMP in Pig Coronary Arteries. *J Biol Chem* **267**, 1015–1019.
- Jiang H, Quilley J, Reddy LM, Falck JR, Wong PYK & McGiff JC (2005). Red blood cells: Reservoirs of cis- and trans-epoxyeicosatrienoic acids. *Prostaglandins Other Lipid Mediat* **75**, 65–78.
- Jiang H, Zhu AG, Mamczur M, Falck JR, Lerea KM & McGiff JC (2007). Stimulation of rat erythrocyte P2X 7 receptor induces the release of epoxyeicosatrienoic acids. *Br J Pharmacol* **151**, 1033–1040.
- Jordan J, Shannon JR, Diedrich a., Black B, Costa F, Robertson D & Biaggioni I (2000). Interaction of Carbon Dioxide and Sympathetic Nervous System Activity in the Regulation of Cerebral Perfusion in Humans. *Hypertension* **36**, 383–388.
- Joshi S, Mangla S, Wang M, Sciacca RR & Young WL (2002). Intra-arterial Xe-133 measurements suggest a dose-dependent increase in cerebral blood flow during intracarotid infusion of adenosine in nonhuman primates. *J Neurosurg Anesthesiol* **14**, 108–113.
- Joshi S, Young WL, Duong DH, Ostapkovich ND, Aagaard BD, Hashimoto T & Pile-Spellman J (2000). Intracarotid infusion of the nitric oxide synthase inhibitor, L-NMMA, modestly decreases cerebral blood flow in human subjects. *Anesthesiology* **93**, 699–707.
- Joshi S, Young WL, Pile-Spellman J, Duong DH, Vang MC, Hacin-bey L, Lee HT & Ostapkovich N (1998). The Feasibility of Intracarotid Adenosine for the Manipulation of Human Cerebrovascular Resistance. *Neurosurg Anesth* **87**, 1291–1298.
- Kajita Y, Dietrich HH & Dacey RG (1996). Effects of oxyhemoglobin on local and propagated vasodilatory responses induced by adenosine, adenosine diphosphate, and adenosine triphosphate in rat cerebral arterioles. *J Neurosurg* **85**, 908–916.
- Kakkar R, Raju RVS & Sharma RK (1999). Calmodulin-dependent cyclic nucleotide phosphodiesterase (PDE1). *Cell Mol Life Sci* **55**, 1164–1186.

- Kalaria RN & Harik SI (1988). Adenosine receptors and the nucleoside transporter in human brain vasculature. *J Cereb Blood Flow Metab* **8**, 32–39.
- Kalsi KK & González-Alonso J (2012). Temperature-dependent release of ATP from human erythrocytes: mechanism for the control of local tissue perfusion. *Exp Physiol* **97**, 419–432.
- Kantor H & Hampton M (1978). Indomethacin in submicromolar concentrations inhibits cyclic AMP-dependent protein kinase. *Nature* **276**, 841–842.
- Karnik R, Valentin A, Winkler WB, Khaffaf N, Donath P & Slany J (1996). Sex-related differences in acetazolamide-induced cerebral vasomotor reactivity. *Stroke* **27**, 56–58.
- Kastrup A, Thomas C, Hartmann C & Schabet M (1997). Sex dependency of cerebrovascular CO<sub>2</sub> reactivity in normal subjects. *Stroke* **28**, 2353–2356.
- Kastrup A, Dichgans J, Niemeier M & Schabet M (1998). Changes of cerebrovascular CO<sub>2</sub> reactivity during normal aging. *Stroke* **29**, 1311–1314.
- Kastrup A, Happe V, Hartmann C & Schabet M (1999a). Gender-related effects of indomethacin on cerebrovascular CO<sub>2</sub> reactivity. *J Neurol Sci* **162**, 127–132.
- Kastrup A, Krüger G, Glover GH, Neumann-Haefelin T & Moseley ME (1999b). Regional variability of cerebral blood oxygenation response to hypercapnia. *Neuroimage* **10**, 675–681.
- Kawano T, Zoga V, Kimura M, Liang M-Y, Wu H-E, Gemes G, McCallum JB, Kwok W-M, Hogan QH & Sarantopoulos CD (2009). Nitric Oxide Activates ATP-Sensitive Potassium Channels in Mammalian Sensory Neurons: Action by Direct S-Nitrosylation. *Mol Pain* **5**, 1744-8069-5–12.
- Kellawan JM, Harrell JW, Schrauben EM, Hoffman CA, Roldan-Alzate A, Schrage WG & Wieben O (2015). Quantitative cerebrovascular 4D flow MRI at rest and during hypercapnia challenge. *Magn Reson Imaging* **34**, 422–428.
- Kellawan MJ, Harrell JW, Roldan-Alzate A, Wieben O & Schrage WG (2016). Regional hypoxic cerebral vasodilation facilitated by diameter changes primarily in anterior versus posterior circulation. *J Cereb Blood Flow Metab* **37**, 2025–2034.
- Kellie G (1824). An account of the appearances observed in the dissection of two of three individuals presumed to have perished in the storm of the 3rd, and whose bodies were

- discovered in the vicinity of Leith on the morning of the 4th, November 1821: with some reflectio. *Trans Medico-Chirurgical Soc Edinburgh* 82–169.
- Kerrick WG & Hoar PE (1981). Inhibition of smooth muscle tension by cyclic AMP-dependent protein kinase. *Nature* **292**, 253–255.
- Kety S & Schmidt C (1945). The determination of cerebral blood flow in man by the use of nitrous oxide in low concentrations. *Am J Physiol* **143**, 53–66.
- Kety SS & Schmidt CF (1948a). The Nitrous Oxide Method for the Quantitative Determination of Cerebral Blood Flow in Man: Theory, Procedure and Normal Values. *J Clin Invest* **27**, 476–483.
- Kety SS & Schmidt CF (1948b). the Effects of Altered Arterial Tensions of Carbon Dioxide and Oxygen on Cerebral Blood Flow and Cerebral Oxygen Consumption of Normal Young Men. *J Clin Invest* **27**, 484–492.
- Kety SS & Schmidt CF (1948c). The effects of altered arterial tensions of carbon dioxide and oxygen on cerebral blood flow and cerebral oxygen consumption of normal young men. *J Clin Invest* **27**, 484–492.
- Kielstein JT, Donnerstag F, Gasper S, Menne J, Kielstein A, Martens-Lobenhoffer J, Scalera F, Cooke JP, Fliser D & Bode-Böger SM (2006). ADMA increases arterial stiffness and decreases cerebral blood flow in humans. *Stroke* **37**, 2024–2029.
- Kielstein JT, Impraim B, Simmel S, Bode-Böger SM, Tsikas D, Frölich JC, Hoepfer MM, Haller H & Fliser D (2004). Cardiovascular Effects of Systemic Nitric Oxide Synthase Inhibition with Asymmetrical Dimethylarginine in Humans. *Circulation* **109**, 172–177.
- Kikuchi Y (1979). Reduced Deformability of Erythrocytes Exposed to Hypercapnia. *Experientia* **35**, 343–344.
- Kinoshita H & Katusic ZS (1997). Role of potassium channels in relaxations of isolated canine basilar arteries to acidosis. *Stroke* **28**, 433–437.
- Kitano M, Oldendorf WH & Cassen B (1964). The Elasticity of the Cranial Blood Pool. *J Nucl Med* **5**, 613–625.
- Kleiser B & Widdern B (1992). Course of cerebrovascular reactivity in patients with carotid artery occlusions. *Stroke* **23**, 171–174.
- Klößner U & Isenberg G (1994a). Calcium channel current of vascular smooth muscle cells:

- extracellular protons modulate gating and single channel conductance. *J Gen Physiol* **103**, 665–678.
- Klößner U & Isenberg G (1994b). Intracellular pH modulates the availability of vascular L-type Ca<sup>2+</sup> channels. *J Gen Physiol* **103**, 647–663.
- Koehler RC & Traystman RJ (1982). Bicarbonate ion modulation of cerebral blood flow during hypoxia and hypercapnia. *Am J Physiol* **243**, H33-40.
- Koller A & Toth P (2012). Contribution of flow-dependent vasomotor mechanisms to the autoregulation of cerebral blood flow. *J Vasc Res* 375–389.
- Kontos HA, Raper AJ & Patterson JL (1977a). Analysis of vasoactivity of local pH, PCO<sub>2</sub> and bicarbonate on pial vessels. *Stroke* **8**, 358–360.
- Kontos HA & Wei EP (1996). Arginine analogues inhibit responses mediated by ATP-sensitive K<sup>+</sup> channels. *Am J Physiol* **271**, H1498-506.
- Kontos HA, Wei EP, Ellis EF, Jenkins LW, Povlishock JT, Rowe GT & Hess ML (1985). Appearance of superoxide anion radical in cerebral extracellular space during increased prostaglandin synthesis in cats. *Circ Res* **57**, 142–151.
- Kontos HA, Wei EP, Povlishock JT & Christman CW (1984). Oxygen radicals mediate the cerebral arteriolar dilation from arachidonate and bradykinin in cats. *Circ Res* **55**, 295–303.
- Kontos HA, Wei EP, Povlishock JT, Dietrich WD, Magiera CJ & Ellis EF (1980). Cerebral Arteriolar Damage by Arachidonic Acid and Prostaglandin G<sub>2</sub>. *Science (80- )* **209**, 1242–1245.
- Kontos HA, Wei EP, Raper AJ & Patterson JL (1977b). Local mechanism of CO<sub>2</sub> action of cat pial arterioles. *Stroke* **8**, 226–229.
- Kooijman M, Thijssen DHJ, de Groot PCE, Bleeker MWP, van Kuppevelt HJM, Green DJ, Rongen GA, Smits P & Hopman MTE (2008). Flow-mediated dilatation in the superficial femoral artery is nitric oxide mediated in humans. *J Physiol* **586**, 1137–1145.
- Korosue K & Heros RC (1992). Mechanism of cerebral blood flow augmentation by hemodilution in rabbits. *Stroke* **23**, 1487-1492; discussion 1492-1493.
- Korosue K, Ishida K, Matsuoka H, Nagao T, Tamaki N & Matsumoto S (1988). Clinical, hemodynamic, and hemorheological effects of isovolemic hemodilution in acute

- cerebral infarction. *Neurosurgery* **23**, 148–153.
- Koźniewska E, Oseka M & Styś T (1992). Effects of endothelium-derived nitric oxide on cerebral circulation during normoxia and hypoxia in the rat. *J Cereb blood flow Metab* **12**, 311–317.
- Kruuse C, Jacobsen TB, Thomsen LL, Hasselbalch SG, Frandsen EK, Dige-Petersen H & Olesen J (2000). Effects of the non-selective phosphodiesterase inhibitor pentoxifylline on regional cerebral blood flow and large arteries in healthy subjects. *Eur J Neurol* **7**, 629–638.
- Kukreja RC, Kontos HA, Hess ML & Ellis EF (1986). PGH synthase and lipoxygenase generate superoxide in the presence of NADH or NADPH. *Circ Res* **59**, 612–619.
- Kulik TB, Aronhime SN, Echeverry G, Beylin A & Winn HR (2010). The relationship between oxygen and adenosine in astrocytic cultures. *Glia* **58**, 1335–1344.
- Kunze H & Vogt W (1971). Significance of Phospholipase A for Prostaglandin Formation. *Ann N Y Acad Sci* **180**, 123–125.
- Kupper TEAH, Strohl KP, Hoefler M, Gieseler U, Netzer CM & Netzer NC (2008). Low-dose theophylline reduces symptoms of acute mountain sickness. *J Travel Med* **15**, 307–314.
- Kurtz A (1987). Adenosine Stimulates Guanylate Cyclase Activity in Vascular Smooth Muscle Cells. *J Biol Chem* **262**, 6296–6300.
- Kuschinsky W, Wahl M, Bosse O & Thureau K (1972). Perivascular Potassium and pH as Determinants of Local Pial Arterial Diameter in Cats: A MICROAPPLICATION STUDY. *Circ Res* **31**, 240–247.
- Kuwabara Y, Sasaki M, Hirakata H, Koga H, Nakagawa M, Chen T, Kaneko K, Masuda K & Fujishima M (2002). Cerebral blood flow and vasodilatory capacity in anemia secondary to chronic renal failure. *Kidney Int* **61**, 564–569.
- Lahiri S & Milledge JS (1965). Sherpa physiology. *Nature* **207**, 610–612.
- Lahousse L, Tiemeier H, Ikram MA & Brusselle GG (2015). Chronic obstructive pulmonary disease and cerebrovascular disease: A comprehensive review. *Respir Med* **109**, 1371–1380.
- Lambertsen CJJ, Gelfand R, Semple SJG, Smyth MG & Gelfand R (1961). H<sup>+</sup> and pCO<sub>2</sub> as chemical factors in respiratory and cerebral circulatory control. *J Appl Physiol* **16**, 473–

- Lammertsma AA, Brooks DJ, Beaney RP, Turton DR, Kensett MJ, Heather JD, Marshall J & Jones T (1984). In Vivo Measurement of Regional Cerebral Haematocrit Using Positron Emission Tomography. *J Cereb Blood Flow Metab* **4**, 317–322.
- Langill L & O'Donnell F (1986). Reductions in Arterial Diameter Produced by Chronic Decreases in Blood Flow are Endothelium Dependent. *Science (80- )* **231**, 405–407.
- Lassen LH, Sperling B, Andersen AR & Olesen J (2005). The effect of i.v. L-NG methylarginine hydrochloride (L-NMMA: 546C88) on basal and acetazolamide (Diamox®) induced changes of blood velocity in cerebral arteries and regional cerebral blood flow in man. *Cephalalgia* **25**, 344–352.
- Lassen NA (1959). Cerebral Blood Flow and Oxygen Consumption in Man. *Physiol Rev.*
- Lavi S (2006). Impaired cerebral CO<sub>2</sub> vasoreactivity: association with endothelial dysfunction. *AJP Hear Circ Physiol* **291**, H1856–H1861.
- Lavi S, Egbarya R, Lavi R & Jacob G (2003). Role of nitric oxide in the regulation of cerebral blood flow in humans: Chemoregulation versus mechanoregulation. *Circulation* **107**, 1901–1905.
- Lawley JS, Levine BD, Williams MA, Malm J, Eklund A, Polaner DM, Subudhi AW, Hackett PH & Roach RC (2015). Cerebral spinal fluid dynamics: Effect of hypoxia and implications for high-altitude illness. *J Appl Physiol* [jap.00370.2015](#).
- Lawley JS, Macdonald JH, Oliver SJ & Mullins PG (2017). Unexpected reductions in regional cerebral perfusion during prolonged hypoxia. *J Physiol* **595**, 935–947.
- St. Lawrence KS, Ye FQ, Lewis BK, Weinberger DR, Frank JA & McLaughlin AC (2002). Effects of indomethacin on cerebral blood flow at rest and during hypercapnia: An arterial spin tagging study in humans. *J Magn Reson Imaging* **15**, 628–635.
- Leffler C & Busija D (1985). Prostanoids in cortical subarachnoid cerebrospinal fluid and pial arterial diameter in newborn pigs. *Circ Res* **57**, 689–694.
- Leffler C & Busija D (1987). Prostanoids and pial arteriolar diameter in hypotensive newborn pigs. *Am J Physiol Heart Circ Physiol* **252**, 687–691.
- Leffler C, Mirro R, Pharris LJ & Shibata M (1994). Permissive role of prostacyclin in cerebral vasodilation to hypercapnia in newborn pigs. *Am J Physiol Heart Circ Physiol*

**267**, H285–H291.

Leffler CW & Balabanova L (2001). Mechanism of permissive prostacyclin action in cerebrovascular smooth muscle. *Prostaglandins Other Lipid Mediat* **66**, 145–153.

Leffler CW, Busija DW, Armstead WM, Shanklin DR, Mirro R & Thelin O (1990). Activated oxygen and arachidonate on newborn cerebral arterioles. *Am J Physiol Heart Circ Physiol* **259**, 1230–1238.

Leffler CW & Fedinec AL (1997). Newborn piglet cerebral microvascular responses to epoxyeicosatrienoic acids. *Am J Physiol Heart Circ Physiol* **273**, H333–H338.

Leffler CW, Mirro R, Shibata M, Parfenova H, Armstead WM & Zuckerman S (1993). Effects of indomethacin on cerebral vasodilator responses to arachidonic acid and hypercapnia in newborn pigs. *Pediatr Res* **33**, 609–614.

Leffler CW, Mirro R, Thompson C, Shibata M, Armstead WM, Pourcyrous M & Thelin O (1991). Activated oxygen species do not mediate hypercapnia-induced cerebral vasodilation in newborn pigs. *Am J Physiol Circ Physiol* **261**, H335–H342.

Leffler CW & Parfenova H (1997). Cerebral arteriolar dilation to hypoxia: role of prostanoids. *Am J Physiol* **272**, H418–H424.

Leffler CW, Parfenova H, Jaggar JH, Wang R, Leffler CW, Parfenova H, Jaggar JH, Wang R, Charles W, Parfenova H, Jaggar JH & Wang R (2006). Carbon monoxide and hydrogen sulfide: gaseous messengers in cerebrovascular circulation. *J Appl Physiol* **100**, 1065–1076.

Leffler CW, Smith JS, Edrington JL, Zuckerman SL & Parfenova H (1997). Mechanisms of hypoxia-induced cerebrovascular dilation in the newborn pig. *Am J Physiol* **272**, H1323–H1332.

Leiper J & Vallance P (1999). Biological significance of endogenous methlarginines that inhibit nitric oxide synthases. *Cardiovasc Res* **43**, 542–548.

LeMarbre G, Stauber S, Khayat RN, Puleo DS, Skatrud JB & Morgan BJ (2003). Baroreflex-induced sympathetic activation does not alter cerebrovascular CO<sub>2</sub> responsiveness in humans. *J Physiol* **551**, 609–616.

Lennox WG & Gibbs EL (1932). The blood flow in the brain and the leg of man, and the changes induced by alteration of blood gases. *J Clin Invest* **1** 1155–1177.

- Leoni RF, Oliveira IAF, Pontes-Neto OM, Santos AC & Leite JP (2017). Cerebral blood flow and vasoreactivity in aging: an arterial spin labeling study. *Brazilian J Med Biol Res* **50**, 1–9.
- Leuenberger U a, Gray K & Herr MD (1999). Adenosine contributes to hypoxia-induced forearm vasodilation in humans. *J Appl Physiol* **87**, 2218–2224.
- Lewis NCS, Bailey DM, Dumanoir GR, Messinger L, Lucas SJE, Cotter JD, Donnelly J, McEneny J, Young IS, Stembridge M, Burgess KR, Basnet AS & Ainslie PN (2014a). Conduit artery structure and function in lowlanders and native highlanders: relationships with oxidative stress and role of sympathoexcitation. *J Physiol* **592**, 1009–1024.
- Lewis NCS, Messinger L, Monteleone B & Ainslie PN (2014b). Effect of acute hypoxia on regional cerebral blood flow: effect of sympathetic nerve activity. *J Appl Physiol* **116**, 1189–1196.
- Liao WC, Lin CL, Chang SN, Tu CY & Kao CH (2015). The association between chronic obstructive pulmonary disease and dementia: A population-based retrospective cohort study. *Eur J Neurol* **22**, 334–340.
- Lima B, Forrester MT, Hess DT & Stamler JS (2010). S-nitrosylation in cardiovascular signaling. *Circ Res* **106**, 633–646.
- Lin Y-F, Raab-Graham K, Jan YN & Jan LY (2004). NO stimulation of ATP-sensitive potassium channels: Involvement of Ras/mitogen-activated protein kinase pathway and contribution to neuroprotection. *Proc Natl Acad Sci U S A* **101**, 7799–7804.
- Lincoln TM, Cornwell TL & Taylor AE (1990). cGMP-dependent protein kinase mediates the reduction of Ca<sup>2+</sup> by cAMP in vascular smooth muscle cells. *Am J Physiol Cell Physiol* **258**, C399–C407.
- Lindauer U, Vogt J, Schuh-Hofer S, Dreier JP & Dirnagl U (2003). Cerebrovascular Vasodilation to Extraluminal Acidosis Occurs via Combined Activation of ATP-Sensitive and Ca<sup>2+</sup>-Activated Potassium Channels. *J Cereb Blood Flow Metab* **23**, 1227–1238.
- Liu J, Liu Y, Ren L, Li L, Wang Z, Liu S, Li S & Cao T (2016). Effects of race and sex on cerebral hemodynamics, oxygen delivery and blood flow distribution in response to high altitude. *Sci Rep* **6**, 30500.

- Liu W, Liu J, Lou X, Zheng D, Wu B, Wang DJJ & Ma L (2017). A longitudinal study of cerebral blood flow under hypoxia at high altitude using 3D pseudo-continuous arterial spin labeling. *Sci Rep* **7**, 43246.
- Liu X, Gebremedhin D, Harder DR & Koehler RC (2015). Contribution of epoxyeicosatrienoic acids to the cerebral blood flow response to hypoxemia. *J Appl Physiol* **119**, 1202–1209.
- Liu X, Li C, Falck JR, Harder DR & Koehler RC (2012a). Relative contribution of cyclooxygenases, epoxyeicosatrienoic acids, and pH to the cerebral blood flow response to vibrissal stimulation. *AJP Hear Circ Physiol* **302**, H1075–H1085.
- Liu X, Li C, Falck JR, Harder DR & Koehler RC (2012b). Relative contribution of cyclooxygenases, epoxyeicosatrienoic acids, and pH to the cerebral blood flow response to vibrissal stimulation. *AJP Hear Circ Physiol* **302**, H1075–H1085.
- LTOTTR TL-TOTTR (2017). A Randomized Trial of Long-Term Oxygen for COPD with Moderate Desaturation. *N Engl J Med* **375**, 1617–1627.
- Lu D et al. (2016). Ancestral Origins and Genetic History of Tibetan Highlanders. 580–594.
- Lu H, Xu F, Rodrigue KM, Kennedy KM, Cheng Y, Flicker B, Hebrank AC, Uh J & Park DC (2011). Alterations in cerebral metabolic rate and blood supply across the adult lifespan. *Cereb Cortex* **21**, 1426–1434.
- Lucas SJE, Burgess KR, Thomas KN, Donnelly J, Peebles KC, Lucas RAI, Fan J-L, Cotter JD, Basnyat R & Ainslie PN (2011). Alterations in cerebral blood flow and cerebrovascular reactivity during 14 days at 5050 m. *J Physiol* **589**, 741–753.
- Lucas SJE, Tzeng YC, Galvin SD, Thomas KN, Ogoh S & Ainslie PN (2010). Influence of changes in blood pressure on cerebral perfusion and oxygenation. *Hypertension* **55**, 698–705.
- MacArthur PH, Shiva S & Gladwin MT (2007). Measurement of circulating nitrite and S-nitrosothiols by reductive chemiluminescence. *J Chromatogr B Anal Technol Biomed Life Sci* **851**, 93–105.
- Macintyre I (2014). A hotbed of medical innovation: George Kellie (1770-1829), his colleagues at Leith and the Monro-Kellie doctrine. *J Med Biogr* **22**, 93–100.
- Madden J & Christman N (1999). Integrin signaling, free radicals, and tyrosine kinase

- mediate flow constriction in isolated cerebral arteries. *Am J Physiol Heart Circ Physiol* **277**, H2264–H2271.
- Madureira J, Castro P & Azevedo E (2017). Demographic and Systemic Hemodynamic Influences in Mechanisms of Cerebrovascular Regulation in Healthy Adults. *J Stroke Cerebrovasc Dis* **26**, 500–508.
- Magnussen I & Hoedt-Rasmussen K (1977). The effect of intraarterial administered aminophylline on cerebral hemodynamics in man. *Acta Neurol Scand* **55**, 131–136.
- Mandell DM, Han JS, Poublanc J, Crawley AP, Stainsby JA, Fisher JA & Mikulis DJ (2008). Mapping cerebrovascular reactivity using blood oxygen level-dependent MRI in patients with arterial steno-occlusive disease: Comparison with arterial spin labeling MRI. *Stroke* **39**, 2021–2028.
- Mardimae A, Balaban DY, Machina M a, Battisti-Charbonney A, Han JS, Katznelson R, Minkovich LL, Fedorko L, Murphy PM, Wasowicz M, Naughton F, Meineri M, Fisher J a & Duffin J (2012). The interaction of carbon dioxide and hypoxia in the control of cerebral blood flow. *Pflugers Arch* **464**, 345–351.
- Markus H & Cullinane M (2001). Severely impaired cerebrovascular reactivity predicts stroke and TIA risk in patients with carotid artery stenosis and occlusion. *Brain* **124**, 457–467.
- Markus HS (2000). Transcranial Doppler ultrasound. *Br Med Bull* **56**, 378–388.
- Markus HS, Vallance P & Brown MM (1994). Differential effect of three cyclooxygenase inhibitors on human cerebral blood flow velocity and carbon dioxide reactivity. *Stroke* **25**, 1760–1764.
- Marsh EE, Shaw ND, Klingman KM, Tiamfook-Morgan TO, Yialamas MA, Sluss PM & Hall JE (2011). Estrogen levels are higher across the menstrual cycle in African-American women compared with Caucasian women. *J Clin Endocrinol Metab* **96**, 3199–3206.
- Martin W, Cusack NJ, Carleton JS & Gordon JL (1985). Specificity of P2-purinoceptor that mediates endothelium-dependent relaxation of the pig aorta. *Eur J Pharmacol* **108**, 295–299.
- Mashour GA & Boock RJ (1999). Effects of shear stress on nitric oxide levels of human

- cerebral endothelial cells cultured in an artificial capillary system. *Brain Res* **842**, 233–238.
- Matteis M, Troisi E, Monaldo BC, Caltagirone C & Silvestrini M (1998). Age and Sex Differences in Cerebral Hemodynamics A Transcranial Doppler Study. *Stroke* **29**, 963–967.
- McCalden TA, Nath RG & Thiele K (1984). The role of prostacyclin in the hypercapnic and hypoxic cerebrovascular dilations. *Life Sci* **34**, 1801–1807.
- McLaren AT, David Mazer C, Zhang H, Liu E, Mok L & Hare GMT (2009). A potential role for inducible nitric oxide synthase in the cerebral response to acute hemodilution. *Can J Anesth* **56**, 502–509.
- McVerry F, Liebeskind DS & Muir KW (2012). Systematic review of methods for assessing leptomeningeal collateral flow. *AJNR Am J Neuroradiol* **33**, 576–582.
- Meno JR, Crum a V & Winn HR (2001). Effect of adenosine receptor blockade on pial arteriolar dilation during sciatic nerve stimulation. *Am J Physiol Heart Circ Physiol* **281**, H2018-27.
- Messina EJ, Sun D, Koller A, Wolin MS & Kaley G (1992). Role of endothelium-derived prostaglandins in hypoxia-elicited arteriolar dilation in rat skeletal muscle. *Circ Res* **71**, 790–796.
- Miekisiak G, Kulik T, Kusano Y, Kung D, Chen J-F & Winn HR (2008). Cerebral blood flow response in adenosine 2a receptor knockout mice during transient hypoxic hypoxia. *J Cereb blood flow Metab* **28**, 1656–1664.
- Miki N, Kawabe Y & Kuriyama K (1977). Activation of Cerebral Guanylate Cyclase by Nitric Oxide. *Biochem Biophys Res Commun* **75**, 851–856.
- Mikulis DJ, Krolczyk G, Desal H, Logan W, deVeber G, Dirks P, Tymianski M, Crawley A, Vesely A, Kassner A, Preiss D, Somogyi R & Fisher JA (2005). Preoperative and postoperative mapping of cerebrovascular reactivity in moyamoya disease by using blood oxygen level—dependent magnetic resonance imaging. *J Neurosurg* **103**, 347–355.
- Van Mil AHM, Spilt A, Van Buchem MA, Bollen ELEM, Teppema L, Westendorp RGJ & Blauw GJ (2002a). Nitric oxide mediates hypoxia-induced cerebral vasodilation in

- humans. *J Appl Physiol* **92**, 962–966.
- Van Mil AHM, Spilt A, Buchem MA Van, Bollen ELEM, Teppema L, Westendorp RGJ, Blauw GJ, Querido JS, Kennedy PM, Sheel AW, Physiol JA, Jawad AF, Tomaszewski M & Melhem ER (2002b). Nitric oxide mediates hypoxia-induced cerebral vasodilation in humans. *J Appl Physiol* **92**, 962–966.
- Milledge JS & Sorensen SC (1972). Cerebral arteriovenous difference in man native to high altitude. *J Appl Physiol* **32**, 687–689.
- Mishra A, Reynolds JP, Chen Y, Gourine A V, Rusakov D a & Attwell D (2016). Astrocytes mediate neurovascular signaling to capillary pericytes but not to arterioles. *Nat Neurosci* **19**, 1619–1627.
- Miyazaki M & Kato K (1965). Measurement of cerebral blood flow by ultrasonic Doppler technique; hemodynamic comparison of right and left carotid artery in patients with hemiplegia. *Jpn Circ J* **29**, 383–386.
- Miyoshi H, Nakaya Y & Moritoki H (1994). Nonendothelial-derived nitric oxide activates the ATP-sensitive K<sup>+</sup> channel of vascular smooth muscle cells. *FEBS Lett* **345**, 47–49.
- Modin A, Björne H, Herulf M, Alving K, Weitzberg E & Lundberg JON (2001). Nitrite-derived nitric oxide: A possible mediator of “acidic-metabolic” vasodilation. *Acta Physiol Scand* **171**, 9–16.
- Møller K (2010). Every breath you take: acclimatisation at altitude. *J Physiol* **588**, 1811–1812.
- Momoi H, Ikomi F & Ohhashi T (2003). Estrogen-induced augmentation of endothelium-dependent nitric oxide-mediated vasodilation in isolated rat cerebral small arteries. *Jpn J Physiol* **53**, 193–203.
- Monro A (1783). Observations on the structure and functions of the nervous system. *Edinburgh*.
- Moody DM, Bell MA & Challa VR (1990). Features of the cerebral vascular pattern that predict vulnerability to perfusion or oxygenation deficiency: An anatomic study. *Am J Neuroradiol* **11**, 431–439.
- Moore LG (2017). Measuring High-Altitude Adaptation. *J Appl Physiol*; DOI: 10.1152/jappphysiol.00321.2017.

- Morii S, Ngai C & Winn HR (1986). Reactivity of rat pial arterioles and venules to adenosine and carbon dioxide: with detailed description of the closed cranial window technique in rats. *J Cereb Blood Flow Metab* **6**, 34–41.
- Morii S, Ngai AC, Ko KR & Winn HR (1987a). Role of adenosine in regulation of cerebral blood flow: effects of theophylline during normoxia and hypoxia. *Am J Physiol Circ Physiol* **253**, H165–H175.
- Morii S, Ngai AC, Ko KR & Winn HR (1987b). Role of adenosine in regulation of cerebral blood flow: effects of theophylline during normoxia and hypoxia. *Am J Physiol Hear Circ Physiol* **22**, H165–H175.
- Morikawa T, Kajimura M, Nakamura T, Hishiki T, Nakanishi T, Yukutake Y, Nagahata Y, Ishikawa M, Hattori K, Takenouchi T, Takahashi T, Ishii I, Matsubara K, Kabe Y, Uchiyama S, Nagata E, Gadalla MM, Snyder SH & Suematsu M (2012). Hypoxic regulation of the cerebral microcirculation is mediated by a carbon monoxide-sensitive hydrogen sulfide pathway. *Proc Natl Acad Sci U S A* **109**, 1293–1298.
- Mosso A (1880). Sulla circolazione del sangue nel cervello dell'uomo. *Atti R Accad Lincei Mem Cl Sci Fis Mat Nat* **237–358**.
- Mosso A (1884). Applicazione della bilancia allo studio della circolazione sanguigna dell'uomo. *Atti R Accad Lincei Mem Cl Sci Fis Mat Nat* **XIX**, 531–543.
- Mosso A & Glinzer I (1892). Die Ermüdung: Aus dem italienischen übersetzt von J.glinzer.
- MRCWP (1981). Long Term Ddomiciliary Oxygen Therapy In Chronic Hypoxic Cor Pulmonale Complicating Chronic Bronchitis And Emphysema. Report of the Medical Research Council Working Party. *Lancet* **317**, 681–686.
- Mühling J, Dehne MG, Sablotzki A & Hempelmann G (1999). Cerebral blood flow velocity during isovolemic hemodilution and subsequent autologous blood retransfusion. *Can J Anaesth* **46**, 550–557.
- Muizelaar JP, Wei EP, Kontos HA & Becker DP (1986). Cerebral blood flow is regulated by changes in blood pressure and in blood viscosity alike. *Stroke* **17**, 44–48.
- Mullen MJ, Kharbanda RK, Cross J, Donald AE, Taylor M, Vallance P, Deanfield JE & MacAllister RJ (2001). Heterogenous nature of flow-mediated dilatation in human conduit arteries in vivo: relevance to endothelial dysfunction in hypercholesterolemia.

*Circ Res* **88**, 145–151.

Murkin JM (2005). Neurocognitive outcomes: the year in review. *Curr Opin Anaesthesiol* **18**, 57–62.

Nagao T, Ibayashi S, Sadoshima S, Fujii K, Fujii K, Ohya Y & Fujishima M (1996). Distribution and Physiological Roles of ATP-Sensitive K<sup>+</sup> Channels in. *Circ Res* **78**, 238–243.

Nakahata K, Kinoshita H, Hirano Y, Kimoto Y, Iranami H & Hatano Y (2003). Mild hypercapnia induces vasodilation via adenosine triphosphate-sensitive K<sup>+</sup> channels in parenchymal microvessels of the rat cerebral cortex. *Anesthesiology* **99**, 1333–1339.

Naqvi TZ & Hyuhn HK (2009). Cerebrovascular mental stress reactivity is impaired in hypertension. *Cardiovasc Ultrasound* **7**, 1–14.

Narumiya S, Sugimoto Y, Ushikubi F & Conclusions VI (1999). Prostanoid Receptors : Structures , Properties , and Functions. **79**, 1193–1226.

Nelson M, Patlak J, Worley J & Standen N (1990a). Calcium channels, potassium channels, and voltage dependence of arterial smooth muscle tone. *Am J Physiol* **259**, C3-18.

Nelson MT, Patlak JB, Worley JF & Standen NB (1990b). Calcium channels, potassium channels, and voltage dependence of arterial smooth muscle tone. *Am J Physiol* **259**, C3–C18.

Newell DW & Aaslid R (1992). Transcranial Doppler: clinical and experimental uses. *Cerebrovasc Brain Metab Rev* **4**, 122–143.

Ngai AC, Coyne EF, Meno JR, West GA & Winn HR (2001). Receptor subtypes mediating adenosine-induced dilation of cerebral arterioles. *Am J Physiol Hear Circ Physiol* **280**, H2329-35.

Nicolakakis N & Hamel E (2011). Neurovascular function in Alzheimer’s disease patients and experimental models. *J Cereb blood flow Metab* **31**, 1354–1370.

Nilsson GE & Lutz PL (2004). Anoxia Tolerant Brains. *J Cereb Blood Flow Metab* **475–486**.

Nirkko AC & Baumgartner RW (1996). Sex-Related Differences in Acetazolamide-Induced Cerebral Vasomotor Reactivity: A Statistical Misinterpretation? *Stroke* **27**, 56–58.

Nishimura M, Yoshioka A, Yamamoto M, Akiyama Y, Miyamoto K & Kawakami Y (1993). Effect of theophylline on brain tissue oxygenation during normoxia and hypoxia in

- humans. *J Appl Physiol* **74**, 2724–2728.
- Nishimura N, Schaffer CB, Friedman B, Lyden PD & Kleinfeld D (2007). Penetrating arterioles are a bottleneck in the perfusion of neocortex. *Proc Natl Acad Sci* **104**, 365–370.
- Niwa K, Haensel C, Ross ME & Iadecola C (2001). Cyclooxygenase-1 Participates in Selected Vasodilator Responses of the Cerebral Circulation. *Circ Res* **88**, 600–608.
- Niwa K, Lindauer U, Villringer a & Dirnagl U (1993). Blockade of nitric oxide synthesis in rats strongly attenuates the CBF response to extracellular acidosis. *J Cereb Blood Flow Metab* **13**, 535–539.
- Nobili F, Rodriguez G, Marengo S, De CF, Gambaro M, Castello C, Pontremoli R & Rosadini G (1993). Regional cerebral blood flow in chronic hypertension. A correlative study. *Stroke* **24**, 1148–1153.
- Nordstrom CH, Rehrna S, Siesjo BK & Westerberg E (1977). Adenosine in Rat Cerebral Cortex: Its Determination, Normal Values, and Correlation to AMP and Cyclic AMP during Shortlasting Ischemia. *Acta Physiol Scand* **101**, 63–71.
- NOTTG (1980). Continuous or nocturnal oxygen therapy in hypoxemic chronic obstructive lung disease: a clinical trial. *Ann Intern Med* **93**, 391–398.
- Numan T, Bain AR, Hoiland RL, Smirl JD, Lewis NC & Ainslie PN (2014). Static autoregulation in humans: a review and reanalysis. *Med Eng Phys* **36**, 1487–1495.
- Obrist WD, Thompson HK, Wang HS & Wilkinson WE (1975). Regional Cerebral Blood Flow Estimated by 133Xenon Inhalation. *Stroke* **6**, 245–256.
- Ogawa S, Handa N, Matsumoto M, Etani H, Yoneda S, Kimura K & Kamada T (1988). Carbon dioxide reactivity of the blood flow in human basilar artery estimated by the transcranial doppler method in normal men: a comparison with that of the middle cerebral artery. *Ultrasound Med Biol* **14**, 479–483.
- Ogoh S & Ainslie P (2009). Cerebral blood flow during exercise: mechanisms of regulation. *J Appl Physiol* 1370–1380.
- Ogoh S, Sato K, Nakahara H, Okazaki K, Subudhi AW & Miyamoto T (2013a). Effect of acute hypoxia on blood flow in vertebral and internal carotid arteries. *Exp Physiol* **98**, 692–698.

- Ogoh S, Sato K, Nakahara H, Okazaki K, Subudhi AW & Miyamoto T (2013b). Effect of acute hypoxia on blood flow in vertebral and internal carotid arteries. *Exp Physiol* **98**, 692–698.
- Ogoh S, Washio T, Sasaki H, Petersen LG, Secher NH & Sato K (2016). Coupling between arterial and venous cerebral blood flow during postural change. *Am J Physiol - Regul Integr Comp Physiol* **311**, R1255–R1261.
- Okamoto H, Hudetz a G, Roman RJ, Bosnjak ZJ & Kampine JP (1997). Neuronal NOS-derived NO plays permissive role in cerebral blood flow response to hypercapnia. *Am J Physiol* **272**, H559–H566.
- Oshima T, Karasawa F & Satoh T (2002). Effects of propofol on cerebral blood flow and the metabolic rate of oxygen in humans. *Acta Anaesthesiol Scand* **46**, 831–835.
- Ospina JA, Duckles SP & Krause DN (2003). 17 $\beta$ -Estradiol decreases vascular tone in cerebral arteries by shifting COX-dependent vasoconstriction to vasodilation. *Am J Physiol - Hear Circ Physiol* **285**, H241–H250.
- Oudegeest-Sander MH, van Beek AHEA, Abbink K, Olde Rikkert MGM, Hopman MTE & Claassen JAHR (2014). Assessment of dynamic cerebral autoregulation and cerebrovascular CO<sub>2</sub> reactivity in ageing by measurements of cerebral blood flow and cortical oxygenation. *Exp Physiol* **99**, 586–598.
- Pandit JJ, Mohan RM, Paterson ND & Poulin MJ (2003). Cerebral blood flow sensitivity to CO<sub>2</sub> measured with steady-state and Read's rebreathing methods. *Respir Physiol Neurobiol* **137**, 1–10.
- Panerai RB (2003). The critical closing pressure of the cerebral circulation. *Med Eng Phys* **25**, 621–632.
- Paola MD, Bozzali M, Fadda L, Musicco M, Sabatini U & Caltagirone C (2008). Reduced oxygen due to high-altitude exposure relates to atrophy in motor-function brain areas. *Eur J Neurol* **15**, 1050–1057.
- Paravicini TM, Miller A a, Drummond GR & Sobey CG (2006). Flow-induced cerebral vasodilatation in vivo involves activation of phosphatidylinositol-3 kinase, NADPH-oxidase, and nitric oxide synthase. *J Cereb Blood Flow Metab* **26**, 836–845.
- Parfenova H, Hsu P & Leffler CW (1995a). Dilator Prostanoid-induced cyclic AMP

- formation and release by Cerebral Microvascular Smooth Muscle Cells: Inhibition by indomethacin. *J Pharmacol Exp Ther* **272**, 44–52.
- Parfenova H & Leffler C (1996). Effects of hypercapnia on prostanoid and cAMP production by cerebral microvascular cell cultures. *Am J Physiol Cell Physiol* **270**, C1503–C1510.
- Parfenova H, Shibata M, Zuckerman S & Leffler CW (1994). CO<sub>2</sub> and cerebral circulation in newborn pigs: cyclic nucleotides and prostanoids in vascular regulation. *Am J Physiol Heart Circ Physiol* **266**, H1494–H1501.
- Parfenova H, Shibata M, Zuckerman S, Mirro R & Leffler CW (1993). cyclic nucleotides and cerebrovascular tone in newborn pigs. *Am J Physiol Heart Circ Physiol* **265**, H1972–H1982.
- Parfenova H, Zuckerman S & Leffler CW (1995*b*). Inhibitory effect of indomethacin on prostacyclin receptor-mediated cerebral vascular responses. *Am J Physiol Heart Circ Physiol* **268**, H1884–H1890.
- Park CW, Sturzenegger M, Douville CM, Aaslid R & Newell DW (2003). Autoregulatory response and CO<sub>2</sub> reactivity of the basilar artery. *Stroke* **34**, 34–39.
- Parsons AA & Whalley ET (1989). Effects of Prostanoids on Human and Rabbit Basilar Arteries Precontracted In Vitro. *Cephalalgia* **9**, 165–171.
- Patterson JL, Heyman A & Duke TW (1952). cerebral circulation and metabolism in chronic pulmonary emphysema. *Am J Med* **12**, 382–387.
- Paul KS, T WE, Forster C, Lye R & Dutton J (1982). Prostacyclin and cerebral vessel relaxation. *J Neurosurg* **57**, 334–340.
- Paul SM, Mytelka DS, Dunwiddie CT, Persinger CC, Munos BH, Lindborg SR & Schacht AL (2010). How to improve R&D productivity: the pharmaceutical industry's grand challenge. *Nat Rev Drug Discov*; DOI: 10.1038/nrd3078.
- Paulson OB, Parving HH, Olesen J & Skinhoj E (1973). Influence of carbon monoxide and of hemodilution on cerebral blood flow and blood gases in man. *J Appl Physiol* **35**, 111–116.
- Pearce WJ, Ashwal S & Cuevas J (1989). Direct effects of graded hypoxia on intact and denuded rabbit cranial arteries. *Am J Physiol* **257**, H824–H833.
- Pearce WJ, Reynier-Rebuffel AM, Lee J, Aubineau P, Ignarro L & Seylaz J (1990). Effects

- of methylene blue on hypoxic cerebral vasodilatation in the rabbit. *J Pharmacol Exp Ther* **254**, 616–625.
- Peebles KC, Ball OG, MacRae B a., Horsman HM & Tzeng YC (2012). Sympathetic regulation of the human cerebrovascular response to carbon dioxide. *J Appl Physiol* **113**, 700–706.
- Peebles KC, Richards AM, Celi L, McGrattan K, Murrell CJ & Ainslie PN (2008). Human cerebral arteriovenous vasoactive exchange during alterations in arterial blood gases. *J Appl Physiol* **105**, 1060–1068.
- Pelligrino DA, Koenig HM & Albrecht RF (1993). Nitric oxide synthesis and regional cerebral blood flow responses to hypercapnia and hypoxia in the rat. *J Cereb Blood Flow Metab* **13**, 80–87.
- Pelligrino DA & Wang Q (1998). Cyclic nucleotide crosstalk and the regulation of cerebral vasodilation. *Prog Neurobiol* **56**, 1–18.
- Pelligrino DA, Wang Q, Koenig HM & Albrecht RF (1995a). Role of nitric oxide, adenosine, N-methyl-D-aspartate receptors, and neuronal activation in hypoxia-induced pial arteriolar dilation in rats. *Brain Res* **704**, 61–70.
- Pelligrino DA, Wang Q, Koenig HM & Albrecht RF (1995b). Role of nitric oxide, adenosine, N-methyl-d-aspartate receptors, and neuronal activation in hypoxia-induced pial arteriolar dilation in rats. *Brain Res* **704**, 61–70.
- Pelligrino DA, Ye S, Tan F, Santizo RA, Feinstein DL & Wang Q (2000). Nitric-oxide-dependent pial arteriolar dilation in the female rat: Effects of chronic estrogen depletion and repletion. *Biochem Biophys Res Commun* **269**, 165–171.
- Peltonen GL, Harrell JW, Aleckson BP, LaPlante KM, Crain MK & Schrage WG (2016). Cerebral blood flow regulation in women across menstrual phase: differential contribution of cyclooxygenase to basal, hypoxic, and hypercapnic vascular tone. *Am J Physiol Integr Comp Physiol* **311**, R222–R231.
- Peltonen GL, Harrell JW, Rousseau CL, Ernst BS, Marino ML, Crain MK & Schrage WG (2015). Cerebrovascular regulation in men and women: stimulus-specific role of cyclooxygenase. *Physiol Rep* **3**, e12451.
- Peng HG, Arsen AI V, Nilsson H & Aalkjler C (1998). On the cellular mechanism for the

effect of acidosis on vascular tone. 517–525.

Phillips AA, Chan FH, Zheng MMZ, Krassioukov A V & Ainslie PN (2016). Neurovascular coupling in humans: Physiology, methodological advances and clinical implications. *J Cereb Blood Flow Metab* **36**, 647–664.

Phillis JW & DeLong RE (1987). An involvement of adenosine in cerebral blood flow regulation during hypercapnia. *Gen Pharmacol* **18**, 133–139.

Phillis JW & O'Regan MH (2003). Effects of adenosine receptor antagonists on pial arteriolar dilation during carbon dioxide inhalation. *Eur J Pharmacol* **476**, 211–219.

Phillis JW, O'Regan MH & Perkins LM (1993). Adenosine 5'-triphosphate release from the normoxic and hypoxic in vivo rat cerebral cortex. *Neurosci Lett* **151**, 94–96.

Pickard J & MacKenzie E (1973). Inhibition of prostaglandin synthesis and the response of baboon cerebral circulation to carbon dioxide. *Nature* **245**, 187–188.

Pickles H, Brown MM, Thomas M, Hewazy a H, Redmond S, Zilkha E & Marshall J (1984). Effect of indomethacin on cerebral blood flow, carbon dioxide reactivity and the response to epoprostenol (prostacyclin) infusion in man. *J Neurol Neurosurg Psychiatry* **47**, 51–55.

Pinard E, Puiroud S & Seylaz J (1989). Role of adenosine in cerebral hypoxic hyperemia in the unanesthetized rabbit. *Brain Res* **481**, 124–130.

Pinder AG, Rogers SC, Khalatbari A, Ingram TE & James PE (2009). The Measurement of Nitric Oxide and Its Metabolites in Biological Samples by Ozone-Based Chemiluminescence. In *Methods in Molecular Biology, Redox-Mediated Signal Transduction*, pp. 11–28. Available at: <http://link.springer.com/10.1007/978-1-59745-129-1>.

Pitsikoulis C, Bartels MN, Gates G, Rebmann RA, Layton AM & De Meersman RE (2008). Sympathetic drive is modulated by central chemoreceptor activation. *Respir Physiol Neurobiol* **164**, 373–379.

Pohl U, Herlan K, Huang A & Bassenge E (1991). EDRF-mediated shear-induced dilation opposes myogenic vasoconstriction in small rabbit arteries. *Am J Physiol* **261**, H2016-23.

Pohl U, Holtz J, Busse R & Basenge E (1986). Crucial Role of Endothelium in the

- Vasodilator Response to Increased Flow in Vivo. *Hypertension* **2**, 37–44.
- Poison JB, Krzanowski JJ, Goldman AL & Szentivanyi A (1978). Inhibition of Human Pulmonary Phosphodiesterase Activity By Therapeutic Levels of Theophylline. *Clin Exp Pharmacol Physiol* **5**, 535–539.
- Portegies MLP, de Bruijn RFAG, Hofman A, Koudstaal PJ & Ikram MA (2014). Cerebral vasomotor reactivity and risk of mortality: the Rotterdam Study. *Stroke* **45**, 42–47.
- Portegies MLP, Lahousse L, Joos GF, Hofman A, Koudstaal PJ, Stricker BH, Brusselle GG & Arfan Ikram M (2016). Chronic obstructive pulmonary disease and the risk of stroke the Rotterdam study. *Am J Respir Crit Care Med* **193**, 251–258.
- Poublanc J, Crawley AP, Sobczyk O, Montandon G, Sam K, Mandell DM, Dufort P, Venkatraghavan L, Duffin J, Mikulis DJ & Fisher JA (2015). Measuring cerebrovascular reactivity: The dynamic response to a step hypercapnic stimulus. *J Cereb Blood Flow Metab* **35**, 1746–1756.
- Poulin MJ, Fatemian M, Tansley JG, Connor DFO & Robbins PA (2002). Changes in cerebral blood flow during and after 48 h of both isocapnic and poikilocapnic hypoxia in humans. *Exp Physiol* **87**, 633–642.
- Poulin MJ, Liang PJ & Robbins P a (1996). Dynamics of the cerebral blood flow response to step changes in end-tidal PCO<sub>2</sub> and PO<sub>2</sub> in humans. *J Appl Physiol* **81**, 1084–1095.
- Poulin MJ, Liang PJ & Robbins P a (1998). Fast and slow components of cerebral blood flow response to step decreases in end-tidal PCO<sub>2</sub> in humans. *J Appl Physiol* **85**, 388–397.
- Price AK, Fischer DJ, Martin RS & Spence DM (2004). Deformation-induced release of ATP from erythrocytes in a poly(dimethylsiloxane)-based microchip with channels that mimic resistance vessels. *Anal Chem* **76**, 4849–4855.
- Price AK, Martin RS & Spence DM (2006). Monitoring erythrocytes in a microchip channel that narrows uniformly: Towards an improved microfluidic-based mimic of the microcirculation. *J Chromatogr A* **1111**, 220–227.
- Pries AR, Neuhaus D & Gaetgens P (1992). Blood viscosity in tube flow: dependence on diameter and hematocrit. *Am J Physiol Circ Physiol* **263**, H1770–H1778.
- Prince M, Bryce R, Albanese E, Wimo A, Ribeiro W & Ferri CP (2013). The global prevalence of dementia: A systematic review and metaanalysis. *Alzheimer's Dement* **9**,

63–75.

Prinz F, Schlange T & Asadullah K (2011). Believe it or not: How much can we rely on published data on potential drug targets? *Nat Rev Drug Discov* **10**, 712–713.

Przybyłowski T, Bangash M-F, Reichmuth K, Morgan BJ, Skatrud JB & Dempsey JA (2003). Mechanisms of the cerebrovascular response to apnoea in humans. *J Physiol* **548**, 323–332.

Pulsinelli WA (1985). Selective neuronal vulnerability: morphological and molecular characteristics. *Prog Brain Res* **63**, 29–37.

Purkayastha S & Sorond F (2014). Transcranial Doppler Ultrasound: Technique and Application. *Semin Neurol* **32**, 411–420.

Pyke KE & Tschakovsky ME (2007). Peak vs. total reactive hyperemia: which determines the magnitude of flow-mediated dilation? *J Appl Physiol* **102**, 1510–1519.

Qaseem A, Wilt TJ, Weinberger SE, Hanania NA, Criner G, van der Molen T, Marciniuk DD, Denberg T, Schunemann H, Wedzicha W, MacDonald R, Shekelle P & for the American College of Physicians the AC of CP (2011). Diagnosis and Management of Stable Chronic Obstructive Pulmonary Disease: A Clinical Practice Guideline Update from the American College of Physicians, American College of Chest Physicians, American Thoracic Society, and European Respiratory Society. *Ann Intern Med* **155**, 179–191.

Querido JS, Ainslie PN, Foster GE, Henderson WR, Halliwill JR, Ayas NT & Sheel AW (2013). Dynamic cerebral autoregulation during and following acute hypoxia: role of carbon dioxide. *J Appl Physiol* **114**, 1183–1190.

Querido JS, Godwin JB & Sheel AW (2008). Intermittent hypoxia reduces cerebrovascular sensitivity to isocapnic hypoxia in humans. *Respir Physiol Neurobiol* **161**, 1–9.

Querido JS, Kennedy PM & Sheel a W (2010). Hyperoxia attenuates muscle sympathetic nerve activity following isocapnic hypoxia in humans. *J Appl Physiol* **108**, 906–912.

Rahn H & Otis AB (1949). Man's respiratory response during acclimatization to high altitude. *Am J Physiol* **157**, 445–462.

Raichle ME & Gusnard DA (2002). Appraising the brain's energy budget. *Proc Natl Acad Sci U S A* **99**, 10237–10239.

- Raichlen DA & Polk JD (2013). Linking brains and brawn: exercise and the evolution of human neurobiology. *Proc Biol Sci* **280**, 20122250.
- Raignault A, Bolduc V, Lesage F & Thorin E (2016). Pulse pressure-dependent cerebrovascular eNOS regulation in mice. *J Cereb Blood Flow Metab*; DOI: 10.1177/0271678X16629155.
- Ramsay SC, Murphy K, Shea SA, Friston KJ, Lammertsma AA, Clark JC, Adams L, Guz A & Frackowiak RS (1993). Changes in global cerebral blood flow in humans: effect on regional cerebral blood flow during a neural activation task. *J Physiol* **471**, 521–534.
- Rapoport RM, Draznin MB & Murad F (1983). Endothelium-dependent relaxation in rat aorta may be mediated through cyclic GMP-dependent protein phosphorylation. *Nature* **306**, 174–176.
- Rapoport RM & Murad F (1983). Agonist-Induced Endothelium-Dependent Relaxation in Rat Thoracic Aorta May Be Mediated through cGMP. *Circ Res* **52**, 352–357.
- Rebel A, Lenz C, Krieter H, Waschke KF, Van Ackern K & Kuschinsky W (2001). Oxygen delivery at high blood viscosity and decreased arterial oxygen content to brains of conscious rats. *Am J Physiol Heart Circ Physiol* **280**, H2591–H2597.
- Rebel A, Ulatowski JA, Kwansa H, Bucci E & Koehler RC (2003). Cerebrovascular response to decreased hematocrit: effect of cell-free hemoglobin, plasma viscosity, and CO<sub>2</sub>. *Am J Physiol Heart Circ Physiol* **285**, H1600–H1608.
- Regan RE, Fisher JA & Duffin J (2014). Factors affecting the determination of cerebrovascular reactivity. *Brain Behav* **4**, 775–788.
- Reich T & Rusinek H (1989). Cerebral Cortical and White Matter Reactivity to Carbon Dioxide. *Stroke* **20**, 453–457.
- Reichmuth KJ, Dopp JM, Barczy SR, Skatrud JB, Wojdyla P, Hayes D & Morgan BJ (2009). Impaired vascular regulation in patients with obstructive sleep apnea: Effects of continuous positive airway pressure treatment. *Am J Respir Crit Care Med* **180**, 1143–1150.
- Reid JM, Davies AG, Ashcroft FM & Paterson DJ (1995). Effect of L-NMMA, cromakalim, and glibenclamide on cerebral blood flow in hypercapnia and hypoxia. *Am J Physiol* **269**, H916–22.

- Reid JM, Paterson DJ, Ashcroft FM & Bergel DH (1993). The effect of tolbutamide on cerebral blood flow during hypoxia and hypercapnia in the anaesthetized rat. *Pflügers Arch Eur J Physiol* **425**, 362–364.
- Reinhard M, Schwarzer G, Briel M, Altamura C, Palazzo P, King A, Bornstein NM, Petersen N, Motschall E, Hetzel A, Marshall RS, Klijn CJM, Silvestrini M, Markus HS & Vernieri F (2014). Cerebrovascular reactivity predicts stroke in high-grade carotid artery disease. *Neurology* **83**, 1424–1431.
- Ringelstein EB, Sievers C, Ecker S, Schneider PA & Otis SM (1988). Noninvasive assessment of CO<sub>2</sub>-induced cerebral vasomotor response in normal individuals and patients with internal carotid artery occlusions. *Stroke* **19**, 963–969.
- Roach RC, Bartsch P, Oelz O & Hackett PH (1993). The Lake Louise scute mountain sickness scoring system. In *Hypoxia and Molecular Medicine*, ed. Sutton JR, Houston CS & Coates G, pp. 272–274. Queen City Press, Burlington, VT.
- Roach RC, Koskolou MD, Calbet J a & Saltin B (1999). Arterial O<sub>2</sub> content and tension in regulation of cardiac output and leg blood flow during exercise in humans. *Am J Physiol* **276**, H438–H445.
- Robertson BE, Schubert R, Hescheler J & Nelson MT (1993). cGMP-dependent protein kinase activates Ca-activated K channels in cerebral artery smooth muscle cells. *Am J Physiol* **265**, 299–303.
- Rosenblum W (1983a). Effects of free radical generation on mouse pial arterioles: probable role of hydroxyl radicals. *Am J Physiol*.
- Rosenblum WI (1983b). Effects of free radical generation on mouse pial arterioles: probable role of hydroxyl radicals. *Am J Physiol* **245**, H139-42.
- Rosenblum WI (1987). Hydroxyl radical mediates the endothelium-dependent relaxation produced by bradykinin in mouse cerebral arterioles. *Circ Res* **61**, 601–603.
- Rosenblum WI (2003). ATP-sensitive potassium channels in the cerebral circulation. *Stroke* **34**, 1547–1552.
- Rosenblum WI, Wei EP & Kontos HA (2002). Dilation of rat brain arterioles by hypercapnia in vivo can occur even after blockade of guanylate cyclase by ODC. *Eur J Pharmacol* **448**, 201–206.

- Rossen R, Kabat H & Anderson JP (1943). Acute arrest of cerebral circulation in man. *Arch Neurol Psychiatry* **50**, 510–528.
- Rousseeuw PJ, Ruts I & Tukey JW (1999). The Bagplot: A Bivariate Boxplot. *Am Stat* **53**, 382–387.
- Roy CS & Sherrington CS (1890). On the regulation of the blood supply of the brain. *J Physiol* **11**, 85–108.
- Rubanyi GM, Romero JC & Vanhoutte PM (1986). Flow-induced release of endothelium-derived relaxing factor. *Am J Physiol* **250**, H1145-9.
- Rupp T, Esteve F, Bouzat P, Lundby C, Levy P & Robach P (2014). Cerebral hemodynamic and ventilatory responses to hypoxia, hypercapnia, and hypocapnia during 5 days at 4,350 m. *J Cereb Blood Flow Metab* **34**, 52–60.
- Ryan BJ, Wachsmuth NB, Schmidt WF, Byrnes WC, Julian CG, Lovering AT, Subudhi AW & Roach RC (2014). Altitudeomics: Rapid hemoglobin mass alterations with early acclimatization to and de-acclimatization from 5260 m in healthy humans. *PLoS One* **9**, e108788.
- Rybalkin SD, Yan C, Bornfeldt KE & Beavo JA (2003). Cyclic GMP phosphodiesterases and regulation of smooth muscle function. *Circ Res* **93**, 280–291.
- Sagoo RS, Hutchinson CE, Wright A, Handford C, Parsons H, Sherwood V, Wayte S, Nagaraja S, NgAndwe E, Wilson MH & Imray CH (2016). Magnetic Resonance investigation into the mechanisms involved in the development of high-altitude cerebral edema. *J Cereb Blood Flow Metab* **37**, 319–331.
- Sakabe T & Siesjö BK (1979). The effect of indomethacin on the blood flow-metabolism couple in the brain under normal, hypercapnic and hypoxic conditions. *Acta Physiol Scand* **107**, 283–284.
- Sakai F, Nakazawa K, Tazaki Y, Ishii K, Hino H, Igarashi H & Kanda T (1985). Regional cerebral blood volume and hematocrit measured in normal human volunteers by single-photon emission computed tomography. *J Cereb Blood Flow Metab* **5**, 207–213.
- Salminen A, Kauppinen A & Kaarniranta K (2017). Hypoxia/ischemia activate processing of Amyloid Precursor Protein: impact of vascular dysfunction in the pathogenesis of Alzheimer's disease. *J Neurochem* **140**, 536–549.

- Salomon JA, Wang H, Freeman MK, Vos T, Flaxman AD, Lopez AD & Murray CJL (2012). Healthy life expectancy for 187 countries, 1990-2010: A systematic analysis for the Global Burden Disease Study 2010. *Lancet* **380**, 2144–2162.
- Sam K, Poublanc J, Sobczyk O, Han JS, Battisti-Charbonney A, Mandell DM, Tymianski M, Crawley AP, Fisher JA & Mikulis DJ (2015). Assessing the effect of unilateral cerebral revascularisation on the vascular reactivity of the non-intervened hemisphere: A retrospective observational study. *BMJ Open* **5**, 1–8.
- Sandor P, Komjati K, Reivich M & Nyary I (1994). Major role of nitric oxide in the mediation of regional CO<sub>2</sub> responsiveness of the cerebral and spinal cord vessels of the cat. *J Cereb Blood Flow Metab* **14**, 49–58.
- Sandrone S, Bacigaluppi M, Galloni MR, Cappa SF, Moro A, Catani M, Filippi M, Monti MM, Perani D & Martino G (2014). Weighing brain activity with the balance: Angelo Mosso's original manuscripts come to light. *Brain* **137**, 621–633.
- Santa N, Kitazono T, Ago T, Ooboshi H, Kamouchi M, Wakisaka M, Ibayashi S & Iida M (2003). ATP-sensitive potassium channels mediate dilatation of basilar artery in response to intracellular acidification in vivo. *Stroke* **34**, 1276–1280.
- Santizo R, Baughman VL & Pelligrino DA (2000). No relative contributions from neuronal and endothelial nitric oxide synthases to regional cerebral blood flow changes during forebrain ischemia in rats. *Neuroreport* **11**, 1549–1553.
- Sato K, Sadamoto T, Hirasawa A, Oue A, Subudhi AW, Miyazawa T & Ogoh S (2012a). Differential blood flow responses to CO<sub>2</sub> in human internal and external carotid and vertebral arteries. *J Physiol* **590**, 3277–3290.
- Sato K, Sadamoto T, Hirasawa A, Oue A, Subudhi AW, Miyazawa T & Ogoh S (2012b). Differential blood flow responses to CO<sub>2</sub> in human internal and external carotid and vertebral arteries. *J Physiol* **590**, 3277–3290.
- Sattin A & Rall TW (1970). The effect of adenosine and adenine nucleotides on the cyclic adenosine 3', 5'-phosphate content of guinea pig cerebral cortex slices. *Mol Pharmacol* **6**, 13–23.
- Scharrer E (1940). Arteries and Veins in the Mammalian Brain. *Anat Rec* **78**, 173–196.
- Scheel P, Ruge C, Petrich UR & Schöning M (2000a). Color Duplex Measurement of

- Cerebral Blood Flow VOLUME in Healthy Adults. *Stroke* **31**, 147–150.
- Scheel P, Ruge C & Schöning M (2000b). Flow Velocity and Flow Volume Measurements in the Extracranial Carotid and Vertebral Arteries in Healthy Adults: Reference Data and the Effects of Age. *Ultrasound Med Biol* **26**, 1261–1266.
- Schell RM & Cole DJ (2000). Cerebral monitoring: jugular venous oximetry. *Anesth Analg* **90**, 559–566.
- Schmetterer L, Findl O, Strenn K, Graselli U, Kastner J, Eichler HG & Wolzt M (1997). Role of NO in the O<sub>2</sub> and CO<sub>2</sub> responsiveness of cerebral and ocular circulation in humans. *Am J Physiol* **273**, R2005–R2012.
- Schoenemann PT (2006). Evolution of the Size and Functional Areas of the Human Brain. *Annu Rev Anthropol* **35**, 379–406.
- Schöning M, Walter J & Scheel P (1994). Estimation of Cerebral Blood Flow Through Color Duplex Sonography of the Carotid and Vertebral Arteries in Healthy Adults. *Stroke* **25**, 17–22.
- Schoonman GG, Sándor PS, Nirikko AC, Lange T, Jaermann T, Dydak U, Kremer C, Ferrari MD, Boesiger P & Baumgartner RW (2008). Hypoxia-induced acute mountain sickness is associated with intracellular cerebral edema: a 3 T magnetic resonance imaging study. *J Cereb Blood Flow & Metab* **28**, 198–206.
- Schubert R, Krien U & Gagov H (2001). Protons inhibit the BK(Ca) channel of rat small artery smooth muscle cells. *JVascRes* **38**, 30–38.
- Schulz JM, Al-khazraji BK, Shoemaker JK & Shoemaker JK (2018). Sodium nitroglycerin induces middle cerebral artery vasodilation in young, healthy adults Running title : Sodium Nitroglycerin and Cerebrovascular Dilation □□ What is the central question of this study? Nitric oxide causes dilation in peripheral vessels. *Exp Physiol*; DOI: 10.1113/EP087022.
- Scott DA, Evered LA & Silbert BS (2014). Cardiac surgery, the brain, and inflammation. *J Extra Corpor Technol* **46**, 15–22.
- Secomb TW (2016). Hemodynamics. *Compr Physiol* **6**, 975–1003.
- Secomb TW & Pries AR (2013). Blood Viscosity in Microvessels: Experiment and Theory. *C R Phys* **14**, 470–478.

- Serrador JM, Picot PA, Rutt BK, Shoemaker JK & Bondar RL (2000). MRI Measures of Middle Cerebral Artery Diameter in Conscious Humans During Simulated Orthostasis. *Stroke* **31**, 1672–1678.
- Severinghaus J (1979a). Simple, accurate equations for human blood O<sub>2</sub> dissociation computations. *J Appl Physiol* **46**, 599–602.
- Severinghaus JJW (1979b). Simple, accurate equations for human blood O<sub>2</sub> dissociation computations. *J Appl Physiol* **46**, 599–602.
- Severinghaus JW, Chiodi H, Eger E I II, Brandstater B & Hornbein TF (1966a). Cerebral Blood Flow In Man at High Altitude: Role of Cerebrospinal Fluid pH in Normalization of Flow in Chronic Hypocapnia. *Circ Res* **19**, 274–282.
- Severinghaus JW, Chiodi H, Eger E I II, Brandstater B, Hornbein TF, Eger EI, Brandstater B & Hornbein TF (1966b). Cerebral Blood Flow In Man at High Altitude. Role of cerebrospinal fluid pH in normalization of flow in chronic hypocapnia. *Circ Res* **19**, 274–282.
- Shapiro HM, Stromberg DD, Lee DR & Wiederhielm CA (1971). Dynamic pressures in the pial arterial microcirculation. *Am J Physiol* **221**, 279–283.
- Shapiro W, Wasserman AJ, Baker JP & Patterson JL (1970). Cerebrovascular response to acute hypocapnic and eucapnic hypoxia in normal man. *J Clin Invest* **49**, 2362–2368.
- Shapiro W, Wasserman AJ & Patterson JL (1966). Mechanism and Pattern of Human Cerebrovascular Regulation after Rapid Changes in Blood CO<sub>2</sub> Tension. *J Clin Invest.*
- Sharma RK (1995). Signal transduction: regulation of cAMP concentration in cardiac muscle by calmodulin- dependent cyclic nucleotide phosphodiesterase. *Mol Cell Biochem* **149**, 241–247.
- Sherwood CC, Subiaul F & Zawidzki TW (2008). A natural history of the human mind: tracing evolutionary changes in brain and cognition. *J Anat* **212**, 426–454.
- Sheth SA & Liebeskind DS (2015). Collaterals in endovascular therapy for stroke. *Curr Opin Neurol* **28**, 10–15.
- Siebenmann C, Cathomen A, Hug M, Keiser S, Lundby A-KM, Hilty MP, Goetze JP, Rasmussen P & Lundby C (2015). Hemoglobin mass and intravascular volume kinetics during and after exposure to 3,454 m altitude. *J Appl Physiol* **119**, 1194–1201.

- Siero JCW, Hartkamp NS, Donahue MJ, Hartevelde AA, Compter A, Petersen ET & Hendrikse J (2015). Neuronal activation induced BOLD and CBF responses upon acetazolamide administration in patients with steno-occlusive artery disease. *Neuroimage* **105**, 276–285.
- Silvestrini M, Pasqualetti P, Baruffaldi R, Bartolini M, Handouk Y, Matteis M, Moffa F, Provinciali L & Vernieri F (2006). Cerebrovascular reactivity and cognitive decline in patients with Alzheimer disease. *Stroke* **37**, 1010–1015.
- Simonson TS (2015). Altitude Adaptation: A Glimpse Through Various Lenses. *High Alt Med Biol* **16**, 125–137.
- Simpson RE & Phillis JW (1991). Adenosine deaminase reduces hypoxic and hypercapnic dilatation of rat pial arterioles: evidence for mediation by adenosine. *Brain Res* **553**, 305–308.
- Skow RJ, MacKay CM, Tymko MM, Willie CK, Smith KJ, Ainslie PN & Day TA (2013a). Differential cerebrovascular CO<sub>2</sub> reactivity in anterior and posterior cerebral circulations. *Respir Physiol Neurobiol* **189**, 76–86.
- Skow RJ, MacKay CM, Tymko MM, Willie CK, Smith KJ, Ainslie PN & Day TA (2013b). Differential cerebrovascular CO<sub>2</sub> reactivity in anterior and posterior cerebral circulations. *Respir Physiol Neurobiol* **189**, 76–86.
- Slessarev M, Han J, Mardimae A, Prisman E, Preiss D, Volgyesi G, Ansel C, Duffin J & Fisher J a (2007). Prospective targeting and control of end-tidal CO<sub>2</sub> and O<sub>2</sub> concentrations. *J Physiol* **581**, 1207–1219.
- Smirl JD, Lucas SJE, Lewis NCS, DuManoir GR, Dumanior GR, Smith KJ, Bakker A, Basnyat AS & Ainslie PN (2014). Cerebral pressure-flow relationship in lowlanders and natives at high altitude. *J Cereb blood flow Metab* **34**, 248–257.
- Smith BA, Clayton EW & Robertson D (2011). Experimental arrest of cerebral blood flow in human subjects: the red wing studies revisited. *Perspect Biol Med* **54**, 121–131.
- Smith JJ, Hillard CJ, Lee JG, Hudetz AG, Bosnjak ZJ & Kampine JP (1997a). The Role of Nitric Oxide in the Cerebrovascular to Hypercapnia. *Anesth Analg* **84**, 363–369.
- Smith JJ, Lee JG, Hudetz AG, Hillard CJ, Bosnjak ZJ & Kampine JP (1997b). The Role of Nitric Oxide in the Cerebrovascular Response to Hypercapnia. *Neurosurg Anesth* **84**,

363–369.

Smith KJ & Ainslie PN (2017). Regulation of cerebral blood flow and metabolism during exercise. *Exp Physiol* 1–35.

Smith KJ, Hoiland RL, Grove R, McKirdy H, Naylor L, Ainslie PN & Green DJ (2017). Matched increases in cerebral artery shear stress, irrespective of stimulus, induce similar changes in extra-cranial arterial diameter in humans. *J Cereb Blood Flow Metab* 0271678X1773922.

Smith KJ, MacLeod D, Willie CK, Lewis NCS, Hoiland RL, Ikeda K, Tymko MM, Donnelly J, Day T a., MacLeod N, Lucas SJE & Ainslie PN (2014). Influence of high altitude on cerebral blood flow and fuel utilization during exercise and recovery. *J Physiol* **592**, 5507–5527.

Smith KJ, Wildfong KW, Hoiland RL, Harper M, Lewis NC, Pool A, Smith SL, Kuca T, Foster GE & Ainslie PN (2016). Role of CO<sub>2</sub> in the cerebral hyperemic response to incremental normoxic and hyperoxic exercise. *J Appl Physiol*; DOI: 10.1152/jappphysiol.00490.2015.

Smith WL (1992). Prostanoid biosynthesis and mechanisms of action. *Am J Physiol* **263**, F181-91.

Smith WL, Marnett LJ & DeWitt DL (1991). prostaglandin and thromboxane biosynthesis. *Pharmacol Ther.*

Sobczyk O, Battisti-Charbonney A, Fierstra J, Mandell DM, Poublanc J, Crawley AP, Mikulis DJ, Duffin J & Fisher JA (2014). A conceptual model for CO<sub>2</sub>-induced redistribution of cerebral blood flow with experimental confirmation using BOLD MRI. *Neuroimage* **92**, 56–68.

Sokoloff L, Reivich M, Kennedy C, Rosiers MH Des, Patlak CS, Pettigrew KD, Sakurada O, Shinohara M, Des Rosiers MH, Patlak CS, Pettigrew KD, Sakurada O & Shinohara M (1977). The [<sup>14</sup>C]Deoxyglucose Method for the Measurement of Local Cerebral Glucose Utilization: Theory, Procedure, and Normal Values in the Conscious and Anesthetized Albino Rat. *J Neurochem* **28**, 897–916.

Song Y & Simard M (1995). Beta-Adrenoceptor stimulation activates large. Conductance Ca<sup>2+</sup>-activated K<sup>+</sup> channels in smooth muscle cells from basilar artery of guinea pig. *Pflugers Arch* **430**, 984–993.

- Sprague RS, Ellsworth ML, Stephenson AH & Lonigro AJ (1996). ATP: the red blood cell link to NO and local control of the pulmonary circulation. *Am J Physiol* **271**, H2717–H2722.
- Sprague RS, Ellsworth ML, Stephenson AH, Kleinhenz ME & Lonigro AJ (1998). Deformation-induced ATP release from red blood cells requires CFTR activity. *Am J Physiol* **275**, H1726–H1732.
- Sprung R, Sprague R & Spence D (2002). Determination of ATP release from erythrocytes using microbore tubing as a model of resistance vessels in vivo. *Anal Chem* **74**, 2274–2278.
- Stamler JS, Jaraki O, Osborne J, Simon DI, Keaney J, Vita J, Singel D, Valeri CR & Loscalzo J (1992). Nitric oxide circulates in mammalian plasma primarily as an S-nitroso adduct of serum albumin. *Proc Natl Acad Sci U S A* **89**, 7674–7677.
- Stamler JS, Jia L, Eu JP, McMahon TJ, Demchenko IT, Bonaventura J, Gernert K & Piantadosi CA (1997a). Blood flow regulation by S-nitrosohemoglobin in the physiological oxygen gradient. *Science* **276**, 2034–2037.
- Stamler JS, Jia L, Eu JP, McMahon TJ, Demchenko IT, Bonaventura J, Gernert K & Piantadosi CA (1997b). Blood flow regulation by S-nitrosohemoglobin in the physiological oxygen gradient. *Science* **276**, 2034–2037.
- Statland BE & Demas TJ (1980). Serum caffeine half-lives. Healthy subjects vs. patients having alcoholic hepatic disease. *Am J Clin Pathol* **73**, 390–393.
- Steinback CD, Breskovic T, Banic I, Dujic Z & Shoemaker JK (2010a). Autonomic and cardiovascular responses to chemoreflex stress in apnoea divers. *Auton Neurosci* **156**, 138–143.
- Steinback CD, Breskovic T, Frances M, Dujic Z & Shoemaker JK (2010b). Ventilatory restraint of sympathetic activity during chemoreflex stress. 1407–1414.
- Steinback CD, Salzer D, Medeiros PJ, Kowalchuk J & Shoemaker JK (2009). Hypercapnic vs. hypoxic control of cardiovascular, cardiovagal, and sympathetic function. *Am J Physiol Regul Integr Comp Physiol* **296**, R402–10.
- Steiner LA, Balestreri M, Johnston AJ, Coles JP, Chatfield DA, Pickard JD, Menon DK & Czosnyka M (2005). Effects of moderate hyperventilation on cerebrovascular pressure-

- reactivity after head injury. *Acta Neurochir Suppl* **17**–20.
- Stewart A (1983). Modern quantitative acid- base chemistry. *Can J Physiol Pharmacol* **61**, 1444–1461.
- Stromberg DD & Fox JR (1972). Pressures in the Pial Arterial Microcirculation of the Cat during Changes in Systemic Arterial Blood Pressure. *Circ Res* **31**, 229–239.
- Subudhi AW et al. (2014a). AltitudeOmics: The integrative physiology of human acclimatization to hypobaric hypoxia and its retention upon reascent. *PLoS One* **9**, e92191.
- Subudhi AW, Fan J-L, Evero O, Bourdillon N, Kayser B, Julian CG, Lovering AT & Roach RC (2014b). AltitudeOmics: Effect of ascent and acclimatization to 5260 m on regional cerebral oxygen delivery. *Exp Physiol* **5**, 772–781.
- Swenson ER, Robertson HT & Hlastala MP (1994). Effects of inspired carbon dioxide on ventilation-perfusion matching in normoxia, hypoxia, and hyperoxia. *Am J Respir Crit Care Med* **149**, 1563–1569.
- Symon L (1968). Experimental Evidence for “Intracerebral Steal” Following CO<sub>2</sub> Inhalation. *Scandinavian J Clin Lab Investig* **102**, XIII.
- Szabo K, Lako E, Juhasz T, Rosengarten B, Csiba L & Olah L (2011). Hypocapnia induced vasoconstriction significantly inhibits the neurovascular coupling in humans. *J Neurol Sci* **309**, 58–62.
- Szabo K, Rosengarten B, Juhasz T, Lako E, Csiba L & Olah L (2014). Effect of non-steroid anti-inflammatory drugs on neurovascular coupling in humans. *J Neurol Sci* **336**, 227–231.
- Takeuchi S & Karino T (2010). Flow patterns and distributions of fluid velocity and wall shear stress in the human internal carotid and middle cerebral arteries. *World Neurosurg* **73**, 174–185.
- Takuwa H, Matsuura T, Bakalova R, Obata T & Kanno I (2010). Contribution of nitric oxide to cerebral blood flow regulation under hypoxia in rats. *J Physiol Sci* **60**, 399–406.
- Tan CO (2012). Defining the characteristic relationship between arterial pressure and cerebral flow. *J Appl Physiol* **113**, 1194–1200.
- Tang SC, Huang YW, Shieh JS, Huang SJ, Yip PK & Jeng JS (2008). Dynamic cerebral

- autoregulation in carotid stenosis before and after carotid stenting. *J Vasc Surg* **48**, 88–92.
- Tarumi T & Zhang R (2017). Cerebral Blood Flow in Normal Aging Adults: Cardiovascular Determinants, Clinical Implications, and Aerobic Fitness. *J Neurochem* 1–14.
- Telischak NA, Detre JA & Zaharchuk G (2015). Arterial spin labeling MRI: Clinical applications in the brain. *J Magn Reson Imaging* **41**, 1165–1180.
- Thakur N, Blanc PD, Julian LJ, Yelin EH, Katz PP, Sidney S, Iribarren C & Eisner MD (2010). COPD and cognitive impairment: the role of hypoxemia and oxygen therapy. *Int J Chron Obstruct Pulmon Dis* **5**, 263–269.
- Thijssen DHJ, Black MA, Pyke KE, Padilla J, Atkinson G, Harris R a, Parker B, Widlansky ME, Tschakovsky ME & Green DJ (2011). Assessment of flow-mediated dilation in humans: a methodological and physiological guideline. *Am J Physiol Heart Circ Physiol* **300**, H2–H12.
- Thomas BP, Liu P, Park DC, van Osch MJP & Lu H (2014). Cerebrovascular Reactivity in the Brain White Matter: Magnitude, Temporal Characteristics, and Age Effects. *J Cereb Blood Flow Metab* **34**, 242–247.
- Thomas BP, Yezhuvath US, Tseng BY, Liu P, Levine BD, Zhang R & Lu H (2013). Life-long aerobic exercise preserved baseline cerebral blood flow but reduced vascular reactivity to CO<sub>2</sub>. *J Magn Reson Imaging* **38**, 1177–1183.
- Thomas DJ, Du Boulay GH, Marshall J, Pearson TC, Ross Russell RW, Symon L, Wetherley-Mein G & Zilkha E (1977a). Cerebral blood flow in polycythemia. *Lancet* **2**, 161–163.
- Thomas DJ, Marshall J, Ross Russell RW, Wetherley-Mein G, Du Boulay GH, Pearson TC, Symon L & Zilkha E (1977b). Effect of hematocrit on cerebral blood flow in man. *Lancet* **2**, 941–943.
- Thomas KN, Lewis NCS, Hill BG & Ainslie PN (2015). Technical recommendations for the use of carotid duplex ultrasound for the assessment of extracranial blood flow. *Am J Physiol Regul Integr Comp Physiol* **309**, R707–R720.
- Thomas SR, Witting PK & Drummond GR (2008). Redox Control of Endothelial Function and Dysfunction: Molecular Mechanisms and Therapeutic Opportunities. *Antioxid*

*Redox Signal* **10**, 1713–1766.

Thompson BG, Pluta RM, Girton ME & Oldfield EH (1996). Nitric oxide mediation of chemoregulation but not autoregulation of cerebral blood flow in primates. *J Neurosurg* **84**, 71–78.

Tian R, Vogel P, Lassen NA, Mulvany MJ, Andreassen F & Aalkjaer C (1995). Role of extracellular and Intracellular Acidosis for Hypercapnia-Induced Inhibition of Tension of Isolated Rat Cerebral Arteries. *Circ Res* **76**, 269–275.

Toda N (1974a). The Action of Vasodilating Drugs on Isolated Basilar, Coronary, and Mesenteric Arteries of the Dog. *J Pharmacol Exp Ther* **191**, 139–146.

Toda N (1974b). The action of vasodilation drugs on isolated basilar, coronary and mesenteric arteries of the dog. *J Pharmacol Exp Ther* **191**, 139–146.

Toda N, Ayajiki K, Enokibori M & Sciences M (1993). Monkey cerebral arterial relaxation caused by hypercapnic acidosis and hypertonic bicarbonate. *Am J Physiol* **265**, 929–933.

Toda N, Ayajiki K & Okamura T (2009). Cerebral Blood Flow Regulation by Nitric Oxide: Recent Advances. *Pharmacol Rev* **61**, 62–97.

Toda N, Hatano Y & Mori K (1989). Mechanisms underlying response to hypercapnia and bicarbonate of isolated dog cerebral arteries. *Am J Physiol* **257**, H141-6.

Toda N & Miyazaki M (1978). Responses of isolated dog cerebral and peripheral arteries to prostaglandins after application of aspirin and polyphloretin phosphate. *Stroke* **9**, 490–498.

Todd MM, Farrell S & Wu B (1997). Cerebral blood flow during hypoxemia and hemodilution in rabbits: different roles for nitric oxide? *J Cereb Blood Flow Metab* **17**, 1319–1325.

Todd MM, Weeks JB & Warner DS (1992). Cerebral blood flow, blood volume, and brain tissue hematocrit during isovolemic hemodilution with hetastarch in rats. *Am J Physiol* **263**, H75-82.

Todd MM, Wu B, Maktabi M, Hindman BJ & Warner DS (1994). Cerebral blood flow and oxygen delivery during hypoxemia and hemodilution: role of arterial oxygen content. *Am J Physiol* **267**, H2025-31.

Toksvang LN & Berg RMG (2013). Using a classic paper by Robin Fahraeus and Torsten

- Lindqvist to teach basic hemorheology. *AJP Adv Physiol Educ* **37**, 129–133.
- Tomiyama Y, Brian JE & Todd MM (2000). Plasma viscosity and cerebral blood flow. *Am J Physiol Heart Circ Physiol* **279**, H1949-54.
- Tomiyama Y, Brian Jr JE & Todd MM (1999a). Cerebral blood flow during hemodilution and hypoxia in rats : role of ATP-sensitive potassium channels. *Stroke* **30**, 1942–1948.
- Tomiyama Y, Jansen K, Brian JE & Todd MM (1999b). Hemodilution, cerebral O<sub>2</sub> delivery, and cerebral blood flow: a study using hyperbaric oxygenation. *Am J Physiol* **276**, H1190–H1196.
- Tran CHT & Gordon GR (2015). Astrocyte and microvascular imaging in awake animals using two-photon microscopy. *Microcirculation* **22**, 219–227.
- Triner L, Nahas GG, Vulliemoz Y, Overweg NIA, Verosky M, Habib D V. & Ngai SH (1971). Cyclic Amp and Smooth Muscle Function. *Ann N Y Acad Sci* **185**, 458–476.
- Tsai AG, Johnson PC & Intaglietta M (2003). Oxygen gradients in the microcirculation. *Physiol Rev* **83**, 933–963.
- Tsoukias NM (2008). Nitric Oxide Bioavailability in the Microcirculation: Insights from Mathematical Models. *Microcirculation* **15**, 813–834.
- Tu YK & Liu HM (1996). Effects of isovolemic hemodilution on hemodynamics, cerebral perfusion, and cerebral vascular reactivity. *Stroke* **27**, 441–445.
- Tulain U & Nisar-Ur-Rahman (2008). Comparative bioavailability and in vitro in vivo correlation of two sustained release brands of theophylline: Tablets and pellets. *Pak J Pharm Sci* **21**, 131–138.
- Tymko MM, Ainslie PN, Macleod DB, Willie CK & Foster GE (2015). End-tidal-to-arterial CO<sub>2</sub> and O<sub>2</sub> gas gradients at low- and high-altitude during dynamic end-tidal forcing. *Am J Physiol - Regul Integr Comp Physiol* **308**, R895-906.
- Tymko MM, Hoiland RL, Kuca T, Boulet LM, Tremblay JC, Pinske BK, Williams AM & Foster GE (2016a). Measuring the human ventilatory and cerebral blood flow response to CO<sub>2</sub>: A technical consideration for the end-tidal-to-arterial gas gradient. *J Appl Physiol*; DOI: 10.1152/jappphysiol.00787.2015.
- Tymko MM, Hoiland RL, Kuca T, Boulet LM, Tremblay JC, Pinske BK, Williams AM & Foster GE (2016b). Measuring the human ventilatory and cerebral blood flow response

- to CO<sub>2</sub>: A technical consideration for the end-tidal-to-arterial gas gradient. *J Appl Physiol* **120**, 282–296.
- Tzeng Y, Willie CK, Atkinson G, Lucas SJE, Wong A & Ainslie PN (2010). Cerebrovascular Regulation During Transient Hypotension and Hypertension in Humans. *Hypertension* **56**, 268–273.
- Tzeng YC & Ainslie PN (2014). Blood pressure regulation IX: Cerebral autoregulation under blood pressure challenges. *Eur J Appl Physiol* **114**, 545–559.
- Uski T, Andersson K, Brandt L, Edvinsson L & Ljunggren B (1983). Responses of Isolated Feline and Human Cerebral Arteries to Prostacycliri and Some of Its Metabolites. 238–245.
- Valdueza JM, Balzer JO, Villringer A, Vogl TJ, Kutter R & Einhüpl KM (1997). Changes in blood flow velocity and diameter of the middle cerebral artery during hyperventilation: assessment with MR and transcranial Doppler sonography. *Am J Neuroradiol* **18**, 1929–1934.
- Verbree J, Bronzwaer A, van Buchem M, Daemen M, van Lieshout J & van Osch M (2017). Middle cerebral artery diameter changes during rhythmic handgrip exercise in humans. *J Cereb Blood Flow Metab* **37**, 2921–2927.
- Verbree J, Bronzwaer AGT, Ghariq E, Versluis MJ, Daeman MJAP, van Buchem MA, Dahan A, van Lieshout JJ & van Osch MJP (2014). Assessment of middle cerebral artery diameter during hypocapnia and hypercapnia in humans using ultra high-field MRI. *J Appl Physiol* **117**, 1084–1089.
- Vestbo J, Hurd SS, Agusti AG, Jones PW, Vogelmeier C, Anzueto A, Barnes PJ, Fabbri LM, Martinez FJ, Nishimura M, Stockley RA, Sin DD & Rodriguez-Roisin R (2013). Global strategy for the diagnosis, management, and prevention of chronic obstructive pulmonary disease GOLD executive summary. *Am J Respir Crit Care Med* **187**, 347–365.
- Vestergaard MB, Lindberg U, Aachmann-andersen NJ, Lisbjerg K, Christensen SJ, Law I, Rasmussen P, Olsen N V & Larsson HBW (2015). Acute hypoxia increases the cerebral metabolic rate – a magnetic resonance imaging study. *J Cereb Blood Flow Metab* **in press.**, 10.1177/0271678X15606460.
- Vianna LC, Deo SH, Jensen AK, Holwerda SW, Zimmerman MC & Fadel PJ (2011).

- Impaired dynamic cerebral autoregulation during isometric exercise in patients with type 2 diabetes. *Am J Physiol Hear Circ Physiol* **25**, .
- Vorstrup S, Lass P, Waldemar G, Brandi L, Schmidt JF, Johnsen A & Paulson OB (1992). Increased cerebral blood flow in anemic patients on long-term hemodialytic treatment. *J Cereb Blood Flow Metab* **12**, 745–749.
- Vriens EM, Kraaier V, Musbach M, Wieneke GH & van Huffelen AC (1989). Transcranial pulsed doppler measurements of blood velocity in the middle cerebral artery: Reference values at rest and during hyperventilation in healthy volunteers in relation to age and sex. *Ultrasound Med Biol* **15**, 1–8.
- Wade JP (1983). Transport of oxygen to the brain in patients with elevated haematocrit values before and after venesection. *Brain* **106 (Pt 2)**, 513–523.
- Wade JP, du Boulay GH, Marshall J, Pearson TC, Russell RW, Shirley JA, Symon L, Wetherley-Mein G & Zilkha E (1980). Cerebral blood flow, haematocrit and viscosity in subjects with a high oxygen affinity haemoglobin variant. *Acta Neurol Scand* **61**, 210–215.
- Wade JP, Pearson TC, Russell RW & Wetherley-Mein G (1981). Cerebral blood flow and blood viscosity in patients with polycythaemia secondary to hypoxic lung disease. *Br Med J (Clin Res Ed)* **283**, 689–692.
- Wagerle LC & Mishra OP (1988). Mechanism of CO<sub>2</sub> response in cerebral arteries of the newborn pig: role of phospholipase, cyclooxygenase, and lipoxygenase pathways. *Circ Res* **62**, 1019–1026.
- Wahl M, Deetjen P, Thureau K, Ingvar DH & Lassen NA (1970). Micropuncture evaluation of the importance of perivascular pH for the arteriolar diameter on the brain surface. *Pflügers Arch Eur J Physiol* **316**, 152–163.
- Wahl M & Kuschinsky W (1976). The dilatatory action of adenosine on pial arteries of cats and its inhibition by theophylline. *Pflugers Arch* **362**, 55–59.
- Wahl M, Kuschinsky W, Bosse O & Thureau K (1973). Dependency of Pial Arterial and Arteriolar on Perivascular Osmolarity in the Cat: A microapplication study. *Circ Res* **32**, 162–170.
- Wahl M, Schilling L & Whalley ET (1989). Cerebrovascular effects of prostanoids: In-situ

- studies in pial arteries of the cat. *Naunyn Schmiedebergs Arch Pharmacol* **340**, 314–320.
- Wan J, Ristenpart WD & Stone HA (2008). Dynamics of shear-induced ATP release from red blood cells. *Proc Natl Acad Sci* **105**, 16432–16437.
- Wang Q, Bryan RM & Pelligrino DA (1998). Calcium-dependent and ATP-sensitive potassium channels and the “permissive” function of cyclic GMP in hypercapnia-induced pial arteriolar relaxation. *Brain Res* **793**, 187–196.
- Wang Q, Paulson OB & Lassen NA (1992). Effect of nitric oxide blockade by NG-Nitro-L-Arginine on cerebral blood flow response to changes in carbon dioxide tension. *J Cereb blood flow Metab* **12**, 947–953.
- Wang Q, Pelligrino DA, Koenig HM & Albrecht RF (1994a). The role of endothelium and nitric oxide in rat pial arteriolar dilatory responses to CO<sub>2</sub> in vivo. *J Cereb Blood Flow Metab* **14**, 944–951.
- Wang Q, Pelligrino DA, Baughman VL, Koenig HM & Albrecht RF (1995). The role of neuronal nitric oxide synthase in regulation of cerebral blood flow in normocapnia and hypercapnia in rats. *J Cereb Blood Flow Metab* **15**, 774–778.
- Wang Q, Pelligrino DA, Paulson OB & Lassen NA (1994b). Comparison of the effects of NG-nitro-L-arginine and indomethacin on the hypercapnic cerebral blood flow increase in rats. *Brain Res* **641**, 257–264.
- Wang X, Wu J, Li L, Chen F, Wang R & Jiang C (2003). Hypercapnic acidosis activates KATP channels in vascular smooth muscles. *Circ Res* **92**, 1225–1232.
- Warnert EA, Hart EC, Hall JE, Murphy K & Wise RG (2015). The major cerebral arteries proximal to the Circle of Willis contribute to cerebrovascular resistance in humans. *J Cereb Blood Flow Metab* 0271678X15617952.
- Warnert EA, Rodrigues JC, Burchell AE, Neumann S, Ratcliffe LE, Manghat NE, Harris AD, Adams ZH, Nightingale AK, Wise RG, Paton JF & Hart EC (2016). Is High Blood Pressure Self-Protection for the Brain? *Circ Res* **119**, e140–e151.
- Waschke KF, Krieter H, Hagen G, Albrecht DM, Van Ackern K & Kuschinsky W (1994). Lack of dependence of cerebral blood flow on blood viscosity after blood exchange with a Newtonian O<sub>2</sub> carrier. *J Cereb blood flow Metab* **14**, 871–876.
- Wechsler RL, Kleiss LM & Kety SS (1950). The effects of intravenously administered

- aminophylline on cerebral circulation and metabolism in man. *J Clin Invest* **29**, 28–30.
- Wei E, Ellis E & Kontos H (1980). Role of prostaglandins in pial arteriolar response to CO<sub>2</sub> and hypoxia. *Am J Physiol Heart Circ Physiol* **238**, H226–H230.
- Wei EP, Christman CW, Kontos HA & Povlishock JT (1985). Effects of oxygen radicals on cerebral arterioles. *Am J Physiol* **248**, 157–162.
- Wei HS, Kang H, Rasheed ID, Xu C, Wei HS, Kang H, Rasheed ID, Zhou S, Lou N & Gershteyn A (2016). Erythrocytes Are Oxygen-Sensing Regulators of the Cerebral Microcirculation. *Neuron* **91**, 851–862.
- Weitzberg E & Lundberg JON (1998). Nonenzymatic Nitric Oxide Production in Humans. *Nitric Oxide* **2**, 1–7.
- Weksler BB, Marcus AJ & Jaffe EA (1977). Synthesis of prostaglandin I<sub>2</sub> (prostacyclin) by cultured human and bovine endothelial cells. *Proc Natl Acad Sci* **74**, 3922–3926.
- Welch K, Knowles L & Spira P (1974). local effect of prostaglandins on cat pial arteries. *Eur J Pharmacol* **25**, 155–158.
- Wennmalm A, Carlsson I, Edlund A, Eriksson S, Kaijser L & Nowak J (1984). Central and peripheral haemodynamic effects of non-steroidal anti-inflammatory drugs in man. *Arch Toxicol Suppl* **7**, 350–359.
- West GA, Leppla DC & Simard JM (1992). Effects of external pH on ionic currents in smooth muscle cells from the basilar artery of the guinea pig. *Circ Res* **71**, 201–209.
- Whalley ET, Schilling L & Wahl M (1989). Cerebrovascular Effects of Prostanoids: IN-VITRO Studies in Middle Cerebral and Basilar Artery. *Prostaglandins* **38**, 625–634.
- White RP, Deane C, Vallance P & Markus HS (1998). Nitric oxide synthase inhibition in humans reduces cerebral blood flow but not the hyperemic response to hypercapnia. *Stroke* **29**, 467–472.
- White RP, Hindley C, Bloomfield PM, Cunningham VJ, Vallance P, Brooks DJ & Markus HS (1999). The effect of the nitric oxide synthase inhibitor L-NMMA on basal CBF and vasoneuronal coupling in man: a PET study. *J Cereb Blood Flow Metab* **19**, 673–678.
- Willette RN, Shiloh AO, Sauermelch CF, Sulpizio A, Michell MP, Cieslinski LB, Torphy TJ & Ohlstein EH (1997). Identification, characterization, and functional role of phosphodiesterase type IV in cerebral vessels: Effects of selective phosphodiesterase

- inhibitors. *J Cereb Blood Flow Metab* **17**, 210–219.
- Williams DS, Detre JA, Leigh JS & Koretsky AP (1992). Magnetic resonance imaging of perfusion using spin inversion of arterial water. *Proc Natl Acad Sci* **89**, 212–216.
- Willie CK, Colino FL, Bailey DM, Tzeng YC, Binsted G, Jones LW, Haykowsky MJ, Bellapart J, Ogoh S, Smith KJ, Smirl JD, Day TA, Lucas SJ, Eller LK & Ainslie PN (2011). Utility of transcranial Doppler ultrasound for the integrative assessment of cerebrovascular function. *J Neurosci Methods* **196**, 221–237.
- Willie CK, Macleod DB, Shaw AD, Smith KJ, Tzeng YC, Eves ND, Ikeda K, Graham J, Lewis NC, Day TA & Ainslie PN (2012). Regional brain blood flow in man during acute changes in arterial blood gases. *J Physiol* **59014**, 3261–3275.
- Willie CK, MacLeod DB, Smith KJ, Lewis NC, Foster GE, Ikeda K, Hoiland RL & Ainslie PN (2015a). The contribution of arterial blood gases in cerebral blood flow regulation and fuel utilization in man at high altitude. *J Cereb Blood Flow Metab* **35**, 873–881.
- Willie CK, MacLeod DB, Smith KJ, Lewis NC, Foster GE, Ikeda K, Hoiland RL & Ainslie PN (2015b). The contribution of arterial blood gases in cerebral blood flow regulation and fuel utilization in man at high altitude. *J Cereb Blood Flow Metab*; DOI: 10.1038/jcbfm.2015.4.
- Willie CK, Smith KJ, Day TA, Ray LA, Lewis NCS, Bakker A, Macleod DB & Ainslie PN (2014a). Regional cerebral blood flow in humans at high altitude: gradual ascent and 2 wk at 5,050 m. *J Appl Physiol* **116**, 905–910.
- Willie CK, Tzeng Y-C, Fisher JA & Ainslie PN (2014b). Integrative regulation of human brain blood flow. *J Physiol* **592**, 841–859.
- Willie CK, Tzeng Y-CC, Fisher JA & Ainslie PN (2014c). Integrative regulation of human brain blood flow. *J Physiol* **592**, 841–859.
- Willis T (1664). *Cerebri Anatome: Cui accessit nervorum description et usus* (thesis).
- Wilson MH, Edsell MEG, Davagnanam I, Hirani SP, Martin DS, Levett DZH, Thornton JS, Golay X, Strycharczuk L, Newman SP, Montgomery HE, Grocott MPW & Imray CHE (2011). Cerebral artery dilatation maintains cerebral oxygenation at extreme altitude and in acute hypoxia - an ultrasound and MRI study. *J Cereb Blood Flow Metab* **31**, 2019–2029.

- Wilson MH & Imray CHE (2016). The cerebral venous system and hypoxia. *J Appl Physiol* **120**, 244–250.
- Winn HR, Rubio R & Berne RM (1979). Brain adenosine production in the rat during 60 seconds of ischemia. *Circ Res* **45**, 486–492.
- Winn HR, Rubio R & Berne RM (1981a). Brain adenosine concentration during hypoxia in rats. *Am J Physiol* **241**, H235-42.
- Winn HR, Rubio R & Berne RM (1981b). Brain adenosine hypoxia in rats concentration during. *Am J Physiol Heart Circ Physiol* **241**, 235–242.
- Winn HR, Rubio RG & Berne RM (1981c). The role of adenosine in the regulation of cerebral blood flow. *Cereb Blood Flow Metab* **1**, 239–244.
- Winslow RM, Chapman KW, Gibson CC, Samaja M, Monge CC, Goldwasser E, Sherpa M, Blume FD & Santolaya R (1989). Different hematologic responses to hypoxia in Sherpas and Quechua Indians. *J Appl Physiol* **66**, 1561–1569.
- Wolff HG & Lennox WG (1930). The Effect On Pial Vessels Of Variations In The Oxygen And Carbon Dioxide Content Of The Blood. *Arch Neurol Psychiatry* **23**, 1097–1120.
- Woodman RJ, Playford DA, Watts GF, Cheetham C, Reed C, Taylor RR, Puddey IB, Beilin LJ, Burke V, Mori T a & Green D (2001). Improved analysis of brachial artery ultrasound using a novel edge-detection software system. *J Appl Physiol* **91**, 929–937.
- Wright IK, Amirchetty-Rao S & Kendall DA (1994). Potentiation by forskolin of both SNP- and ANP-stimulated cyclic GMP accumulation in porcine isolated palmar lateral vein. *Br J Pharmacol* **112**, 1146–1150.
- Xie A, Skatrud JB, Morgan B, Chenuel B, Khayat R, Reichmuth K, Lin J & Dempsey JA (2006a). Influence of cerebrovascular function on the hypercapnic ventilatory response in healthy humans. *J Physiol* **577**, 319–329.
- Xie A, Skatrud JB, Morgan B, Chenuel B, Khayat R, Reichmuth K, Lin J & Dempsey JA (2006b). Influence of cerebrovascular function on the hypercapnic ventilatory response in healthy humans. *J Physiol* **577**, 319–329.
- Xie A, Skatrud JB, Puleo DS & Morgan BJ (2001). Exposure to hypoxia produces long-lasting sympathetic activation in humans. *J Appl Physiol* **91**, 1555–1562.
- Xu F, Liu P, Pekar JJ & Lu H (2015). Does acute caffeine ingestion alter brain metabolism in

- young adults? *Neuroimage* **110**, 39–47.
- Xu K & Lamanna JC (2006). Regulation of the Cerebral Circulation Chronic hypoxia and the cerebral circulation. 725–730.
- Yamal J-M, Rubin ML, Benoit JS, Tilley BC, Gopinath S, Hannay HJ, Doshi P, Aisiku IP & Robertson CS (2015). Effect of Hemoglobin Transfusion Threshold on Cerebral Hemodynamics and Oxygenation. *J Neurotrauma*; DOI: 10.1089/neu.2014.3752.
- Yamauchi H, Fukuyama H, Ogawa M, Ouchi Y & Kimura J (1993). Hemodilution improves cerebral hemodynamics in internal carotid artery occlusion. *Stroke* **24**, 1885–1890.
- Yeoh TY, Venkatraghavan L, Fisher JA & Meineri M (2017). Internal jugular vein blood flow in the upright position during external compression and increased central venous pressure: an ultrasound study in healthy volunteers. *Can J Anesth Can d'anesthésie* **64**, 854–859.
- Yoon S, Zuccarello M & Rapoport RM (2012). pCO<sub>2</sub> and pH regulation of cerebral blood flow. *Front Physiol* **3**, 1–8.
- You J, Johnson TD, Childres WF & Bryan RM (1997). Endothelial-mediated dilations of rat middle cerebral arteries by ATP and ADP. *Am J Physiol* **273**, H1472-7.
- You J, Johnson TD, Marrelli SP & Bryan RM (1999). Functional heterogeneity of endothelial P<sub>2</sub> purinoceptors in the cerebrovascular tree of the rat. *Am J Physiol* **277**, H893–H900.
- You JP, Wang Q, Zhang W, Paulson B, Lassen NA & Edvinsson L (1994). HYPERCAPNIC VASODILATATION IN ISOLATED RAT BASILAR ARTERIES IS EXERTED VIA LOW pH AND DOES NOT INVOLVE NITRIC OXIDE SYNTHASE STIMULATION OR CYCLIC GMP PRODUCTION. *Acta Physiol Scand* **152**, 391–397.
- Yu Y, Mizushige K, Ueda T, Nishiyama Y, Seki M, Aoyama T, Ohkawa M & Matsuo H (2000). Effect of olprinone, phosphodiesterase III inhibitor, on cerebral blood flow assessed with technetium-99m-ECD SPECT. *J Cardiovasc Pharmacol* **35**, 422–426.
- Zarrinkoob L, Ambarki K, Wåhlin A, Birgander R, Eklund A & Malm J (2015). Blood flow distribution in cerebral arteries. *J Cereb Blood Flow & Metab* **35**, 648–654.
- Zhang C et al. (2017). Differentiated demographic histories and local adaptations between Sherpas and Tibetans. 1–18.
- Zhang DD & Li SH (2002). Optical dating of Tibetan human hand- and footprints: An

implication for the palaeoenvironment of the last glaciation of the Tibetan Plateau. *Geophys Res Lett* **29**, 3–5.

Zhang H, Wang X, Lin J, Sun Y, Huang Y, Yang T, Zheng S, Fan M & Zhang J (2013). Reduced regional gray matter volume in patients with chronic obstructive pulmonary disease: a voxel-based morphometry study. *AJNR Am J Neuroradiol* **34**, 334–339.

Zhou Y, Rodgers ZB & Kuo AH (2015). Cerebrovascular reactivity measured with arterial spin labeling and blood oxygen level dependent techniques. *Magn Reson Imaging* **33**, 566–576.

Zhu Y-S, Tarumi T, Tseng BY, Palmer DM, Levine BD & Zhang R (2013). Cerebral Vasomotor Reactivity during Hypo- and Hypercapnia in Sedentary Elderly and Masters Athletes. *J Cereb Blood Flow Metab* **33**, 1190–1196.

Zweier JL, Wang P, Samouilov A & Kuppusamy P (1995). Enzyme-independent formation of nitric oxide in biological tissues. *Nat Med* **1**, 804–809.

## APPENDICES

### APPENDIX A: SHEAR-MEDIATED DILATION OF THE INTERNAL CAROTID ARTERY OCCURS INDEPENDENT OF HYPERCAPNIA

**Hoiland RL, Smith KJ, Carter HH, Lewis NCS, Tymko MM, Wildfong KW, Bain AR, Green DJ, Ainslie PN.** Shear-mediated dilation of the internal carotid artery occurs independent of hypercapnia. *Am J Physiol - Hear Circ Physiol* 313: 24–31, 2017.

Reproduced with permission. Copyright © 2017 the American Physiological Society

## INTRODUCTION

The endothelium is integral to the maintenance of vascular health and function in humans. Endothelial dysfunction is an early and integral event in the pathogenesis of atherosclerosis as well as cardio- and cerebro-vascular diseases (Heitzer *et al.*, 2001). In the peripheral and coronary vasculature, flow mediated dilation (FMD) has been used as a functional bioassay to assess endothelial health. The FMD test strongly predicts cardiac events (Green *et al.*, 2011), potentially allowing for pre-clinical detection of future cardiovascular disease (Celermajer *et al.*, 1992). While the conventional FMD test is based on the notion that a healthy endothelium produces autocooids (e.g. nitric oxide) that induce a quantifiable dilator response to an imposed increase in shear stress (Green *et al.*, 2014), there is currently no equivalent assessment of cerebrovascular function in humans. Although standard carbon dioxide (CO<sub>2</sub>) reactivity tests using transcranial Doppler are predictive of cerebrovascular events (i.e. stroke) in individuals with pre-existing carotid stenosis (Gupta *et al.*, 2012), its use is limited as it does not provide significant predictive value pertaining to stroke risk in apparently healthy individuals (Portegies *et al.*, 2014). Other metrics of cerebrovascular function such as neurovascular coupling (Phillips *et al.*, 2016) and cerebral autoregulation (Tang *et al.*, 2008; Vianna *et al.*, 2011) are similarly impaired in clinical populations, but are not predictive of risk in apparently healthy individuals. Therefore, the development of an FMD-type test that could potentially provide an index of cerebrovascular endothelial function may prove to be clinically impactful.

Recently, our group has provided the first evidence in humans of shear-mediated dilation in the internal carotid artery (ICA) (Carter *et al.*, 2016a). Here, we demonstrated that vascular

responsiveness to CO<sub>2</sub> was related to the rise in intra-arterial shear stress, leading to vasodilation with a similar time dependency to that of peripheral FMD. However, the carotid vasodilation observed in that study coincided with elevated arterial PCO<sub>2</sub> levels and we could not partition the effects of shear stress from those occurring secondary to sustained hypercapnia [e.g. elevated blood pressure (Regan *et al.*, 2014), cardiac output (Balanos *et al.*, 2003), chemoreceptor-mediated sympathoactivation (Pitsikoulis *et al.*, 2008), potential direct vasomotor effects of CO<sub>2</sub> (Kontos *et al.*, 1977a; Willie *et al.*, 2012; Hoiland *et al.*, 2016b)]. As a result, the contribution of shear-dependent mechanisms to human CBF regulation and carotid dilator function requires further investigation *in vivo*.

Therefore, the primary purpose of this experiment was to extend our previous findings (Carter *et al.*, 2016a), using a test without sustained hypercapnia, to quantify the role that shear stress-dependent mechanisms play in carotid dilation in response to CO<sub>2</sub> reactivity. It was hypothesized that transient (30-second) increases in end-tidal PCO<sub>2</sub> (P<sub>ET</sub>CO<sub>2</sub>) would produce an ICA shear response similar to that of a *peripheral* FMD test (i.e. bell-curve). We further reasoned that upon return of P<sub>ET</sub>CO<sub>2</sub> to baseline values, and consequent withdrawal of the direct effects of CO<sub>2</sub>, a time dependent dilation of the ICA would occur (e.g. 30-60 second delay from shear onset), implying a shear-specific mechanism that is consistent with that observed in peripheral vessels of young healthy individuals (Black *et al.*, 2008).

## **MATERIALS AND METHODS**

### **Ethical Approval**

This study was approved by the University of British Columbia Clinical Research Ethics Board and the University of Western Australia Human Research Ethics Committee, and data was subsequently collected at both institutions. Prior to participation in the study, all participants completed written informed consent. All procedures conformed to the standards set by the Declaration of Helsinki.

## Research Participants

Twenty-seven healthy (twenty two male, five female), young volunteers (mean $\pm$ SD; 22 $\pm$ 3 years; body mass index=22 $\pm$ 2 kg/m<sup>2</sup>) were recruited to participate in this study. Following written informed consent and familiarization the participants attended the laboratory on one occasion having fasted for  $\geq$ 2 hours and refrained from exercise, alcohol and caffeine for 24 hours. During familiarization, participants were screened to ensure that reliable ICA ultrasound images and middle cerebral artery (MCA) signals could be obtained. Participants were familiarized with the remaining experimental equipment and procedures during this session. All participants were free of cardiovascular, respiratory, and cerebrovascular disease, were non-diabetic, and were not taking any prescription drugs (other than oral contraceptives; n=4) at their time of participation, as determined by a screening questionnaire. All females were tested in days 1-3 of their follicular phase. Of the 27 participants recruited, 24 completed both CO<sub>2</sub> protocols, while three only completed the transient CO<sub>2</sub> protocol.

## Experimental Measures

### *Cardiorespiratory Measures.*

All cardiorespiratory variables were sampled continuously at 1KHz via an analogue-to-digital converter (Powerlab, 16/30; ADInstruments, Colorado Springs, CO). Heart rate (HR) was measured by 3-lead electrocardiogram (ADI bioamp ML132), while beat-to-beat blood pressure was measured by finger photoplethysmography (Finometer PRO, Finapres Medical Systems, Amsterdam, Netherlands). The Finometer reconstructed brachial waveform was used for the calculation of mean arterial pressure (MAP) after values were back calibrated to the average of three automated brachial blood pressure measurements made over 5-minutes at rest (Tango+; SunTech, Morrisville, NC). Both P<sub>ET</sub>CO<sub>2</sub> and the end-tidal partial pressure of O<sub>2</sub> (P<sub>ET</sub>O<sub>2</sub>) were sampled at the mouth and recorded by a calibrated gas analyzer (model ML206, ADInstruments), while respiratory flow was measured by a pneumotachograph (model HR 800L, HansRudolph, Shawnee, KS) connected in series to a bacteriological filter. All data were interfaced with LabChart (Version 7).

### *Dynamic End-Tidal Forcing.*

The  $P_{ET}O_2$  and  $P_{ET}CO_2$  were controlled by a portable dynamic end-tidal forcing system that has been previously described in detail (Tymko *et al.*, 2015, 2016b). Our end-tidal forcing system effectively controls end-tidal gases through wide ranges of  $P_{ET}CO_2$  and  $P_{ET}O_2$  independent of ventilation (Tymko *et al.*, 2015, 2016b) and has been previously used for similar  $P_{ET}CO_2$  manipulations (Hoiland *et al.*, 2016b).

### *Cerebrovascular Measures.*

Blood velocity in the right MCA (MCAv) was measured using a 2MHz transcranial Doppler ultrasound (TCD; Spencer Technologies, Seattle, WA). The TCD probe was fixed to a headpiece (model M600 bilateral head frame, Spencer Technologies) and secured into place. The MCA was insonated through the middle trans-temporal window, using previously described location and standardization techniques (Willie *et al.*, 2011).

### *Internal Carotid Artery Measurements*

Right ICA blood velocity (ICAv) and vessel diameter were measured using a 10MHz multi-frequency linear array duplex ultrasound (Terason T3200, Teratech, Burlington, MA). Specifically, B-mode imaging was used to measure arterial diameter, while pulse-wave mode was used to concurrently measure peak blood velocity. Diameter and velocity of the ICA were measured at least 1.5 cm distal to the common carotid bifurcation to eliminate recordings of turbulent and retrograde flow and non-uniform shear. Great care was taken to ensure that the insonation angle ( $60^\circ$ ) was unchanged throughout each test. Further, upon acquisition of the first ultrasound image (i.e., resting baseline) there was no alteration of B-mode gain to avoid any artificial changes in arterial wall brightness/thickness. All recordings were made in accordance with published guidelines (Thomas *et al.*, 2015).

All recordings were screen captured and stored as video files for offline analysis. This analysis involved concurrent determination of arterial diameter and peak blood velocity at 30Hz, using customized edge detection and wall tracking software (BloodFlow Analysis, Version 5.1) designed to mitigate observer bias (Woodman *et al.*, 2001). Our *within* day coefficient of

variation for the assessment of ICA diameter is 1.5% using this technique (Hoiland *et al.*, 2016b). Blood flow and shear rate were subsequently calculated as previously described (Black *et al.*, 2008; Hoiland *et al.*, 2016b).

## **Experimental Protocol**

### *Carotid Shear-Mediated Dilation Tests*

Prior to commencing the study, pilot testing was ran to determine the optimal  $P_{ETCO_2}$  change required to elicit a maximal transient shear stress response. Although it is well established that the cerebral blood flow response is linear with elevations in  $P_{ETCO_2}$  (Ainslie & Duffin, 2009), we determined that there was no appreciable difference in the transient test shear response between a targeted  $P_{ETCO_2}$  stimuli of +9 or +15mmHg. Given that +15 leads to a greater extent of participant discomfort, and a larger ventilatory response, which would increase the difficulty of acquiring ultrasound recordings of the ICA, we reasoned that a +9mmHg stimulus would be better suited to address our research question. In addition, the +9mmHg stimulus is roughly comparable to what would be induced by an  $F_{ICO_2}$  of 0.05 – this level is commonly used in other studies (Ainslie & Duffin, 2009).

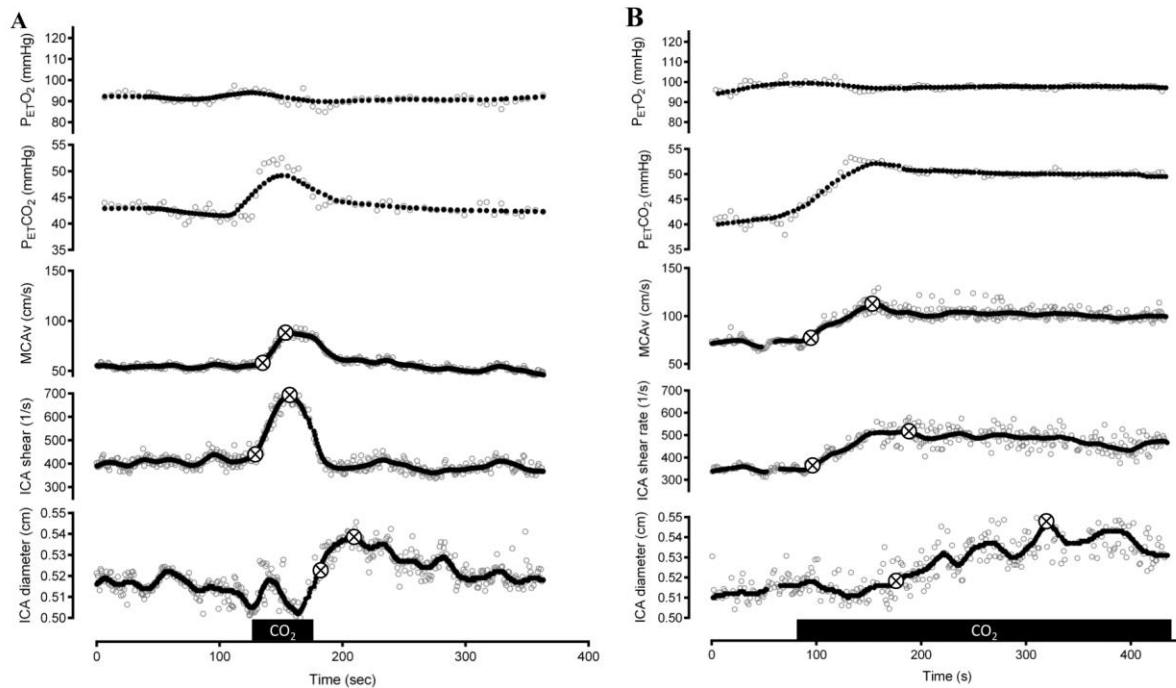


**Figure 1. Representative traces for the transient and steady state CO<sub>2</sub> tests.**

Panel A depicts a typical response for the transient CO<sub>2</sub> test and panel B depicts a typical response for the steady state CO<sub>2</sub> test. Each panel displays P<sub>ET</sub>CO<sub>2</sub>, P<sub>ET</sub>O<sub>2</sub>, MCAv, ICA shear rate, and ICA diameter, with the raw data represented by the open grey circles, and the smoothed data represented by the closed black circles. The circled X's indicate the response start and subsequent peak value of each hemodynamic variable, while the black bar denotes the duration of CO<sub>2</sub> manipulation. Reproduced from (Hoiland *et al.*, 2017c), permission not required.

Two separate CO<sub>2</sub> tests were utilized to assess the influence of shear and flow on ICA vascular tone: 1) a transient CO<sub>2</sub> test (+9 mmHg P<sub>ET</sub>CO<sub>2</sub>) to simulate the shear dynamics characteristic of a post occlusion brachial cuff release in standardized peripheral FMD tests (Thijssen *et al.*, 2011) (Figures 1 & 2), and 2) a steady state CO<sub>2</sub> test to determine maximal reactivity/dilation to the same +9mmHg stimulus. The steady state CO<sub>2</sub> test was conducted fifteen minutes following the transient test.

- 1) *Transient CO<sub>2</sub> Test*: Participants lay supine, while breathing room air. Following five minutes of resting data collection, participants breathed simulated room air delivered from the end-tidal forcing system (i.e. P<sub>ET</sub>O<sub>2</sub> & P<sub>ET</sub>CO<sub>2</sub> did not change) for two minutes. Participants were then paced at 20 breaths per minute through verbal coaching and visual feedback while end-tidal values were maintained (i.e. did not change) for an additional two minutes. Breathing was maintained at 20 breaths per minute for the remainder of the trial. This approach was utilized to improve the end-tidal forcing systems ability to abruptly manipulate P<sub>ET</sub>CO<sub>2</sub> in a controlled fashion, as a higher breathing rate allows for quicker gas manipulations. Further, this eliminated the potential for abrupt changes in V<sub>E</sub> due to CO<sub>2</sub> chemosensitivity, which could interfere with ultrasound imaging (e.g., large neck muscle movements) and act as a confounding physiological factor. At the two minute mark, P<sub>ET</sub>CO<sub>2</sub> was abruptly (~five seconds) elevated to +9 mmHg above baseline for 30-seconds and then quickly returned to baseline values, which were maintained for three additional minutes. Reported data are from the last minute of hyperventilation onwards.
  
- 2) *Steady State CO<sub>2</sub> Test*: Participants lay supine, while breathing room air. Following five minutes of resting data collection, the participant breathed simulated room air on the end-tidal forcing system. Following two minutes of steady breathing, P<sub>ET</sub>CO<sub>2</sub> was abruptly (~five seconds) elevated to +9 mmHg above baseline and maintained for four minutes. Following four minutes, participants returned to room air breathing.

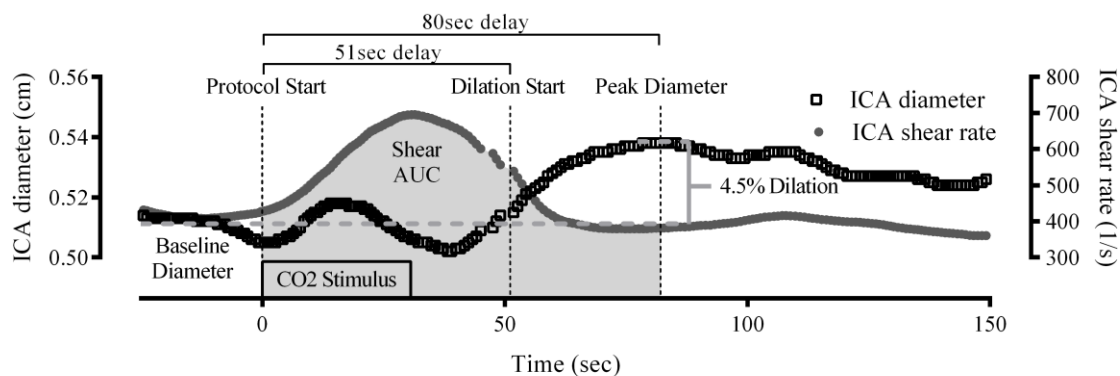


**Figure 2. Shear rate and diameter during the transient CO<sub>2</sub> test.**

This figure highlights the temporal dynamics of the 30-second transient CO<sub>2</sub> test in one subject. Time zero represents the onset of the 30-second CO<sub>2</sub> stimulus (+9mmHg P<sub>ET</sub>CO<sub>2</sub>). The increase in CO<sub>2</sub> produced an increase in CBF and therefore cerebral shear rate (grey circles) which mirrors that subsequent to brachial cuff release during a peripheral FMD test [see figure 2 in (Thijssen *et al.*, 2011)]. Shear rate area under the curve is highlighted in grey. Following the transient increase in shear rate, ICA diameter (open squares) increased approximately 30 seconds after peak shear rate was reached (51-seconds from CO<sub>2</sub> onset). Peak diameter was reached approximately 60-seconds after peak shear occurred (80-seconds from CO<sub>2</sub> onset). Reproduced from (Hoiland *et al.*, 2017c), permission not required.

## Data Analysis

### *Data Extraction and Carotid Shear-Mediated Dilation Software*

All data from LabChart (e.g. MCAV, MAP, P<sub>ET</sub>CO<sub>2</sub> and P<sub>ET</sub>O<sub>2</sub>) were down sampled to 50Hz and exported into Microsoft Excel. Vascular data were interpolated at 50Hz and exported into the same excel spreadsheet and time-aligned with the LabChart data. The excel spreadsheet was re-opened as a LabChart data file and all cardiovascular/cerebrovascular data were exported to a new excel spreadsheet in beat-by-beat averages, while all respiratory variables were exported on a breath-by-breath basis. These variables were subsequently analyzed using custom designed shear-mediated dilation software (Labview®) as previously explained in detail (Carter *et al.*, 2016a). In brief, the data were filtered and the following variables were automatically detected and calculated: 1) Baseline values; 2) Peak responses, and; 3) Relative

(%) changes. In addition, a threshold selection algorithm was applied to each data array (e.g., ICA shear, ICA diameter,), which identified threshold points for the increase in each variable following the onset of CO<sub>2</sub> administration. Once the software had automatically detected the threshold points, they were depicted on the filtered and raw data array and visually inspected to ensure they met the following criteria: a) the algorithm-detected threshold point occurred prior to the peak value and, b) the variable did not decrease below the algorithm-detected threshold point prior to the peak value occurring. Of the 240 responses analyzed, 151 met the agreed criteria and their automatically detected points were accepted. In the remaining 89 cases (37%) the threshold points were manually adjusted by two independent investigators to a point where each deemed there was a clear deviation from baseline that met the above criteria. The mean of these manually assessed points were entered in the analysis. The coefficient of variation for the analysis of the threshold points detected using the above systematic approach was 4.2% overall, and 11.2% between the 89 manually adjusted files. Shear rate area under the curve (AUC) was also calculated for both the transient and steady state trials, in accordance with the analytical methods used for brachial FMD (Black *et al.*, 2008; Thijssen *et al.*, 2011) (i.e., from the onset of CO<sub>2</sub> stimulus until peak dilation occurred).

#### *Data Exclusion Criteria*

Of the subjects tested, four trials were excluded from analysis of the steady state CO<sub>2</sub> tests while seven were excluded from the transient CO<sub>2</sub> tests. Additionally, there were three subjects who only completed the transient CO<sub>2</sub> test (not both trials). Thus, the resulting samples sizes were n=20 for both the steady state CO<sub>2</sub> and transient CO<sub>2</sub> tests, with 13 subjects having repeated measures across both trials. Ultrasound videos were visually inspected prior to analyses and were excluded based upon the following criteria: 1) the occurrence of an overt angle change (n=2); 2) excessive movement of the vessel [e.g., due to high ventilation (n=3)]; and 3) overall poor image quality [e.g., blurry vessel walls (n=4)]. In two cases a test was excluded following video analysis due to low fidelity wall tracking despite the visual appearance of a clear vessel wall. Therefore, sample size is noted throughout the text for all statistical comparisons.

## Statistical Analyses

No statistical differences were found between male and female vascular responses in the current study; therefore, data were pooled for analyses. Sample sizes were based off of previous research by our group investigating vasomotion of the ICA (Willie *et al.*, 2012; Carter *et al.*, 2016b; Hoiland *et al.*, 2016b). Comparisons between baseline and peak values within trial were made using two-tailed paired t-tests. Due to the differing participants for each trial (see *Data Exclusion Criteria*), between trial comparisons were made using a linear mixed model analysis with a compound symmetry covariance structure (Fixed factor: steady state vs. transient test) to account for this drop out. Pearson correlations were used to assess the relationship between vasodilatory responses during the transient and steady state CO<sub>2</sub> protocols in the subjects with repeated measures (n=13), and to determine the relationship between shear AUC and dilation in each trial (transient n=19; steady state n=20). For the shear AUC and dilation bivariate analysis, a statistical outlier was determined utilizing bagplot analysis (Rousseeuw *et al.*, 1999). All statistical analyses were performed using SPSS (IBM statistics, Version 22.0).

## RESULTS

### Carotid Shear-Mediated Dilation

From the onset of elevated P<sub>ET</sub>CO<sub>2</sub> (Figure 3), the delay for ICA shear to increase was 16.8±13.2s in the transient trial and 18.2±14.2s (P=0.61) in the steady state trial. Peak shear occurred at 42.2±9.9s in the transient trial and 163.6±87.5s in the steady state trial (P<0.01). The onset of dilation in the transient trial occurred 59.4±60.3s from onset of elevated P<sub>ET</sub>CO<sub>2</sub>, while the delay was 110.3±79.6s in the steady state trial (P=0.047). Peak dilation occurred 110.3±69.1s and 283.6±56.1s in the transient and steady state trial, respectively (P<0.01). In both the steady state (18.2±14.2 vs. 110.3±79.6s; P<0.01) and transient test (16.8±13.2 vs. 59.4±60.3s; P<0.01) the increase in ICA shear preceded ICA dilation (Figure 3).

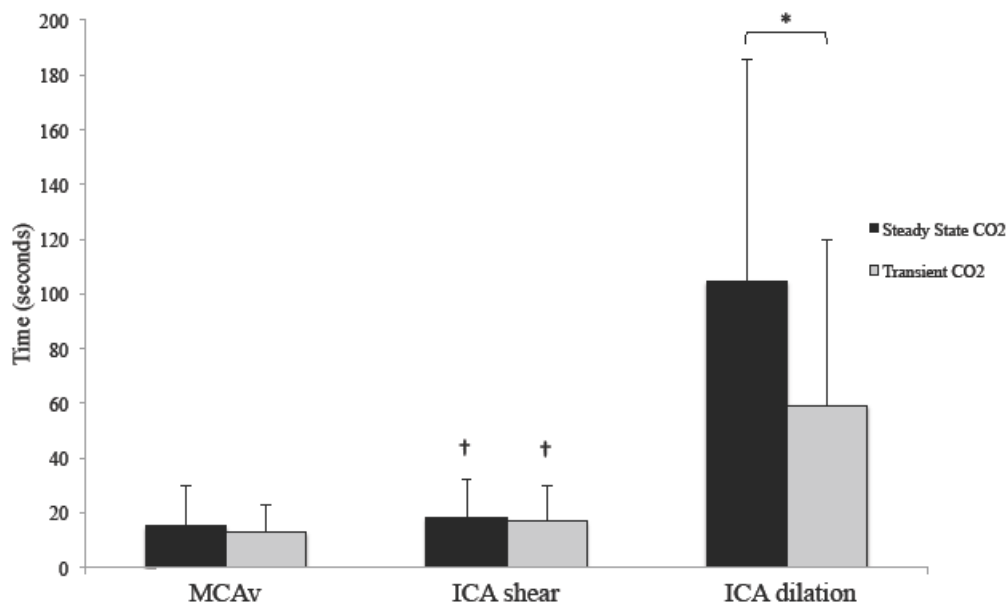


**Figure 3. The time course of cerebral vascular responses to steady state and transient CO<sub>2</sub> breathing.**

The presented data represents the threshold at which middle cerebral artery blood velocity (MCAv), internal carotid artery (ICA) shear, and ICA diameter begin to deviate (increase) from baseline. \* Denotes a significant difference between steady state CO<sub>2</sub> and transient CO<sub>2</sub> response times. † Denotes a significant difference in the time delay between ICA shear and ICA dilation *within* a trial. Reproduced from (Hoiland *et al.*, 2017c), permission not required.

During the transient and steady state hypercapnic tests the ICA dilated by  $3.3 \pm 1.9\%$  ( $n=20$ ;  $P<0.01$ ) and  $5.3 \pm 2.9\%$  ( $n=20$ ;  $P<0.01$ ), respectively. The steady state elevation in  $P_{ET}CO_2$  produced the greatest dilation as reflected in a 60% greater increase ( $P=0.03$ ; Figure 4). Shear rate increased from  $330.0 \pm 74.2 s^{-1}$  to a peak value of  $448.5 \pm 111.7 s^{-1}$  ( $n=20$ ;  $P<0.01$ ) in the transient CO<sub>2</sub> trial and from  $337.3 \pm 56.6 s^{-1}$  to  $526.8 \pm 83.5 s^{-1}$  ( $n=20$ ;  $P<0.01$ ) in the steady state trial. The increase in shear rate during the steady state trial was greater than during the transient test ( $189.5 \pm 49.9 s^{-1}$  vs.  $118.5 \pm 53.8 s^{-1}$ ;  $P<0.01$ ). Shear rate AUC for the transient trial was  $43,053 \pm 21,277 s^{-1}$  ( $n=19$ ), and  $131,476 \pm 30,880 s^{-1}$  ( $n=20$ ) in the steady state trial ( $p<0.01$ ; independent samples t-test). Shear rate AUC was correlated to the magnitude of vasodilation in the transient test ( $r^2=0.44$ ;  $P<0.01$ ;  $n=19$ ); however, this relationship was not present in the steady state trial ( $r^2=0.02$ ;  $P=0.53$ ) (Figure 5).

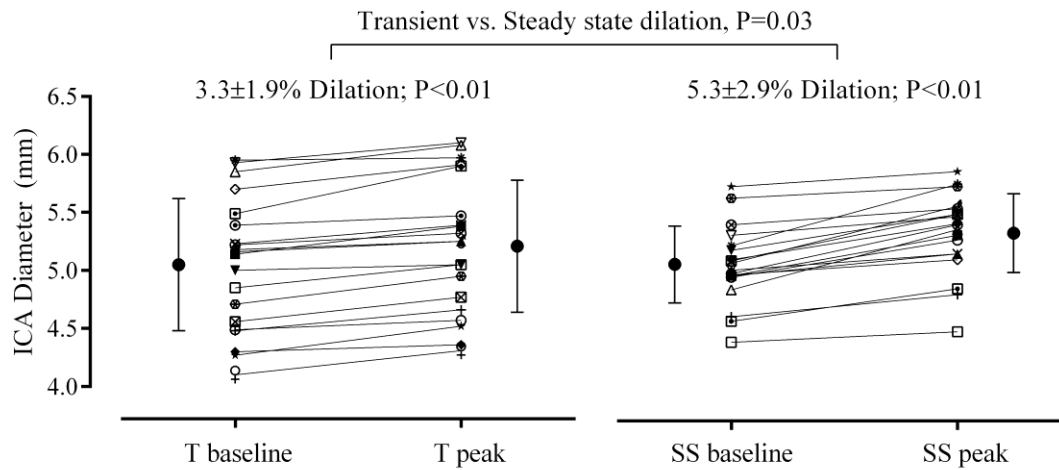


**Figure 4. Peak internal carotid artery dilation during the steady state and transient CO<sub>2</sub> tests.**

The left panel shows the change in diameter of the internal carotid artery (ICA) from baseline to peak dilation after a transient 30-second period of hypercapnia (+9mmHg) for 20 subjects. The right panel shows the change in diameter of the ICA from baseline to peak dilation during four minutes of steady state hypercapnia (+9mmHg) for 20 subjects. The %change in diameter in the steady state trial was greater than the %change in diameter in the transient 30-second trial (comparison of deltas between trials, P=0.03). Mean±SD is indicated for each trial by the filled circles (●) and error bars. Reproduced from (Hoiland *et al.*, 2017c), permission not required.

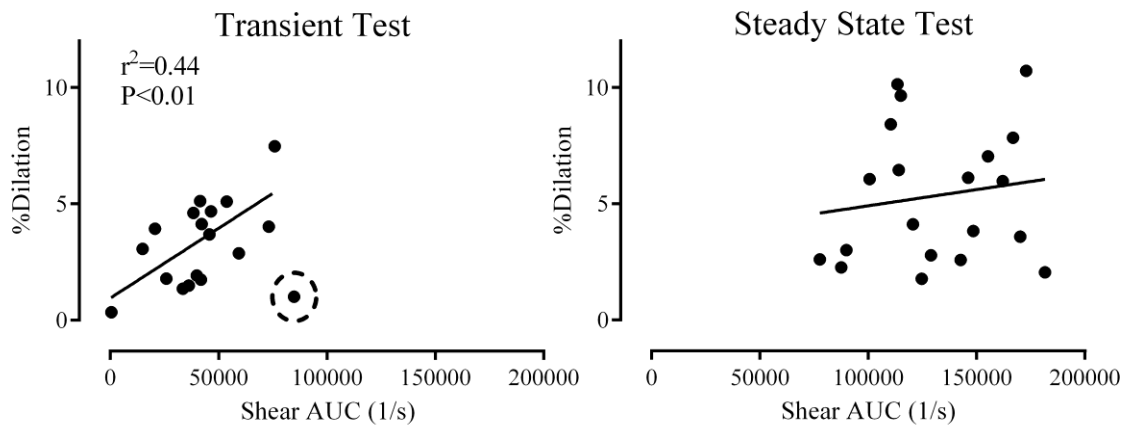


**Figure 5. The relationship between shear AUC and ICA dilation in the transient and steady state CO<sub>2</sub> trials.**

The present data represent the stimulus-response relationship between shear area under the curve (AUC) and ICA vasodilation. In the transient trial, following removal of the statistical outlier (circled), shear area AUC was positively correlated with ICA vasodilation ( $r^2=0.44$ ;  $P<0.01$ ). No relationship was present between shear AUC and ICA vasodilation in the steady state trial ( $r^2=0.02$ ;  $P=0.53$ ). Reproduced from (Hoiland *et al.*, 2017c), permission not required.

### **Intra- vs. Extra-Cranial Cerebral Hemodynamics**

Elevations in MCAv occurred at the same time as ICAv following the onset of hypercapnia in the transient ( $13.0\pm 10.0$  vs.  $16.7\pm 14.5$ ;  $P=0.18$ ) and steady state trials ( $15.1\pm 14.9$  vs.  $16.9\pm 13.9$ s;  $P=0.11$ ), respectively (Figure 3). Peak MCAv and ICAv occurred at the same time in the transient ( $40.1\pm 7.5$  vs.  $42.8\pm 9.3$ s;  $P=0.09$ ) and steady state ( $182.1\pm 99.0$  vs.  $199.6\pm 91.3$ s;  $P=0.24$ ) trials. In the transient and steady state tests, peak ICA flow occurred  $41.7\pm 9.5$ s and  $234.2\pm 84.3$ s following the onset of CO<sub>2</sub> breathing, respectively.

### **Blood Pressure Regulation**

During the transient CO<sub>2</sub> test, MAP increased from  $94.6\pm 12.5$ mmHg to peak value of  $104.2\pm 13.6$ mmHg ( $P<0.01$ ), while the time of occurrence for peak MAP ( $81.2\pm 73.1$ s) was not

statistically different from the time of peak dilation ( $110.1 \pm 69.1$  s;  $P=0.20$ ). However, the time to peak MAP and dilation were not related *within* subject ( $r^2=0.14$ ;  $P=0.06$ ), nor was the magnitude of dilation and change in MAP ( $r^2=0.09$ ;  $P=0.22$ ). During the steady state hypercapnia, MAP increased from  $94.2 \pm 10.4$  mmHg to a peak value of  $105.8 \pm 11.3$  mmHg ( $P<0.01$ ), while the time of occurrence for peak MAP ( $169.0 \pm 96.3$  s) was earlier than that for peak dilation ( $283.6 \pm 56.1$  s;  $P<0.01$ ). There was no relationship in the time to peak dilation and peak MAP ( $R^2=0.002$ ;  $P=0.43$ ).

## DISCUSSION

The present study outlines a novel experimental design aimed at: 1) assessing shear-mediated dilation of cerebral conduit arteries without the confounding influence of sustained increases in PaCO<sub>2</sub>, and 2) reinforcing the existence of shear mediated dilation of the ICA (Carter *et al.*, 2016a; Hoiland *et al.*, 2016b). We observed dilation of the ICA in response to both transient and steady state hypercapnia. Under both conditions, increases in shear stress preceded dilation of the ICA in a time-dependent manner. Vasodilation of the ICA in the transient trial was strongly correlated to the increase in shear AUC, implicating shear as the primary stimulus for dilation, consistent with observations in the brachial, femoral, and coronary arteries (Pyke & Tschakovsky, 2007).

The assessment of FMD in peripheral arteries dates back >20 years to the landmark study by Celermajer *et al.*, 1992 (Celermajer *et al.*, 1992). This technique evolved into a method for assessing the function and health of endothelial cells in the general circulation (Green *et al.*, 2014). However, to date, there is no equivalent method of assessing cerebral conduit artery shear-mediated regulation. In humans, the ICA conveys blood flow to the brain and bilaterally this accounts for ~70% of global CBF (Zarrinkoob *et al.*, 2015). In addition to serving as cerebral conduit vessels, the ICAs regulate CBF (Willie *et al.*, 2014c) and provide the most accessible avenue (Thomas *et al.*, 2015) to assess cerebral endothelial function using duplex ultrasound. Therefore, the measurement of ICA diameter during a controlled and transient elevation in shear stress may provide a valid paradigm and for the specific assessment of cerebral conduit artery endothelial function (or dysfunction) (Thijssen *et al.*, 2011). Whilst ischemia-induced hyperemia is utilized in *peripheral* FMD tests, this is obviously not possible in the cerebral vasculature (Smith *et al.*, 2011). However, the present study indicates that

hypercapnia-induced vasodilation, in particular utilizing transient exposure, induces ICA dilation following increases in intra-vascular shear stress of a similar manner and profile to post-occlusion cuff release (Carter *et al.*, 2016a). Given the congruent shear dynamics of a peripheral FMD test and the current carotid FMD test, in addition to the strong relationship between shear AUC and vasodilation, it appears that transient elevations in CO<sub>2</sub> provide a robust (and relatively specific) method to perturb shear-mediated regulation of CBF. We therefore propose a novel technique to assess “cerebrovascular FMD” in the present study; however, pharmacological inhibition of endothelial NO synthase is necessary to confirm the potential applicability of this technique. The lack of correlation between shear AUC and dilation in the steady state trial indicates that sustained hypercapnia is likely not an adequate method to assess shear-mediated regulation of the ICA due to a larger influence of confounding factors (increased blood pressure etc.,).

Our data implicate shear dependent mechanisms as key contributors to vasodilation in the ICA during a CO<sub>2</sub> reactivity test (Figures 4 & 5) in accordance with previous study (Carter *et al.*, 2016a). Considering the transient CO<sub>2</sub> test elicited a more rapid, albeit lower, ICA dilation compared to the steady state test, our findings suggest that ICA dilation in the transient test is less influenced by extraneous factors (e.g., BP, sympathetic nervous activity, metabolism, direct effects of CO<sub>2</sub>/pH etc.,) As depicted in figure 5, the relationship between shear AUC and dilation occurs within a range between 0-100,000s<sup>-1</sup>, but in the steady state trial where shear AUC is >100,000s<sup>-1</sup> this relationship is lost. This may be due to two potential factors: 1) a ceiling effect of shear on ICA vasodilation, and 2) that as previously mentioned, sustained CO<sub>2</sub> engages other confounding physiological responses (e.g., elevated BP) that obscures the relationship between Shear AUC and vasodilation. Therefore, it appears the transient trial more closely resembles the NO-mediated FMD observed in the peripheral vasculature (Thijssen *et al.*, 2011; Green *et al.*, 2014), which is further supported by observations that other endothelial derived relaxing factors [e.g. prostaglandins (Hoiland *et al.*, 2016b)] do not possess an obligatory role in hypercapnic cerebral vasodilation. That the percent dilation was only modestly correlated *within* subjects between the transient and steady state CO<sub>2</sub> tests indicates that distinct mechanisms may be evoked differentially in response to varying stimuli (i.e. time of hypercapnia). This is consistent with findings from the peripheral FMD test, where five minutes of ischemia induces a largely NO-mediated dilation, whereas longer periods of ischemia induce compensatory redundant mechanisms resulting in less NO dependency

(Mullen *et al.*, 2001). However, it must be stressed that studies pharmacologically inhibiting endothelial nitric oxide synthase activity have not consistently demonstrated a role for NO in hypercapnic vasodilation (Schmetterer *et al.*, 1997; White *et al.*, 1998; Ide *et al.*, 2007). These variable findings may be related to the use of velocity indices of cerebral blood flow (CBF) [i.e. TCD; discussed in (Ainslie & Hoiland, 2014)], which are unable to detect and quantify changes in vessel diameter. In addition, systemic administration of NO blockers such as L-NMMA have both direct, and indirect reflex, effects on vasomotor tone and these are countervailing, making the impacts of such drugs difficult to interpret.

A delayed response (~60sec) to reach maximal steady state CBF for a given step change in  $P_{ET}CO_2$  has been demonstrated previously (Shapiro *et al.*, 1966; Carter *et al.*, 2016a). Further, steady state hypercapnia is reported to elicit higher cerebrovascular reactivity than non-steady state tests [e.g., rebreathing (Pandit *et al.*, 2003)]. This disparity in reactivity may be explained by the time dependent nature of endothelial NO synthase upregulation and consequent NO mediated vasodilation, which may not be fully engaged at the termination of a progressive and dynamic stimulus. By quantifying the maximal dilation to a steady-state  $CO_2$  stimulus in addition to the vasomotor reaction to a transient elevation in  $CO_2$  and shear, we have provided insight into the percent contribution of shear-dependent mechanisms to total  $CO_2$  reactivity. Further, this highlights that ~40% of  $CO_2$  reactivity is not explained by shear, and may be partially attributable to changes in MAP (Przybyłowski *et al.*, 2003; Ainslie *et al.*, 2012; Peebles *et al.*, 2012), increases in cardiac output, and/or direct effects of  $PaCO_2$  /pH. The difference in time to peak dilation during the transient and steady-state  $CO_2$  test likely indicates a different time course of these mechanism(s) on vasomotor tone. Therefore, while shear mechanisms likely acted in the same time course between tests, it is the additional stimuli that results in a further and delayed maximal dilation during steady state elevations in  $CO_2$ .

When considering the contribution of shear dependent mechanisms to cerebrovascular dilation one must also consider the potential for myogenic influences during hypercapnia-mediated increases in MAP (Faraci *et al.*, 1989). Increases in cerebral perfusion pressure have been shown to produce cerebral vasoconstriction (Fog, 1939); therefore, myogenic constriction may have masked vasodilation to some degree (resulting in underestimation of shear-mediated vasodilation), and/or be related to the variable contribution of shear dependent mechanisms to hypercapnia mediated vasodilation. The opposing forces of shear-mediated dilation and

myogenic constriction has been previously demonstrated in peripheral vessels (Pohl *et al.*, 1991; Atkinson *et al.*, 2015).

### *Methodological considerations*

Recently it has become convention to normalize peripheral FMD tests via logarithmic transformation of baseline diameter, peak diameter, and shear rate AUC to allometrically scale for artery size and account for between subject variations in the shear stimulus (Atkinson & Batterham, 2013; Atkinson *et al.*, 2013). The purpose of these corrections is to better estimate the endothelial responsiveness to a shear stimulus. Here, we have not scaled for baseline diameter and shear AUC between trials as the purpose of the current study was not to evoke and subsequently quantify a change in endothelial function, but to determine the experimental feasibility of a transient increase in ICA shear (via elevated  $P_{ET}CO_2$ ) in eliciting a measureable change in arterial diameter. Indeed endothelial function should not be different between the two trials given no intervention was present.

While we have used dynamic end-tidal forcing to control  $P_{ET}CO_2$ , determining the efficacy of the Douglas bag technique for a 30-second manipulation of  $CO_2$  may provide great utility, given the reduced technical demand and consequently easier transition into a clinical setting. Further determining the within and between-day variation in transient  $CO_2$  mediated ICA vasodilation will help determine its potential translation into a clinical setting.

### *Perspective*

Turbulent flow and non-uniform shear stress, which are characteristic of the carotid bulb and ICA, render the carotid vasculature a ‘high risk’ area for atherogenesis, wall thickening, and consequent vascular dysfunction (Glagov *et al.*, 1988; Takeuchi & Karino, 2010; Bijari *et al.*, 2014). Therefore, the present carotid FMD test may possess future potential to detect early carotid and cerebral vascular dysfunction, before the development of overt wall thickening or intractable plaque deposition. Analogous to the peripheral FMD approaches, which predict future cardiovascular events (Green *et al.*, 2011), our carotid test may provide a useful clinical window into sub-clinical atherogenesis and also enable treat-to-target assessment of management efficacy. While steady state  $CO_2$  reactivity tests have shown a strong ability to

predict cerebral vascular events in clinical populations [e.g., carotid stenosis (Gupta *et al.*, 2012)], they have yet to demonstrate predictive value relative to cerebral vascular risk in healthy individuals (Portegies *et al.*, 2014). The inability to specifically predict cerebral vascular risk may be related to several factors including: 1) previous use of velocity indices of CBF and consequent inability to directly quantify vasomotion (Ainslie & Hoiland, 2014; Coverdale *et al.*, 2014), and 2) the confounding nature of the myriad physiological consequences secondary to sustained hypercapnia [i.e., elevated blood pressure (Regan *et al.*, 2014) and cardiac output (Balanos *et al.*, 2003), chemoreceptor mediated sympathoactivation (Pitsikoulis *et al.*, 2008), and the potential for direct vasodilatory effects of CO<sub>2</sub>/pH (Kontos *et al.*, 1977a; Willie *et al.*, 2012; Hoiland *et al.*, 2016b)]. Our approach mitigates these limitations by directly visualizing arterial diameter change and quantifying the magnitude and profile of the shear stimulus. It is tailored to perturb *cerebrovascular* endothelial function with reduced input from confounding physiological factors and couples concurrent measurement of cerebral conduit artery diameter, flow and shear at high temporal and spatial resolution. Future research should aim to 1) determine the influence of transiently elevated shear on ICA vasodilation prior to and following NO blockade to confirm endothelial involvement, and 2) determine the magnitude by which carotid shear-mediated dilation may be reflective of cerebral vascular health and risk of cerebrovascular events.